UNVEILING THE IMPACT OF LOCAL OR SYSTEMIC THERAPEUTIC STRATEGIES ON THE TUMOR MICROENVIRONMENT

EDITED BY: Jian Huang, Chao Ni, Liu Yang, Kevin J. Ni and Hengyu Li
PUBLISHED IN: Frontiers in Cell and Developmental Biology and
Frontiers in Oncology

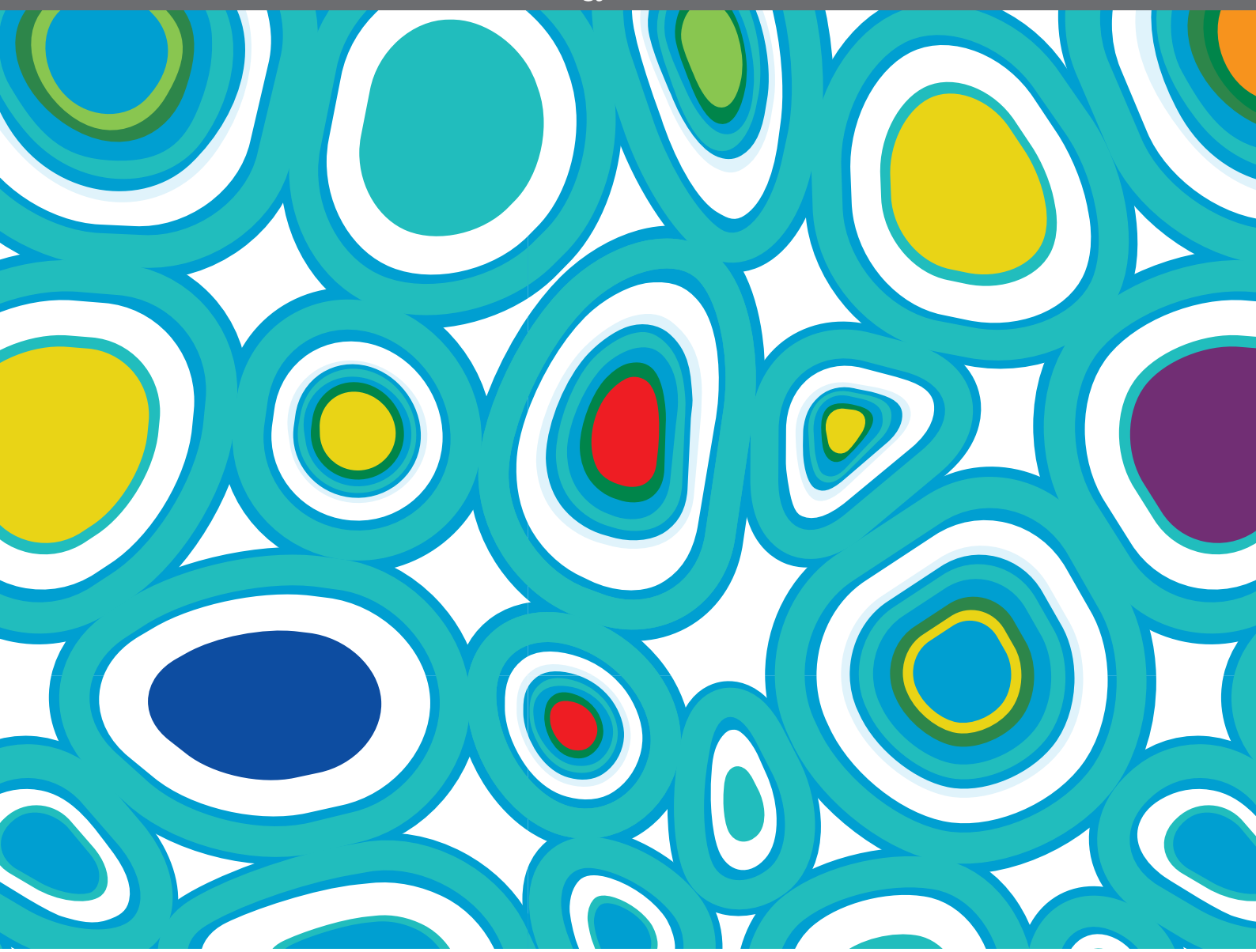

frontiers Research Topics

ISSN 1664-8714
ISBN 978-2-88974-255-4
DOI 10.3389/978-2-88974-255-4

About Frontiers

Frontiers is more than just an open-access publisher of scholarly articles: it is a pioneering approach to the world of academia, radically improving the way scholarly research is managed. The grand vision of Frontiers is a world where all people have an equal opportunity to seek, share and generate knowledge. Frontiers provides immediate and permanent online open access to all its publications, but this alone is not enough to realize our grand goals.

Frontiers Journal Series

The Frontiers Journal Series is a multi-tier and interdisciplinary set of open-access, online journals, promising a paradigm shift from the current review, selection and dissemination processes in academic publishing. All Frontiers journals are driven by researchers for researchers; therefore, they constitute a service to the scholarly community. At the same time, the Frontiers Journal Series operates on a revolutionary invention, the tiered publishing system, initially addressing specific communities of scholars, and gradually climbing up to broader public understanding, thus serving the interests of the lay society, too.

Dedication to Quality

Each Frontiers article is a landmark of the highest quality, thanks to genuinely collaborative interactions between authors and review editors, who include some of the world's best academicians. Research must be certified by peers before entering a stream of knowledge that may eventually reach the public - and shape society; therefore, Frontiers only applies the most rigorous and unbiased reviews.
Frontiers revolutionizes research publishing by freely delivering the most outstanding research, evaluated with no bias from both the academic and social point of view. By applying the most advanced information technologies, Frontiers is catapulting scholarly publishing into a new generation.

What are Frontiers Research Topics?

Frontiers Research Topics are very popular trademarks of the Frontiers Journals Series: they are collections of at least ten articles, all centered on a particular subject. With their unique mix of varied contributions from Original Research to Review Articles, Frontiers Research Topics unify the most influential researchers, the latest key findings and historical advances in a hot research area! Find out more on how to host your own Frontiers Research Topic or contribute to one as an author by contacting the Frontiers Editorial Office: frontiersin.org/about/contact

UNVEILING THE IMPACT OF LOCAL OR SYSTEMIC THERAPEUTIC STRATEGIES ON THE TUMOR MICROENVIRONMENT

Topic Editors:
Jian Huang, Zhejiang University, China
Chao Ni, Zhejiang University, China
Liu Yang, Zhejiang Provincial People's Hospital, China
Kevin J. Ni, St George Hospital, Australia
Hengyu Li, Second Military Medical University, China

Citation: Huang, J., Ni, C., Yang, L., Ni, K. J., Li, H., eds. (2022). Unveiling the Impact of Local or Systemic Therapeutic Strategies on the Tumor Microenvironment. Lausanne: Frontiers Media SA. doi: 10.3389/978-2-88974-255-4

Table of Contents

frontiers in Oncology

EDITORIAL
published: 25 January 2022
doi: 10.3389/fonc.2021.832036

Editorial: Unveiling the Impact of Local or Systemic Therapeutic Strategies on the Tumor Microenvironment

Yun-Wang Chen[1,2], *Jia-Hong Jiang*[1], *Zhe-Ling Chen*[1]* *and Liu Yang*[1,2]*

[1] Cancer Center, Department of Medical Oncology, Zhejiang Provincial People's Hospital, Affiliated People's Hospital, Hangzhou Medical College, Hangzhou, China, [2] The Medical College, The Qingdao University, Qingdao, China

Keywords: tumor microenvironment, microenvironment-targeting therapy, oncology precision therapy, treatment, immunotherapy

Editorial on the Research Topic

Unveiling the Impact of Local or Systemic Therapeutic Strategies on the Tumor Microenvironment

In cancer treatment, chemotherapy and immunotherapy are two important systemic treatments. Yet both of the above treatments are affected by tumor microenvironment (TME). TME is not only the "soil" that supports tumor growth, but also a complex and dynamically changing integrated system, including fibroblasts, immune-inflammatory cells and glial cells, as well as interstitial cells, microvascular system, and infiltrating biomolecules in the adjacent area. TME in a highly immunosuppressive state can significantly attenuate anti-tumoral responses induced by immunotherapy. Some components of TME, such as cancer-associated fibroblasts (CAFs), cytokines, and chemokines secreted by CAFs, can protect tumor cells from the effects of conventional chemotherapy, leading to tumor progression and chemotherapy resistance. Therefore, it is necessary to incorporate microenvironment-targeting therapy into the comprehensive treatment of tumors. In addition, some cells or molecules that make up TME can also be used as potential indicators to predict cancer prognosis and evaluate the efficacy of chemotherapy or immunotherapy.

TME manifests as an acidic microenvironment, characterized by hypoxia, angiogenesis, inflammation, and immunosuppression. Tumor cells are able to overcome the above TME hardships during the growth phase to achieve a stronger growth advantage than normal cells. The tumor microenvironment-targeting therapies aimed at its complex biological characteristics and various components of TME have achieved good therapeutic outcomes. Hypoxia-activated prodrugs have been widely investigated for targeting hypoxic tumor cells. Canakinumab, a selective IL-1 β inhibitor, can inhibit the related inflammatory response in TME and reduce immunosuppression. According to the CANTOS study, compared with the placebo group, canakinumab treatment could significantly reduce the incidence rates and mortality of lung cancer (1). The immunosuppressive environment in TME can attenuate the antitumor activity of natural killer (NK) cells. Metabolic flexibility determines NK cell functional fate in TME (2). Compared with the original NK cells, the expanded NK cells with complete metabolic flexibility have stronger tumor killing in TME. Except for non-cellular components, tumor-associated macrophages (TAMs), Tregs, myeloid-derived suppressor cells (MDSCs), and other cellular components with immunosuppressive effects in TME play an important role in tumor

OPEN ACCESS

Edited and reviewed by:
Luisa Lanfrancone, European Institute of Oncology (IEO), Italy

***Correspondence:**
Liu Yang
yangliu@hmc.edu.cn
Zhe-Ling Chen
chenzheling@hmc.edu.cn

Specialty section:
This article was submitted to Molecular and Cellular Oncology, a section of the journal Frontiers in Oncology

Received: *09 December 2021*
Accepted: *30 December 2021*
Published: *25 January 2022*

Citation:
Chen Y-W, Jiang J-H, Chen Z-L and Yang L (2022) Editorial: Unveiling the Impact of Local or Systemic Therapeutic Strategies on the Tumor Microenvironment. Front. Oncol. 11:832036. doi: 10.3389/fonc.2021.832036

proliferation, migration, invasion, metastasis, and chemoresistance. Targeted blocking of the above components could kill tumors and reverse chemotherapy resistance. TME provides the "soil" for tumor to "grow", which leads to the production of nonsynonymous mutation of tumor cells, namely neoantigens. Neoantigens are also the high-quality targets for microenvironment-targeting therapies. Individualized neoantigen peptide vaccines can induce sustained T cell responses (3). At the same time, microenvironment-targeting therapies may also have synergistic effects with routine chemotherapy, immunotherapy, and other targeted treatment strategies. In addition to tumor microenvironment targeting therapies, it also makes sense to predict chemotherapy and immunotherapy by TME related indicators. Analyzing the changes of immune status before and after anti-tumor treatment or developing a visualization tool of personalized treatment based on genomics are important elements and tools for precision tumor therapy (4). This Research Topic includes three review articles and five original research articles on TME.

Wang et al. summarized the TME of esophageal cancer (EC) and the latest progress in microenvironment-targeting therapies. This paper summarized that some stromal components and important signaling pathways in TME played an important role in the evolution of EC. It also pointed out that suppressing inflammation in TME, anti-angiogenesis, and improving the hypoxic microenvironment could achieve the aim of preventing and treating tumors. Guo et al. have developed a novel NK cell expansion method utilizing OX40L armed NK-92 cell with secreting neoleukin-2/15 (Neo-2/15). These cells have high cytotoxicity against Raji cells and against HepG2 (liver cancer), A427 (lung cancer), and CAVO3 (ovarian cancer) *in vivo*. The complex TME of solid tumor can block the infiltration of NK cells, and the NK92-Neo2/15-OX40L expanded NK cells have stronger infiltration ability and antitumor activity. Cao et al. summarized the characteristics and functions of some key cellular components of TME. On this basis, this article explored the potential treatment strategies of targeted therapy for the above factors in order to eliminate drug resistance and increase therapeutic efficacy. Zhang et al. identified and analyzed multiple neoantigens by whole-exome sequencing of tumor specimens from three patients with non-small cell lung cancer (NSCLC). Neoantigens from three patients successfully induced neoantigen-reactive T cells (NRTs), which showed satisfactory results and anti-tumor effects, as demonstrated with mouse model. The treatment method aiming at the specific antigen produced by tumor cells can efficiently control and even cure the tumor, so as to achieve the purpose of oncology precision therapy. Turinetto et al. summarized the effects of poly (ADP-ribose) polymerase inhibitors (PARPi) on TME in ovarian cancer from the perspectives of hypoxia, cGAS-cGAMP-STING pathway, and upregulation of PDL-1. It shows that PARP inhibitors plus other target therapies or immunotherapy can improve the prognosis by influencing the immune system and the TME.

Wang et al. collected immunological indexes before and after neoadjuvant chemotherapy in 262 breast cancer patients and selected five of these indexes for analysis to form a prediction model, named NeoAdjuvant Therapy Immune Model (NATIM). Three indexes - CD4+/CD8+ T cell ratio (a/b), CD3+CD8+ cytotoxic T cell percent (a/b), and lymphosum of T, B, and NK cells (a/b) - were thought to be effective predictors of neoadjuvant chemotherapy. Using bioinformatics and cytological tests Aili et al. confirmed that knockdown of PBRM1 was associated with the reduction of CD4 T cells in clear cell renal cell carcinoma (ccRCC) TME and anti-PD-1 immunotherapy can increase the infiltration of T cells in both PBRM1 high and PBRM1 low tumors, but to different degrees. High PBRM1 expression levels imply more T cells in TME and PBRM1 expression levels can influence and predict the efficacy of anti-PD-1 immunotherapy. Zhang et al. performed comprehensive bioinformatics analysis of the published datasets of head and neck squamous cell carcinoma (HNSCC) and proposed a novel molecular subtype classification strategy that can predict disease prognosis and guide treatment allocation.

Microenvironment-targeting therapies improve the therapeutic efficacy of existing tumor methods and reverse drug resistance. Analyzing various immunological indexes in TME and classifying molecular subtypes including TME can guide treatment allocation and predict disease prognosis, so as to achieve the purpose of personalized oncology precision therapy. However, there are still many problems to be solved about the clinical guidance of the TME in the future. Future research does not only need more in-depth excavation of the ingredients in the TME but also needs to develop an accurate treatment for microenvironment targets. With this Research Topic, the editors hope to inspire subsequent research for TME and the further development of microenvironment-targeting therapies.

AUTHOR CONTRIBUTIONS

LY and Z-LC contributed to the conception of the article. Y-WC integrated all information and wrote the manuscript. LY and Z-LC provided critical guidance, revisions for J-HJ throughout the writing process. Y-WC, J-HJ, and LY compiled information and revised the manuscript. All authors read and approved the final manuscript.

REFERENCES

1. Ridker PM, MacFadyen JG, Thuren T, Everett BM, Libby P, Glynn RJ, et al. Effect of Interleukin-1β Inhibition With Canakinumab on Incident Lung Cancer in Patients With Atherosclerosis: Exploratory Results From a Randomised, Double-Blind, Placebo-Controlled Trial. *Lancet* (2017) 390(10105):1833–42. doi: 10.1016/s0140-6736(17)32247-x
2. Poznanski SM, Singh K, Ritchie TM, Aguiar JA, Fan IY, Portillo AL, et al. Metabolic Flexibility Determines Human NK Cell Functional Fate in the Tumor Microenvironment. *Cell Metab* (2021) 33(6):1205–20.e1205. doi: 10.1016/j.cmet.2021.03.023

3. Hu Z, Leet DE, Allesoe RL, Oliveira G, Li S, Luoma AM, et al. Personal Neoantigen Vaccines Induce Persistent Memory T Cell Responses and Epitope Spreading in Patients With Melanoma. *Nat Med* (2021) 27(3):515–25. doi: 10.1038/s41591-020-01206-4
4. Bagaev A, Kotlov N, Nomie K, Svekolkin V, Gafurov A, Isaeva O, et al. Conserved Pan-Cancer Microenvironment Subtypes Predict Response to Immunotherapy. *Cancer Cell* (2021) 39(6):845–65.e847. doi: 10.1016/j.ccell.2021.04.014

Conflict of Interest: The authors declare that the research was conducted in the absence of any commercial or financial relationships that could be construed as a potential conflict of interest.

Publisher's Note: All claims expressed in this article are solely those of the authors and do not necessarily represent those of their affiliated organizations, or those of the publisher, the editors and the reviewers. Any product that may be evaluated in this article, or claim that may be made by its manufacturer, is not guaranteed or endorsed by the publisher.

frontiers in Cell and Developmental Biology

ORIGINAL RESEARCH
published: 18 March 2021
doi: 10.3389/fcell.2021.656981

Circadian Rhythm Gene PER3 Negatively Regulates Stemness of Prostate Cancer Stem Cells via WNT/β-Catenin Signaling in Tumor Microenvironment

Qilin Li[1], Ding Xia[2], Zhihua Wang[2], Bo Liu[3], Jing Zhang[3], Ping Peng[3], Qiujun Tang[3], Jie Dong[3], Juan Guo[3], Dong Kuang[4], Weimin Chen[1], Jing Mao[1], Qiuhui Li[5]* and Xin Chen[3]**

[1] Department of Stomatology, Tongji Hospital, Tongji Medical College, Huazhong University of Science and Technology, Wuhan, China, [2] Department of Urology, Tongji Hospital, Tongji Medical College, Huazhong University of Science and Technology, Wuhan, China, [3] Department of Oncology, Tongji Hospital, Tongji Medical College, Huazhong University of Science and Technology, Wuhan, China, [4] Department of Pathology, Tongji Hospital, Tongji Medical College, Huazhong University of Science and Technology, Wuhan, China, [5] State Key Laboratory Breeding Base of Basic Science of Stomatology (Hubei-MOST) and Key Laboratory for Oral Biomedicine of Ministry of Education (KLOBM), School and Hospital of Stomatology, Wuhan University, Wuhan, China

OPEN ACCESS

Edited by:
Kevin J. Ni,
St George Hospital, Australia

Reviewed by:
Dhyan Chandra,
University at Buffalo, United States
Qi-En Wang,
The Ohio State University,
United States

***Correspondence:**
Xin Chen
dr.chenxin@tjh.tjmu.edu.cn
orcid.org/0000-0002-0566-7678
Qiuhui Li
qiuhui.li@whu.edu.cn
orcid.org/0000-0003-4825-7772
Jing Mao
maojing@hust.edu.cn
orcid.org/0000-0001-6353-9992

Specialty section:
This article was submitted to Molecular and Cellular Oncology, a section of the journal Frontiers in Cell and Developmental Biology

Received: 21 January 2021
Accepted: 10 February 2021
Published: 18 March 2021

Citation:
Li Q, Xia D, Wang Z, Liu B, Zhang J, Peng P, Tang Q, Dong J, Guo J, Kuang D, Chen W, Mao J, Li Q and Chen X (2021) Circadian Rhythm Gene PER3 Negatively Regulates Stemness of Prostate Cancer Stem Cells via WNT/β-Catenin Signaling in Tumor Microenvironment. Front. Cell Dev. Biol. 9:656981. doi: 10.3389/fcell.2021.656981

Prostate cancer (PCa) cells are heterogeneous, containing a variety of cancer cells with phenotypical and functional discrepancies in the tumor microenvironment, where prostate cancer stem cells (PCSCs) play a vital role in PCa development. Our earlier studies have shown that $ALDH^{hi}CD44^{+}$ (DP) PCa cells and the corresponding $ALDH^{lo}CD44^{-}$ (DN) PCa cells manifest as PCSCs and non-PCSCs, respectively, but the underlying mechanisms regulating stemness of the PCSCs are not completely understood. To tackle this issue, we have performed RNA-Sequencing and bioinformatic analysis in DP (versus DN) cells in this study. We discovered that, PER3 (period circadian regulator 3), a circadian rhythm gene, is significantly downregulated in DP cells. Overexpression of PER3 in DP cells significantly suppressed their sphere- and colony-forming abilities as well as tumorigenicity in immunodeficient hosts. In contrast, knockdown of PER3 in DN cells dramatically promoted their colony-forming and tumor-initiating capacities. Clinically, PER3 is downregulated in human prostate cancer specimens and PER3 expression levels are highly correlated with the prognosis of the PCa patient. Mechanistically, we observed that low levels of PER3 stimulates the expression of BMAL1, leading to the phosphorylation of β-catenin and the activation of the WNT/β-catenin pathway. Together, our results indicate that PER3 negatively regulates stemness of PCSCs via WNT/β-catenin signaling in the tumor microenvironment, providing a novel strategy to treat PCa patients.

Keywords: prostate cancer stem cells, prostate cancer, tumor microenvironment, PER3, Wnt/β-catenin signaling

Abbreviations: ALDH, aldehyde dehydrogenase; AML, acute myeloid leukemia; CSCs, cancer stem cells; DN cells, $ALDH^{lo}CD44^{-}$ cells; DP cells, $ALDH^{hi}CD44^{+}$ cells; FACS, fluorescence-activated cell sorting; GSCs, glioblastoma stem cells; IHC, immunohistochemical staining; KIRC, kidney renal clear cell carcinoma; LDAs, limiting dilution assays; mCRPC, metastatic castration resistant prostate cancer; OS, overall survival; PCa, prostate cancer; PCSCs, prostate cancer stem cells; PER3, period circadian regulator 3; RNA-seq, RNA-sequencing; s.c., subcutaneous; TIF, tumor-initiating frequency; TMA, tissue microarray; TME, tumor microenvironment; ULA, ultra-low attachment.

INTRODUCTION

Human prostate cancer (PCa) is the most malignant cancers affecting men worldwide with an increasing incidence and high mortality. It has been estimated that there were 191,930 new cases and 33,330 deaths from PCa in the United States during 2020 (Siegel et al., 2020). Surgery and/or radiation are often curative in the initial stages, but many patients eventually develop metastatic castration resistant prostate cancer (mCRPC) that is incurable and fatal (Rycaj and Tang, 2017; Li et al., 2018). At the moment, the etiology for PCa development is still not completely understood, and novel regiments for treating PCa metastasis and recurrence still need to be developed.

Prostate cancer is a heterogenous malignancy, consisting of cancer cells with functional and phenotypical differences in the tumor microenvironment (TME) (Skvortsov et al., 2018). Tumor cell heterogeneity results from clone evolution and/or cancer stem cell (CSC) models (Tang, 2012; Prager et al., 2019). Like many other solid tumors, emerging evidence has shown that there are subsets of PCa cells with stem cell properties in TME, i.e., prostate cancer stem cells (PCSCs), responsible for PCa initiation, progression, therapy resistance and metastasis (Chen et al., 2013; Skvortsov et al., 2018). Hence, a better understanding of PCSCs in TME will result in better treatment for PCa patients. On the other hand, TME is vital for PCSCs. Recent studies have suggested that certain signaling pathways in TME may play a critical role in regulating PCSCs for their SC properties, metastatic traits and resistance to treatment, including the CXCL12/CXCR4 and WNT/β-catenin signaling pathways (Trautmann et al., 2014; Cojoc et al., 2015). However, it is not completely clear which molecules are required to activate these signaling pathways that regulate PCSCs in TME.

The circadian clock is a molecular pacemaker and an evolutionally conserved mechanism that governs biological and physiological processes, which is located in the hypothalamus suprachiasmatic nucleus (Shafi and Knudsen, 2019). The circadian rhythm is generated by positive and negative transcription-translation feedback loops (Young and Kay, 2001). In general, the positive loop is composed of the basic helix-loop-helix heterodimeric transcriptional factors, BMAL1 and CLOCK, which drive the clock and are highly associated with the regulation of the immune response and various cellular pathways (Dong et al., 2019). In addition, the BMAL1/CLOCK complex regulate the expression of the negative regulators of the loop, including *Period* (*PER1*, *PER2*, *PER3*) and *Cryptochromes* (*CRY1* and *CRY2*) gene, which in turn repress BMAL1/CLOCK activity (Shafi and Knudsen, 2019). Recent evidence has reported that circadian rhythm disruption is related to increased cancer incidence (Dickerman et al., 2016; Markt et al., 2016; Wendeu-Foyet and Menegaux, 2017) and poor efficacy of cancer management (Sancar et al., 2015), although the pertinent mechanisms are incompletely understood. Importantly, very recent studies have suggested that uncovering the underlying mechanisms of circadian clock regulation in cancer development may explore a future direction in cancer treatment (Sancar and Van Gelder, 2021).

Whether circadian rhythm genes regulate stemness of CSCs is incompletely understood, and dysregulation of circadian clock in CSCs are correlated to cancer development. For instance, Puram et al. (2016) have indicated that altered circadian regulation in leukemia stem cells may be associated with cancer progression. In solid tumors, targeting CSCs in brain tumors via disruption of the circadian clock genes may be a novel strategy for targeted therapy of glioblastoma patients (Dong et al., 2019). Based on this background, we started this project to understand the molecular impact of circadian regulation in PCSCs. In this study, we performed a deep RNA-sequencing to compare gene expression profiles, using $ALDH^{hi}CD44^{+}$ (DP) PCa cells and $ALDH^{lo}CD44^{-}$ (DN) PCa cells, which have been shown to function as PCSCs and non-PCSCs, respectively (Li et al., unpublished). We found that: (1) PER3 (Period Circadian Regulator 3), a circadian rhythm gene, is markedly downregulated in DP PCa cells. (2). PER3 overexpression in DP PCa cells significantly inhibits their clonogenicity and tumorigenicity, whereas PER3 knockdown in DN cells dramatically promotes their colony-forming and tumor-initiating abilities. (3) PER3 is downregulated in human PCa specimens, and its level is related with better patient survival. (4) Mechanistically, low expression levels of PER3 stimulates the expression of BMAL1, resulting in the phosphorylation of β-catenin and the activation of the WNT/β-catenin pathway. Collectively, this study identifies that PER3 is a negative regulator for PCSCs via the activation of WNT/β-catenin signaling in TME, providing a potential and novel strategy for PCa treatment.

MATERIALS AND METHODS

Cell Lines and Reagents

Human prostate cancer cell lines, PC3 and DU145, were purchased and authenticated from Cell Bank (Chinese Academy of Sciences, Shanghai, China). Cells were cultured in DMEM (Invitrogen, CA, United States) with 10% FBS (Gibco, United States) and 10,000 U/ml penicillin, and incubated in 5% CO2 incubator at 37°C. All cells were tested for mycoplasma free via a mycoplasma detection kit (Thermo Fisher Scientific, United States).

Purification of Double Marker Cells by Fluorescence-Activated Cell Sorting (FACS)

Basic procedures were previously described (Chen et al., 2016). In brief, all cells were first digested into single cells by trypsin containing 0.25% EDTA, and resuspended in PBS. Cells were incubated with a PE-conjugated anti-CD44 antibody (cat#: 550392, BD Pharmingen) at 4°C for 30 min, and then incubated with an ALDEFLUOR assay kit (Stemcell Technologies, #01700) at 37°C for 45 min, according to the manufacturer's instructions. The top 10% and bottom 10% gated cells were resolved and debris was abducted by gates in the light scatter SSC versus FSC diagrams.

DP PCa cells and the corresponding DN PCa cells were sorted by a FACS sorter (Aria II, BD Biosciences, United States).

Sphere and Colony-Formation Assays

Basic procedures were previously described (Chen et al., 2016). For sphere-formation assay, purified PC3 DP and DN cells were seeded (1,000 cells/well) in 96-well ultra-low attachment plates (Corning) and incubated using DMEM/F12 (Invitrogen, United States) supplemented with B27 (GIBCO) and bFGF (Stem Cell Technology). For the sphere passage, spheres were collected with a 40 μm diameter cell strainer, and then digested with 0.25% EDTA trypsin for 15 min into single cells for the next cycle. Spheres (diameter >40 μm) were counted, photographed and scored under an inverted microscope (Olympus CKX41, Tokyo, Japan) to determine the sphere forming efficiency. For the colony-formation assay, purified PC3 DP and DN cells were resuspended in Matrigel (BD Biosciences, Cat#: 354256) and seeded into 24-well culture plates (1,000 cells/well). After 30 min at 37°C, colony-formation culture medium was added to the wells: 50 ng/ml recombinant human EGF (Sigma), 10 nM Gastrin (Sigma), DMEM/F12 (Invitrogen, United States) supplemented with 1× B27 (GIBCO) and 500 nM A83-01 (Miltenyi Biotec). To determine the colony-forming efficiency, colonies (diameters >100 μm) were numerated, photographed and scored after 1 week.

Animal Studies

NOD/SCID male mice (4-week-old) were purchased from Beijing HFK Bioscience Co., Ltd (Beijing, China). Our animal work was conducted under the protocols approved by the IACUC of Huazhong University of Science and Technology (HUST; Wuhan, China, IACUC No. S2348). Basic procedures have been previously described (Chen et al., 2016). For limiting-dilution tumor regeneration assays (LDA), cells at increasing doses (100 to 1,000 cells/injection) were injected subcutaneously into NOD/SCID male mice. At the endpoint, mice were anesthetized and sacrificed according to AVMA guidelines, and tumors were harvested. The tumor-initiating frequency (TIF) in this study was calculated[1].

RT-qPCR

Basic procedures were previously described (Chen et al., 2016). Total RNA from PC3 DP and DN cells was extracted using the RNAiso Plus (Takara, Japan, Cat#: 9108), and cDNA was synthesized using cDNA Synthesis Kit (Thermo Scientific, United States, Cat#: 11754050). RT-qPCR analysis was performed using Maxima SYBR Green/ROX Mix (Thermo Scientific, United States) according to the manufacturer's instructions. Glyceraldehyde-3-phosphate dehydrogenase (GAPDH) was used as an internal control. GAPDH: 5′-TCGTGGAAGGACTCATGACC-3′ (forward) and 5′TCC ACCACCCTGTTGCTGTA-3′ (reverse); CD44: 5′-ATGG ACAAGTTTTGGTGGCACGC-3′ (forward) and 5′-AAGATGT AACCTCCTGAAGTGCTGC-3′ (reverse); ALDH1A1: 5′-ATCT TTGCTGACTGTGACCT-3′ (forward) and 5′-GCACCTCTT xCTACCACTCTC-3′ (reverse); PER3: 5′-AGCTACCTGCACC CTGAAGA-3′ (forward) and 5′-CGAACTTTATGCCGACC AAT-3′ (reverse); CD133: 5′-TGGATGCAGAACTTGACAA CGT-3′ (forward) and 5′-ATACCTGCTACGACAGTCGTGGT-3′ (reverse).

Immunofluorescence

Procedures for immunofluorescent staining was carried out as previously described (Chen et al., 2016). In brief, purified PC3 DP and DN cells were cultured in glass-bottomed 24-well dishes overnight, and incubated with primary antibodies (anti-PER3, Abcam, Cat#: ab67862, 1:100, or anti-β-catenin, Cell Signaling Technology, Cat#2951, 1:100) followed by secondary antibodies conjugated to Streptavidin-Cy3 (1:100; Thermo Fisher Scientific, Cat#:A12421) or Alexa Fluor 488 (1:100; Invitrogen, Cat#:A21202). Finally, cellular nuclei were stained with DAPI dye (4′,6-dynamiting-2-phenylamine, Sigma, Cat#: D9542) at room temperature for 10 min. Images were captured under a fluorescence microscope (Olympus, Tokyo, Japan).

Western Blotting

Procedures for western blotting have been previously described (Li et al., 2018). Primary antibodies used for western blotting are as follows: anti-GAPDH (Abcam, Cat#: ab9484, 1:5,000), anti-CD44 (Abcam, Cat#: ab157107, 1:5,000), anti-PER3 (Abcam, Cat#: ab177482, 1:5,000), anti-ALDH1 (Cell Signaling Technology, Cat#:5741, 1:5,000), anti-total β-catenin (Cell Signaling Technology, Cat#:2951, 1:5,000), anti-phosphorylated β-catenin (Cell Signaling Technology, Cat#: 176, 1:5,000).

Gene Overexpression and Knockdown With Lentiviral Vectors

Basic procedures were previously described (Chen et al., 2016). Briefly, PER3-shRNA lentivirus, pGMLV-PE1-PER3 lentiviral vectors were purchased from Shanghai SBO Medical Biotechnology (Shanghai, China). Purified PC3 DP and DN cells were purified via FACS and seeded in 6-well plates (50, 000 cells/well) and cultured for 24 h. PC3 DP were infected with pGMLV-PE1-PER3 lentiviral vectors, and PC3 DN cells were infected with PER3 shRNA-encoding viral vectors, at a multiplicity of infection (MOI) of 20 for 48 h, respectively.

Evaluation of WNT Activity

A TCF/LEF lentiviral reporter, tagged the gene expressing GFP (termed as TOP-GFP), has been widely used for evaluating WNT activity (Vermeulen et al., 2010). Lentivirus generating from the TCF/LEF reporter was purchased from Shanghai SBO Medical Biotechnology (Shanghai, China), and used for cell infection at the MOI of 20 for 48 h. To evaluate WNT activity, the intensity of GFP were detected via a fluorescent imaging system (Olympus Corp.).

RNA-Sequencing (RNA-seq)

Procedures for RNA-Seq have been previously described (Li et al., 2018). FACS was used to purify PC3 DP and DN cells, and the total RNA was extracted (RNeasy mini kit, Qiagen). A 1 μg of RNA was used for cDNA libraries per manufacturer's

[1]http://bioinf.wehi.edu.au/software/elda/

instructions (NEBNext® UltraTM RNA Library Prep Kit for Illumina®, NEB, United States). TruSeq PE Cluster Kit v3-cBot-HS (Illumia) was used for Clustering of the index-coded samples, and the library preparations were then sequenced on an Illumina NovaSeq platform with 150 bp paired-end reads generated. Gene model annotation files and reference genome were downloaded[2]. Hisat 2 v2.0.5 was used to build an index of the reference genome. Cluster 3.0 and Java Tree View were used for Heatmaps.

Bioinformatic Analysis

Basic procedures were previously described (Li et al., 2018). KEGG was used to analyze pathways that are preferentially enriched in PC3 DP or DN cells. Gene Set Enrichment Analysis (GSEA) was performed at version 4.0.3. The software was run per the user's guide. An FDR < 0.25 is considered as statistically significant.

Tissue Microarray (TMA) and Immunohistochemical Staining (IHC)

Basic procedures were previously described (Li et al., 2018). We purchased tissue microarrays (TMA) from http://www.avilabio.com (Shanxi, China), which consist of 16 normal/benign prostatic tissues and 32 prostate tumor cores. IHC for PER3 (Abcam, #ab67862, 1:100) staining was conducted and PER3 scoring was calculated by two experienced pathologists via an Image-pro Plus 6.0 system (Media Cybernetics, Inc., United States).

Statistical Analysis

In this study, the unpaired two-tailed Student's *t*-test was used to compare significance in sphere- and colony-forming efficiencies, tumor weight, and knockdown efficiency. Survival curve was generated from TCGA database. At least three independent experiments were performed for mean standard deviation. $P < 0.05$ was considered statistically significant.

Data Availability

The raw RNA-seq data is deposited in Sequence Read Archive (SRA) database[3] (accession number: PRJNA671757).

RESULTS

PC3 Double-Positive ($ALDH^{hi}CD44^{+}$) Prostate Cancer Cells Bear PCSC Properties in TME

Emerging evidence has shown that PCSCs are enriched by different phenotypic markers, including expression of $CD44^{+}$, aldehyde dehydrogenase (ALDH), $CD44^{+}\alpha2\beta1^{hi}CD133^{+}$, $PSA^{-/lo}$, and $CD166^{+}$ (Chen et al., 2013; Skvortsov et al., 2018). Using HPCa treatment-naïve samples, we reported earlier that FACS-purified $ALDH^{hi}CD44^{+}$ PCa cells (double-positive/DP) seem to have higher colony-forming abilities than the isogenic $ALDH^{lo}CD44^{-}$ (double-negative/DN) cells in androgen-deprived cultured conditions (Chen et al., 2016), suggesting that $ALDH^{hi}CD44^{+}$ PCa cells may enrich for PCSCs in TME.

To validate this suggestion, we used FACS to purify DP and corresponding DN cells in the PC3 cell line, and tested their sphere- and colony-forming abilities. We found that PC3 DP cells have a higher sphere-forming capacity compared to DN cells (**Figures 1A,C**). For example, in the 1° generation, PC3 DP cells demonstrated ∼4.7-fold higher sphere-forming ability compared to PC3 DN cells (**Figures 1A,C**) in ultra-low attachment plate (ULA). In the 2° generation, PC3 DP cells generated bigger and more spheres than PC3 DN cells (**Figures 1A,C**), and this trend continued to the 3° generation (**Figures 1A,C**). Moreover, PC3 DP cells exhibited higher clonogenic activities than the DN cells for three consecutive generations by generating more and larger colonies in Matrigel (**Figures 1B,D**). Furthermore, we purified PC3 DP and DN cells and performed RT-qPCR analysis of the stem cell associated genes. This analysis revealed that PC3 DP cells expressed higher levels of *CD44*, *ALDH1A1*, and *CD133* mRNA levels (**Figure 1E**). Thus, PC3 DP cells bear CSC features *in vitro*.

As *in vivo* limiting-dilution tumor regeneration assay (LDA) is widely accepted as the standard strategy for examining the tumor-initiating frequency in a candidate CSC population (Chen et al., 2013), we freshly sorted PC3 DP and isogenic DN cells and subcutaneously (s.c.) injected these cells in male NOD/SCID mice at different doses (from 100 to 1,000; **Figures 1F,G**). Expectedly, as few as 100 PC3 DP cells generated 6/10 tumors, while 100 DN cells gave rise to 2/10 tumors (**Figures 1F,G**). Overall, PC3 DP cells have ∼4-fold higher tumor-initiating ability than DN cells (TIF 1/109 vs. 1/472, respectively, $P = 0.0121$, **Figure 1G**). Together, those results showed that PC3 DP cells bear PCSC characteristics.

RNA-Seq Identifies PER3 Prominently Downregulated in PC3 DP Cells

Previous studies have proposed that PCSCs play vital roles in TME (Skvortsov et al., 2018), but the exact regulatory mechanisms are not completely understood. To tackle this issue, we ran an RNA-Sequencing (RNA-Seq) assay using freshly purified PC3 DP and corresponding DN cells (**Figure 2A**; **Supplementary Figure 1**). RNA-Seq studies found that 5,053 differentially expressed genes (DEGs) are upregulated in DP cells, whereas 4,672 DEGs are downregulated in DP cells ($P < 0.05$; $|\log_2\text{Fold Change}| > 0$). Moreover, bioinformatic analysis using KEGG revealed novel signaling pathways significantly downregulated in PC3 DP cells (**Figure 2B**). Surprisingly, KEGG demonstrated that the circadian entrainment pathway is among the notably downregulated pathways, as recent evidence has suggested that circadian rhythm genes have potential roles in TME (Zhou et al., 2020; **Figure 2B**). Remarkably, PER3 (Period Circadian Regulator 3), a circadian rhythm gene, which seems to play a vital role in other solid tumors (Wang et al., 2012), is significantly downregulated in PC3 DP cells (**Figure 2C**). With a fold change (FC) ≥ 2 and a P value < 0.05, we found that a total of 2,693 DEGs were identified

[2] ftp://ftp.ensembl.org/pub/, GRCh38.p12

[3] www.ncbi.nlm.nih.gov/sra/

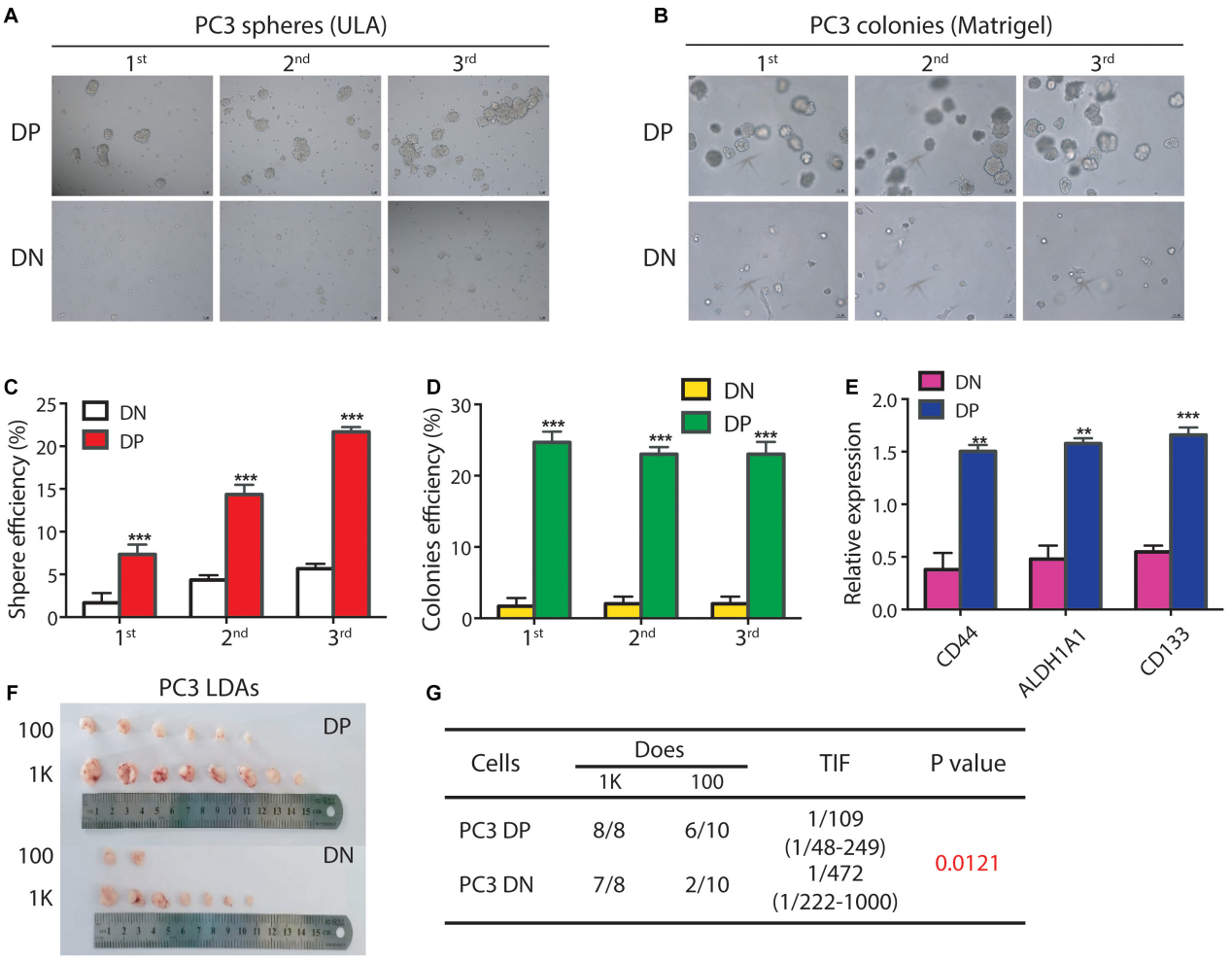

Cells	Does		TIF	P value
	1K	100		
PC3 DP	8/8	6/10	1/109 (1/48-249)	0.0121
PC3 DN	7/8	2/10	1/472 (1/222-1000)	

FIGURE 1 | The PC3 ALDH^{hi}CD44^{+} PCa cells enrich for PCSCs. **(A,B)** The PC3 ALDH^{hi}CD44^{+} (DP) PCa cells have higher clonogenicity than isogenic ALDH^{lo}CD44^{-} (DN) PCa cells. **(A)** For sphere assays, PC3 DP and corresponding DN cells were freshly purified by FACS and seeded in ultra-low attachment (ULA) plates (1,000 cells/well). Spheres were counted and photographed 12 days later. The 1° spheres were harvested and passaged for 2° spheres (1,000 cells/well) in ULA plates, which were then harvested for 3° spheres. **(B)**. For colony formation assays, PC3 DP and DN cells were mixed with Matrigel (1,000 cells/well) in 24-well cell culture plates. The 1° colonies were harvested and passaged for 2° colony-formation assays (1,000 cells/well), which were then harvested for 3° clonogenic assays. Data is presented from three separate experiments. Scale bars, 100 μm. **(C)** Spheres were counted for sphere formation assays **(A)** and the sphere efficiency was presented for three generations. $^{***}P < 0.001$. **(D)** Colonies were enumerated for colony-formation assays **(B)** and the colony efficiency was shown for 3 generations. $^{***}P < 0.001$. **(E)** Expression of mRNA levels for *CD44*, *ALDH1A1*, and *CD133* is much higher in PC3 DP cells (vs. DN cells). GAPDH was served as a loading control. Data was collected from there independent experiments. $^{**}P < 0.01$, $^{***}P < 0.001$. **(F,G)** PC3 DP cells are more tumorigenic than PC3 DN cells in male NOD/SCID mice. PC3 DP and DN cells were freshly sorted via FACS, and injected subcutaneously in male NOD/SCID mice for limiting dilution assays (LDAs). Six weeks after implanting, tumors were harvested. Tumor images, incidence and tumor-initiating frequency (TIF) were recorded. TIF was calculated using Extreme Limiting Dilution Analysis (ELDA) software (http://bioinf.wehi.edu.au/software/elda/index.html).

between PC3 DP and DN cells, and PER3 was still among the most downregulated DEGs in DP cells (**Supplementary Table 1**). In support, PC3 DP cells have lower levels of PER3 than isogenic DN cells at the protein level, whereas CSC markers (ALDH1 and CD44) are significantly upregulated in PC3 DP cells (**Figure 2D**). Furthermore, GSEA (Gene Set Enrichment Analysis) was applied to explore the signaling pathways associated with TME, and the results revealed that PC3 DP cells are enriched in stem cell pathways, including KRAS signaling, JAK/STAT3 signaling, and STAT5 signaling (**Figure 2E**; **Supplementary Figure 2A**). Additionally, PC3 DP cells showed an increased inflammatory and interferon response (**Figure 2E**; **Supplementary Figure 2B**). Combined, these data suggest that PER3 is a potentially important factor for regulating PCSCs in TME.

PER3 Negatively Regulates Stemness of PC3 DP Cells

To functionally study PER3 regulation of PCSCs, we overexpressed PER3 in PC3 DP cells (**Figures 3A,B**) and found that PER3 overexpression (OE) in PC3 DP cells significantly inhibited their sphere-forming abilities in ultra-low attachment

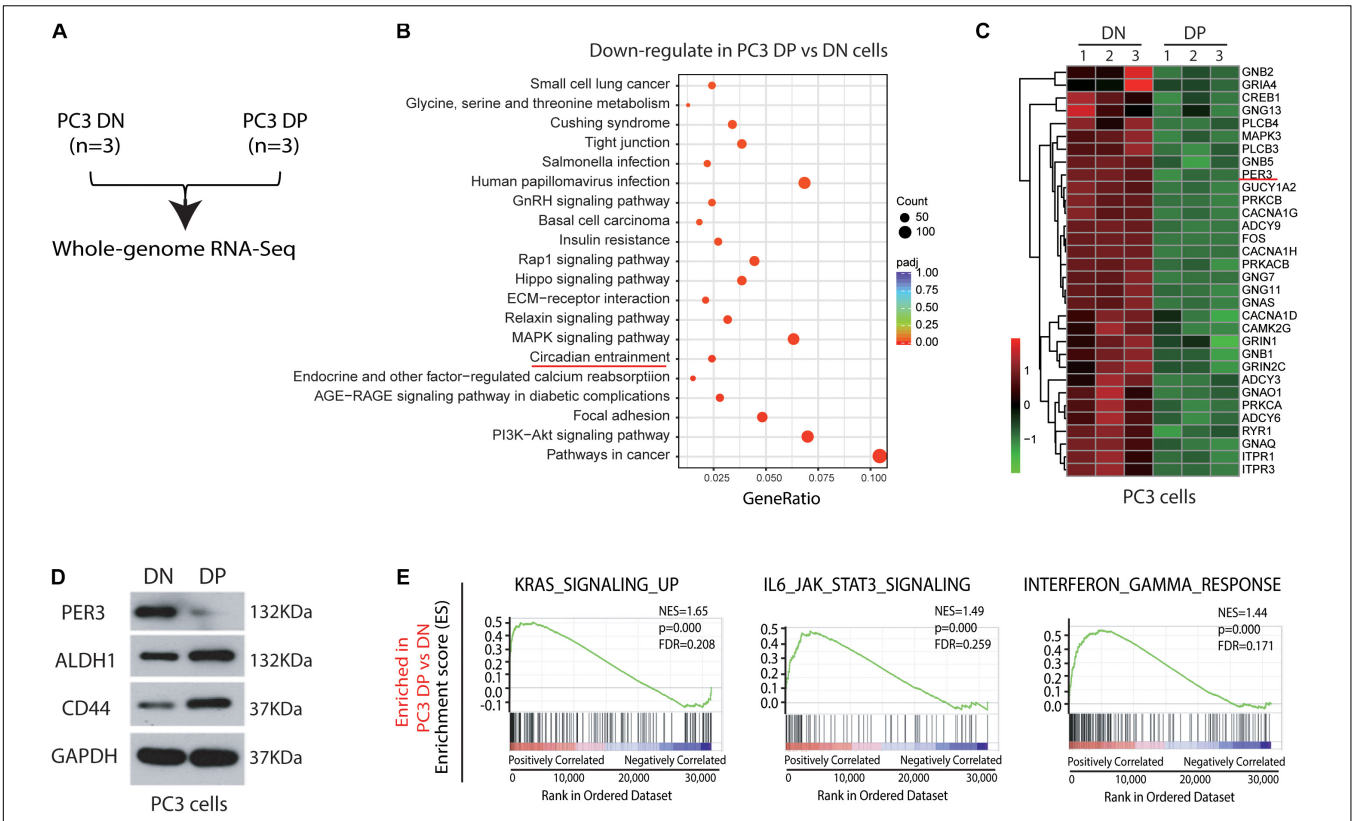

FIGURE 2 | RNA-Sequencing and bioinformatic analysis identify circadian rhythm genes as potential regulators for PCSCs in TME. **(A)** Experimental plan for RNA-Seq in PC3 cell model. **(B)** KEGG enrichment of 4,672 DEGs that were downregulated in PC3 DP cells (vs. PC3 DP cells) ($P < 0.05$; $|\log_2\text{Fold Change}| > 0$) identified 20 significantly down-regulated pathways. In particular, the circadian entrainment pathway was marked in red. **(C)** Heatmaps showing representative circadian rhythm genes downregulated in PC3 DP cells compared to DN cells. **(D)** PER3 level is downregulated in PC3 DP cells at the protein level, whereas CD44 and ALDH1 are upregulated in PC3 DP cells (vs. DN cells). **(E)** GSEA showing that PC3 DP cells are enriched in gene sets preferentially expressed in stem cell pathways, including KRAS signaling, and IL6/JAK/STAT3 signaling, and also in interferon responses. Data are presented from three independent experiments.

(ULA) plates (**Figures 3C,D**). In contrast, knocking down PER3 in PC3 DN cells (**Figures 3A,B**) led to bigger and more spheres (**Figures 3C,D**). Furthermore, PER3 OE in PC3 DP cells suppressed their colony-forming abilities by generating smaller and fewer colonies in Matrigel (**Figures 3E,F**), but PER3 KD in DN cells promoted colony formation (**Figures 3E,F**). Together, these data indicate that PER3 negatively regulates stem cell features of DP cells *in vitro*.

More importantly, we attempted to test if PER3 is functionally involved in PCa development. PER3 OE in PC3 DP cells decreased tumor initiating capacities as compared to controls (TIF 1/392 vs. 1/29, respectively, $P = 0.00000315$; **Figures 4A,B**). However, PER3 KD in PC3 DN cells promoted tumor formation (TIF 1/97 vs. 1/526, $P = 0.000696$, **Figures 4C,D**). Collectively, these results indicate that PER3 is causally important for regulating SC traits.

PER3 Is a Potentially Prognostic Marker for PCa Patients

To explore the clinical significance of PER3 in PCa, we used IHC to examine PER3 expression level in a tissue microarray (TMA) consisting of hormone naïve 32 PCa patients and 16 benign/normal prostate tissue cores. Our results revealed that PER3 levels are downregulated in HPCa tissues as compared to benign/normal tissues (**Figures 5A,B**). Furthermore, PCa samples in TCGA database expressed lower levels of *PER3* mRNA in HPCa tissues ($n = 499$) than normal tissues ($n = 52$) (**Figures 5C,D**). Moreover, the *PER3* mRNA levels are positively correlated with PCa patients' overall survival (OS) (**Figure 5E**). Notably, PCa patients with higher *PER3* mRNA levels have better recurrence free survival ($P = 0.019$) (**Figure 5F**). Altogether, our findings suggest that PER3 has significant clinical relevance, and is a potential prognostic marker for PCa patients.

Low Levels of PER3 Regulate Stemness of PCSCs by Activating WNT/β-Catenin Signaling

Emerging evidence has suggested that several signaling pathways play vital roles in TME for PCa development, in particular, WNT/β-catenin signaling pathways (Skvortsov et al., 2018). Surprisingly, our RNA-seq of Du145 cells revealed that the WNT/β-catenin pathway appears to be activated in PCa DP cells, but not in isogenic DN cells (Li et al., unpublished). However, it

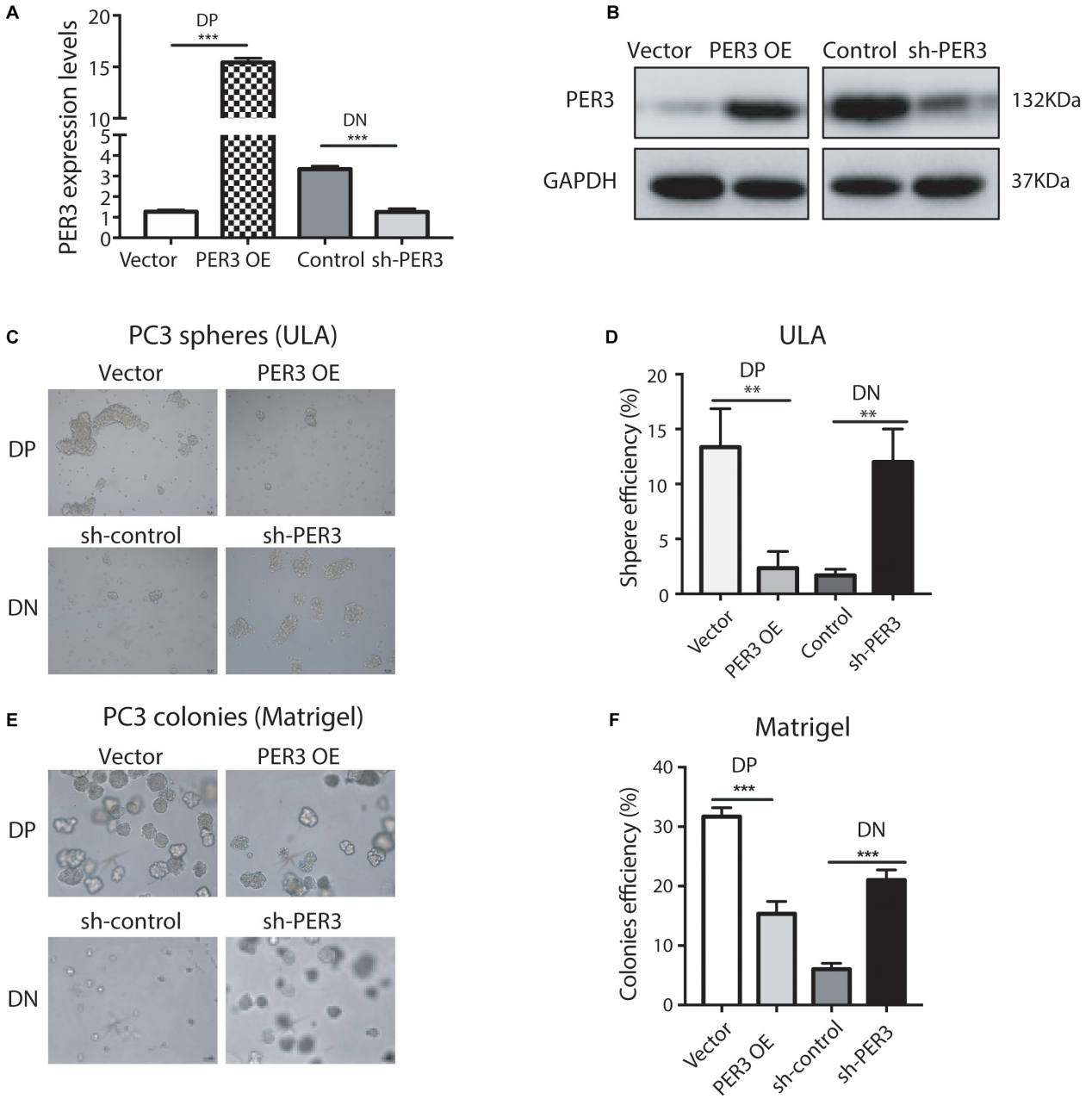

FIGURE 3 | PER3 regulates stemness of PC3 DP cells *in vitro*. **(A)** RT-qPCR analysis was used to evaluate efficiency of *PER3* overexpression (OE) and knockdown (KD, or sh-PER3) in PC3 DP and PC3 DN cells, respectively. **(B)** Western blotting was performed to examine PER3 levels of PER3 OE in PC3 DP cells and PER3 KD in PC3 DN cells, respectively. **(C,D)** In sphere formation assays, *PER3* OE in PC3 cells impairs their sphere-forming abilities whereas *PER3* KD in PC3 DN cells improved their sphere formation. A total of 1,000 cells for each well were seeded in ULA plates. Spheres were imaged **(C)** and counted **(D)** for sphere efficiency 1–2 weeks later. **(E,F)** In colony formation assays, *PER3* OE in PC3 DP cells abrogates their colony-forming abilities whereas *PER3* KD in PC3 DN cells improved their clonogenicity. A total of 1,000 cells for each well were mixed with Matrigel and plated in 24-well culture plates. Colonies were imaged **(E)** and counted **(F)** for colonies efficiency 1–2 weeks later. Data are presented from three independent experiments. Scale bars, 100 μm. $^{**}P < 0.01$, $^{***}P < 0.001$.

is not clear which key molecules are involved in triggering the activation of the WNT/β-catenin pathway in DP cells.

To solve this issue, we first performed GO (Gene Ontology) enrichment analysis on the PC3 DP versus DN cells, and found that WNT/β-catenin pathway related genes are significantly enriched in PC3 DP cells (**Figure 6A**), further supporting our observations that the WNT/β-catenin pathway may be involved in the regulation of SC features of PCa DP cells. Furthermore, we employed a TOP-GFP viral vector, a TCF/LEF reporter, which has been widely used to evaluate WNT activity (Vermeulen et al., 2010). Notably, PER3 OE in PC3 DP cells decreased GFP expression, indicating the

A

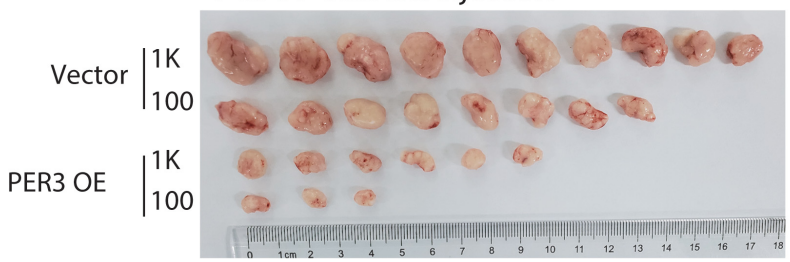

B

PC3 DP cells	Cell Dose		TIF	P value
	1K	100		
Vector	10/10	8/10	1/29(1/63-135)	0.00000315
PER3 OE	6/10	3/10	1/392(1/805-1652)	

C

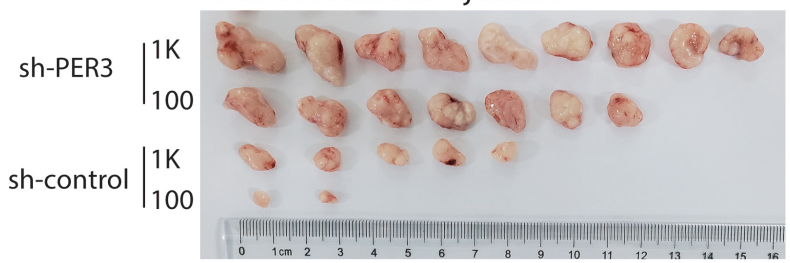

D

PC3 DN cells	Cell Dose		TIF	P value
	1K	100		
sh-PER3	9/10	7/10	1/97(1/219-494)	0.000696
sh-control	5/10	2/10	1/526(1/1149-2509)	

FIGURE 4 | PER3 regulates stemness of PC3 DP cells *in vivo*. **(A,B)** *PER3* OE in PC3 DP cells inhibits tumor formation. DP cells freshly purified from PC3 cell line were infected with the pGMLV-PE1-PER3 lentiviral vectors (MOI = 20, 48 h) and injected subcutaneously into male NOD/SCID mice at increasing cell doses. Six weeks after implanting, tumors were harvested. Tumor images, incidence and TIF were recorded. **(C,D)** *PER3* KD in PC3 DN cells promoted their tumorigenicity. DN cells freshly purified from PC3 cell line were infected with lentiviral vectors (MOI = 20, 48 h) and subcutaneously injected into male NOD/SCID mice at increasing cell doses. Tumors were harvested after 6 weeks after injection. Tumor images, incidence and TIF were recorded.

inactivation of WNT/β-catenin pathway, whereas PER3 KD in PC3 DN cells increased GFP expression (**Figure 6B**; data not shown). More importantly, our results revealed that PER3 KD in PC3 DN cells led to the translocation of cytoplasmic β-catenin into the nucleus (**Figure 6C**), indicating that the activation of WNT/β-catenin signaling pathway. In addition, PER3 KD in PC3 DN cells resulted in the upregulation of BMAL1, which is a transcriptional activator for circadian clock genes and related to the WNT/β-catenin signaling pathway from earlier reports (Lecarpentier et al., 2019) (**Figure 6D**). On the other hand, PER3 OE in PC3 DP cells led to the downregulation of BMAL1 (data not shown). Finally, PER3 KD in PC3 DN cells resulted in the phosphorylation of β-catenin, whereas PER3 OE in PC3 DP cells downregulated the level of phosphorylated β-catenin (**Figure 6E**). Taken together, these data suggest that PER3 negatively regulates stemness of PCSCs, probably via WNT/β-catenin signaling pathway.

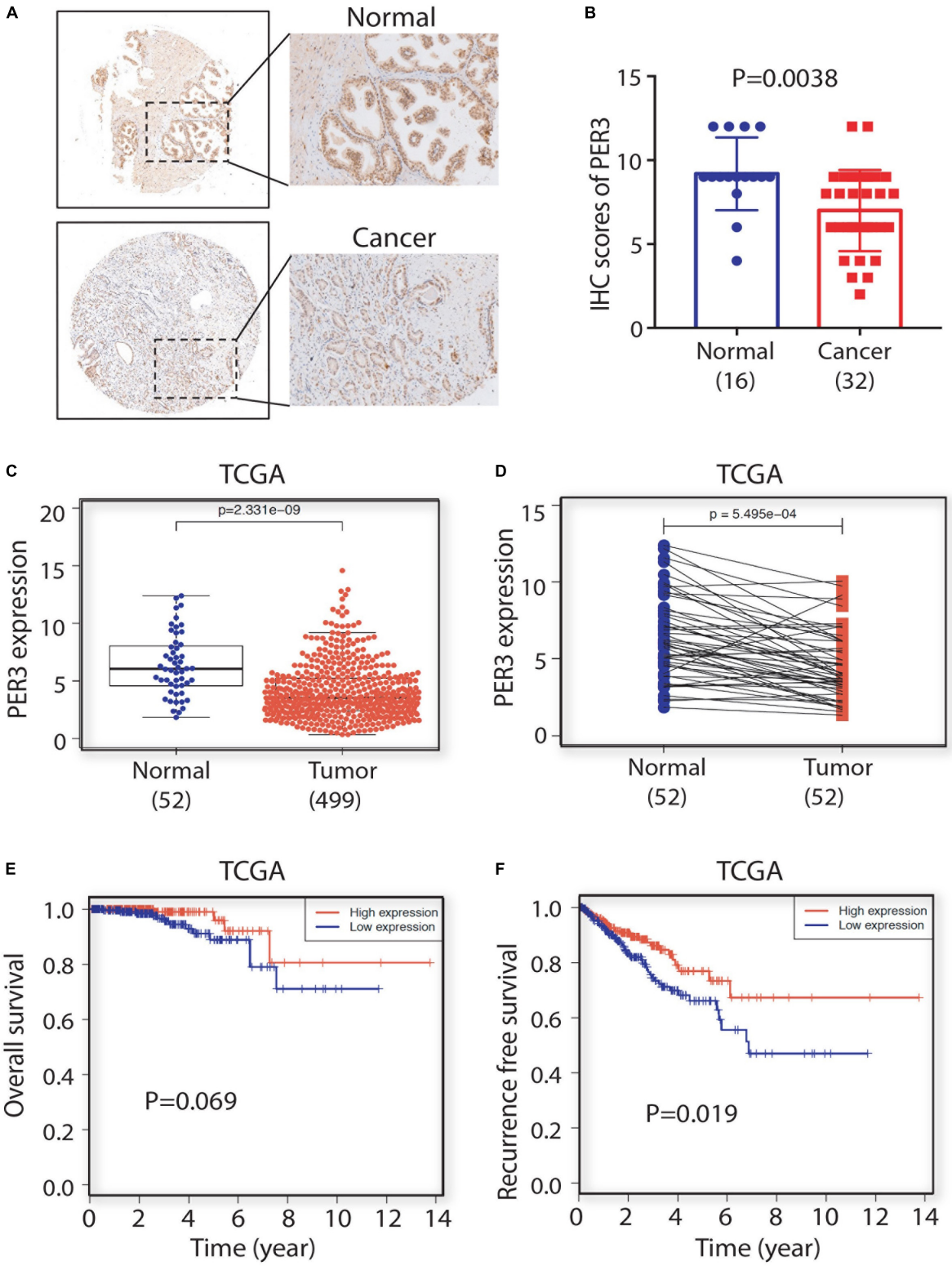

FIGURE 5 | PER3 is a potentially prognostic factor for prostate cancer. **(A)** Representative IHC images of PER3 expression in benign/normal prostatic tissues and prostate cancers. **(B)** Characterizations of PER3 from a tissue microarray (TMA, Pro-01019) containing 32 untreated PCa patient and 16 normal prostate tissue cores. **(C)** *PER3* mRNA levels were downregulated in PCa in TCGA database. A total of 52 prostatic benign/normal and 499 prostate tumor tissues were compared **(C)**, and 52 matched normal and tumor pairs were compared **(D)**. **(E,F)** Kaplan-Meier analysis of the correlation of PER3 mRNA levels for overall survival rate (OS) and recurrence free survival rate in PCa patients from TCGA database.

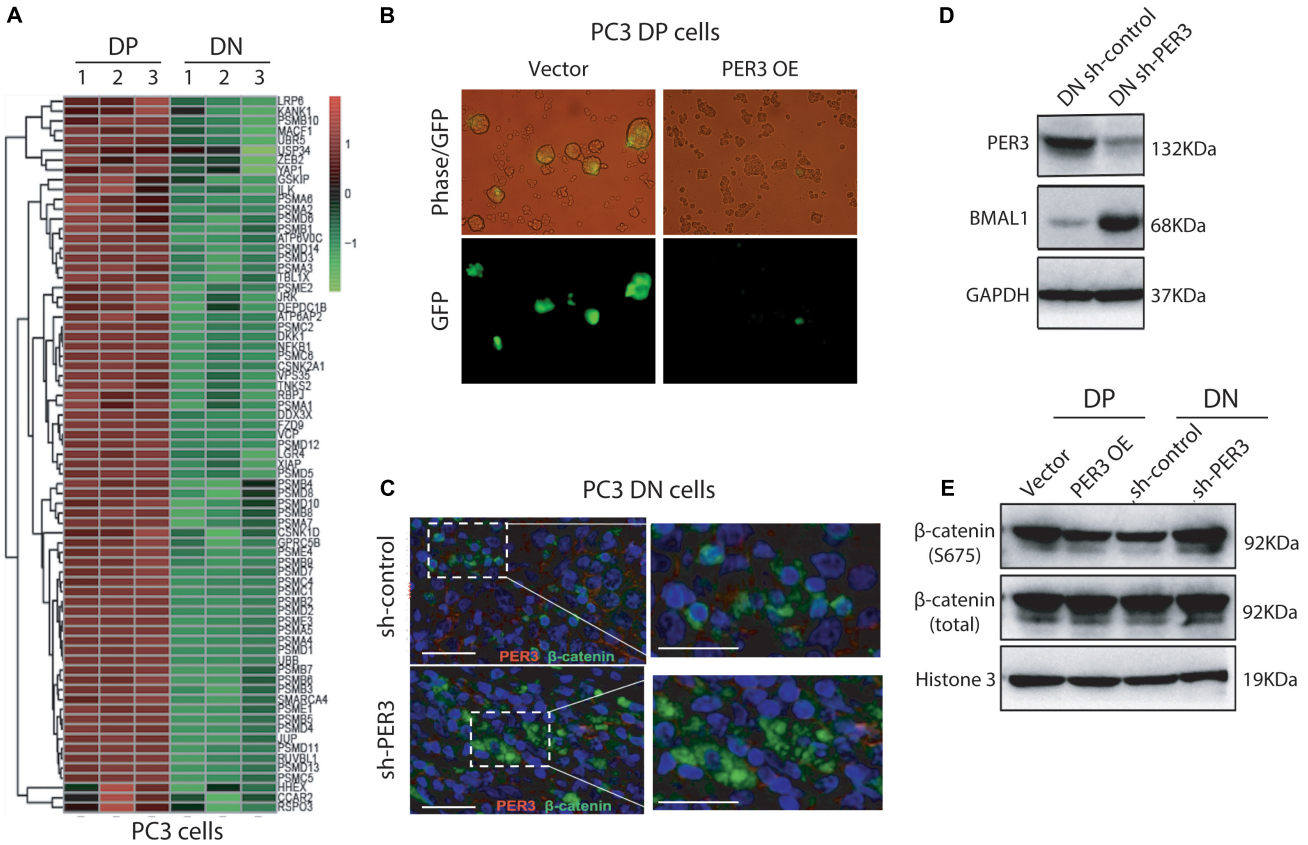

FIGURE 6 | Low levels of PER3 activate WNT/β-catenin pathway. **(A)** Heatmap enrichment of genes associated with WNT/β-catenin signaling pathway in PC3 DP cells and PC3 DN cells. **(B)** Representative images showed TOP-GFP expression in PC3 DP cells transfected with the TOP-GFP lentivirus vector. Scale bars, 100 μm. **(C)** Immunofluorescent staining of PER3 and β-catenin in PC3 DN cells after PER3 KD revealed that PER3 KD promoted translocation of β-catenin from cytoplasm into nucleus. Scale bars, left: 100 μm, right: 200 μm. **(D)** PER3 KD in PC3 DN cells led to the upregulation of BMAL1. Shown are western blotting of the molecules indicated. GAPDH was used as the control. **(E)** PER3 OE in PC3 DP cells resulted in the downregulation of phosphorylated β-catenin expression level, but PER3 KD in PC3 DN cells upregulated levels of phosphorylated β-catenin. GAPDH was used as the loading control at the western blotting.

DISCUSSION

Like many solid tumors, prostate cancer cells are heterogeneous (Tang, 2012), and this cancer cell heterogeneity can be explained by both clonal evolution and/or CSC models (Lytle et al., 2018; Prager et al., 2019). In prostate cancer, emerging evidence has shown the existence of PCSCs, which are important for prostate cancer development at every stage (Deng and Tang, 2015). Through both *in vivo* and *in vitro* methods, PCSCs have also been identified in numerous studies (Skvortsov et al., 2018). For instance, human prostate tumor cells with $CD44^{+}\alpha2\beta1^{hi}CD133^{+}$ phenotype represent potential PCSCs *in vitro* (Collins et al., 2005). Using PCa xenograft tumors, $CD44^{+}$ PCa cells are shown to have stem-like cancer cell properties (Patrawala et al., 2006), and $CD44^{+}\alpha2\beta1^{+}$ PCa cells are further enriched in tumor-initiating cells (Patrawala et al., 2007). In addition, $PSA^{-/lo}$ PCa cells are reported to serially propagate tumor regeneration and are resistant to androgen deprivation therapy (Qin et al., 2012). Moreover, PCa cells bearing high levels of aldehyde dehydrogenase (ALDH) activity are enriched in tumor-initiating and metastasis-imitating cells (van den Hoogen et al., 2010). Furthermore, PCSCs are reported to be responsible for therapy resistance and castration resistant prostate cancer (CRPC) (Domingo-Domenech et al., 2012; Chen et al., 2016). Recently, we have found that hormone naïve HPCa cells with $ALDH^{hi}CD44^{+}$ (DP) phenotype can give rise to bigger and more colonies or spheres than HPCa cells with $ALDH^{lo}CD44^{-}$ (DN) phenotype (Chen et al., 2016), hinting that these cells may be the cellular target for PCa treatment. To further explore this possibility, we have shown that PC3 DP cells can self-renew, and are more clonogenic and tumorigenic than the corresponding DN cells (**Figure 1**), consistent to our previous observations that DP cells in Du145 cell model also bear significantly enhanced metastatic potential, clonogenicity and tumorigenicity than isogenic Du145 DN cells (data not shown). These data together suggest that PCa DP cells are a subpopulation of PCSCs.

Recent evidence has suggested that the circadian clock is associated with TME in solid tumors with clinical values and therapeutic potentials, although the underlying mechanisms are not clear. For example, Zhou et al. (2020) found that a wide range of circadian clock genes are changed epigenetically in kidney renal clear cell carcinoma (KIRC), and have a prognostic

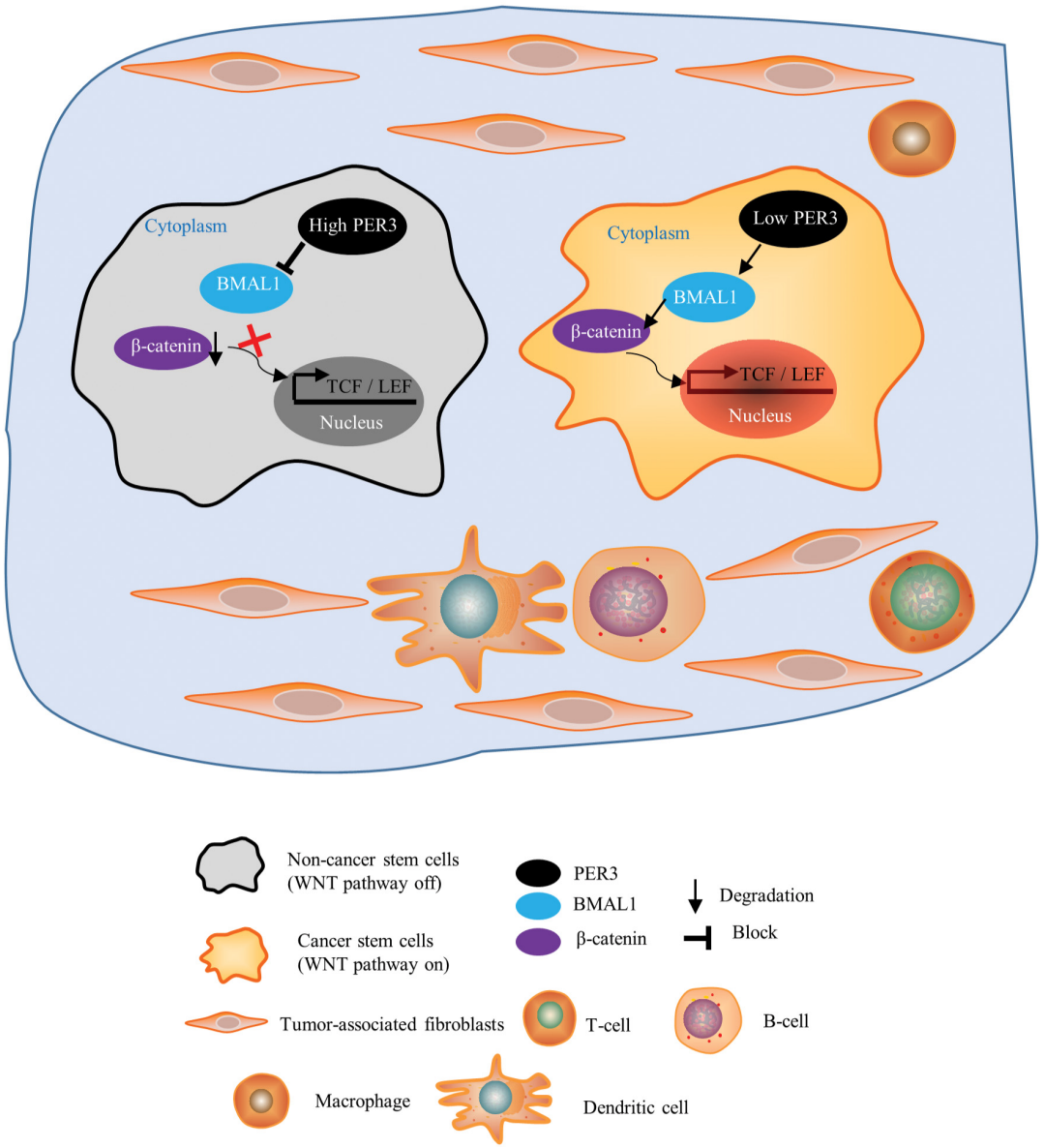

FIGURE 7 | A model depicting that PER3 regulates stemness of PCSCs via WNT/β-catenin pathway. Our results suggest that in PCa TME, PCa DN cells (non-PCSCs) bear high levels of PER3, which downregulates the expression of BMAL1 and prevents the translocation of β-catenin from cytoplasm into nucleus to activate WNT/β-catenin pathway. On the other hand, PCa DP cells (PCSCs) have low levels of PER3, which upregulates BMAL1 expression, leading to the translocation of β-catenin from cytoplasm into nucleus to eventually activate WNT/β-catenin signaling pathway.

value. KIRC patients expressing high levels of *PER2*, *PER3*, *CLOCK*, *CRY2*, and *RORA* have a better overall survival and disease-free survival (Zhou et al., 2020). In addition, circadian clock genes are implicated in various signaling pathways, such as apoptosis and cell cycle, as well as in immune cell infiltration (Zhou et al., 2020). Similarly, by multi-omics computation techniques, several core circadian clock genes are found changed epigenetically in lung adenocarcinomas and lung squamous cell carcinomas, which are involved in cell cycle and apoptosis, such as *PER2* and *RORA* (Yang et al., 2019). By applying MC38, a colorectal cancer cell line, in a syngeneic mouse model of liver metastasis, $Per1^{-/-}Per2^{-/-}$ mice had reduced liver metastasis, and $Per2^{-/-}$ livers had less cancer-associated fibroblasts infiltration and collagen deposition (Shaashua et al., 2020). Further characterizations revealed that stromal *Per2* is also required for primary tumor formation (Shaashua et al., 2020). This finding implies the importance of PER family genes in TME.

How circadian rhythm genes regulate CSCs remains unknown. In a mouse model of acute myeloid leukemia (AML), *in vivo* RNAi screening identified that the circadian rhythm genes (Bmal1 and Clock) are required for AML cell growth, and targeting the circadian machinery showed therapeutic effects by depleting leukemia stem cells and impaired cell proliferation (Puram et al., 2016). In solid tumors, glioblastoma stem cells (GSCs) dependent on core circadian clock transcription factors, BMAL1 and CLOCK, for their cell growth, and targeting core clock factors in GSCs suppresses their tumor growth (Dong et al., 2019). Moreover, Bmal1 KO reduced the development of murine skin tumors by reducing tumor-initiating cells and enhancing the expression of tumor suppressor genes (Janich et al., 2011). These studies, together with many others, have highlighted the impact of circadian clock genes on CSCs.

In this study, we are the first to report the biological effect of circadian clock genes on PCSCs. We have made several novel findings. First, using deep RNA-Seq and applying systematic bioinformatic analysis, we found that the circadian rhythm pathway is significantly downregulated in PC3 DP cells (vs. PC3 DN cells). Among PER family members, PER3 is markedly downregulated in PC3 DP cells, suggesting that circadian clock genes may regulate PCSCs. Second, RNA-Seq in PC3 DP cells (compared to PC3 DN cells) also revealed that PC3 DP cells are enriched in stem cell pathways (including KRAS, JAK/STAT3, and STAT5 signaling pathways), inflammatory response and interferon response (**Figure 2E**; **Supplementary Figure 2**). In support, our recent RNA-Seq in Du145 DP cells (vs. isogenic DN cells) identified that Du145 DP cells are enriched in EMT, angiogenesis, metabolisms and stem cell signaling pathways (including human embryonic stem cell pluripotency, STAT3, WNT/β-catenin signaling pathways) (Li et al., unpublished). These data suggest that PCa DP cells play vital roles in PCa TME. Third, we explored if PER3 is a key molecule to regulate PCSCs through detailed *in vitro* and *in vivo* characterizations. In colony-formation and sphere-formation assays, overexpressing PER3 in PC3 DP cells significantly suppresses clonogenicity by generating smaller and fewer colonies and/or spheres, while knocking down PER3 in PC3 DN cells markedly improves their clonogenicity. In animal studies, PER3 OE dramatically inhibits tumor initiation of PC3 DP cells, whereas PER3 KD in PC3 DN cells notably promotes their tumorigenicity (**Figure 3** and **Figure 4**). These results altogether indicate that PER3 regulates stem cell characteristics of PCSCs. Fourth, patients with higher levels of PER3 have a better survival and disease-free rate, implying the prognostic value of PER3 in PCa. In other solid tumors, low levels of PER3 are identified in colon cancers vs. normal tissues, which are associated with colon cancer incidence and development (Wang et al., 2012). Further studies revealed that PER3 may be important in regulating the stemness of colorectal CSCs by inhibiting NOTCH and β-catenin signaling (Zhang et al., 2017), supporting our findings that the importance of PER3 in regulating PCSCs. Moreover, a study from Cai et al. (2018) reported that PER3 expression is lower in paclitaxel-resistant PCa cells, and PER3 OE in PCa resistant cells inhibits cell proliferation, arrests the cell cycle and increases apoptosis, which induce therapeutic sensitivity to paclitaxel by downregulating NOTCH1 signaling pathway, further supporting our suggestion that PER3 is of clinical and therapeutic value. Mechanistically, our GO enrichment analysis identified that many genes related to WNT/β-catenin pathway are significantly enriched in PC3 DP cells, as WNT/β-catenin signaling pathways have been shown to be imperative for PCSC regulation (Skvortsov et al., 2018). More importantly, PER3 KD in PC3 DN cells increases the expression of BMAL1, resulting in the phosphorylation of β-catenin and translocation of β-catenin from the cytoplasm into the nucleus to activate the WNT/β-catenin pathway (**Figure 7**). On the contrary, PER3 OE in PC3 DP cells inhibits the expression of BMAL1, leading to the inactivation of the WNT/β-catenin pathway (**Figure 7**). The exact mechanisms of how PER3 regulates stemness of PCSCs via WNT/β-catenin pathway will be further clarified.

Circadian clock dysfunction may play a role in cancer development, and this relationship may be instrumental in the development of targeted treatments for cancer patients (Sancar and Van Gelder, 2021). Our ongoing work is to elucidate the exact mechanisms of the circadian clock genes (PER3) on PCSCs, which hopefully can be translated into clinical management in the future.

DATA AVAILABILITY STATEMENT

The datasets presented in this study can be found in online repositories. The names of the repository/repositories and accession number(s) can be found below: The RNA-Seq data presented in the study are deposited in the Sequence Read Archive (SRA) (www.ncbi.nlm.nih.gov/sra/), Accession number: PRJNA671757.

ETHICS STATEMENT

The animal study was reviewed and approved by the IACUC of Huazhong University of Science and Technology.

AUTHOR CONTRIBUTIONS

QLL, QHL, and XC designed all the experiments and the concept of this manuscript. QLL performed the major experiments. DX, ZHW, BL, JZ, PP, QJT, JD, JG, and DK provided technical support. WMC and JM provided scientific suggestions. QLL and XC drafted the manuscript. JM and XC co-supervised QLL to complete this project. All authors listed have read and approved the manuscript before submission.

FUNDING

This study was supported by grants from the National Natural Science Foundation of China (No. 81602592) for XC. QHL was supported, in part, by the National Natural Science Foundation of China (No. 81802973) and the general project of the Natural Science Foundation of Hubei Province (No. 2020CFB844). JM was supported in part by the Key Project of the Health Commission of Hubei Province (No. WJ2019Z006).

ACKNOWLEDGMENTS

We thank animal core of Tongji Hospital for their animal care. We thank Mr. Kevin Lin at the Department of Epigenetics and Molecular Carcinogenesis of MD Anderson Cancer Center (United States) for assistance in RNA-Seq analysis, and Mr. Alex Zacharek at the Department of Neurology Research of Henry Ford Hospital (United States) for suggestions of our manuscript. We also thank Dr. Jichao Qin at the Department of Surgery at the Tongji Hospital for technical support and helpful suggestions. We apologize to the colleagues whose work was not cited due to space limitations.

SUPPLEMENTARY MATERIAL

The Supplementary Material for this article can be found online at: https://www.frontiersin.org/articles/10.3389/fcell.2021.656981/full#supplementary-material

Supplementary Figure 1 | Bioinformatic analysis of RNA-Seq in PC3 DP cells compared to PC3 DN cells. **(A)** High consistency in the biological triplicates were shown in the correlation plot. **(B)** Proper distribution of fpkm of each analyzed sample was shown in the violin plot.

Supplementary Figure 2 | GSEA shows enrichment of gene signatures in PC3 DP cells compared to DN cells in TME. **(A)** GSEA shows enrichment of gene signatures related to CSCs, including IL-2/STAT5 pathway. **(B)** GSEA shows enrichment of gene signatures pertinent to inflammatory response.

REFERENCES

Cai, D. W., Chen, D., Sun, S. P., Liu, Z. J., Liu, F., Xian, S. Z., et al. (2018). Overexpression of PER3 reverses paclitaxel resistance of prostate cancer cells by inhibiting the Notch pathway. *Eur. Rev. Med. Pharmacol. Sci.* 22, 2572–2579. doi: 10.26355/eurrev_201805_14950

Chen, X., Li, Q., Liu, X., Liu, C., Liu, R., Rycaj, K., et al. (2016). Defining a population of stem-like human prostate cancer cells that can generate and propagate castration-resistant prostate cancer. *Clin. Cancer Res.* 22, 4505–4516. doi: 10.1158/1078-0432.CCR-15-2956

Chen, X., Rycaj, K., Liu, X., and Tang, D. G. (2013). New insights into prostate cancer stem cells. *Cell Cycle* 12, 579–586. doi: 10.4161/cc.23721

Cojoc, M., Peitzsch, C., Kurth, I., Trautmann, F., Kunz-Schughart, L. A., Telegeev, G. D., et al. (2015). Aldehyde dehydrogenase is regulated by beta-Catenin/TCF and promotes radioresistance in prostate cancer progenitor cells. *Cancer Res.* 75, 1482–1494. doi: 10.1158/0008-5472.CAN-14-1924

Collins, A. T., Berry, P. A., Hyde, C., Stower, M. J., and Maitland, N. J. (2005). Prospective identification of tumorigenic prostate cancer stem cells. *Cancer Res.* 65, 10946–10951. doi: 10.1158/0008-5472.CAN-05-2018

Deng, Q., and Tang, D. G. (2015). Androgen receptor and prostate cancer stem cells: biological mechanisms and clinical implications. *Endocr. Relat. Cancer* 22, T209–T220. doi: 10.1530/ERC-15-0217

Dickerman, B. A., Markt, S. C., Koskenvuo, M., Hublin, C., Pukkala, E., Mucci, L. A., et al. (2016). Sleep disruption, chronotype, shift work, and prostate cancer risk and mortality: a 30-year prospective cohort study of Finnish twins. *Cancer Causes Control.* 27, 1361–1370. doi: 10.1007/s10552-016-0815-5

Domingo-Domenech, J., Vidal, S. J., Rodriguez-Bravo, V., Castillo-Martin, M., Quinn, S. A., Rodriguez-Barrueco, R., et al. (2012). Suppression of acquired docetaxel resistance in prostate cancer through depletion of notch- and hedgehog-dependent tumor-initiating cells. *Cancer Cell* 22, 373–388. doi: 10.1016/j.ccr.2012.07.016

Dong, Z., Zhang, G., Qu, M., Gimple, R. C., Wu, Q., Qiu, Z., et al. (2019). Targeting glioblastoma stem cells through disruption of the circadian clock. *Cancer Discov.* 9, 1556–1573. doi: 10.1158/2159-8290.CD-19-0215

Janich, P., Pascual, G., Merlos-Suarez, A., Batlle, E., Ripperger, J., Albrecht, U., et al. (2011). The circadian molecular clock creates epidermal stem cell heterogeneity. *Nature* 480, 209–214. doi: 10.1038/nature10649

Lecarpentier, Y., Schussler,O., Hébert, J. L., Vallée, A. (2019). Multiple Targets of the Canonical WNT/β-Catenin Signaling in Cancers. *Front. Oncol.* 9:1248. doi: 10.3389/fonc.2019.01248

Li, Q., Deng, Q., Chao, H. P., Liu, X., Lu, Y., Lin, K., et al. (2018). Linking prostate cancer cell AR heterogeneity to distinct castration and enzalutamide responses. *Nat. Commun.* 9:3600. doi: 10.1038/s41467-018-06067-7

Lytle, N. K., Barber, A. G., and Reya, T. (2018). Stem cell fate in cancer growth, progression and therapy resistance. *Nat. Rev. Cancer* 18, 669–680. doi: 10.1038/s41568-018-0056-x

Markt, S. C., Flynn-Evans, E. E., Valdimarsdottir, U. A., Sigurdardottir, L. G., Tamimi, R. M., Batista, J. L., et al. (2016). Sleep duration and disruption and prostate cancer risk: a 23-year prospective study. *Cancer Epidemiol. Biomark. Prev.* 25, 302–308. doi: 10.1158/1055-9965.EPI-14-1274

Patrawala, L., Calhoun, T., Schneider-Broussard, R., Li, H., Bhatia, B., Tang, S., et al. (2006). Highly purified CD44+ prostate cancer cells from xenograft human tumors are enriched in tumorigenic and metastatic progenitor cells. *Oncogene* 25, 1696–1708. doi: 10.1038/sj.onc.1209327

Patrawala, L., Calhoun-Davis, T., Schneider-Broussard, R., and Tang, D. G. (2007). Hierarchical organization of prostate cancer cells in xenograft tumors: the CD44+α2β1+ cell population is enriched in tumor-initiating cells. *Cancer Res.* 67, 6796–6805. doi: 10.1158/0008-5472.CAN-07-0490

Prager, B. C., Xie, Q., Bao, S., and Rich, J. N. (2019). Cancer stem cells: the architects of the tumor ecosystem. *Cell Stem Cell* 24, 41–53. doi: 10.1016/j.stem.2018.12.009

Puram, R. V., Kowalczyk, M. S., De Boer, C. G., Schneider, R. K., Miller, P. G., Mcconkey, M., et al. (2016). Core circadian clock genes regulate leukemia stem cells in AML. *Cell* 165, 303–316. doi: 10.1016/j.cell.2016.03.015

Qin, J., Liu, X., Laffin, B., Chen, X., Choy, G., Jeter, C. R., et al. (2012). The PSA(-/lo) prostate cancer cell population harbors self-renewing long-term tumor-propagating cells that resist castration. *Cell Stem Cell* 10, 556–569. doi: 10.1016/j.stem.2012.03.009

Rycaj, K., and Tang, D. G. (2017). Molecular determinants of prostate cancer metastasis. *Oncotarget* 8, 88211–88231. doi: 10.18632/oncotarget.21085

Sancar, A., Lindsey-Boltz, L. A., Gaddameedhi, S., Selby, C. P., Ye, R., Chiou, Y. Y., et al. (2015). Circadian clock, cancer, and chemotherapy. *Biochemistry* 54, 110–123. doi: 10.1021/bi5007354

Sancar, A., and Van Gelder, R. N. (2021). Clocks, cancer, and chronochemotherapy. *Science* 371:eabb0738. doi: 10.1126/science.abb0738

Shaashua, L., Mayer, S., Lior, C., Lavon, H., Novoselsky, A., and Scherz-Shouval, R. (2020). Stromal expression of the core clock gene period 2 is essential for tumor initiation and metastatic colonization. *Front. Cell Dev. Biol.* 8:587697. doi: 10.3389/fcell.2020.587697

Shafi, A. A., and Knudsen, K. E. (2019). Cancer and the circadian clock. *Cancer Res.* 79, 3806–3814. doi: 10.1158/0008-5472.CAN-19-0566

Siegel, R. L., Miller, K. D., and Jemal, A. (2020). Cancer statistics, 2020. *CA Cancer J. Clin.* 70, 7–30. doi: 10.3322/caac.21590

Skvortsov, S., Skvortsova, I., Tang, D. G., and Dubrovska, A. (2018). Concise review: prostate cancer stem cells: current understanding. *Stem Cells* 36, 1457–1474. doi: 10.1002/stem.2859

Tang, D. G. (2012). Understanding cancer stem cell heterogeneity and plasticity. *Cell Res.* 22, 457–472. doi: 10.1038/cr.2012.13

Trautmann, F., Cojoc, M., Kurth, I., Melin, N., Bouchez, L. C., Dubrovska, A., et al. (2014). CXCR4 as biomarker for radioresistant cancer stem cells. *Int. J. Radiat. Biol.* 90, 687–699. doi: 10.3109/09553002.2014.906766

van den Hoogen, C., Van Der Horst, G., Cheung, H., Buijs, J. T., Lippitt, J. M., Guzman-Ramirez, N., et al. (2010). High aldehyde dehydrogenase activity identifies tumor-initiating and metastasis-initiating cells in human prostate cancer. *Cancer Res.* 70, 5163–5173. doi: 10.1158/0008-5472.CAN-09-3806

Vermeulen, L., De Sousa, E. M. F., Van Der Heijden, M., Cameron, K., De Jong, J. H., Borovski, T., et al. (2010). Wnt activity defines colon cancer stem cells and is regulated by the microenvironment. *Nat. Cell Biol.* 12, 468–476. doi: 10.1038/ncb2048

Wang, X., Yan, D., Teng, M., Fan, J., Zhou, C., Li, D., et al. (2012). Reduced expression of PER3 is associated with incidence and development of colon cancer. *Ann. Surg. Oncol.* 19, 3081–3088. doi: 10.1245/s10434-012-2279-5

Wendeu-Foyet, M. G., and Menegaux, F. (2017). Circadian disruption and prostate cancer risk: an updated review of epidemiological evidences. *Cancer Epidemiol. Biomarkers Prev.* 26, 985–991. doi: 10.1158/1055-9965.EPI-16-1030

Yang, Y., Yuan, G., Xie, H., Wei, T., Zhu, D., Cui, J., et al. (2019). Circadian clock associates with tumor microenvironment in thoracic cancers. *Aging (Albany NY)* 11, 11814–11828. doi: 10.18632/aging.102450

Young, M. W., and Kay, S. A. (2001). Time zones: a comparative genetics of circadian clocks. *Nat. Rev. Genet.* 2, 702–715. doi: 10.1038/35088576

Zhang, F., Sun, H., Zhang, S., Yang, X., Zhang, G., and Su, T. (2017). Overexpression of PER3 inhibits self-renewal capability and chemoresistance of colorectal cancer stem-like cells via inhibition of notch and beta-catenin signaling. *Oncol. Res.* 25, 709–719. doi: 10.3727/096504016X14772331883976

Zhou, L., Luo, Z., Li, Z., and Huang, Q. (2020). Circadian clock is associated with tumor microenvironment in kidney renal clear cell carcinoma. *Aging (Albany NY)* 12, 14620–14632. doi: 10.18632/aging.103509

Conflict of Interest: The authors declare that the research was conducted in the absence of any commercial or financial relationships that could be construed as a potential conflict of interest.

frontiers in Cell and Developmental Biology

ORIGINAL RESEARCH
published: 01 April 2021
doi: 10.3389/fcell.2021.640476

A Comprehensive Investigation to Reveal the Relationship Between Plasmacytoid Dendritic Cells and Breast Cancer by Multiomics Data Analysis

Saisai Tian[1†], Li Yan[1†], Lu Fu[1†], Zhen Zhang[1], Jinbo Zhang[1,3], Guofeng Meng[2] and Weidong Zhang[1,2]*

[1] School of Pharmacy, Second Military Medical University, Shanghai, China, [2] Institute of Interdisciplinary Integrative Medicine Research, Shanghai University of Traditional Chinese Medicine, Shanghai, China, [3] Department of Pharmacy, Tianjin Rehabilitation and Recuperation Center, Joint Logistics Support Force, Tianjin, China

OPEN ACCESS

Edited by:
Hengyu Li,
Second Military Medical University, China

Reviewed by:
Xiaoqing Guan,
Cancer Research Institute, Zhejiang Cancer Hospital, China
Ying Jing,
Shanghai Jiao Tong University, China

****Correspondence:***
Weidong Zhang
wdzhangy@hotmail.com

[†] These authors have contributed equally to this work

Specialty section:
This article was submitted to Molecular and Cellular Oncology, a section of the journal Frontiers in Cell and Developmental Biology

Received: *11 December 2020*
Accepted: *02 March 2021*
Published: *01 April 2021*

Citation:
Tian S, Yan L, Fu L, Zhang Z, Zhang J, Meng G and Zhang W (2021) A Comprehensive Investigation to Reveal the Relationship Between Plasmacytoid Dendritic Cells and Breast Cancer by Multiomics Data Analysis. Front. Cell Dev. Biol. 9:640476. doi: 10.3389/fcell.2021.640476

Plasmacytoid dendritic cells (pDC) are an essential immune microenvironment component. They have been reported for crucial roles in linking the adaptive and immune systems. However, the prognostic role of the pDC in breast cancer (BRCA) was controversial. In this work, we collected large sample cohorts and did a comprehensive investigation to reveal the relationship between pDC and BRCA by multiomics data analysis. Elevated pDC levels were correlated with prolonged survival outcomes in BRCA patients. The distinct mutation landscape and lower burden of somatic copy number alterations (SCNA) and lower intratumoral heterogeneity were observed in the high pDC abundance group. Additionally, a more sensitive immune response and chemotherapies response were observed in the high pDC group, which implicates that patients with high pDC abundance can be benefited from the combination of chemotherapy and immunotherapy. In conclusion, the correlation between pDC abundance and BRCA patients' overall survival (OS) was found to be positive. We identified the molecular profiles of BRCA patients with pDC abundance. Our findings may be beneficial in aiding in the development of immunotherapy and elucidating on the precision treatment for BRCA.

Keywords: breast cancer, immunotherapy, plasmacytoid dendritic cells, prognosis, bioinformatics analysis

INTRODUCTION

Breast cancer (BRCA) is a pathological state in which breast epithelial cells proliferate out of control under the action of multiple carcinogens. The International Agency for Research on Cancer (IARC) documented that in 2018, BRCA has an incidence rate of 24.2% among females globally and is the most susceptible malignant tumor for women. There are four breast subtypes: lumina A (cavity surface A), lumina B (cavity surface B), HER-2 positive, and triple-negative. Although the overall survival (OS) for early BRCA patients continues to increase, the vast majority of advanced BRCA

patients cannot be cured. As a new star in the field of oncology, immunotherapy has drawn lots of attention. In the treatment of solid tumors, such as liver cancer, lung cancer, pancreatic cancer, and ovarian cancer, immunotherapy has been shown to exert a strong anti-tumor activity (Steven et al., 2016; Odunsi, 2017; Banerjee et al., 2018; Emens, 2018). The Food and Drug Administration (FDA) has approved several tumor immunotherapy drugs for clinical application (Riley et al., 2019). Moreover, immunotherapy has been used for advanced BRCA, but only for specific subtypes, such as programmed death-ligand 1 (PD-L1) monoclonal antibody atezolizumab for triple-negative BRCA. Phase III clinical studies have confirmed that the combination of chemotherapy and immunotherapy can improve the curative effect and improve the OS (Schmid et al., 2018).

However, only relying on a PD-L1 test will definitely miss some patients who can also benefit from immunotherapy. Concurrently, current research enthusiasm concentrated on T cells, and less attention paid to other types of immune cells. Hollern's team confirmed for the first time that the production of antibodies by B cells plays a crucial role in anti-tumor immune response (Hollern et al., 2019). This shows that different immune cell types have unique importance in the immune system and immunotherapy still needs to seek more breakthroughs for general patients with BRCA. Based on lineage-negative cells with dendritic cell (DC)-like morphology (Chehimi et al., 1989; O'Doherty et al., 1993), upon stimulation with influenza or herpes simplex viruses, the plasmacytoid dendritic cells (pDC) were found to be the key type I interferon (IFN)-secreting cells in circulation (Cella et al., 1999; Siegal et al., 1999). Therefore, these cells play a crucial role in adaptive and innate immune defenses against viruses, other pathogens, and autoimmune diseases as well as in anti-tumor immunity.

However, the role of the pDC is different among different tumor types (Han et al., 2017; Schuster et al., 2019; Wagner et al., 2019; Zhou et al., 2019). Studies on the role of the pDC on the clinical outcomes of BRCA patients have not found a binding conclusion (Sawant et al., 2012; Sisirak et al., 2012, 2013; Faget et al., 2013; Sawant and Ponnazhagan, 2013; Kini Bailur et al., 2016; Wu et al., 2017; Gadalla et al., 2019). This study aimed at evaluating the role of the pDC in BRCA patients. First, we measured the tumor-infiltrating immune cells (TIICs) of BRCA by the Single-Sample Gene Set Enrichment Analysis (ssGSEA) algorithm and constructed the interaction networks of the TIICs. Then, we conducted a detailed analysis to determine the potential role of the pDC from a multiomics view including somatic copy number alterations (SCNA), burden of SCNA, somatic mutation, and intratumoral heterogeneity. Finally, we revealed the influences of the pDC in BRCA and offered potential therapeutic strategies for the precise treatment of different molecular subtypes of BRCA. In short, we evaluated the roles of the pDC, pDC-associated genes, as well as immunotherapeutic outcomes in BRCA using machine learning and bioinformatics models. Our findings reveal probable therapeutic targets and elucidate on the molecular mechanisms of the BRCA microenvironment.

MATERIALS AND METHODS

Patients and Samples

The Cancer Genome Atlas (TCGA)-BRCA mRNA count data and their relevant clinical information were retrieved from the GDC data portal[1]. In this paper, 1,097 BRCA samples with corresponding clinical information were available in TCGA. Simultaneously, the somatic mutation data (VarScan2 Variant Aggregation and Masking) were retrieved from TCGA database. Moreover, SCNA were downloaded from the Firehose database[2]. Another two independent cohorts, including GSE20685 and GSE86166, were obtained from the Gene Expression Omnibus (GEO) database[3] to confirm the performance of the prognostic pDC. The detailed TCGA clinical information is shown in **Table 1**. **Figure 1** shows the workflow of this study, that is, data pre-processing, estimation of the immune cell abundance, analysis of SCNA, and the immunotherapeutic and chemotherapeutic response prediction.

[1]https://portal.gdc.cancer.gov
[2]http://www.firehose.org/
[3]https://www.ncbi.nlm.nih.gov/geo

TABLE 1 | Clinical characteristics of BRCA patients in TCGA.

Characteristic	TCGA
Age	
Median	58
Range	19–90
Sex	
Male	12
Female	1,085
M stage	
M0	907
M1	190
N stage	
N0	514
N1	365
N2	120
N3	78
NX	20
T stage	
T1	280
T2	637
T3	137
T4	40
Unknown	3
pTNM stage	
Stage I	181
Stage II	625
Stage III	250
Stage IV	20
Stage X	13
Unknown	8
Vital status	
Living	943
Dead	154

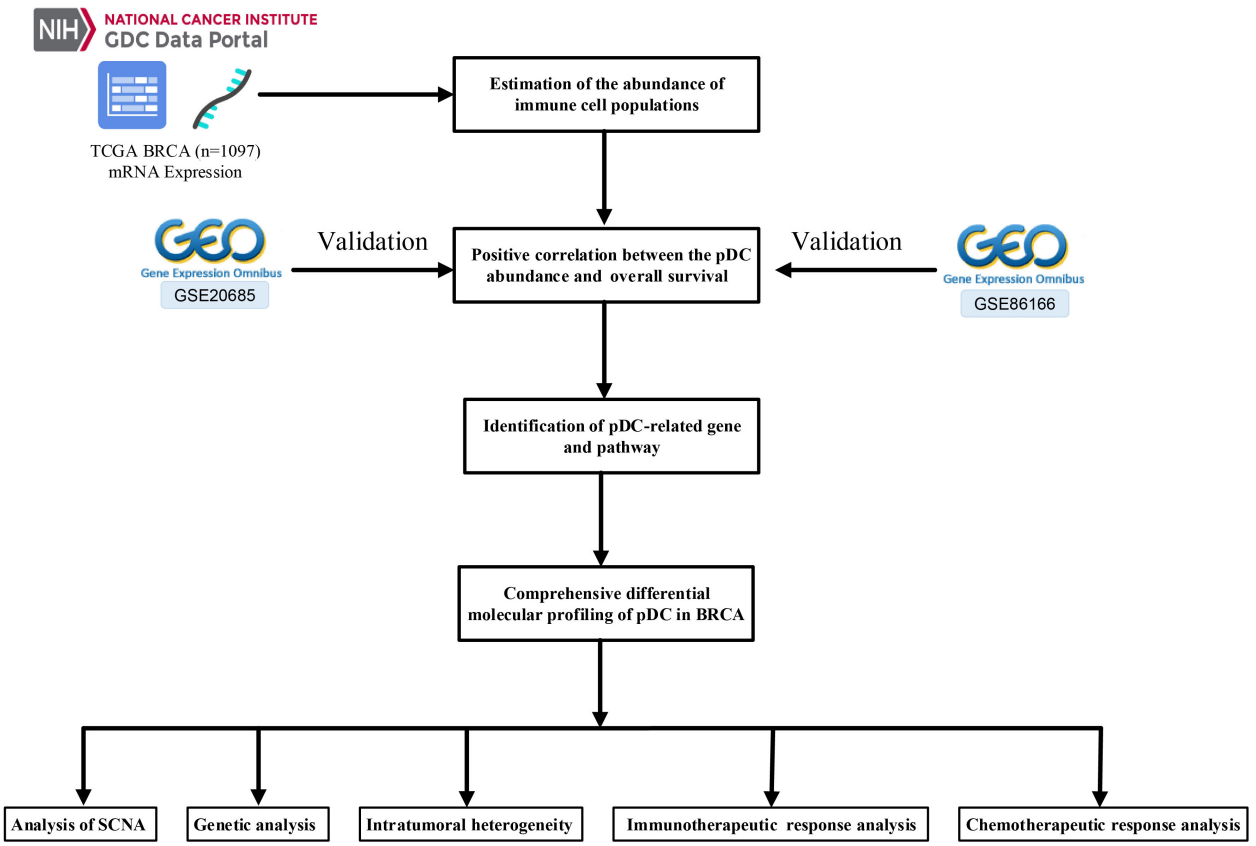

FIGURE 1 | Schematic presentation of the study design.

Pre-Processing of Gene Expression Data

We first transformed the Ensembl IDs to gene symbols and preserved protein-coding genes. Given that transcripts per kilobase million (TPM) values were similar to the results generating from microarray, we computed the TPM values. For the GEO datasets, we normalized the expression datasets by Robust Multiarray Average with the R package "affy" (Gautier et al., 2004). Mean value was selected in cases where multiple probes were mapped to the same gene.

Estimation of the Abundance of Immune Cell Populations

Gene signatures of 24 TIICs, including adaptive and innate immunity, were used to calculate the infiltration level of immune cell through the ssGSEA algorithm (Bindea et al., 2013). In brief, ssGSEA applied the special signatures of immune cells to determine the abundance of immune cell populations in every sample. In our research, we did ssGSEA to estimate the infiltration levels of 24 kinds of TIICs in BRCA samples, which was implemented in the R package GSVA (Hänzelmann et al., 2013). The correlations and heatmap between the infiltration levels of the TIICs were established to show the relationship between the TIICs using the corrplot and ComplexHeatmap packages (Gu, 2015; Wei et al., 2017).

Survival Analysis of TIICs Abundance of BRCA

After establishing the abundance of the TIICs in BRCA samples by the GSVA package, we further identified whether the TIICs have prognostic value. For TCGA and GEO datasets, the TIICs' infiltration levels data of patients and clinical data are combined into a matrix. Then, using the survminer package in R (Kassambara et al., 2017), we determined the optimal cut-off point for group division. Using the cut-off value, the samples were assigned into the pDC^{high} group and the pDC^{low} group. Finally, using the survival package (Therneau and Lumley, 2014; Tian et al., 2019b), the R software was used to show the influence of the abundance of the TIICs on OS. Given that the pDC play crucial roles in investigating adaptive and innate immune responses, the results also showed that the tumor-infiltrating pDC were positively correlated with OS; therefore, we aimed at evaluating the effect of the pDC on the BRCA microenvironment.

Identification of Differentially Expressed Genes Associated With the pDC

In TCGA dataset, we used the limma package to calculate the differentially expressed genes (DEGs) between the pDC^{high} and pDC^{low} groups at the cut-off $|\log FC| > 0.585$ and adj.P.Val < 0.05 (p-value was attuned for multiple tests using

the Benjamini–Hochberg method) (Smyth, 2005; Tian et al., 2019b). The heatmap and volcano map were drawn, where highly expressed genes were marked in red, whereas genes with suppressed expression levels were marked in blue. The Gene Ontology (GO) and Kyoto Encyclopedia of Genes and Genomes (KEGG) analyses were performed for gene set annotation, whereas the GSEA algorithm was applied to identify the key pathways and biological process of the pDC-related genes using the R package "clusterProfiler" (Yu et al., 2012; Tian et al., 2019a).

Survival Analysis of Hub Genes Based on the DEGs

For the DEGs between the pDC^{high} and pDC^{low} groups, we used the Search Tool for the Retrieval of Interacting Genes (STRING, version 11.0)[4] online database with the cut-off criterion of combined score > 0.4 to establish the protein–protein interaction (PPI) networks (Mering et al., 2003). In addition, three network topology parameters, including degree, betweenness, and closeness, were used to filter the key genes, and the top 10 key gene relationship networks were built using cytoHubba plugin (Chin et al., 2014). Finally, a Venny map was built to show the hub gene, and survival analysis also was performed to show whether the hub genes have prognostic value.

Analysis of SCNA

SCNA data of BRCA were downloaded from Firehose[5] and, based on pDC abundance, were distributed into two groups. The GISTIC 2.0 module of GenePattern (Mermel et al., 2011) was used to analyze the SCNA data of the pDC^{high} group and the pDC^{low} group. In this paper, the hg19.mat data with a threshold of 0.1 were selected. In addition, we calculated the burden of SCNA including gain as well as loss at the focal and arm levels.

Genetic Analysis and Intratumoral Heterogeneity

The MutSigCV_v1.41[6] was used in the identification of significantly mutated genes ($q < 0.05$) more than expected by chance with default parameters (Lawrence et al., 2013). Fisher's exact test was used to discover differentially mutated genes between the pDC^{high} and pDC^{low} groups. The R package "ComplexHeatmap" was used to draw the mutation landscape oncoprint. Concurrently, we also calculated the intratumoral heterogeneity score by the R package maftools (Mroz and Rocco, 2013; Mayakonda et al., 2018). The specific calculation formula was shown as:

$$\mathrm{MATH} = 100 \times \mathrm{MAD}/\mathrm{median}.$$

The MATH score of each individual was calculated based on median of mutant-allele fractions and median absolute deviation (MAD). In somatic mutations, the MATH score could quantify the genetic heterogeneity by the normalized variance of the frequency distribution of mutant alleles.

[4]http://string-db.org

[5]http://www.firehose.org/

[6]www.broadinstitute.org

Immunotherapeutic and Chemotherapeutic Response Prediction

Using two prediction methods, we further explored the possibility of clinical responses to immune checkpoint blockade. The Tumor Immune Dysfunction and Exclusion (TIDE) algorithm as well as the subtype mapping method were employed to evaluate each sample likelihood of responding to immunotherapy (Hoshida et al., 2007; Jiang et al., 2018). Moreover, using the R package "pRRophetic," chemotherapeutic responses of each sample were predicted using the largest public pharmacogenomics database, that is, the Genomics of Drug Sensitivity in Cancer (GDSC) database[7] (Geeleher et al., 2014b). Based on the GDSC dataset, the pRRopheticPredict function was used to predict the half-maximal inhibitory concentration (IC50) of each sample using ridge regression. The 10-fold cross-validation method was used to evaluate the prediction accuracy. Using ComBat function, we eliminated batch effects between cell lines for analysis (Geeleher et al., 2014a).

Statistical Analysis

Statistical analysis was performed using the R software. The survival package was used for survival analysis. The difference of OS was assessed using Kaplan–Meier plots and log-rank tests. The correlation between defined groups and categorical clinical information was assessed using chi-square. $p \leq 0.05$ was set as the threshold for statistical significance.

RESULTS

High pDC Abundance in BRCA Is Correlated With Better Survival Outcomes

Figure 1 shows the workflow of the whole analysis. First, the ssGSEA approach was used to calculate the richness of 24 immune cell populations in BRCA samples. In order to show the immune phenotype landscape in the tumor microenvironment (TME) of BRCA, the TME cell correlations network and their effects on the OS of patients were constructed by hierarchical cluster analysis. As is shown in **Figure 2A**, the TME immune cells, drawing an overall landscape of TME interactions, were clustered into four clusters, and the relationship between OS and clusters was analyzed by the pairwise log-rank test. Using an optimal cut-off value determined by the survminer package in R, we divided BRCA samples into the pDC^{high} group and the pDC^{low} group. Specifically, the pDC^{high} group, comprising 751 samples, was distinguished from the pDC^{low} group, containing 346 samples. The survival analysis suggested that the abundance of the pDC was strongly positively associated with patient's clinical outcome, which means that the elevated abundance of the pDC benefited the survival outcomes of BRCA patients included in TCGA cohorts (**Figure 2B**). Additionally, two external cohorts (GSE20685 and GSE86166) were used to verify the association between the pDC and the survival of BRCA

[7]https://www.cancerrxgene.org/

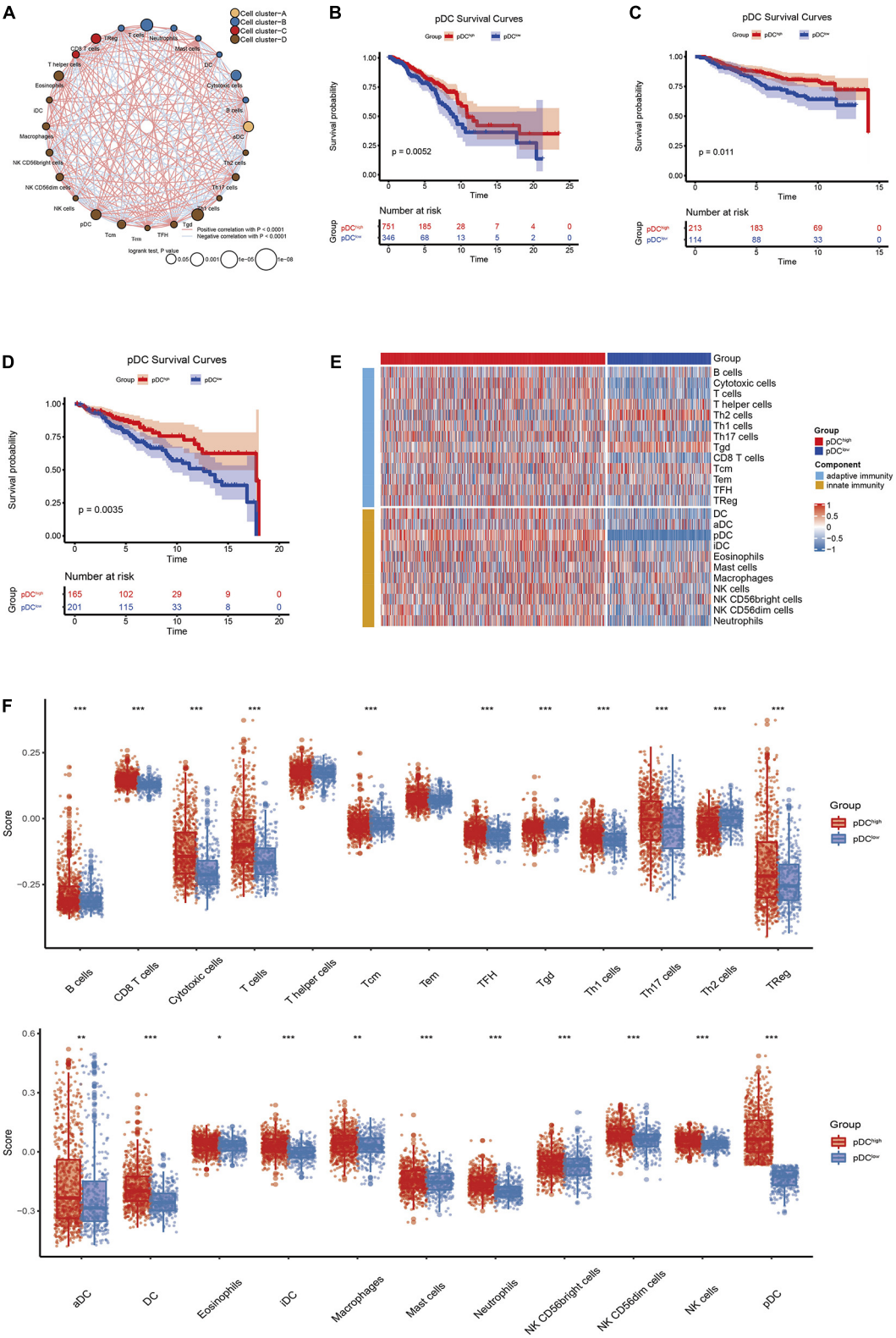

FIGURE 2 | The correlation between clinical outcomes and pDC abundance in BRCA patients. **(A)** Correlations among immune cell populations. **(B–D)** Kaplan–Meier curves for the OS of BRCA patients revealed that patients with elevated pDC abundance exhibited favorable clinical outcomes when compared with patients with low pDC abundance in TCGA, GSE20685, and GSE86166 cohorts. **(E,F)** The immune infiltration levels between the two groups, including adaptive immune signatures and innate immune signatures. The meaning of the statistical difference is as follows: * represents $p \leq 0.05$, ** represents $p \leq 0.01$, and *** represents $p \leq 0.001$.

patients (**Figures 2C,D**). In addition, adaptive immunity and innate immunity were compared. The pDC^{high} group was highly enriched in adaptive and innate immunity (**Figures 2E,F**).

Identification and Functional Enrichment Analysis of the DEGs Associated With the pDC

Using the "limma" R package, we performed a differential expression analysis of two pDC groups at the cut-off $|\log FC| > 0.585$ and adj.*P*.Val < 0.05 in TCGA. Then, 542 DEGs (95 down-regulated and 447 up-regulated genes) were identified for further analysis in TCGA. The heatmap and volcano plots of the DEGs are shown in **Figures 3A,B**. In order to characterize the pathway differences between the two groups, KEGG and GO were utilized for functional enrichment analysis by GSEA. The results showed that the pDC^{high} group was enriched with immune-related pathways, such as T cells, B cells, natural killer (NK) cells, PD-L1, chemokines, and tumor necrosis factor (TNF) signaling pathways, and biological processes, such as activation of immune response, T cell activation, and adaptive immune responses, whereas the pDC^{low} group was enriched with cellular senescence, cell cycle, renal cell carcinoma, and several metabolic processes (e.g., carbon metabolism, inositol phosphate metabolism) (**Figures 3C–F**). The detailed parameters of the related results are shown in **Tables 2**, **3**, which indicate that these two groups play different roles—therefore, they have different effects on the prognosis of patients.

Screening for Hub Genes

The PPI network of all DEGs was established based on the network annotation of the STRING database under default parameters. The network, which consisted of 499 nodes and 4,353 edges, was visualized using the cytoscape software[8] (**Supplementary Figure 1**). Then, using the top 10 key genes, three subnetworks were built by three network topology parameters, including degree, betweenness, and closeness. The cytoHubba plugin was used to select the three subnetworks of PPI, and the results are shown in **Supplementary Figure 2**. Four hub genes, including CD34, IL6, SPI1, and SELL, were selected (**Supplementary Figure 3**). Then, we examined the correlation between the expression of the four hub genes and immune cell infiltration levels in BRCA. As depicted in **Figure 4A**, the expression of the four hub genes was closely associated with the most TIICs abundance in BRCA patients, which also suggested that the four hub genes were closely associated with immunity. The survival analysis of the four hub genes was further analyzed (**Figures 4B–E**). The results show that the overexpression of SPI1 and SELL due to pDC abundance was significantly associated with good clinical outcomes in BRCA patients ($p < 0.05$). Another two hub genes (CD34 and IL6) showed no significant prognostic value.

In addition, the pan-cancer expression of the hub genes was further analyzed, and the data on the hub gene expression were extracted from the TIMER database, which is an in-depth resource for systematic analyses across multiple malignancies. Among the results, the expression levels of CD34, IL6, SPI1, and SELL showed significant expression differences in 16, 12, 12, and 11 cancer types, respectively, especially in BRCA (**Supplementary Figure 4**).

Analysis of Copy Number Aberrations Between the pDC Groups

Using the GISTIC 2.0 module of GenePattern, we also assessed the difference in alterations in somatic copy numbers between the pDC^{high} group and the pDC^{low} group. The 22 chromosomes in the two groups exhibited a similarity in chromosomal aberrations, and the distribution of the frequency across all chromosomes in these groups is shown in **Figure 5A**. As is shown in **Figure 5B**, many focal amplifications (e.g., 6p21.1, 8q23.3, and 11q12.2) and deletions (e.g., 1p36.13, 11q23.3, and 19p13.3) within chromosomal regions were detected in the higher pDC abundance group. In addition, we compared the DEGs with copy number aberrations in the high pDC abundance group, and only a few genes showed a similar mode with its expression level as shown in **Figure 5C**. This implies that most of the DEGs were not affected by SCNA. In other words, differential gene expression between the pDC^{high} group and the pDC^{low} group occurred without the effects of SCNA.

To evaluate the impact of SCNA on the pDC, we examined the differences of the burden of copy number alterations in arm level and focal level between these distinct groups (**Figure 5D**). Compared with those in the pDC^{high} group, the pDC^{low} group demonstrated a higher burden of SCNA in focal and arm levels. These results above suggested that SCNA contributed to differences in immune cell infiltration in BRCA, and the patients of the pDC^{high} group may be more sensitive to immunotherapy.

Differential Somatic Mutation Landscape Between the pDC Subgroups

After analyzing the transcriptional alterations and copy number aberrations between the two groups, we further investigated the differences in somatic mutations between the pDC^{high} group and the pDC^{low} group. Somatic mutations data were downloaded from TCGA portal using the R package TCGAbiolinks. By MutSigCV_v1.41 tools, among all BRCA samples, we identified 10 significantly mutated genes, including TP53, PIK3CA, CDH1, GATA3, MAP3K1, MUC4, DMD, PTEN, NCOR1, and NF1, after removing genes whose non-silent mutation rate was less than 5% (**Figure 6A**). Additionally, 30 differentially mutated genes between the two groups were identified by using the mafCompare() function in the R package "maftools" (**Figure 6B**). Additionally, 3 of these differentially mutated genes, including TP53, PIK3CA, and CDH1, were consistent with 10 significantly mutated genes among all BRCA samples above. In addition, we determined 333 and 309 significant mutation genes by MutSigCV for the pDC^{high} group and the pDC^{low} group, respectively, at a loose cut-off of $p < 0.05$, and only 40 significant mutation genes were shared (**Figure 6C**).

Moreover, the intratumoral heterogeneity of each sample was determined by the MATH value and was the ratio of MAD

[8]http://www.cytoscape.org/

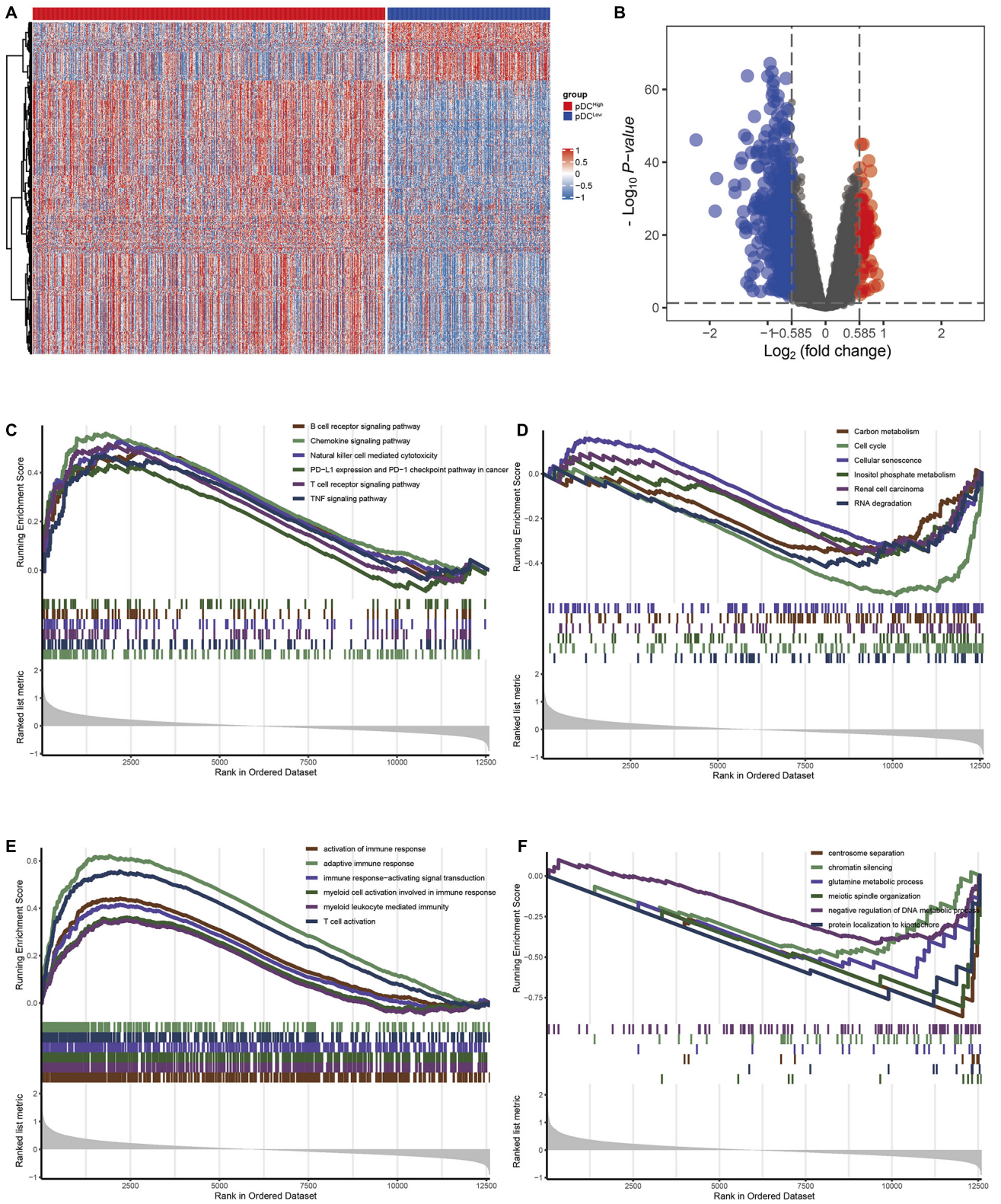

FIGURE 3 | The DEGs and pathways between the two groups. **(A)** Heatmap of the DEGs between the two groups. **(B)** The volcano plot of the DEGs between the two groups. **(C)** KEGG analysis in the pDC^{high} group. **(D)** KEGG analysis in the pDC^{low} group. **(E)** GO analysis demonstrated in the pDC^{high} group. **(F)** GO analysis in the pDC^{low} group.

TABLE 2 | The enriched KEGG pathways associated with the pDC in TCGA.

ID	Description	Set size	NES	*p* value	Group
hsa04662	B cell receptor signaling pathway	74	1.961	0.001	pDC^{high}
hsa04062	Chemokine signaling pathway	158	2.404	0.001	pDC^{high}
hsa04650	Natural killer cell-mediated cytotoxicity	86	2.08	0.001	pDC^{high}
hsa05235	PD-L1 expression and PD-1 checkpoint pathway in cancer	76	1.688	0.001	pDC^{high}
hsa04660	T cell receptor signaling pathway	90	2.048	0.001	pDC^{high}
hsa04668	TNF signaling pathway	101	1.893	0.001	pDC^{high}
hsa01200	Carbon metabolism	92	−1.659	0.003	pDC^{low}
hsa04110	Cell cycle	121	−2.587	0.004	pDC^{low}
hsa04218	Cellular senescence	143	−1.639	0.004	pDC^{low}
hsa00562	Inositol phosphate metabolism	70	−1.637	0.007	pDC^{low}
hsa05211	Renal cell carcinoma	62	−1.531	0.016	pDC^{low}
hsa03018	RNA degradation	67	−1.818	0.003	pDC^{low}

TABLE 3 | The enriched GO pathways associated with the pDC in TCGA.

ID	Description	Set size	NES	*p* value	Group
GO:0002253	Activation of immune response	451	2.078	0.001	pDC^{high}
GO:0002250	Adaptive immune response	294	2.806	0.001	pDC^{high}
GO:0002757	Immune response-activating signal transduction	400	1.937	0.001	pDC^{high}
GO:0002275	Myeloid cell activation involved in immune response	445	1.698	0.001	pDC^{high}
GO:0002444	Myeloid leukocyte-mediated immunity	450	1.643	0.001	pDC^{high}
GO:0042110	T cell activation	374	2.579	0.001	pDC^{high}
GO:0051299	Centrosome separation	10	−2.225	0.002	pDC^{low}
GO:0006342	Chromatin silencing	40	−1.924	0.003	pDC^{low}
GO:0006541	Glutamine metabolic process	18	−1.930	0.003	pDC^{low}
GO:0000212	Meiotic spindle organization	10	−2.072	0.002	pDC^{low}
GO:0051053	Negative regulation of DNA metabolic process	101	−1.942	0.004	pDC^{low}
GO:0034501	Protein localization to kinetochore	10	−2.059	0.002	pDC^{low}

to the median of mutant-allele fractions. For MATH data, the difference between the pDC^{high} group and the pDC^{low} group was determined using the Wilcoxon test (Mann–Whitney test). There was a significant difference between the two groups ($p < 0.001$), and lower intratumoral heterogeneity existed in the pDC^{high} group, as shown in **Figure 6D**.

Differential Sensitivity Analysis of Immuno/Chemotherapies Between the pDC Groups

According to our knowledge, the effect of immunotherapy is closely related to the burden of SCNA and intratumoral heterogeneity. Then, the likelihood of immunotherapeutic responses was determined using two methods. First, using the subclass mapping method, we compared the expression profiles of the two groups with a dataset of 47 melanoma patients who responded to immunotherapy. It demonstrated that the higher pDC group was more sensitive to anti-PD-1 therapy ($p = 0.039$) (**Figure 7A**). The likelihood of immunotherapeutic responses was also predicted using the TIDE algorithm. Significant differences between the two groups were shown ($p < 0.01$). According to previous results, it also was consistent that patients with a lower burden of somatic copy number variations (SCNV) and lower intratumoral heterogeneity in the pDC^{high} group were more sensitive to immunotherapy.

In BRCA clinical practice, chemotherapy is a common method to treat the tumor. Thus, four chemo drugs, gemcitabine, camptothecin, lapatinib, and paclitaxel, were used to assess the different responses to chemotherapy between the two pDC groups. Firstly, cell line data from the GDSC database were downloaded. Then, using the ridge regression, we trained a predictive model method and determined the predictive accuracy by 10-fold cross-validation. We calculated the IC50 values for gemcitabine, camptothecin, lapatinib, and paclitaxel of each patient by the predictive model. Finally, we found that there was a significant difference in sensitivity to gemcitabine, camptothecin, lapatinib, and paclitaxel, as shown in **Figure 7B**.

Demographic Characteristics

According to the cut-off point confirmed previously, 751 cases were classified into the pDC^{high} group and 346 into the pDC^{low} group. Then, we performed a series of chi-square tests to inspect the correlation between the abundance of the pDC and clinicopathological characteristics. Most of the clinicopathological characteristics, including patient age, gender, and pathological stage, were not different between the two groups, except M stage, N stage, and T stage (**Supplementary Table 1**). Concurrently, univariate and multivariate Cox regression analyses were conducted to assess whether the prognostic ability of the pDC was independent of other clinical features. The result of univariate Cox regression indicated that the risk score was significantly associated with OS [pDC^{low} group vs. pDC^{high} group, hazard ratio (HR) = 1.579, 95% CI 1.143–2.182, $p < 0.01$]. Additionally, in multivariable Cox regression, the pDC have a significant relationship with OS (pDC^{low} group vs. pDC^{high} group, HR = 1.570, 95% CI 1.131–2.178, $p < 0.01$) (**Supplementary Table 2**). These results demonstrated that the prognostic ability of the pDC was independent of other clinical features. In addition, the relationship between clinical features (tumor stage and age) and pDC abundance was explored. The analyzed results suggested that pDC abundance showed no significant difference in tumor stage and age, which is consistent with previous results in **Supplementary Table 1** (**Supplementary Figure 5**).

DISCUSSION

DCs are the most important antigen-presenting cells (APC). The migration ability of immature DCs has been documented to be strong. Mature DCs effectively activate initial T cells and regulate and maintain the central link of the immune response. This maturation occurs in tandem with antigen uptake, processing, as well as presentation to activate T cells.

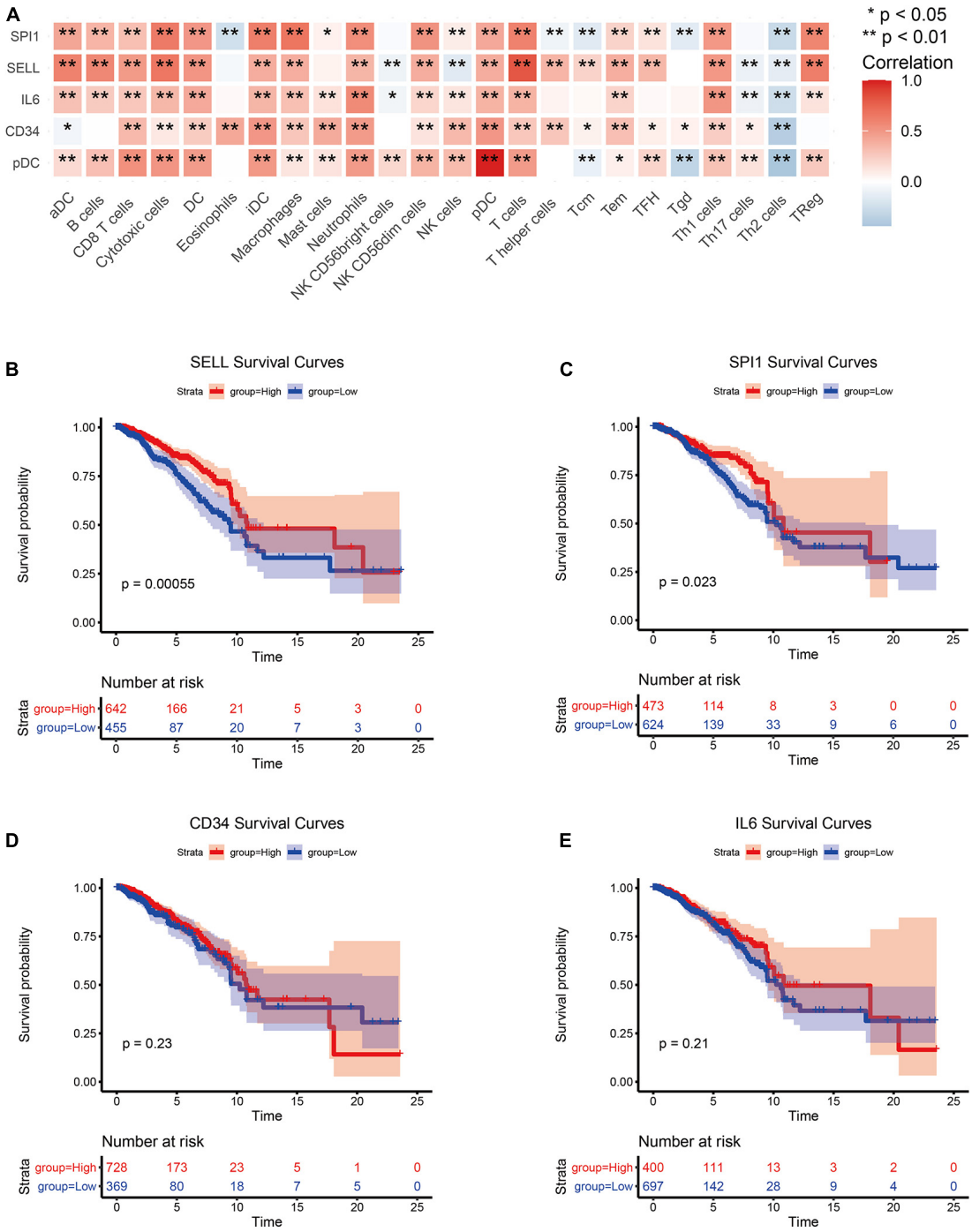

FIGURE 4 | Screening of hub genes and correlation analysis. **(A)** Correlation analysis between hub genes and TIICs. **(B–E)** Survival analysis of hub genes.

Otherwise, DCs induce antigen-specific T cell tolerance or silencing. On the one hand, the secondary products of the pDC, especially type I IFNs, exhibit both tolerogenic and immunogenic effects in tumor immunity. These factors enhance the cytotoxicity of T cells and NK cells, help activate B cells to differentiate into plasma cells, enhance the maturation and activation of DCs as well as pro-inflammatory macrophages, and finally jointly contribute to an immune-activated TME. On the one hand, the pDC also recruit Treg cells or induce the expression of immune regulatory molecules to create an immunosuppressive TME.

The complex roles of the pDC allow them to perform different functions in BRCA. It has been documented that, through TRAIL and Granzyme B, the activated pDC can kill

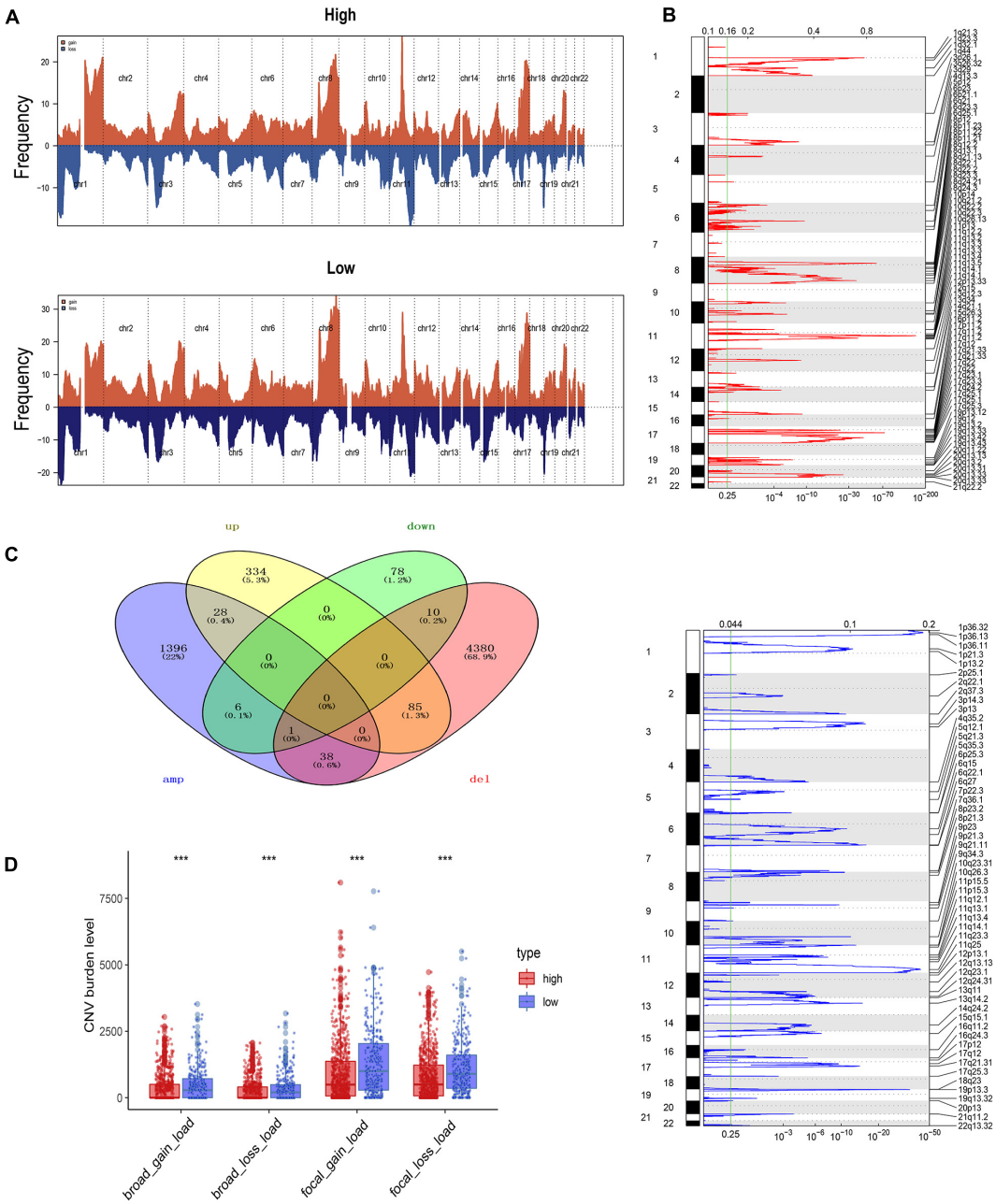

FIGURE 5 | Somatic copy number aberration across the pDC groups. **(A)** The copy number amplifications and deletions between the two groups. **(B)** Detailed cytoband with focal amplification (top) and focal deletion (bottom) in the pDC^{high} group generated with GISTIC_2.0. **(C)** Venn diagram of the genes with SCNA and the DEGs in the pDC^{high} group. **(D)** The burden of SCNA between the pDC^{high} group and the pDC^{low} group. The meaning of the statistical difference is as follows: *** represents $p \leq 0.001$.

breast tumor cells. Furthermore, the pDC initiate the sequential activation of CD8 + T cells as well as NK cells and ultimately suppress BRCA growth (Wu et al., 2017). Kini studied 75 newly diagnosed BRCA patients aged 28–87 and found a positive correlation between higher than median levels of circulating pDC and 5-year survival (Kini Bailur et al., 2016). While another study has revealed that pDC infiltration would lead to poor prognosis because the pDC promote lymph node metastasis *via* the CXCR4/SDF-1 axis (Gadalla et al., 2019). These studies prove that the pDC can predict the prognosis of BRCA, but the specific role is still controversial. Therefore, we determined the potential role of the pDC-associated genes in BRCA. The abundance of the pDC was calculated by the ssGSEA algorithm in three cohorts. In this research, BRCA samples were assigned into two groups based on the abundance of the pDC. An elevated abundance of the pDC

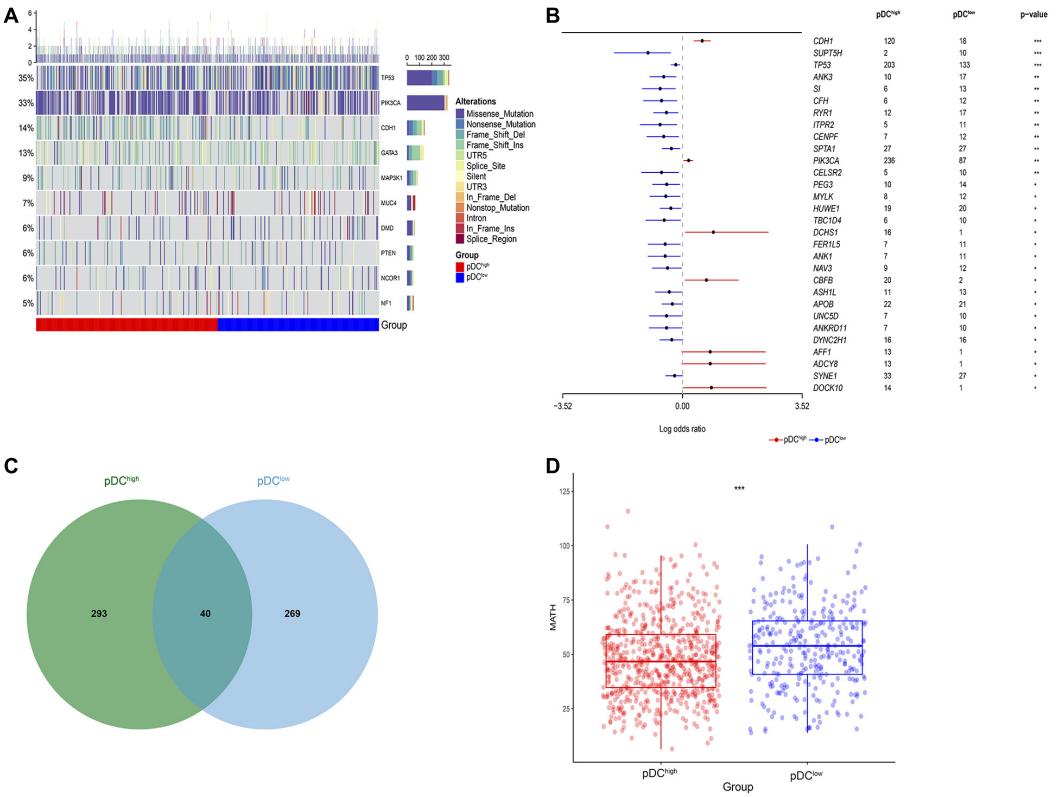

FIGURE 6 | Genetic alteration across the pDC groups. **(A)** Somatic mutation landscape of significantly mutated genes in TCGA. **(B)** Differentially mutated genes between the pDC^{high} group and the pDC^{low} group. **(C)** Shared significantly mutated genes between the pDC^{high} group and the pDC^{low} group. **(D)** Boxplot of intratumoral heterogeneity between the two groups. The meaning of the statistical difference is as follows: * represents $p \leq 0.05$, ** represents $p \leq 0.01$, and *** represents $p \leq 0.001$.

was correlated with better survival outcomes in BRCA patients. Concurrently, this conclusion also was confirmed by another two external cohorts.

Then, further analysis identified 542 DEGs between the groups. KEGG pathway annotation and GO annotation were conducted by the GSEA algorithm, and the results indicated that the pDC^{high} group was more related to immune response. In order to select the hub genes associated with the pDC, the PPI network was conducted through the STRING database, three subnetworks were filtered out, and finally, we identified four hub genes. Among the four hub genes, we also found that two hub genes (SELL, SPI1) related to the pDC have independent prognostic significance. These two genes are potential prognostic biomarkers with therapeutic implications. Selectin is a type of Ca^{2+}-dependent cell adhesion molecule, which can recognize and bind to specific glycosyl groups, involved in the recognition and adhesion between white blood cells and vascular endothelial cells. The selectin family has three members: E-selectin, L-selectin, and P-selectin. L-selectin (SELL) was first discovered as a homing receptor on lymphocytes and later found to be expressed on various white blood cells. Chu et al. documented that SELL immunodepletion inhibited MDA-MB-231 cell migration (Laubli and Borsig, 2010; Geng et al., 2013; Chu et al., 2014). SPI1 transcription factors are closely related to developmental processes. It is a major regulator hematopoiesis and limits hematopoietic stem cell self-renewal. Deregulation of its activity or expression is associated with leukemia, in which SpI1 can act as either an oncogene or a tumor suppressor. Delestre et al. (2017) documented that senescence is an anti-proliferative mechanism induced by SpI1 that may inhibit the pathogenesis of acute myeloid leukemia. Moreover, the stemness of T-ALL leukemia stem cell is epigenetically regulated by SPI1 (Zhu et al., 2018). In addition, the expression of SpI1 can promote the early myeloid development of zebrafish (Yu et al., 2018). Although the other two genes (IL6, CD34) did not show significant prognostic value, they are still crucial for the occurrence and development of BRCA. Interleukin 6 (IL6)/STAT3 signaling enhances BRCA metastasis by interfering with estrogen receptor (ER) alpha (Hu et al., 2020; Siersbaek et al., 2020). The expression of CD34 in BRCA tissues is positively correlated with angiogenesis, and its high expression will promote cancer cell infiltration and metastasis (Shpall et al., 1994; Schulman et al., 1999; Westhoff et al., 2020).

SCNA analysis also was performed by the GISTIC 2.0 module of GenePattern. There was clear similarity between chromosomal aberrations in two groups. However, the burden of copy number alterations in arm level and focal level also

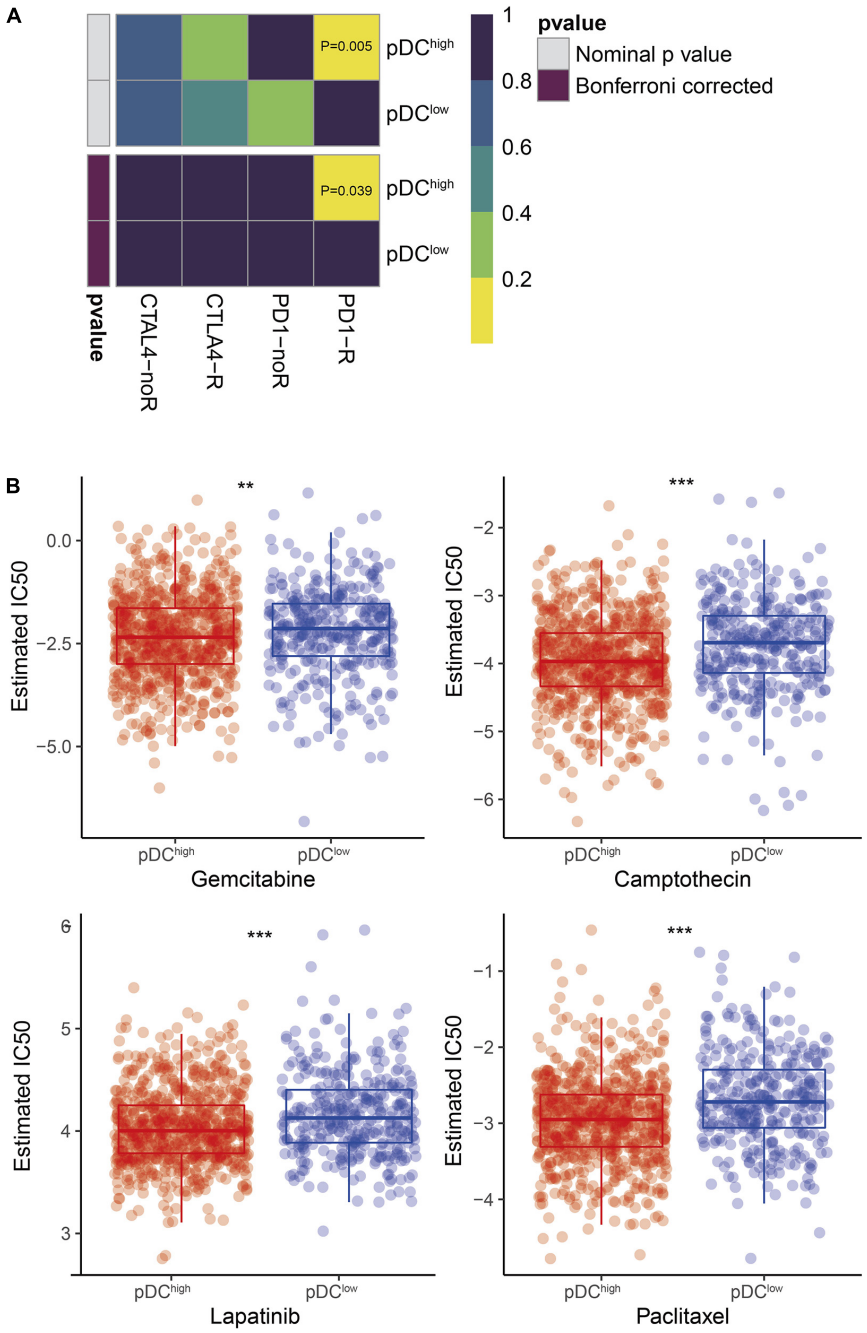

FIGURE 7 | Differential putative immunotherapeutic and chemotherapeutic response prediction. **(A)** Submap analysis in two groups. **(B)** The box plots of chemotherapeutic response in two groups. The meaning of the statistical difference is as follows: ** represents $p \leq 0.01$ and *** represents $p \leq 0.001$.

was calculated, and the pDC^{high} group exhibited a lower burden of SCNV that could contribute to the difference in immunotherapy response between the two groups. Furthermore, the genomic analysis revealed a distinct mutation landscape. In this paper, 3 differentially mutated genes, including TP53, PIK3CA, and CDH1, were overlapped with 10 significantly mutated genes among all BRCA samples. The differentially mutated gene TP53 was discoverd in the pDC^{high} group. TP53 is the tumor suppressor gene with the highest correlation with human tumors discovered so far. More than 50% of tumor patients have p53 gene mutations. In the cell cycle, normal p53 is activated when DNA damage or hypoxia causes the cell cycle to stagnate in the G1/S phase and perform DNA repair. Failure to repair will activate downstream genes to start cell apoptosis. PIK3CA gene is responsible for encoding the p110α protein, which is a subunit of the PI3K enzyme. The

main function of the PI3K enzyme is phosphorylation, which triggers a series of intracellular signal transmission through phosphorylation of other proteins. These signals are related to cell activities, including cell proliferation, migration, survival, as well as new protein production and intracellular material transport. The pathway that PI3K participates in is the PI3K–AKT–mTOR pathway. Pathogenic mutations in PIK3CA will cause it to encode abnormal p110α subunits, which will keep the PI3K enzyme in a state of continuous activation, which enhances the signal transduction in the cell, leading to uncontrolled cell proliferation and thus the formation of tumors. The classic cadherin of the cadherin superfamily is encoded by the *CDH1* gene. Alternative splicing can lead to multiple transcriptional variants. This calcium-dependent intercellular adhesion protein is composed of a transmembrane region, five extracellular cadherin repeats, and a cytoplasmic tail that is highly conserved. It has been documented that mutations affecting the *CDH1* gene result in several types of cancers including ovarian, thyroid, colorectal, breast, and gastric cancers. Loss of function of *CDH1* promotes the progression of cancers and metastasis.

In conclusion, to the best of our knowledge, this is the first comprehensive differential molecular profiling of BRCA that is based on the abundance of the pDC. Molecular differences may be beneficial in aiding in the development of immunotherapy and opened up a new world for the precision treatment of BRCA. However, this study is associated with some limitations. First, the conclusion is based on *in silico* analysis only. Prospective population-based studies should be performed to verify our findings. Second, a larger sample size should be used to identify the potential differences in clinicopathological features. Finally, the response to chemotherapy is just based on the GDSC dataset, and more datasets should be used to validate the observation in future work.

DATA AVAILABILITY STATEMENT

Publicly available datasets were analyzed in this study. This data can be found here: https://portal.gdc.cancer.gov, https://www.ncbi.nlm.nih.gov/geo.

AUTHOR CONTRIBUTIONS

ST, LY, and LF contributed equally to this article, collected and analyzed data, and drafted and revised the manuscript. WZ designed the study. ZZ, JZ, and GM collected data and revised the manuscript. All authors read and approved the final manuscript.

FUNDING

The work was financially supported by the National Key Research and Development Program of China (2019YFC1711000 and 2017YFC1700200), Professor of Chang Jiang Scholars Program, NSFC (82004003, 81520108030, and 21472238), Shanghai Engineering Research Center for the Preparation of Bioactive Natural Products (16DZ2280200), Scientific Foundation of Shanghai China (13401900103 and 13401900101), and the Shanghai Sailing Program (20YF1459000).

SUPPLEMENTARY MATERIAL

The Supplementary Material for this article can be found online at: https://www.frontiersin.org/articles/10.3389/fcell.2021.640476/full#supplementary-material

Supplementary Figure 1 | The PPI network for all DEGs.

Supplementary Figure 2 | The three subnetworks of PPI according to **(A)** degree, **(B)** betweenness, and **(C)** closeness.

Supplementary Figure 3 | Venn diagram of three subnetworks.

Supplementary Figure 4 | CD34, IL6, SPI1, and SELL expression in different cancer types. **(A–D)** The expression levels of CD34, IL6, SPI1, and SELL in TCGA are shown. The meaning of the statistical difference is as follows: ns represents not significant ($p > 0.05$), * represents $p \leq 0.05$, ** represents $p \leq 0.01$, and *** represents $p \leq 0.001$.

Supplementary Figure 5 | The relationship between clinical features and pDC abudance. **(A)** Tumor stage. **(B)** Age.

Supplementary Table 1 | Demographic characteristics of two groups.

Supplementary Table 2 | Univariate and multivariate Cox regression analyses of the pDC in TCGA set. Abbreviations: HR, hazard ratio; CI, confidence interval.

REFERENCES

Banerjee, K., Kumar, S., Ross, K. A., Gautam, S., Poelaert, B., Nasser, M. W., et al. (2018). Emerging trends in the immunotherapy of pancreatic cancer. *Cancer Lett.* 417, 35–46. doi: 10.1016/j.canlet.2017.12.012

Bindea, G., Mlecnik, B., Tosolini, M., Kirilovsky, A., Waldner, M., Obenauf, A. C., et al. (2013). Spatiotemporal dynamics of intratumoral immune cells reveal the immune landscape in human cancer. *Immunity* 39, 782–795.

Cella, M., Jarrossay, D., Facchetti, F., Alebardi, O., Nakajima, H., Lanzavecchia, A., et al. (1999). Plasmacytoid monocytes migrate to inflamed lymph nodes and produce large amounts of type I interferon. *Nat. Med.* 5, 919–923. doi: 10.1038/11360

Chehimi, J., Starr, S. E., Kawashima, H., Miller, D. S., Trinchieri, G., Perussia, B., et al. (1989). Dendritic cells and IFN-alpha-producing cells are two functionally distinct non-B, non-monocytic HLA-DR+ cell subsets in human peripheral blood. *Immunology* 68, 486–490.

Chin, C.-H., Chen, S.-H., Wu, H.-H., Ho, C.-W., Ko, M.-T., and Lin, C.-Y. (2014). cytoHubba: identifying hub objects and sub-networks from complex interactome. *BMC Syst. Biol.* 8:S11.

Chu, J. E., Xia, Y., Chin-Yee, B., Goodale, D., Croker, A. K., and Allan, A. L. (2014). Lung-derived factors mediate breast cancer cell migration through CD44 receptor-ligand interactions in a novel ex vivo system for analysis of organ-specific soluble proteins. *Neoplasia* 16, 180–191. doi: 10.1593/neo.132076

Delestre, L., Cui, H., Esposito, M., Quiveron, C., Mylonas, E., Penard-Lacronique, V., et al. (2017). Senescence is a Spi1-induced anti-proliferative mechanism in primary hematopoietic cells. *Haematologica* 102, 1850–1860. doi: 10.3324/haematol.2016.157636

Emens, L. A. (2018). Breast cancer immunotherapy: facts and hopes. *Clin. Cancer Res.* 24, 511–520. doi: 10.1158/1078-0432.CCR-16-3001

Faget, J., Sisirak, V., Blay, J. Y., Caux, C., Bendriss-Vermare, N., and Menetrier-Caux, C. (2013). ICOS is associated with poor prognosis in breast cancer as it promotes the amplification of immunosuppressive CD4(+) T cells by

plasmacytoid dendritic cells. *Oncoimmunology* 2:e23185. doi: 10.4161/onci.23185

Gadalla, R., Hassan, H., Ibrahim, S. A., Abdullah, M. S., Gaballah, A., Greve, B., et al. (2019). Tumor microenvironmental plasmacytoid dendritic cells contribute to breast cancer lymph node metastasis via CXCR4/SDF-1 axis. *Breast Cancer Res. Treat.* 174, 679–691. doi: 10.1007/s10549-019-05129-8

Gautier, L., Cope, L., Bolstad, B. M., and Irizarry, R. A. (2004). affy—analysis of Affymetrix GeneChip data at the probe level. *Bioinformatics* 20, 307–315.

Geeleher, P., Cox, N. J., and Huang, R. S. (2014a). Clinical drug response can be predicted using baseline gene expression levels and in vitro drug sensitivity in cell lines. *Genome Biol.* 15:R47.

Geeleher, P., Cox, N., and Huang, R. S. (2014b). pRRophetic: an R package for prediction of clinical chemotherapeutic response from tumor gene expression levels. *PLoS ONE* 9:e107468.

Geng, Y., Takatani, T., Yeh, K., Hsu, J. W., and King, M. R. (2013). Targeting underglycosylated MUC1 for the selective capture of highly metastatic breast cancer cells under flow. *Cell Mol. Bioeng.* 6, 148–159. doi: 10.1007/s12195-013-0282-y

Gu, Z. (2015). *Complexheatmap: Making Complex Heatmaps. Peckage Version 1.0.0.*

Han, N., Zhang, Z., Liu, S., Ow, A., Ruan, M., Yang, W., et al. (2017). Increased tumor-infiltrating plasmacytoid dendritic cells predicts poor prognosis in oral squamous cell carcinoma. *Arch. Oral. Biol.* 78, 129–134. doi: 10.1016/j.archoralbio.2017.02.012

Hänzelmann, S., Castelo, R., and Guinney, J. (2013). GSVA: gene set variation analysis for microarray and RNA-seq data. *BMC Bioinformatics* 14:7. doi: 10.1186/1471-2105-14-17

Hollern, D. P., Xu, N., Thennavan, A., Glodowski, C., Garcia-Recio, S., Mott, K. R., et al. (2019). B cells and T follicular helper cells mediate response to checkpoint inhibitors in high mutation burden mouse models of breast cancer. *Cell* 179, 1191.e1121–1206.e1121. doi: 10.1016/j.cell.2019.10.028

Hoshida, Y., Brunet, J.-P., Tamayo, P., Golub, T. R., and Mesirov, J. P. (2007). Subclass mapping: identifying common subtypes in independent disease data sets. *PLoS One* 2:e1195. doi: 10.1371/journal.pone.0001195

Hu, G., Cheng, P., Pan, J., Wang, S., Ding, Q., Jiang, Z., et al. (2020). An IL6-adenosine positive feedback loop between CD73(+) gammadeltaTregs and CAFs promotes tumor progression in human breast cancer. *Cancer Immunol Res* 8, 1273–1286. doi: 10.1158/2326-6066.CIR-19-0923

Jiang, P., Gu, S., Pan, D., Fu, J., Sahu, A., Hu, X., et al. (2018). Signatures of T cell dysfunction and exclusion predict cancer immunotherapy response. *Nat. Med.* 24, 1550–1558.

Kassambara, A., Kosinski, M., Biecek, P., and Fabian, S. (2017). *Package 'survminer'.*

Kini Bailur, J., Gueckel, B., and Pawelec, G. (2016). Prognostic impact of high levels of circulating plasmacytoid dendritic cells in breast cancer. *J. Transl. Med.* 14:151. doi: 10.1186/s12967-016-0905-x

Laubli, H., and Borsig, L. (2010). Selectins as mediators of lung metastasis. *Cancer Microenviron.* 3, 97–105. doi: 10.1007/s12307-010-0043-6

Lawrence, M. S., Stojanov, P., Polak, P., Kryukov, G. V., Cibulskis, K., Sivachenko, A., et al. (2013). Mutational heterogeneity in cancer and the search for new cancer-associated genes. *Nature* 499, 214–218.

Mayakonda, A., Lin, D.-C., Assenov, Y., Plass, C., and Koeffler, H. P. (2018). Maftools: efficient and comprehensive analysis of somatic variants in cancer. *Genome Res.* 28, 1747–1756.

Mering, C. V., Huynen, M., Jaeggi, D., Schmidt, S., Bork, P., and Snel, B. (2003). STRING: a database of predicted functional associations between proteins. *Nucleic Acids Res.* 31, 258–261.

Mermel, C. H., Schumacher, S. E., Hill, B., Meyerson, M. L., Beroukhim, R., and Getz, G. (2011). GISTIC2. 0 facilitates sensitive and confident localization of the targets of focal somatic copy-number alteration in human cancers. *Genome Biol.* 12:R41.

Mroz, E. A., and Rocco, J. W. (2013). MATH, a novel measure of intratumor genetic heterogeneity, is high in poor-outcome classes of head and neck squamous cell carcinoma. *Oral Oncol.* 49, 211–215.

O'Doherty, U., Steinman, R. M., Peng, M., Cameron, P. U., Gezelter, S., Kopeloff, I., et al. (1993). Dendritic cells freshly isolated from human blood express CD4 and mature into typical immunostimulatory dendritic cells after culture in monocyte-conditioned medium. *J. Exp. Med.* 178, 1067–1076. doi: 10.1084/jem.178.3.1067

Odunsi, K. (2017). Immunotherapy in ovarian cancer. *Ann. Oncol.* 28, viii1–viii7. doi: 10.1093/annonc/mdx444

Riley, R. S., June, C. H., Langer, R., and Mitchell, M. J. (2019). Delivery technologies for cancer immunotherapy. *Nat. Rev. Drug. Discov.* 18, 175–196. doi: 10.1038/s41573-018-0006-z

Sawant, A., Hensel, J. A., Chanda, D., Harris, B. A., Siegal, G. P., Maheshwari, A., et al. (2012). Depletion of plasmacytoid dendritic cells inhibits tumor growth and prevents bone metastasis of breast cancer cells. *J. Immunol.* 189, 4258–4265. doi: 10.4049/jimmunol.1101855

Sawant, A., and Ponnazhagan, S. (2013). Role of plasmacytoid dendritic cells in breast cancer bone dissemination. *Oncoimmunology* 2:e22983. doi: 10.4161/onci.22983

Schmid, P., Adams, S., Rugo, H. S., Schneeweiss, A., Barrios, C. H., Iwata, H., et al. (2018). Atezolizumab and Nab-Paclitaxel in Advanced Triple-Negative Breast Cancer. *N. Engl. J. Med.* 379, 2108–2121. doi: 10.1056/NEJMoa1809615

Schulman, K. A., Birch, R., Zhen, B., Pania, N., and Weaver, C. H. (1999). Effect of CD34(+) cell dose on resource utilization in patients after high-dose chemotherapy with peripheral-blood stem-cell support. *J. Clin. Oncol.* 17:1227. doi: 10.1200/JCO.1999.17.4.1227

Schuster, P., Lindner, G., Thomann, S., Haferkamp, S., and Schmidt, B. (2019). Prospect of Plasmacytoid Dendritic Cells in Enhancing Anti-Tumor Immunity of Oncolytic Herpes Viruses. *Cancers* 11:651. doi: 10.3390/cancers11050651

Shpall, E. J., Jones, R. B., Bearman, S. I., Franklin, W. A., Archer, P. G., Curiel, T., et al. (1994). Transplantation of enriched CD34-positive autologous marrow into breast cancer patients following high-dose chemotherapy: influence of CD34-positive peripheral-blood progenitors and growth factors on engraftment. *J. Clin. Oncol.* 12, 28–36. doi: 10.1200/JCO.1994.12.1.28

Siegal, F. P., Kadowaki, N., Shodell, M., Fitzgerald-Bocarsly, P. A., Shah, K., Ho, S., et al. (1999). The nature of the principal type 1 interferon-producing cells in human blood. *Science* 284, 1835–1837. doi: 10.1126/science.284.5421.1835

Siersbaek, R., Scabia, V., Nagarajan, S., Chernukhin, I., Papachristou, E. K., Broome, R., et al. (2020). IL6/STAT3 Signaling hijacks estrogen receptor alpha enhancers to drive breast cancer metastasis. *Cancer Cell* 38, 412.e419–423.e419. doi: 10.1016/j.ccell.2020.06.007

Sisirak, V., Faget, J., Gobert, M., Goutagny, N., Vey, N., Treilleux, I., et al. (2012). Impaired IFN-alpha production by plasmacytoid dendritic cells favors regulatory T-cell expansion that may contribute to breast cancer progression. *Cancer Res.* 72, 5188–5197. doi: 10.1158/0008-5472.CAN-11-3468

Sisirak, V., Faget, J., Vey, N., Blay, J. Y., Menetrier-Caux, C., Caux, C., et al. (2013). Plasmacytoid dendritic cells deficient in IFNalpha production promote the amplification of FOXP3(+) regulatory T cells and are associated with poor prognosis in breast cancer patients. *Oncoimmunology* 2, e22338. doi: 10.4161/onci.22338

Smyth, G. K. (2005). "Limma: linear models for microarray data," in *Bioinformatics and Computational Biology Solutions using R and Bioconductor*, ed. R. Gentleman et al. (Berlin: Springer), 397–420.

Steven, A., Fisher, S. A., and Robinson, B. W. (2016). Immunotherapy for lung cancer. *Respirology* 21, 821–833. doi: 10.1111/resp.12789

Therneau, T. M., and Lumley, T. (2014). *Package 'survival'*, Vol. 2. 3.

Tian, S., Huang, P., Gu, Y., Yang, J., Wu, R., Zhao, J., et al. (2019a). Systems biology analysis of the effect and mechanism of Qi-Jing-Sheng-Bai granule on leucopenia in mice. *Front. Pharmacol.* 10:408. doi: 10.3389/fphar.2019.00408 eCollection 2019

Tian, S., Meng, G., and Zhang, W. (2019b). A six-mRNA prognostic model to predict survival in head and neck squamous cell carcinoma. *Cancer Manag. Res.* 11, 131–142.

Wagner, F., Holig, U., Wilczkowski, F., Plesca, I., Sommer, U., Wehner, R., et al. (2019). Neoadjuvant radiochemotherapy significantly alters the phenotype of plasmacytoid dendritic cells and 6-sulfo LacNAc(+) monocytes in rectal cancer. *Front. Immunol.* 10:602. doi: 10.3389/fimmu.2019.00602

Wei, T., Simko, V., Levy, M., Xie, Y., Jin, Y., and Zemla, J. (2017). *Package 'corrplot'*, Vol. 56. e24.

Westhoff, C. C., Jank, P., Jacke, C. O., Albert, U. S., Ebrahimsade, S., Barth, P. J., et al. (2020). Prognostic relevance of the loss of stromal CD34 positive fibroblasts in invasive lobular carcinoma of the breast. *Virchows Arch.* 477, 717–724. doi: 10.1007/s00428-020-02835-3

Wu, J., Li, S., Yang, Y., Zhu, S., Zhang, M., Qiao, Y., et al. (2017). TLR-activated plasmacytoid dendritic cells inhibit breast cancer cell growth in vitro and in vivo. *Oncotarget* 8, 11708–11718. doi: 10.18632/oncotarget.14315

Yu, G., Wang, L.-G., Han, Y., and He, Q.-Y. (2012). clusterProfiler: an R package for comparing biological themes among gene clusters. *OMICS* 16, 284–287.

Yu, S. H., Zhu, K. Y., Zhang, F., Wang, J., Yuan, H., Chen, Y., et al. (2018). The histone demethylase Jmjd3 regulates zebrafish myeloid development by promoting spi1 expression. *Biochim. Biophys. Acta Gene Regul. Mech.* 1861, 106–116. doi: 10.1016/j.bbagrm.2017.12.009

Zhou, Z. J., Xin, H. Y., Li, J., Hu, Z. Q., Luo, C. B., and Zhou, S. L. (2019). Intratumoral plasmacytoid dendritic cells as a poor prognostic factor for hepatocellular carcinoma following curative resection. *Cancer Immunol. Immunother.* 68, 1223–1233. doi: 10.1007/s00262-019-02355-3

Zhu, H., Zhang, L., Wu, Y., Dong, B., Guo, W., Wang, M., et al. (2018). T-ALL leukemia stem cell 'stemness' is epigenetically controlled by the master regulator SPI1. *Elife* 7:e38314. doi: 10.7554/eLife.38314

Conflict of Interest: The authors declare that the research was conducted in the absence of any commercial or financial relationships that could be construed as a potential conflict of interest.

frontiers in Cell and Developmental Biology

REVIEW
published: 13 April 2021
doi: 10.3389/fcell.2021.646981

Immune Response: A Missed Opportunity Between Vitamin D and Radiotherapy

*Xinyue Yu, Baocai Liu, Ning Zhang, Qian Wang and Guanghui Cheng**

Department of Radiation Oncology, China–Japan Union Hospital of Jilin University, Changchun, China

Radiotherapy (RT) is a mainstay treatment in several types of cancer and acts by mediating various forms of cancer cell death, although it is still a large challenge to enhance therapy efficacy. Radiation resistance represents the main cause of cancer progression, therefore, overcoming treatment resistance is now the greatest challenge for clinicians. Increasing evidence indicates that immune response plays a role in reprogramming the radiation-induced tumor microenvironment (TME). Intriguingly, radiation-induced immunosuppression possibly overwhelms the ability of immune system to ablate tumor cells. This induces an immune equilibrium, which, we hypothesize, is an opportunity for radiosensitizers to make actions. Vitamin D has been reported to act in synergistic with RT by potentiating antiproliferative effect induced by therapeutics. Additionally, vitamin D can also regulate the TME and may even lead to immunostimulation by blocking immunosuppression following radiation. Previous reviews have focused on vitamin D metabolism and epidemiological trials, however, the synergistic effect of vitamin D and existing therapies remains unknown. This review summarizes vitamin D mediated radiosensitization, radiation immunity, and vitamin D-regulated TME, which may contribute to more successful vitamin D-adjuvant radiotherapy.

Keywords: vitamin D, calcitriol, radiation, radiotherapy, immune response, tumor microenvironment

OPEN ACCESS

Edited by:
Kevin J. Ni,
St George Hospital, Australia

Reviewed by:
Xi Yang,
Fudan University, China
Guo-Kai Feng,
Sun Yat-sen University Cancer Center, China

***Correspondence:**
Guanghui Cheng
chenggh@jlu.edu.cn

Specialty section:
This article was submitted to Molecular and Cellular Oncology, a section of the journal Frontiers in Cell and Developmental Biology

Received: *28 December 2020*
Accepted: *24 March 2021*
Published: *13 April 2021*

Citation:
Yu X, Liu B, Zhang N, Wang Q and Cheng G (2021) Immune Response: A Missed Opportunity Between Vitamin D and Radiotherapy. Front. Cell Dev. Biol. 9:646981. doi: 10.3389/fcell.2021.646981

INTRODUCTION

Radiotherapy (RT) is usually the definitive treatment for many types of tumors, including but not limited to colorectal cancer, nasopharyngeal carcinoma, and cervical cancer (Chen et al., 2019; Cohen et al., 2019; Dekker et al., 2019). Resistance to radiation is considered to be an important reason for tumor recurrence and local failure, different cell molecular mechanisms are involved in intrinsic and acquired resistance of cancer cells to therapeutics. Although some strategies, such as radiosensitizers, have been investigated recently, sensitizers have been limited to preclinical studies due to the toxic effects of these agents.

Vitamin D, which is a fat-soluble secosteroid mediating numerous physiological functions (Maurya et al., 2020), has been demonstrated to participate in antitumor activity in many cancers (Keum et al., 2019). Moreover, accumulating data suggest that vitamin D employs several mechanisms to enhance the elimination of irradiated tumor cells (Sundaram and Gewirtz, 1999; Chaudhry et al., 2001; Bristol et al., 2012; Sharma et al., 2014). Thus, a deeper understanding of how

vitamin D functions in combination with RT in cancer may help in developing effective sensitizers to overcome radioresistance.

It is worth noting that the immune system plays an important role in the response to RT (Chen et al., 2019). Radiation can lead to both positive and negative regulation of the immune response, and this has been observed not only in tumor cells but also in the tumor microenvironment (TME). Importantly, vitamin D is also involved in the immune microenvironment (Charoenngam and Holick, 2020), although the underlying mechanism has not been clearly elucidated.

Although there is growing awareness of the importance of vitamin D in tumor cell response to radiation, there have been few reviews to report the underlying mechanisms. In this review, we briefly introduce vitamin D and the mechanisms influencing radiosensitivity. Additionally, we discuss how the immune response is regulated in response to RT. Finally, we present the modulation of TME by vitamin D and speculate on the intricate association among vitamin D, radiation, and anti-tumor immunity.

VITAMIN D METABOLISM AND EPIDEMIOLOGY

Vitamin D is produced from 7-dehydrocholesterol in the human skin after exposure to ultraviolet radiation in sunlight, therefore, it can be influenced by season, latitude, skin pigmentation, and cultural habits. In addition, dietary habits and supplementation can also affect vitamin D levels (Amrein et al., 2020). A two-step catalysis mediated by cytochrome P450 is the crucial process in the production of the steroid hormone calcitriol (biologically active form of vitamin D) (Jones et al., 2014). The less active form of vitamin D, $25(OH)D_3$, is generated after the first hydroxylation by vitamin D 25-hydroxylase (CYP2R1 and CYP27A1) in the liver (Bikle, 2014). $25(OH)D_3$ is found to be the major circulating form of vitamin D in the blood, however, general agreement on the threshold levels has not been defined. Recently, 25(OH)D levels of 75-150 nmol/L (30-60 ng/mL) have been proposed to be the optimal range for vitamin D (Bischoff-Ferrari et al., 2016). The association between 25(OH)D level and cancer risk has been described in several solid cancers (Yao et al., 2017; Ramakrishnan et al., 2019; Yuan et al., 2019), and higher 25(OH)D circulating level contributes to better prognosis in colorectal cancer (Markotic et al., 2019). Subsequently, the kidneys utilize the circulating $25(OH)D_3$ as a substrate and convert it into 1,25-dihydroxy-vitamin D3, which is hydroxylated by CYP27B1 (Jones et al., 2014).

Previous finding supports the role of CYP24A1 in catabolizing 25(OH)D and preventing the formation of $1,25(OH)_2D_3$ (Jones et al., 2012). Interestingly, either activation of the catabolic enzyme CYP24A1 by calcidol or calcitriol or inactivation of CYP27B1 by calcitriol can lead to a negative feedback loop to regulate the vitamin D level, broadening the role of CYP24A1 as an important mediator of the rate limiting step of not only vitamin D generation but also hormone self-regulation, thus potentially ameliorating hypercalcemia. The hypercalcemia induced by an increased concentration of calcitriol or insufficiency in the blood due to its instability can undoubtedly limit its clinical application. This has eventually led to the exploration of calcitriol analogs that can exert equipotent or increased anticancer actions with less side effects (Jones, 2010).

$1,25(OH)_2D_3$ is able to regulate the expression of several genes depending on the tissues, cell types, and context (Carlberg and Munoz, 2020). By binding to vitamin D receptor (VDR), $1,25(OH)_2D_3$ facilitates dimerization with the retinoid X receptor (RXR), which fosters nuclear translocation of this complex, and subsequent binding to the vitamin D response elements (VDREs) in the target gene, followed by recruitment of co-modulators. Therefore, calcitriol can interfere with target gene expression in the genomic pathway (Carlberg and Munoz, 2020). It functions in the genomic way by which $1,25(OH)_2D_3$-VDR-RXR complex is involved, and the non-genomic way, by which a 1,25D-membrane-associated, rapid response steroid-binding protein (1,25D-MARRS) is involved (Hii and Ferrante, 2016).

Several studies have confirmed the ability of vitamin D to affect cell proliferation and differentiation (Feldman et al., 2014; Fernandez-Barral et al., 2020a), and that it has an important role in decreasing the risk of developing multiple cancers (Wu et al., 2019). The association between $1,25(OH)_2D_3$ and cancer was initially detected in 1981, when inhibition of melanoma cells and differentiation induction of myeloid leukemic cells were reported (Abe et al., 1981; Colston et al., 1981). Since then, anticancer properties of vitamin D have been increasingly confirmed through *in vitro* and *in vivo* studies (Lappe et al., 2017; Jeon and Shin, 2018). Recent research has identified the crucial impact of vitamin D on carcinoma cells, especially in colon and breast cancers (Grant, 2020). In line with the antiproliferative effects of $1,25(OH)_2D_3$, high VDR expression has also been shown in association with favorable prognosis (Feldman et al., 2014; Carlberg and Munoz, 2020). Although these previous studies have shown the positive role of VDR in patient prognosis, VDR has also been found to be associated with increased cancer risk (Zheng et al., 2017), indicating the controversial role of VDR. Thus, VDR may be a possible prognostic biomarker in patients. Furthermore, several findings support that vitamin D supplementation contributes to favorable prognosis (Ng et al., 2019; Urashima et al., 2019; Yonaga et al., 2019), especially the prognosis improvement compared to those with treatment alone (Wesselink et al., 2020).

ROLE OF VITAMIN D IN RADIOSENSITIVITY

More recently, accumulating evidence has confirmed the anticancer role of vitamin D in several cancer models. In addition to the induction of differentiation and proliferation inhibition, the role of vitamin D as a magnifier of radiation response is emerging. Evaluation of combined therapy was performed in preclinical studies, showing synergistic or additive antitumor effectiveness. To date, the molecular mechanisms by which vitamin D potentiates the antitumor effects of RT are only partially known, and need further clarification. The antitumor actions of vitamin D are carried out through several mechanisms,

such as induction of apoptosis, inhibition of proliferation, and suppression of angiogenesis. Additionally, vitamin D can also potentiate the antitumor effects of RT through different pathways. A summary of previous literature on the role of vitamin D to enhance radiation sensitization in cancer is presented in **Figure 1**.

Apoptosis

Cancer relapse occurs through multiple mechanisms, most of which are mediated by insufficient apoptosis. Increased DNA fragmentation induced by additive EB1089 in MDA-MB-231 cells was associated with increased responsiveness to radiation (Sundaram and Gewirtz, 1999). Although the number of apoptotic cells triggered by radiation alone appeared to be minimal in MCF-7 cells, the rate and extent of cytotoxicity in irradiated cells were enhanced when combined with ILX-23-7553 (vitamin D analog) (Chaudhry et al., 2001). It is important to emphasize that vitamin D3 and EB1089 promote the inactivation of BCL-2 (Simboli-Campbell et al., 1997), which is an anti-apoptotic protein. Additionally, high radiation doses have been correlated with more adverse events. In prostate cancer, vitamin D3 achieved equal therapeutic efficacy by inducing apoptosis along with marked attenuation of the radiation dose, thereby mitigating the side effects associated with a high radiation dose (Dunlap et al., 2003). In preclinical studies, these high-dose strategies show a weaker relationship with clinical RT, necessitating an experimental fractionation dose. The combination of ILX-23-7553 with fractionated radiation (5×2Gy, 3 days) demonstrated an advantage in inducing the apoptosis of MCF-7 cells; conversely, it appeared to have no impact on normal human fibroblasts, thus supporting the tumor-specific role of ILX-23-7553 (Polar et al., 2003). Similarly, a relationship between fractionated radiation and EB1089 has been reported in breast cancer: combination treatment led to a higher apoptotic rate than that with radiation alone and showed no detectable toxicity in normal breast epithelial cells or BJ fibroblast cells (DeMasters et al., 2004).

Moreover, it is known that radiation can directly induce cell death by DNA damage or indirectly by production of reactive oxygen species (ROS). When intrinsic resistance develops in tumor cells, ROS clearance is enhanced to ameliorate the oxidative stress. Xu et al. (2007) showed that RelB triggered by radiation resulted in the protection of irradiated cells, whereas vitamin D3 ablated this protection. As a member of the NF-κB family, RelB can be inactivated by VDR-mediated transcriptional repression. Similarly, in breast cancer cells pre-treated with vitamin D3, sensitivity to radiation was increased accompanied with down-regulation of RelB (Mineva et al., 2009), again indicating that RelB was a target gene regulated by vitamin D in response to radiation.

Autophagy

As a source of cellular stress, radiation can also induce autophagy, which is a homeostasis mechanism for cellular stress and is mediated by a series of autophagy-related proteins. This process could also be influenced by vitamin D. Gewirtz (2014) first summarized the four faces of autophagy, which are the different types of autophagy that may play crucial roles in response to conventional therapies: (i) cytotoxic autophagy, (ii) cytoprotective autophagy, (iii) cytostatic autophagy, and (iv) non-protective autophagy.

Cytotoxic Autophagy

Demasters et al. (2006) indicated that autophagic cell death could be an important tumor cell elimination mechanism for combinatorial EB1089 and radiation in breast cancer. Cytotoxic autophagy is characterized by enhanced cell death, which is accompanied with earlier occurrence and greater extent of autophagosome, but no other apparent cell death type.

Cytoprotective Autophagy

Response to a single or combination treatment is not simply the result of a uniform type of autophagy, there is evidence that cytoprotective autophagy induced by radiation alone may be converted to cytotoxic autophagy when combined with vitamin D3 (Wilson et al., 2011). This further supports the view that dual functions of autophagy may be exhibited concomitantly. The cytoprotective form of autophagy is often considered as a mechanism of drug and radiation resistance in tumors (Ko et al., 2014). Consequently, autophagy inhibitors have been proposed to counteract the elevated cytoprotective autophagy induced by RT to improve radiosensitivity. Several studies have indicated that vitamin D3 shifted the autophagy type from cytoprotective to cytotoxic, which has been considered an autophagic switch (Wilson et al., 2011; Bristol et al., 2012).

Cytostatic Autophagy

Both cytotoxic and cytoprotective autophagy are closely related to the alteration of the autophagy flux level, whereas a cytostatic form of autophagy has been shown to exert beneficial antitumor effects on non-small cell lung carcinoma independent of the autophagy flux alteration. In a study by Sharma et al. (2014), EB1089 was revealed to increase radiation sensitization by inducing a growth-arrest status with no autophagy alteration or direct cell killing; interestingly, pharmacological inhibition or genetic silencing of autophagy rescued the tumor cells from the cytostatic status. EB1089 is possibly effective in switching the autophagy to cytostatic mode which appears to be involved in growth arrest. Therefore, autophagy primarily induced by radiation can be maintained, whereas the nature can be shifted to antitumor activity.

Non-protective Autophagy

Unlike cytoprotective autophagy, where autophagy inhibition results in an enhanced response to treatment, or cytotoxic and cytostatic autophagy where autophagy inhibition leads to reduced therapy efficiency, inhibition of non-protective autophagy shows no association with response to therapeutics. A study by Chakradeo et al. (2015) confirmed this finding by investigating whether cytoprotective autophagy induced by radiation in multiple cell lines was blocked by pharmacological inhibition or genetic silencing of autophagy genes. They found that inhibition of autophagy failed to influence the radiation sensitivity of p53 null cells, which seems to support the mysterious non-protective form of autophagy.

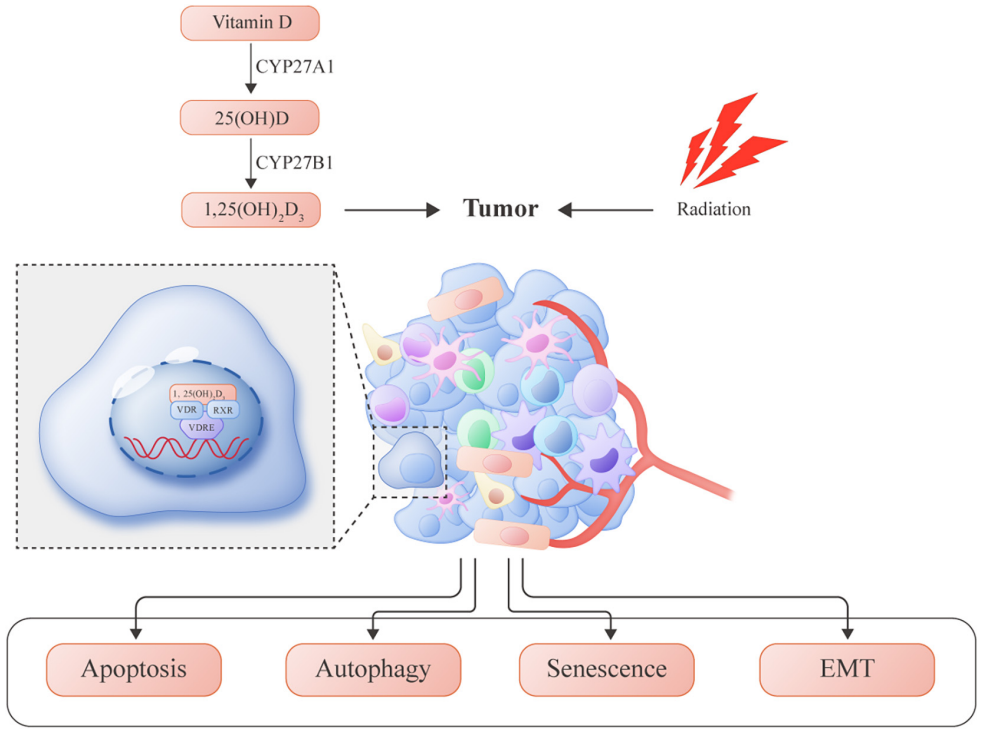

FIGURE 1 | Vitamin D-induced molecular mechanisms involved in enhancing radiosensitivity in several tumors.

Senescence

In a previous study, EB1089 was found to enhance cell apoptosis in response to radiation; the study also claimed that EB1089 had no perceptible effect on preventing senescence but only delayed the emergence of senescence (DeMasters et al., 2004). Similar studies on vitamin D3 mediated radiosensitivity also mentioned the occurrence of cell senescence (Demasters et al., 2006; Wilson et al., 2011).

Therapy-Induced Senescence

Traditionally, senescence was considered irreversible; however, recently, the focus has been on the capability to regain proliferation instead of quiescence in response to radiation. TIS was an accelerated form of senescence (or premature), different from the replicative senescence in aging cells. There is increasing evidence that low-dose radiation interferes with TIS (Yu et al., 2018). Under this condition, senescent cells can escape from direct damage due to RT and enter temporary dormancy; once re-activated, the surviving cells re-emerge from the dormant state and develop into a more aggressive phenotype (Rodier and Campisi, 2011). This is also termed "pseudo-senescence" or "senescence-like arrest." Some clinical reports have demonstrated that patient prognosis was negatively correlated with the expression of senescence markers when exposed to radiation (Fischer et al., 2011).

Senescence-Associated Secretory Phenotype

Radiation influences not only irradiated cells but also the TME, or the so called SASP (Faget et al., 2019). SASP can influence the neighboring non-irradiated cells by releasing a series of pro-inflammatory chemokines and cytokines such as IL-1β, IL-6, and CXCL1 into the surrounding environment (Acosta et al., 2013). Such molecules can hinder the success of RT. This bystander effect induced by radiation might be the mechanism by which a tumor treated with primary therapy becomes refractory to further treatment. This premise has been supported by Huang et al. (2014), who established a bystander model by treating non-irradiated cells with a conditioned medium acquired from irradiated senescent MDA-MB-231-2A cells. They demonstrated that the conditioned medium could lead to the invasion and migration of neighboring cells mediated by the JAK2-dependent AKT and STAT3 pathways. This non-targeted effect of radiation requires potential therapeutics for a better regulation between the target site and the surrounding microenvironment.

Vitamin D and Senescence

Studies on the elimination of TIS are underway for the prevention of disease relapse (Gorgoulis et al., 2019; Short et al., 2019). Notably, VDRE is a promoter of the gene encoding p21; thus, vitamin D3 could directly regulate p21 by binding to VDRE (Ylikomi et al., 2002). Elevated levels of IL-6 and IL-8 are associated with paracrine secretion in the SASP phenotype, and vitamin D3 has been proven to exert anti-inflammatory effects in prostate cancer through the inhibition of IL-6, IL-8, and TNF-α (Giangreco et al., 2015). Mechanistically, vitamin D was shown to inhibit the IL-6 production through the inactivation of p38MAPK (Nonn et al., 2006). These observations imply that vitamin D3 may be a potential senolytic that

can eliminate senescence-related effects, thereby enhancing sensitization to radiation.

Epithelial-to-Mesenchymal Transition

EMT is a reversible process, which usually involves an initial loss of the differentiated phenotype to the migratory phenotype as circulating form in the bloodstream, and subsequent mesenchymal–epithelial transition (MET) for initial colonization leading to metastatic niches, thus generating intratumoral phenotypic heterogeneity (Angela Nieto, 2017). Usually, EMT is accompanied with diminished apoptosis and increased stemness, and both effects are linked to resistance to conventional therapies (Dongre and Weinberg, 2019). Data on colorectal cancer have shown that calcitriol significantly enhanced the therapeutic effects of radiation regulated by EMT (Findlay et al., 2014). In this study, Slug was involved, and overexpression of Slug in calcitriol-sensitive cell lines abrogated the radiosensitization effect. DNA damage repair is a major regulator of treatment response and also involved in radioresistance. ZEB1 was reported to promote DNA damage repair (Zhang et al., 2014). Besides, the presence of Snail was correlated with decreased apoptosis mediated by p53 (Kurrey et al., 2009). Furthermore, upregulation of Slug by IR reversely contributed to inhibition of PUMA, thus decreasing apoptosis (Wu et al., 2005). These data establish EMT as a sensitization switch which regulates the treatment response, and harness of EMT related transcriptional factors may be a potential strategy for enhancing response to RT. Additionally, there is evidence that calcitriol can directly influence tumor-initiating cells (TICs, also known as cancer stem cells), which demonstrated that calcitriol in combination with radiation could inhibit spheroid formation more than either treatment alone; furthermore, this effect could be abolished by the overexpression of β-catenin (Jeong et al., 2015). It has been postulated that non-cancer stem cells are more sensitive to treatment, and EMT can directly characterize epithelial cells of the stem-cell properties, therefore, understanding the impact of calcitriol on EMT and CSCs might provide a novel insight into its effect on radiosensitivity.

Nevertheless, the scant molecular data have revealed that vitamin D may enhance the response to radiation at different levels. The reported molecular mechanisms involve the potentiation of existing apoptosis and the inhibition of protective autophagy. Moreover, the role of vitamin D in senescence and EMT transition requires further investigation. The available evidence strongly suggests that $1,25(OH)_2D_3$ could be considered for combination therapy for cancer.

RADIATION IMMUNITY

As summarized above, vitamin D demonstrates a synergistic effect with radiation through various mechanisms. However, given the complexity of the direct impact of radiation on tumor cells and the indirect impact on the TME, it is worth noting the role that immune response plays in the response to RT. It has been traditionally thought that RT is an approach to suppress the immune system when harnessed for allogeneic transplantation (Rodier and Campisi, 2011). Recently, reactivation of the immune system, or the 6th R of radiobiology, has been proclaimed as the emerging target for RT (Fischer et al., 2011). RT participates in numerous steps of the immunological process (**Figure 2**). Therefore, the ultimate impact of vitamin D may be dependent, in part, on the radiation-induced TME, and the role that the immune system plays in the overall TME.

RT Induced Immuno-Stimulation

Immunogenic Cell Death

Evidence shows that ICD is the dominant process responsible for the higher therapeutic efficacy of concurrent chemoradiotherapy than single chemotherapy (Formenti and Demaria, 2008). The effects of RT are far beyond tumor size reduction; RT converts the irradiated site into an immunogenic hub by releasing damage associated molecular patterns (DAMPs), the so-called "*in situ* vaccine" that contributes to the priming of the systemic immune response (Carvalho and Villar, 2018). Increasingly, evidence indicates that radiation-induced DAMPs can exert adjuvanticity by converting the "immune-cold" tumor into the "immune-hot" tumor (Whiteside et al., 2016). "Cold" tumor normally does not respond to conventional therapies. This conversion relies on the ability of RT to induce primary tumor to be the immunogenic hub, thus significantly improving the effector T cell response (Zheng et al., 2016). A better appreciation of the intricate interaction between immune cold-to-hot conversion and radiotherapy is emerging (Galon and Bruni, 2019), which could shed light on tumors respond poorly to existing treatments. The mechanism of ICD includes CRT translocation to the dendritic cell (DC) surface promoting antigen presentation, release of HMGB1 from the dying cells to activate the Toll-like receptor 4 (TLR4) pathway, and ATP binding to the P2X7 receptor in DCs (Apetoh et al., 2007; Obeid et al., 2007; Ghiringhelli et al., 2009). Radiation can potentiate ICD through any of these three steps (Golden et al., 2014). Various DAMPs can be induced by radiation. HMGB1, as one of the DAMPs, has been shown to boost antigen presentation by DCs; other factors such as TLR4, which contributes to the binding of HMGB1 to DCs, are also triggered in response to radiation (Apetoh et al., 2007).

Antigenicity

Tumors with a higher antigen load have a greater tendency to induce the activation of naive T cells by DCs, leading to the possibility of low-immunogenic tumors inducing an immune response (Galluzzi et al., 2017). Following the release of tumor associated antigens (TAA) such as DAMPs, tumor-specific T cells are trafficked back to the tumor site, and the radiation-triggered immune response can therefore be amplified (individualized vaccination) (Vanpouille-Box et al., 2017). Radiation has been proven to lead to the upregulation of MHC-I, which further enhances the efficacy of antigen presentation (Reits et al., 2006). A similar effect has been observed in DCs, manifesting as improved maturation and recruitment of DCs to the irradiated site. The T cell function in response to RT was first described by Stone et al. (1979), who demonstrated that the attenuation of the radiation efficacy correlated with immune insufficiency. Experimental data have shown that the antitumor immune

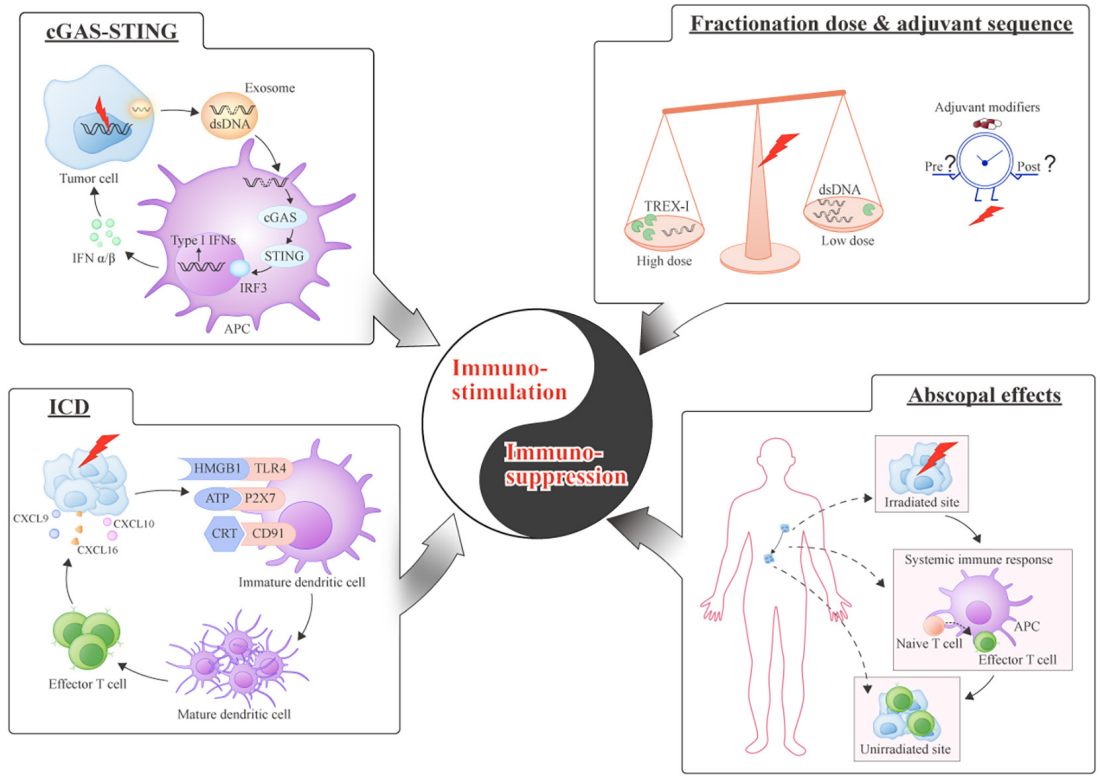

FIGURE 2 | Equilibrium between immuno-stimulation and immuno-suppression induced by radiation. Immuno-stimulation (Left): (cGAS-STING) cGAS-STING-mediated type I interferons (IFNs) are released by sensing double-stranded DNA (dsDNA) and contribute to the immune response; (Immunogenic cell death [ICD]) A schematic of the series of molecules binding to their receptors during immunogenic cell death. Immuno-suppression (Right): (Fractionation dose and sequence) The dose of RT influences immunomodulation through the production of Three-Prime Repair Exonuclease 1 (TREX1); the introduction of immune modifiers should be optimally timed; (Abscopal effects): The priming of antitumor immunity by local RT causes the distant tumor sites to shrink by activating systemic immune response.

effects of RT could be attributed to CD8+ T cell infiltration (Lee et al., 2009).

Chemokines and Cytokines

Specific chemokines and chemokine receptors are crucial for T-cell trafficking to the tumor site. For instance, irradiated tumors secrete C-X-C motif ligand 9 (CXCL9), CXCL10, and CXCL16, which bind to their receptors C-X-C chemokine receptor type 3 (CXCR3) or CXCR6 expressed on T cells or T helper 1 cells (T_H1), and can facilitate the homing of CD8 T-cells to the irradiated site (McLaughlin et al., 2020). DNA damage has recently been identified to play a novel role in anti-tumor immunity induced by RT (Harding et al., 2017; Mackenzie et al., 2017), and the presence of double-stranded DNA (dsDNA), a recognized type I interferon (IFN-I) initiator, has been shown to elicit a tumor-specific T cell response (Deng et al., 2014; Vanpouille-Box et al., 2017). The cGAS-STING (cyclic GMP-AMP synthase-stimulator of interferon genes) pathway is of great significance as it is involved in dsDNA sensing and production of IFN-I during the radiation response (Deng et al., 2014; Harding et al., 2017; Mackenzie et al., 2017). The micronuclei derived from the damaged DNA can be transported by the nucleic acid sensors, cyclic GMP-AMP (cGAMP), to the STING dependent pathway and promote IFN-I production. Three-Prime Repair Exonuclease 1 (TREX1), upstream of cGAS, is a known exonuclease that can be transferred by exosome and has been shown to be associated with the degradation of dsDNA in irradiated cells (Diamond et al., 2018). Exosome is a particular form of extracellular vesicles with a size range of 40 to 160 nm in diameter and carries different types of cargoes inside (Kalluri and LeBleu, 2020). Previous evidence indicates that radioresistance is correlated with tumor derived exosomes (Ni et al., 2019). The most straightforward reply for how exosome respond to radiation is the alteration of its content because of altered TME induced by radiation (Diamond et al., 2018). The production of TREX1 is radiation dose-dependent and may lead to immune failure when receiving RT at a dose more than 12 Gy (Vanpouille-Box et al., 2017). Therefore, the commonly seen therapeutic resistance in response to high-dose RT may result from concentration-dependent TREX1, which can modulate cytosolic dsDNA and thus influence the immune response. It is important to understand that the tumor-cell-intrinsic sensing remains unclear. There is evidence that caspase 9 (CASP9) signaling hijacked by the irradiated tumor cells can result in acquired resistance to radiation by the inhibition of innate DNA sensing (Han et al., 2020). When CASP9 was blocked using a pan-caspase inhibitor, a thousand-fold increase

in IFN-I appeared in response to RT. Caspase appears to be involved in the immune response to radiation mediated by the innate DNA sensor.

RT Induced Immuno-Suppression

Immuno-Suppression

Since cancer is commonly based on the equilibrium between pro-immune and anti-immune effects in a degree sufficient to cause substantial cell death, T cells can induce successful immunization for achieving tumor elimination. An inhibitory TME often acts as a signal for immunosuppression, and this aberrant milieu influences the intrinsic properties of the surrounding cells. Specific immune suppressive cytokines are important for this milieu. Transforming growth factor-β (TGF-β), which can be induced by radiation, has been shown to impair antigen-presentation by DCs and can impede effector T cell differentiation (Tauriello et al., 2018). A study has indicated that T cell-mediated tumor rejection was acquired only when combined with anti-TGF-β (Vanpouille-Box et al., 2015). In addition, the remarkable myeloid-derived suppressor cells (MDSCs) induced by RT can also lead to immunosuppression mediated by TGF-β (Vatner and Formenti, 2015). Meanwhile, up-regulation of MDSCs in response to radiation is also associated with increased anti-programmed death-ligand 1 (PD-L1) expression on the cell surface of MDSCs (Dovedi et al., 2017). MDSCs can differentiate into mature macrophages, and there is evidence that radiation can cause the macrophage polarization into the M2 phenotype, thus attenuating the response to therapy (Tsai et al., 2007). Moreover, suppressive chemokines such as C-C motif chemokine 2 (CCL2) or CCL5 released from irradiated cells can recruit MDSCs and regulatory CD4 T cells (Tregs) to the tumor site (Connolly et al., 2016). Intriguingly, although IFN-I derived from the cGAS-STING pathway plays an important role in the antitumor immune response induced by RT, long-term chronic interferon-driven basal interferon-stimulated gene (ISG) was also correlated with T cell dysfunction (McLaughlin et al., 2020). Thus, the dual target roles of IFN-I need further investigation for effectively mitigating immunosuppression.

Abscopal Effect

The ability of RT to inhibit tumor growth far from the irradiated site is called the abscopal effect (Formenti and Demaria, 2009). The link between the abscopal effect and systemic immunity was first reported by Demaria et al. (2004), who claimed that the antitumor immune response triggered by radiation can also elicit effective eradication of the non-irradiated tumor site. As an immunogenic hub, the field directly exposed to radiation sustains the *in situ* vaccine effect; however, this may be insufficient. The possible theories regarding how radiation can trigger the abscopal effect are based on the equilibrium between the immunostimulatory and immunosuppressive effects. As explained above, radiation not only has an immunostimulatory effect on the irradiated site but also promotes an immunosuppressive response in the surrounding environment. In a preclinical experiment, the abscopal effect was observed under blockade of immunosuppression (Levy et al., 2016), which supports the potential use of immune modifiers for this effect. Logically, TAAs play the role of mediators in the abscopal effect by shuttling outside the radiation field; however, when administered alone, radiation or immune checkpoint inhibitors (ICIs) did not inhibit growth in all the metastatic niches, suggesting that the antigenic overlap between the irradiated and non-irradiated sites was required to elicit an abscopal effect (Formenti et al., 2018). Activation of systemic antitumor immunity undergoes numerous processes including neoantigens releasing and priming of T cell infiltration. Notably, the abscopal effect is previously rare and single-site irradiation only shows some modest success, does not substantially increase the response rate (Luke et al., 2018). Therefore, we should rethink the importance of tumor heterogeneity. Radiation to multiple sites has been suggested to surmount this barrier and lead to optimal effectiveness of RT, which can be a meaningful strategy to prime systemic immune response (Brooks and Chang, 2019).

Radiation Fractionation and Sequence

Of note, the promotion or inhibition of the immune response triggered by radiation depends on various factors, such as the fractionation dose. A radiation dose of more than 7.5 Gy but not 5 Gy was revealed to stimulate the systemic immune response in a low immunogenic tumor (Stone et al., 1979), and a mathematical model appeared to allow the maximum immunity level in a range of 10-13 Gy (Lee et al., 2009). Conventional dose fractionation or single high-dose RT increases the amount of MDSCs, conversely, this can be reverted by hypofractionation (McLaughlin et al., 2020). There is evidence that 8 Gy × 3 fractions or 6 Gy × 5 fractions, but not a single high dose, can activate the immune response more intensively (Apetoh et al., 2007). Furthermore, a single dose of 20 Gy did not have a synergistic effect with additive immune modifiers. TREX1 induced by RT might help to elucidate the abrogation of the immune response (Nonn et al., 2006). Commonly, antitumor immune response with radiation alone has a limited effect, and optimal stimulation of the adaptive immunity requires the aid of ICIs. Recently, immune checkpoints, such as the programmed cell death protein 1 (PD-1) or cytotoxic T lymphocyte-associated protein 4 (CTLA-4), as co-inhibitory receptors on T lymphocytes, have been selected as targets to reactivate T cell function (Harding et al., 2017). This application of ICIs can make the paradigm shift to RT and vice versa. Additionally, the increased antitumor activity also depends on whether the immune modifiers are administered, before, after, or concurrently with RT. This might be due to the functional mechanisms of modifiers to inhibit immunosuppression. For example, therapeutic benefit could be acquired only when anti-PD-L1 was applied concomitantly with RT (Mackenzie et al., 2017). It seems that the effectiveness of anti-PD-L1 therapy depends on the upregulation of PD-L1 on the cell surface, which should be first activated by radiation.

A likely explanation for the mixed results is that a specific therapeutic window is needed for RT to remove the immune barriers when acting synergistically with immune adjuvants. Additional evidence on how conventional fractionation or hypofractionation influences the immune system should be acquired for harnessing the benefits of combination treatment. There is a very delicate balance between the immunostimulation

and immunosuppression induced by RT; consequently, effective cancer treatment is determined by an optimal fractionation scheme combined with specific immune modifiers along with suitable timing.

VITAMIN D AND IMMUNITY

Although the crucial role of the TME during RT is widely accepted, studies on how the radiation-induced TME can be reprogrammed by adjuvants are scarce. Recent study has demonstrated that vitamin D can also modulate tumor stromal cells (Sherman et al., 2014), and the excellent review has summarized the effects of vitamin D on the TME (Wu et al., 2019). The primary association between vitamin D and immunity is mainly thought to be based on energy metabolism and defense against infections. However, in recent years, vitamin D has been shown to be a multifaceted regulator of the immune system (Hanel and Carlberg, 2020). Vitamin D has been used for the treatment of autoimmune disorders by attenuation of the inflammatory immune response (Dimitrov et al., 2017), and it has also been shown to benefit organ transplant patients by inhibiting autoimmunity (Zhou et al., 2017). In fact, although vitamin D induces partial immunosuppression in normal tissues, the long-term effect of chronic inflammation control prevents tumorigenesis, allowing for the antitumor immunity induced by vitamin D.

Study has shown that the immune system can also affect vitamin D production (Liu et al., 2006). A high level of $25(OH)D_3$ in plasma led to a lower risk in the colorectal cancer subtype with an intense immune reaction, but had no effect on low degree reaction subtypes (Song et al., 2016). This further supports that sufficient immunity is necessary for vitamin D to exert its antitumor effect. Apart from kidney tubular cells, immune cells also express CYP27B1 and VDR, which reinforces the important role of vitamin D in regulating immune functions (Wei and Christakos, 2015; Christakos et al., 2016). Many types of immune cells such as DCs, CD4, and CD8 T cells expressing VDR (Lu et al., 2018) and CYP27B1 can produce the active metabolite $1,25(OH)_2D_3$, which can maintain a healthy immune system (Barragan et al., 2015).

Inflammation

Not only the infiltrating immune cells but also cytokines and chemokines in the TME usually influence the tumor response to treatment (Diakos et al., 2014). Vitamin D regulates the inflammatory microenvironment through several mechanisms (Liu et al., 2018). NF-κB plays an important role in regulating immune response (Miraghazadeh and Cook, 2018), and evidence supports the role of VDR antagonist in suppressing p65 activation (Tse et al., 2010). It was also found that vitamin D increased the infiltration of CD8+ T cells, and this was due to the suppression of IL-6 in the TME (Karkeni et al., 2019). Moreover, $1,25(OH)_2D_3$ was effective in suppressing IL-8, which was based on the inhibition of NF-κB activation (Yang et al., 2018).

Cancer-Associated Fibroblasts

CAFs are a heterogeneous population of cells in the TME, derived from tumor cells or tumor stroma cells, and are usually involved in tumor progression and therapeutic resistance (Augsten, 2014). Therefore, a strategy to target the CAFs is necessary (Chen and Song, 2019). Recent data indicate that calcipotriol (VDR agonist) can enhance the therapeutic efficacy by reducing inflammation and fibrosis in pancreatic cancer (Sherman et al., 2014). In line with these data, analyses of patients have reported that high VDR expression in CAFs is associated with better prognosis (Ferrer-Mayorga et al., 2017). These findings are clinically relevant, which indicates that VDR agonists can exert antitumor actions on tumor stromal cells and patients in carcinoma VDR-negative status may still benefit from vitamin D treatment. In recent years, recognition of the crucial role played by exosome in cancer has led to the novel insight for selectively targeting cancer cells (Knox et al., 2020). In this context, a study (Kong et al., 2019) reported that vitamin D decreased the amount of exosomes secreted by the CAFs and thus inhibited the tumor promoter miR-10a-5p in pancreatic cancer.

Cancer Stem Cells

CSCs are a subpopulation of cells characterized by self-renewal due to the accumulation of genetic and epigenetic alterations, and possibly make an important contribution to therapeutic resistance. Moreover, inhibition of CSCs by vitamin D has been described in prostate and breast malignancies as a promising treatment strategy (So and Suh, 2015). $1,25(OH)_2D_3$ has been found to reduce sphere formation in breast cancer, with downregulation of stem cell markers and NOTCH pathway genes (Shan et al., 2017). Organoids have been proposed to represent the *in vivo* situation, as three-dimensional structures generated by primary normal or cancer stem cells isolated from the patients. On the one hand, $1,25(OH)_2D_3$ can induce cell differentiation in colon tumor organoids and lead to a more epithelial phenotype (Fernandez-Barral et al., 2020b). On the other hand, $1,25(OH)_2D_3$ upregulates stemness-related genes and downregulates differentiation genes in normal rectum organoids (Costales-Carrera et al., 2020). These results demonstrate the different roles of vitamin D in normal stem cells and colon CSCs. Recently, it has been demonstrated that vitamin D induced significant downregulation of stemness-related genes compared to imatinib alone, indicating the apparent amplified function of vitamin D on CSCs (Kotlarz et al., 2019). Likewise, reduction of MCF-7 stem cell subpopulation can be induced by VDR overexpression, which elevates sensitivity to tamoxifen (Zheng et al., 2018).

The above data clearly demonstrate that $1,25(OH)_2D_3$ can suppress tumor progression by modulating the TME. Initially, it has been shown that immune cells and tumor stromal cells express VDR, which contributes to $1,25(OH)_2D_3$ responsiveness. Supporting this, vitamin D correlates inversely with the CAFs in the surrounding TME. In addition, the inhibition of CSCs is probably also a consequence of TME regulation by $1,25(OH)_2D_3$. Similar functional effects were observed on the novel three-dimensional structures of organoids. Taken together, vitamin D modulates the TME in diverse ways, which strongly indicates the multi-level anticancer actions of vitamin D in various cancers.

FUTURE PERSPECTIVES

This review aimed to bring together two different fields, namely, vitamin D and radiation, which have rarely been linked before. We used the TME as the bridge between the two fields. However, further investigation is required before we can fully elucidate the impact of vitamin D on radiation. Notable evidence reported in previous studies has highlighted the importance of the TME in the treatment response of cancer. Molecular scenarios induced by radiation in cancer also demonstrate the remarkable functions of the TME. We hypothesize that, if the immunosuppression caused by radiation can be weakened or subtracted by vitamin D, the equilibrium will be broken and immunostimulation will be in dominancy. Supporting this, suitable vitamin D intervention in combination with radiation can induce an antiproliferative additive effect, and this effect of RT may be derived from not only directly causing cancer cell death but also indirectly reprogramming the TME. This may widen the perspective on vitamin D with regard to its immune modulatory role, which is essential for the treatment of autoimmune disorders. Overall, radiation therapy is complex with the involvement of intricate immune modulation and multiple types of cancer cell death. Additional research is needed to elucidate the underlying mechanisms and the potential utility of vitamin D in RT.

Nonetheless, more investigations are needed to confirm whether there is existing resistance to vitamin D itself, accompanied with the detection of a vitamin D response-dependent biomarker, which could facilitate the selection of patients with a higher likelihood of response to vitamin D, and decide the biologically optimal dose of vitamin D for achieving maximum health benefit. Is there a scheme to satisfy the target doses by controlling the local concentration of calcitriol? For greater benefits, the development of VDR agonists is recommended, which is deemed to acquire the equi-effective but less hypercalcaemia effect. The timing of vitamin D initiation during combination therapy is another important issue. For best regimen, whether the agent should be supplemented continuously or not? Does radiation alter vitamin D metabolism indirectly? These explorations may contribute to the discovery of potential cost-effective and efficient agent for combination treatment with conventional therapeutics.

AUTHOR CONTRIBUTIONS

GC conceptualized and supervised the conception of the manuscript. GC and XY coordinated and performed the literature search with BL, NZ, and QW contribution. XY and GC designed and performed figures, and wrote the manuscript with important inputs from all authors. All authors reviewed and agreed with the content of the manuscript.

FUNDING

This work was supported by grants from the National Natural Science Foundation of China (grant numbers 82073331 and 82003208), the Jilin Province Science and Technology Development Plan Project (grant number 20200201599JC), and the Project of Science and Technology Department of Jilin Province (grant number 20190303151SF).

REFERENCES

Abe, E., Miyaura, C., Sakagami, H., Takeda, M., Konno, K., Yamazaki, T., et al. (1981). Differentiation of mouse myeloid leukemia cells induced by 1 alpha,25-dihydroxyvitamin D3. *Proc. Natl. Acad. Sci. U.S.A.* 78, 4990–4994. doi: 10.1073/pnas.78.8.4990

Acosta, J. C., Banito, A., Wuestefeld, T., Georgilis, A., Janich, P., Morton, J. P., et al. (2013). A complex secretory program orchestrated by the inflammasome controls paracrine senescence. *Nat. Cell Biol.* 15, 978–990. doi: 10.1038/ncb2784

Amrein, K., Scherkl, M., Hoffmann, M., Neuwersch-Sommeregger, S., Koestenberger, M., Berisha, A. T., et al. (2020). Vitamin D deficiency 2.0: an update on the current status worldwide. *Eur. J. Clin. Nut.* 74, 1498–1513. doi: 10.1038/s41430-020-0558-y

Angela Nieto, M. (2017). Context-specific roles of EMT programmes in cancer cell dissemination. *Nat. Cell Biol.* 19, 416–418. doi: 10.1038/ncb3520

Apetoh, L., Ghiringhelli, F., Tesniere, A., Obeid, M., Ortiz, C., Criollo, A., et al. (2007). Toll-like receptor 4-dependent contribution of the immune system to anticancer chemotherapy and radiotherapy. *Nat. Med.* 13, 1050–1059.

Augsten, M. (2014). Cancer-associated fibroblasts as another polarized cell type of the tumor microenvironment. *Front. Oncol.* 4:62. doi: 10.3389/fonc.2014.00062

Barragan, M., Good, M., and Kolls, J. K. (2015). Regulation of dendritic cell function by Vitamin D. *Nutrients* 7, 8127–8151. doi: 10.3390/nu7095383

Bikle, D. D. (2014). Vitamin D Metabolism, mechanism of action, and clinical applications. *Chem. Biol.* 21, 319–329. doi: 10.1016/j.chembiol.2013.12.016

Bischoff-Ferrari, H. A., Dawson-Hughes, B., Orav, J., Staehelin, H. B., Meyer, O. W., Theiler, R., et al. (2016). Monthly high-dose Vitamin D treatment for the prevention of functional decline A randomized clinical trial. *Jama Int. Med.* 176, 175–183. doi: 10.1001/jamainternmed.2015.7148

Bristol, M. L., Di, X., Beckman, M. J., Wilson, E. N., Henderson, S. C., Maiti, A., et al. (2012). Dual functions of autophagy in the response of breast tumor cells to radiation Cytoprotective autophagy with radiation alone and cytotoxic autophagy in radiosensitization by vitamin D-3. *Autophagy* 8, 739–753. doi: 10.4161/auto.19313

Brooks, E. D., and Chang, J. Y. (2019). Time to abandon single-site irradiation for inducing abscopal effects. *Nat. Rev. Clin. Oncol.* 16, 123–135. doi: 10.1038/s41571-018-0119-7

Carlberg, C., and Munoz, A. (2020). An update on vitamin D signaling and cancer. *Semin. Cancer Biol.* S1044-S1579, 30114–30110.

Carvalho, H. D. A., and Villar, R. C. (2018). Radiotherapy and immune response: the systemic effects of a local treatment. *Clinics* 73:e557s.

Chakradeo, S., Sharma, K., Alhaddad, A., Bakhshwin, D., Le, N., Harada, H., et al. (2015). Yet another function of p53–the switch that determines whether radiation-induced autophagy will be cytoprotective or nonprotective: implications for autophagy inhibition as a therapeutic strategy. *Mol. Pharmacol.* 87, 803–814. doi: 10.1124/mol.114.095273

Charoenngam, N., and Holick, M. F. (2020). Immunologic effects of Vitamin D on human health and disease. *Nutrients* 12:2097. doi: 10.3390/nu12072097

Chaudhry, M., Sundaram, S., Gennings, C., Carter, H., and Gewirtz, D. A. (2001). The vitamin D-3 analog, ILX-23-7553, enhances the response to Adriamycin and irradiation in MCF-7 breast tumor cells. *Cancer Chemother. Pharmacol.* 47, 429–436. doi: 10.1007/s002800000251

Chen, X., and Song, E. (2019). Turning foes to friends: targeting cancer-associated fibroblasts. *Nat. Rev. Drug Discov.* 18, 99–115. doi: 10.1038/s41573-018-0004-1

Chen, Y.-P., Chan, A. T. C., Quynh-Thu, L., Blanchard, P., Sun, Y., and Ma, J. (2019). Nasopharyngeal carcinoma. *Lancet* 394, 64–80.

Christakos, S., Dhawan, P., Verstuyf, A., Verlinden, L., and Carmeliet, G. (2016). Vitamin D: metabolism, molecular mechanism of action, and pleiotropic effects. *Physiol. Rev.* 96, 365–408. doi: 10.1152/physrev.00014.2015

Cohen, P. A., Jhingran, A., Oaknin, A., and Denny, L. (2019). Cervical cancer. *Lancet* 393, 169–182.

Colston, K., Colston, M. J., and Feldman, D. (1981). 1,25-dihydroxyvitamin D3 and malignant melanoma: the presence of receptors and inhibition of cell growth in culture. *Endocrinology* 108, 1083–1086. doi: 10.1210/endo-108-3-1083

Connolly, K. A., Belt, B. A., Figueroa, N. M., Murthy, A., Patel, A., Kim, M., et al. (2016). Increasing the efficacy of radiotherapy by modulating the CCR2/CCR5 chemokine axes. *Oncotarget* 7, 86522–86535. doi: 10.18632/oncotarget.13287

Costales-Carrera, A., Fernandez-Barral, A., Bustamante-Madrid, P., Dominguez, O., Guerra-Pastrian, L., Cantero, R., et al. (2020). Comparative study of organoids from patient-derived normal and tumor colon and rectal tissue. *Cancers* 12:2302. doi: 10.3390/cancers12082302

Dekker, E., Tanis, P. J., Vleugels, J. L. A., Kasi, P. M., and Wallace, M. B. (2019). Colorectal cancer. *Lancet* 394, 1467–1480.

Demaria, S., Ng, B., Devitt, M. L., Babb, J. S., Kawashima, N., Liebes, L., et al. (2004). Ionizing radiation inhibition of distant untreated tumors (abscopal effect) is immune mediated. *Int. J. Radiat. Oncol. Biol. Phys.* 58, 862–870. doi: 10.1016/j.ijrobp.2003.09.012

Demasters, G., Di, X., Newsham, I., Shiu, R., and Gewirtz, D. A. (2006). Potentiation of radiation sensitivity in breast tumor cells by the vitamin D3 analogue, EB 1089, through promotion of autophagy and interference with proliferative recovery. *Mol. Cancer Ther.* 5, 2786–2797. doi: 10.1158/1535-7163.mct-06-0316

DeMasters, G. A., Gupta, M. S., Jones, K. R., Cabot, M., Wang, H., Gennings, C., et al. (2004). Potentiation of cell killing by fractionated radiation and suppression of proliferative recovery in MCF-7 breast tumor cells by the Vitamin D3 analog EB 1089. *J. Steroid. Biochem. Mol. Biol.* 92, 365–374. doi: 10.1016/j.jsbmb.2004.07.011

Deng, L., Liang, H., Xu, M., Yang, X., Burnette, B., Arina, A., et al. (2014). STING-Dependent cytosolic DNA sensing promotes radiation-induced Type I interferon-dependent antitumor immunity in immunogenic tumors. *Immunity* 41, 843–852. doi: 10.1016/j.immuni.2014.10.019

Diakos, C. I., Charles, K. A., McMillan, D. C., and Clarke, S. J. (2014). Cancer-related inflammation and treatment effectiveness. *Lancet Oncol.* 15, E493–E503.

Diamond, J. M., Vanpouille-Box, C., Spada, S., Rudqvist, N. P., Chapman, J. R., Ueberheide, B. M., et al. (2018). Exosomes Shuttle TREX1-Sensitive IFN-Stimulatory dsDNA from irradiated cancer cells to DCs. *Cancer Immunol. Res.* 6, 910–920. doi: 10.1158/2326-6066.cir-17-0581

Dimitrov, V., Bouttier, M., Boukhaled, G., Salehi-Tabar, R., Avramescu, R. G., Memari, B., et al. (2017). Hormonal vitamin D up-regulates tissue-specific PD-L1 and PD-L2 surface glycoprotein expression in humans but not mice. *J. Biol. Chem.* 292, 20657–20668. doi: 10.1074/jbc.m117.793885

Dongre, A., and Weinberg, R. A. (2019). New insights into the mechanisms of epithelial-mesenchymal transition and implications for cancer. *Nat. Rev. Mol. Cell Biol.* 20, 69–84. doi: 10.1038/s41580-018-0080-4

Dovedi, S. J., Cheadle, E. J., Popple, A. L., Poon, E., Morrow, M., Stewart, R., et al. (2017). Fractionated radiation therapy stimulates antitumor immunity mediated by both resident and infiltrating polyclonal T-cell populations when combined with PD-1 blockade. *Clin. Cancer Res.* 23, 5514–5526. doi: 10.1158/1078-0432.ccr-16-1673

Dunlap, N., Schwartz, G. G., Eads, D., Cramer, S. D., Sherk, A. B., John, V., et al. (2003). 1alpha,25-dihydroxyvitamin D(3) (calcitriol) and its analogue, 19-nor-1alpha,25(OH)(2)D(2), potentiate the effects of ionising radiation on human prostate cancer cells. *Br. J. Cancer* 89, 746–753. doi: 10.1038/sj.bjc.6601161

Faget, D. V., Ren, Q., and Stewart, S. A. (2019). Unmasking senescence: context-dependent effects of SASP in cancer. *Nat. Rev. Cancer* 19, 439–453. doi: 10.1038/s41568-019-0156-2

Feldman, D., Krishnan, A. V., Swami, S., Giovannucci, E., and Feldman, B. J. (2014). The role of vitamin D in reducing cancer risk and progression. *Nat. Rev. Cancer* 14, 342–357. doi: 10.1038/nrc3691

Fernandez-Barral, A., Bustamante-Madrid, P., Ferrer-Mayorga, G., Barbachano, A., Larriba, M. J., and Munoz, A. (2020a). Vitamin D effects on cell differentiation and stemness in cancer. *Cancers* 12:2413. doi: 10.3390/cancers12092413

Fernandez-Barral, A., Costales-Carrer, A., Buira, S. P., Jung, P., Ferrer-Mayorga, G., Larriba, M. J., et al. (2020b). Vitamin D differentially regulates colon stem cells in patient-derived normal and tumor organoids. *FEBS J.* 287, 53–72. doi: 10.1111/febs.14998

Ferrer-Mayorga, G., Gomez-Lopez, G., Barbachano, A., Fernandez-Barral, A., Pena, C., Pisano, D. G., et al. (2017). Vitamin D receptor expression and associated gene signature in tumor stromal fibroblasts predict clinical outcome in colorectal cancer. *Gut* 66, 1449–1462. doi: 10.1136/gutjnl-2015-310977

Findlay, V. J., Moretz, R. E., Wang, C., Vaena, S. G., Bandurraga, S. G., Ashenafi, M., et al. (2014). Slug expression inhibits calcitriol-mediated sensitivity to radiation in colorectal cancer. *Mol. Carcinog.* 53(Suppl. 1), E130–E139.

Fischer, C. A., Jung, M., Zlobec, I., Green, E., Storck, C., Tornillo, L., et al. (2011). Co-overexpression Of P21 And Ki-67 in head and neck squamous cell carcinoma relative to a significantly poor prognosis. *Head Neck* 33, 267–273. doi: 10.1002/hed.21440

Formenti, S. C., and Demaria, S. (2008). Effects of chemoradiation on tumor-host interactions: the immunologic side. *J. Clin. Oncol.* 26, 1562–1563. doi: 10.1200/jco.2007.15.5499

Formenti, S. C., and Demaria, S. (2009). Systemic effects of local radiotherapy. *Lancet Oncol.* 10, 718–726. doi: 10.1016/s1470-2045(09)70082-8

Formenti, S. C., Rudqvist, N.-P., Golden, E., Cooper, B., Wennerberg, E., Lhuillier, C., et al. (2018). Radiotherapy induces responses of lung cancer to CTLA-4 blockade. *Nat. Med.* 24, 1845–1851. doi: 10.1038/s41591-018-0232-2

Galluzzi, L., Buque, A., Kepp, O., Zitvogel, L., and Kroemer, G. (2017). Immunogenic cell death in cancer and infectious disease. *Nat. Rev. Immunol.* 17, 97–111. doi: 10.1038/nri.2016.107

Galon, J., and Bruni, D. (2019). Approaches to treat immune hot, altered and cold tumors with combination immunotherapies. *Nat. Rev. Drug Discov.* 18, 197–218. doi: 10.1038/s41573-018-0007-y

Gewirtz, D. A. (2014). The four faces of autophagy: implications for cancer therapy. *Cancer Res.* 74, 647–651. doi: 10.1158/0008-5472.can-13-2966

Ghiringhelli, F., Apetoh, L., Tesniere, A., Aymeric, L., Ma, Y., Ortiz, C., et al. (2009). Activation of the NLRP3 inflammasome in dendritic cells induces IL-1 beta-dependent adaptive immunity against tumors. *Nat. Med.* 15, 1170–1178. doi: 10.1038/nm.2028

Giangreco, A. A., Dambal, S., Wagner, D., Van der Kwast, T., Vieth, R., Prins, G. S., et al. (2015). Differential expression and regulation of vitamin D hydroxylases and inflammatory genes in prostate stroma and epithelium by 1,25-dihydroxyvitamin D in men with prostate cancer and an in vitro model. *J. Steroid Biochem. Mol. Biol.* 148, 156–165. doi: 10.1016/j.jsbmb.2014.10.004

Golden, E. B., Frances, D., Pellicciotta, I., Demaria, S., Barcellos-Hoff, M. H., and Formenti, S. C. (2014). Radiation fosters dose-dependent and chemotherapy-induced immunogenic cell death. *Oncoimmunology* 3:e28518. doi: 10.4161/onci.28518

Gorgoulis, V., Adams, P. D., Alimonti, A., Bennett, D. C., Bischof, O., Bishop, C., et al. (2019). Cellular senescence: defining a path forward. *Cell* 179, 813–827. doi: 10.1016/j.cell.2019.10.005

Grant, W. B. (2020). Review of recent advances in understanding the role of Vitamin D in reducing cancer risk: breast, colorectal, prostate, and overall cancer. *Anticancer Res.* 40, 491–499. doi: 10.21873/anticanres.13977

Han, C., Liu, Z., Zhang, Y., Shen, A., Dong, C., Zhang, A., et al. (2020). Tumor cells suppress radiation-induced immunity by hijacking caspase 9 signaling. *Nat. Immunol.* 21, 546–554. doi: 10.1038/s41590-020-0641-5

Hanel, A., and Carlberg, C. (2020). Vitamin D and evolution: pharmacologic implications. *Biochem. Pharmacol.* 173:113595. doi: 10.1016/j.bcp.2019.07.024

Harding, S. M., Benci, J. L., Irianto, J., Discher, D. E., Minn, A. J., and Reenberg, R. A. G. (2017). Mitotic progression following DNA damage enables pattern recognition within micronuclei. *Nature* 548, 466–470. doi: 10.1038/nature23470

Hii, C. S., and Ferrante, A. (2016). The non-genomic actions of Vitamin D. *Nutrients* 8:135. doi: 10.3390/nu8030135

Huang, Y. H., Yang, P. M., Chuah, Q. Y., Lee, Y. J., Hsieh, Y. F., Peng, C. W., et al. (2014). Autophagy promotes radiation-induced senescence but inhibits bystander effects in human breast cancer cells. *Autophagy* 10, 1212–1228. doi: 10.4161/auto.28772

Jeon, S.-M., and Shin, E.-A. (2018). Exploring vitamin D metabolism and function in cancer. *Exp. Mol. Med.* 50:20.

Jeong, Y., Swami, S., Krishnan, A. V., Williams, J. D., Martin, S., Horst, R. L., et al. (2015). Inhibition of mouse breast tumor-initiating cells by calcitriol and dietary Vitamin D. *Mol. Cancer Ther.* 14, 1951–1961. doi: 10.1158/1535-7163.mct-15-0066

Jones, G. (2010). Vitamin D analogs. endocrinology and metabolism. *Clin. North Am.* 39, 447–472. doi: 10.1016/j.ecl.2010.02.003

Jones, G., Prosser, D. E., and Kaufmann, M. (2012). 25-Hydroxyvitamin D-24-hydroxylase (CYP24A1): its important role in the degradation of vitamin D. *Arch. Biochem. Biophys.* 523, 9–18. doi: 10.1016/j.abb.2011.11.003

Jones, G., Prosser, D. E., and Kaufmann, M. (2014). Thematic review series: fat-soluble Vitamins: Vitamin D Cytochrome P450-mediated metabolism of vitamin D. *J. Lipid Res.* 55, 13–31.

Kalluri, R., and LeBleu, V. S. (2020). The biology, function, and biomedical applications of exosomes. *Science* 367:eaau6977. doi: 10.1126/science.aau6977

Karkeni, E., Morin, S. O., Tayeh, B. B., Goubard, A., Josselin, E., Castellano, R., et al. (2019). Vitamin D controls tumor growth and CD8+T cell infiltration in breast cancer. *Front. Immunol.* 10:1307. doi: 10.3389/fimmu.2019.01307

Keum, N., Lee, D. H., Greenwood, D. C., Manson, J. E., and Giovannucci, E. (2019). Vitamin D supplementation and total cancer incidence and mortality: a meta-analysis of randomized controlled trials. *Ann. Oncol.* 30, 733–743. doi: 10.1093/annonc/mdz059

Knox, M. C., Ni, J., Bece, A., Bucci, J., Chin, Y., Graham, P. H., et al. (2020). A clinician's guide to cancer-derived exosomes: immune interactions and therapeutic implications. *Front. Immunol.* 11:1612. doi: 10.3389/fimmu.2020.01612

Ko, A., Kanehisa, A., Martins, I., Senovilla, L., Chargari, C., Dugue, D., et al. (2014). Autophagy inhibition radiosensitizes in vitro, yet reduces radioresponses in vivo due to deficient immunogenic signalling. *Cell Death Differ.* 21, 92–99. doi: 10.1038/cdd.2013.124

Kong, F., Li, L., Wang, G., Deng, X., Li, Z., and Kong, X. (2019). VDR signaling inhibits cancer-associated-fibroblasts' release of exosomal miR-10a-5p and limits their supportive effects on pancreatic cancer cells. *Gut* 68, 950–951. doi: 10.1136/gutjnl-2018-316627

Kotlarz, A., Przybyszewska, M., Swoboda, P., Neska, J., Miloszewska, J., Grygorowicz, M. A., et al. (2019). Imatinib inhibits the regrowth of human colon cancer cells after treatment with 5-FU and cooperates with vitamin D analogue PRI-2191 in the downregulation of expression of sternness-related genes in 5-FU refractory cells. *J. Steroid Biochem. Mol. Biol.* 189, 48–62. doi: 10.1016/j.jsbmb.2019.02.003

Kurrey, N. K., Jalgaonkar, S. P., Joglekar, A. V., Ghanate, A. D., Chaskar, P. D., Doiphode, R. Y., et al. (2009). Snail and slug mediate radioresistance and chemoresistance by antagonizing p53-Mediated apoptosis and acquiring a stem-like phenotype in ovarian cancer cells. *Stem Cells* 27, 2059–2068. doi: 10.1002/stem.154

Lappe, J., Garland, C., and Gorham, E. (2017). Vitamin D supplementation and cancer risk reply. *JAMA J. Am. Med. Assoc.* 318, 299–300. doi: 10.1001/jama.2017.7833

Lee, Y., Auh, S. L., Wang, Y., Burnette, B., Wang, Y., Meng, Y., et al. (2009). Therapeutic effects of ablative radiation on local tumor require CD8+ T cells: changing strategies for cancer treatment. *Blood* 114, 589–595. doi: 10.1182/blood-2009-02-206870

Levy, A., Chargari, C., Marabelle, A., Perfettini, J.-L., Magne, N., and Deutsch, E. (2016). Can immunostimulatory agents enhance the abscopal effect of radiotherapy? *Eur. J. Cancer* 62, 36–45. doi: 10.1016/j.ejca.2016.03.067

Liu, P. T., Stenger, S., Li, H. Y., Wenzel, L., Tan, B. H., Krutzik, S. R., et al. (2006). Toll-like receptor triggering of a vitamin D-mediated human antimicrobial response. *Science* 311, 1770–1773. doi: 10.1126/science.1123933

Liu, W., Zhang, L., Xu, H.-J., Li, Y., Hu, C.-M., Yang, J.-Y., et al. (2018). The anti-inflammatory effects of Vitamin D in tumorigenesis. *Int. J. Mol. Sci.* 19:2736. doi: 10.3390/ijms19092736

Lu, M., Taylor, B. V., and Korner, H. (2018). Genomic effects of the Vitamin D receptor: potentially the link between Vitamin D, immune cells, and multiple sclerosis. *Front. Immunol.* 9:477. doi: 10.3389/fimmu.2018.00477

Luke, J. J., Lemons, J. M., Karrison, T. G., Pitroda, S. P., Melotek, J. M., Zha, Y., et al. (2018). Safety and clinical activity of pembrolizumab and multisite stereotactic body radiotherapy in patients with advanced solid tumors. *J. Clin. Oncol.* 36, 1611–1618. doi: 10.1200/jco.2017.76.2229

Mackenzie, K. J., Carroll, P., Martin, C.-A., Murina, O., Fluteau, A., Impson, D. J. S., et al. (2017). cGAS surveillance of micronuclei links genome instability to innate immunity. *Nature* 548, 461–465. doi: 10.1038/nature23449

Markotic, A., Langer, S., Kelava, T., Vucic, K., Turcic, P., Tokic, T., et al. (2019). Higher post-operative serum Vitamin D Level is associated with better survival outcome in colorectal cancer patients. *Nutr. Cancer Int. J.* 71, 1078–1085. doi: 10.1080/01635581.2019.1597135

Maurya, V. K., Bashir, K., and Aggarwal, M. (2020). Vitamin D microencapsulation and fortification: trends and technologies. *J. Steroid Biochem. Mol. Biol.* 196:105489. doi: 10.1016/j.jsbmb.2019.105489

McLaughlin, M., Patin, E. C., Pedersen, M., Wilkins, A., Dillon, M. T., Melcher, A. A., et al. (2020). Inflammatory microenvironment remodelling by tumor cells after radiotherapy. *Nat. Rev. Cancer* 20, 203–217. doi: 10.1038/s41568-020-0246-1

Mineva, N. D., Wang, X., Yang, S., Ying, H., Xiao, Z. X., Holick, M. F., et al. (2009). Inhibition of RelB by 1,25-dihydroxyvitamin D3 promotes sensitivity of breast cancer cells to radiation. *J. Cell Physiol.* 220, 593–599. doi: 10.1002/jcp.21765

Miraghazadeh, B., and Cook, M. C. (2018). Nuclear Factor-kappaB in autoimmunity: man and mouse. *Front. Immunol.* 9:613. doi: 10.3389/fimmu.2018.00613

Ng, K., Nimeiri, H. S., McCleary, N. J., Abrams, T. A., Yurgelun, M. B., Cleary, J. M., et al. (2019). Effect of high-dose vs Standard-Dose Vitamin D-3 supplementation on progression-free survival among patients with advanced or metastatic colorectal cancer the SUNSHINE randomized clinical trial. *JAMA J. Am. Med. Assoc.* 321, 1370–1379. doi: 10.1001/jama.2019.2402

Ni, J., Bucci, J., Malouf, D., Knox, M., Graham, P., and Li, Y. (2019). Exosomes in cancer radioresistance. *Front. Oncol.* 9:869. doi: 10.3389/fonc.2019.00869

Nonn, L., Peng, L. H., Feldman, D., and Peehl, D. M. (2006). Inhibition of p38 by vitamin D reduces interleukin-6 production in normal prostate cells via mitogen-activated protein kinase phosphatase 5: implications for prostate cancer prevention by vitamin D. *Cancer Res.* 66, 4516–4524. doi: 10.1158/0008-5472.can-05-3796

Obeid, M., Tesniere, A., Ghiringhelli, F., Fimia, G. M., Apetoh, L., Perfettini, J.-L., et al. (2007). Calreticulin exposure dictates the immunogenicity of cancer cell death. *Nat. Med.* 13, 54–61. doi: 10.1038/nm1523

Polar, M. K., Gennings, C., Park, M., Gupta, M. S., and Gewirtz, D. A. (2003). Effect of the vitamin D3 analog ILX 23-7553 on apoptosis and sensitivity to fractionated radiation in breast tumor cells and normal human fibroblasts. *Cancer Chemother. Pharmacol.* 51, 415–421. doi: 10.1007/s00280-003-0606-z

Ramakrishnan, S., Steck, S. E., Arab, L., Zhang, H., Bensen, J. T., Fontham, E. T. H., et al. (2019). Association among plasma 1,25(OH)(2)D, ratio of 1,25(OH)(2)D to 25(OH)D, and prostate cancer aggressiveness. *Prostate* 79, 1117–1124. doi: 10.1002/pros.23824

Reits, E. A., Hodge, J. W., Herberts, C. A., Groothuis, T. A., Chakraborty, M., Wansley, E. K., et al. (2006). Radiation modulates the peptide repertoire, enhances MHC class I expression, and induces successful antitumor immunotherapy. *J. Exp. Med.* 203, 1259–1271. doi: 10.1084/jem.20052494

Rodier, F., and Campisi, J. (2011). Four faces of cellular senescence. *J. Cell Biol.* 192, 547–556. doi: 10.1083/jcb.201009094

Shan, N. L., Wahler, J., Lee, H. J., Bak, M. J., Das Gupta, S., Maehr, H., et al. (2017). Vitamin D compounds inhibit cancer stem-like cells and induce differentiation in triple negative breast cancer. *J. Steroid Biochem. Mol. Biol.* 173, 122–129. doi: 10.1016/j.jsbmb.2016.12.001

Sharma, K., Goehe, R. W., Di, X., Hicks, M. A. II, Torti, S. V., Torti, F. M., et al. (2014). A novel cytostatic form of autophagy in sensitization of non-small cell lung cancer cells to radiation by vitamin D and the vitamin D analog, EB 1089. *Autophagy* 10, 2346–2361. doi: 10.4161/15548627.2014.993283

Sherman, M. H., Yu, R. T., Engle, D. D., Ding, N., Atkins, A. R., Tiriac, H., et al. (2014). Vitamin D receptor-mediated stromal reprogramming suppresses pancreatitis and enhances pancreatic cancer therapy. *Cell* 159, 80–93. doi: 10.1016/j.cell.2014.08.007

Short, S., Fielder, E., Miwa, S., and von Zglinicki, T. (2019). Senolytics and senostatics as adjuvant tumor therapy. *Ebiomedicine* 41, 683–692. doi: 10.1016/j.ebiom.2019.01.056

Simboli-Campbell, M., Narvaez, C. J., van Weelden, K., Tenniswood, M., and Welsh, J. (1997). Comparative effects of 1,25(OH)2D3 and EB1089 on cell cycle kinetics and apoptosis in MCF-7 breast cancer cells. *Breast Cancer Res. Treatm.* 42, 31–41. doi: 10.1023/a:1005772432465

So, J. Y., and Suh, N. (2015). Targeting cancer stem cells in solid tumors by vitamin D. *J. Steroid Biochem. Mol. Biol.* 148, 79–85.

Song, M., Nishihara, R., Wang, M., Chan, A. T., Qian, Z. R., Inamura, K., et al. (2016). Plasma 25-hydroxyvitamin D and colorectal cancer risk according to tumor immunity status. *Gut* 65, 296–304.

Stone, H. B., Peters, L. J., and Milas, L. (1979). Effect of host immune capability on radiocurability and subsequent transplantability of a murine fibrosarcoma. *J. Natl. Cancer Inst.* 63, 1229–1235.

Sundaram, S., and Gewirtz, D. A. (1999). The vitamin D-3 analog EB 1089 enhances the response of human breast tumor cells to radiation. *Radiat. Res.* 152, 479–486.

Tauriello, D. V. F., Palomo-Ponce, S., Stork, D., Berenguer-Llergo, A., Badia-Ramentol, J., Iglesias, M., et al. (2018). TGF beta drives immune evasion in genetically reconstituted colon cancer metastasis. *Nature* 554, 538–543.

Tsai, C.-S., Chen, F.-H., Wang, C.-C., Huang, H.-L., Jung, S.-M., Wu, C.-J., et al. (2007). Macrophages from irradiated tumors express higher levels of iNOS, Arginase-I and COX-2, and promote tumor growth. *Int. J. Radiat. Oncol. Biol. Phys.* 68, 499–507.

Tse, A. K.-W., Zhu, G.-Y., Wan, C.-K., Shen, X.-L., Yu, Z.-L., and Fong, W.-F. (2010). 1 alpha,25-Dihydroxyvitamin D-3 inhibits transcriptional potential of nuclear factor kappa B in breast cancer cells. *Mol. Immunol.* 47, 1728–1738.

Urashima, M., Ohdaira, H., Akutsu, T., Okada, S., Yoshida, M., Kitajima, M., et al. (2019). Effect of Vitamin D supplementation on relapse-free survival among patients with digestive tract cancers the AMATERASU randomized clinical trial. *JAMA J. Am. Med. Assoc.* 321, 1361–1369.

Vanpouille-Box, C., Alard, A., Aryankalayil, M. J., Sarfraz, Y., Diamond, J. M., Schneider, R. J., et al. (2017). DNA exonuclease Trex1 regulates radiotherapy-induced tumor immunogenicity. *Nat. Commun.* 8:15618.

Vanpouille-Box, C., Diamond, J. M., Pilones, K. A., Zavadil, J., Babb, J. S., Formenti, S. C., et al. (2015). TGF beta is a master regulator of radiation therapy-induced antitumor immunity. *Cancer Res.* 75, 2232–2242.

Vatner, R. E., and Formenti, S. C. (2015). Myeloid-derived cells in tumors: effects of radiation. *Semin. Radiat. Oncol.* 25, 18–27.

Wei, R., and Christakos, S. (2015). Mechanisms underlying the regulation of innate and adaptive immunity by Vitamin D. *Nutrients* 7, 8251–8260.

Wesselink, E., Bours, M. J. L., de Wilt, J. H. W., Aquarius, M., Breukink, S. O., Hansson, B., et al. (2020). Chemotherapy and vitamin D supplement use are determinants of serum 25-hydroxyvitamin D levels during the first six months after colorectal cancer diagnosis. *J. Steroid Biochem. Mol. Biol.* 199:105577.

Whiteside, T. L., Demaria, S., Rodriguez-Ruiz, M. E., Zarour, H. M., and Melero, I. (2016). Emerging opportunities and challenges in cancer immunotherapy. *Clin. Cancer Res.* 22, 1845–1855.

Wilson, E. N., Bristol, M. L., Di, X., Maltese, W. A., Koterba, K., Beckman, M. J., et al. (2011). A switch between cytoprotective and cytotoxic autophagy in the radiosensitization of breast tumor cells by chloroquine and vitamin D. *Horm. Cancer* 2, 272–285.

Wu, W. S., Heinrichs, S., Xu, D., Garrison, S. P., Zambetti, G. P., Adams, J. M., et al. (2005). Slug antagonizes p53-mediated apoptosis of hematopoietic progenitors by repressing puma. *Cell* 123, 641–653.

Wu, X., Hu, W., Lu, L., Zhao, Y., Zhou, Y., Xiao, Z., et al. (2019). Repurposing vitamin D for treatment of human malignancies via targeting tumor microenvironment. *Acta Pharm. Sin. B* 9, 203–219.

Xu, Y., Fang, F., St. Clair, D. K., Josson, S., Sompol, P., Spasojevic, I., et al. (2007). Suppression of RelB-mediated manganese superoxide dismutase expression reveals a primary mechanism for radiosensitization effect of 1 alpha,25-dihydroxyvitamin D-3 in prostate cancer cells. *Mol. Cancer Ther.* 6, 2048–2056.

Yang, J., Yan, J., and Liu, B. (2018). Targeting veGF/veGFR to modulate antitumor immunity. *Front. Immunol.* 9:978. doi: 10.3389/fimmu.2018.00978

Yao, S., Kwan, M. L., Ergas, I. J., Roh, J. M., Cheng, T.-Y. D., Hong, C.-C., et al. (2017). Association of serum level of Vitamin D at diagnosis with breast cancer survival a case-cohort analysis in the pathways study. *JAMA Oncol.* 3, 351–357.

Ylikomi, T., Laaksi, I., Lou, Y. R., Martikainen, P., Miettinen, S., Pennanen, P., et al. (2002). Antiproliferative action of vitamin D. *Vitam. Horm.* 64, 357–406.

Yonaga, H., Okada, S., Akutsu, T., Ohdaira, H., Suzuki, Y., and Urashima, M. (2019). Effect modification of Vitamin D supplementation by histopathological characteristics on survival of patients with digestive tract cancer: post hoc analysis of the AMATERASU randomized clinical trial. *Nutrients* 11:2547.

Yu, X., Liu, Y., Yin, L., Peng, Y., Peng, Y., Gao, Y., et al. (2018). Radiation-promoted CDC6 protein stability contributes to radioresistance by regulating senescence and epithelial to mesenchymal transition. *Oncogene* 38, 549–563.

Yuan, C., Sato, K., Hollis, B. W., Zhang, S., Niedzwiecki, D., Ou, F.-S., et al. (2019). Plasma 25-Hydroxyvitamin D Levels and survival in patients with advanced or metastatic colorectal cancer: findings from CALGB/SWOG 80405 (Alliance). *Clin. Cancer Res.* 25, 7497–7505.

Zhang, P., Wei, Y., Wang, L., Debeb, B. G., Yuan, Y., Zhang, J., et al. (2014). ATM-mediated stabilization of ZEB1 promotes DNA damage response and radioresistance through CH K1. *Nat. Cell Biol.* 16, 864–875.

Zheng, W., Duan, B., Zhang, Q., Ouyang, L., Peng, W., Qian, F., et al. (2018). Vitamin D-induced vitamin D receptor expression induces tamoxifen sensitivity in MCF-7 stem cells via suppression of Wnt/beta-catenin signaling. *Biosci. Rep.* 38:BSR20180595.

Zheng, W., Skowron, K. B., Namm, J. P., Burnette, B., Fernandez, C., Arina, A., et al. (2016). Combination of radiotherapy and vaccination overcomes checkpoint blockade resistance. *Oncotarget* 7, 43039–43051.

Zheng, Y., Trivedi, T., Lin, R. C. Y., Fong-Yee, C., Nolte, R., Manibo, J., et al. (2017). Loss of the vitamin D receptor in human breast and prostate cancers strongly induces cell apoptosis through downregulation of Wnt/beta-catenin signaling. *Bone Res.* 5:17023.

Zhou, Q., Qin, S., Zhang, J., Zhon, L., Pen, Z., and Xing, T. (2017). 1,25(OH)(2)D-3 induces regulatory T cell differentiation by influencing the VDR/PLC-gamma 1/TGF-beta 1/pathway. *Mol. Immunol.* 91, 156–164.

Conflict of Interest: The authors declare that the research was conducted in the absence of any commercial or financial relationships that could be construed as a potential conflict of interest.

frontiers in Oncology

ORIGINAL RESEARCH
published: 13 April 2021
doi: 10.3389/fonc.2021.628456

Personal Neoantigens From Patients With NSCLC Induce Efficient Antitumor Responses

Wei Zhang[1†], Qi Yin[2†], Haidong Huang[1†], Jingjing Lu[2], Hao Qin[1], Si Chen[2], Wenjun Zhang[3], Xiaoping Su[4], Weihong Sun[5], Yuchao Dong[1*] and Qiang Li[2*]*

[1] Department of Pulmonary and Critical Care Medicine, Shanghai Changhai Hospital, Second Military Medical University, Shanghai, China, [2] Department of Pulmonary and Critical Care Medicine, Shanghai East Hospital, Tongji University, Shanghai, China, [3] Department of Emergency, Shanghai Changhai Hospital, Second Military Medical University, Shanghai, China, [4] School of Basic Medicine, Wenzhou Medical University, Wenzhou Tea Mountain Higher Education Park, Wenzhou, China, [5] Biotherapy Center, Qingdao Central Hospital, The Second Affiliated Hospital, Qingdao University, Qingdao, China

OPEN ACCESS

Edited by:
Chao Ni,
Zhejiang University, China

Reviewed by:
Ana Paula Lepique,
University of São Paulo, Brazil
Heng Xu,
Sichuan University, China
Taigo Kato,
Osaka University, Japan

***Correspondence:**
Weihong Sun
sunweihong@126.com
Yuchao Dong
dongyc1020@aliyun.com
Qiang Li
liqressh@hotmail.com

[†]These authors have contributed equally to this work

Specialty section:
This article was submitted to Molecular and Cellular Oncology, a section of the journal Frontiers in Oncology

Received: 12 November 2020
Accepted: 23 March 2021
Published: 13 April 2021

Citation:
Zhang W, Yin Q, Huang H, Lu J, Qin H, Chen S, Zhang W, Su X, Sun W, Dong Y and Li Q (2021) Personal Neoantigens From Patients With NSCLC Induce Efficient Antitumor Responses. Front. Oncol. 11:628456. doi: 10.3389/fonc.2021.628456

Objective: To develop a neoantigen-targeted personalized cancer treatment for non-small cell lung cancer (NSCLC), neoantigens were obtained from collected human lung cancer samples, and the utility of neoantigen and neoantigen-reactive T cells (NRTs) was assessed.

Methods: Tumor specimens from three patients with NSCLC were obtained and analyzed by whole-exome sequencing, and neoantigens were predicted accordingly. Dendritic cells and T lymphocytes were isolated, NRTs were elicited and IFN-γ ELISPOT tests were conducted. HLA-A2.1/K^b transgenic mice were immunized with peptides from HLA-A*02:01$^+$patient with high immunogenicity, and NRTs were subjected to IFN-γ, IL-2 and TNF-α ELISPOT as well as time-resolved fluorescence assay for cytotoxicity assays to verify the immunogenicity *in vitro*. The HLA-A*02:01$^+$lung cancer cell line was transfected with minigene and inoculated into the flanks of C57BL/$6^{nu/nu}$ mice and the NRTs induced by the immunogenic polypeptides from autologous HLA-A2.1/K^b transgenic mice were adoptively transfused to verify their immunogenicity *in vivo*.

Results: Multiple putative mutation-associated neoantigens with strong affinity for HLA were selected from each patient. Immunogenic neoantigen were identified in all three NSCLC patients, the potency of ACAD8-T105I, BCAR1-G23V and PLCG1-M425L as effective neoantigen to active T cells in suppressing tumor growth was further proven both *in vitro* and *in vivo* using HLA-A2.1/Kb transgenic mice and tumor-bearing mouse models.

Conclusion: Neoantigens with strong immunogenicity can be screened from NSCLC patients through the whole-exome sequencing of patient specimens and machine-learning-based neoantigen predictions. NRTs shown efficient antitumor responses in transgenic mice and tumor-bearing mouse models. Our results indicate that the development of neoantigen-based personalized immunotherapies in NSCLC is possible.

Precis: Neoantigens with strong immunogenicity were screened from NSCLC patients. This research provides evidence suggesting that neoantigen-based therapy might serve as feasible treatment for NSCLC.

Keywords: neoantigen, neoantigen-reactive T cells (NRTs), non-small cell lung cancer (NSCLC), tumor vaccine, immunotherapy

INTRODUCTION

Non-small cell lung cancer (NSCLC) is the most common cause of cancer related death worldwide, accounting for more than one million deaths annually. The current standard treatment for NSCLC is oncogene-targeted therapy or debulking surgery combined with paclitaxel and carboplatin chemotherapy. Despite a good initial response, most patients relapse and ultimately develop resistance, and no curative therapeutic options are currently available (1, 2). Immunotherapies that boost the ability of endogenous T cells to destroy cancer cells have demonstrated therapeutic efficacy in a variety of human malignancies (3). Immunotherapy using agents such as immune-checkpoint inhibitors (ICI) has been a focus of attention (4) and their effectiveness in the treatment of NSCLC has been reported (5–10). The emergence of these therapeutic agents has greatly advanced the treatment of lung cancer. However, even for patients with PD-1 ligand (PD-L1) expression ≥50%, only 30% of them can benefit from anti-PD-1 treatment. So, it is very important to explore new immunotherapy methods for NSCLC.

In cancer, mutations are the source of neoantigens that can be recognized by the immune system as foreign-like peptides called 'neoepitopes' presented on major histocompatibility complex (MHC) molecules (11). However, the nature of the antigens that allow the immune system to distinguish cancer cells from noncancer cells has long remained elusive. Recent technological innovations have made it possible to dissect the immune response to patient-specific neoantigens that arise as a consequence of tumor-specific mutations, and emerging lines of data suggest that the recognition of such neoantigens is a major factor contributing to the activity of clinical immunotherapies. In melanoma and glioblastoma, the targeting of select neoepitopes by vaccination has demonstrated high immunogenicity and signs of clinical efficacy (12, 13). Although the cancer mutanome is considered a possible source of potent tumor antigens for cancer immunotherapy, it has remained largely out of reach for decades due to the lack of suitable genomic and proteomic methods to identify actionable mutations. Lung cancer genomes harbor somatic mutations that are caused by exposure to mutagens such as smoking (14). The density of somatic mutations and neoantigens was recently shown to correlate with long-term benefits from immune checkpoint blockade in non-small cell lung cancer (NSCLC) (15). However, the study and application of neoantigen-based immunotherapy in NSCLC have been rarely reported (16, 17).

In this study, tumor specimens and blood samples from three NSCLC patients were collected, and whole exome and transcriptome sequencing were conducted. Gene mutations, gene expression, and patient HLA typing were analyzed using various software programs, and the aberrant peptides were prioritized according to the identified mutation, HLA typing and gene expression information. Multiple putative mutation-associated neoantigens with strong affinity for HLA were selected from each patient, and *in vitro* experiments and NRT-induced cytotoxicity *in vivo* evaluation assays were performed. All the patients developed NRT cells responses against multiple vaccine neo-epitopes. Our study demonstrates that individual mutations can be exploited in NSCLC, and this finding opens a path toward personalized immunotherapy for patients with NSCLC.

MATERIALS AND METHODS

Patient Material and Cell Lines

Tumor samples from NSCLC patients were obtained from biopsy specimens. A portion of the sample was removed for formalin fixation and paraffin embedding (FFPE). The remainder of the tissue was immediately frozen in aliquots and stored in vapor-phase liquid nitrogen.

PBMCs obtained for immune monitoring or as starting material for the manufacturing process were isolated by Ficoll-Hypaque (Amersham Biosciences) density gradient centrifugation from buffy coats of healthy donors or from peripheral blood samples of NSCLC patients. Immature dendritic cells (DCs) were generated as described previously (18, 19). T2 and H522 cells (ATCC) were cultured under standard conditions. T2 and H522cells were stably transfected with the A2.1/Kb chimeric gene (T2/Kb, H522/Kb) for mice experiments. T2/Kb and H522/kb cells were stable transfectants and express the product of the HLA-A*02:01/Kb chimeric gene (the α1 and α2 domains from HLA-A*0201 and the α3 domain of H-2K^b (20). Cell banks were generated and tested for mycoplasma. The cells were reauthenticated short tandem repeat (STR) profiling at ATCC.

Next-Generation Sequencing

For WES sequencing, DNA from fresh frozen tumor samples or cells was extracted using the DNeasy Blood and Tissue Kit, which was purchased from Qiagen. The genomic DNA was sheared, end-repaired, ligated to barcoded Illumina sequencing adapters, amplified, and size-selected. Whole-exome capture was performed using an Agilent Sure Select Human All Exon 44-Mb version 2.0 bait set (Agilent Technologies) (21). The resulting libraries were then quantified by qPCR, pooled, and sequenced

using 76-basepaired-end reads obtained with HiSeq 2000 or 2500 sequencers (Illumina).

For RNA sequencing, RNA from fresh frozen tumor samples was extracted using the RNeasy Mini Kit. RNA-seq libraries were prepared using an Illumina TruSeq Stranded mRNA Library Prep Kit (for cell suspensions). Flow cell cluster amplification and sequencing were performed according to the manufacturer's instructions using either a HiSeq2500.

The sequencing data have been deposited in the NCBI Sequence Read Archive (SRA) database under the accession code SRP (https://submit.ncbi.nlm.nih.gov/subs/sra/SUB8559404/overview).

Bioinformatics and Mutation Discovery

All mutanome-related data analysis steps for a single patient were coordinated by a software pipeline implemented in the Python programming language. At least $150\times 10^6$and 75×10^6 paired-end 50 nt reads were required for the DNA and RNA libraries, respectively. For mutation detection, the DNA reads were aligned to the reference genome hg19 with BWA (22). Duplicate exomes from tumor and matched normal samples were analyzed for single-nucleotide variants. Loci with putative homozygous genotypes in the normal samples were identified and filtered to retain high-confidence calls for single-nucleotide variants. The remaining sites were further inspected for a putative homozygous or heterozygous mutational event. The suspected sites were filtered to remove potential false positives, and replicates were incorporated by testing both the sum of replicates and the replicates separately. The final list of single-nucleotide variants was composed of high-confidence homozygous sites in the normal samples and high-confidence heterozygous or homozygous mutational events in the tumor samples. The genomic coordinates of identified variants were compared with known gene transcript coordinates detailed in the UCSC Genome Browser to determine the association of the variants with genes, transcripts, potential amino acid sequence changes and RNA-seq-derived expression values.

For RNA-seq, RNA reads were aligned to the hg19 reference genome and transcriptome using Bowtie (23), and the gene expression levels were determined by comparison with known gene transcript and exon coordinates detailed in UCSC followed by normalization to RPKM units (16).

HLA TYPING

The HLA alleles of each patient were inferred from the WES data using OptiType (24) with the default settings after the reads were filtered by aligning to the HLA region using RazerS version 3.4.0 (25).

NEOANTIGEN IDENTIFICATION

Non-synonymous somatic mutations, including SNVs, insertion, deletion and frameshift, were used to predict neoantigens following the previous procedure with modification (26). First, 8-11-amino-acid long mutant peptides were generated for MHC I-restricted neoantigen prediction, and 12-15-amino-acid long mutant peptides were generated for MHC II-restricted neoantigen prediction. Then HLA binding affinity for each peptide was calculated by NetMHCpan4.0 (27) and NetMHCIIpan3.2 (28) for MHC I and MHC II molecules respectively. Expression level of mutant genes was derived from RNA-seq data in transcripts per million (TPM). The number of mismatches between the mutant and normal peptides was considered as the similarity to self-peptides. Mutant allele frequency was detected by the variant caller MuTect2 (29). Each peptide was given a priority score based on HLA binding affinity, expression level, similarity to self-peptides, the final score for each neoantigen was calculated as follows:

$$\textbf{NeoantigenScore}\,(\mathbf{p}) = \text{affinityMutantScore ExpressionScore VAF Normal Exact Match Penalty}$$

$$\textbf{affinity Mutant Score} = 1/(1+\text{math}.\exp(5*(\text{float}(\text{rank\_mutant})-2)))$$

$$\textbf{ExpressionScore} = \begin{cases} 1, \text{ if TPM} > \text{upper quartile} \\ 0.5, \text{ if lower quartile} < \text{TPM} < \text{upper quartile} \\ 0.25, \text{ if TPM} < \text{lower quartile} \\ 0, \text{ TPM} = 0 \end{cases}$$

$$\textbf{NormalExactMatchPenalty} = \text{Normal exact match penalty}: 0 \text{ if mutated peptide matches } 100\,\% \text{ to any peptide in the reference proteome, else } 1.$$

Peptides with priority score larger than 0 were selected as neoantigen candidates. Peptides with a %rank less than 0.5 were considered strong binders and peptides with a %rank larger than 0.5 were considered weak binders.

SYNTHESIS OF LONG PEPTIDES AND FINAL VACCINE PREPARATION

Peptides with purity greater than 95% were synthesized by GL Biochem (Shanghai, China) using fluorenyl methoxy carbonyl chemistry by reverse-phase high-performance liquid chromatography and were confirmed by mass spectrometry. The lyophilized peptides were dissolved in dimethyl sulfoxide, diluted in phosphate-buffered saline (pH 7.4) to a concentration of 10 mM and stored as aliquots at −80°C as described previously.

Minigenes

A tandem minigene (TMG) was constructed as previously described (30). Minigenes were included in each TMG construct used in this study. Plasmids encoding the minigenes were linearized with the restriction enzyme NsiI, and each linearized plasmid was used as a template for *in vitro* transcription using the mMESSAGE mMACHINE T7 Transcription Kit (Thermo Fisher Scientific) according to the manufacturer's instructions.

Induction of Neoantigen-Reactive T Cells by Coculture With NSCLC Patient-Derived Peripheral Blood Lymphocytes (PBLs) *In Vitro*

The autologous PBMCs from the patients were harnessed to evaluate the immunogenicity of the candidate neoantigens *in vitro*. An established simple and effective culture protocol with a few modifications (31, 32) was applied to detect and monitor the antigen peptide-specific cytotoxic T lymphocyte precursors (CTL-P) in the circulation. Briefly, heparinized blood samples were obtained from patients with relapsed/refractory tumors for the isolation of PBMCs by centrifugation on a Ficoll density gradient, and the isolated PBMCs were suspended in AIM-V medium (Gibco). In each U-bottomed well of a plate, 1×10^5 PBMCs were incubated with a corresponding peptide (25 μM) in 200μl of culture medium, which was applied to facilitate cell-to-cell contact. The culture medium consisted of AIM-V medium, 10% FCS (Gibco), and IL-2 (100 U/ml; PeproTech). For peptide stimulation, half of the culture medium was replaced with fresh medium containing the corresponding peptide (25 μM) and IL-2 (100 U/ml) at 3-day intervals. After three cycles of peptide stimulation followed by overnight re-stimulation, the specific T cell responses to each peptide were evaluated through an ELISPOT assay on day 10. The recognition of each single antigen was tested in comparison with the no-peptide control (medium only), and phytohemagglutinin was used as the positive control. In some cases, the reactivity of T cells was evaluated by peptide pulsing of DCs cocultured with T cells. Mature DCs were pulsed with 10 μM peptide for 4–6 hours at 37°C, washed with prewarmed PBS, and then incubated overnight with T cells at a stimulator/effector ratio of 1:10 in complete AIM-V medium. IFN-γ-secreting cells was determined by IFN-γ ELISPOT assay.

Generation of Neoantigen-Specific T Cells in HLA-A2.1/K^{b}Tg Mice

The preparation of bone marrow-derived DCs from Tg mice and the vaccination of HLA-A2.1/K^{b}Tg mice (10 mice per group) with peptide-pulsed DCs were performed as described previously (33). On day 7 after the last immunization with peptide-pulsed DCs, all the immune splenocytes from the same group of primed mice were collected, cultured at a density of 1×10^7 cells per well in six-well plates and stimulated with peptides (20 μM) for 7 days *in vitro*. The bulk populations were functionally tested by enzyme-linked immunospot assay (ELISPOT), enzyme-linked immunosorbent assay (ELISA), intracellular staining assays, and time-resolved fluorescence assays.

ELISPOT Assay

ELISPOT kits (Dakewei) was used to determine the amount of cytokine-secreting T cells after overnight activation with a peptide (34). In this study, a multiple culture protocol was used to analyze the T cell response as described above. Briefly, the peptide-stimulated PBMCs or the DC-pulsed peptide coculture with T cells (10^5 per well) were added to duplicate wells for 18–20 hours. The plates were washed before addition of the diluted detection antibody (1:100 dilution) and then incubated for 1 hour at 37°C. After the plates were washed, streptavidin–HRP (1:100 dilution) was added, and the plates were incubated at 37°C for 1 hour. 3-Amino-9-ethylcarbazole (AEC) solution mix was then added to each well, and the plates were left in the dark for approximately 15–25 minutes at room temperature. Deionized water was then added to stop the reaction, and the plates were subsequently scanned using an ELISPOT CTL Reader (Cellular Technology Inc.). The results were analyzed with ELISPOT software (AID). Spots with a size that were more than twofold greater than that of the no-peptide control (medium only) were considered positive for T cell reactivity.

In Vitro T Cell Cytotoxicity Assay

Cytotoxicity assays were performed using time-resolved fluorescence assay as previously described (35, 36). Briefly, target cells were labeled with a fluorescence enhancing ligand (BADTA)and co-incubated with NRT cells for 2h. The supernatants were then measured by time-resolved fluorometry (EnVision 2014Multilabel reader, PerkinElmer). The percent specific lysis was determined according to the following formula: (experimental release −spontaneous release)/(maximum release −spontaneous release)) × 100% and the percent spontaneous release was calculated from(spontaneous release – background signal)/(maximum release – background signal) × 100%.

Adoptive Immunotherapy in Tumor-bearing Nude Mice

Splenocytes from each group of immunized HLA-A2.1/K^b mice were stimulated with 20 μMACAD8-T105I, BCAR1-G23V or PLCG1-M425Lfor 7 days as described in the section detailing the protocol used for the cytotoxicity assay. HLA-A*02:01$^+$H522/Kb-minigene tumor cells (5×10^6) were injected s.c. into the flanks of C57BL/6nu/nu mice, which formed homogeneous tumors in 100% of the mice. Three days later (37–41), the mice were intravenously injected with splenocytes (1×10^8 cells per mouse) from each group of immunized HLA-A2.1/K^b mice that were stimulated with 20 μM ACAD8-T105I, BCAR1-G23V and PLCG1-M425L for 7 days as described in the section detailing the protocol used for the cytotoxicity assay. This adoptive transfer was performed twice at 1-week intervals and was followed by the intraperitoneal administration of 2000 U of hIL-2 every 2 days. The control mice received splenocytes from HLA-A2.1/K^b mice immunized with irrelevant peptide -pulsed DCs or only IL-2. The tumor size and body weight were measured in two perpendicular dimensions three times at weekly intervals. The mice were killed 80 days after tumor inoculation.

Statistical Analysis

GraphPad Prism 5.0 (GraphPad Software) was used for all statistical analyses. The data samples were compared using two-tailed Student's t test, and a P value less than 0.05 was considered significant.

RESULTS

Immunogenic Neoantigens Were Predicted and Identified From NSCLC Patients

Whole-exome sequencing of tumor specimens and matched normal samples from three NSCLC patients (Clinico pathological characteristics of the subjects were presented in **Supplementary Table 3**) was performed after DNA extraction, and the resulting genetic mutations and HLA typing information were then analyzed (**Supplementary Table 1**). RNA was also extracted, and transcriptome sequencing was performed to confirm the genetic mutations and identify mutant gene expression level. Patient somatic mutations and RNA expression were analyzed by MuPeXI to identify neoantigen candidates. An average of 184 non-synonymous somatic mutations were detected (**Figure 1A**) and an average of 145MHC I-restricted neoantigens (range of 97-226) and an average of 38 MHC II-restricted neoantigens (range of 32-46) were identified in 3 NSCLC patients (**Supplementary Table 2**). An average of 34 neoantigens were considered as strong binders with %rank less than 0.5, and an average of 150 neoantigens were considered as weaker binders with %rank larger than 0.5 (**Figure 1B**). Ten putative mutation-associated long peptides (27 aa) with strong HLA affinity were selected from each patient and produced by chemosynthesis (**Table 1**).

In order to identify the neoantigen with high immunogenicity, an established simple and effective polypeptide immunogenicity assay with a few modifications (31) was applied to test the immunogenicity of the synthesized neoantigen polypeptides based on NSCLC patient-derived PBMCs. The neoantigens GPM6B-C94F, DMXL1-L2124F,TPBG-P57L,HACE1-T20S and COQ3-T91A from HLA-0206$^+$ Patient 01 (P01), OPLAH-G890D, BCAR1-V64L,GBF1-D1478Y,SNX16-C318Y and UPF3A-R380T fromHLA-0207$^+$ and HLA-3303$^+$ Patient 02 (P02) andACAD8-T105I, BCAR1-G23V,SCLC7A1-A349S, SSH1-R470C and PLCG1-M425L from HLA-0201$^+$ Patient 03 (P03) elicited more obvious peptide-specific T-cell responses than the no-peptide control (medium only) or the irrelevant peptide control (VSV-NP43-69, STKVALNDLRAYVYQGIKSGNP SILHI), as shown by ELISPOT assay (**Figures 2A–C**). GPM6B-C94F and TPBG-P57L from P01, OPLAH-G890D, BCAR1-V64L, GBF1-D1478Y and UPF3A-R380Tfrom P02, and ACAD8-T105I, BCAR1-G23V, and PLCG1-M425Lfrom P03manifestedparticularly distinct peptide-specific T-cell responses.

Neoantigen-Specific T Responses Can Be Induced *In Vitro* From PBLs of HLA-A*02:01$^+$Patient 03 With NSCLC

In order to explore the role of NRT in patients with NSCLC.DCs from P03 (HLA-A*02:01$^+$) loaded with ACAD8-T105I, BCAR1-G23V and PLCG1-M425L were cocultured with PBLs to generate mutated peptide-specific NRTs *in vitro*, and the immune responses were compared with the WT peptide-induced NRTs. As shown by ELISPOT assay, the means spots of IFN-γ-producing T cells were significantly greater in NRTs elicited by the aberrant peptides than in those induced by the WT peptides (**Figures 3A, B**).

Mutant peptide-pulsed HLA-A*02:01$^+$ T2 cells and minigene-nucleofected H522 cells (HLA-A*02:01$^+$, H522-minigene) were used as peptide-specific targets to further examine the cytotoxic effect of the corresponding NRTs. The killing activity of NRTs at different ratios of effective cells to target cells is shown in **Figures 3C–E**. Bulk NRTs against ACAD8-T105I, BCAR1-G23V and PLCG1-M425L, particularly NRTs against BCAR1-G23V and PLCG1- M425L, exerted significant cytotoxic effects toward target cells expressing corresponding antigens. No significant cytotoxic effect was detected with T2 cells that did not pulse any peptides or pulsed irrelevant peptides (VSV-NP43-69) and H522 cells that did not express any mutant peptides.

HLA-A2.1-Restricted Neoantigens Can Induce NRT Cells in HLA-A2.1/k^b Mice *In Vivo*

To evaluate the immunogenicity of the candidate polypeptides *in vivo*, the polypeptides ACAD8-T105I, BCAR1-G23V and PLCG1-M425L from P03 (HLA-A*02:01$^+$), whose immunogenicity was previously proven *in vitro*, were selected

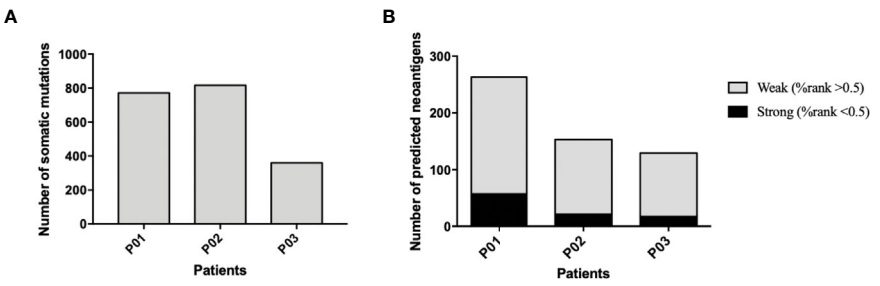

FIGURE 1 | Frequency of somatic mutations and predicted neoantigens in 3NSCLC patients. **(A)** WES and RNA-seq were performed in 3 patients with NSCLC. Tumor-specific non-synonymous somatic mutations were identified. The frequency of somatic mutations of each patient is shown. **(B)** Neoantigen prediction was performed for each patient. The frequency of neoantigens as well as strong binder (%rank <0.5) and weak binder (0.5< %rank <2) of each patient is shown.

TABLE 1 | *In silico* prediction of mutations of three NSCLC patients with favorable HLA class I or II binding properties.

Patient	Gene	HLA restriction	Mutated sequence[a]	Substitution (WT, AA#, Mut)	HLA- I or -IIScores[b]
	POLE	B*1502	SRYFHIPIGNLPE**Y**ISTFGSDLFFARH	D1663Y	88
	FHL1	A*0206	CFTCSNCKQVIGT**V**SFFPKGEDFYCVT	G139V	86
	GPM6B	DQA1*0401	TILCFSGVALFCG**F**GHVALAGTVAILE	C94F	81
	LRP5	B*8101	CSHICIAKGDGTP**L**CSCPVHLVLLQNL	R1237L	80
P01	DMXL1	B*1502	QLRENFQEKRQWL**F**KYQSLLRMFLSYC	L2124F	78
	TP53	B*8101	CMGGMNRRPILTI**F**TLEDSSGNLLGRN	I3123F	70
	TPBG	A*0206	SAPFLASAVSAQP**L**LPDQCPALCECSE	P57L	84
	HACE1	DRB1*1101	QLNRLTRSLRRAR**S**VELPEDNETAVYT	T20S	70
	COQ3	A*0206	RYPWARLYSTSQT**A**VDSGEVKTFLALA	T91A	68
	RAB4A	DRB1*1101	ERMGSGIQYGDAA**F**RQLRSPRRAQAPN	L199F	53
	ITFG1	A*0207	CVFILAIIGILHW**L**EKKADDREKRQEA	Q591L	39
	OPLAH	DQA1*0501	EGAVFLSFKLVQG**D**VFQEEAVTEALRA	G890D	49
	BCAR1	DPA1*0202	RQGIVPGNRLKIL**L**VVPTRVGQGYVYE	V64L	31
	TP53	A*3303	TIITLEDSSGNLL**V**RNSFEVRVCACPG	G266V	32
P02	GBF1	B*1501	SSQHASRGGQSDD**Y**EDEGVPASYHTVS	D1478Y	25
	COP1	B*5801	ILWDGFTGQRSKV**S**QEHEKRCWSVDFN	Y485S	31
	ATP11B	DQA1*0301	LKNTKEIFGVAVY**S**GMETKMALNYKSK	T262S	29
	UPF3A	A*3303	GSQDSGAPGEAME**T**LGRAQRCDDSPAP	R380T	26
	IER5L	A*0207	LHKNLLVSYVLRN**T**RQLYLSERYAELY	A43T	30
	SNX16	B*5801	QDVWMRSRADNKP**Y**LSFSEPENAVSEI	C318Y	27
	OSBPL6	A*0201	EVLLSASSSENEA**L**DDESYISDVSDNI	S513L	19
	NFE2L2	A*0201	AFFAQLQLDEETG**Q**FLPIQPAQHIQSE	E82Q	18
	SLX4	A*0201	SPTKEAPPGLNDD**G**QIPASQESVATSV	A1694G	18
	ACAD8	A*0201	QTDVGGSGLSRLD**I**SVIFEALATGCTS	T105I	31
	MTREX	A*0201	EMPKLTEQLAGPL**C**QMQECAKRIAKVS	R933C	15
P03	BCAR1	A*0201	VLLSWKVLDFSGP**V**PQGTGQPCSCGHW	G23V	37
	SLC7A1	A*0201	KYAVAVGSLCALS**S**SLLGSMFPMPRVI	A349S	28
	PLCG1	A*0201	SIEDHCSIAQQRN**L**AQYFKKVLGDTLL	M425L	23
	PIF1	A*0201	EADLFDKLEAVAR**G**VRQQNKPFGGIQL	A325G	3
	SSH1	A*0201	ILDASKQRHNKLW**C**QQTDSSLQQPVDD	R470C	2

NSCLC, nonsmall cell lung cancer. [a]Mutated residues are highlighted in hold. WT, wide type; AA#, position of mutated amino acid; Mut, mutation. [b]HLA class I and II binding affinity are predicted by netMHCpan 4.0 and netMHCIIpan 3.2, respectively.

for the immunization of HLA-A2.1/k^b mice. On days 0 and 7, ACAD8-T105I, BCAR1-G23V and PLCG1-M425L (100 μg per peptide) were mixed with 50 μg of poly (I:C), and the mixture was subcutaneously injected into transgenic mice for immunization. Splenocytes were collected 7 days after the last immunization. Some of the splenocytes were used for IFN-γ, TNF-αand IL-2 ELISPOT assay. The rest of the splenocytes were cultured for another 7 days with the corresponding peptides, and T cells were then isolated for cytotoxicity detection. NRTs against ACAD8-T105I, BCAR1-G23V and PLCG1-M425L from HLA-A2.1/K^b mice contained more IFN-γ, TNF-α and IL-2-producing T cells than those obtained using the WT epitopes, as demonstrated by ELISPOT assay (**Figures 4A–D**). The no-peptide control (culture medium only) and the irrelevant peptide control (VSV-NP43-69) only induced baseline-level secretory responses. In the cytotoxicity assay, the neoantigen-induced NRTs, particularly those induced with BCAR1-G23V and PLCG1-M425L, presented higher cytotoxicity against T2/Kb cells and H522/Kb-minigene cells carrying or expressing the corresponding mutant peptides. No significant cytotoxicity was detected in T2/Kb cells that were not loaded with the peptide or were loaded with irrelevant peptides or H522/Kb cells that did not express mutant peptides (**Figures 4E–G**).

ADOPTIVE NRT IMMUNOTHERAPY OF C57BL/$6^{NU/NU}$ MICE BEARING HUMAN NSCLC

To further investigate whether ACAD8-T105I, BCAR1-G23V and PLCG1-M425L peptides can serve as potent vaccines against tumor growth *in vivo*, HLA-A2.1/K^b transgenic mouse-derived NRTs were adoptively transferred into H522/Kb-minigene human lung cancer-bearing C57BL/6 nude mice. As shown in **Figure 5A**, tumor-bearing nude mice treated with neoantigen (ACAD8-T105I, BCAR1-G23V and PLCG1-M425L)-induced NRTs exhibited significantly delayed tumor growth, whereas the irrelevant peptide-induced NRTs did not restrict tumor growth. In addition, 6/10 (60%) of the BCAR1-G23V vaccination group, 5/10 (50%) of the PLCG1-M425L vaccination group and 3/10 (30%) of the ACAD8-T105I vaccination group exhibited prolonged long-term survival (over 80 days) after tumor inoculation (**Figure 5B**), whereas all the mice in the control groups died between days 19 and 40. With regard to the toxicity as detected by the loss of body weight, adoptive NRT immunotherapy seemed to be well tolerated because no appreciable body weight loss were observed in all treatment groups (**Figure 5C**). The above-mentioned findings indicated that the neoantigens ACAD8-T105I, BCAR1-G23V and PLCG1-

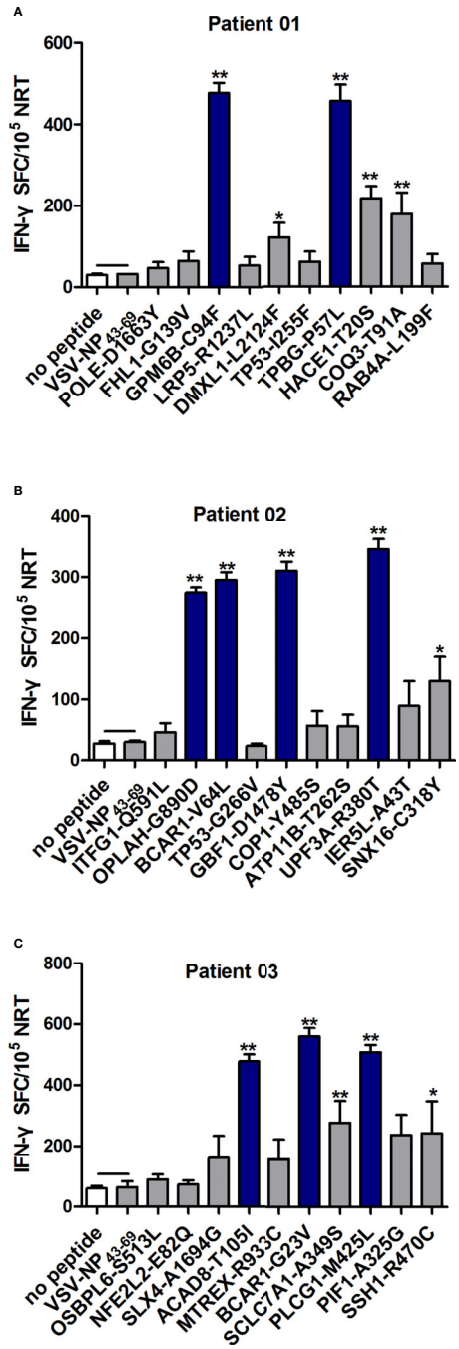

FIGURE 2 | Evaluation of the immunogenicity of neoantigens from patients with NSCLC. Autologous PBMCs were stimulated with candidate mutated peptides every 3 days in the presence of IL-2, and on day 10, the T cell responses to each antigen were measured by IFN-γ ELISPOT assay. The PBMCs in **A–C** were obtained from NSCLC patients 01, 02, and 03, respectively. Stimulation with the no-peptide control (medium only) or irrelevant peptide VSV-NP_{43-69}(STKVALNDLRAYVYQGIKSGNPSILHI) was performed as controls. The data are presented as the means ± s.e.m.s from three independent experiments. $^{**}P<0.01$ and $^{*}P<0.05$ were obtained for the comparison of IFN-γ production by PBMCs stimulated without a peptide or with irrelevant peptide VSV-NP_{43-69}. SFC, spot-forming cell; VSV-NP, vesicular stomatitis virus expressing influenza nucleoprotein.

M425L can potently and safely induce anti-tumor responses *in vivo*.

DISCUSSION

Tumor-specific somatic mutations are considered ideal targets for tumor immunotherapy, but the study and application of neoantigen-based immunotherapy in NSCLC have not been reported. To develop neoantigen-targeted personalized cancer treatments for NSCLC, samples of human lung cancer were collected, and the potential use of selected neoantigens as targets for NSCLC immunotherapy was tested. In accordance with our research, immunogenic neoantigen were identified in all three NSCLC patients. Additionally, T cells activated by neoantigens from patient 03 (HLA-A*02:01^{+}) showed anti-tumor potency, as demonstrated with HLA-A2.1/K^{b} transgenic mice and tumor-bearing mouse models.

With the rapid development of immunotherapy, numerous studies have attempted to develop cancer vaccines (42). Neoantigens are a series of immunogenic peptides derived from tumor-specific mutations or viral open reading frames rather than from the normal human genome (43–45). Neoantigens are highly immunogenic and can escape from central thymic tolerance. Four successful phase I clinical trials were recently and have attracted much attention for use in the development of personalized neoantigen vaccines (12, 13, 46, 47). Although neoantigens represent the optimal choice for anti-tumor immunotherapy, their application is hindered by the unique neoantigen landscape of individualized tumors. The density of somatic mutations and neoantigens was recently shown to correlate with long-term benefits from immune checkpoint blockade in NSCLC (48). Neoantigen loss is observed during immune checkpoint blockade and has implications for the development of immune therapies that target tumor neoantigens (15). Karasaki et al. (14). found a median of 46potential neoantigens (pNeoAgs) (range of 13-659) for adenocarcinoma and 95.5 pNeoAgs(range of 10-145) for squamous cell carcinoma (SCC) in NSCLC. It was previously shown that the selection pressures from a diverse tumor microenvironment affect neoantigen presentation, tumor-intrinsic mechanisms that lead to immune escape and their respective effects on clinical outcomes in NSCLC (49). These studies have confirmed the existence of abundant neoantigens in lung cancer. However, the role of neoantigens in lung cancer remains unclear. Neoantigens were predicted from all three lung cancer patients, and nine from thirty selected neoantigens, which induce significant specific T cell responses with a patient's own PBMC cells, were also confirmed in our study. Our results shown higher positive ratio than the average level reported by Daniel K. et al. (50), which may be related to the cancer type, ethnic specificity, health/immune condition, and randomization effect (51).

Recently, increasing evidence has shown that adoptive T cell therapy, specific for neoantigens, has been successfully used to treat many human solid cancers (16, 52). Rosenberg led his

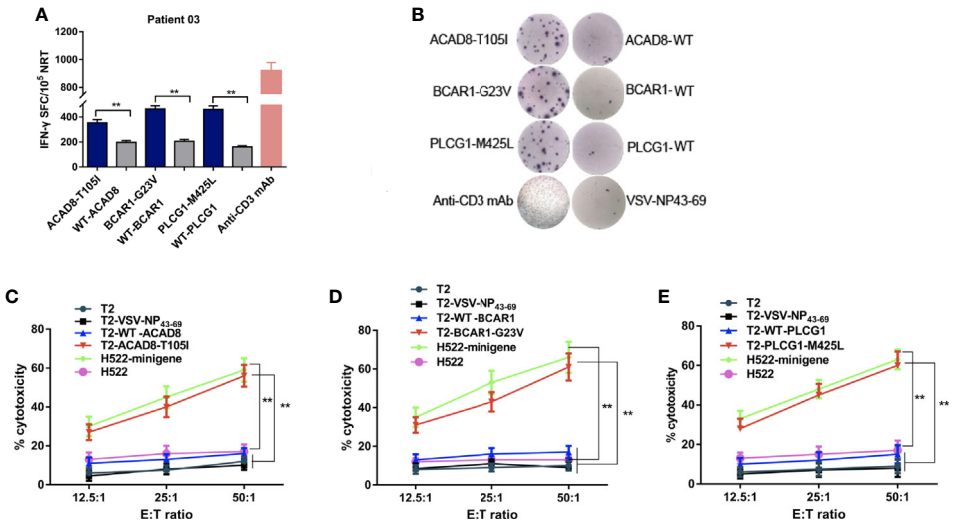

FIGURE 3 | Cytotoxicity of NRTs obtained from the *in vitro* stimulation of PBLs of HLA-A*0201-positive patient 03 with NSCLC. NRTs were induced with autologous ACAD8-T105I, BCAR1-G23V and PLCG1-M425L-pulsed DCs from PBLs of Patient 03 (P03). Seven days after the third stimulation, the NRTs were harvested for analysis. **(A, B)** IFN-γ secretion by neoantigen-reactive T cell lines against mutated and wild-type peptides. IFN-γ-positive SFCs/10^5 NRTs detected by cytokine-specific ELISPOT assay. Stimulation with anti-CD3-mAb was used as positive control. **(C–E)** Cytotoxicity at the indicated E:T ratios measured using time-resolved fluorescence assay. Mutant peptide-pulsed T2 cells and minigene-nucleofected H522 cells (HLA-A2.1$^+$, H522-minigene) were used as peptide-specific targets, whereas irrelevant peptideVSV-NP43-69-pulsed T2 cells,T2 cells alone and H522 cells were used as controls. The data are presented as the means ± s.e.m.s from three independent experiments. $^{**}P<0.01$. NRTs, neoantigen-reactive T cells; WT, wild-type peptide; E:T, effector: target; PBL, peripheral blood lymphocyte; SFC, spot-forming cell; VSV-NP, vesicular stomatitis virus nucleoprotein.

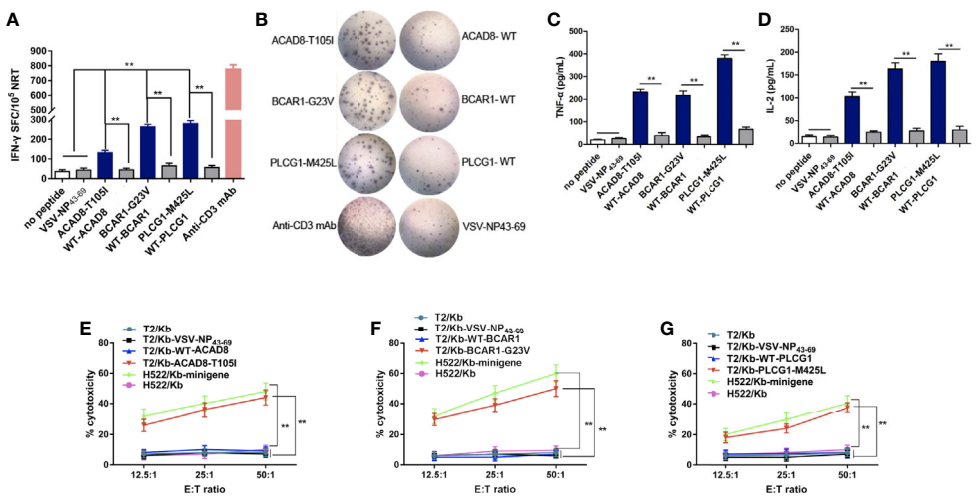

FIGURE 4 | ACAD8-T105I, BCAR1-G23V and PLCG1-M425Linduce more efficient NRT responses than WT epitopes in HLA-A2.1/K^bTg mice. **(A–D)** Splenocytes of mice(n=5) vaccinated with mutated peptides were tested by ELISPOT assay for the recognition of mutated peptides compared with the corresponding wild-type sequences. The data are presented as the means ± s.e.m.s from three independent experiments. $^{**}P < 0.01$ was obtained in the comparison of IFN-γ **(A, B)**, TNF-α **(C)** and IL-2 **(D)** production by splenocytes stimulated without a peptide or with VSV-NP43-69. **(E–G)** Splenocytes from HLA-A2.1/K^bTg mice immunized with mutated peptides were re-stimulated *in vitro* with the corresponding mutated peptide for 7 days. The ex vivo cytotoxicity against the corresponding mutated peptide-pulsed T2/Kb cells and minigene-nucleofected H522/Kb cells at the indicated E:T ratio was examined using time-resolved fluorescence assay. Irrelevant peptide VSV-NP43-69-pulsed T2/Kb cells, T2/Kb cells alone or H522/Kb cells were used as controls. Stimulation with anti-CD3-mAb was used as positive control. The data are presented as the means ± s.e.m.s from three independent experiments. $^{**}P<0.01$. E:T, effector: target; SFC, spot-forming cell; VSV-NP, vesicular stomatitis virus nucleoprotein.

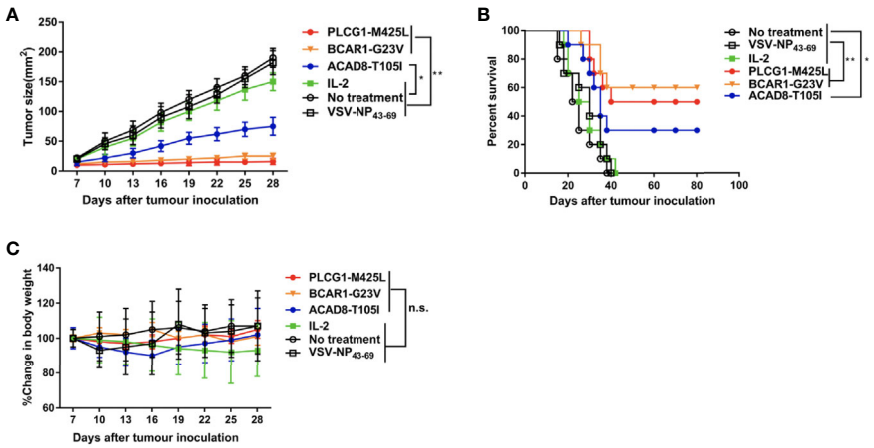

FIGURE 5 | Adoptive immunotherapy of minigene-nucleofectedH522/Kb tumor-bearing nude mice. Minigene-nucleofected H522/Kb tumor cells (5×10^6 cells/mouse) were injected into the flanks of C57BL/$6^{nu/nu}$ mice. Three days later, splenocytes (1×10^8 cells/mouse) from ACAD8-T105I-, BCAR1-G23V- or PLCG1-M425L-immunized HLA-A2.1/K^bTg mice were injected as described in the Materials and methods section. The mice in the control groups received IL-2 alone or did not receive treatment. **(A)** Tumor growth was observed every 3 days and recorded as the mean tumor size (mm 2). **(B)** Survival of mice after tumor inoculation (n = 10 mice/group). **(C)** The effect of different treatments on mouse body weight. (*P<0.05; **P<0.01).

research team to identify neoantigens in a patient with metastatic cholangiocarcinoma who exhibited radiotherapy and chemotherapy failure using a whole-exome sequencing-based approach (30).Subsequently, the same research team published another paper in NEJM describing the successful application of adoptive TIL cell therapy in a patient with metastatic colorectal (53). In another study, Chen F. et al. (16) successfully treated advanced cancer patients with multiple metastases using personalized peptide vaccines in combination with NRT adoptive therapy, and these results further verified the application of individualized tumor therapy based on NRTs. All these observations verified the potency of putative neoantigens in the induction of NRTs, which also indicated the potential of patient-specific immunotherapy approaches, particularly adoptive T cell transfer, in the treatment of lung cancer. In accordance with our research, *in vitro* experiments and NRT-induced cytotoxicity *in vivo* evaluation assays showed that all the NSCLC patients developed NRT cell responses against multiple vaccine neo-epitopes.

Our research confirms the presence of large amounts of neoantigens in NSCLC. Functional neoantigens were successfully screened through gene sequencing, software prediction and other evaluations. Specific NRTs were successfully elicited, and their cytotoxicity was confirmed both *in vitro* and *in vivo*. Our study provides evidence showing that neoantigen-based therapy might serve as feasible treatment for NSCLC that show great potential for achieving maximal therapeutic specificity, overcoming immune tolerance, and minimizing the risk of autoimmunity. Taken together, the results obtained in this study demonstrate that tumors can be efficiently controlled and cured in the evolving field of precision medicine, particularly through the application of personalized immunotherapy.

DATA AVAILABILITY STATEMENT

The datasets presented in this study can be found in online repositories. The names of the repository/repositories and accession number(s) can be found in the article/ **Supplementary Material**.

ETHICS STATEMENT

The studies involving human participants were reviewed and approved by Medical Ethics Committee of Shanghai East Hospital. The patients/participants provided their written informed consent to participate in this study. The animal study was reviewed and approved by Biotherapy Center, Qingdao Central Hospital, The Second Affiliated Hospital, Qingdao University.

AUTHOR CONTRIBUTIONS

WZ, QY, and HH designed and performed experiments, analyzed data, and wrote the paper. JL, HQ, WZ, and XS performed experiments. SC translated the paper. WS and YD designed experiments, oversaw the data analysis and wrote the paper. QL conceived the study and wrote the paper. All authors contributed to the article and approved the submitted version.

FUNDING

This work was supported by Clinical Plateau Discipline Project in Shanghai Pudong New Area(PWYgy2018-06), Scientific Research Project by Shanghai Science and Technology

Committee(19411950400) and Qingdao Outstanding Health Professional Development Fund; Qingdao Science and Technology Project (for Benefiting the People, 19-6-1-27-nsh).

ACKNOWLEDGEMENTS

We appreciate the help of neoantigen screening and data analysis by the P&PMed Biotechnology Co. Ltd. (Shanghai, China. http://www.pnp-med.com/).

SUPPLEMENTARY MATERIAL

The Supplementary Material for this article can be found online at: https://www.frontiersin.org/articles/10.3389/fonc.2021.628456/full#supplementary-material

Supplementary Figure 1 | Immunogenicity of Cancer-associated mutations in HLA-A2.1/KbTg mice. Splenocytes of mice vaccinated with peptides and polyinosinic: polycytidylic acid (polyI: C) were tested for recognition of mutated peptides by flow cytometry.

Supplementary Figure 2 | Expression of HLA-A*0201/Kb chimeric gene in T2/Kb and H522/Kb cells. T2/Kb and H522/Kb cells were stable transfectants and express the product of the HLA-A*0201/Kb chimeric gene (the α1 and α2 domains from HLA-A*0201 and the α3 domain of H-2Kb)

Supplementary Figure 3 | Immunogenicity of peptides-containing neoantigen at different various concentrations. Peptide titration of the NRT lines specific for PLACG1-M425L, BCAR1-G23V and ACAD8-T105I peptides. The immune splenocytes from HLA-0201/Kb vaccinated animals were stimulated with various concentrations (100, 10 or 1 μM) of PLACG1-M425L, BCAR1-G23V and ACAD8-T105I peptides. After 4 h of incubation, frequency of IFN-γ-secreting cells was measured. The data are presented as the means ± s.e.m.s from three independent experiments.

REFERENCES

1. Lovly CM, Iyengar P, Gainor JF. Managing Resistance to EFGR- and ALK-Targeted Therapies. *Am Soc Clin Oncol Educ Book* (2017) 37:607–18. doi: 10.1200/EDBK_176251
2. Dittrich C, Papai-Szekely Z, Vinolas N, Sederholm C, Hartmann JT, Behringer D, et al. A randomised phase II study of pemetrexed versus pemetrexed+erlotinib as second-line treatment for locally advanced or metastatic non-squamous non-small cell lung cancer. *Eur J Cancer* (2014) 50(9):1571–80. doi: 10.1016/j.ejca.2014.03.007
3. Duraiswamy J, Freeman GJ, Coukos G. Therapeutipc PD-1 pathway blockade augments with other modalities of immunotherapy T-cell function to prevent immune decline in ovarian cancer. *Cancer Res* (2013) 73(23):6900–12. doi: 10.1158/0008-5472.CAN-13-1550
4. Melosky B, Chu Q, Juergens R, Leighl N, McLeod D, Hirsh V. Pointed Progress in Second-Line Advanced Non-Small-Cell Lung Cancer: The Rapidly Evolving Field of Checkpoint Inhibition. *J Clin Oncol* (2016) 34 (14):1676–88. doi: 10.1200/JCO.2015.63.8049
5. Brahmer J, Reckamp KL, Baas P, Crino L, Eberhardt WE, Poddubskaya E, et al. Nivolumab versus Docetaxel in Advanced Squamous-Cell Non-Small-Cell Lung Cancer. *N Engl J Med* (2015) 373(2):123–35. doi: 10.1056/NEJMoa1504627
6. Borghaei H, Paz-Ares L, Horn L, Spigel DR, Steins M, Ready NE, et al. Nivolumab versus Docetaxel in Advanced Nonsquamous Non-Small-Cell Lung Cancer. *N Engl J Med* (2015) 373(17):1627–39. doi: 10.1056/NEJMoa1507643
7. Herbst RS, Baas P, Kim DW, Felip E, Perez-Gracia JL, Han JY, et al. Pembrolizumab versus docetaxel for previously treated, PD-L1-positive, advanced non-small-cell lung cancer (KEYNOTE-010): a randomised controlled trial. *Lancet* (2016) 387(10027):1540–50. doi: 10.1016/S0140-6736(15)01281-7
8. Rittmeyer A, Barlesi F, Waterkamp D, Park K, Ciardiello F, von Pawel J, et al. Atezolizumab versus docetaxel in patients with previously treated non-small-cell lung cancer (OAK): a phase 3, open-label, multicentre randomised controlled trial. *Lancet* (2017) 389(10066):255–65. doi: 10.1016/S0140-6736(16)32517-X
9. Reck M, Rodriguez-Abreu D, Robinson AG, Hui R, Csoszi T, Fulop A, et al. Pembrolizumab versus Chemotherapy for PD-L1-Positive Non-Small-Cell Lung Cancer. *N Engl J Med* (2016) 375(19):1823–33. doi: 10.1056/NEJMoa1606774
10. Mok TSK, Wu YL, Kudaba I, Kowalski DM, Cho BC, Turna HZ, et al. Pembrolizumab versus chemotherapy for previously untreated, PD-L1-expressing, locally advanced or metastatic non-small-cell lung cancer (KEYNOTE-042): a randomised, open-label, controlled, phase 3 trial. *Lancet* (2019) 393(10183):1819–30. doi: 10.1016/S0140-6736(18)32409-7
11. Campbell BB, Light N, Fabrizio D, Zatzman M, Fuligni F, de Borja R, et al. Comprehensive Analysis of Hypermutation in Human Cancer. *Cell* (2017) 171(5):1042–56.e1010. doi: 10.1016/j.cell.2017.09.048
12. Ott PA, Hu Z, Keskin DB, Shukla SA, Sun J, Bozym DJ, et al. An immunogenic personal neoantigen vaccine for patients with melanoma. *Nature* (2017) 547 (7662):217–21. doi: 10.1038/nature22991
13. Hilf N, Kuttruff-Coqui S, Frenzel K, Bukur V, Stevanovic S, Gouttefangeas C, et al. Actively personalized vaccination trial for newly diagnosed glioblastoma. *Nature* (2019) 565(7738):240–5. doi: 10.1038/s41586-018-0810-y
14. Karasaki T, Nagayama K, Kawashima M, Hiyama N, Murayama T, Kuwano H, et al. Identification of Individual Cancer-Specific Somatic Mutations for Neoantigen-Based Immunotherapy of Lung Cancer. *J Thorac Oncol* (2016) 11 (3):324–33. doi: 10.1016/j.jtho.2015.11.006
15. Anagnostou V, Smith KN, Forde PM, Niknafs N, Bhattacharya R, White J, et al. Evolution of Neoantigen Landscape during Immune Checkpoint Blockade in Non-Small Cell Lung Cancer. *Cancer Discov* (2017) 7(3):264–76. doi: 10.1158/2159-8290.CD-16-0828
16. Chen F, Zou Z, Du J, Su S, Shao J, Meng F, et al. Neoantigen identification strategies enable personalized immunotherapy in refractory solid tumors. *J Clin Invest* (2019) 129(5):2056–70. doi: 10.1172/JCI99538
17. Ding Z, Li Q, Zhang R, Xie L, Shu Y, Gao S, et al. Personalized neoantigen pulsed dendritic cell vaccine for advanced lung cancer. *Signal Transduct Target Ther* (2021) 6(1):26. doi: 10.1038/s41392-020-00448-5
18. Liu S, Yu Y, Zhang M, Wang W, Cao X. The involvement of TNF-alpha-related apoptosis-inducing ligand in the enhanced cytotoxicity of IFN-beta-stimulated human dendritic cells to tumor cells. *J Immunol* (2001) 166 (9):5407–15. doi: 10.4049/jimmunol.166.9.5407
19. Wu Y, Wan T, Zhou X, Wang B, Yang F, Li N, et al. Hsp70-like protein 1 fusion protein enhances induction of carcinoembryonic antigen-specific CD8 + CTL response by dendritic cell vaccine. *Cancer Res* (2005) 65(11):4947–54. doi: 10.1158/0008-5472.CAN-04-3912
20. Irwin MJ, Heath WR, Sherman LA. Species-restricted interactions between CD8 and the alpha 3 domain of class I influence the magnitude of the xenogeneic response. *J Exp Med* (1989) 170(4):1091–101. doi: 10.1084/jem.170.4.1091
21. Gnirke A, Melnikov A, Maguire J, Rogov P, LeProust EM, Brockman W, et al. Solution hybrid selection with ultra-long oligonucleotides for massively parallel targeted sequencing. *Nat Biotechnol* (2009) 27(2):182–9. doi: 10.1038/nbt.1523
22. Li H, Durbin R. Fast and accurate short read alignment with Burrows-Wheeler transform. *Bioinformatics* (2009) 25(14):1754–60. doi: 10.1093/bioinformatics/btp324
23. Ghosh S, Chan CK. Analysis of RNA-Seq Data Using TopHat and Cufflinks. *Methods Mol Biol* (2016) 1374:339–61. doi: 10.1007/978-1-4939-3167-5_18
24. Szolek A, Schubert B, Mohr C, Sturm M, Feldhahn M, Kohlbacher O. OptiType: precision HLA typing from next-generation sequencing data. *Bioinformatics* (2014) 30(23):3310–6. doi: 10.1093/bioinformatics/btu548

25. Weese D, Holtgrewe M, Reinert K. RazerS 3: faster, fully sensitive read mapping. *Bioinformatics* (2012) 28(20):2592–9. doi: 10.1093/bioinformatics/bts505
26. Bjerregaard AM, Nielsen M, Hadrup SR, Szallasi Z, Eklund AC. MuPeXI: prediction of neo-epitopes from tumor sequencing data. *Cancer Immunol Immunother* (2017) 66(9):1123–30. doi: 10.1007/s00262-017-2001-3
27. Jurtz V, Paul S, Andreatta M, Marcatili P, Peters B, Nielsen M. NetMHCpan-4.0: Improved Peptide-MHC Class I Interaction Predictions Integrating Eluted Ligand and Peptide Binding Affinity Data. *J Immunol* (2017) 199 (9):3360–8. doi: 10.4049/jimmunol.1700893
28. Jensen KK, Andreatta M, Marcatili P, Buus S, Greenbaum JA, Yan Z, et al. Improved methods for predicting peptide binding affinity to MHC class II molecules. *Immunology* (2018) 154(3):394–406. doi: 10.1111/imm.12889
29. Cibulskis K, Lawrence MS, Carter SL, Sivachenko A, Jaffe D, Sougnez C, et al. Sensitive detection of somatic point mutations in impure and heterogeneous cancer samples. *Nat Biotechnol* (2013) 31(3):213–9. doi: 10.1038/nbt.2514
30. Tran E, Turcotte S, Gros A, Robbins PF, Lu YC, Dudley ME, et al. Cancer immunotherapy based on mutation-specific CD4+ T cells in a patient with epithelial cancer. *Science* (2014) 344(6184):641–5. doi: 10.1126/science.1251102
31. Hida N, Maeda Y, Katagiri K, Takasu H, Harada M, Itoh K. A simple culture protocol to detect peptide-specific cytotoxic T lymphocyte precursors in the circulation. *Cancer Immunol Immunother* (2002) 51(4):219–28. doi: 10.1007/s00262-002-0273-7
32. Noguchi M, Sasada T, Itoh K. Personalized peptide vaccination: a new approach for advanced cancer as therapeutic cancer vaccine. *Cancer Immunol Immunother* (2013) 62(5):919–29. doi: 10.1007/s00262-012-1379-1
33. Liu S, Yi L, Ling M, Jiang J, Song L, Liu J, et al. HSP70L1-mediated intracellular priming of dendritic cell vaccination induces more potent CTL response against cancer. *Cell Mol Immunol* (2018) 15(2):135–45. doi: 10.1038/cmi.2016.33
34. Su S, Hu B, Shao J, Shen B, Du J, Du Y, et al. CRISPR-Cas9 mediated efficient PD-1 disruption on human primary T cells from cancer patients. *Sci Rep* (2016) 6:20070. doi: 10.1038/srep20070
35. Blomberg K, Hautala R, Lovgren J, Mukkala VM, Lindqvist C, Akerman K. Time-resolved fluorometric assay for natural killer activity using target cells labelled with a fluorescence enhancing ligand. *J Immunol Methods* (1996) 193 (2):199–206. doi: 10.1016/0022-1759(96)00063-4
36. Tagod MSO, Mizuta S, Sakai Y, Iwasaki M, Shiraishi K, Senju H, et al. Determination of human gammadelta T cell-mediated cytotoxicity using a non-radioactive assay system. *J Immunol Methods* (2019) 466:32–40. doi: 10.1016/j.jim.2019.01.003
37. Averbook BJ, Cleveland RP, Viscusi C, Papay R. Coinfusion of irradiated splenocytes with low titer tumor-infiltrating lymphocytes augments antitumor efficacy in adoptive immunotherapy. *J Immunother* (1999) 22(2):124–34. doi: 10.1097/00002371-199903000-00004
38. Sun W, Wei X, Niu A, Ma X, Li JJ, Gao D. Enhanced anti-colon cancer immune responses with modified eEF2-derived peptides. *Cancer Lett* (2015) 369(1):112–23. doi: 10.1016/j.canlet.2015.08.002
39. Kaluza KM, Kottke T, Diaz RM, Rommelfanger D, Thompson J, Vile R. Adoptive transfer of cytotoxic T lymphocytes targeting two different antigens limits antigen loss and tumor escape. *Hum Gene Ther* (2012) 23(10):1054–64. doi: 10.1089/hum.2012.030
40. Schmidt J, Ryschich E, Sievers E, Schmidt-Wolf IG, Buchler MW, Marten A. Telomerase-specific T-cells kill pancreatic tumor cells in vitro and in vivo. *Cancer* (2006) 106(4):759–64. doi: 10.1002/cncr.21655
41. Proietti E, Greco G, Garrone B, Baccarini S, Mauri C, Venditti M, et al. Importance of cyclophosphamide-induced bystander effect on T cells for a successful tumor eradication in response to adoptive immunotherapy in mice. *J Clin Invest* (1998) 101(2):429–41. doi: 10.1172/JCI1348
42. Jaroslawski S, Toumi M. Sipuleucel-T (Provenge((R)))-Autopsy of an Innovative Paradigm Change in Cancer Treatment: Why a Single-Product Biotech Company Failed to Capitalize on its Breakthrough Invention. *BioDrugs* (2015) 29(5):301–7. doi: 10.1007/s40259-015-0140-7
43. Liu XS, Mardis ER. Applications of Immunogenomics to Cancer. *Cell* (2017) 168(4):600–12. doi: 10.1016/j.cell.2017.01.014
44. Tran E, Robbins PF, Rosenberg SA. 'Final common pathway' of human cancer immunotherapy: targeting random somatic mutations. *Nat Immunol* (2017) 18(3):255–62. doi: 10.1038/ni.3682
45. Schumacher TN, Schreiber RD. Neoantigens in cancer immunotherapy. *Science* (2015) 348(6230):69–74. doi: 10.1126/science.aaa4971
46. Sahin U, Derhovanessian E, Miller M, Kloke BP, Simon P, Lower M, et al. Personalized RNA mutanome vaccines mobilize poly-specific therapeutic immunity against cancer. *Nature* (2017) 547(7662):222–6. doi: 10.1038/nature23003
47. Keskin DB, Anandappa AJ, Sun J, Tirosh I, Mathewson ND, Li S, et al. Neoantigen vaccine generates intratumoral T cell responses in phase Ib glioblastoma trial. *Nature* (2019) 565(7738):234–9. doi: 10.1038/s41586-018-0792-9
48. Rizvi NA, Hellmann MD, Snyder A, Kvistborg P, Makarov V, Havel JJ, et al. Cancer immunology. Mutational landscape determines sensitivity to PD-1 blockade in non-small cell lung cancer. *Science* (2015) 348(6230):124–8. doi: 10.1126/science.aaa1348
49. Rosenthal R, Cadieux EL, Salgado R, Bakir MA, Moore DA, Hiley CT, et al. Neoantigen-directed immune escape in lung cancer evolution. *Nature* (2019) 567(7749):479–85. doi: 10.1038/s41586-019-1032-7
50. Wells DK, van Buuren MM, Dang KK, Hubbard-Lucey VM, Sheehan KCF, Campbell KM, et al. Key Parameters of Tumor Epitope Immunogenicity Revealed Through a Consortium Approach Improve Neoantigen Prediction. *Cell* (2020) 183(3):818–34.e813. doi: 10.1016/j.cell.2020.09.015
51. Garcia-Garijo A, Fajardo CA, Gros A. Determinants for Neoantigen Identification. *Front Immunol* (2019) 10:1392. doi: 10.3389/fimmu.2019.01392
52. Zacharakis N, Chinnasamy H, Black M, Xu H, Lu YC, Zheng Z, et al. Immune recognition of somatic mutations leading to complete durable regression in metastatic breast cancer. *Nat Med* (2018) 24(6):724–30. doi: 10.1038/s41591-018-0040-8
53. Tran E, Robbins PF, Lu YC, Prickett TD, Gartner JJ, Jia L, et al. T-Cell Transfer Therapy Targeting Mutant KRAS in Cancer. *N Engl J Med* (2016) 375(23):2255–62. doi: 10.1056/NEJMoa1609279

Conflict of Interest: The authors declare that the research was conducted in the absence of any commercial or financial relationships that could be construed as a potential conflict of interest.

frontiers in Oncology

ORIGINAL RESEARCH
published: 15 April 2021
doi: 10.3389/fonc.2021.632540

Proliferation of Highly Cytotoxic Human Natural Killer Cells by OX40L Armed NK-92 With Secretory Neoleukin-2/15 for Cancer Immunotherapy

Meng Guo[1†], Chen Sun[2†], Yuping Qian[2†], Liye Zhu[1], Na Ta[2], Guangjian Wang[3], Jianming Zheng[2], Fengfu Guo[3*] and Yanfang Liu[1,2*]*

[1] National Key Laboratory of Medical Immunology & Institute of Immunology, Navy Medical University, Shanghai, China, [2] Department of Pathology, Changhai Hospital, Navy Medical University, Shanghai, China, [3] Department of Urology, The Linyi People's Hospital, Linyi, China

Adoptive natural killer (NK) cell transfer has been demonstrated to be a promising immunotherapy approach against malignancies, but requires the administration of sufficient activated cells for treatment effectiveness. However, the paucity of clinical-grade to support the for large-scale cell expansion limits its feasibility. Here we developed a feeder-based NK cell expansion approach that utilizes OX40L armed NK-92 cell with secreting neoleukin-2/15 (Neo-2/15), a hyper-stable mimetic with a high affinity to IL-2Rβγ. The novel feeder cells (NK92-Neo2/15-OX40L) induced the expansion of NK cells with a 2180-fold expansion (median; 5 donors; range, 1767 to 2719) after 21 days of co-culture without added cytokines. These cells were highly cytotoxic against Raji cells and against several solid tumors *in vivo*. Mechanistically, NK92-Neo2/15-OX40L induced OX40 and OX40L expression on expanded NK cells and promoted the OX40-OX40L positive feedback loop, thus boosting NK cell function. Our data provided a novel NK cell expansion mechanism and insights into OX40-OX40L axis regulation of NK cell expansion.

Keywords: neoleukin-2/15, OX40 ligand, cytotoxic activity, NK cell expansion, immunotherapy

OPEN ACCESS

Edited by:
Kevin J. Ni,
St. George Hospital, Australia

Reviewed by:
Jian Zhang,
Shandong University, China
Duck Cho,
Sungkyunkwan University, South Korea
Ping Zhou,
Fudan University, China

****Correspondence:***
Yanfang Liu
Liuyanfang00215@163.com
Fengfu Guo
Guoff892@163.com
Jianming Zheng
Jmzheng1962@smmu.edu.cn

[†]These authors have contributed equally to this work and share first authorship

Specialty section:
This article was submitted to Molecular and Cellular Oncology, a section of the journal Frontiers in Oncology

Received: *23 November 2020*
Accepted: *22 March 2021*
Published: *15 April 2021*

Citation:
Guo M, Sun C, Qian Y, Zhu L, Ta N, Wang G, Zheng J, Guo F and Liu Y (2021) Proliferation of Highly Cytotoxic Human Natural Killer Cells by OX40L Armed NK-92 With Secretory Neoleukin-2/15 for Cancer Immunotherapy. Front. Oncol. 11:632540. doi: 10.3389/fonc.2021.632540

INTRODUCTION

As innate "sentinels", NK cells serve an important role in the immune surveillance for pathogens and cancerous cells, implying that NK cells infusion is promising cellular immunotherapy for cancer (1). Therefore, the development of clinical-grade and low-cost approaches for large-scale NK cell expansion is essential to improve on its feasibility and clinical benefit. NK cells constitute approximately 5-25% of the lymphocytes with limited life-span, thus, obtaining enough cells is a major obstacle for NK cell immunotherapy, and the process is expensive and time-consuming.

Studies showed cytokines are essential in the induction of NK cell proliferation and cytotoxic activity (2–4). IL-2 or other cytokine combinations, such as IL-15 and IL-21, have been used to

expand NK cell. However, natural cytokines only exhibit moderate affinity with IL-2Rβγ and are relatively unstable, thus the culture system requires continuous supplementation of cytokines, which greatly increases the cost of NK cell expansion. A recently designed IL-2 mimetics Neo-2/15 with a high affinity and specificity for IL-2Rβγ was reported to maintain T cell proliferation in kilo-picogram per milliliter scale (5). However, the effects of Neo-2/15 on NK cell expansion have not been reported.

Cytokine combination usually results in minimal NK cell expansion (1). One alternative approach would be to co-culture with feeder cells. K562 cells expressing costimulatory molecules in combinations with IL-2/15 greatly enhanced NK cell proliferation (6, 7). However, several studies reported that K562 reduced the cytotoxic activity of certain subpopulations of NK cells (8, 9). Therefore, it is necessary to find a more suitable feeder system for NK expansion. NK-92 is an NK cell line which considered to be a suitable allogeneic cell source for clinical application and its safety has been assessed in many clinical trials for tumor immunotherapy. The results imply that NK-92 can be suitable for NK cell feeders.

In this study, we found a novel approach to expand NK cells using NK-92 cells expressing OX40L and Neo-2/15, which enhanced *in vitro* and *in vivo* NK cell-mediated proliferation and cytotoxicity, respectively. Besides, we presented a possible mechanism of NK cell expansion through homotypic interaction of OX40-OX40L positive feedback loop.

MATERIALS AND METHODS

Mice and Mice Models

NOD/SCID mice and nude mice were purchased from Cavens Experimental Animal Company (Changzhou, China). All mice were housed in specific pathogen-free conditions. Mice were maintained under a 12-hour light-dark cycle at 23°C, and had free access to water and standard rodent diet. Before surgery, mice were anesthetized with 2% isoflurane.

Lung cancer model: 50 μL HBSS containing 5×10^6 A427 (luciferase Knock-in) cells were mixed with 50 μL Matrigel. The mixture was injected at a distance of 1.5 cm along the superior border of the rib into the left lung of male NOD/SCID mice, and unplugged after 10s.18 days after initial tumor growth, mice with similar tumor burden were selected by IVIS and randomly grouped.

Liver cancer model: HepG2 (luciferase Knock-in) cells were resuspended in HBSS with a density of 5×10^7cell/mL. After anesthesia, male NOD/SCID mice were laterally laparotomized below the xiphoid to expose part of the liver, and 100 μL cell suspension was injected into the liver. Vetbond Tissue Adhesive (3M, 1469SB) was used to close the wound while withdrawing needle. The lobe was relocated followed by the closure of the peritoneum and abdominal wall. After 16 days of tumor growth, mice with similar tumor burden were randomly grouped.

Ovarian cancer model: CAOV3 (luciferase Knock-in) xenografts were obtained from subcutaneous tumor cells of female nude mice and prepared as $1mm^3$ blocks. A left subcostal incision was made to expose the left ovary of female NOD/SCID mice, and the xenograft was stitched to the ovarian capsule using 7/0 suture and sealed by Vetbond. After 25 days, mice with similar tumor burden were randomly grouped.

Cells and Culture

Peripheral blood mononuclear cells (PBMCs) were isolated by Lymphoprep™ (StemCell, 07851) gradient centrifugation in SepMate™ (StemCell, 85450) Tubes. Primary Human NK cells were isolated from PBMCs by magnetic bead CD3 depletion (MiltenyiBiotec, 130-050-101) followed by CD56 (MiltenyiBiotec, 130-111-553) isolation. FACS analysis of anti-CD56 antibody revealed more than 90% purity of the NK cell population (Data not shown).

Purified NK cells were cultured in AIM-V Medium (GIBCO, 12055091) supplemented with indicated cytokines or feeder cells. 100ng/mL OKT3 (Muromonab) in the first culture cycle to deplete potential contaminated T or NKT cells.

NK-92 cells were purchased from American Type Culture Collection (ATCC). The complete medium for NK-92 was Alpha Minimum Essential medium (BasalMedia, L540KJ) with final a concentration of 0.2 mM inositol, 0.1 mM 2-mercaptoethanol; 0.02 mM folic acid, 20ng/ml recombinant IL-2 (Novoprotein, C013), 12.5% horse serum (Gibco, 26050088) and 12.5% fetal bovine serum (Gibco, 10091).

A427 was obtained from Boyu Biotechnology, while HepG2, CAOV3 and K562 were obtained from the Cell Bank of Type Culture Collection of the Chinese Academy of Sciences. A427, HepG2 and CAOV3 were cultured in α-MEM with 10% FBS. K562 was cultured in RPMI1640 with 10% FBS. A427, HepG2, and CAOV3 were labeled with luciferase (Genechem, GV633) as previously described (10).

Generation of Engineered Cells Expressing Membrane-Bound Protein

OX40L (NM_003326.5) and 4-1BBL (NM_009404.3) sequences were fused with his-tag and then cloned into pLVX-EF1a-IRES-Puro (Addgene, 85132). The neo-2/15 sequence was fused with Flag-tag and cloned into pLVX-IRES-ZsGreen1 (Fenghui, BR021). The lentivirus was produced by co-transfection with the packaging plasmid psPAX2 and pMD2.G into lenti-X-293 cells cultured in DMEM medium with 10% FBS. The K562 or NK-92 were seeded into 24-well plates at 1×10^5 cells/well and then infected at MOI=10. The cells were harvested 7 days post-infection and subsequently sorted by flow cytometry, resulting in GFP-positive or His-positive monoclonal cell lines. Anti-Flag-PE and anti-His-APC were obtained from BioLegend. NK92-based feeder cells were acclimatized in AIM-V medium after establishment.

Cytotoxicity Assays

In vitro cytotoxicity assay of the expanded NK cells against target tumor cells (Raji, A427, HepG2 and CAOV3) was measured by

FACS. Targeted cells were labeled using 0.5 μM CFSE (Sigma, 21888) at 37°C in PBS for 10min. 2×10^5 CFSE-stained target cells were seeded into 96-well U-bottom plates in triplicate and subsequently mixed with expanded NK cells at the indicated effector-to-target ratios. Co-cultured cells were stained with 7-AAD (ThermoFisher, A1310) according to the manufacturer's instructions. Dead target cells were detected as double-positive CFSE/7-AAD cells.

In vivo cytotoxicity assays were performed by quantification of xenograft tumor burden after NK cells administration. Optical images were analyzed using Living Image 4.3 software (PerkinElmer) as described previously (11).

Western-Blot

The cells were lysed with cell lysis buffer (CST, 9803) supplemented with a protease inhibitor cocktail (Roche, 11873580001). The total protein concentration was measured using the BCA assay (Pierce, 23225). Proteins were separated by SDS-PAGE and then electrophoretically transferred onto nitrocellulose membranes. Subsequently, the blots were incubated with primary antibodies at 4°C overnight, then incubated with HRP conjugated secondary antibodies at room temperature for 2 hours. ECL reagent was used for imaging the blots (12). The antibody was obtained from CST: *#9936T* for NF-κB assay, *#41658* for TRAF5, *#15123* for OX40 and *#19541* for 4-1BB; #7074 and #7074 HRP-linked Abs for secondary antibodies.

Ex Vivo Expansion of Human NK Cells

Purified NK cells were cultured in AIM-V Medium (GIBCO, 12055091) supplemented with indicated cytokines or irradiated feeder cells (1:5, 1000cGry for NK92 and 5000cGy for K562). Cultures were refreshed with half-volume media changes every three days and re-stimulated using feeder cells at a ratio of 1:1 every 7 days. When needed, a fraction of expanded NK cells were cryopreserved or discarded, and the remaining cells were carried forward for subsequent stimulations.

Analysis of NK Cell Function

ELISA: The cell supernatant of feeder cells or cytotoxicity assay was collected to measure the levels of IFN-γ or Neo-2/15(Flag-tag) using their respective kits according to standard practice (R&D #DIF50C for IFN-γ, Abcam#ab125243 for Neo-2/15).

Flow cytometry: Flow cytometry was performed using the BD FACSAria system. Cells were incubated with indicated antibodies for 30 min at 4°C avoiding light. Cells were washed with DPBS and resuspended in FACS buffer before being subjected to FACS assay. Data were analyzed using FlowJo (version 10). The antibodies were from BioLegend and listed as follows: anti-CD107a-APC (328620), anti-OX40L-PE (326308), anti-CD56-PE (355504), anti-CD56-AlexaFluor488 (362518), anti-CD16-FITC (302006), anti-CD94-PE/Cy7 (305516), anti-NKG2A-APC (375108), anti-NKG2C-PE (375004), anti-NKG2D-FITC (320820), anti-KIR2DL2/L3-Percp/Cy5.5 (312614), anti-KIR2DL1/S1/S3/S5-FITC (339504), anti-KIR3DL-BrilliantViolet421(312714), anti-NKp30-BrilliantViolet785 (325230), anti-NKp44-PE/Cy7 (325116), anti-NKp46-BrilliantViolet605 (137619).

Regulatory Approvals

Peripheral blood used in this study was provided by M.G, C.S, Y.Q, L.Z and N.T in the author list (age 26~33). The experiments using primary NK cells were performed according to the guidelines of human subjects at Navy Medical University and approved by Scientific Investigation Board. All animal experiments were approved by the Scientific Investigation Board of Navy Medical University (Shanghai, China).

Statistical Analysis

A two-tailed unpaired, student *t-test* was used to determine significance. One-way ANOVA with a Bonferroni post-test was used to compare the different groups. Survival analysis was performed by Kaplan-Meier survival analysis.

RESULTS

The Stimulatory Effect of Feeder Cells With Secretory Neoleukin-2/15 on Human Natural Killer Cells

Neo-2/15 has been reported as a type of IL-2 mimic, which binds to human IL-2Rβγ with extremely high affinity (Kd=18.8nM) and cause significant expansion of T cells at low doses (5). To determine the Neo-2/15 effect on NK cell expansion, dose-dependent experiments were performed, and the fold expansion of NK cells with Neo-2/15 was higher than cells with IL-2, even at a concentration of 1.25ng/mL. This allowed NK cell expansion to solely rely on feeder-derived cytokines (**Figure 1A**).

To identify cell lines that could be beneficial in promoting NK cell expansion, K562 cells and NK-92 cells, stably transfected with Neo-2/15 lentivirus particles, were constructed and individual clones were picked. Neo-2/15 expression in the clones was identified by FACS. Clone NK92-N02 and N10, clone K562-K13 and K14 showed higher expression of Neo-2/15 (**Figures 1B, C**). Then the life-span of irradiated feeder cells in the AIM-V medium was measured by CCK8 assay. The cell viability of irradiated N02 and N10 cells was slightly lower than that of K13 and K14 cells after 6 days (**Figure 1C**). However, Neo-2/15 production in the supernatants showed no significant difference (**Figure 1D**).

Subsequently, we compared the fold expansion and NK cells cytotoxicity after co-culture with either K562-Neo2/15 (K13) or NK92-Neo2/15 (N02) feeder cells. Compared with NK92-Neo2/15, the fold expansion of NK cells co-cultured with K562-Neo2/15 was slightly higher by the end of the third week (**Figure 1E**), but NK92-Neo-2/15 expanded NK cells had greater cytotoxicity (**Figure 1F**). A possible explanation is that K562 could produce minimal amounts of TGF-β after co-culture with NK-cells (**Supplementary Figure 1**).

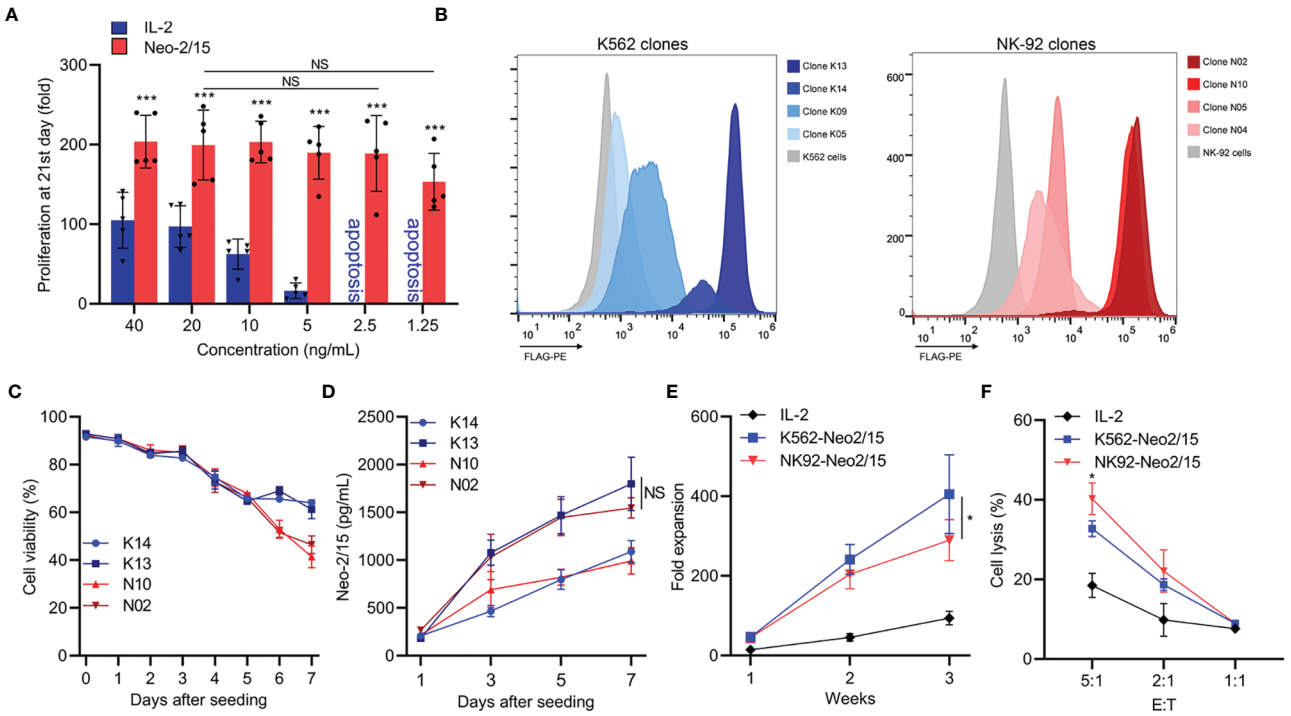

FIGURE 1 | Generation and characterization of feeder cells expressing secretory Neoleukin-2/15 (*p<0.05, ***p<0.001; NS indicates no significant difference). **(A)** In vitro expansion of the NK cells from 5 volunteers by IL-2 or Neo-2/15 at the indicated concentration. **(B)** Genetically Engineered K562 or NK92 clones expressing secretory neoleukin-2/15 were analyzed by flow cytometry. **(C)** The survival of irradiated clones cultured in AIM-V medium and examined over one week. **(D)** Neo-2/15 secretion by indicated clones was measured. **(E)** NK cells were co-cultured with irradiated K562-Neo2/15 or NK92-Neo2/15, cell expansion fold was measured. **(F)** Cytotoxicity assay to measure NK-mediated cell killing in Raji cell at indicated effector-to-target ratios.

OX40L Armed Feeder Cells Improve NK Cell Expansion

The optimal proliferation of NK cells requires both costimulatory signals and cytokines. TNFR superfamily mediated signal transduction has been reported to be involved in this process, including 4-1BB and OX40. To furtherly improve the expansion and cytotoxicity of NK cells, we transferred 4-1BBL or OX40L into NK92-Neo2/15 cells and selected two clones with similar expression levels (**Figure 2A**). The NK92-Neo2/15-OX40L-supported NK cells showed higher fold expansion compared to NK92-Neo2/15-41BBL-supported (1767-2719 *vs.* 833-2275 fold) at the third week (**Figure 2B**). Cytotoxicity of the expanded NK cells was then tested against Raji targets. Target cell lysis was significantly increased after NK92-Neo2/15-OX40L expanded NK treatment at a 5:1 E/T ratio (**Figure 2C**). Consistently, NK92-Neo2/15-OX40L-supported cells presented a higher positive rate of CD107a, and IFN-γ production in the supernatant (**Figures 2D, E**). We evaluated the cytotoxicity of expanded NK cells from three donors against a panel of human tumor cell lines for liver cancer, lung cancer, and ovarian cancer cell lines. We found moderate to high cytotoxicity against all cell lines tested (**Figure 2F**).

We next examined the phenotypes of expanded NK cells expanded upon NK92-Neo2/15-OX40L or IL-2 treatment. The data indicated that proportions of $CD16^+$ NK cells, which are responsible for cytotoxicity, increased in NK92-Neo2/15-OX40L group (**Figure 3A**). Two inhibitory receptors, NKG family member NKG2A and KIR family member KIR2DL2/L3, were less expressed in NK92-Neo2/15-OX40L group (**Figures 3B, C**). NKp44 and NKp46 from NCR family which mediate cytolytic activity against target cells presented a higher expression in NK92-Neo2/15-OX40L group (**Figure 3D**).

OX40 and OX40L Are Highly Induced on NK Cells During Expansion With NK92-Neo2/15-ox40l

To gain insights into the mechanism of NK cell proliferation mediated by OX40L, 4-1BBL or OX40L were overexpressed in NK-92 cells, and two clones with similar expression levels were selected (**Supplementary Figure 2A**) and the doubling time of feeder cells was shown in **Supplementary Figure 2B**. The cells were used as feeders and combined with IL-2 or Neo-2/15 to treat NK cells. Western blotting analysis showed that neither OX40L nor 4-1BBL modified feeder was able to effectively activate NF-κB when combined with IL-2. Notably, NK92-

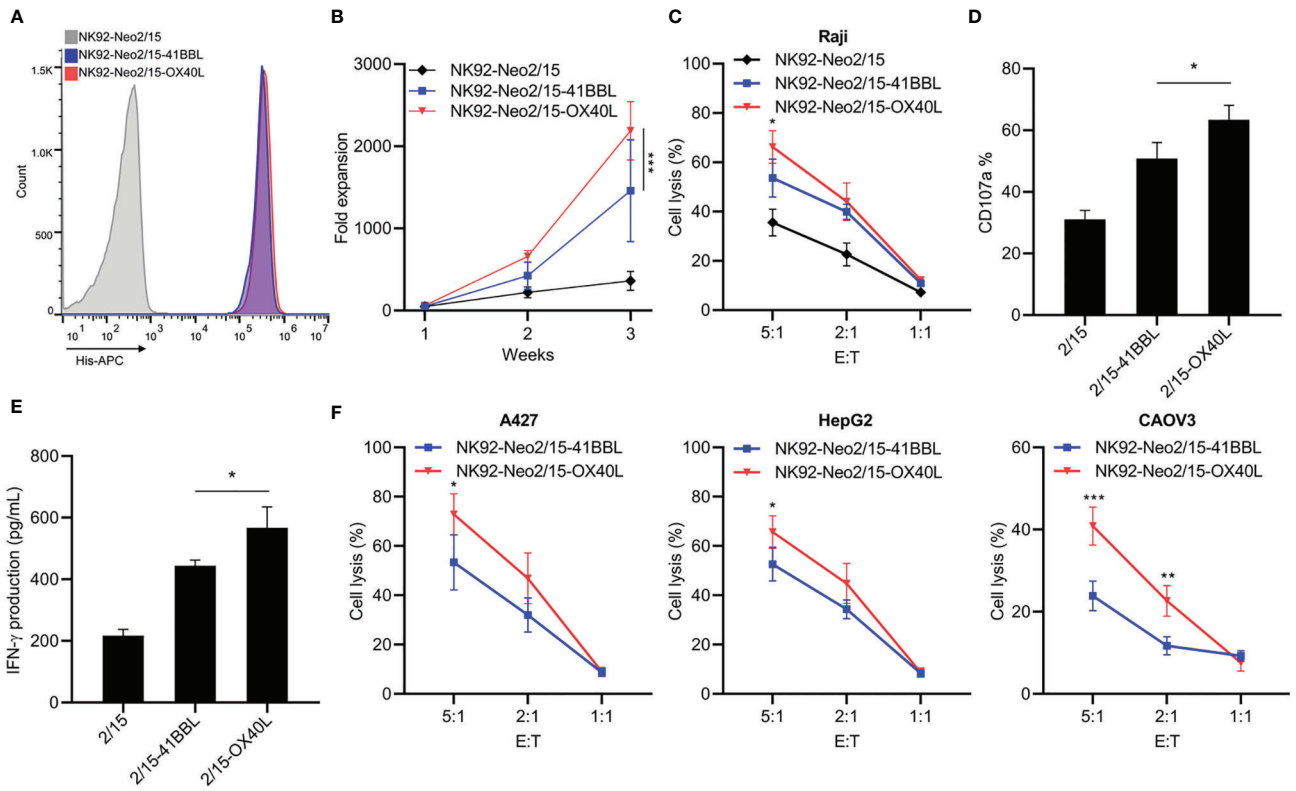

FIGURE 2 | Generation and characterization of OX40L or 4-1BBL armed feeder cells (*p<0.05, **p<0.01, ***p<0.001). **(A)** Genetically knock-in OX40L or 4-1BBL in NK92-Neo2/15 clone N02 and analyzed by flow cytometry. **(B)** NK cells co-cultured with irradiated NK92-Neo2/15-41BBL or NK92-Neo2/15- OX40L, cell expansion fold was measured. **(C)** Cytotoxicity assay to measure NK92-Neo2/15-41BBL or NK92-Neo2/15- OX40L expanded NK cells in Raji cell. **(D)** NK cell activation of E:T=5:1 was determined by FACS staining for CD107a expression. **(E)** IFN-γ production in the supernatants of E:T=5:1 were evaluated by ELISA. **(F)** *In vitro* cytotoxicity assay to measure NK92-Neo2/15-41BBL or NK92-Neo2/15- OX40L expanded NK cells in A427, HepG2 and CAOV3 cells.

OX40L can more strongly activated NF-κB when combined with Neo-2/15 (**Figure 4A**). Subsequently, Neo-2/15 stimulated NK cells from five donors, then 4-1BB and OX40 expression was determined by western blot analysis. Neo-2/15 was found to strongly induce the OX40 expression on the NK cell surface (**Figure 4B**). Although 4-1BB expression was also promoted, the fold-change was significantly lower compared with OX40 (**Figure 4C**). In addition, immunoblotting was performed to detect TRAF5, p-p65, and total p65 in OX40 cascade at indicated day after NK92-Neo2/15-OX40L feeder co-culture. Continuous activation of OX40 cascade in expanded NK cells is shown in **Figure 4D**.

To dissect the mechanism of OX40/OX40L interaction, flow cytometry was performed to investigate the OX40L expression following NK92-Neo2/15-OX40L co-culture. After three days of co-culture, more than 90% of expanded NK cells had positive OX40L expression (**Figure 4E**). Finally, we added IL-2 expanded cells or NK92-Neo2/15-OX40L expanded cells to Neo-2/15 pre-treated NK cells. Immunoblotting showed that NK92-Neo2/15-OX40L-supported cells significantly promoted p65 phosphorylation (**Figure 4F**), further demonstrating that NK92-Neo2/15-OX40L induced OX40 and OX40L expression on NK cells and promoted OX40-OX40L positive feedback loop.

Importantly, we compared NK92-Neo2/15-OX40L expansion ability with NK92-OX40L plus IL-2/IL-15 or NK92-OX40L plus IL-2/IL-21, results indicated NK92-Neo2/15-OX40L performed maximum expansion (**Supplementary Figure 3**).

NK92-Neo2/15-OX40L Improves NK Cells Antitumor Activity *In Vivo*

To evaluate the therapeutic efficacy of NK92-Neo2/15-OX40L expanded NK cells *in vivo*, killing assays were performed on HepG2 (liver cancer), A427 (lung cancer) and CAVO3 (ovarian cancer) derived xenograft models. Here, we compared IL-2 expanded cells and NK92-Neo2/15-OX40L expanded cells. To allow the most consistent comparisons between multiple cancers and across multiple tumors bearing mice, NK cells from the same donor were used. The expansion began 14 days before modeling, and tumor growth was monitored by bioluminescent imaging (**Figure 5A**). Compared with untreated tumor-bearing mice, three murine models treated with NK cells showed a significant reduction in tumor burden after 14 days, with maximal anti-tumor activity seen in NK92-Neo2/15-OX40L-supported cells (**Figures 5B–D**). Increased numbers of infiltrating $CD56^+$ cells were also present in the Feeder-expanded NK treated xenografts (**Supplementary Figure 4**).

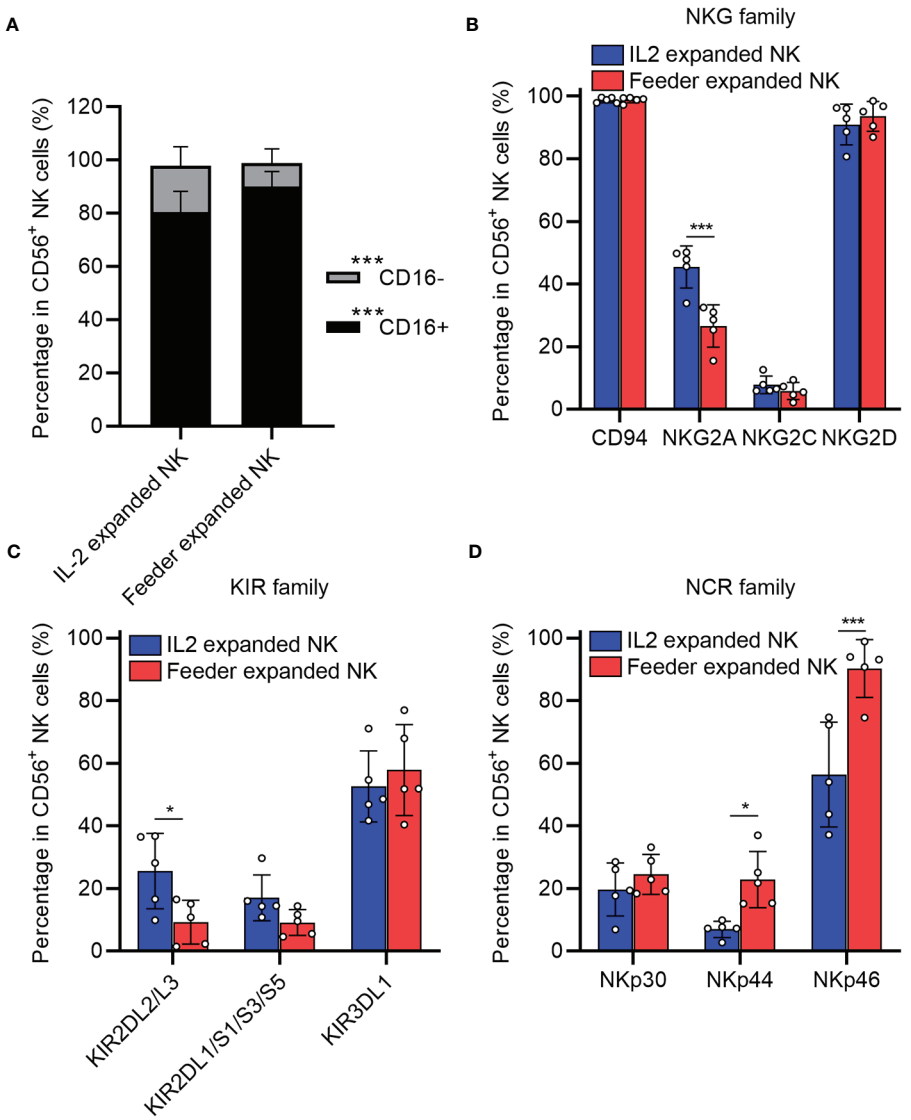

FIGURE 3 | Phenotypic profiling of feeder expanded NK cells (*$p < 0.05$, ***$p < 0.001$). **(A)** Frequency of $CD16^-$ and $CD16^+$ NK cell subsets in the expanded cells. **(B)** Expression of natural killer receptors (NKG, CD94/NKG2A/NKG2C/NKG2D) in the expanded cells. **(C)** Expression of killer inhibitory receptors (KIRs, KIR2DL1/L2/L3/S1/S3/S5/KIR3DL1) in the expanded cells. **(D)** Expression of natural cytotoxicity triggering receptor (NCRs, NKp30/NKp44/NKp46) in the expanded cells.

DISCUSSION

Numerous studies of adoptive transfer of NK cells have indicated responses in a wide range of malignancies (13, 14). However, the large-scale clinical application of NK cell immunotherapy has been limited by the lack of robust and low-cost methods for cell expansion. Here, we designed and evaluated a novel cytokine-free method using feeder cells to expand human PBMC-derived NK cell's proliferation ability and cytotoxic function.

IL-2 family cytokines are essential for the proliferation and activation of NK cells (2–4). IL-2 is the most commonly used cytokines for NK cell expansion, but IL-2 dose potentially promotes Treg expansion, which contributes to tumor tolerance (4). Substitution of cytokines such as IL-15 or IL-21 may also help in Treg expansion, but inducible NKG2A expression can weaken NK cell cytotoxicity (15). In addition, natural IL-2 family cytokines lack both stability and high affinity to IL-2Rβγ, resulting in continuous supplementation of cytokines in long-term cultivation. Neo-2/15 is reported to be a hyper-stable artificial peptide, binding human IL-2Rβγ with higher affinity than the natural cytokines, and maintains T cell proliferation at a concentration of 3.1 ng/mL (5). Our results showed that Neo-2/15 can significantly promote NK cell proliferation even at a concentration of 1.25ng/mL, while a similar concentration of IL-2 could not even maintain NK cell survival. This data allowed us to consider the use of feeder cells to maintain a cytokine-free culture system.

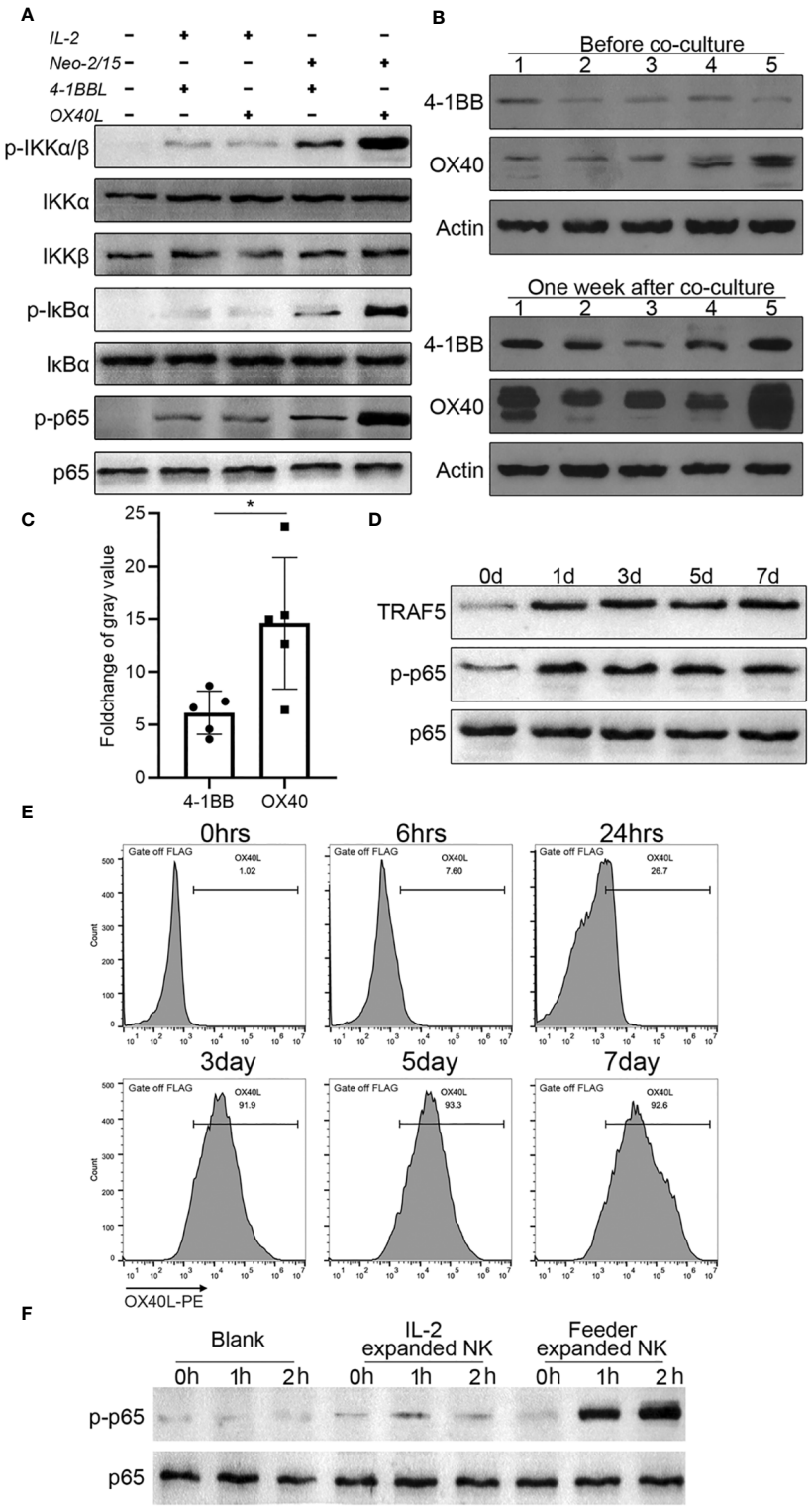

FIGURE 4 | NK92-Neo2/15-OX40L promotes an OX40-OX40L positive feedback loop (*p < 0.05). **(A)** Western-blot detection of NK-κB activation for indicated treatment. **(B)** 4-1BB and OX40 expression in expanded NK cells from 5 donors, measured by Western-blot before and after feeder cell treatment. **(C)** Relative gray value statistics of protein level in **(B)**. **(D)** Immunoblot of TRAF5, phosphorylated-p65, and p65 was detected. **(E)** FACS analysis of OX40L expression on expanded NK. **(F)** NK cells from PBMC, treated by IL-2 or NK92-Neo2/15-OX40L expanded NK cells at a ratio of 19:1, freshly collected NK cells were used as control. Phosphorylated p65 were determined by western blot.

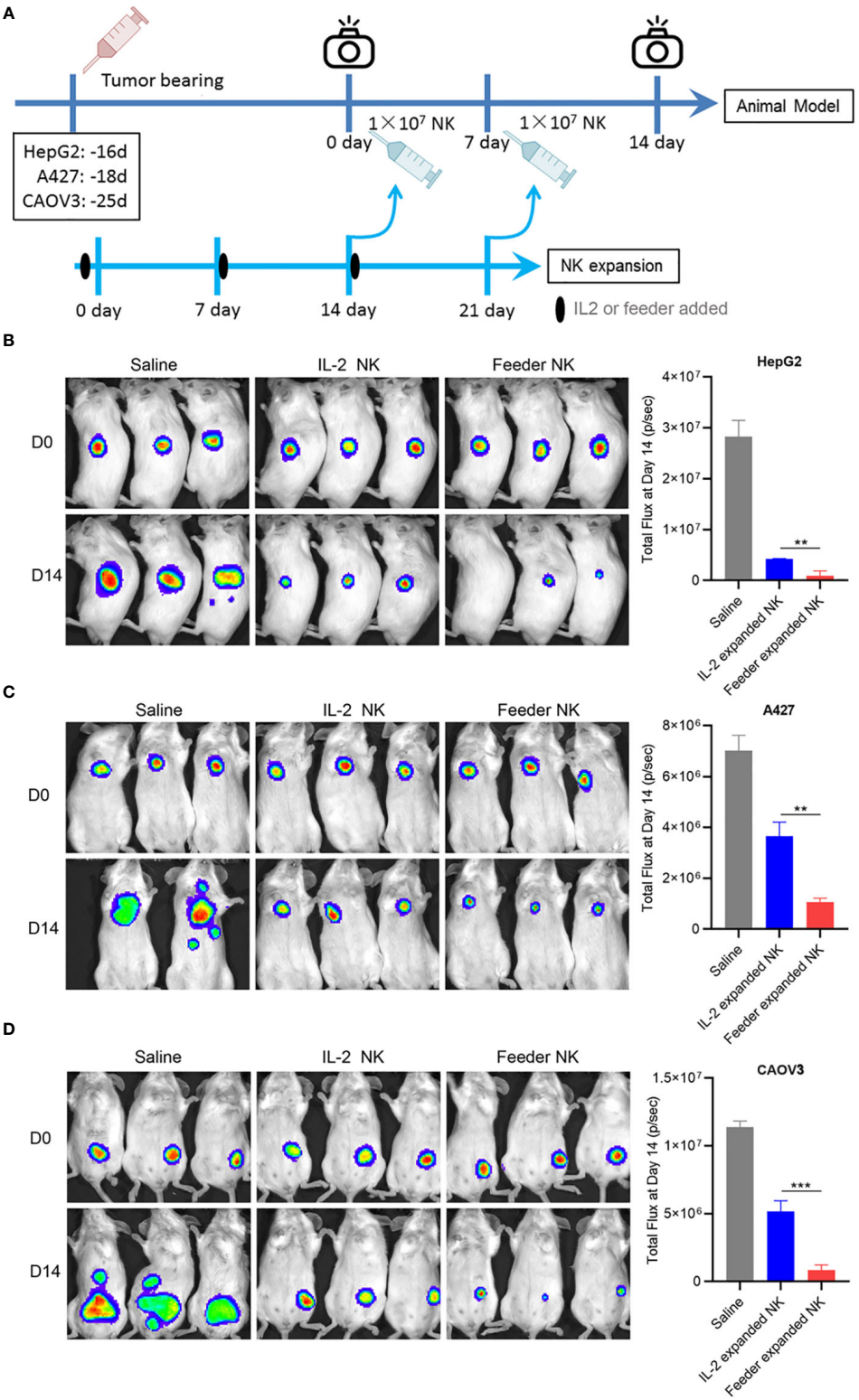

FIGURE 5 | NK92-Neo2/15-OX40L improves antitumor activity of NK cells *in vivo* (**p < 0.01, ***p < 0.001). **(A)** Experimental setup schematics. **(B)** NOD/SCID mice treated as in **(A)**, HepG2 tumors were visualized by IVIS SpectrumCT, and the tumor size was assessed by bioluminescence. **(C)** NOD/SCID mice treated as in **(A)**, A427 tumors were visualized by IVIS SpectrumCT, and the tumor size was assessed by bioluminescence. **(D)** NOD/SCID mice treated as in **(A)**, CAOV3 tumors were visualized by IVIS SpectrumCT, and the tumor size was assessed by bioluminescence.

Several cancer cell lines, like human myelogenous leukemia K562 and human Burkitt's lymphoma cell line Daudi, have been used as feeder cells for NK expansion (6, 7). Nevertheless NK-92, an NK cell line assessed in numerous clinical immunotherapy trials, has not been used as feeder cells. In this study, we used NK-92 as a candidate for expanding NK cells and compared it with K562. Although the NK92-based feeder showed slightly lower expansion potential than K562, the expanded cells had higher cytotoxic activity. This difference may be related to the expression of TGF-β in K562 cells, which is consistent with a previous study reporting that K562 reduced the cytotoxic activity of certain subpopulations of NK cells (8, 9). Therefore, although NK-92 as a feeder cell has a slightly lower ability to expand NK cells than that K562, it has significant advantages in enhancing cytotoxic activity.

IL-2R cascade appears to be necessary but not the only source for NK expansion, and costimulatory signals are also required for optimal proliferation (16). TNFR superfamily ligands (TNFRSFL) are key co-stimulants for the preferential expansion of NK cells. Fujisaki H et al. reported a 21.6-fold expansion of NK cells after co-culture with modified K562 to express membrane-bound form IL-15 and 41BBL (7). In addition, OX40L, a member of TNFRSF, has also been reported to promote NK cell function *via* the OX40 cascade (17–19). Based on NK92-Neo2/15, we furtherly constructed two feeder cells NK92-Neo2/15-41BBL and NK92-Neo2/15-OX40L. Results showed that NK92-Neo2/15-OX40L expanded NK cells not only exhibited higher proliferative and cytotoxic capacity but also mediated significantly higher secretion levels of IFN-γ when compared to NK92-Neo2/15-41BBL expanded cells. OX40L and Neo2/15 were found to be the best combination for NK cell production and expansion.

Studies have shown that both 4-1BB and OX40 are expressed on the surface of activated NK cells, and their expression intensity is regulated by activation signals (17, 20). Our study found that the expression of OX40 in NK cells was strongly induced by Neo-2/15 compared with the 4-1BB signal. This phenomenon can partially explain why is OX40L is more efficient in promoting NK cell proliferation. However, feeder cells added weekly may not provide sufficient OX40L for rapid cell proliferation. Previous studies reported inducible OX40L expression on activated NK cells (21). Consistently, in this study, we observed the same phenomenon that NK92-Neo2/15-OX40L induced the expression of OX40L on NK cells. Over 90% of NK cells were OX40L positive after co-culture. Notably, co-incubation of PBMC-derived NK cells with feeder-expanded NK could also activate the NK-κB pathway. This evidence indicates that NK92-Neo2/15-OX40L significantly induces the expression of OX40 and OX40L on the surface of NK cells and form a positive feedback loop.

Solid tumors, unlike hematological malignancies, have a complex immune microenvironment which blocks NK cells infiltration and subsequently caused the limited efficacy against solid tumors (13). Our *in vivo* results showed that NK92-Neo2/15-OX40L expanded NK cells showed stronger infiltration ability and initiate a marked higher antitumor effect compared with IL-2 expanded NK cells. In conclusion, the NK92-Neo2/15-OX40L feeder triggers the expansion of NK cells with highly cytotoxicity through the formation of an OX40L/OX40 positive feedback loop. Therefore, this study provides a novel NK cell expansion mechanism and insights into OX40-OX40L axis regulation of NK cell expansion.

DATA AVAILABILITY STATEMENT

The raw data supporting the conclusions of this article will be made available by the authors, without undue reservation.

ETHICS STATEMENT

The studies involving human participants were reviewed and approved by Scientific Investigation Board of Navy Medical University. The patients/participants provided their written informed consent to participate in this study. The animal study was reviewed and approved by Scientific Investigation Board of Navy Medical University.

AUTHOR CONTRIBUTIONS

YL, FG, and JZ designed this study and supervised the research. MG and CS performed the research, analyzed data, and wrote the paper. YQ contributed in animal model and IVIS. LZ and NT contributed in technical support. GW contributed in improvement of language and artwork. All authors contributed to the article and approved the submitted version.

FUNDING

This work was supported by the National Natural Science Foundation of China (No.82071799, No.81972683, and No.81971503) and Shanghai Science and Technology Development Funds (No.20ZR1469900).

ACKNOWLEDGMENTS

We thank Chenxi Guo, junior high school student from Junior Middle School of No. 2 High School Affiliated to East China Normal University, for helping cell culture and plasmid preparation.

SUPPLEMENTARY MATERIAL

The Supplementary Material for this article can be found online at: https://www.frontiersin.org/articles/10.3389/fonc.2021.632540/full#supplementary-material

REFERENCES

1. Lee DA. Cellular therapy: Adoptive immunotherapy with expanded natural killer cells. *Immunol Rev* (2019) 290(1):85–99. doi: 10.1111/imr.12793
2. Dunne J, Lynch S, O'Farrelly C, Todryk S, Hegarty JE, Feighery C, et al. Selective expansion and partial activation of human NK cells and NK receptor-positive T cells by IL-2 and IL-15. *J Immunol* (2001) 167(6):3129–38. doi: 10.4049/jimmunol.167.6.3129
3. Parrish-Novak J, Dillon SR, Nelson A, Hammond A, Sprecher C, Gross JA, et al. Interleukin 21 and its receptor are involved in NK cell expansion and regulation of lymphocyte function. *Nature* (2000) 408(6808):57–63. doi: 10.1038/35040504
4. Ageitos AG, Singh RK, Ino K, Ozerol I, Tarantolo S, Reed EK, et al. IL-2 expansion of T and NK cells from growth factor-mobilized peripheral blood stem cell products: monocyte inhibition. *J Immunother* (1998) 21(6):409–17. doi: 10.1097/00002371-199811000-00002
5. Silva DA, Yu S, Ulge UY, Spangler JB, Jude KM, Labao-Almeida C, et al. De novo design of potent and selective mimics of IL-2 and IL-15. *Nature* (2019) 565(7738):186–91. doi: 10.1038/s41586-018-0830-7
6. Denman CJ, Senyukov VV, Somanchi SS, Phatarpekar PV, Kopp LM, Johnson JL, et al. Membrane-bound IL-21 promotes sustained ex vivo proliferation of human natural killer cells. *PloS One* (2012) 7(1):e30264. doi: 10.1371/journal.pone.0030264
7. Fujisaki H, Kakuda H, Shimasaki N, Imai C, Ma J, Lockey T, et al. Expansion of highly cytotoxic human natural killer cells for cancer cell therapy. *Cancer Res* (2009) 69(9):4010–7. doi: 10.1158/0008-5472.CAN-08-3712
8. Jewett A, Bonavida B. Target-induced anergy of natural killer cytotoxic function is restricted to the NK-target conjugate subset. *Cell Immunol* (1995) 160(1):91–7. doi: 10.1016/0008-8749(95)80013-9
9. Jewett A, Cavalcanti M, Bonavida B. Pivotal role of endogenous TNF-alpha in the induction of functional inactivation and apoptosis in NK cells. *J Immunol* (1997) 159(10):4815–22.
10. Guo M, Han S, Liu Y, Guo W, Zhao Y, Liu F, et al. Inhibition of allogeneic islet graft rejection by VISTA-conjugated liposome. *Biochem Biophys Res Commun* (2019) 516(3):914–20. doi: 10.1016/j.bbrc.2019.05.188
11. Liu Y, Gu Y, Han Y, Zhang Q, Jiang Z, Zhang X, et al. Tumor Exosomal RNAs Promote Lung Pre-metastatic Niche Formation by Activating Alveolar Epithelial TLR3 to Recruit Neutrophils. *Cancer Cell* (2016) 30(2):243–56. doi: 10.1016/j.ccell.2016.06.021
12. Teng F, Guo M, Liu F, Wang C, Dong J, Zhang L, et al. Treatment with an SLC12A1 antagonist inhibits tumorigenesis in a subset of hepatocellular carcinomas. *Oncotarget* (2016) 7(33):53571–82. doi: 10.18632/oncotarget.10670
13. Chiossone L, Dumas PY, Vienne M, Vivier E. Natural killer cells and other innate lymphoid cells in cancer. *Nat Rev Immunol* (2018) 18(11):671–88. doi: 10.1038/s41577-018-0061-z
14. Guillerey C, Huntington ND, Smyth MJ. Targeting natural killer cells in cancer immunotherapy. *Nat Immunol* (2016) 17(9):1025–36. doi: 10.1038/ni.3518
15. Andre P, Denis C, Soulas C, Bourbon-Caillet C, Lopez J, Arnoux T, et al. Anti-NKG2A mAb Is a Checkpoint Inhibitor that Promotes Anti-tumor Immunity by Unleashing Both T and NK Cells. *Cell* (2018) 175(7):1731–43.e13. doi: 10.1016/j.cell.2018.10.014
16. Granzin M, Wagner J, Kohl U, Cerwenka A, Huppert V, Ullrich E. Shaping of Natural Killer Cell Antitumor Activity by Ex Vivo Cultivation. *Front Immunol* (2017) 8:458. doi: 10.3389/fimmu.2017.00458
17. Pollmann J, Gotz JJ, Rupp D, Strauss O, Granzin M, Grunvogel O, et al. Hepatitis C virus-induced natural killer cell proliferation involves monocyte-derived cells and the OX40/OX40L axis. *J Hepatol* (2018) 68(3):421–30. doi: 10.1016/j.jhep.2017.10.021
18. Kweon S, Phan MT, Chun S, Yu H, Kim J, Kim S, et al. Expansion of Human NK Cells Using K562 Cells Expressing OX40 Ligand and Short Exposure to IL-21. *Front Immunol* (2019) 10:879. doi: 10.3389/fimmu.2019.00879
19. Turaj AH, Cox KL, Penfold CA, French RR, Mockridge CI, Willoughby JE, et al. Augmentation of CD134 (OX40)-dependent NK anti-tumour activity is dependent on antibody cross-linking. *Sci Rep* (2018) 8(1):2278. doi: 10.1038/s41598-018-20656-y
20. Ward-Kavanagh LK, Lin WW, Sedy JR, Ware CF. The TNF Receptor Superfamily in Co-stimulating and Co-inhibitory Responses. *Immunity* (2016) 44(5):1005–19. doi: 10.1016/j.immuni.2016.04.019
21. Zingoni A, Sornasse T, Cocks BG, Tanaka Y, Santoni A, Lanier LL. Cross-talk between activated human NK cells and CD4+ T cells via OX40-OX40 ligand interactions. *J Immunol* (2004) 173(6):3716–24. doi: 10.4049/jimmunol.173.6.3716

Conflict of Interest: The authors declare that the research was conducted in the absence of any commercial or financial relationships that could be construed as a potential conflict of interest.

frontiers in Cell and Developmental Biology

ORIGINAL RESEARCH
published: 21 April 2021
doi: 10.3389/fcell.2021.670019

α-Enolase Lies Downstream of mTOR/HIF1α and Promotes Thyroid Carcinoma Progression by Regulating CST1

Yang Liu, Lida Liao, Changming An, Xiaolei Wang, Zhengjiang Li, Zhengang Xu, Jie Liu and Shaoyan Liu**

Department of Head and Neck Surgical Oncology, National Cancer Center/National Clinical Research Center for Cancer/Cancer Hospital, Chinese Academy of Medical Sciences and Peking Union Medical College, Beijing, China

Novel therapy strategies are crucial for thyroid carcinoma treatment. It is increasingly important to clarify the mechanism of thyroid carcinoma progression. Several studies demonstrate that α-Enolase (ENO1) participates in cancer development; nevertheless, the role of ENO1 in thyroid carcinoma progression remains unclear. In the present study, we found that the expression of ENO1 was upregulated in thyroid carcinoma samples. Proliferation and migration of thyroid carcinoma cells were suppressed by depletion of ENO1; conversely, ENO1 overexpression promoted thyroid carcinoma cell growth and invasion. To elucidate the mechanisms, we found that the hypoxia-related mTOR/HIF1 pathway regulated ENO1 expression. ENO1 regulated the expression of CST1; knockdown of CST1 reversed the tumorigenicity enhanced by ENO1 overexpression. Taken together, our findings provide a theoretical foundation for thyroid carcinoma treatment.

Keywords: ENO1, thyroid carcinoma, CST1, mTOR, HIF1α

OPEN ACCESS

Edited by:
Kevin J. Ni,
St. George Hospital, Australia

Reviewed by:
Xiaofang Xing,
Peking University Cancer Hospital, China
Xuan Zhou,
Tianjin Medical University Cancer Institute and Hospital, China

****Correspondence:***
Shaoyan Liu
ncclsy@126.com
Jie Liu
liuj@cicams.ac.cn

Specialty section:
This article was submitted to Molecular and Cellular Oncology, a section of the journal Frontiers in Cell and Developmental Biology

Received: *19 February 2021*
Accepted: *29 March 2021*
Published: *21 April 2021*

Citation:
Liu Y, Liao L, An C, Wang X, Li Z, Xu Z, Liu J and Liu S (2021) α-Enolase Lies Downstream of mTOR/HIF1α and Promotes Thyroid Carcinoma Progression by Regulating CST1. Front. Cell Dev. Biol. 9:670019. doi: 10.3389/fcell.2021.670019

INTRODUCTION

The thyroid gland is the largest endocrine organ in humans; it regulates systemic metabolism (Kondo et al., 2006). Thyroid carcinoma (THCA) is the most frequent malignancy in endocrine organs (Hundahl et al., 1998; Parkin et al., 2005; Kondo et al., 2006; Sipos and Mazzaferri, 2010). More than 85% of thyroid carcinomas arise from follicular epithelial cells, most of which are indolent tumors that can be cured with surgical resection or a combination of radioactive-iodine ablation (Kondo et al., 2006; Paschke et al., 2015). Nevertheless, there is a subset of aggressive thyroid tumors that cannot be treated effectively with current therapies (Kondo et al., 2006). To more efficiently manage thyroid carcinomas, additional effective therapeutic strategies are needed.

A better understanding of thyroid carcinoma means better diagnosis and effective therapy; thus, thyroid carcinoma mortality will further decrease. Over recent decades, the increased incidence of thyroid carcinoma is most likely the result of a better understanding of the genetic pathogenesis and more efficient detection methods (Kondo et al., 2006; Sipos and Mazzaferri, 2010; La Vecchia et al., 2015; Davies, 2016). For example, the incidence increased 311% from 1975 to 2013 in the United States and 150% from 1998 to 2010 in Germany (Paschke et al., 2015; Lim et al., 2017). Meanwhile, thyroid carcinoma mortality has declined (Sipos and Mazzaferri, 2010;

La Vecchia et al., 2015; Paschke et al., 2015), primarily due to more sensitive diagnostic tools and more effective therapies, especially rapidly emerging novel targeted strategies (Sipos and Mazzaferri, 2010; La Vecchia et al., 2015). Thus, there is a very high 5-year survival rate (93% for women and 88% for men) for well-differentiated thyroid carcinoma (Paschke et al., 2015).

Clarifying the mechanism of thyroid carcinoma progression is critical for targeted therapy strategy. To date, at least four thyroid carcinoma types have been reported: papillary thyroid carcinoma (PTC), follicular thyroid carcinoma (FTC), anaplastic thyroid carcinoma, and medullary thyroid carcinoma (Sipos and Mazzaferri, 2010; Saiselet et al., 2012). Various mutations causing increased cellular proliferation and dedifferentiation have been characterized for each thyroid carcinoma type (Catalano et al., 2010). *BRAF* point mutations and RET/PTC rearrangements account for 40–60% and 20% of PTC, respectively; these markers can be used to diagnose and treat the most aggressive PTC (Kondo et al., 2006; Xing, 2010). For FTC, the most frequent mutations are RAS point mutations (45% of cases) and PAX8/PPARγ rearrangements (35% of cases). For RAS mutations, MAPK and PI3K pathways could be therapeutic targets (Saavedra et al., 2000; Mitsutake et al., 2005; Knauf et al., 2006). Other mutations have also been described in FTC, including the tumor suppressor gene PTEN (10% of cases) and the PI3KCA oncogenes (10% of cases) (Saiselet et al., 2012). Nevertheless, these are insufficient; more targeted genes and pathways need to be identified.

Cancer cell prefers to metabolize glucose through glycolysis pathway even when oxygen is abundant, a phenomenon called "aerobic glycolysis" or "Warburg effect" (Koppenol et al., 2011). Aerobic glycolysis is driven by activation or upregulation of glycolytic enzymes, such as hexokinase (HK) isoforms, enolase (ENO), and pyruvate kinase (PK). It is well documented that HK2/PKM2 activation of glycolysis contributes to the development of thyroid carcinoma (Coelho et al., 2018). However, the significance of a-Enolase (ENO1) is less unknown in thyroid carcinogenesis. ENO1 is another critical enzyme of the glycolytic pathway expressed in nearly all kinds of tissues (Pancholi, 2001; Zakrzewicz et al., 2014). ENO1 plays critical and multifunctional roles in various physiological and pathological processes (Pancholi, 2001; Ejeskar et al., 2005; Diaz-Ramos et al., 2012; Principe et al., 2015; Capello et al., 2016), including tumorigenesis, cancer invasion, and metastasis (Hsiao et al., 2013; Song et al., 2014). Upregulation of ENO1 was detected in cancers of the stomach, breast, lung, colorectal, brain, kidney, liver, pancreas, and eye, as well as in non-Hodgkin's lymphoma (Nakajima et al., 1986; Tu et al., 2010; Song et al., 2014; Fu et al., 2015; Liu et al., 2015; Principe et al., 2015; Zhu et al., 2015, 2018; Niccolai et al., 2016; Qian et al., 2017; Zhan et al., 2017). Ectopic ENO1 overexpression promoted tumor formation and tumor chemoresistance (Tu et al., 2010; Song et al., 2014; Fu et al., 2015; Principe et al., 2017; Qian et al., 2017; Zhan et al., 2017; Sun et al., 2019; Chen et al., 2020). Conversely, ENO1 silencing in tumor cells significantly decreased malignant biological behavior (Fu et al., 2015; Principe et al., 2015; Zhao et al., 2015; Capello et al., 2016; Cappello et al., 2017; Huang et al., 2019). Several lines of evidence suggest that ENO1 may be a therapeutic target for endometrial carcinoma (Principe et al., 2015; Zhao et al., 2015; Yin et al., 2018). Nevertheless, the role of ENO1 in human thyroid carcinoma and its putative targets have not been investigated. Therefore, exploring the upstream regulator, the downstream effector and the role of ENO1 in thyroid carcinoma can help the oncologists gain more insights into molecular events during the development of thyroid carcinoma.

mTOR (mechanistic target of rapamycin) is a master regulator of glucose metabolism whose action is mediated by activation of HIF1a (Majumder et al., 2004; Semenza, 2011; Chi, 2012; Cheng et al., 2014; Courtnay et al., 2015; Yang et al., 2015; Xiao et al., 2017). The hypoxia-related mTOR/HIF1α pathway also promotes cell proliferation and metastasis (Xiao et al., 2017; Wei et al., 2018; Pan et al., 2019; Zhang et al., 2019). Nevertheless, it is unclear whether the hypoxia-related mTOR/HIF1α pathway participates in thyroid carcinoma progression. CST1 (cystatin 1), a type 2 cystatin superfamily member, is a specific inhibitor of cysteine proteases (Dai et al., 2017; Oh et al., 2017; Jiang et al., 2018; Liu et al., 2019). Several studies demonstrated that CST1 was closely associated with cell proliferation and metastasis in various cancers, including cancer of the stomach, breast, colorectum, pancreas, and bile duct (Jiang et al., 2018; Cui et al., 2019; Liu et al., 2019; Wang et al., 2020). Wang et al. (2020) predicted that CST1 was a biomarker and therapeutic target for gastric cancer. Nevertheless, the role of CST1 in thyroid carcinoma has not yet been investigated.

In the present study, we demonstrated that ENO1 plays an oncogenic role in thyroid carcinoma progression. First, ENO1 was upregulated in thyroid carcinoma samples. Then, downregulation of ENO1 suppressed cell proliferation, invasion, and *in vivo* tumorigenicity by regulating the cell cycle and apoptosis. ENO1 overexpression promoted proliferation, invasion, and inhibited apoptosis. These findings suggested that ENO1 was an oncogene.

Regarding mechanism, we showed that ENO1 acted downstream of the hypoxia-related mTOR/HIF1a pathway. We demonstrated that ENO1 regulated CST1 expression and that these two proteins acted synergistically in thyroid carcinoma progression. In conclusion, we were the first to identify an oncogenic role of ENO1 in thyroid carcinoma; this will pave the way for a more efficient diagnosis and thyroid carcinoma therapy.

MATERIALS AND METHODS

Patients and Specimens

All clinical tissue samples from patients with PTC and normal adjacent tissues were obtained from populations in China and were collected at the Department of Head and Neck Surgical Oncology, Cancer Hospital, Chinese Academy of Medical Sciences and Peking Union Medical College between 2016 and 2019. The research was approved by the Ethics Committee of National Cancer Center/National Clinical Research Center for Cancer/Cancer Hospital, Chinese Academy of Medical Sciences and Peking Union Medical College and conducted under the guidance of the Declaration of Helsinki. Informed consent regarding the use of specimens was obtained from all patients.

Cell Culture and Transfection

TPC1 cells and BCPAP cells were cultured in DMEM/F-12 medium (Gibco, Thermo Fisher Scientific) supplemented with 2 mM glutamine, 10% fetal bovine serum (Gibco, Thermo Fisher Scientific), and 100 U/ml penicillin/streptomycin (Sigma, St. Louis, MO, United States). The cells were maintained at 37°C in a humidified atmosphere containing 5% CO_2. Rapamycin (Sirolimus) was purchased from Selleck (Shanghai, China).

The siRNAs of ENO1 and CST1 were purchased from GenePharma. siCtrl: 5′-UUCUCCGAACGUGUCACGU-3′; siENO1#1: 5′-CGUACCGCUUCCUUAGAACUU-3′; siENO1 #2:5′-GAAUGUCAUCAAGGAGAAAUA-3′; siCST1#1:5′-CC ACCAAAGAUGACUACUA-3′; siCST1#2:5′-GCUCUUUCGAG AUCUACGA-3′; siCST4#1:5′-CUUUCGAGAUCUACGAAGU UCTT-3′; siCST1#2:5′-CCAUCAGCGAGUACAACAATT-3′. According to the manufacturer's protocol, Lipofectamine RNAiMAX transfection reagent (Invitrogen; Thermo Fisher Scientific) was used for transfection of siRNA. Lipofectamine 3000 (Thermo Fisher Scientific) was used for plasmid overexpression.

CCK-8 Cell Viability Assay

CCK-8 reagent was purchased from Sigma. Cells seeded into a 96-well plate with a density of 2000 cells per well were maintained for the indicated days, followed by 10 μl CCK-8 reagent added to each well and incubated at 37°C for 3 h. The absorbance at 450 nm was measured using a microplate reader.

Colony Formation

TPC1 and BCPAP cells were seeded into 6-well plates at 1,000 cells/well, and fresh culture medium was changed every 3 days. Colonies formed after culturing the cells for 14 days. After washing in phosphate-buffered saline (PBS) three times, colonies were fixed in 4% paraformaldehyde for 20 min and stained with GIEMSA staining solution for 20 min. Groups of more than 50 cells were identified as colonies.

RNA Extraction, Reverse Transcription, and Quantitative Real-Time PCR (qRT-PCR)

TRIzol (Thermo Fisher Scientific) was used for the isolation of total RNAs from cells. The RNAs were reverse-transcribed using M-MLV-RTase (Promega) following the manufacturer's protocol. The qRT-PCR analysis was performed using SYBR Master Mixture (TAKARA) on the Agilent MX3000p real-time PCR system. qRT-PCR primers were as follows: ENO1 forward, 5′-AAAGCTGGTGCCGTTGAGAA-3′ and reverse, 5′-GGTTGTGGTAAACCTCTGCTC-3′; CST1 forward 5′-GCCTGCGCCAAGAGACA-3′ and reverse, 5′-CCCTGC TGAGCAACAAAGGA-3′; CST4 forward 5′-CCTCTGTGTAC CCTGCTACTC-3′ and reverse, 5′-CTTCGGTGGCCTTG TTGTACT-3′; β-actin forward, 5′-GAGCTGCGTGTGGC TCCC-3′ and reverse, 5′-CCAGAGGCGTACAGGGAT AGCA-3′.

Apoptosis Analysis

The eBioscience™ Annexin V-FITC apoptosis detection kit (Thermo Fisher Scientific) was used to measure apoptosis. Suspending cells were incubated with 5 μL annexin V-FITC for 10–15 min. After incubation, cells were washed in 1× binding buffer, then resuspended in 1× binding buffer. Resuspended cells were incubated with propidium iodide (20 μg/mL). Finally, samples were subjected to flow cytometry.

Cell Cycle Analysis

FxCycle PI/RNase Staining Solution (Thermo Fisher Scientific) was used to analyze the cell cycle according to the manufacturer's protocol. Briefly, cells were trypsinized and centrifuged at 13,000 rpm for 5 min. After washing in iced D-Hanks (pH = 7.2–7.4) buffer, cells were fixed with iced 75% ethanol for at least 1 h. Then, cells were centrifuged and washed in D-Hanks, followed by incubation in 0.5 mL of FxCycle PI/RNase staining solution for 15–30 min at room temperature. Finally, without washing, the analysis was performed using 488-nm excitation and 585/42-nm emission or the equivalent on the Guava easyCyte HT system (Millipore).

Western Blot Analysis

Cells were lysed with RIPA buffer with proteinase inhibitors. Protein concentrations were measured using the Bradford reagent (Sigma; Merck). Subsequently, 20 μg of total protein was subjected to 10% SDS-PAGE. Then proteins were transferred to nitrocellulose membranes and blocked with 5% non-fat milk at room temperature for 1 h. Membranes were incubated with antibodies against ENO1 (ABclonal, 1:2,000), HIF1a (Sigma, 1:2,000), β-actin (Sigma A5316, 1:5,000), and GAPDH (Proteintech, 1:5,000) at 4°C overnight, followed by secondary antibody (Thermo Fisher Scientific) at room temperature for 60 min.

Transwell Assay

We seeded 3.0×10^4 cells/well into the upper chamber of 24-well Corning® FluoroBlok TM Cell Culture Inserts (NY, United States) to measure cell migration. The lower chambers were filled with DMEM/F-12 medium supplemented with 10% fetal bovine serum to serve as a chemoattractant. Finally, cells that migrated to the other side of the filter were stained with 0.5% crystal violet and counted under an inverted fluorescence microscope.

Wound Healing Assay

Cells were plated in 96-well plate and cultured overnight. Wounds were made in confluent monolayer cells using 96 Wounding Replicator (VP Scientific) and cells were cultured in medium supplemented with 1% FBS. Wound healing was detected at 0, 24 h or 0, 48 h for overexpression or knockdown, respectively. The representative fields at different time points were photographed.

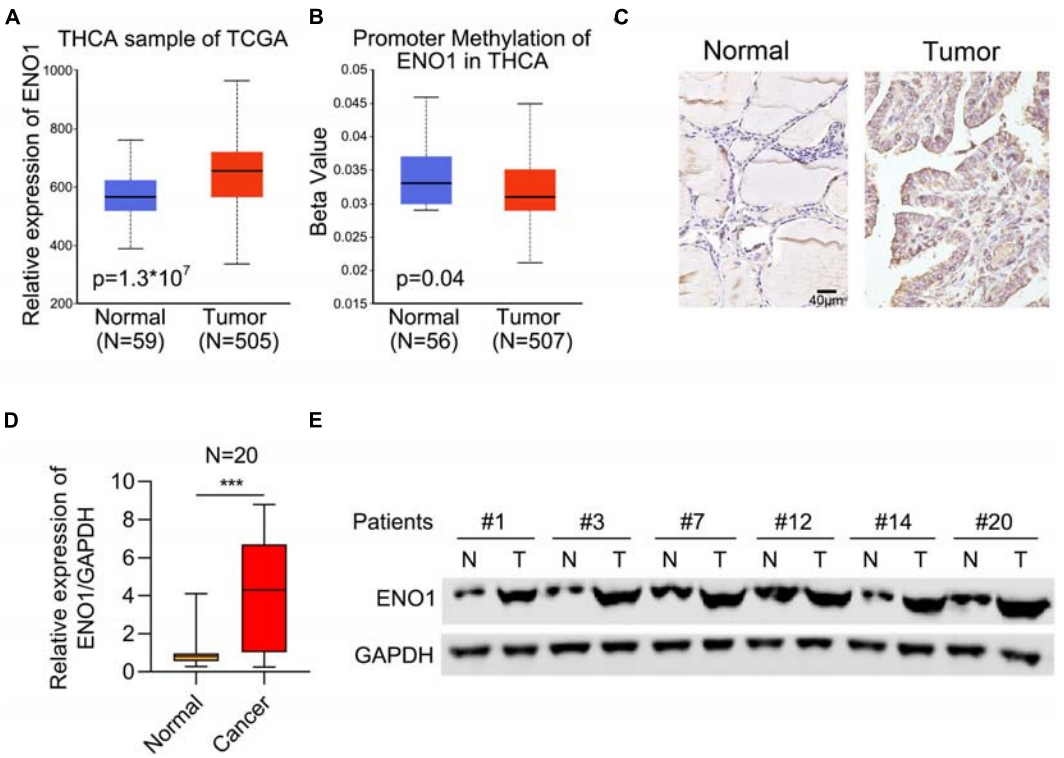

FIGURE 1 | Upregulation of ENO1 in thyroid carcinoma. **(A)** Analysis of ENO1 expression in thyroid carcinoma (n = 505) and normal samples (n = 59) from THCA. **(B)** Analysis of promoter methylation of ENO1 in thyroid carcinoma (n = 507) and normal samples (n = 56) from THCA. **(C)** IHC analysis of ENO1 expression in normal and thyroid carcinoma tissues. **(D)** qRT-PCR analysis of ENO1 expression in normal and thyroid carcinoma tissues. **(E)** Western blotting analysis of ENO1 expression in normal and thyroid carcinoma tissues. GAPDH serves as a loading control. ***$p < 0.001$.

Vector Construction and Luciferase Assay

The TargetScan database[1] was used to predict potential targets of HIF1a (Jaiswal et al., 2019). The 3′ untranslated region (UTR) of the ENO1 sequence was amplified and cloned into a pGL4.10-report vector (Promega Corporation, Madison, WI, United States). Equal quantities of the pGL4.10-3UTR-ENO1 and Renilla expression vector pRL-TK (Promega Corporation) were co-transfected into 293T cells. The luciferase activity was measured at 48 h post-transfection using the Dual-Glo Luciferase Assay system (Promega Corporation).

Tumor Xenograft Experiments

We subcutaneously injected 2×10^6 transfected TPC1 cells into the forelegs of immunodeficient nude mice (male BALB/c, 4-week-old). At the indicated times, thyroid tumors were isolated and weighed following international criteria. Animal studies were conducted in compliance with the regulations on management of animal welfare set by the Ethics Committee of National Cancer Center/National Clinical Research Center for Cancer/Cancer Hospital, Chinese Academy of Medical Sciences and Peking Union Medical College. The protocol for animal experiments was approved by the Ethics Committee of National Cancer Center/National Clinical Research Center for Cancer/Cancer Hospital, Chinese Academy of Medical Sciences and Peking Union Medical College.

[1] targetscan.org

RNA Sequencing

Total RNA was extracted from TPC1 cells incubated with exosomes using TRIzol reagent (Invitrogen, Carlsbad, CA, United States). Agarose electrophoresis was used to determine the total RNA's integrity, and a NanoDrop (Thermo Scientific NanoDrop 2000 Microvolume Spectrophotometer, RRID:SCR_018042) was used for quality control and quantification. A sequencing library was constructed using an RNA library construction kit (NEB, United States). Their sequences were analyzed using Illumina HiSeq™ 2000 (Wistar Genomics Facility, RRID:SCR_010205; Illumina Inc., San Diego, CA, United States).

Chromatin Immunoprecipitation (Ch-IP)

TPC1 cells were fixed in 1% formaldehyde for 10 min at 4°C. Cells were then sonicated to shear genomic DNA, followed by incubating overnight with 5 μg of Rb IgG or HIF1α antibody (Sigma, 1:2,000). The resulting complexes were precipitated using Fastflow G-Sepharose beads (GE Healthcare, Little Chalfont, United Kingdom), eluted, purified, and analyzed using PCR.

Gene-Set-Enrichment Analysis (GSEA)

According to their *P*-values, a GSEA algorithm was used to identify the enrichment of specific functions in the list of genes pre-ranked to test differences in expression between cell lines. The statistical significance of the enrichment score was calculated by permuting the genes 1,000 times as performed by the GSEA software. To collapse each probe set on the array to a single gene, we selected the probe with the highest variance among multiple probes corresponding to the same gene. Gene sets were derived from the REACTOME pathway database.

Bioinformatics Analysis

The StarBase V3.0 project[2] was used to analyze expression levels of ENO1 and CST1. Correlation between ENO1 and CST1 was obtained from 510 samples in thyroid carcinoma.

Statistical Analysis

The analysis was performed using GraphPad Prism 6.0 software. Differences were analyzed using the Student's *t*-test or one-way ANOVA. Differences were statistically significant when $P < 0.05$.

RESULTS

Upregulation of ENO1 in Thyroid Carcinoma

To study the function of ENO1 in thyroid carcinoma, we first analyzed the THCA database to determine the relevance of ENO1 in thyroid carcinoma. We found upregulation of ENO1 in thyroid carcinoma compared with normal samples (**Figure 1A**). And we also found that the higher level of methylation of ENO1's promoter in normal group than tumor group (**Figure 1B**). IHC staining showed that ENO1 was upregulated in thyroid carcinoma samples as compared with normal samples (**Figure 1C** and **Table 1**). The expression ENO1 was not associated with age, gender, T classification and lymph node metastasis (**Table 2**). qRT-PCR and western blotting were also performed to confirm these results; there were higher ENO1 mRNA and protein levels in thyroid carcinoma samples (**Figures 1D,E**). These findings suggest that ENO1 might be an oncogene.

Downregulation of ENO1 Suppresses Cell Proliferation, Invasion, and *in vivo* Tumorigenicity

To elucidate the role of ENO1 in thyroid carcinoma progression, small interfering RNAs were identified to downregulate ENO1 expression in TPC1 and BCPAP cells. Western blotting showed high knockdown efficiency of siENO1 in both cell lines (**Figure 2A**). Then, a CCK8 assay was performed to measure cell proliferation. Depletion of ENO1 suppressed TPC1 and BCPAP thyroid carcinoma cells' proliferation to nearly half that of control cells (**Figure 2B**). The colony formation assay demonstrated that fewer colonies were formed in siENO1 cells (**Figures 2C,D**).

Regarding migration ability, transwell results showed that the percentage of migration cells was decreased (greater than 50% in both cells) with ENO1 depletion compared to control cells (**Figures 2E,F**). In addition, wound healing assays demonstrated that ENO1 knockdown suppressed the migration capacity of TPC1 and BCPAP cells (**Supplementary Figure 1A**). To explore the function of ENO1 *in vivo*, a tumor formation assay was performed. We used ENO1 shRNA to downregulate the expression of ENO1, and the tumor was isolated for measurements at indicated times. Isolated tumors only weighed 0.1 g in shENO1 samples compared with 0.4 g in the control samples (**Figures 2G–I**). These findings further suggest an oncogenic role for ENO1.

ENO1 Regulates the Cell Cycle and Apoptosis

Because the cell cycle is frequently disturbed by oncogenes, we performed flow cytometry. The depletion of ENO1 decreased the number of cells in the S phase, while the G0/G1 cells' percentage increased (**Figure 3A**). Apoptotic cells significantly increased with ENO1 depletion. Compared with control cells, the percentage of apoptosis nearly doubled in siENO1 cells in bPC1 and BCPAP cells (**Figure 3B**). These findings suggest that cell cycle progression was severely impaired by ENO1 depletion.

ENO1 Overexpression Promotes Proliferation and Invasion and Inhibits Apoptosis

To confirm the knockdown results, we performed overexpression experiments. We performed qRT-PCR and western blotting to demonstrate high overexpression levels of ENO1 in both TPC1 and BCPAP cells (**Figures 4A–C**). Next, the CCK8 assay demonstrated that ENO1 overexpression significantly improved

[2]http://starbase.sysu.edu.cn/

TABLE 1 | The expression of ENO1 in Normal tissue and thyroid carcinoma by IHC.

	Normal	Tumor	χ^2	*P* Value
ENO1 high expression	17	31	8.75	0.003
ENO1 low expression	28	14		
Total	45	45		

TABLE 2 | Correlation of ENO1 expression with clinicopathological characteristics in 45 patients of thyroid carcinoma.

	Characteristic	ENO1 expression		*P* value
		High	Low	
Age	<55	14	12	0.787
	≥55	11	8	
Gender	Male	5	6	0.803
	Female	14	20	
T classification	T1–T2	6	8	0.457
	T3–T4	17	14	
Lymph node metastasis	Yes	20	9	0.098
	No	7	9	

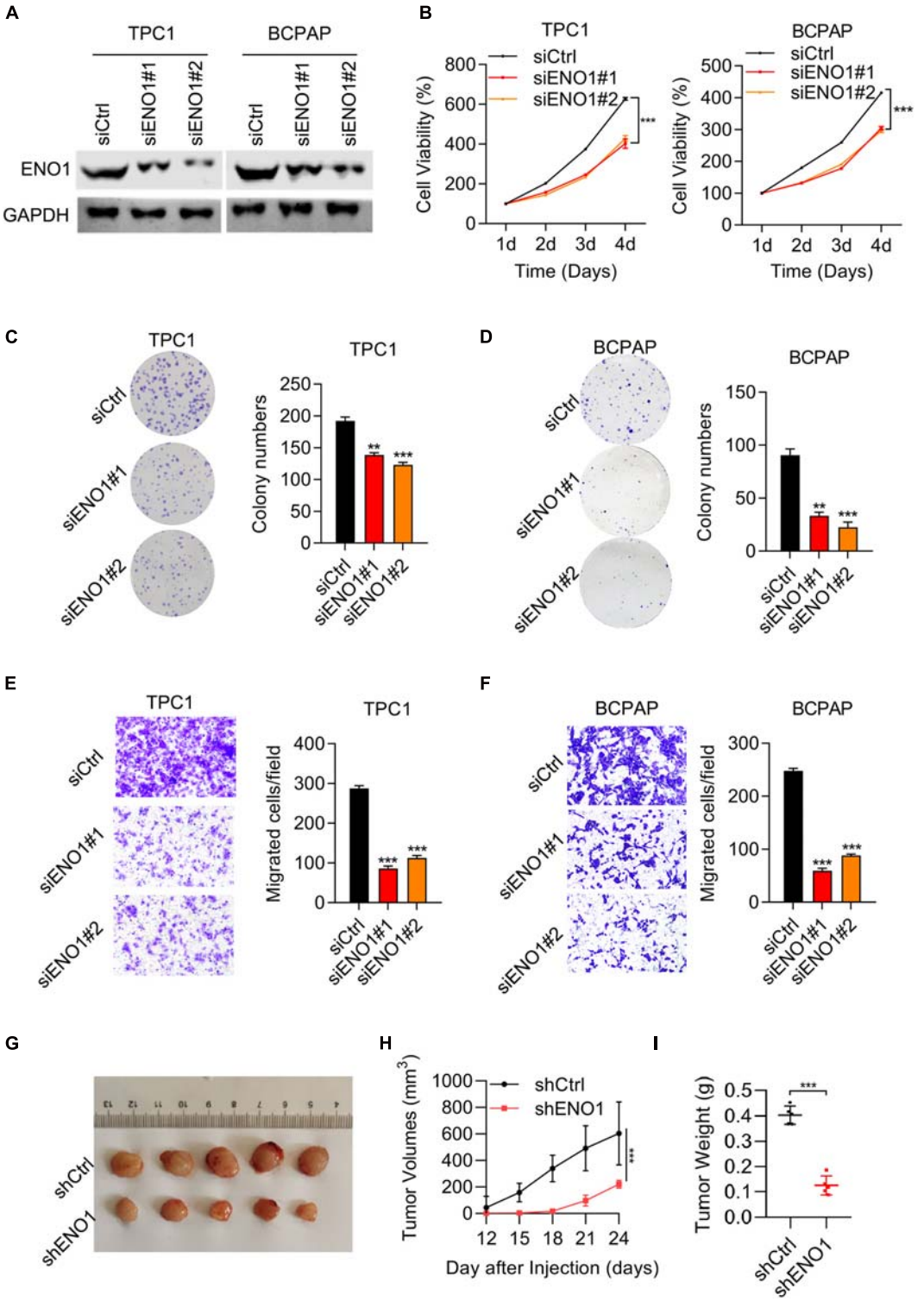

FIGURE 2 | Downregulation of ENO1 suppresses cell proliferation, invasion, and *in vivo* tumorigenicity. **(A)** Western blotting analysis of ENO1 knockdown efficiency in TPC1 and BCPAP cells. GAPDH was used as a loading control. **(B)** CCK8 analysis of cell proliferation in TPC1 cells and BCPAP cells transfected with siCtrl, siENO1#1, and siENO1#2. **(C,D)** Colony formation assay in TPC1 **(C)** and BCPAP **(D)** cells transfected with siCtrl, siENO1#1, and siENO1#2. $^{*}P < 0.05$, $^{**}P < 0.01$, $^{***}P < 0.001$. **(E,F)** Transwell invasion analysis in TPC1 **(E)** and BCPAP **(F)** cells transfected with siCtrl, siENO1#1, and siENO1#2. $^{***}P < 0.001$. **(G–I)** Athymic nude mice ($n = 5$) injected with TPC1 cell lines expressing shCtrl or shENO1 were analyzed for tumor formation. Representative image **(G)**, tumor growth curve **(H)** and weight **(I)** of xenografted tumors are shown.

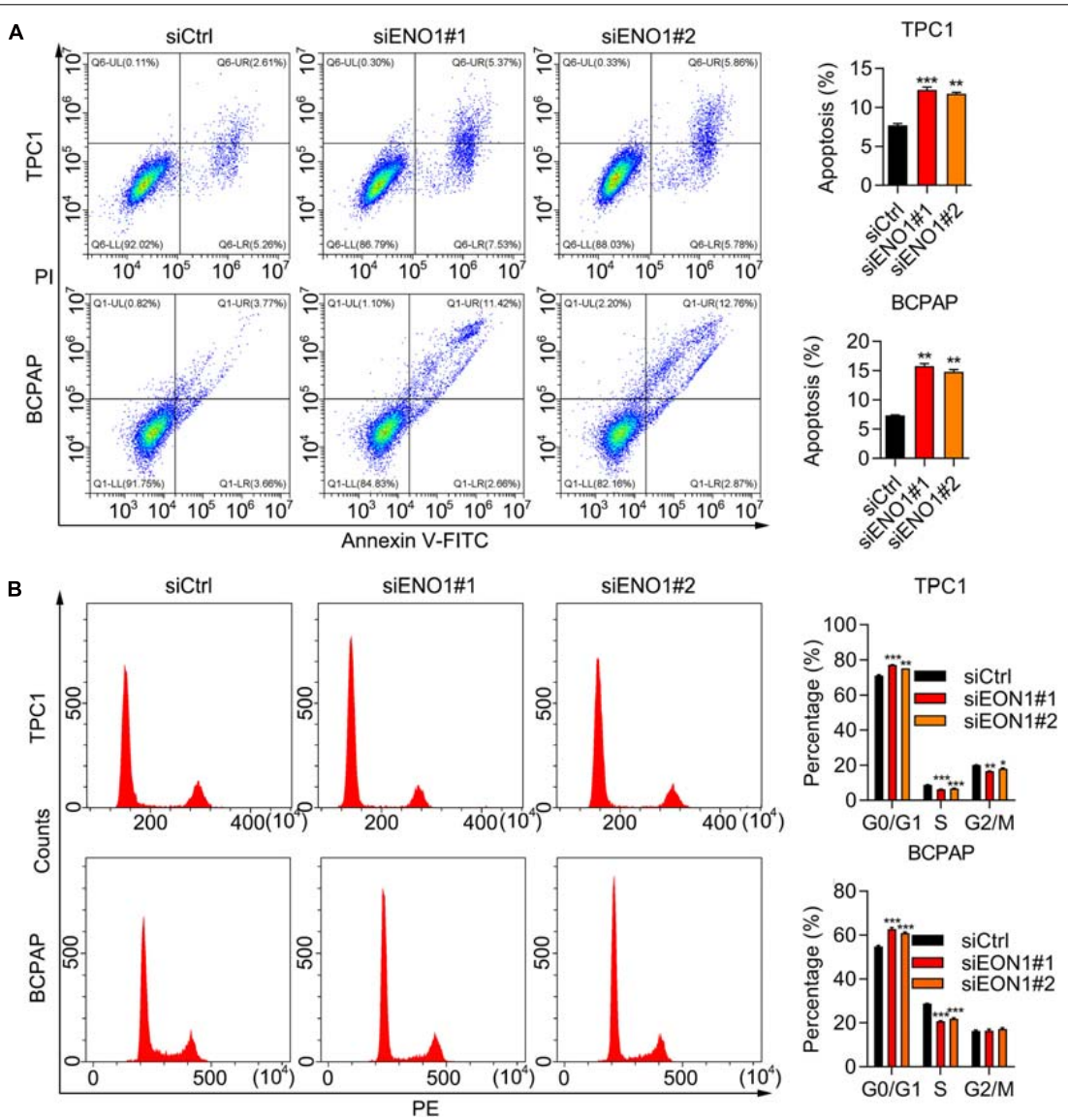

FIGURE 3 | ENO1 regulates cell cycle and apoptosis. **(A)** Cell cycle analysis using PI staining and flow cytometry in siCtrl, siENO1#1, and siENO1#2 transfected into TPC1 and BCPAP cells. $^{**}P < 0.01$, $^{***}P < 0.001$. **(B)** Flow cytometry analysis of apoptosis using annexin V-FITC and PI staining in TPC1 and BCPAP cells transfected with siCtrl, siENO1#1, and siENO1#2. $^{***}P < 0.001$, $^{**}P < 0.01$, $^{*}p < 0.05$.

cell viability compared with control cells from 1 to 4 days (**Figures 4D,E**). The ability of colony formation (**Figures 4F,G**) and Transwell migration (**Figures 4H,I**) in ENO1 overexpressing cells were consistent with the knockdown results (**Figures 2D–F**). Wound healing results also showed that ENO1 overexpression enhanced the migration capacity of TPC1 and BCPAP cells (**Supplementary Figure 1B**). We also performed flow cytometry analysis. Apoptosis was inhibited with ENO1 overexpression in both TPC1 and BCPCP cells (**Figures 4J,K**). Never the less, ENO1 accelerated cell cycle progression, with S stage cells increasing and G0/G1 stage cells decreasing (**Figures 4L,M**). These findings suggest that ENO1 regulates the cell cycle and apoptosis to promote cancer cell progression, functioning as an oncogene.

mTOR/HIF1α Regulates Expression of ENO1

Next, we elucidated the mechanism of ENO1's oncogenic role. ENO1 is a glycolysis-associated enzyme that participates in various cancers (Nakajima et al., 1986; Tu et al., 2010; Song et al., 2014; Fu et al., 2015; Liu et al., 2015; Principe et al., 2015; Zhu et al., 2015, 2018; Niccolai et al., 2016; Qian et al., 2017; Zhan et al., 2017); therefore, we focused on glycolysis-associated pathways; the mTOR/HIF1α pathway is also involved in glycolysis (Majumder et al., 2004; Semenza, 2011; Chi, 2012; Cheng et al., 2014; Courtnay et al., 2015; Yang et al., 2015; Xiao et al., 2017). Therefore, we examined ENO1 expression in TSC1 knockout MEF cells and found

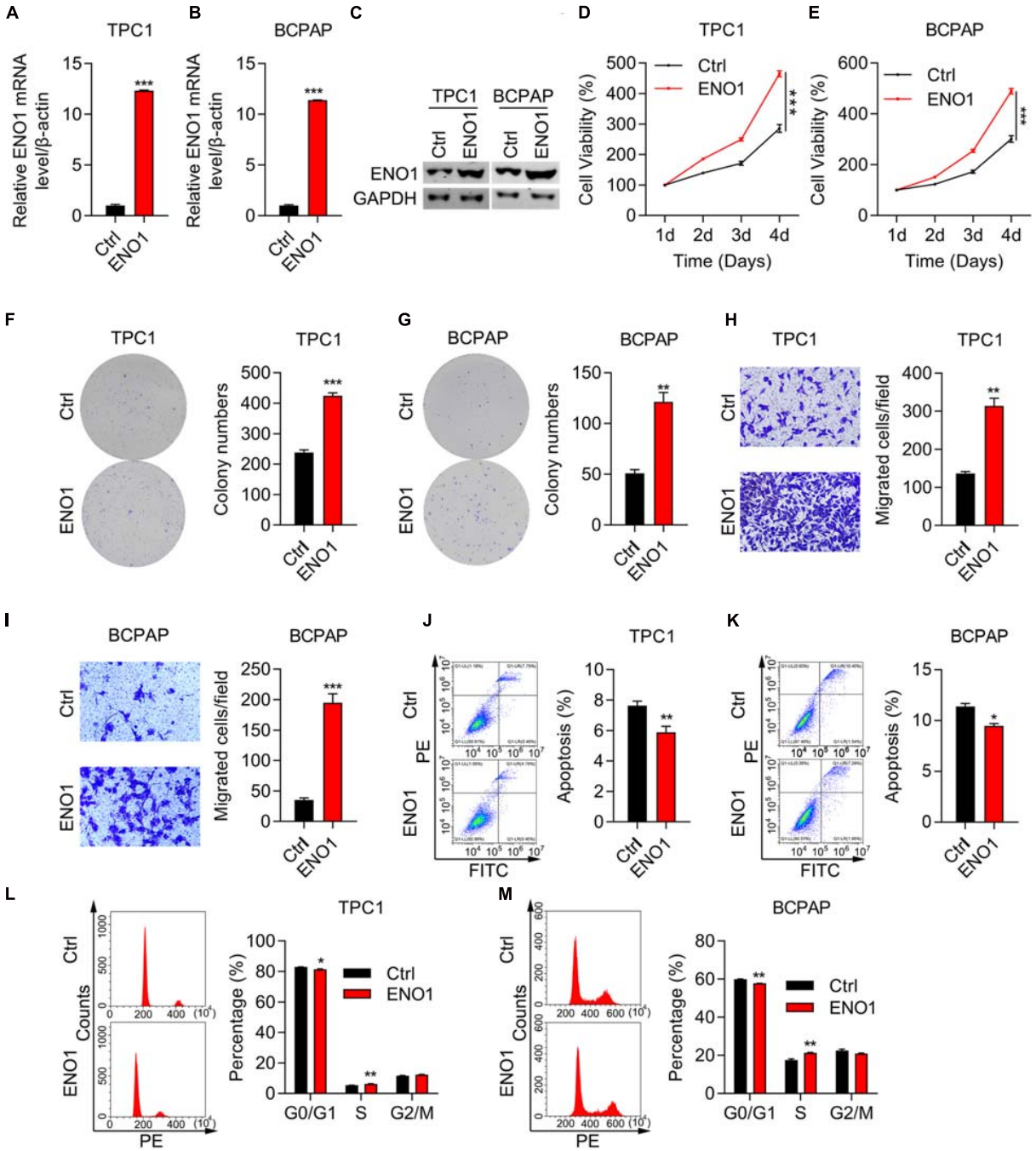

FIGURE 4 | ENO1 overexpression promotes proliferation and invasion and inhibits apoptosis. **(A,B)** qRT-PCR analysis of ENO1 overexpression in TPC1 **(A)** and BCPAP **(B)** cells. β-actin was used for normalization, $^{***}P < 0.001$. **(C)** Western blotting analysis of ENO1 overexpression in TPC1 and BCPAP cells. GAPDH was used as a loading control. **(D,E)** CCK8 cell viability analysis of control or ENO1-overexpressed TPC1 **(D)** and BCPAP **(E)** cells, $^{***}P < 0.001$. **(F,G)** Colony formation assay of control or ENO1-overexpressed TPC1 **(F)** and BCPAP **(G)** cells. $^{**}P < 0.01$, $^{***}P < 0.001$. **(H,I)** Transwell invasion analysis of control or ENO1-overexpressed TPC1 **(H)** and BCPAP **(I)** cells. $^{***}P < 0.001$, $^{**}P < 0.01$. **(J,K)** Flow cytometry analysis of apoptosis using Annexin V-FITC and PI staining in control or ENO1-overexpressed TPC1 **(J)** and BCPAP **(K)** cells. $^{*}P < 0.05$, $^{**}P < 0.01$. **(L,M)** Cell cycle was measured using PI staining and flow cytometry in control or ENO1-overexpressed TPC1 **(L)** and BCPAP **(M)** cells, $^{*}P < 0.05$, $^{**}P < 0.01$.

that TSC1 depletion aberrantly activated the mTOR pathway (Cao et al., 2020). Western blotting showed that knockout of TSC1 upregulated ENO1 expression and the phosphorylation of S6, the downstream of mTOR pathway (**Figure 5A**), as did HIF1α, another downstream molecule of the mTOR/HIF1α pathway. To confirm these results, we used rapamycin to inhibit

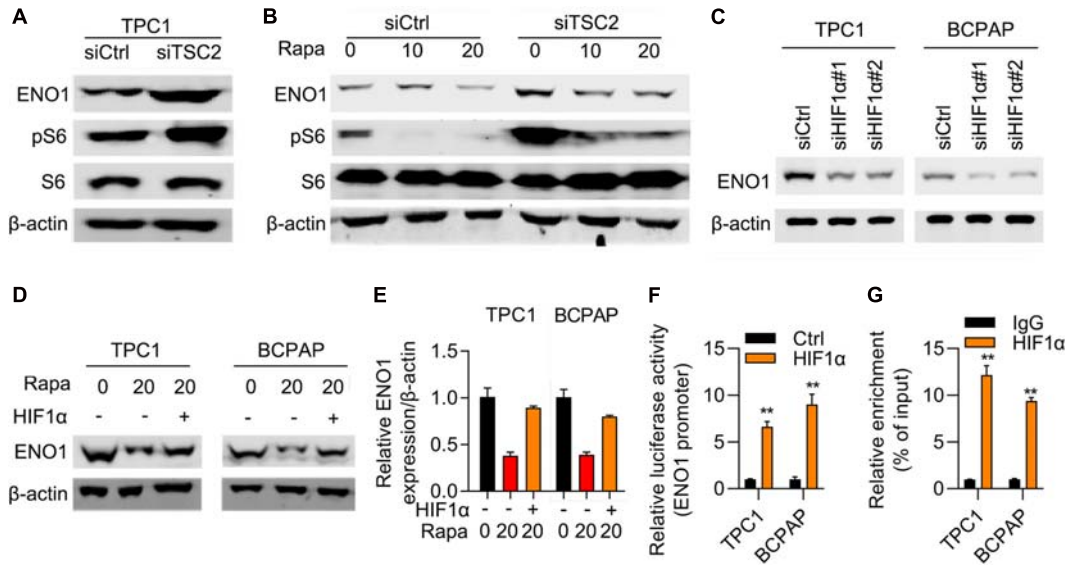

FIGURE 5 | mTOR/HIF1α regulates expression of ENO1. **(A)** ENO1 and phosphorylated S6 was upregulated in TSC1 knockout TPC1 cells. β-actin was used as a loading control. **(B)** ENO1 was downregulated with rapamycin treatment. β-actin was used as a loading control. **(C)** Depletion of HIF1α downregulated expression of ENO1. β-actin was used as a loading control. **(D–E)** HIF1α rescued downregulation of ENO1 with rapamycin treatment. Western blotting **(D)** and qRT-PCR **(E)** were shown. $^{**}P < 0.01$. **(F)** ENO1 luciferase assay in control and HIF1α transfected cells. $^{**}P < 0.01$. **(G)** HIF1α targeted the promoter region of ENO1. ChIP-qPCR results are shown. $^{**}P < 0.01$.

the mTOR pathway (Edwards and Wandless, 2007). ENO1 was downregulated upon rapamycin addition, more significantly in TSC1-depleted cells (**Figure 5B**).

To explore the relationship between ENO1 and HIF1α, an RNA interference assay was performed. With HIF1α depletion, ENO1 was downregulated in both TPC1 and BCPAP cells (**Figure 5C**). The addition of rapamycin further reduced ENO1 expression. Overexpression of HIF1α rescued ENO1 expression both at the protein and mRNA levels (**Figure 5D**). We also performed a luciferase assay. The luciferase activity increased in HIF1α-transfected cells compared with control cells (**Figure 5E**). The ChIP-qPCR assay demonstrated that the *HIF1α* targeted the promoter region of *ENO1* (**Figures 5F,G**). These findings suggest that ENO1 is located downstream of and is regulated by the mTOR/ HIF1α pathway.

ENO1 Regulates the Expression of CST1 and CST4

To further explore the mechanism, we performed differential expression analysis between ENO1-depleted cells and control cells. Variations of mRNA expression between the two groups were plotted, and CST1 and CST4 are the most decreased genes by ENO1 knockdown (**Figure 6A**). GESA analysis showed that ENO1 depletion altered downregulated including G2M checkpoints and glycolysis signaling pathways (**Figure 6B**). We chose the genes with a maximum difference for further analysis (**Figure 6C**). Correlation analysis of the THCA database showed that CST1 and CST4 expression were positively correlated with ENO1 expression (**Figures 6D,E**). qRT-PCR and immunoblotting confirmed that depletion of ENO1 downregulated CST1 and CST4 expression at the mRNA and protein levels (**Figure 6F**).

Depletion of CST1, but Not CST4, Inhibits Proliferation and Invasion and Promotes Apoptosis

CST1 and CST4 were previously reported to be oncogenes (Jiang et al., 2018; Cui et al., 2019; Liu et al., 2019; Wang et al., 2020). Next, we studied the role of CST1 and CST4 in thyroid carcinoma. Western blotting confirmed the high knockdown efficiency of siCST1 in both TPC1 and BCPAP cells (**Figure 7A**). Cell viability analysis with CCK8 assay showed that depletion of CST1 significantly reduced cell viability (**Figure 7B**). However, we found that knockdown of CST4 could not affect the proliferation of THCA cells (**Supplementary Figure 2**). Colony numbers also decreased in siCST1 cells (**Figures 7C,D**). Invasion ability was also inhibited with CST1 depletion, decreasing to nearly half of the control cell levels (**Figures 7E,F**). These findings suggest that CST1 is an oncogene in thyroid carcinoma.

Proliferation, Invasion, and Tumorigenicity Enhanced by ENO1 Overexpression Is Attenuated by CST1 Depletion

To further clarify the relationship between ENO1 and CST1 in thyroid carcinoma, we combined overexpression and knockdown assays in TPC1 cells. Western blotting showed that ENO1 overexpression upregulated CST1 expression and reduced it after shCST1 treatment (**Figure 8A**). Next, cell viability and colony formation assays were performed. Knockdown of CST1 significantly reduced cell viability enhanced with ENO1 overexpression to control level (**Figures 8B,C**). Invasion ability

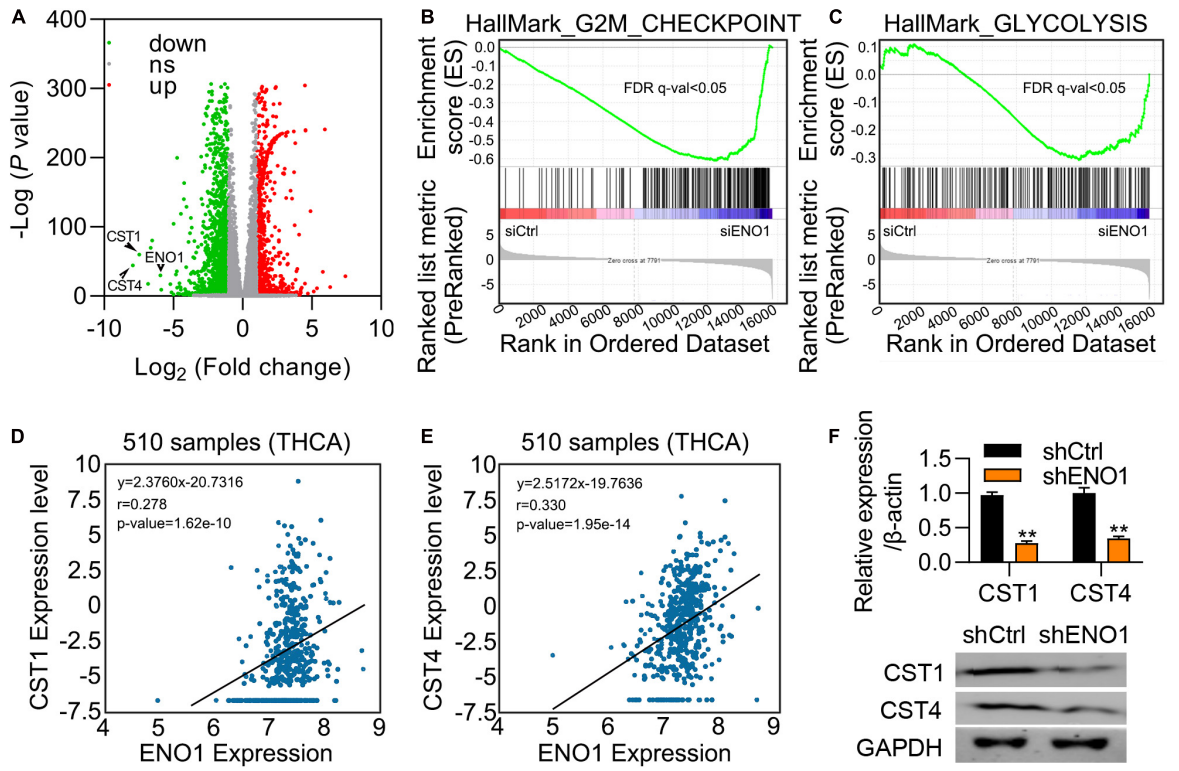

FIGURE 6 | ENO1 regulates the expression of CST1. **(A)** Differential expression of mRNAs between control and siENO1 cells. The abscissa was log2, and the ordinate was -log10. The red and green dots represent upregulated and downregulated genes, respectively. The gray dots represent genes that were not differentially expressed between the two groups. **(B,C)** Selected enriched gene sets from the GSEA. The green tracing shows the enrichment score based on hits of genes in the ordered list of differentially regulated genes resulting from the comparison of control and ENO1 depletion cells. **(D,E)** Correlation between ENO1 and CST1 **(D)** and CST4 **(E)** expression (510 samples) in TCGA database. **(F)** Downregulation of CST1 and CST4 expression by ENO1 depletion. qRT-PCR are shown. β-actin was used for normalization. $^{**}P < 0.01$.

was also attenuated by CST1 depletion (**Figure 8D**). Finally, *in vivo* tumorigenicity was measured. Following the previous result (**Figure 2G**), overexpression of ENO1 resulted in larger tumor sizes (**Figures 8E–G**), suggesting that ENO1 was an oncogene. As predicted, tumor size enlargement was reduced to control levels with shCST1 treatment (**Figures 8E–G**). These findings suggest a synergistic role between ENO1 and CST1 in thyroid carcinoma progression.

DISCUSSION

Traditional therapy strategies such as radioactive-iodine ablation and surgical resection are essential for thyroid carcinoma treatment. Currently, novel targeted strategies play increasingly essential roles in thyroid carcinoma treatment, especially for aggressive thyroid tumors (Kondo et al., 2006). Therefore, more potential targeted genes need to be identified, and their mechanisms need to be further clarified. Our study demonstrated that ENO1 was an oncogene in thyroid carcinoma that acted downstream of mTOR/HIF1α and accelerated thyroid carcinoma progression via regulating CST1. Because ENO1 has been identified as an oncogene in several cancers (Nakajima et al., 1986; Tu et al., 2010; Song et al., 2014; Fu et al., 2015; Liu et al., 2015; Principe et al., 2015; Zhu et al., 2015, 2018; Niccolai et al., 2016; Qian et al., 2017; Zhan et al., 2017), it could be a potential novel target for thyroid carcinoma. Our study paves the way for targeted strategies of thyroid carcinoma treatment.

Enolase has three isoforms in higher eukaryotes: ENO1 is widely expressed in nearly all tissues, whereas ENO2 and ENO3 are specifically expressed in neurons and muscles, respectively (Chen et al., 2020). Although there have been several reports of ENO1, the functions of ENO2 and ENO3 have been rarely reported. Whether ENO2 and ENO3 function as oncogenes in neurons and muscles needs to be clarified. We also need to understand whether the functions of the three ENOs are synergistic or antagonistic.

The localization of ENO1 varies depending on its function. In the cytoplasm, ENO1 maintains ATP levels and associates with the cytoskeleton. At the cell membrane, ENO1 activates the plasminogen system to accelerate tumor cell invasion. ENO1 also localizes in the nucleus to regulate c-myc expression and impede tumor growth (Cappello et al., 2017; Yin et al., 2018). To further explore the mechanism of ENO1 as an oncogene, the precise localization of ENO1 in thyroid carcinoma cells needs to be identified.

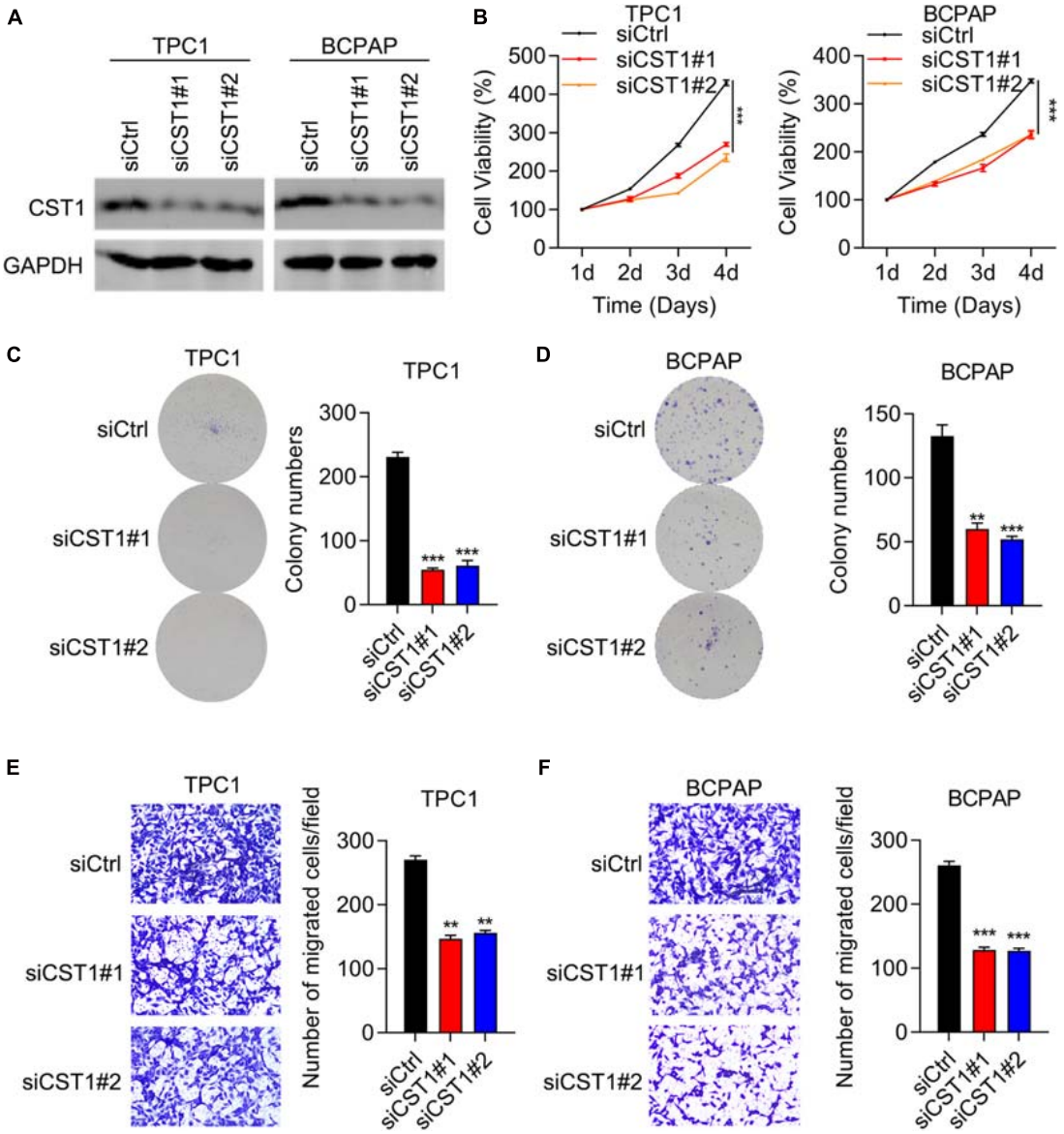

FIGURE 7 | Depletion of CST1 inhibits proliferation and invasion and promotes apoptosis. **(A)** Effective knockdown of CST1 in TPC1 and BCPAP cells. Western blot of TPC1 and BCPAP cells transfected with siCtrl, siCST1#1, and siCST1#2. GAPDH served as a loading control. **(B)** Cell viability analysis of siCtrl, siCST1#1, and siCST1#2 transfected into TPC1 and BCPAP cells using the CCK8 assay. ***$P < 0.001$. **(C,D)** Colony formation analysis of siCtrl, siCST1#1, and siCST1#2 transfected into TPC1 **(C)** and BCPAP **(D)** cells. **$P < 0.01$; ***$P < 0.001$. **(E,F)** Invasion analysis of siCtrl, siCST1#1, and siCST1#2 transfected into TPC1 **(E)** and BCPAP **(F)** cells. **$P < 0.01$; ***$P < 0.001$.

The Warburg effect occurs in most tumor cells (Warburg et al., 1927). In these cells, glycolysis is enhanced. The tricarboxylic acid cycle is inhibited even in abundant oxygen because enhanced glycolysis can provide more efficient glucose consumption to promote tumor cell growth (Lunt and Vander Heiden, 2011). As a glycolytic enzyme, ENO1 overexpression enhances the glycolytic pathway (Yin et al., 2018). There are also reports that PI3K/AKT/ mTOR/HIF1α upregulates the expression of glucose transporters and glycolytic enzymes (Majumder et al., 2004; Semenza, 2011; Chi, 2012; Cheng et al., 2014; Courtnay et al., 2015; Yang et al., 2015; Xiao et al., 2017); HIF1α also targets ENO1 (Qian et al., 2017). Therefore, enhanced glycolysis may be the reason why mTOR/HIF1α/ENO1 promotes thyroid carcinoma progression. The mTOR/HIF1α/ENO1 pathway can also enhance glycolysis in other cancers. However, all these effects need to be further clarified.

Type 2 cystatin superfamily, consisting of CST1, CST2, CST3, CST4, and CST5, exerts cysteine proteases inhibitor effect and is widely expressed in multiple organs. Increasing evidences have demonstrated that dysregulation of CST1 contributes to the development of various cancers. For instance, CST1 expression was elevated in and conferred poor prognosis of breast cancer

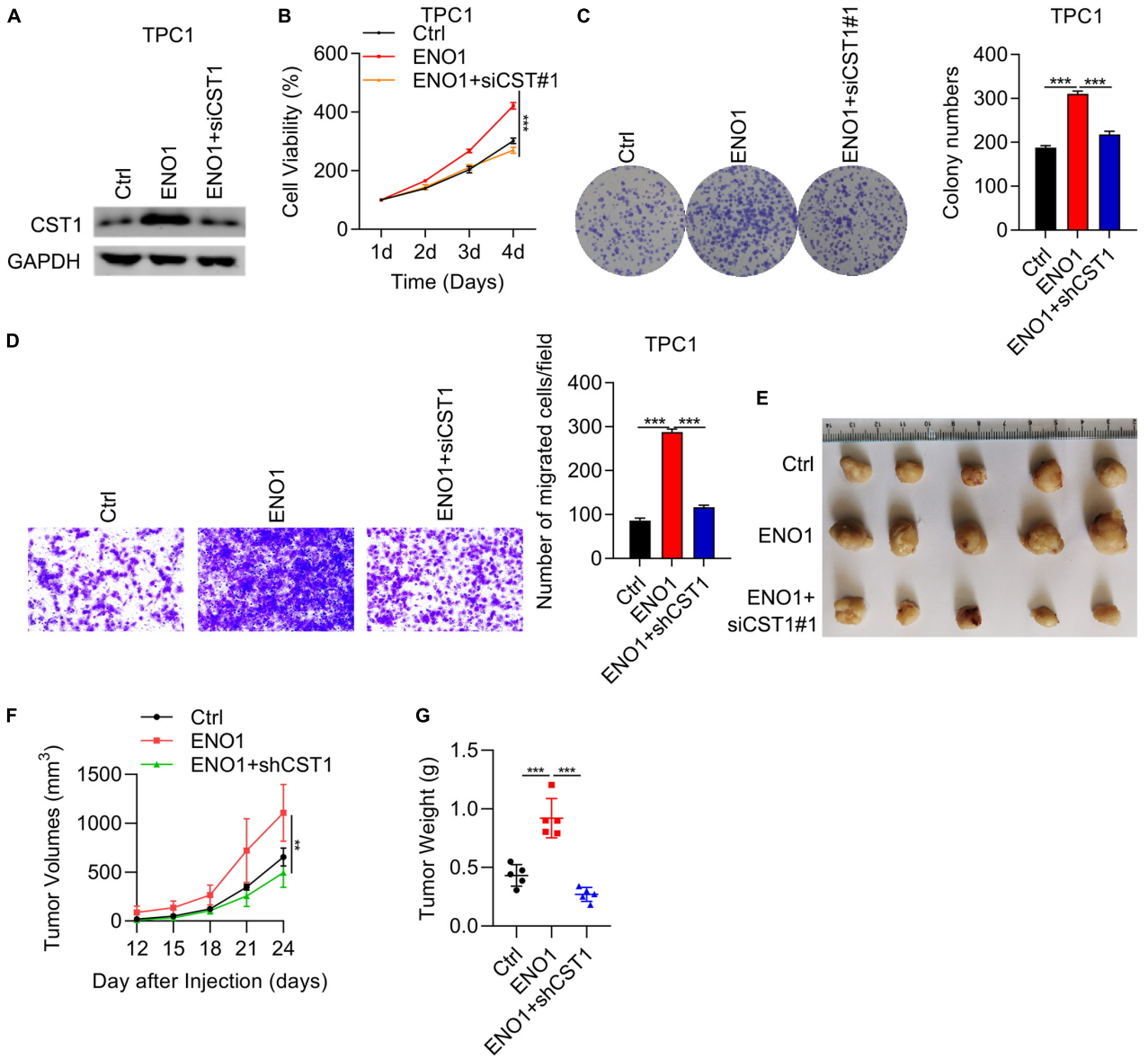

FIGURE 8 | Proliferation, invasion, and tumorigenicity enhanced by ENO1 overexpression is attenuated by CST1 depletion. **(A)** Western blot analysis of CST1 in TPC1 cells transfected with control, ENO1, and ENO1+shCST1. GAPDH was used as a loading control. **(B)** CCK8 cell viability analysis of TPC1 cells transfected with control, ENO1, and ENO1+shCST1. ***$P < 0.001$. **(C)** Colony formation analysis of TPC1 cells transfected with control, ENO1, and ENO1+shCST1. ***$P < 0.001$. **(D)** Invasion ability analysis of TPC1 cells transfected with control, ENO1, and ENO1+shCST1. ***$P < 0.001$. **(E–G)** Tumor formation analysis in athymic nude mice ($n = 5$) injected with TPC1 cell lines expressing control, ENO1, and ENO1+shCST1. Representative image **(E)**, tumor growth curve **(F)** and tumor **(G)** weight of xenografted tumors are shown. **$P < 0.01$; ***$P < 0.001$.

patients. CST1 also promoted the malignant function of breast cancer cells (Dai et al., 2017). Overexpression of CST1 also contributed colorectal cancer growth via reducing intracellular reactive oxygen species (ROS) production (Oh et al., 2017). In addition, upregulation of CST1 promoted hepatocellular carcinogenesis and predicted worse prognosis for the patients (Cui et al., 2019). Besides, elevation of CST1 is a promising diagnostic biomarker for other cancer types, including pancreatic cancer (Jiang et al., 2015), esophageal squamous cell carcinoma (Chen et al., 2013), and gastric cancer (Choi et al., 2009). Nevertheless, the significance of CST1 in thyroid carcinoma and the upstream regulator of CST1 remain to be determined. In this study, we presented the data that ENO1 positively regulated the expression of CST1 and CST4 in thyroid carcinoma cells. There was a positive correlation between ENO1 and CST1/CST4 in human thyroid carcinoma tissues. Functional experiments demonstrated that knockdown of CST1, but not CST4, suppressed the growth of growth of thyroid carcinoma cells. Furthermore, knockdown of CST1 reduced the migration capacity of thyroid carcinoma cells. Importantly, CST1 silencing

reversed the oncogenic function of ENO1 on thyroid carcinoma cell growth, migration and tumorigenic capacity. These results suggested that ENO1 upregulation of CST1 contributed to thyroid carcinoma growth, migration and tumor development.

In summary, although many complicated questions have not been answered, our study was the first to identify the mTOR/HIF1α/ENO1 pathway in thyroid carcinoma progression and ENO1 as a regulator of CST1, thereby paving the way for early diagnosis and efficient therapy of thyroid carcinoma.

DATA AVAILABILITY STATEMENT

The data presented in the study are deposited in the NCBI Short Read Archive (SRA) repository, accession number is SUB9428898, and the BioProject ID is PRJNA719990.

ETHICS STATEMENT

The studies involving human participants were reviewed and approved by the Ethics Committee of National Cancer Center/National Clinical Research Center for Cancer/Cancer Hospital, Chinese Academy of Medical Sciences and Peking Union Medical College. The patients/participants provided their written informed consent to participate in this study. The animal study was reviewed and approved by the Ethics Committee of National Cancer Center/National Clinical Research Center for Cancer/Cancer Hospital, Chinese Academy of Medical Sciences and Peking Union Medical College.

AUTHOR CONTRIBUTIONS

SL, JL, and YL designed the original study. YL performed the most experiments. LL performed the *in vivo* assay. CA assisted with statistical analysis. XW, ZL, and ZX collected the clinical samples. YL wrote and revised the manuscript draft. All authors read and approved the final manuscript.

FUNDING

This study was funded by the National Natural Science Foundation of China (Grant No. 81902728).

SUPPLEMENTARY MATERIAL

The Supplementary Material for this article can be found online at: https://www.frontiersin.org/articles/10.3389/fcell.2021.670019/full#supplementary-material

REFERENCES

Cao, H., Luo, J., Zhang, Y., Mao, X., Wen, P., Ding, H., et al. (2020). Tuberous sclerosis 1 (Tsc1) mediated mTORC1 activation promotes glycolysis in tubular epithelial cells in kidney fibrosis. *Kidney Int.* 98, 686–698. doi: 10.1016/j.kint.2020.03.035

Capello, M., Ferri-Borgogno, S., Riganti, C., Chattaragada, M. S., Principe, M., Roux, C., et al. (2016). Targeting the Warburg effect in cancer cells through ENO1 knockdown rescues oxidative phosphorylation and induces growth arrest. *Oncotarget* 7, 5598–5612. doi: 10.18632/oncotarget.6798

Cappello, P., Principe, M., Bulfamante, S., and Novelli, F. (2017). Alpha-Enolase (ENO1), a potential target in novel immunotherapies. *Front. Biosci.* 22:944–959. doi: 10.2741/4526

Catalano, M. G., Poli, R., Pugliese, M., Fortunati, N., and Boccuzzi, G. (2010). Emerging molecular therapies of advanced thyroid cancer. *Mol. Aspects Med.* 31, 215–226. doi: 10.1016/j.mam.2010.02.006

Chen, J. M., Chiu, S. C., Chen, K. C., Huang, Y. J., Liao, Y. A., and Yu, C. R. (2020). Enolase 1 differentially contributes to cell transformation in lung cancer but not in esophageal cancer. *Oncol. Lett.* 19, 3189–3196. doi: 10.3892/ol.2020.11427

Chen, Y., Ma, G., Cao, X., Luo, R., He, L., He, J., et al. (2013). Overexpression of cystatin SN positively affects survival of patients with surgically resected esophageal squamous cell carcinoma. *BMC Surg.* 13:15. doi: 10.1186/1471-2482-13-15

Cheng, S. C., Quintin, J., Cramer, R. A., Shepardson, K. M., Saeed, S., Kumar, V., et al. (2014). mTOR- and HIF-1alpha-mediated aerobic glycolysis as metabolic basis for trained immunity. *Science* 345:1250684. doi: 10.1126/science.1250684

Chi, H. (2012). Regulation and function of mTOR signalling in T cell fate decisions. *Nat. Rev. Immunol.* 12, 325–338. doi: 10.1038/nri3198

Choi, E., Kim, J., Kim, J., Kim, S., Song, E., Kim, J., et al. (2009). Upregulation of the cysteine protease inhibitor, cystatin SN, contributes to cell proliferation and cathepsin inhibition in gastric cancer. *Clin. Chim. Acta* 406, 45–51. doi: 10.1016/j.cca.2009.05.008

Coelho, R., Fortunato, R., and Carvalho, D. (2018). Metabolic reprogramming in thyroid carcinoma. *Front. Oncol.* 8:82. doi: 10.3389/fonc.2018.00082

Courtnay, R., Ngo, D. C., Malik, N., Ververis, K., Tortorella, S. M., and Karagiannis, T. C. (2015). Cancer metabolism and the Warburg effect: the role of HIF-1 and PI3K. *Mol. Biol. Rep.* 42, 841–851. doi: 10.1007/s11033-015-3858-x

Cui, Y., Sun, D., Song, R., Zhang, S., Liu, X., Wang, Y., et al. (2019). Upregulation of cystatin SN promotes hepatocellular carcinoma progression and predicts a poor prognosis. *J. Cell. Physiol.* 234, 22623–22634. doi: 10.1002/jcp.28828

Dai, D. N., Li, Y., Chen, B., Du, Y., Li, S. B., Lu, S. X., et al. (2017). Elevated expression of CST1 promotes breast cancer progression and predicts a poor prognosis. *J. Mol. Med.* 95, 873–886. doi: 10.1007/s00109-017-1537-1

Davies, L. (2016). Overdiagnosis of thyroid cancer. *BMJ* 355:i6312. doi: 10.1136/bmj.i6312

Diaz-Ramos, A., Roig-Borrellas, A., Garcia-Melero, A., and Lopez-Alemany, R. (2012). alpha-Enolase, a multifunctional protein: its role on pathophysiological situations. *J. Biomed. Biotechnol.* 2012:56795. doi: 10.1155/2012/156795

Edwards, S. R., and Wandless, T. J. (2007). The rapamycin-binding domain of the protein kinase mammalian target of rapamycin is a destabilizing domain. *J. Biol. Chem.* 282, 13395–13401. doi: 10.1074/jbc.M700498200

Ejeskar, K., Krona, C., Caren, H., Zaibak, F., Li, L., Martinsson, T., et al. (2005). Introduction of in vitro transcribed ENO1 mRNA into neuroblastoma cells induces cell death. *BMC Cancer* 5:161. doi: 10.1186/1471-2407-5-161

Fu, Q. F., Liu, Y., Fan, Y., Hua, S. N., Qu, H. Y., Dong, S. W., et al. (2015). Alpha-enolase promotes cell glycolysis, growth, migration, and invasion in non-small cell lung cancer through FAK-mediated PI3K/AKT pathway. *J. Hematol. Oncol.* 8:22. doi: 10.1186/s13045-015-0117-5

Hsiao, K. C., Shih, N. Y., Fang, H. L., Huang, T. S., Kuo, C. C., Chu, P. Y., et al. (2013). Surface alpha-enolase promotes extracellular matrix degradation and tumor metastasis and represents a new therapeutic target. *PLoS One* 8:e69354. doi: 10.1371/journal.pone.0069354

Huang, Z., Lin, B., Pan, H., Du, J., He, R., Zhang, S., et al. (2019). Gene expression profile analysis of ENO1 knockdown in gastric cancer cell line MGC-803. *Oncol. Lett.* 17, 3881–3889. doi: 10.3892/ol.2019.10053

Hundahl, S. A., Fleming, I. D., Fremgen, A. M., and Menck, H. R. (1998). A National cancer data base report on 53,856 cases of thyroid carcinoma treated in the U.S., 1985-1995 [see commetns]. *Cancer* 83, 2638–2648. doi: 10.1002/(sici)1097-0142(19981215)83:12<2638::aid-cncr31<3.0.co;2-1

Jaiswal, P. K., Koul, S., Palanisamy, N., and Koul, H. K. (2019). Eukaryotic translation initiation factor 4 Gamma 1 (EIF4G1): a target for cancer therapeutic intervention? *Cancer Cell Int.* 19:224. doi: 10.1186/s12935-019-0947-2

Jiang, J., Liu, H., Liu, Z., Tan, S., and Wu, B. (2015). Identification of cystatin SN as a novel biomarker for pancreatic cancer. *Tumour Biol.* 36, 3903–3910. doi: 10.1007/s13277-014-3033-3

Jiang, J., Liu, H. L., Tao, L., Lin, X. Y., Yang, Y. D., Tan, S. W., et al. (2018). Let7d inhibits colorectal cancer cell proliferation through the CST1/p65 pathway. *Int. J. Oncol.* 53, 781–790. doi: 10.3892/ijo.2018.4419

Knauf, J. A., Ouyang, B., Knudsen, E. S., Fukasawa, K., Babcock, G., and Fagin, J. A. (2006). Oncogenic RAS induces accelerated transition through G2/M and promotes defects in the G2 DNA damage and mitotic spindle checkpoints. *J. Biol. Chem.* 281, 3800–3809. doi: 10.1074/jbc.M511690200

Kondo, T., Ezzat, S., and Asa, S. L. (2006). Pathogenetic mechanisms in thyroid follicular-cell neoplasia. *Nat. Rev. Cancer* 6, 292–306. doi: 10.1038/nrc1836

Koppenol, W., Bounds, P., and Dang, C. (2011). Otto Warburg's contributions to current concepts of cancer metabolism. *Nat. Rev. Cancer* 11, 325–337. doi: 10.1038/nrc3038

La Vecchia, C., Malvezzi, M., Bosetti, C., Garavello, W., Bertuccio, P., Levi, F., et al. (2015). Thyroid cancer mortality and incidence: a global overview. *Int. J. Cancer* 136, 2187–2195. doi: 10.1002/ijc.29251

Lim, H., Devesa, S. S., Sosa, J. A., Check, D., and Kitahara, C. M. (2017). Trends in thyroid cancer incidence and mortality in the United States, 1974-2013. *JAMA* 317, 1338–1348. doi: 10.1001/jama.2017.2719

Liu, Y., Ma, H., Wang, Y., Du, X., and Yao, J. (2019). Cystatin SN affects cell proliferation by regulating the ERalpha/PI3K/AKT/ERalpha loopback pathway in breast cancer. *Onco Targets Ther.* 12, 11359–11369. doi: 10.2147/OTT.S234328

Liu, Y. Q., Huang, Z. G., Li, G. N., Du, J. L., Ou, Y. P., Zhang, X. N., et al. (2015). Effects of alpha-enolase (ENO1) over-expression on malignant biological behaviors of AGS cells. *Int. J. Clin. Exp. Med.* 8, 231–239.

Lunt, S. Y., and Vander Heiden, M. G. (2011). Aerobic glycolysis: meeting the metabolic requirements of cell proliferation. *Annu. Rev. Cell Dev. Biol.* 27, 441–464. doi: 10.1146/annurev-cellbio-092910-154237

Majumder, P. K., Febbo, P. G., Bikoff, R., Berger, R., Xue, Q., Mcmahon, L. M., et al. (2004). mTOR inhibition reverses Akt-dependent prostate intraepithelial neoplasia through regulation of apoptotic and HIF-1-dependent pathways. *Nat. Med.* 10, 594–601. doi: 10.1038/nm1052

Mitsutake, N., Knauf, J. A., Mitsutake, S., Mesa, C. Jr., Zhang, L., and Fagin, J. A. (2005). Conditional BRAFV600E expression induces DNA synthesis, apoptosis, dedifferentiation, and chromosomal instability in thyroid PCCL3 cells. *Cancer Res.* 65, 2465–2473. doi: 10.1158/0008-5472.CAN-04-3314

Nakajima, T., Kato, K., Kaneko, A., Tsumuraya, M., Morinaga, S., and Shimosato, Y. (1986). High concentrations of enolase, alpha- and gamma-subunits, in the aqueous humor in cases of retinoblastoma. *Am. J. Ophthalmol.* 101, 102–106. doi: 10.1016/0002-9394(86)90471-x

Niccolai, E., Cappello, P., Taddei, A., Ricci, F., D'elios, M. M., Benagiano, M., et al. (2016). Peripheral ENO1-specific T cells mirror the intratumoral immune response and their presence is a potential prognostic factor for pancreatic adenocarcinoma. *Int. J. Oncol.* 49, 393–401. doi: 10.3892/ijo.2016.3524

Oh, B. M., Lee, S. J., Cho, H. J., Park, Y. S., Kim, J. T., Yoon, S. R., et al. (2017). Cystatin SN inhibits auranofin-induced cell death by autophagic induction and ROS regulation via glutathione reductase activity in colorectal cancer. *Cell Death Dis.* 8:e2682. doi: 10.1038/cddis.2017.100

Pan, C., Liu, Q., and Wu, X. (2019). HIF1alpha/miR-520a-3p/AKT1/mTOR feedback promotes the proliferation and glycolysis of gastric cancer cells. *Cancer Manag. Res.* 11, 10145–10156. doi: 10.2147/CMAR.S223473

Pancholi, V. (2001). Multifunctional alpha-enolase: its role in diseases. *Cell. Mol. Life Sci.* 58, 902–920. doi: 10.1007/pl00000910

Parkin, D. M., Bray, F., Ferlay, J., and Pisani, P. (2005). Global cancer statistics, 2002. *CA Cancer J. Clin.* 55, 74–108. doi: 10.3322/canjclin.55.2.74

Paschke, R., Lincke, T., Muller, S. P., Kreissl, M. C., Dralle, H., and Fassnacht, M. (2015). The treatment of well-differentiated thyroid carcinoma. *Dtsch. Arztebl. Int.* 112, 452–458. doi: 10.3238/arztebl.2015.0452

Principe, M., Borgoni, S., Cascione, M., Chattaragada, M. S., Ferri-Borgogno, S., Capello, M., et al. (2017). Alpha-enolase (ENO1) controls alpha v/beta 3 integrin expression and regulates pancreatic cancer adhesion, invasion, and metastasis. *J. Hematol. Oncol.* 10:16. doi: 10.1186/s13045-016-0385-8

Principe, M., Ceruti, P., Shih, N. Y., Chattaragada, M. S., Rolla, S., Conti, L., et al. (2015). Targeting of surface alpha-enolase inhibits the invasiveness of pancreatic cancer cells. *Oncotarget* 6, 11098–11113. doi: 10.18632/oncotarget.3572

Qian, X., Xu, W., Xu, J., Shi, Q., Li, J., Weng, Y., et al. (2017). Enolase 1 stimulates glycolysis to promote chemoresistance in gastric cancer. *Oncotarget* 8, 47691–47708. doi: 10.18632/oncotarget.17868

Saavedra, H. I., Knauf, J. A., Shirokawa, J. M., Wang, J., Ouyang, B., Elisei, R., et al. (2000). The RAS oncogene induces genomic instability in thyroid PCCL3 cells via the MAPK pathway. *Oncogene* 19, 3948–3954. doi: 10.1038/sj.onc.1203723

Saiselet, M., Floor, S., Tarabichi, M., Dom, G., Hebrant, A., van Staveren, W. C., et al. (2012). Thyroid cancer cell lines: an overview. *Front. Endocrinol.* 3:133. doi: 10.3389/fendo.2012.00133

Semenza, G. L. (2011). Hypoxia-inducible factor 1: regulator of mitochondrial metabolism and mediator of ischemic preconditioning. *Biochim. Biophys. Acta* 1813, 1263–1268. doi: 10.1016/j.bbamcr.2010.08.006

Sipos, J. A., and Mazzaferri, E. L. (2010). Thyroid cancer epidemiology and prognostic variables. *Clin. Oncol. (R. Coll. Radiol.)* 22, 395–404. doi: 10.1016/j.clon.2010.05.004

Song, Y., Luo, Q., Long, H., Hu, Z., Que, T., Zhang, X., et al. (2014). Alpha-enolase as a potential cancer prognostic marker promotes cell growth, migration, and invasion in glioma. *Mol. Cancer* 13:65. doi: 10.1186/1476-4598-13-65

Sun, L., Lu, T., Tian, K., Zhou, D., Yuan, J., Wang, X., et al. (2019). Alpha-enolase promotes gastric cancer cell proliferation and metastasis via regulating AKT signaling pathway. *Eur. J. Pharmacol.* 845, 8–15. doi: 10.1016/j.ejphar.2018.12.035

Tu, S. H., Chang, C. C., Chen, C. S., Tam, K. W., Wang, Y. J., Lee, C. H., et al. (2010). Increased expression of enolase alpha in human breast cancer confers tamoxifen resistance in human breast cancer cells. *Breast Cancer Res. Treat.* 121, 539–553. doi: 10.1007/s10549-009-0492-0

Wang, W., He, Y., Zhao, Q., Zhao, X., and Li, Z. (2020). Identification of potential key genes in gastric cancer using bioinformatics analysis. *Biomed. Rep.* 12, 178–192. doi: 10.3892/br.2020.1281

Warburg, O., Wind, F., and Negelein, E. (1927). The metabolism of tumors in the body. *J. Gen. Physiol.* 8, 519–530. doi: 10.1085/jgp.8.6.519

Wei, J., Wu, J., Xu, W., Nie, H., Zhou, R., Wang, R., et al. (2018). Salvianolic acid B inhibits glycolysis in oral squamous cell carcinoma via targeting PI3K/AKT/HIF-1alpha signaling pathway. *Cell Death Dis.* 9:599. doi: 10.1038/s41419-018-0623-9

Xiao, Y., Peng, H., Hong, C., Chen, Z., Deng, X., Wang, A., et al. (2017). PDGF promotes the Warburg effect in pulmonary arterial smooth muscle cells via activation of the PI3K/AKT/mTOR/HIF-1alpha signaling pathway. *Cell. Physiol. Biochem.* 42, 1603–1613. doi: 10.1159/000479401

Xing, M. (2010). Prognostic utility of BRAF mutation in papillary thyroid cancer. *Mol. Cell. Endocrinol.* 321, 86–93. doi: 10.1016/j.mce.2009.10.012

Yang, X., Cheng, Y., Li, P., Tao, J., Deng, X., Zhang, X., et al. (2015). A lentiviral sponge for miRNA-21 diminishes aerobic glycolysis in bladder cancer T24 cells via the PTEN/PI3K/AKT/mTOR axis. *Tumour Biol.* 36, 383–391. doi: 10.1007/s13277-014-2617-2

Yin, H., Wang, L., and Liu, H. L. (2018). ENO1 overexpression in pancreatic cancer patients and its clinical and diagnostic significance. *Gastroenterol. Res. Pract.* 2018:3842198. doi: 10.1155/2018/3842198

Zakrzewicz, D., Didiasova, M., Zakrzewicz, A., Hocke, A. C., Uhle, F., Markart, P., et al. (2014). The interaction of enolase-1 with caveolae-associated proteins regulates its subcellular localization. *Biochem. J.* 460, 295–307. doi: 10.1042/BJ20130945

Zhan, P., Zhao, S., Yan, H., Yin, C., Xiao, Y., Wang, Y., et al. (2017). alpha-enolase promotes tumorigenesis and metastasis via regulating AMPK/mTOR pathway in colorectal cancer. *Mol. Carcinog.* 56, 1427–1437. doi: 10.1002/mc.22603

Zhang, X., Wang, S., Wang, H., Cao, J., Huang, X., Chen, Z., et al. (2019). Circular RNA circNRIP1 acts as a microRNA-149-5p sponge to promote gastric cancer progression via the AKT1/mTOR pathway. *Mol. Cancer* 18:20. doi: 10.1186/s12943-018-0935-5

Zhao, M., Fang, W., Wang, Y., Guo, S., Shu, L., Wang, L., et al. (2015). Enolase-1 is a therapeutic target in endometrial carcinoma. *Oncotarget* 6, 15610–15627. doi: 10.18632/oncotarget.3639

Zhu, W., Li, H., Yu, Y., Chen, J., Chen, X., Ren, F., et al. (2018). Enolase-1 serves as a biomarker of diagnosis and prognosis in hepatocellular carcinoma patients. *Cancer Manag. Res.* 10, 5735–5745. doi: 10.2147/CMAR.S182183

Zhu, X., Miao, X., Wu, Y., Li, C., Guo, Y., Liu, Y., et al. (2015). ENO1 promotes tumor proliferation and cell adhesion mediated drug resistance (CAM-DR) in Non-Hodgkin's Lymphomas. *Exp. Cell Res.* 335, 216–223. doi: 10.1016/j.yexcr.2015.05.020

Conflict of Interest: The authors declare that the research was conducted in the absence of any commercial or financial relationships that could be construed as a potential conflict of interest.

frontiers in Oncology

ORIGINAL RESEARCH
published: 27 April 2021
doi: 10.3389/fonc.2021.651809

An Immune Model to Predict Prognosis of Breast Cancer Patients Receiving Neoadjuvant Chemotherapy Based on Support Vector Machine

Mozhi Wang[1†], Zhiyuan Pang[2†], Yusong Wang[1], Mingke Cui[2], Litong Yao[1], Shuang Li[2], Mengshen Wang[1], Yanfu Zheng[2], Xiangyu Sun[1], Haoran Dong[1], Qiang Zhang[2] and Yingying Xu[1*]*

[1] Department of Breast Surgery, The First Affiliated Hospital of China Medical University, Shenyang, China, [2] Department of Breast Surgery, Cancer Hospital of China Medical University, Liaoning Cancer Hospital & Institute, Shenyang, China

OPEN ACCESS

Edited by:
Hengyu Li,
Second Military Medical University, China

Reviewed by:
Ke-Da Yu,
Fudan University, China
Zhidong Lv,
The Affiliated Hospital of Qingdao University, China

***Correspondence:**
Yingying Xu
xuyingying@cmu.edu.cn
Qiang Zhang
zhangqiang8220@163.com

[†]These authors have contributed equally to this work

Specialty section:
This article was submitted to Molecular and Cellular Oncology, a section of the journal Frontiers in Oncology

Received: 11 January 2021
Accepted: 22 February 2021
Published: 27 April 2021

Citation:
Wang M, Pang Z, Wang Y, Cui M, Yao L, Li S, Wang M, Zheng Y, Sun X, Dong H, Zhang Q and Xu Y (2021) An Immune Model to Predict Prognosis of Breast Cancer Patients Receiving Neoadjuvant Chemotherapy Based on Support Vector Machine. Front. Oncol. 11:651809. doi: 10.3389/fonc.2021.651809

Tumor microenvironment has been increasingly proved to be crucial during the development of breast cancer. The theory about the conversion of cold and hot tumor attracted the attention to the influences of traditional therapeutic strategies on immune system. Various genetic models have been constructed, although the relation between immune system and local microenvironment still remains unclear. In this study, we tested and collected the immune index of 262 breast cancer patients before and after neoadjuvant chemotherapy. Five indexes were selected and analyzed to form the prediction model, including the ratio values between after and before neoadjuvant chemotherapy of $CD4^+/CD8^+$ T cell ratio; lymphosum of T, B, and natural killer (NK) cells; $CD3^+CD8^+$ cytotoxic T cell percent; $CD16^+CD56^+$ NK cell absolute value; and $CD3^+CD4^+$ helper T cell percent. Interestingly, these characters are both the ratio value of immune status after neoadjuvant chemotherapy to the baseline. Then the prediction model was constructed by support vector machine (accuracy rate = 75.71%, area under curve = 0.793). Beyond the prognostic effect and prediction significance, the study instead emphasized the importance of immune status in traditional systemic therapies. The result provided new evidence that the dynamic change of immune status during neoadjuvant chemotherapy should be paid more attention.

Keywords: neoadjuvant chemotherapy, prediction, immunity, breast cancer, support vector machine

INTRODUCTION

Breast cancer (BC) has been the most common cancer in women, giving rise to 30% of new cases (1). Although the overall mortality of BC is second to lung cancers, it has been the first leading cause of cancer death among females aged 20 to 59 years. With the improved treatment strategies including endocrine therapy, targeted therapy, radiotherapy, and chemotherapy, the mortality of BC declines significantly. However, the descent slowed from previous years in contrast to the accelerating decline of lung cancer and melanoma, which may be owing to a wake of immune therapy for advanced cancers. Since ipilimumab was approved by the

Food and Drug Administration in 2011 (2), immune checkpoint inhibitors have become the promising therapy strategy in the past decades. As a result of low somatic mutation burden, BC showed poor response to immune therapy, traditionally regarded as an immune desert (3). Thus, the diagnosis and treatment of BC have gotten stuck in a bottleneck.

Surprisingly, immune checkpoint inhibitors were proven to function on some certain subpopulation of BC (4, 5). Atezolizumab, a programmed death 1 ligand (PD-L1) inhibitor, was suggested to prolong of overall survival (OS) in advanced triple-negative BC (TNBC) patients whose PD-L1 expressed positive. Despite the low immunogenicity, some BC patients could receive benefit from combination treatment of immune therapy and chemotherapy. Thus, the cold tumor is likely to be turned into hot tumor when treated with traditional therapeutic approaches, such as chemotherapy, radiotherapy, and targeted therapy (6). Therefore, the immune status before and after chemotherapy should be clear to unveil the key indexes that work against the malignant progression and indicate outcomes.

The increasing improvement of BC outcome is in virtue of early diagnosis, and various predictive models emerge as the times require. Clinical characteristics, including grades, TNM stages, and lymph node invasion, are essential prognostic factors besides imaging examination and have been widely used for the diagnosis and treatment (7, 8). During the past years, high-throughput sequencing made it possible to reveal the landscape of cancer transcriptome and genome. Groups of proteins, transcripts, and genes were screened to formulate new types of prediction models. The support vector machine (SVM) is a supervised learning algorithm that can achieve binary classification by linear or non-linear decision boundary. A relatively accurate maximum-margin hyperplane could be trained, even though the sample size is small. These years, many predictive models were directly constructed by SVM using high-dimensional profiles, as there are various public datasets concluding the number of presented samples, clinical information, and follow-up information (9, 10). However, genome and transcriptome data of tumor tissue samples can only reflect regional microenvironment status (11). Compared with local immune infiltration detected on sample, peripheral blood examination is much more accessible.

Hence, this study retrospectively enrolled 262 women with BC, collecting immune function indexes before and after neoadjuvant chemotherapy (NAC). And we performed univariate analysis to select independent indicators and used SVM to train a model that can predict prognosis of patients, named as NeoAdjuvant Therapy Immune Model (NATIM).

MATERIALS AND METHODS

Patients and Preprocessing

The flowchart of the study is shown in **Figure 1**. The study has been approved by the Ethics Committee of the Cancer Hospital of China Medical University. As shown in **Figure 1**, the total cohort included 262 patients from the Breast Surgery Department of Cancer Hospital of China Medical University who received NAC during the period of 2014 and 2018. The clinical and pathological features were collected as follows: age;

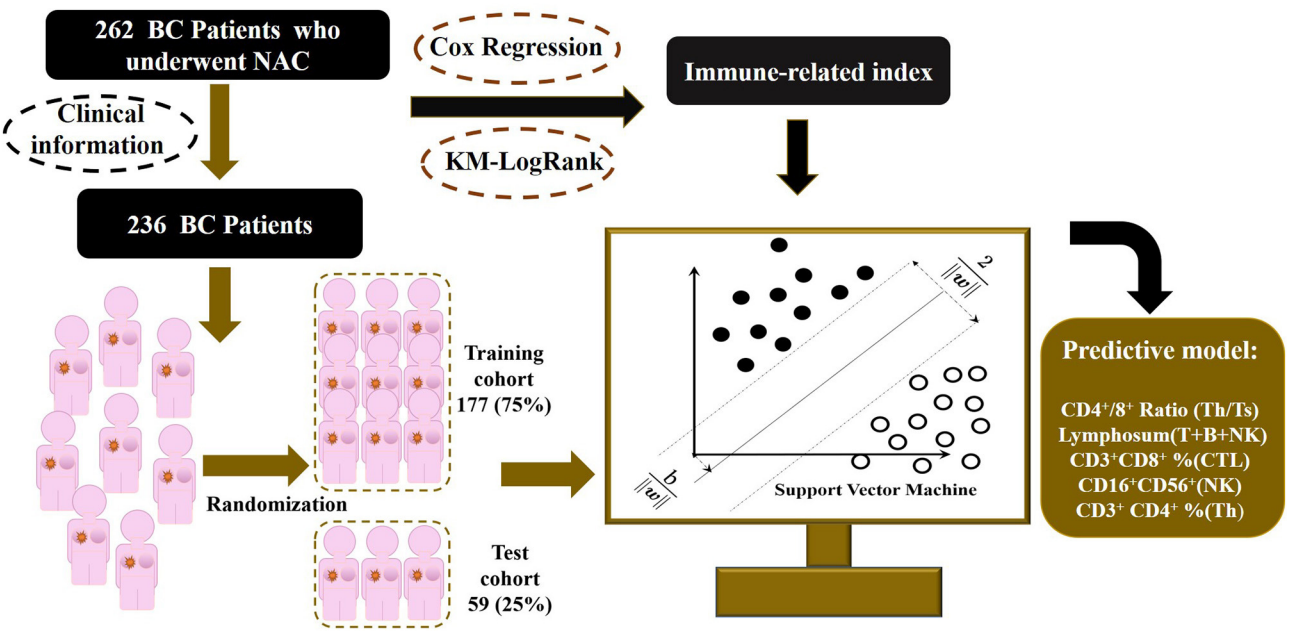

FIGURE 1 | Outline of the SVM-NATIM model flow. The study enrolled 262 women with breast cancer, collecting immune function indexes before and after neoadjuvant chemotherapy. After data processing, 236 patients were put into modeling procedure. Univariate analysis and supporting vector machine were performed to select independent indicators and train a predictive model, named as NeoAdjuvant Therapy Immune Model (NATIM).

TABLE 1 | Clinicopathological characteristics of patients when diagnosed.

Characteristics	Number	Percent (%)
All patients	262	100
Age, years		
≤50	104	39.7
>50	158	60.3
Grade		
1	3	1.1
2	118	45.0
3	14	5.3
Unknown	127	48.5
cT		
1	3	1.1
2	220	84.0
3	21	8.0
Unknown	18	6.9
N		
−	159	60.7
+	14	5.3
Unknown	89	34.0
ER		
−	104	39.7
+	145	55.3
Unknown	13	5.0
PR		
−	150	57.2
+	99	37.8
Unknown	13	5.0
HER2		
−	147	56.1
+	63	24.0
Unknown	52	19.9
Ki67, %		
≤20	57	21.7
>20	192	73.3
Unknown	13	5.0
Subtype		
Luminal A	35	13.4
Luminal B	81	30.9
Her2 positive	45	17.2
TNBC	49	18.7
Unknown	52	19.8
NAC		
Anthracycline- and taxane-based	238	90.8
Taxane-based only	22	8.4
Unknown	2	0.8
MP grade		
1	11	4.2
2	87	33.2
3	103	39.3
4	39	14.9
5	12	4.6
Unknown	10	3.8

ER, estrogen receptor; PR, progesterone receptor; HER2, human epidermal growth factor receptor; TNBC, triple-negative breast cancer; NAC, neoadjuvant chemotherapy; MP, Miller–Payne.

gender; grade; clinical primary tumor (T) and regional nodes (N) stage at diagnosed; grade; pathological T and N stage at surgery; estrogen receptor (ER), progesterone receptor (PR), human epidermal growth factor receptor (HER2), and Ki67 percentage before and after NAC; Miller–Payne (MP) grade; and therapeutic plans of NAC. The histopathological diagnosis and histochemical examination were performed on tumor biopsy before NAC and tumor specimens at surgery after NAC, and TNM stage followed the eighth edition of AJCC TNM staging. The follow-up data including death and date were collected every 6 months by telephone and OS was calculated from the date of surgery to the date of death or the latest follow-up.

Patients whose information was missed had been excluded, resulting in a total of 236 patients enrolled finally. To minimize the bias, outliers were assessed and winsorized. Characteristics that were unknown for more than 10% of overall patients had been deleted, whereas missed items that remained were assigned as average values.

Immune Status of Patients

All immune-related indexes in peripheral blood that reflected lymphocytic immune function were examined by clinical laboratory of Cancer Hospital of China Medical University before and after NAC. Immune-related indexes include $CD4^+/CD8^+$T cell ratio, $CD16^+CD56^+$ natural killer (NK) cell percent, $CD16^+CD56^+$ NK cell absolute value, $CD19^+$ B cell percent, $CD19^+$B cell absolute value, $CD3^+$ T cell percent, $CD3^+$ T cell absolute value, $CD3^+CD4^+$ helper T cell percent, $CD3^+CD4^+$ helper T cell absolute value, $CD3^+CD8^+$ cytotoxic T cell percent, $CD3^+CD8^+$ cytotoxic T cell absolute value, $CD45^+$ T cell absolute value, and lymphosum of T, B, and NK cells.

Statistical Programs and Software

Statistical analyses were performed with R version 3.5.3 and SPSS version 19. The SVM algorithm was built using the LIBSVM program 27 based on MATLAB 2017a (MathWorks), and the source code was uploaded to Github (https://github.com/zjslp218/NATIM-SVM-model).

RESULTS

Change of Characteristics of Peripherally Immune Status Before and After NAC

We collected the information of 262 BC patients who received NAC before surgery (**Table 1**) and sorted out 236 patients whose clinical characteristics and immune function examination results before and after NAC were both accessible. As shown in **Tables 2**, **3**, after NAC, $CD4^+/CD8^+$ T cell ratio elevated to 7.01 ± 72.19 from 1.95 ± 0.85 and lymphosum of T, B, and NK cell reached to 216.28 ± 750.71 from 128.7 ± 326.24. On the contrary, $CD16^+CD56^+$ NK cell absolute value, $CD19^+$ B cells, and $CD45^+$ T cells were decreased, among which $CD19^+$ B cell absolute value and percent decreased most.

The relationship of peripherally immune status before and after NAC and pathological indexes when first diagnosed were additionally assessed (**Supplementary Tables 1**–**3**). The change of $CD3^+$ T cell percent (after NAC vs. baseline) was significantly

TABLE 2 | Statistical distribution of immune function indexes before NAC.

	Average ± SD	Range	Percentage		
			25%	Median	75%
$CD4^+/CD8^+$ T cell ratio	1.95 ± 0.85	0.6–4.99	1.27	1.82	2.37
$CD16^+CD56^+$ NK cell percent	20.68 ± 8.1	4.03–48.03	15.15	19.36	25.46
$CD16^+CD56^+$ NK cell absolute value	465.25 ± 290.26	24.09–1,655.28	287.08	383.74	603.43
$CD19^+$ B cell percent	10.92 ± 10.32	2.17–157.59	7.58	9.63	12.77
$CD19^+$B cell absolute value	223.66 ± 128.89	14.22–975.57	134.52	197.00	278.00
$CD3^+$ T cell percent	71.28 ± 48.98	6.44–802.65	63.65	69.62	74.50
$CD3^+$ T cell absolute value	1,532.19 ± 938.8	43.62–9,479.66	1,055.26	1,314.25	1,752.82
$CD3^+CD4^+$ helper T cell percent	55.65 ± 144.9	19.54–1,750.31	34.67	40.95	45.60
$CD3^+CD4^+$ helper T cell absolute value	900.42 ± 636.94	23.15–6,294.57	584.80	761.20	1,033.00
$CD3^+CD8^+$ cytotoxic T cell percent	33.42 ± 87.46	7.51–1,076.42	18.56	23.52	28.71
$CD3^+CD8^+$ cytotoxic T cell absolute value	539.65 ± 412.78	7.77–4,121.23	328.50	471.28	613.45
$CD45^+$ T cell absolute value	2,243.73 ± 1,235.11	478.1–11,715.49	1,587.53	1,984.50	2,519.49
Lymphosum of T, B, and NK cells	128.7 ± 326.24	30.24–4,321.96	99.53	99.77	99.86

NK cell, natural killer cell.

TABLE 3 | Statistical distribution of immune function indexes after NAC.

	Average ± SD	Range	Percentage		
			25%	Median	75%
$CD4^+/CD8^+$ T cell ratio	7.01 ± 72.19	7.01–72.19	7.01	72.19	7.01
$CD16^+CD56^+$ NK cell percent	364.14 ± 5,289.26	364.14–5,289.26	364.14	5,289.26	364.14
$CD16^+CD56^+$ NK cell absolute value	346.03 ± 279.22	346.03–279.22	346.03	279.22	346.03
$CD19^+$ B cell percent	5.13 ± 18.66	5.13–18.66	5.13	18.66	5.13
$CD19^+$B cell absolute value	69.78 ± 74.85	69.78–74.85	69.78	74.85	69.78
$CD3^+$ T cell percent	78 ± 28.68	78–28.68	78.00	28.68	78.00
$CD3^+$ T cell absolute value	1,330.41 ± 952.48	1,330.41–952.48	1,330.41	952.48	1,330.41
$CD3^+CD4^+$ helper T cell percent	50.61 ± 113.48	50.61–113.48	50.61	113.48	50.61
$CD3^+CD4^+$ helper T cell absolute value	2,322.06 ± 23,648.54	2,322.06–23,648.54	2,322.06	23,648.54	2,322.06
$CD3^+CD8^+$ cytotoxic T cell percent	27.45 ± 8.67	27.45–8.67	27.45	8.67	27.45
$CD3^+CD8^+$ cytotoxic T cell absolute value	498.25 ± 406.11	498.25–406.11	498.25	406.11	498.25
$CD45^+$ T cell absolute value	1,748 ± 1,187.9	1,748–1,187.9	1,748.00	1,187.90	1,748.00
lymphosum of T, B, and NK cells	216.28 ± 750.71	216.28–750.71	216.28	750.71	216.28

NK cell, natural killer cell.

increased in ER-positive subgroup when compared to ER-negative subgroup (1.26 ± 1.05 vs. 1.18 ± 0.93, $P = 0.031$). In addition to $CD3^+$ T cell percent (1.33 ± 1.28 vs. 1.16 ± 0.78, $P = 0.023$), the change of $CD16^+CD56^+$ NK cell percent (after NAC vs. baseline) circulating in periphery blood was much in the PR-positive subgroup than in the PR-negative subgroup (52.67 ± 485.31 vs. 1.02 ± 0.3, $P = 0.048$). Dissimilarly, the ratio of $CD3^+CD4^+$ helper T cell percent and $CD19^+$ B cell percent after NAC to that of baseline was less in HER2-positive subpopulation rather than HER2-negative subpopulation ($CD3^+CD4^+$ helper T cell percent, 1.01 ± 0.26 vs. 1.34 ± 3.14, $P = 0.019$; $CD19^+$ B cell percent, 0.38 ± 0.33 vs. 0.61 ± 2.68, $P = 0.046$). Above distribution and change intimated the different immune cell populations evoked by NAC in peripheral blood.

Then, we analyzed correlation between the peripheral immune indexes before and after NAC (**Supplementary Figures 1**, **2**). Spearman correlation was performed, and it suggested that $CD45^+$ T cell absolute value, $CD3^+$ T cell absolute value, and $CD3^+CD4^+$ helper T cell absolute value were strongly related to each other positively. And $CD16^+CD56^+$ NK cell absolute value was negatively related to $CD3^+$ T cell percent.

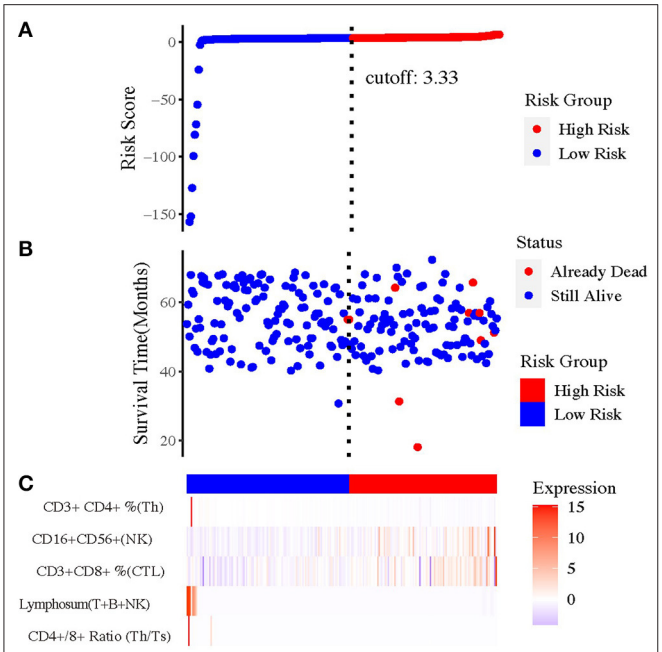

FIGURE 2 | The prognostic value of risk model of the five immune-related indexes. **(A)** The risk curve based on the model with the largest area under curve (AUC). **(B)** The scatterplot based on the survival status of each sample. The blue and red plots represent low risk and high risk, respectively. **(C)** The heatmap showed the enrichment level of immune-related indexes in peripheral blood in high- and low-risk subgroups.

Selection of Related Immune Index

To select the most appropriate immune function indexes, we calculated the ratio of each immune function index after NAC to the baseline and put them as independent indexes, besides the direct value before and after NAC. To distinguish the three values of each index, the values before and after NAC were named as Index(b) and Index(a), whereas the ratio values were Index(a/b) below. Subsequently, we performed Cox regression and Kaplan–Meier (KM) analysis on all lymphocytic immune function indexes in peripheral blood for univariate analysis (**Supplementary Figures 3B–F**). And forest plot was drawn and inferred that the indexes (a/b) showed overall better interaction with prognosis (**Supplementary Figure 4**). Under help of SVM, the most optimal combination that consisted of five indexes were sorted out (**Figure 2**), including $CD4^+/CD8^+$ T cell ratio (a/b); lymphosum of T, B, and NK cells (a/b); $CD3^+CD8^+$ cytotoxic T cell percent (a/b); $CD16^+CD56^+$ NK cell absolute value (a/b); and $CD3^+CD4^+$ helper T cell percent (a/b).

Construction and Evaluation of the NATIM

To better classify the patients with different prognosis, the population was divided into two subgroups by the comprehensive assessment of live status and OS. Those who lived for more than 5 years were assigned as low-risk population, whereas those who were dead within 5 years or lived for <5 years were assigned as high-risk population. Because of the lack of external validation cohort, training cohort and test cohort were randomly selected and formed by division of original cohort. After training of training set and adjustment of parameters, SVM was applied to construct the best-performing model with Gaussian kernel. The accuracy reached 75.71% (134/177) in the training set, and the area under curve (AUC) reached 0.794, highlighting the well-prognostic effectiveness of NATIM (**Figures 3A,B**). Then we used randomized testing cohort to test the efficacy and obtained an accuracy of 67.80% (40/59) and AUC of 0.653 in the testing cohort (**Figures 3C,D**). Furthermore, the KM plot was shown to validate the effective of NATIM to classify the high- and low-risk subpopulation ($P = 0.0018$) (**Figure 3E**).

Therefore, we drew the receiver operating characteristic curve and calculated the AUC of each single immune index (**Supplementary Figure 3A**). All the AUCs of single immune indexes were lower than that of NATIM (*P*-value of $CD4^+/CD8^+$ T cell ratio; lymphosum of T, B, and NK cell; and $CD3^+CD8^+$ cytotoxic T cell percent were both <0.05). Accordingly, the above results claimed that NATIM can provide an independent approach to predict the prognosis, more effective than any single immune cell model.

DISCUSSION

In recent decades, immune therapy has become the most promising strategy. Since reaching several peaks that contributed by clinical and preclinical breakthroughs, progresses against BC slow down. Distinct from other metastatic cancers including non-small cell lung cancer, melanoma, and gastric cancer, BCs react inertly to systemic and local immune mobilization. In TONIC trial (NCT02499367), 67 patients who were diagnosed as having advanced TNBC randomly received a 2-week inducible therapy and sequenced by three cycles of nivolumab, a programmed death 1 (PD-1) inhibitor (12). Surprisingly, doxorubicin and cisplatin were found to induce T cell infiltration and subsequently acquire the highest clinical response rate. Afterward, researches about the effect of traditional treatment on microenvironment came out one after the other. Chemotherapy was proved to impact individual resistance to different types of drugs by activating, recruiting, and polarizing tumor-related immune cells in addition to immunogenic cell death (13). Chemotherapy could directly kill immunosuppressive cells and effective cells, increasing infiltration of tumor-related macrophages and then induced drug resistance (14, 15). The dual effect of chemotherapy on immunity leaves the mechanism complex and potential to be targeted as diagnostic and therapeutic markers. Our results showed that $CD4^+/CD8^+$ T cell ratio increased from immune suppressive status to an active status, indicating an elevated neoantigen-recognitive and killing capacity of regional immune cells.

Outcome prediction and treatment benefit models relied on clinical features as mainly elements were variously developed and validated around the 20th century (16). With the rapid development of next-generation sequencing and single cell sequencing, genome and transcriptome of cancer patients have been profiled accurately. Diverse models and biomarkers have been built up to describe and predict immune status,

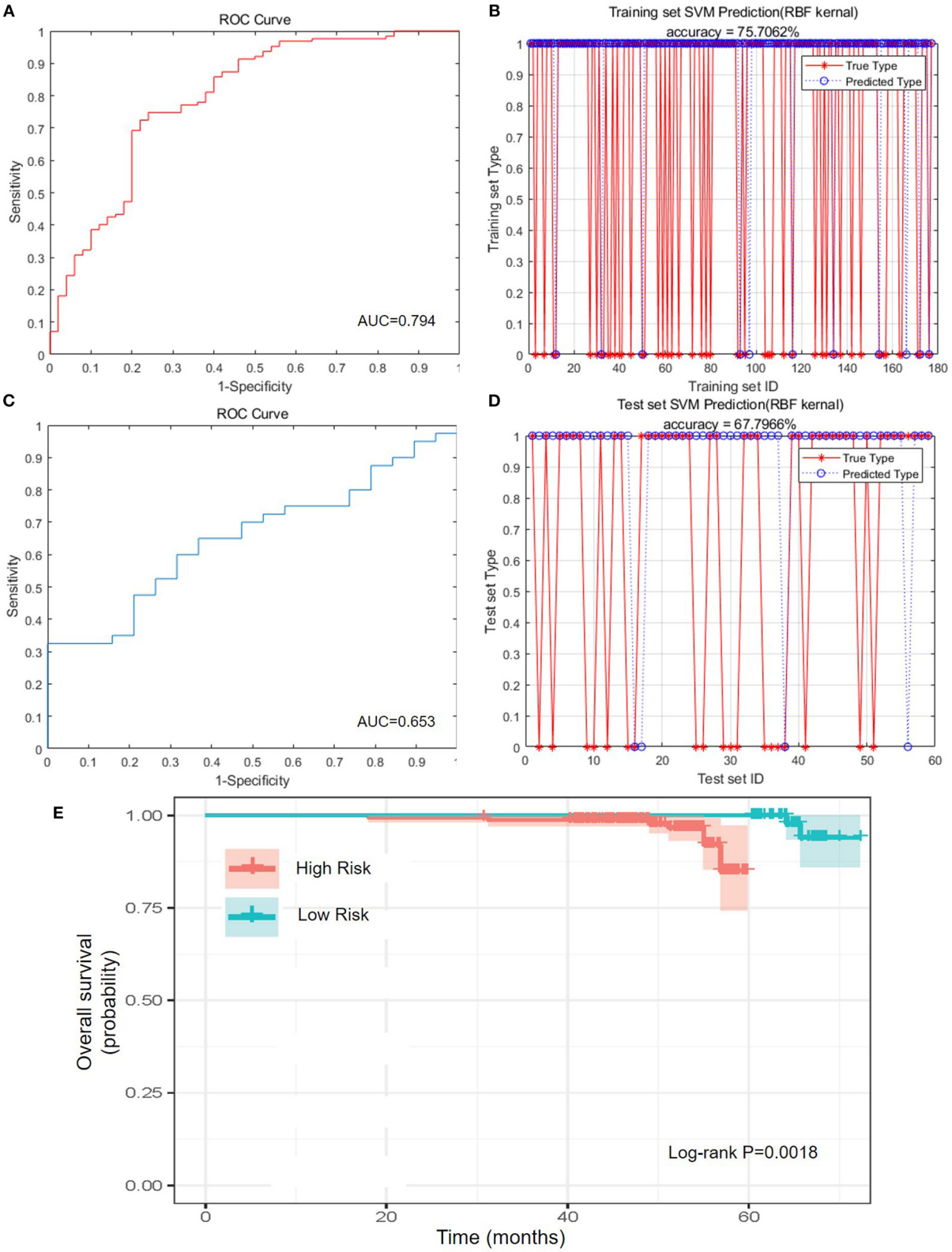

FIGURE 3 | Predictive efficacy of NATIM. **(A)** Receiver operating characteristic (ROC) curve and area under curve (AUC) of NeoAdjuvant Therapy Immune Model (NATIM) in training cohort. **(B)** Prediction accuracy of NATIM in training cohort. **(C)** ROC and AUC of NATIM in test cohort. **(D)** Prediction accuracy of NATIM in test cohort. **(E)** Kaplan–Meier plot of NATIM between high- and low-risk population.

drug response, and prognosis (17–19). Shao et al. analyzed transcriptional expression atlas of TNBC, selected eight mRNAs and two lncRNAs, and constructed a predictive model that can forecast chemotherapy response and outcome of TNBC patients based on the above 10 transcripts (20). A 13-epigenetic characteristics were also formed as a model to distinct low- and high-risk BC population, along with the transcription (21). Moreover, distant metastatic sites of TNBC could be well-predicted by eight signatures in paraffin-embedded tissues likewise (22). However, immunity includes not only microenvironment surrounding the tumor cells, but also the peripherally immune cells that reflect the systemic immunity. Supervision of immune components of peripheral blood is unneglectable. Axelrod et al. performed single cell sequencing on PD-1–high $CD8^+$ T cells in peripheral blood along with the exploration on tumor immune microenvironment of tumor tissues from advanced BC patients who ever received NAC (23). The result at the genetic level suggested the opposite status of peripheral blood and local immune microenvironment.

We collected 262 patients and finally enrolled 236 BC patients who underwent immune function examination in peripheral blood before and after NAC. KM log rank and Cox regression were adopted for the univariate analysis. Three dynamic indexes that reflect changes caused by NAC, $CD4^+/CD8^+$ T cell ratio (a/b), $CD3^+CD8^+$ cytotoxic T cell percent (a/b), and lymphosum of T, B, and NK cells (a/b) were proven to be an effective predictive factor. Then, we randomly divided the cohort into training cohort and validation cohort and used SVM to train the best model, which arrives at an accuracy of 0.75. SVM is an important kind of machine learning algorithm regarded as the best classifier suitable for training sets whose sample size is too small. SVM is a generalized linear regression model for linear subscenarios. And for non-linear subscenarios, the samples of low-dimensional feature space could be mapped to high-dimensional space by nuclear technique to achieve linear analysis of non-linear samples. The theoretical basis of the SVM method is non-linear mapping by using kernel functions instead of non-linear mapping to high-dimensional space. In addition, the optimization goal of SVM is to minimize the structured risk instead of the empirical risk, avoiding the problem of overfit. Then it got the structured description of the data distribution through the margin concept, reducing the requirements of data size and data distribution, leading excellent generalization ability. Consequently, SVM can get more accurate results on small sample training sets than other algorithms.

Neoadjuvant therapy is an appropriate period to evaluate the change of immune status caused by chemotherapy, avoiding the traumatic immune response caused by any other treatment including operation. Furthermore, patients who undergo neoadjuvant therapy are at earlier stages with an improved immunity rather than those who are at advanced stages. Additionally, peripheral blood examination is much easier and cheaper to perform for both doctors and patients, which is an important element for a well-used predictive model. It is worth noting that the indexes sorted by regression with best distinction for prognosis are both the ratio value of immune status after NAC to the baseline. The used studies always studied instantaneous status of immune function of cancer patients, but our results first proved that the dynamic change of immune function may demonstrate much more clues.

This study still has some limitations. First, the immune function assessment of peripheral blood was just carried out in the last few years. Clinical cohort with entire immune examination before and after NAC is so rare that external validation is lacking. Hence, more prospective researches or large-scale studies are urgently required to affirm this result. Second, owing to the specificity of data, the overall patients who enrolled are still not adequate enough to be divided for subgroup analysis. Most immune-related clinical experiments focus attention on TNBC or advanced patients in consideration of ethics. However, the systemic and local immune status of each subtype of BCs ought to be distinct to each other and should be profiled accurately. Finally, the present study just states the peripheral other than local microenvironment immune status. Therefore, it would be better to compare the immune status both from peripheral blood and microenvironment correspondingly and describe the systemic and local immune characteristics exactly before and after chemotherapy. We will enlarge the data and update the model in the future.

In conclusion, we constructed a new immune index model of BC by integrating immune cell absolute value and percentage of dissimilar immune cell population. Our peripheral immune index model is practical for predicting the prognosis of BC patients who received NAC. Further studies are warranted to validate these results.

DATA AVAILABILITY STATEMENT

The raw data supporting the conclusions of this article will be made available by the authors, without undue reservation.

AUTHOR CONTRIBUTIONS

MoW wrote the manuscript. YW and MeW studied R-related data and process. LY and HD performed SPSS-related process. XS revised the language. ZP and SL was in charge of the data collecting, while MC and YZ enrolled the patients. YX and QZ designed the study. All authors contributed to the article and approved the submitted version.

FUNDING

This work was supported by National Natural Science Foundation of China [81773083], Scientific and Technological Innovation Leading Talent Project of Liaoning Province [XLYC1802108] and Support Project for Young and Technological Innovation Talents of Shenyang [RC190393].

SUPPLEMENTARY MATERIAL

The Supplementary Material for this article can be found online at: https://www.frontiersin.org/articles/10.3389/fonc.2021.651809/full#supplementary-material

Supplementary Figure 1 | Spearman correlation between the peripheral immune indexes before neoadjuvant chemotherapy.

Supplementary Figure 2 | Spearman correlation between the peripheral immune indexes after neoadjuvant chemotherapy.

Supplementary Figure 3 | Evaluation of single immune index. **(A)** ROC and AUC of single immune index; **(B)** KM plot of CD16+CD56+ NK cell absolute value (a/b); **(C)** KM plot of lymphosum of T cell, B cell and NK cell (a/b); **(D)** KM plot of CD3+ CD8+ cytotoxic T cell percent (a/b); **(E)** KM plot of CD4+/CD8+ T cell ratio (a/b); **(F)** KM plot of CD3+ CD4+ helper T cell percent (a/b).

Supplementary Figure 4 | Forest plot of index selected by Cox regression.

Supplementary Table 1 | Relationship of peripherally immune status change before and after NAC and ER status at diagnosis.

Supplementary Table 2 | Relationship of peripherally immune status change before and after NAC and PR status at diagnosis.

Supplementary Table 3 | Relationship of peripherally immune status change before and after NAC and HER2 status at diagnosis.

REFERENCES

1. Siegel RL, Miller KD, Jemal A. Cancer statistics, 2020. *CA Cancer J Clin.* (2020) 70:7–30. doi: 10.3322/caac.21590
2. Kirkwood JM, Butterfield LH, Tarhini AA, Zarour H, Kalinski P, Ferrone S. Immunotherapy of cancer in 2012. *CA Cancer J Clin.* (2012) 62:309–35. doi: 10.3322/caac.20132
3. Zehir A, Benayed R, Shah RH, Syed A, Middha S, Kim HR, et al. Mutational landscape of metastatic cancer revealed from prospective clinical sequencing of 10,000 patients. *Nat Med.* (2017) 23:703–13. doi: 10.1038/nm.4333
4. Schmid P, Adams S, Rugo HS, Schneeweiss A, Barrios CH, Iwata H, et al. Atezolizumab and nab-paclitaxel in advanced triple-negative breast cancer. *N Engl J Med.* (2018) 379:2108–21. doi: 10.1056/NEJMoa1809615
5. Emens LA, Esteva FJ, Beresford M, Saura C, De Laurentiis M, Kim SB, et al. Trastuzumab emtansine plus atezolizumab versus trastuzumab emtansine plus placebo in previously treated, HER2-positive advanced breast cancer (KATE2): a phase 2, multicentre, randomised, double-blind trial. *Lancet Oncol.* (2020) 21:1283–95. doi: 10.1016/S1470-2045(20)30465-4
6. Galon J, Bruni D. Approaches to treat immune hot, altered and cold tumours with combination immunotherapies. *Nat Rev Drug Discov.* (2019) 18:197–218. doi: 10.1038/s41573-018-0007-y
7. Degnim AC, Winham SJ, Frank RD, Pankratz VS, Dupont WD, Vierkant RA, et al. Model for predicting breast cancer risk in women with atypical hyperplasia. *J Clin Oncol.* (2018) 36:1840–6. doi: 10.1200/JCO.2017.75.9480
8. Yala A, Lehman C, Schuster T, Portnoi T, Barzilay R. A deep learning mammography-based model for improved breast cancer risk prediction. *Radiology.* (2019) 292:60–6. doi: 10.1148/radiol.2019182716
9. Huang S, Cai N, Pacheco PP, Narrandes S, Wang Y, Xu W. Applications of support vector machine (SVM) learning in cancer genomics. *Cancer Genomics Proteomics.* (2018) 15:41–51. doi: 10.21873/cgp.20063
10. Chen Q, Gao P, Song Y, Huang X, Xiao Q, Chen X, et al. Predicting the effect of 5-fluorouracil-based adjuvant chemotherapy on colorectal cancer recurrence: a model using gene expression profiles. *Cancer Med.* (2020) 9:3043–56. doi: 10.1002/cam4.2952
11. Klauschen F, Muller KR, Binder A, Bockmayr M, Hagele M, Seegerer P, et al. Scoring of tumor-infiltrating lymphocytes: from visual estimation to machine learning. *Semin Cancer Biol.* (2018) 52:151–7. doi: 10.1016/j.semcancer.2018.07.001
12. Voorwerk L, Slagter M, Horlings HM. Immune induction strategies in metastatic triple-negative breast cancer to enhance the sensitivity to PD-1 blockade: the TONIC trial. *Nat Med.* (2019) 25:920–8. doi: 10.1038/s41591-019-0432-4
13. Ruffell B, Coussens LM. Macrophages and therapeutic resistance in cancer. *Cancer Cell.* (2015) 27:462–72. doi: 10.1016/j.ccell.2015.02.015
14. Xynos ID, Karadima ML, Voutsas IF, Amptoulach S, Skopelitis E, Kosmas C, et al. Chemotherapy ± cetuximab modulates peripheral immune responses in metastatic colorectal cancer. *Oncology.* (2013) 84:273–83. doi: 10.1159/000343282
15. Takahashi H, Sakakura K, Mito I, Ida S, Chikamatsu K. Dynamic changes in immune cell profile in head and neck squamous cell carcinoma: immunomodulatory effects of chemotherapy. *Cancer Sci.* (2016) 107:1065–71. doi: 10.1111/cas.12976
16. Candido Dos Reis FJ, Wishart GC, Dicks EM, Greenberg D, Rashbass J, Schmidt MK, et al. An updated PREDICT breast cancer prognostication and treatment benefit prediction model with independent validation. *Breast Cancer Res.* (2017) 19:58. doi: 10.1186/s13058-017-0852-3
17. Zeng D, Zhou R, Yu Y, Luo Y, Zhang J, Sun H, et al. Gene expression profiles for a prognostic immunoscore in gastric cancer. *Br J Surg.* (2018) 105:1338–48. doi: 10.1002/bjs.10871
18. Lai J, Wang H, Pan Z, Su F. A novel six-microRNA-based model to improve prognosis prediction of breast cancer. *Aging.* (2019) 11:649–62. doi: 10.18632/aging.101767
19. Kim J, Yu D, Kwon Y, Lee KS, Sim SH, Kong SY, et al. Genomic characteristics of triple-negative breast cancer nominate molecular subtypes that predict chemotherapy response. *Mol Cancer Res.* (2020) 18:253–63. doi: 10.1158/1541-7786.MCR-19-0453
20. Liu YR, Jiang YZ, Xu XE, Hu X, Yu KD, Shao ZM. Comprehensive transcriptome profiling reveals multigene signatures in triple-negative breast cancer. *Clin Cancer Res.* (2016) 22:1653–62. doi: 10.1158/1078-0432.CCR-15-1555
21. Bao X, Anastasov N, Wang Y, Rosemann M. A novel epigenetic signature for overall survival prediction in patients with breast cancer. *J Transl Med.* (2019) 17:380. doi: 10.1186/s12967-019-2126-6
22. Klimov S, Rida PC, Aleskandarany MA, Green AR, Ellis IO, Janssen EA, et al. Novel immunohistochemistry-based signatures to predict metastatic site of triple-negative breast cancers. *Br J Cancer.* (2017) 117:826–34. doi: 10.1038/bjc.2017.224
23. Axelrod ML, Nixon MJ, Gonzalez-Ericsson PI, Bergman RE, Pilkinton MA, Mcdonnell WJ, et al. Changes in peripheral and local tumor immunity after neoadjuvant chemotherapy reshape clinical outcomes in patients with breast cancer. *Clin Cancer Res.* (2020) 26:5668–81. doi: 10.1158/1078-0432.CCR-19-3685

Conflict of Interest: The authors declare that the research was conducted in the absence of any commercial or financial relationships that could be construed as a potential conflict of interest.

frontiers in Cell and Developmental Biology

REVIEW
published: 31 May 2021
doi: 10.3389/fcell.2021.683940

Endoplasmic Reticulum Stress and Tumor Microenvironment in Bladder Cancer: The Missing Link

Zhenyu Nie[1], Mei Chen[1], Xiaohong Wen[1], Yuanhui Gao[1], Denggao Huang[1], Hui Cao[1], Yanling Peng[1], Na Guo[1], Jie Ni[2,3] and Shufang Zhang[1]**

[1]Central Laboratory, Affiliated Haikou Hospital of Xiangya Medical College, Central South University, Haikou, China, [2]Cancer Care Center, St. George Hospital, Sydney, NSW, Australia, [3]St George and Sutherland Clinical School, Faculty of Medicine, UNSW Sydney, Sydney, NSW, Australia

Bladder cancer is a common malignant tumor of the urinary system. Despite recent advances in treatments such as local or systemic immunotherapy, chemotherapy, and radiotherapy, the high metastasis and recurrence rates, especially in muscle-invasive bladder cancer (MIBC), have led to the evaluation of more targeted and personalized approaches. A fundamental understanding of the tumorigenesis of bladder cancer along with the development of therapeutics to target processes and pathways implicated in bladder cancer has provided new avenues for the management of this disease. Accumulating evidence supports that the tumor microenvironment (TME) can be shaped by and reciprocally act on tumor cells, which reprograms and regulates tumor development, metastasis, and therapeutic responses. A hostile TME, caused by intrinsic tumor attributes (e.g., hypoxia, oxidative stress, and nutrient deprivation) or external stressors (e.g., chemotherapy and radiation), disrupts the normal synthesis and folding process of proteins in the endoplasmic reticulum (ER), culminating in a harmful situation called ER stress (ERS). ERS is a series of adaptive changes mediated by unfolded protein response (UPR), which is interwoven into a network that can ultimately mediate cell proliferation, apoptosis, and autophagy, thereby endowing tumor cells with more aggressive behaviors. Moreover, recent studies revealed that ERS could also impede the efficacy of anti-cancer treatment including immunotherapy by manipulating the TME. In this review, we discuss the relationship among bladder cancer, ERS, and TME; summarize the current research progress and challenges in overcoming therapeutic resistance; and explore the concept of targeting ERS to improve bladder cancer treatment outcomes.

Keywords: endoplasmic reticulum stress, unfolded protein response, tumor microenvironment, bladder cancer, therapeutic target

OPEN ACCESS

Edited by:
Chao Ni,
Zhejiang University, China

Reviewed by:
Lei Jin,
The University of Newcastle, Australia
Bo Wang,
Hainan General Hospital, China

****Correspondence:***
Jie Ni
jie.ni@health.nsw.gov.au
Shufang Zhang
zsf66189665@126.com

Specialty section:
This article was submitted to Molecular and Cellular Oncology, a section of the journal Frontiers in Cell and Developmental Biology

Received: *22 March 2021*
Accepted: *28 April 2021*
Published: *31 May 2021*

Citation:
Nie Z, Chen M, Wen X, Gao Y, Huang D, Cao H, Peng Y, Guo N, Ni J and Zhang S (2021) Endoplasmic Reticulum Stress and Tumor Microenvironment in Bladder Cancer: The Missing Link. Front. Cell Dev. Biol. 9:683940. doi: 10.3389/fcell.2021.683940

INTRODUCTION

Bladder cancer is the fourth most common and eighth most lethal malignant tumor in men in the United States, accounting for an estimated number of 81,400 new cases and 17,980 deaths in the United States in 2020 (Siegel et al., 2020). In China, a total of 80,500 new cases and 32,900 deaths were recorded in 2015 (Chen et al., 2016a).

Bladder cancer represents a broad spectrum of diseases, from low-risk, non-invasive lesions to advanced, muscle-invasive tumors. For non-muscle-invasive bladder cancer (NMIBC), although the survival rate is favorable, patients with low and intermediate risk have 5-year recurrence-free survival rates of only 43 and 33%, respectively (Ritch et al., 2020). For muscle-invasive bladder cancer (MIBC), although neoadjuvant chemotherapy provides a significant survival benefit, metastasis remains a devastating problem in a high portion of MIBC cases (50–70%), resulting in a dismal 5-year overall survival (OS) rate of 4.8% (Alfred-Witjes et al., 2017). Thus, novel treatment strategies against aggressive and advanced bladder cancer are clearly needed.

In eukaryotic cells, the synthesis and processing of secreted and membrane proteins take place in the endoplasmic reticulum (ER). The stability of its environment is a prerequisite for the successful synthesis and correct folding of proteins. When unfolded or misfolded proteins accumulate abnormally in the ER, they cause a harmful situation called ER stress (ERS) and usually trigger an intracellular signaling pathway called unfolded protein response (UPR) to restore normal ER protein-folding functionality. If this function is not restored, apoptosis is activated (Clarke et al., 2012). As such, several reports described a multi-faceted and paradoxical role of ERS in various diseases, such as neurological disorders, immune diseases, and cancers (Forouhan et al., 2018; Siwecka et al., 2019; Qin et al., 2020). In particular, whether ERS and UPR prevent or promote tumor growth has been hotly debated and warrants a careful review.

The tumor microenvironment (TME) refers to the environment in which tumor cells are located during tumorigenesis, development, and metastasis. Various cellular components (e.g., fibroblasts and immune cells) and non-cellular components (e.g., the extracellular matrix and physicochemical factors) can act on tumor cells and directly or indirectly regulate their tumorigenic, metastatic, and therapeutic resistance capacities. However, tumor cells can also alter or reshape the TME through autocrine or paracrine effects (Rodvold et al., 2017). Multiple stressors within the TME can cause ERS in tumor cells. They include intrinsic tumor attributes, such as hypoxia, oxidative stress, and nutrient deprivation and external stressors, such as chemotherapy, radiation, and immunotherapy. Cancer cells then utilize effective pathways to respond, adapt, and save themselves from ERS-induced cell death (Wouters and Koritzinsky, 2008; Saito et al., 2009; Tsachaki et al., 2018).

In this work, we review the ERS pathway and its role in bladder cancer; discuss the relationship of bladder cancer, ERS, and TME; highlight the significance of ERS in innate tumoricidal immune response and the efficacy of cancer immunotherapy; summarize the current research progress and challenges in this field; and explore the concept of targeting ERS to improve bladder cancer treatment outcomes in the clinical setting.

ERS AND RELATED SIGNALING PATHWAYS

As mentioned above, multiple physiological and pathological stimuli can cause ERS, thereby triggering UPR. When a mild to moderate (yet persistent) ERS occurs, cells will cause transcriptional and translational changes through homeostatic UPR (hUPR), which promotes cell adaptation and enhances cell survival. As the ERS progresses to a degree where hUPR is inadequate to restore homeostasis, the UPR in the cell will be dominated by terminal UPR (tUPR). This process will actively initiate cell apoptosis to prevent continuous cell damage (Abern et al., 2013; Wallis et al., 2016).

Unfolded protein response relies on signaling cascades mediated by three different transmembrane proteins localized on the ER membrane, namely, inositol-requiring enzyme 1α (IRE1α), protein kinase-like ER kinase (PERK), and activating transcription factor 6 (ATF6; **Figure 1**). When the ER is in a homeostatic state, a chaperone protein called glucose-regulated protein 78 (GRP78) in the ER binds to the intraluminal domains of the three transmembrane proteins and keeps them inactive. When a large number of misfolded and unfolded proteins accumulate in the ER, the three transmembrane proteins will be dissociated from GRP78 and activate three parallel UPR signaling pathways to reduce the burden caused by unfolded or misfolded proteins in the ER. They work by decreasing translation to reduce the folding requirements of newly synthesized proteins or guiding unfolded proteins into the cytoplasm for ubiquitination and destruction through the ER-associated degradation (ERAD) pathway (Ri, 2016; Li et al., 2019).

IRE1α Pathway

IRE1 is a dual-effect protein with endoribonuclease (RNase) and serine/threonine kinase activities. Once the RNase domain of IRE1α is activated, it catalyzes a splicing reaction of X-box binding protein-1 (XBP1) mRNA and generates a resultant splicing variant called XBP1s. XBP1s upregulates the expression of many genes related to UPR, including *ZNF64*, *GPR7*, *PLK*, and *MRPS22* (Ron and Walter, 2007; Peschek et al., 2015), to increase the expression of chaperones and foldase to mitigate ERS. In addition, under persistent and unresolved ERS, XBP1s can initiate a global mRNA degradation to limit the translation of proteins on the ER – a process known as regulated IRE1α-dependent decay, which ultimately induces ER destruction and apoptosis (Tam et al., 2014; Rashid et al., 2017). In bladder cancer, upregulated IRE1α is associated with an immediate UPR to restore protein homeostasis, and if UPR fails to alleviate ERS under prolonged or severe ERS, cells activate apoptosis pathways to eliminate damaged cells (Wu et al., 2019a). On the serine/threonine kinase front, phosphorylated IRE1α activates c-Jun N-terminal kinase (JNK) and NF-κB signaling, regulating a diverse range of cellular processes, such as inflammation, cell proliferation, survival, angiogenesis, and autophagy (Urano et al., 2000; Zhang and Kaufman, 2008; Han et al., 2009).

PERK Pathway

The N-terminal of PERK inside the ER lumen is a stress-sensitive domain that binds to GRP78, whereas its C-terminal region on the cytoplasmic side contains a serine/threonine protein kinase domain that is capable of quickly and effectively inhibiting cell protein translation by phosphorylating the serine

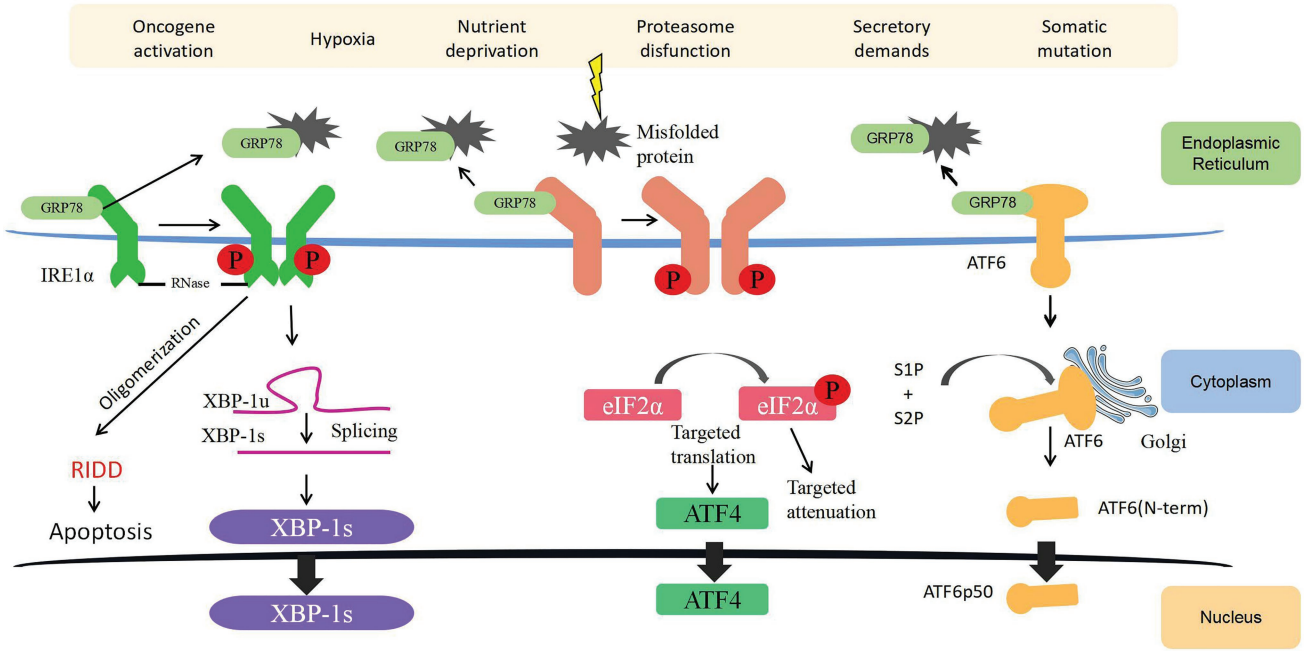

FIGURE 1 | Endoplasmic reticulum (ER) stress (ERS) and unfolded protein response (UPR) signaling. Three ERS sensors (namely, IRE1α, PERK, and ATF6) collectively coordinate UPR signaling. Under normal conditions, GRP78 is attached to ERS sensors rendering them inactive. During ERS, GRP78 dissociates from the three transmembrane proteins on the ER membrane and activates these pathways. Together, the IRE1α, PERK, and ATF6 pathways regulate several genes with the ultimate goal of reinstating ER homeostasis and induce survival, angiogenesis, metastasis, and cell death resistance in cancer. ATF4, activating transcription factor 4; ATF6, activating transcription factor 6; ER, endoplasmic reticulum; eIF2α, eukaryotic initiation factor 2α; GRP78, glucose-regulated protein 78; IRE1α, inositol-requiring enzyme 1; P, phosphorylation; PERK, protein kinase-like ER kinase; RIDD, regulated IRE1α-dependent decay; S1P, Site1 Protease; S2P, Site2 Protease; XBP-1s, spliced X-box binding protein 1; and XBP-1u, unspliced X-box binding protein 1.

51 on eukaryotic initiation factor 2α (eIF2α) upon activation by ERS. Phosphorylated eIF2α is essential for the translation of some UPR-dependent mRNAs through the upstream open reading frame, including activating transcription factor 4 (ATF4). Subsequently, ATF4 has several important target genes, such as the Growth Arrest and DNA Damage-Inducible Protein (GADD34) and C/EBP homologous protein (CHOP), which facilitate cell apoptosis (Lu et al., 2004). In bladder cancer, ERS activates CHOP and GADD34, which then trigger early apoptotic changes, including the dimerization of pro-apoptotic protein BAX (Zhang et al., 2011). On the other hand, the knockdown of CHOP in bladder cancer can partly reverse the pro-apoptotic effect exerted by cytotoxic drugs through blocking the translocation of BAX from the cytoplasm to the mitochondria (Zhang et al., 2018).

ATF6 Pathway

Activating transcription factor 6 has two subtypes, namely, ATF6α and ATF6β. After ERS is activated, ATF6 on the outer side of the ER membrane will be packaged into the transporter and shuttled to the Golgi apparatus. In the Golgi apparatus, Site1 and Site2 Protease (S1P and S2P) will process ATF6 into an active ATF6p50 transcription factor and transport to the nucleus to bind and activate the promoter of UPR target genes (Yamamoto et al., 2004). In addition, ATF6 can achieve specific biological effects by regulating the expression of other transcription factors, such as activating the transcription of CHOP to induce cell apoptosis or activating the unedited expression of XBP1 linked to the IRE1α pathway (Walter et al., 2018). In bladder cancer, Zhang et al. (2021) found that deubiquitinase otubain 1 facilitates bladder cancer progression by inhibiting the ubiquitylation of ATF6 signaling, thereby remodeling the stressed cells through transcriptional regulation.

Association Between UPR Pathway and Classical Signaling Pathways

Mounting evidence have suggested that the genetic alterations of classical cellular signaling pathways can also trigger ERS, and the three parallel yet distinctive UPR pathways interplay with them to determine oncogenic transformation and cell fate. For example, in brown adipocytes of hepatocellular carcinoma (HCC), the inhibition of the PI3K/AKT pathway leads to decreased levels of PERK phosphorylation; downregulates the expression of ATF4 and CHOP; decreases the phosphorylation levels of IRE1, GRP78, and XBP1; and antagonizes the effects of the ERS inducer tunicamycin (Winnay et al., 2020). In addition, PI3K/AKT has been found to positively regulate UPR in a lung fibrosis model (Hsu et al., 2017). During hypoxia, PERK can also be activated as a direct target of AKT (Blaustein et al., 2013). In addition, the activation of PERK can induce cellular autophagy by inhibiting the AKT/TSC/mTOR pathway (Blaustein et al., 2013). However, in the U87 glioblastoma cell

line and SKBR3 breast cancer cell line, the activation of PI3K/AKT leads to the inactivation of PERK and its downstream eIF2α, thereby inhibiting the protective effect of PERK/eIF2α on tumor cells (Mounir et al., 2011). This indicates that the role of UPR is highly dynamic and depends on cells and conditions. In addition, the UPR pathway interacts with the MEK/ERK pathway during ERS. For example, in HCC cell lines (HEP3B and SMMC-7721), ERS inhibits AKT activity, allowing the activation of the MEK/ERK pathway and causing cell proliferation (Dai et al., 2009). IRE1 also activates ERK1/2 (Darling and Cook, 2014), and the inhibition of the MEK/ERK pathway in the breast cancer cell line U0126 renders cancer cells to become more sensitive to ERS-induced apoptosis (Yang et al., 2016). In MAPK-related pathways, UPR can regulate all three signaling axes, including JNK, p38, and ERK1/2. For example, IRE dimers can bind to ASK1 and phosphorylate to activate MKK4/7, thereby activating JNK (Urano et al., 2000). The JNK pathway is usually thought to be associated with apoptosis, but JNK can mediate c-Jun phosphorylation, thereby promoting cell survival (Darling and Cook, 2014). In addition, the activation of the IRE/JNK pathway induced by ERS can bind to Beclin-1 and regulate the occurrence of protective autophagy in cells (Kania et al., 2015; Senft and Ronai, 2015; Lin et al., 2019). ASK1 can also activate MKK3/6, which activates p38, ultimately causing an increase in p38-induced ATF6 expression and activation, as well as CHOP activation, leading to apoptosis (Luo and Lee, 2002).

In summary, obtaining an in-depth understanding of the complex network of oncogenic signaling and the key UPR factors is important, and the existence of this potential complementary and compensatory mechanism needs to be taken into consideration when targeting URP.

ROLES OF ERS IN BLADDER CANCER

ERS and Bladder Cancer Cell Proliferation

Instead of responding to the growth control system, cancer cells grow and divide in an uncontrolled manner, leading to continual unregulated cell proliferation and tumor growth. Rapidly proliferating cells require rapid protein synthesis and ER replication for division. As reviewed earlier, the fate of cells undergoing ERS depends on the intensity and duration of the stress, which will result in a pro-survival or pro-apoptotic effect on cancer cells.

Many studies have proved that ERS closely regulates the proliferation of bladder cancer cells. The ER-related degradation protein-1 (Derlin-1) is a core protein of the ER degradation pathway that can interact with a variety of proteins. Derlin-1 can form a protein complex with protein containing valine (p97), ubiquitin ligase, and ubiquitin protein. Then, it reverses the ERS by co-regulating substrate protein with major histocompatibility complex I and mediates the degradation of unfolded or misfolded proteins (Iida et al., 2011; Christianson and Ye, 2014; Mehnert et al., 2014). Therefore, the increased expression of Derlin-1 can make tumor cells more resistant to ERS. Wu et al. (2016b) showed that the expression of Derlin-1 in bladder cancer tissue is significantly higher than that in adjacent tissues, and its expression is positively correlated with tumor stage, histological grade, lymph node involvement, and muscle invasiveness. The mechanism behind this process (Wu et al., 2016b) may be due to the fact that the overexpression of Derlin-1 can upregulate the expression of matrix metalloproteinase (MMP)-2/MMP-9, and it can also cause extracellular regulated protein kinase (ERK) phosphorylation (Dong et al., 2017a). In addition, Wu et al. (2019a) found that extracellular vesicles (EVs) from bladder cancer cells can induce malignant transformation of susceptible cells adjacent to cancer by stimulating UPR during ERS and inflammation and promoting the proliferation, progression, and recurrence of bladder cancer. This study proposed novel mechanisms of EV-mediated tumorigenesis and ERS initiation (by horizontal transfer of the EV cargo), providing a novel insight into the mechanisms underlying bladder cancer carcinogenesis and recurrence.

ERS and Bladder Cancer Cell Apoptosis

As discussed above, UPR alleviates ERS by suppressing protein synthesis and reinforcing the degradation of unfolded proteins. However, if the stress is beyond the capacity of the adaptive machinery, the cells will undergo apoptosis *via* several tUPR-mediated mechanisms. IRE1α activates JNK and p38-MAPK pathways that promote apoptosis (Ron and Hubbard, 2008). Moreover, p38-MAPK can activate the transcription factor CHOP, which enhances the expression of pro-apoptotic genes such as Bim while reducing the expression of Bcl-2 (Puthalakath et al., 2007). PERK attenuates mRNA translation under ERS by phosphorylating eIF2α, thereby inhibiting polypeptide chain synthesis. In addition, the phosphorylation of eIF2α activates ATF4, followed by CHOP and GADD34 (Lu et al., 2004).

Many drugs exert their tumor-killing effects by regulating ERS-related apoptosis pathways in bladder cancer. Thymoquinone, the major active compound of black seed oil, exhibits cytotoxicity to bladder cancer cells and induces apoptosis by upregulating the phosphorylated eIF2α, IRE1, and CHOP (Zhang et al., 2018). Similarly, flaccidoxide-13-acetate, isolated from cultured soft coral *Sinularia gibberosa*, was found to provoke ERS and activate the PERK–eIF2α–ATF6–CHOP pathway, causing inhibitory effects against the invasion and migration of bladder cancer cells (Wu et al., 2019b). Yuan et al. (2013) found that exposure to licochalcone A (a licorice chalconoid) could induce apoptosis in T24 bladder cancer cells by enhancing GRP78 and CHOP expression.

Euchromatic histone-lysine N-methyltransferase 2 (EHMT2) is an important enzyme in the process of histone modification. It is highly expressed in a variety of malignant tumor tissues, including bladder cancer and promotes tumor cell proliferation and invasion (Milner and Campbell, 1993; Tachibana et al., 2001; Huang et al., 2010; Mund and Lyko, 2010; Cho et al., 2011). BIX-01294 is a specific inhibitor of EHMT2 and has been found to have an inhibitory effect on bladder cancer (Kim et al., 2013). Cui et al. (2015) found that BIX-01294 stimulates ERS and triggers UPR by upregulating the expression of DDIT3, which ultimately causes bladder cancer cell apoptosis.

Interleukin-24 (IL-24) is a unique IL-10 family cytokine that can selectively induce cancer cell apoptosis without damaging normal cells (Gupta et al., 2006). Recently, some researchers have proved that IL-24 exerts its cytotoxic effect through ERS-induced tumor cell apoptosis (Zhang et al., 2016b).

Collectively, these pieces of evidence indicated a convergent role of ERS in regulating cancer cell apoptosis, and these ERS-related pathways can be manipulated to exert therapeutic effects.

ERS and Autophagy in Bladder Cancer

Autophagy is a highly conserved lysosomal degradation pathway that plays an essential role in the maintenance of cellular homeostasis. The by-products and damaged organelles produced by the metabolism of various biochemicals in the cell are swallowed by autophagosomes and transported to lysosomes, where they are degraded and recycled (Klionsky et al., 2021). Similar to other cancers, the role of autophagy in bladder cancer is double-sided (Santoni et al., 2013; Kou et al., 2017; Hua et al., 2018; Li et al., 2018; Schlütermann et al., 2018; Wang et al., 2018). On the one hand, Yang et al. (2018) found that BNIP3, a pro-apoptotic protein that belongs to the Bcl-2 family, can be activated by hypoxia-inducible factor-1α (HIF-1α) under hypoxic conditions and lead to autophagy initiation, which counteracts gemcitabine-induced apoptosis. On the other hand, Li et al. (2018) revealed that NVP-BEZ235, a dual PI3K/mTOR inhibitor, leads to cell death in cisplatin-resistant bladder cancer through autophagic flux activation without inducing apoptosis.

As autophagy is a stress-induced cellular mechanism, it would not be surprising to discover crosstalk between autophagy and ERS. The intertwined molecular mechanisms may vary: Ogata et al. (2006) indicated that ERS triggers autophagy *via* the IRE1–JNK pathway, but not the PERK or ATF6 pathway. However, other studies found that PERK/eIF2α phosphorylation triggers autophagy to adapt to ERS (Harding et al., 2000; Kouroku et al., 2007). Given the data above, several complex signaling pathways may contribute to the crosstalk between autophagy and ERS. Research has shown that ERS-mediated autophagy stimulates the occurrence and development of bladder cancer cells. For example, Liu et al. (2017a) observed a concurrent increase in the expression of ERS-related genes (ATF6, IRE1, EDEM1, and ERdj4) and autophagy-related genes (BECN, ATG3, and ATG5) in bladder cancer cells treated with melatonin and valproic acid. Although the anti-cancer activity of melatonin has long been considered to mediate ERS, melatonin is also an epithelial-mesenchymal transition (EMT) inhibitor, and some researchers have found that the attenuation of EMT signal in tumor tissues is closely related to melatonin-mediated ERS (Wu et al., 2016a; Yu et al., 2016b). Photodynamic therapy uses visible light and a light-absorbing agent to generate cytotoxic reactive oxygen species (ROS) within the tumor, which leads to tumor ablation. Buytaert et al. (2008) have recently used hypericin as a photosensitizer to effectively eradicate bladder cancer cells and subsequently found that autophagy-related genes WIPI1, MAP1LC3B, and ATG12 were upregulated, underpinning the involvement of autophagy in UPR in response to ERS in bladder cancer. Prolyl-4-hydroxylase subunit beta (P4HB) is an autophagy-related protein that is highly expressed in a variety of cancers including bladder cancer (Xu et al., 2014; Lyu et al., 2020). Co-expression network analysis and gene set enrichment analysis from two studies (Lyu et al., 2020; Wang et al., 2020) revealed that P4HB is involved in bladder cancer ERS response and associated with an unfavorable prognosis.

A pressing issue at the time of predicting whether the induction of ERS will activate autophagy in a protective or cytotoxic way is our relative lack of understanding of the molecular mechanisms through which autophagy regulates cell death. Therefore, the cellular context should be considered to understand how different ERS signals are integrated to yield a protective or cytotoxic autophagic response.

ERS and Bladder Cancer Cell Resistance

Chemotherapy remains the mainstay of treatment for patients with muscle-invasive or metastatic bladder cancer (Flaig et al., 2020). Although cisplatin-based combinational chemotherapy is effective in tumor debulking, certain patients show initial response but progressively become unresponsive to the treatment. Therefore, exploring novel drug-resistance mechanisms to overcome chemoresistance is urgently needed for bladder cancer. Recently, an increasing number of chemotherapy resistance mechanisms involved in ERS have been discovered. In addition to its biological effects in promoting the proliferation and invasion of bladder cancer, the high expression of Derlin-1 can also induce bladder cancer cells to become resistant to cisplatin *via* the PI3K/AKT and MMP/ERK pathways. Lowering the expression of Derlin-1 could re-sensitize bladder cancer to cisplatin (Dong et al., 2017a). Gemcitabine is a cytosine analogue that exerts anti-tumor effects by interfering with the metabolism and synthesis of tumor cell genetic materials, which has been used as the first-line chemotherapy for bladder cancer (Schlack et al., 2016). Wang et al. (2020) found that the inhibition of P4HB, an ER chaperone, could sensitize bladder cancer cells to gemcitabine by activating apoptosis and the PERK/eIF2α/ATF4/CHOP pathways. Topoisomerase inhibitors, such as etoposide, can trigger programmed cell death through the caspase-dependent signal cascade in cancer cells (Schuler et al., 2000; Wang et al., 2020). Hence, they have been widely used to treat bladder cancer with a small-cell component histology in a neoadjuvant setting. GRP78 is a protein that binds to unfolded protein and triggers its degradation when ERS occurs. Its high expression can improve the tolerance of the ER to various stressors. Some researchers have found that high expression of GRP78 can cause bladder cancer cells to develop resistance to various topoisomerase inhibitors and protect them from apoptosis (Reddy et al., 2003).

CROSSTALK BETWEEN ERS AND TME

Recent years have witnessed a shift in cancer research and therapeutic strategy from a cancer-centric model to a TME-focused one, as a substantial number of studies have

proved that cellular and non-cellular components in the TME can reprogram tumorigenesis, invasion, metastasis, and response to anti-cancer therapies. On the other hand, the rapidly dividing cancer cells aggressively consume oxygen and glucose and discharge lactic acid waste, which affects the conditions of the TME. Cancer cells respond to stressors, such as hypoxia, nutrient deficiency, and ROS accumulation through a wide variety of mechanisms, one of which is the activation of UPR in ERS. In addition, as the major cellular constituents of the TME, immune cells have also been found to be altered and shaped by ERS, thus influencing the malignant transformation and progression of cancer cells (**Figure 2**).

Hypoxia

Hypoxia is a common feature of the TME (Mazumdar et al., 2009; Jiang et al., 2015), and it can easily cause the accumulation of misfolded proteins as protein folding is an oxygen-dependent process, which makes ER sensitive to hypoxia (Koritzinsky et al., 2013). As UPR in ERS at the initial stages increases cancer cell survival and consequently the tumor mass, this may constitute a positive hypoxia–ERS–tumor growth–hypoxia feedback loop, further aggravating tumor proliferation. Hypoxia stabilizes HIF-1α and results in the activation of the PERK pathway of UPR through the phosphorylation of eIF2α and induction of ATF4 (Koumenis et al., 2002; Fels and Koumenis, 2006). In bladder cancer, HIF-1α has also been demonstrated to play a major role in mediating the cellular responses under low-oxygen conditions, such as promoting glycolysis (Zhang et al., 2016a; Xia et al., 2019), EMT (Lv et al., 2019), and autophagy (Yang et al., 2018), which contribute to tumor growth, invasion, and chemoresistance. Furthermore, hypoxia gene signatures have a strong and independent prognostic value for MIBC patients and can aid in the selection of patients for carbogen and nicotinamide treatment to reverse hypoxia to sensitize bladder cancer to radiotherapy (BCON Trial; Yang et al., 2017b). Of note, EVs that contain genetic materials have recently been recognized as an integral part in mediating the interaction and communication between cancer cells and the TME (Li and Nabet, 2019). On the one hand, the induction of ERS increases the biogenesis and release of EV through the IRE1α and PERK UPR pathways (Kanemoto et al., 2016); on the other hand, bladder cancer-derived EVs were found to activate UPR in ERS to promote malignant transformation (Wu et al., 2019a). Moreover, under hypoxia, bladder cancer cells secrete oncogenic long non-coding RNA-enriched EVs to remodel the TME, facilitating tumor growth and development (Xue et al., 2017). These observations offer novel perspectives as to the interaction and communication between hypoxia and ERS and open a new avenue for the development of targeted therapies, such as engineered EV therapeutics or EV-based small drug delivery.

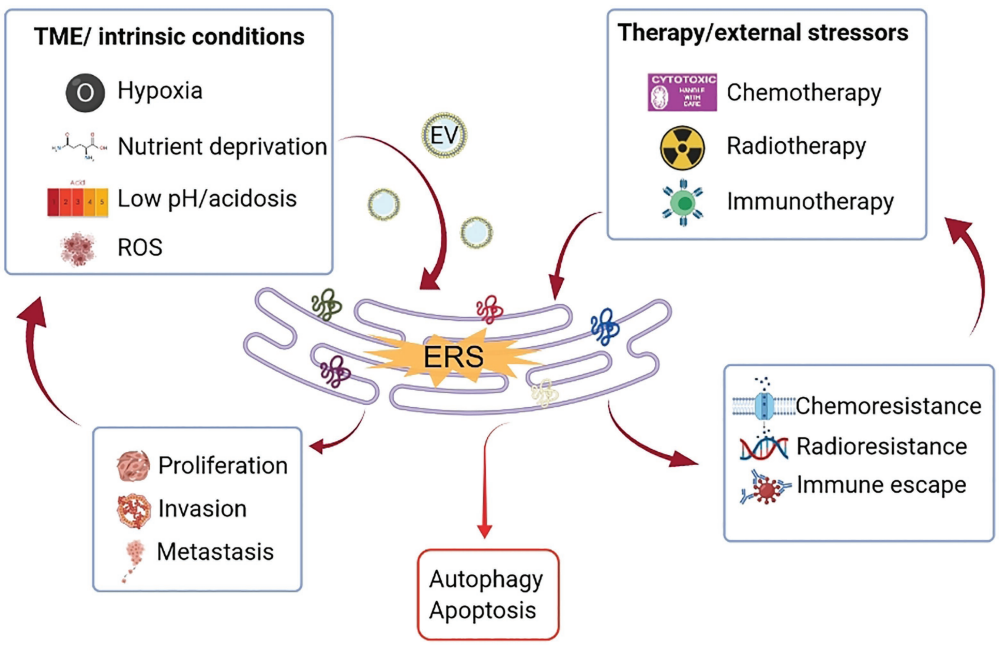

FIGURE 2 | Crosstalk between ERS and TME. Uncontrolled tumor growth generates a hostile TME, characterized by hypoxia, nutritional deficiencies, and localized acidosis, which increase the accumulation of unfolded/misfolded proteins on the ER (partly mediated by EV) and consequently ERS. Therapeutic modalities, such as chemotherapy, radiation, and immunotherapy also trigger ERS. Depending on the intensity and magnitude of ERS, the cells face two different fates through the activation of UPR. If the stressor is persistent and strong that goes beyond the adaptive capacity, UPR will mediate cell death through the induction of apoptosis or autophagy. If the ERS is tolerated, UPR signaling will lead to tumor proliferation, metastasis, and treatment resistance, which in turn aggravate the hostility of the TME. ER, endoplasmic reticulum; ERS, endoplasmic reticulum stress; EV, extracellular vesicle; ROS, reactive oxygen species; TME, tumor microenvironment; and UPR, unfolded protein response.

Nutrient Deficiency

The stability of the ER can be destabilized by nutrient deprivation. For example, uridine diphosphate-N-acetylglucosamine (UDP-GlcNAc) is synthesized by glucose and glutamine *via* the hexosamine biosynthetic pathway (HBP) and necessary for the correct folding of proteins in the ER and for the process of glycosylation. However, glucose or glutamine deficiency blocks the HBP, decreasing the synthesis of UDP-GlcNAc and increasing the precursor product N-acetylglucosamine (NAG). NAG can also bind to proteins in the ER, but triggers UPR because it does not drive the correct folding of proteins (Braakman and Bulleid, 2011; Denzel and Antebi, 2015; Domblides et al., 2018). In bladder cancer, the increase in NAG is induced by a limited supply of glucose, causing ERS and eventually a G2/M phase block (Isono et al., 2013). Similarly, amylo-α-1,6-glucosidase, 4-α-glucanotransferase (AGL), a key enzyme of glycogenolysis, was found to have an inhibitory effect on bladder cancer. Bladder cancer cells with deficient AGL expression have a higher glycolytic activity and glycine synthesis capacity than those with normal expression of AGL, and this capacity can greatly contribute to the proliferation of bladder cancer (Sun et al., 2019). Impaired amino acid metabolism can affect ERS through the action of the TME. Amino acid starvation can induce an integrative stress response (ISR), which is essential for tumor cells to adapt to stressors (Ritterson-Lew et al., 2015), making them resistant to chemotherapeutic agents. The induction of ISR in bladder cancer can cause resistance to the proteasome inhibitor, bortezomib (Pakos-Zebrucka et al., 2016). Interestingly, a high-fat diet can lead to alterations in the size, composition, and fluidity of ER membranes, which can affect functions such as protein glycosylation, thereby promoting ERS (Qi et al., 2013). The level of lipid-derived acetyl coenzyme A was found to be proportional to the proliferative capacity of bladder cancer cells, and excessive intake of acetyl coenzyme A synthase 3 and fatty acids is responsible for this phenomenon (Wei et al., 2006). Even in the presence of sufficient glucose, tumor cells prefer to use the glycolytic pathway to produce lactate for energy. At the same time, tumor cells competitively inhibit the sugar metabolism of immune cells in the microenvironment, thus creating a local acidic microenvironment. This microenvironment not only hampers the clearance of bladder cancer by immune cells, but also promotes tumor proliferation and invasion by fostering neovascularization (Afonso et al., 2020; Zhang et al., 2020).

Reactive Oxygen Species

The accumulation of intracellular ROS can significantly affect the state of proteins within the ER lumen (Dong et al., 2017b). For example, limiting the amount of intracellular glutamine can induce ERS by disrupting glutathione production and thus altering the redox state within the ER lumen (Shimizu and Hendershot, 2009). In bladder cancer, glutamine can promote its proliferation by increasing ROS and regulating the expression of signal transducer and activator of transcription 3 (STAT3; Zhang et al., 2017a). The inner mitochondrial membrane is the main site of ROS production. For example, during β-oxidation of fatty acids, large amounts of ROS are subsequently produced as by-products of the electron transport chain. In addition, some cytokines or growth factors with pro-inflammatory effects can lead to the continuous activation of NADPH oxidases (NOXs), producing large amounts of ROS (Choudhary et al., 2011). The constant activation of NOX, the accumulation of intracellular ROS, and the depletion of glutathione can jointly affect the caspase activity of bladder cancer cells and regulate their apoptosis (Liou and Storz, 2010).

Tumor-Associated Immune Cells

Bacille Calmette–Guérin (BCG) therapy is the current first-line treatment for high-risk NMIBC patients. With this in mind, bladder cancer was one of the earliest cancers where immunotherapy was first utilized. The protective effect of BCG is mediated by increasing the number of macrophages in the TME, urinary bladder wall surrounding the tumor, and urine (Fuge et al., 2015). Tumor-killing macrophages (M1 type) are the main enforcers of the anti-tumor effect of BCG, whereas M2 macrophages may negatively influence the immune response of bladder cancer to BCG (Liu et al., 2019). However, most of the tumor-associated macrophages (TAMs) in bladder cancer are polarized into M2 macrophages, which resist the anti-cancer effect of BCG (Shan et al., 2018; Kobatake et al., 2020), due to their suppressive immune response to cancer and pro-tumor progression (Aljabery et al., 2018; Asano et al., 2018). New and effective strategies are needed to reverse M2 polarization and redirect TAMs to become tumoricidal.

Currently, numerous studies have shown that ERS of tumor cells can influence tumor progression by altering the function of infiltrating immune cells in the TME. Bladder cancer cells subjected to ERS could infiltrate the tumor tissue by the excessive release of specific cytokines and recruitment of myeloid-derived suppressor cells (MDSCs; Zhang et al., 2017b). MDSCs can increase the resistance of bladder cancer cells to cisplatin and the checkpoint inhibitor α-PD-L1 antibody (Takeyama et al., 2020). In addition, MDSCs can cause inflammation and promote angiogenesis within the bladder cancer tissue (Dominguez-Gutierrez et al., 2020). On the other hand, IL-6 enriched in the TME can block MDSCs by triggering IRE1α–XBP1 signaling in macrophages through the activation of STAT3 and STAT6 (Yan et al., 2016; Yang et al., 2017a). ERS-related markers, such as GRP78, ATF6, PERK, and IRE1α can recruit CD68+ macrophages to infiltrate the peritumor tissue and upregulate PD-L1 expression in macrophages *via* EVs, which subsequently inhibit T-cell function and facilitate immune escape (Liu et al., 2019; Xue et al., 2019).

ERS is commonly believed to affect natural killer (NK) cell-dependent tumor recognition (Obiedat et al., 2019), and NK cells are mainly regulated and recruited by IRE1α–XBP1 signaling (Dong et al., 2019) and mediate bladder cancer cell differentiation or death (Ramakrishnan et al., 2019). However, bladder cancer-infiltrating NK cells have a functional defect: they are unable to complete the degranulation process, resulting in the inability to exercise their cytolytic effect; by contrast, circulating NK cells do not have this functional defect (Tsujihashi et al., 1989). BCG may repair this defect and restore the

function of NK cell degranulation (Kleinnijenhuis et al., 2014; García-Cuesta et al., 2015).

T cells are indispensable immune cells in the immune system, and ERS occurring in bladder cancer has been shown to modulate T-cell-mediated cancer cell proliferation, metastasis, and sensitivity to immunotherapy (Chugh et al., 2013; Pommier et al., 2018; Tao et al., 2018). Studies have found that T cells playing various roles are recruited into the bladder cancer TME during disease, including pro-inflammatory T cells (which may be beneficial to the body) and anti-inflammatory T cells (which may be detrimental; Oh et al., 2020; Wu and Abraham, 2021). Thus, regulating T-cell infiltration may be a promising therapeutic strategy to target bladder cancer.

Notably, various stressors in the TME can stimulate ERS not only in cancer cells but also in immune cells; for example, high levels of cholesterol in the TME can activate IRE1α–XBP1 signaling in T cells within cancer tissues, induce programmed death protein 1 (PD-1) expression, and prevent T cells from exerting tumor-killing effect (Ma and Yi, 2019). Furthermore, the accumulation of ROS in the TME promotes ERS in dendritic cells (DCs) and the sustained activation of IRE1α–XBP1, which subsequently inhibits their function of presenting local tumorigenic antigens to intratumoral T cells (Herber et al., 2010; Gao et al., 2015).

CLINICAL IMPLICATIONS

ERS as a Cancer Prognostic Marker

Endoplasmic reticulum stress-related molecular markers have been reported to have prognostic values for cancer patients. The roles of PERK and IRE1α signaling in cancer prognosis depend on cell types, stress conditions, and the TME and thus are inconsistent (Clarke et al., 2014). For example, the expression levels of ERS markers, such as GRP78, PERK, and IRE1α in human HCC tissues are proportional to CD63/PD-L1$^{+/+}$ macrophage infiltration and predict poor clinical prognosis (Liu et al., 2019). Analysis of glioma patient datasets showed that the overexpression of PERK pathway signature is strongly correlated with chemotherapy resistance and poor OS (Del Vecchio et al., 2014). Similarly, another study revealed that high expression of ERS markers within DCs in human ovarian cancer tissues is associated with reduced T-cell infiltration (Cubillos-Ruiz et al., 2015). Song et al. (2018) also found that high expression of XBP1 (from IRE1α signaling) in T cells is associated with less T-cell infiltration and often observed in ascites, which only accumulates in patients with advanced or metastatic diseases. Furthermore, they found that low XBP1 expression exhibits excellent anti-tumor immunity, with a reduced tumor progression and prolonged OS in ovarian cancer mouse models (Song et al., 2018). However, in one study, XBP-1 isoforms were found to be differently associated with the outcome of breast cancer endocrine therapy: high levels of XBP-1u favor tumor cell apoptosis, whereas high levels of XBP-1s favor tumor survival. In bladder cancer, the overexpression of XBP1 has been found to correlate with the poor OS in transitional cell carcinoma patients (Chen et al., 2016b). In addition, ATF6 was also primarily recognized as a protective modulator in cancer during ERS. A growing body of literature has demonstrated that ERS-related ATF6 contributes to poor survival in different types of cancers, including colon cancer (Liu et al., 2018), glioblastoma (Dadey et al., 2016), prostate cancer (Liu et al., 2017b), and osteosarcoma (Yarapureddy et al., 2019).

ERS and UPR as Therapeutic Targets

As aberrant UPR and ERS are major contributors to cancer development, chemoresistance, and poor prognosis, there has been strong interest in clinically influencing this process as a strategy to restrain tumor growth and reverse drug resistance. Two approaches can be used to target the ERS pathways: one being the inhibition of UPR-mediated adaptive responses to interrupt ER homeostasis, the other being the induction of sustained and lethal ERS that leads to cell death. Drugs that modulate the ERS or UPR, either as a monotherapy or in combination with chemotherapy, targeted therapy, and immunotherapy, have shown promising preclinical treatment efficacy and warrant further investigations and trials (Hetz et al., 2019).

IRE1α/XBP-1 Pathway

IRE1 RNase inhibitors (including B-I09, STF083010, MKC3946, and MKC8866) have shown good therapeutic performance in multiple myeloma (MM), breast cancer, prostate cancer, melanoma, lymphoma, and chronic lymphocytic leukemia (Tang et al., 2014; Logue et al., 2018; Xie et al., 2018; Zhao et al., 2018; Sheng et al., 2019; Jin and Saatcioglu, 2020). For example, MKC3946 significantly enhanced cytotoxicity induced by bortezomib (a proteasome inhibitor) in an MM xenograft model (Mimura et al., 2012). As a single agent, MKC8866 shows a significant tumor-suppressing effect; when used with chemotherapy such as paclitaxel and docetaxel, the combination shows surprisingly superior tumor-killing and survival-improving capabilities compared with the chemotherapy agent alone (Logue et al., 2018; Zhao et al., 2018). Of note, these inhibitors are capable of blocking the downstream XBP1 splicing without affecting the upstream IRE1α or PERK or ATF6 pathway, making them superior candidates for clinical trials with good tolerability, which explains that long-term usage of MKC8866 is effective in breast and prostate cancers in preclinical models, without causing substantial toxicity to normal tissues (Zhao et al., 2018; Sheng et al., 2019).

Another group of IRE1α inhibitors, IRE1α kinase inhibitors, also shows significant efficacy in an *in vivo* model of MM xenografts. IRE1α kinase inhibitor compound 18, also known as KIRA8 or AMG-18, inhibits the growth of MM and sensitizes the myeloma to current first-line therapeutic agents, bortezomib, and lenalidomide (an immunomodulatory agent; Harnoss et al., 2019). However, the suppression of XBP1s in MM was shown to induce bortezomib resistance *via* diminishing ER front-loading and cytotoxic susceptibility to inhibition of ERAD (Leung-Hagesteijn et al., 2013). This suggests that IRE1α inhibitors may trigger other UPR pathways *via* a feedback loop and may not fully recapitulate the effects of IRE1α gene

ablation. More surprisingly, Auf et al. (2010) observed in a glioma mouse model that blockade of IRE1 reduces angiogenesis and tumor growth rate but causes extensive invasiveness and angiogenesis. Further investigation of IRE1α signaling is required to unveil the complex relationship between angiogenesis and invasiveness, and the development of highly selective inhibitors may therefore represent a more appropriate approach.

Chen et al. (2016b) discovered a novel natural product analogue CYD 6–17 that has a potent inhibitory effect on multidrug-resistant bladder transitional cell carcinoma by decreasing the binding of XBP1 to the promoter region. The delivery of CYD 6–17 significantly inhibited tumor growth using a xenograft model without detectable side effects.

PERK/eIF2α/ATF4/CHOP Pathway

Direct targeting of CHOP and ATF4 is challenging for conventional inhibitors as CHOP and part of ATF4 molecules are located in the nucleus, rendering the upstream transducer PERK and eIF2α the only viable options.

As a rationale, the inhibition of PERK signaling reversed the multidrug resistance of de-differentiated breast cancer cells (Del Vecchio et al., 2014), and the inhibition of the eIF2α-dependent arm of UPR reversed the tumor radioresistance in a subset of hypoxic glioblastoma cells (Rouschop et al., 2013). Similarly, the knockdown of ATF4 in combination with radiation led to reduced proliferation and colony formation in glioblastoma (Dadey et al., 2018).

On a pharmaceutical front, GSK2606414 and GSK2656157 are two of the most well-studied PERK kinase inhibitors. Of note, GSK2606414 was found to enhance PD-1 blockade efficacy in a sarcoma model (Hurst et al., 2019), and GSK2656157 showed tumor-killing and chemo-sensitizing effects in preclinical models of MM, pancreatic, and colon cancers (Atkins et al., 2013; Shi et al., 2019). In spite of the therapeutic efficacy, the use of GSK2606414 and GSK2656157 comes with significant "on-target" side effects such as diabetes caused by pancreatic β-cell loss (Yu et al., 2015). Moreover, both agents exhibit an "off-target" effect by showing a high inhibitory affinity to receptor-interacting kinase 1, which regulates pro-survival NF-κB signaling and cell death (Rojas-Rivera et al., 2017). The on-target side effects, along with the off-target effects, have largely hindered the clinical translation of GSK2606414 and GSK2656157.

eIF2α is located downstream of PERK and is a convergent node of ISR. The ISR inhibitor (ISRIB) is a potent eIF2α inhibitor that suppresses eIF2α phosphorylation (activation). It has shown a significant tumor-suppressing effect in prostate cancer when used alone in a mouse model *in vivo* (Nguyen et al., 2018) with no overall toxicity. Though ISRIB is difficult to formulate and insoluble given its high potency, it is nevertheless, a promising candidate for pharmaceutical exploration. Some natural compounds have shown treatment advantages in various cancers including bladder cancer *via* this pathway. Arctigenin (Kim et al., 2010), 11-epi-sinulariolide acetate (Lin et al., 2016), and flaccidoxide-13-acetate (Sinclair, 1988) have been proved to kill colon, cervical, or bladder cancer cells through the activation of the PERK/eIF2α/ATF4/CHOP pathway.

ATF6 Pathway

The pharmacological inhibition of ATF6 has not been vastly explored, and it may be attributed to the fact that this pathway relies on ATF6 protein alone to perform its function. Some investigators have found that ceapins, UPR inhibitors, can selectively block ATF6 signaling by impeding the translocation of ATF6α to the Golgi (Gallagher et al., 2016; Gallagher and Walter, 2016). Given that ATF6p50 is translocated to the nucleus once it is successfully sheared, it is difficult to make drugs that can stop ATF6p50 from functioning. However, the successful shearing of ATF6p50 depends on S1P and S2P, so the regulation of S1P and S2P can indirectly affect the function of ATF6. If the expression of S1P is inhibited using an inhibitor (PF-429242), it also reduces the expression of ATF6 and GRP78, which in turn activate IRE1α and PERK signaling, leading to apoptosis (Lebeau et al., 2018). Another herbal extract, baicalin, induces apoptosis through the targeted activation of S2P, and the effect is mitigated by the knockdown of ATF6 (Yu et al., 2016a).

Despite considerable efforts to improve BCG, no existing immunotherapy outperforms BCG for the treatment of high-risk NMIBC to date. Currently, five anti-PD-1/PD-L1 immunotherapeutic drugs (namely, atezolizumab, durvalumab, avelumab, nivolumab, and pembrolizumab) have been approved for the treatment of advanced and metastatic bladder cancer and demonstrated satisfactory efficacy (Powles et al., 2020). New approaches that incorporate emerging immunotherapies might successfully synergize with BCG to improve patient outcomes. In terms of ERS in immunotherapy, disabling ERS sensors or orchestrating UPR pathways can enhance anti-tumor immune responses. For example, Cubillos-Ruiz et al. (2015) found that knockdown of XBP1 in DCs enables the re-activation of CD8+ T cells and prolongs survival in a metastatic ovarian cancer mouse model. This may represent a novel notion to control UPR not only in cancer cells but also in immune cells within the TME for improving the efficacy of cancer immunotherapies. Of course, further studies are warranted to test these new ideas.

Interestingly, recent studies showed that several antiviral drugs, such as lopinavir, ritonavir, and nelfinavir, can inhibit the proliferation of bladder cancer cell line *in vitro* by inducing ERS (Sato et al., 2018; Okubo et al., 2019). However, this inhibitory effect on tumors may have nothing to do with the type of tumor and not be selective as these three drugs are potent inhibitors of proteases, which adaptive UPR relies on in response to ERS.

Overall, drugs that modulate ERS and UPR-related regulators have a great anti-cancer potential, and ERS-related markers are also important in predicting patient prognosis. The use of pharmacological inhibitors of UPR signaling may help to improve the prognosis of cancer patients. However, drugs that exert superior therapeutic potency and minimal side effects in bladder cancer are lacking. An important prerequisite of an ideal anti-cancer drug is that it should be non-toxic to or does not trigger ERS in normal cells. However, some active protein secretory cells, such as pancreatic β-cells mentioned above, require ERS as a rapid control mechanism and thus will have

to be considered carefully. It is also worthwhile to test the synergistic effects of two single inhibitors or investigate the possibility of a dual inhibitor that targets two different UPR pathways to exert enhanced therapeutic potency.

CONCLUSION

In bladder cancer, ERS and UPR are widely involved in multiple cellular processes and cell fate determination, including cell proliferation, autophagy, apoptosis, and therapeutic resistance. A growing body of literature suggested that UPR plays a cytoprotective and pro-oncogenic role in cancer to enable cancer cells to cope with adverse microenvironmental stimuli, such as hypoxia, nutrient deficiency, and ROS. This may represent a mechanism underlying the invasive, resistant, and recurrent behaviors of bladder cancer.

This review has focused on the crosstalk between ERS and TME and demonstrated its roles in bladder cancer and clinical implications. We also shed some light on the roles of EV in ERS–TME interaction and explored the concept of targeting ERS to revive innate tumoricidal immune response and enhance the efficacy of emerging cancer immunotherapy.

Unfolded protein response signaling also interacts with tumor regulatory genes (Rather et al., 2020) and signaling pathways (Oakes, 2020). Recent studies have also revealed that ERS contributes to several hallmarks of cancer (Limia et al., 2019; Pluquet and Galmiche, 2019; Martelli et al., 2020), but the mechanisms are poorly understood. Further studies are needed to elucidate the ambivalent roles of ERS responses in cancer and clarify the complex network between UPR and other signaling pathways. An in-depth understanding of such key players will facilitate the development of novel selective inhibitors with high potency and low toxicity to improve the current bladder cancer treatment.

AUTHOR CONTRIBUTIONS

ZN, JN, and SZ conceived and designed the framework of the study. MC, XW, YG, DH, HC, YP, and NG collected and reviewed the data. ZN wrote the manuscript. JN and SZ reviewed and edited the manuscript. All authors contributed to the article and approved the submitted version.

FUNDING

This work was supported by the National Science Foundation of China (grant number 81760465), the Finance Science and Technology Project of Hainan Province (grant numbers ZDYF2019163 and ZDKJ2017007), the Hainan Provincial Nature Science Foundation of China (grant number 819QN387), and the Cancer Research Trust Fund St George Hospital (JN).

REFERENCES

Abern, M. R., Dude, A. M., Tsivian, M., and Coogan, C. L. (2013). The characteristics of bladder cancer after radiotherapy for prostate cancer. *Urol. Oncol.* 31, 1628–1634. doi: 10.1016/j.urolonc.2012.04.006

Afonso, J., Santos, L. L., Longatto-Filho, A., and Baltazar, F. (2020). Competitive glucose metabolism as a target to boost bladder cancer immunotherapy. *Nat. Rev. Urol.* 17, 77–106. doi: 10.1038/s41585-019-0263-6

Alfred-Witjes, J., Lebret, T., Compérat, E. M., Cowan, N. C., De Santis, M., Bruins, H. M., et al. (2017). Updated 2016 EAU guidelines on muscle-invasive and metastatic bladder cancer. *Eur. Urol.* 71, 462–475. doi: 10.1016/j.eururo.2016.06.020

Aljabery, F., Olsson, H., Gimm, O., Jahnson, S., and Shabo, I. (2018). M2-macrophage infiltration and macrophage traits of tumor cells in urinary bladder cancer. *Urol. Oncol.* 36, 119–159. doi: 10.1016/j.urolonc.2017.11.020

Asano, T., Ohnishi, K., Shiota, T., Motoshima, T., Sugiyama, Y., Yatsuda, J., et al. (2018). CD169-positive sinus macrophages in the lymph nodes determine bladder cancer prognosis. *Cancer Sci.* 109, 1723–1730. doi: 10.1111/cas.13565

Atkins, C., Liu, Q., Minthorn, E., Minthorn, E., Zhang, S.-Y., Moss, K., et al. (2013). Characterization of a novel PERK kinase inhibitor with antitumor and antiangiogenic activity. *Cancer Res.* 73, 1993–2002. doi: 10.1158/0008-5472.CAN-12-3109

Auf, G., Jabouille, A., Guérit, S., Pineau, R., Delugin, M., Bouchecareilh, M., et al. (2010). Inositol-requiring enzyme 1alpha is a key regulator of angiogenesis and invasion in malignant glioma. *Proc. Natl. Acad. Sci. U.S.A.* 107, 15553–15558. doi: 10.1073/pnas.0914072107

Blaustein, M., Pérez-Munizaga, D., Ma, S., Urrutia, C., Grande, A., Risso, G., et al. (2013). Modulation of the Akt pathway reveals a novel link with PERK/eIF2α, which is relevant during hypoxia. *PLoS One* 8:e69668. doi: 10.1371/journal.pone.0069668

Braakman, I., and Bulleid, N. J. (2011). Protein folding and modification in the mammalian endoplasmic reticulum. *Annu. Rev. Biochem.* 80, 71–99. doi: 10.1146/annurev-biochem-062209-093836

Buytaert, E., Matroule, J. Y., Durinck, S., Close, P., Kocanova, S., Vandenheede, J. R., et al. (2008). Molecular effectors and modulators of hypericin-mediated cell death in bladder cancer cells. *Oncogene* 27, 1916–1929. doi: 10.1038/sj.onc.1210825

Chen, W., Zheng, R., Baade, P. D., Zhang, S., Zeng, H., Bray, F., et al. (2016a). Cancer statistics in China, 2015. *CA Cancer J. Clin.* 66, 115–132. doi: 10.3322/caac.21338

Chen, W., Zhou, J., Wu, K., Huang, J., Ding, Y., Yun, E. J., et al. (2016b). Targeting XBP1-mediated β-catenin expression associated with bladder cancer with newly synthetic Oridonin analogues. *Oncotarget* 7, 56842–56854. doi: 10.18632/oncotarget.10863

Cho, H. S., Kelly, J. D., Hayami, S., Toyokawa, G., Takawa, M., Yoshimatsu, M., et al. (2011). Enhanced expression of EHMT2 is involved in the proliferation of cancer cells through negative regulation of SIAH1. *Neoplasia* 13, 676–684. doi: 10.1593/neo.11512

Choudhary, S., Rathore, K., and Wang, H. (2011). Differential induction of reactive oxygen species through Erk1/2 and Nox-1 by FK228 for selective apoptosis of oncogenic H-Ras-expressing human urinary bladder cancer J82 cells. *J. Cancer Res. Clin.* 137, 471–480. doi: 10.1007/s00432-010-0910-z

Christianson, J. C., and Ye, Y. (2014). Cleaning up in the endoplasmic reticulum: ubiquitin in charge. *Nat. Struct. Mol. Biol.* 21, 325–335. doi: 10.1038/nsmb.2793

Chugh, S., Anand, V., Swaroop, L., Sharma, M., Seth, A., and Sharma, A. (2013). Involvement of Th17 cells in patients of urothelial carcinoma of bladder. *Hum. Immunol.* 74, 1258–1262. doi: 10.1016/j.humimm.2013.06.032

Clarke, H. J., Chambers, J. E., Liniker, E., and Marciniak, S. J. (2014). Endoplasmic reticulum stress in malignancy. *Cancer Cell* 25, 563–573. doi: 10.1016/j.ccr.2014.03.015

Clarke, R., Cook, K. L., Hu, R., Facey, C. O. B., Tavassoly, I., Schwartz, J. L., et al. (2012). Endoplasmic reticulum stress, the unfolded protein response, autophagy, and the integrated regulation of breast cancer cell. *Cancer Res.* 72, 1321–1331. doi: 10.1158/0008-5472.CAN-11-3213

Cubillos-Ruiz, J. R., Silberman, P. C., Rutkowski, M. R., Chopra, S., Perales-Puchalt, A., Song, M., et al. (2015). ER stress sensor XBP1 controls

anti-tumor immunity by disrupting dendritic cell homeostasis. *Cell* 161, 1527–1538. doi: 10.1016/j.cell.2015.05.025

Cui, J., Sun, W., Hao, X., Wei, M., Su, X., Zhang, Y., et al. (2015). EHMT2 inhibitor BIX-01294 induces apoptosis through PMAIP1-USP9X-MCL1 axis in human bladder cancer cells. *Cancer Cell Int.* 15:4. doi: 10.1186/s12935-014-0149-x

Dadey, D. Y. A., Kapoor, V., Khudanyan, A., Thotala, D., and Hallahan, D. E. (2018). PERK regulates Glioblastoma sensitivity to ER stress although promoting radiation resistance. *Mol. Cancer Res.* 16, 1447–1453. doi: 10.1158/1541-7786.MCR-18-0224

Dadey, D. Y. A., Kapoor, V., Khudanyan, A., Urano, F., Kim, A. H., Thotala, D., et al. (2016). The ATF6 pathway of the ER stress response contributes to enhanced viability in glioblastoma. *Oncotarget* 7, 2080–2092. doi: 10.18632/oncotarget.6712

Dai, R., Chen, R., and Li, H. (2009). Cross-talk between PI3K/Akt and MEK/ERK pathways mediates endoplasmic reticulum stress-induced cell cycle progression and cell death in human hepatocellular carcinoma cells. *Int. J. Oncol.* 34, 1749–1757. doi: 10.3892/ijo_00000306

Darling, N. J., and Cook, S. J. (2014). The role of MAPK signalling pathways in the response to endoplasmic reticulum stress. *Biochim. Biophys. Acta* 1843, 2150–2163. doi: 10.1016/j.bbamcr.2014.01.009

Del Vecchio, C. A., Feng, Y., Sokol, E. S., Tillman, E. J., Sanduja, S., Reinhardt, F., et al. (2014). De-differentiation confers multidrug resistance via noncanonical PERK-Nrf2 signaling. *PLoS Biol.* 12:e1001945. doi: 10.1371/journal.pbio.1001945

Denzel, M. S., and Antebi, A. (2015). Hexosamine pathway and (ER) protein quality control. *Curr. Opin. Cell Biol.* 33, 14–18. doi: 10.1016/j.ceb.2014.10.001

Domblides, C., Lartigue, L., and Faustin, B. (2018). Metabolic stress in the immune function of T cells. *Cells* 7:68. doi: 10.3390/cells7070068

Dong, H., Adams, N. M., Xu, Y., Cao, J., Allan, D. S. J., Carlyle, J. R., et al. (2019). The IRE1 endoplasmic reticulum stress sensor activates natural killer cell immunity in part by regulating c-Myc. *Nat. Immunol.* 20, 865–878. doi: 10.1038/s41590-019-0388-z

Dong, Q., Fu, L., Zhao, Y., Tan, S., and Wang, E. (2017a). Derlin-1 overexpression confers poor prognosis in muscle invasive bladder cancer and contributes to chemoresistance and invasion through PI3K/AKT and ERK/MMP signaling. *Oncotarget* 8, 17059–17069. doi: 10.18632/oncotarget.15001

Dong, L., Krewson, E. A., and Yang, L. (2017b). Acidosis activates endoplasmic reticulum stress pathways through GPR4 in human vascular endothelial cells. *Int. J. Mol. Sci.* 18:278. doi: 10.3390/ijms18020278

Fels, D. R., and Koumenis, C. (2006). The PERK/eIF2alpha/ATF4 module of the UPR in hypoxia resistance and tumor growth. *Cancer Biol. Ther.* 5, 723–728. doi: 10.4161/cbt.5.7.2967

Flaig, T. W., Spiess, P. E., Agarwal, N., Bangs, R., Boorjian, S. A., Buyyounouski, M. K., et al. (2020). Bladder Cancer, version 3.2020, NCCN clinical practice guidelines in oncology. *J. Natl. Compr. Canc. Netw.* 18, 329–354. doi: 10.6004/jnccn.2020.0011

Forouhan, M., Mori, K., and Boot-Handford, R. P. (2018). Paradoxical roles of ATF6α and ATF6β in modulating disease severity caused by mutations in collagen X. *Matrix Biol.* 70, 50–71. doi: 10.1016/j.matbio.2018.03.004

Fuge, O., Vasdev, N., Allchorne, P., and Green, J. S. (2015). Immunotherapy for bladder cancer. *Res. Rep. Urol.* 7, 65–79. doi: 10.2147/RRU.S63447

Gallagher, C. M., Garri, C., Cain, E. L., Ang, K. K., Wilson, C. G., Chen, S., et al. (2016). Ceapins are a new class of unfolded protein response inhibitors, selectively targeting the ATF6α branch. *eLife* 5:e11878. doi: 10.7554/eLife.11878

Gallagher, C. M., and Walter, P. (2016). Ceapins inhibit ATF6α signaling by selectively preventing transport of ATF6α to the Golgi apparatus during ER stress. *eLife* 5:e11880. doi: 10.7554/eLife.11880

Gao, F., Liu, C., Guo, J., Sun, W., Xian, L., Bai, D., et al. (2015). Radiation-driven lipid accumulation and dendritic cell dysfunction in cancer. *Sci. Rep.* 5:9613. doi: 10.1038/srep09613

García-Cuesta, E. M., López-Cobo, S., Álvarez-Maestro, M., Esteso, G., Romera-Cárdenas, G., Rey, M., et al. (2015). NKG2D is a key receptor for recognition of bladder cancer cells by IL-2-activated NK cells and BCG promotes NK cell activation. *Front. Immunol.* 6:284. doi: 10.3389/fimmu.2015.00284

Gupta, P., Walter, M. R., Su, Z. -Z., Lebedeva, I. V., Emdad, L., Randolph, A., et al. (2006). BiP/GRP78 is an intracellular target for MDA-7/IL-24 induction of cancer-specific apoptosis. *Cancer Res.* 66, 8182–8191. doi: 10.1158/0008-5472.CAN-06-0577

Gutierrez, P. R. D., Kwenda, E. P., Donelan, W., O'Malley, P., Crispen, P. L., and Kusmartsev, S. (2020). Hyal2 expression in tumor-associated myeloid cells mediates cancer-related inflammation in bladder cancer. *Cancer Res.* doi: 10.1158/0008-5472.CAN-20-1144 [Epub ahead of print]

Han, D., Lerner, A. G., Vande-Walle, L., Upton, J. P., Xu, W., Hagen, A., et al. (2009). IRE1alpha kinase activation modes control alternate endoribonuclease outputs to determine divergent cell fates. *Cell* 138, 562–575. doi: 10.1016/j.cell.2009.07.017

Harding, H. P., Zhang, Y., Bertolotti, A., Zeng, H., and Ron, D. (2000). Perk is essential for translational regulation and cell survival during the unfolded protein response. *Mol. Cell* 5, 897–904. doi: 10.1016/s1097-2765(00)80330-5

Harnoss, J. M., Le Thomas, A., Shemorry, A., Marsters, S. A., Lawrence, D. A., Lu, M., et al. (2019). Disruption of IRE1α through its kinase domain attenuates multiple myeloma. *Proc. Natl. Acad. Sci. U.S.A.* 116, 16420–16429. doi: 10.1073/pnas.1906999116

Herber, D. L., Cao, W., Nefedova, Y., Novitskiy, S. V., Nagaraj, S., Tyurin, V. A., et al. (2010). Lipid accumulation and dendritic cell dysfunction in cancer. *Nat. Med.* 16, 880–886. doi: 10.1038/nm.2172

Hetz, C., Axten, J. M., and Patterson, J. B. (2019). Pharmacological targeting of the unfolded protein response for disease intervention. *Nat. Chem. Biol.* 15, 764–775. doi: 10.1038/s41589-019-0326-2

Hsu, H. S., Liu, C. C., Lin, J. H., Hsu, T. W., Hsu, J. W., Su, K., et al. (2017). Involvement of ER stress, PI3K/AKT activation, and lung fibroblast proliferation in bleomycin-induced pulmonary fibrosis. *Sci. Rep.* 7:14272. doi: 10.1038/s41598-017-14612-5

Hua, X., Xu, J., Deng, X., Xu, J., Li, J., Zhu, D., et al. (2018). New compound ChlA-F induces autophagy-dependent anti-cancer effect via upregulating Sestrin-2 in human bladder cancer. *Cancer Lett.* 436, 38–51. doi: 10.1016/j.canlet.2018.08.013

Huang, J., Dorsey, J., Chuikov, S., Zhang, X., Jenuwein, T., Reinberg, D., et al. (2010). G9a and Glp methylate lysine 373 in the tumor suppressor p53. *J. Biol. Chem.* 285, 9636–9641. doi: 10.1074/jbc.M109.062588

Hurst, K. E., Lawrence, K. A., Essman, M. T., Walton, Z. J., Leddy, L. R., and Thaxton, J. E. (2019). Endoplasmic reticulum stress contributes to mitochondrial exhaustion of CD8 T cells. *Cancer Immunol. Res.* 7, 476–486. doi: 10.1158/2326-6066.CIR-18-0182

Iida, Y., Fujimori, T., Okawa, K., Nagata, K., Wada, I., and Hosokawa, N. (2011). SEL1L protein critically determines the stability of the HRD1-SEL1L endoplasmic reticulum-associated degradation (ERAD) complex to optimize the degradation kinetics of ERAD substrates. *J. Biol. Chem.* 286, 16929–16939. doi: 10.1074/jbc.M110.215871

Isono, T., Chano, T., Okabe, H., and Suzaki, M. (2013). Study of global transcriptional changes of N-GlcNAc2 proteins-producing T24 bladder carcinoma cells under glucose deprivation. *PLoS One* 8:e60397. doi: 10.1371/annotation/053f227a-3847-41e2-a8c4-a5530a282a29

Jiang, D., Niwa, M., and Koong, A. C. (2015). Targeting the IRE1α-XBP1 branch of the unfolded protein response in human diseases. *Semin. Cancer Biol.* 33, 48–56. doi: 10.1016/j.semcancer.2015.04.010

Jin, Y., and Saatcioglu, F. (2020). Targeting the unfolded protein response in hormone-regulated cancers. *Trends Cancer* 6, 160–171. doi: 10.1016/j.trecan.2019.12.001

Kanemoto, S., Nitani, R., Murakami, T., Kaneko, M., Asada, R., Matsuhisa, K., et al. (2016). Multivesicular body formation enhancement and exosome release during endoplasmic reticulum stress. *Biochem. Biophys. Res. Commun.* 480, 166–172. doi: 10.1016/j.bbrc.2016.10.019

Kania, E., Pająk, B., and Orzechowski, A. (2015). Calcium homeostasis and ER stress in control of autophagy in cancer cells. *Biomed. Res. Int.* 2015:352794. doi: 10.1155/2015/352794

Kim, J. Y., Hwang, J. H., Cha, M. R., Yoon, M. Y., Son, E. S., Tomida, A., et al. (2010). Arctigenin blocks the unfolded protein response and shows therapeutic antitumor activity. *J. Cell. Physiol.* 224, 33–40. doi: 10.1002/jcp.22085

Kim, Y., Kim, Y. S., Kim, D. E., Lee, J., Song, J., Kim, H. G., et al. (2013). BIX-01294 induces autophagy-associated cell death via EHMT2/G9a dysfunction and intracellular reactive oxygen species production. *Autophagy* 9, 2126–2139. doi: 10.4161/auto.26308

Kleinnijenhuis, J., Quintin, J., Preijers, F., Joosten, L. A., Jacobs, C., Xavier, R. J., et al. (2014). BCG-induced trained immunity in NK cells: role for non-

specific protection to infection. *Clin. Immunol.* 155, 213–219. doi: 10.1016/j.clim.2014.10.005

Klionsky, D. J., Abdel-Aziz, A. K., Abdelfatah, S., Abdellatif, M., Abdoli, A., Abel, S., et al. (2021). Guidelines for the use and interpretation of assays for monitoring autophagy (4th Edn). *Autophagy* 17, 1–382. doi: 10.1080/15548627.2020.1797280

Kobatake, K., Ki, I., Nakata, Y., Yamasaki, N., Ueda, T., Kanai, A., et al. (2020). Kdm6a deficiency activates inflammatory pathways, promotes M2 macrophage polarization, and causes bladder cancer in cooperation with dysfunction. *Clin. Cancer Res.* 26, 2065–2079. doi: 10.1158/1078-0432.CCR-19-2230

Koritzinsky, M., Levitin, F., van den Beucken, T., Rumantir, R. A., Harding, N. J., Chu, K. C., et al. (2013). Two phases of disulfide bond formation have differing requirements for oxygen. *J. Cell Biol.* 203, 615–627. doi: 10.1083/jcb.201307185

Kou, B., Liu, W., Xu, X., Yang, Y., Yi, Q., Guo, F., et al. (2017). Autophagy induction enhances tetrandrine-induced apoptosis via the AMPK/mTOR pathway in human bladder cancer cells. *Oncol. Rep.* 38, 3137–3143. doi: 10.3892/or.2017.5988

Koumenis, C., Naczki, C., Koritzinsky, M., Rastani, S., Diehl, A., Sonenberg, N., et al. (2002). Regulation of protein synthesis by hypoxia via activation of the endoplasmic reticulum kinase PERK and phosphorylation of the translation initiation factor eIF2alpha. *Mol. Cell. Biol.* 22, 7405–7416. doi: 10.1128/MCB.22.21.7405-7416.2002

Kouroku, Y., Fujita, E., Tanida, I., Ueno, T., Isoai, A., Kumagai, H., et al. (2007). ER stress (PERK/eIF2alpha phosphorylation) mediates the polyglutamine-induced LC3 conversion, an essential step for autophagy formation. *Cell Death Differ.* 14, 230–239. doi: 10.1038/sj.cdd.4401984

Lebeau, P., Byun, J., Yousof, T., and Austin, R. C. (2018). Pharmacologic inhibition of S1P attenuates ATF6 expression, causes ER stress and contributes to apoptotic cell death. *Toxicol. Appl. Pharmacol.* 349, 1–7. doi: 10.1016/j.taap.2018.04.020

Leung-Hagesteijn, C., Erdmann, N., Cheung, G., Keats, J. J., Stewart, A. K., Reece, D. E., et al. (2013). Xbp1s-negative tumor B cells and pre-plasmablasts mediate therapeutic proteasome inhibitor resistance in multiple myeloma. *Cancer Cell* 24, 289–304. doi: 10.1016/j.ccr.2013.08.009

Li, J., Li, T. X., Ma, Y., Zhang, Y., Li, D. Y., and Xu, H. (2019). Bursopentin (BP5) induces G1 phase cell cycle arrest and endoplasmic reticulum stress/mitochondria-mediated caspase-dependent apoptosis in human colon cancer HCT116 cells. *Cancer Cell Int.* 19:130. doi: 10.1186/s12935-019-0849-3

Li, I., and Nabet, B. Y. (2019). Exosomes in the tumor microenvironment as mediators of cancer therapy resistance. *Mol. Cancer* 18:32. doi: 10.1186/s12943-019-0975-5

Li, T., Xu, K., and Liu, Y. (2018). Anticancer effect of salidroside reduces viability through autophagy/PI3K/Akt and MMP-9 signaling pathways in human bladder cancer cells. *Oncol. Lett.* 16, 3162–3168. doi: 10.3892/ol.2018.8982

Limia, C. M., Sauzay, C., Urra, H., Hetz, C., Chevet, E., and Avril, T. (2019). Emerging roles of the endoplasmic reticulum associated unfolded protein response in cancer cell migration and invasion. *Cancer* 11:631. doi: 10.3390/cancers11050631

Lin, Y., Jiang, M., Chen, W., Zhao, T., and Wei, Y. (2019). Cancer and ER stress: mutual crosstalk between autophagy, oxidative stress and inflammatory response. *Biomed. Pharmacother.* 118:109249. doi: 10.1016/j.biopha.2019.109249

Lin, J., Wang, R., Chen, J. C., Chiu, C. C., Liao, M., and Wu, Y. (2016). Cytotoxicity of 11-epi-Sinulariolide acetate isolated from cultured soft corals on HA22T cells through the endoplasmic reticulum stress pathway and mitochondrial dysfunction. *Int. J. Mol. Sci.* 17:1787. doi: 10.3390/ijms17111787

Liou, G. Y., and Storz, P. (2010). Reactive oxygen species in cancer. *Free Radic. Res.* 44, 479–496. doi: 10.3109/10715761003667554

Liu, J., Fan, L., Yu, H., Zhang, J., He, Y., Feng, D., et al. (2019). Endoplasmic reticulum stress causes liver cancer cells to release Exosomal miR-23a-3p and up-regulate programmed death ligand 1 expression in macrophages. *Hepatology* 70, 241–258. doi: 10.1002/hep.30607

Liu, C. Y., Hsu, C. C., Huang, T., Lee, C., Chen, J. L., Yang, S., et al. (2018). ER stress-related ATF6 upregulates CIP2A and contributes to poor prognosis of colon cancer. *Mol. Oncol.* 12, 1706–1717. doi: 10.1002/1878-0261.12365

Liu, S., Liang, B., Jia, H., Jiao, Y., Pang, Z., and Huang, Y. (2017a). Evaluation of cell death pathways initiated by antitumor drugs melatonin and valproic acid in bladder cancer cells. *FEBS Open Bio.* 7, 798–810. doi: 10.1002/2211-5463.12223

Liu, J., Xiao, M., Li, J., Wang, D., He, Y., He, J., et al. (2017b). Activation of UPR Signaling pathway is associated With the malignant progression and poor prognosis in prostate cancer. *Prostate* 77, 274–281. doi: 10.1002/pros.23264

Logue, S. E., McGrath, E. P., Cleary, P., Greene, S., Mnich, K., Almanza, A., et al. (2018). Inhibition of IRE1 RNase activity modulates the tumor cell secretome and enhances response to chemotherapy. *Nat. Commun.* 9:3267. doi: 10.1038/s41467-018-05763-8

Lu, P. D., Harding, H. P., and Ron, D. (2004). Translation reinitiation at alternative open reading frames regulates gene expression in an integrated stress response. *J. Cell Biol.* 167, 27–33. doi: 10.1083/jcb.200408003

Luo, S., and Lee, A. S. (2002). Requirement of the p38 mitogen-activated protein kinase signalling pathway for the induction of the 78 kDa glucose-regulated protein/immunoglobulin heavy-chain binding protein by azetidine stress: activating transcription factor 6 as a target for stress-induced phosphorylation. *Biochem. J.* 366, 787–795. doi: 10.1042/BJ20011802

Lv, W.-L., Liu, Q., An, J.-H., and Song, X.-Y. (2019). Scutellarin inhibits hypoxia-induced epithelial-mesenchymal transition in bladder cancer cells. *J. Cell. Physiol.* 234, 23169–23175. doi: 10.1002/jcp.28883

Lyu, L., Xiang, W., Zheng, F., Huang, T., Feng, Y., Yuan, J., et al. (2020). Significant prognostic value of the autophagy-related gene P4HB in bladder Urothelial carcinoma. *Front. Oncol.* 10:1613. doi: 10.3389/fonc.2020.01613

Ma, X., and Yi, Q. (2019). Cholesterol induces T cell exhaustion. *Aging* 11, 7334–7335. doi: 10.18632/aging.102305

Martelli, A. M., Paganelli, F., Chiarini, F., Evangelisti, C., and McCubrey, J. A. (2020). The unfolded protein response: a novel therapeutic target in acute leukemias. *Cancer* 12:333. doi: 10.3390/cancers12020333

Mazumdar, J., Dondeti, V., and Simon, M. C. (2009). Hypoxia-inducible factors in stem cells and cancer. *J. Cell. Mol. Med.* 13, 4319–4328. doi: 10.1111/j.1582-4934.2009.00963.x

Mehnert, M., Sommer, T., and Jarosch, E. (2014). Der1 promotes movement of misfolded proteins through the endoplasmic reticulum membrane. *Nat. Cell Biol.* 16, 77–86. doi: 10.1038/ncb2882

Milner, C. M., and Campbell, R. D. (1993). The G9a gene in the human major histocompatibility complex encodes a novel protein containing ankyrin-like repeats. *Biochem. J.* 290, 811–818. doi: 10.1042/bj2900811

Mimura, N., Fulciniti, M., Gorgun, G., Tai, Y., Cirstea, D., Santo, L., et al. (2012). Blockade of XBP1 splicing by inhibition of IRE1α is a promising therapeutic option in multiple myeloma. *Blood* 119, 5772–5781. doi: 10.1182/blood-2011-07-366633

Mounir, Z., Krishnamoorthy, J. L., Wang, S., Papadopoulou, B., Campbell, S., Muller, W. J., et al. (2011). Akt determines cell fate through inhibition of the PERK-eIF2α phosphorylation pathway. *Sci. Signal.* 4:a62. doi: 10.1126/scisignal.2001630

Mund, C., and Lyko, F. (2010). Epigenetic cancer therapy: proof of concept and remaining challenges. *BioEssays* 32, 949–957. doi: 10.1002/bies.201000061

Nguyen, H. G., Conn, C. S., Kye, Y., Xue, L., Forester, C. M., Cowan, J. E., et al. (2018). Development of a stress response therapy targeting aggressive prostate cancer. *Sci. Transl. Med.* 10:eaar2036. doi: 10.1126/scitranslmed.aar2036

Oakes, S. A. (2020). Endoplasmic reticulum stress Signaling in cancer cells. *Am. J. Pathol.* 190, 934–946. doi: 10.1016/j.ajpath.2020.01.010

Obiedat, A., Seidel, E., Mahameed, M., Berhani, O., Tsukerman, P., Voutetakis, K., et al. (2019). Transcription of the NKG2D ligand MICA is suppressed by the IRE1/XBP1 pathway of the unfolded protein response through the regulation of E2F1. *FASEB J.* 33, 3481–3495. doi: 10.1096/fj.201801350RR

Ogata, M., Hino, S., Saito, A., Morikawa, K., Kondo, S., Kanemoto, S., et al. (2006). Autophagy is activated for cell survival after endoplasmic reticulum stress. *Mol. Cell. Biol.* 26, 9220–9231. doi: 10.1128/MCB.01453-06

Oh, D. Y., Kwek, S. S., Raju, S. S., Li, T., Mccarthy, E., Chow, E., et al. (2020). Intratumoral CD4 T cells mediate anti-tumor cytotoxicity in human bladder cancer. *Cell* 181, 1612–1625. doi: 10.1016/j.cell.2020.05.017

Okubo, K., Isono, M., Asano, T., and Sato, A. (2019). Lopinavir-ritonavir combination induces endoplasmic reticulum stress and kills urological cancer cells. *Anticancer Res.* 39, 5891–5901. doi: 10.21873/anticanres.13793

Pakos-Zebrucka, K., Koryga, I., Mnich, K., Ljujic, M., Samali, A., and Gorman, A. M. (2016). The integrated stress response. *EMBO Rep.* 17, 1374–1395. doi: 10.15252/embr.201642195

Peschek, J., Acosta-Alvear, D., Mendez, A. S., and Walter, P. (2015). A conformational RNA zipper promotes intron ejection during non-conventional

XBP1 mRNA splicing. *EMBO Rep.* 16, 1688–1698. doi: 10.15252/embr.201540955

Pluquet, O., and Galmiche, A. (2019). Impact and relevance of the unfolded protein response in HNSCC. *Int. J. Mol. Sci.* 20:2654. doi: 10.3390/ijms20112654

Pommier, A., Anaparthy, N., Memos, N., Kelley, Z. L., Gouronnec, A., Yan, R., et al. (2018). Unresolved endoplasmic reticulum stress engenders immune-resistant, latent pancreatic cancer metastases. *Science* 360:eaao4908. doi: 10.1126/science.aao4908

Powles, T., Park, S.-H., Voog, E., Claudia, C., Valderrama, B.-P., Gurney, H., et al. (2020). Maintenance avelumab + best supportive care (BSC) versus BSC alone after platinum-based first-line (1L) chemotherapy in advanced urothelial carcinoma (UC): JAVELIN bladder 100 phase III interim analysis. *J. Clin. Oncol.* 38:A1. doi: 10.1200/JCO.2020.38.18_suppl.LBA1

Puthalakath, H., O'Reilly, L. A., Gunn, P., Lee, L., Kelly, P. N., Huntington, N. D., et al. (2007). ER stress triggers apoptosis by activating BH3-only protein Bim. *Cell* 129, 1337–1349. doi: 10.1016/j.cell.2007.04.027

Qi, W., White, M. C., Choi, W., Guo, C., Dinney, C., McConkey, D. J., et al. (2013). Inhibition of inducible heat shock protein-70 (hsp72) enhances bortezomib-induced cell death in human bladder cancer cells. *PLoS One* 8:e69509. doi: 10.1371/journal.pone.0069509

Qin, X., Denton, W. D., Huiting, L. N., Smith, K. S., and Feng, H. (2020). Unraveling the regulatory role of endoplasmic-reticulum-associated degradation in tumor immunity. *Crit. Rev. Biochem. Mol.* 55, 322–353. doi: 10.1080/10409238.2020.1784085

Ramakrishnan, S., Granger, V., Rak, M., Hu, Q., Attwood, K., Aquila, L., et al. (2019). Inhibition of EZH2 induces NK cell-mediated differentiation and death in muscle-invasive bladder cancer. *Cell Death Differ.* 26, 2100–2114. doi: 10.1038/s41418-019-0278-9

Rashid, H.-O., Kim, H.-K., Junjappa, R., Kim, H.-R., and Chae, H.-J. (2017). Endoplasmic reticulum stress in the regulation of liver diseases: involvement of regulated IRE1α and β-dependent decay and miRNA. *J. Gastroenterol. Hepatol.* 32, 981–991. doi: 10.1111/jgh.13619

Rather, R. A., Bhagat, M., and Singh, S. K. (2020). Oncogenic BRAF, endoplasmic reticulum stress, and autophagy: crosstalk and therapeutic targets in cutaneous melanoma. *Mutat. Res.* 785:108321. doi: 10.1016/j.mrrev.2020.108321

Reddy, R. K., Mao, C., Baumeister, P., Austin, R. C., Kaufman, R. J., and Lee, A. S. (2003). Endoplasmic reticulum chaperone protein GRP78 protects cells from apoptosis induced by topoisomerase inhibitors: role of ATP binding site in suppression of caspase-7 activation. *J. Biol. Chem.* 278, 20915–20924. doi: 10.1074/jbc.M212328200

Ri, M. (2016). Endoplasmic-reticulum stress pathway-associated mechanisms of action of proteasome inhibitors in multiple myeloma. *Int. J. Hematol.* 104, 273–280. doi: 10.1007/s12185-016-2016-0

Ritch, C. R., Velasquez, M. C., Kwon, D., Becerra, M. F., Soodana-Prakash, N., Atluri, V. S., et al. (2020). Use and validation of the AUA/SUO risk grouping for nonmuscle invasive bladder cancer in a contemporary cohort. *J. Urol.* 203, 505–511. doi: 10.1097/JU.0000000000000593

Ritterson-Lew, C., Guin, S., and Theodorescu, D. (2015). Targeting glycogen metabolism in bladder cancer. *Nat. Rev. Urol.* 12, 383–391. doi: 10.1038/nrurol.2015.111

Rodvold, J. J., Chiu, K. T., Hiramatsu, N., Nussbacher, J. K., Galimberti, V., Mahadevan, N. R., et al. (2017). Intercellular transmission of the unfolded protein response promotes survival and drug resistance in cancer cells. *Sci. Signal.* 10:eaah7177. doi: 10.1126/scisignal.aah7177

Rojas-Rivera, D., Delvaeye, T., Roelandt, R., Nerinckx, W., Augustyns, K., Vandenabeele, P., et al. (2017). When PERK inhibitors turn out to be new potent RIPK1 inhibitors: critical issues on the specificity and use of GSK2606414 and GSK2656157. *Cell Death Differ.* 24, 1100–1110. doi: 10.1038/cdd.2017.58

Ron, D., and Hubbard, S. R. (2008). How IRE1 reacts to ER stress. *Cell* 132, 24–26. doi: 10.1016/j.cell.2007.12.017

Ron, D., and Walter, P. (2007). Signal integration in the endoplasmic reticulum unfolded protein response. *Nat. Rev. Mol. Cell Biol.* 8, 519–529. doi: 10.1038/nrm2199

Rouschop, K. M., Dubois, L. J., Keulers, T. G., van den Beucken, T., Lambin, P., Bussink, J., et al. (2013). PERK/eIF2α signaling protects therapy resistant hypoxic cells through induction of glutathione synthesis and protection against ROS. *Proc. Natl. Acad. Sci. U.S.A.* 110, 4622–4627. doi: 10.1073/pnas.1210633110

Saito, S., Furuno, A., Sakurai, J., Sakamoto, A., Park, H.-R., Shin-Ya, K., et al. (2009). Chemical genomics identifies the unfolded protein response as a target for selective cancer cell killing during glucose deprivation. *Cancer Res.* 69, 4225–4234. doi: 10.1158/0008-5472.CAN-08-2689

Santoni, M., Amantini, C., Morelli, M. B., Liberati, S., Farfariello, V., Nabissi, M., et al. (2013). Pazopanib and sunitinib trigger autophagic and non-autophagic death of bladder tumour cells. *Br. J. Cancer* 109, 1040–1050. doi: 10.1038/bjc.2013.420

Sato, A., Asano, T., Okubo, K., Isono, M., and Asano, T. (2018). Nelfinavir and ritonavir kill bladder cancer cells synergistically by inducing endoplasmic reticulum stress. *Oncol. Res.* 26, 323–332. doi: 10.3727/096504017X14957929842972

Schlack, K., Boegemann, M., Steinestel, J., Schrader, A. J., and Krabbe, L.-M. (2016). The safety and efficacy of gemcitabine for the treatment of bladder cancer. *Expert Rev. Anticancer. Ther.* 16, 255–271. doi: 10.1586/14737140.2016.1143777

Schlütermann, D., Skowron, M. A., Berleth, N., Böhler, P., Deitersen, J., Stuhldreier, F., et al. (2018). Targeting urothelial carcinoma cells by combining cisplatin with a specific inhibitor of the autophagy-inducing class III PtdIns3K complex. *Urol. Oncol.* 36, 160–161. doi: 10.1016/j.urolonc.2017.11.021

Schuler, M., Bossy-Wetzel, E., Goldstein, J. C., Fitzgerald, P., and Green, D. R. (2000). p53 induces apoptosis by caspase activation through mitochondrial cytochrome c release. *J. Biol. Chem.* 275, 7337–7342. doi: 10.1074/jbc.275.10.7337

Senft, D., and Ronai, Z. A. (2015). UPR, autophagy, and mitochondria crosstalk underlies the ER stress response. *Trends Biochem. Sci.* 40, 141–148. doi: 10.1016/j.tibs.2015.01.002

Shan, G., Tang, T., Qian, H., and Xia, Y. (2018). Certain BCG-reactive responses are associated with bladder cancer prognosis. *Cancer Immunol. Immunother.* 67, 797–803. doi: 10.1007/s00262-018-2127-y

Sheng, X., Nenseth, H. Z., Qu, S., Kuzu, O. F., Frahnow, T., Simon, L., et al. (2019). IRE1α-XBP1s pathway promotes prostate cancer by activating c-MYC signaling. *Nat. Commun.* 10:323. doi: 10.1038/s41467-018-08152-3

Shi, Z., Yu, X., Yuan, M., Lv, W., Feng, T., Bai, R., et al. (2019). Activation of the PERK-ATF4 pathway promotes chemo-resistance in colon cancer cells. *Sci. Rep.* 9:3210. doi: 10.1038/s41598-019-39547-x

Shimizu, Y., and Hendershot, L. M. (2009). Oxidative folding: cellular strategies for dealing with the resultant equimolar production of reactive oxygen species. *Antioxid. Redox Signal.* 11, 2317–2331. doi: 10.1089/ars.2009.2501

Siegel, R. L., Miller, K. D., and Jemal, A. (2020). Cancer statistics, 2020. *CA Cancer J. Clin.* 70, 7–30. doi: 10.3322/caac.21590

Sinclair, J. D. (1988). Biological control systems in health and disease. *N. Z. Med. J.* 101, 702–703.

Siwecka, N., Rozpędek, W., Pytel, D., Wawrzynkiewicz, A., Dziki, A., Dziki, Ł., et al. (2019). Dual role of endoplasmic reticulum stress-mediated unfolded protein response Signaling pathway in carcinogenesis. *Int. J. Mol. Sci.* 20:4354. doi: 10.3390/ijms20184354

Song, M., Sandoval, T. A., Chae, C.-S., Chopra, S., Tan, C., Rutkowski, M. R., et al. (2018). IRE1α-XBP1 controls T cell function in ovarian cancer by regulating mitochondrial activity. *Nature* 562, 423–428. doi: 10.1038/s41586-018-0597-x

Sun, N., Liang, Y., Chen, Y., Wang, L., Li, D., Liang, Z., et al. (2019). Glutamine affects T24 bladder cancer cell proliferation by activating STAT3 through ROS and glutaminolysis. *Int. J. Mol. Med.* 44, 2189–2200. doi: 10.3892/ijmm.2019.4385

Tachibana, M., Sugimoto, K., Fukushima, T., and Shinkai, Y. (2001). Set domain-containing protein, G9a, is a novel lysine-preferring mammalian histone methyltransferase with hyperactivity and specific selectivity to lysines 9 and 27 of histone H3. *J. Biol. Chem.* 276, 25309–25317. doi: 10.1074/jbc.M101914200

Takeyama, Y., Kato, M., Tamada, S., Azuma, Y., Shimizu, Y., Iguchi, T., et al. (2020). Myeloid-derived suppressor cells are essential partners for immune checkpoint inhibitors in the treatment of cisplatin-resistant bladder cancer. *Cancer Lett.* 479, 89–99. doi: 10.1016/j.canlet.2020.03.013

Tam, A. B., Koong, A. C., and Niwa, M. (2014). Ire1 has distinct catalytic mechanisms for XBP1/HAC1 splicing and RIDD. *Cell Rep.* 9, 850–858. doi: 10.1016/j.celrep.2014.09.016

Tang, C., Ranatunga, S., Kriss, C. L., Cubitt, C. L., Tao, J., Pinilla-Ibarz, J. A., et al. (2014). Inhibition of ER stress-associated IRE-1/XBP-1 pathway reduces leukemic cell survival. *J. Clin. Invest.* 124, 2585–2598. doi: 10.1172/JCI73448

Tao, L., Qiu, J., Slavin, S., Ou, Z., Liu, Z., Ge, J., et al. (2018). Recruited T cells promote the bladder cancer metastasis via up-regulation of the estrogen receptor β/IL-1/c-MET signals. *Cancer Lett.* 430, 215–223. doi: 10.1016/j.canlet.2018.03.045

Tsachaki, M., Mladenovic, N., štambergová, H., Birk, J., and Odermatt, A. (2018). Hexose-6-phosphate dehydrogenase controls cancer cell proliferation and migration through pleiotropic effects on the unfolded-protein response, calcium homeostasis, and redox balance. *FASEB J.* 32, 2690–2705. doi: 10.1096/fj.201700870RR

Tsujihashi, H., Matsuda, H., Uejima, S., Akiyama, T., and Kurita, T. (1989). Role of natural killer cells in bladder tumor. *Eur. Urol.* 16, 444–449. doi: 10.1159/000471637

Urano, F., Wang, X., Bertolotti, A., Zhang, Y., Chung, P., Harding, H. P., et al. (2000). Coupling of stress in the ER to activation of JNK protein kinases by transmembrane protein kinase IRE1. *Science* 287, 664–666. doi: 10.1126/science.287.5453.664

Wallis, C. J. D., Mahar, A. L., Choo, R., Herschorn, S., Kodama, R., Shah, P. S., et al. (2016). Second malignancies after radiotherapy for prostate cancer: systematic review and meta-analysis. *BMJ* 352:i851. doi: 10.1136/bmj.i851

Walter, F., O'brien, A., Concannon, C. G., Düssmann, H., and Prehn, J. H. M. (2018). ER stress signaling has an activating transcription factor 6α (ATF6)-dependent "off-switch." *J. Biol. Chem.* 293, 18270–18284. doi: 10.1074/jbc.RA118.002121

Wang, X., Bai, Y., Zhang, F., Yang, Y., Feng, D., Li, A., et al. (2020). Targeted inhibition of P4HB promotes cell sensitivity to gemcitabine in Urothelial carcinoma of the bladder. *Onco. Targets Ther.* 13, 9543–9558. doi: 10.2147/OTT.S267734

Wang, F., Tang, J., Li, P., Si, S., Yu, H., Yang, X., et al. (2018). Chloroquine enhances the radiosensitivity of bladder cancer cells by inhibiting autophagy and activating apoptosis. *Cell. Physiol. Biochem.* 45, 54–66. doi: 10.1159/000486222

Wei, Y., Wang, D., Topczewski, F., and Pagliassotti, M. J. (2006). Saturated fatty acids induce endoplasmic reticulum stress and apoptosis independently of ceramide in liver cells. *Am. J. Physiol. Endocrinol. Metab.* 291, E275–E281. doi: 10.1152/ajpendo.00644.2005

Winnay, J. N., Solheim, M., Sakaguchi, M., Njølstad, P. R., and Kahn, C. R. (2020). Inhibition of the PI 3-kinase pathway disrupts the unfolded protein response and reduces sensitivity to ER stress-dependent apoptosis. *FASEB J.* 34, 12521–12532. doi: 10.1096/fj.202000892R

Wouters, B. G., and Koritzinsky, M. (2008). Hypoxia signalling through mTOR and the unfolded protein response in cancer. *Nat. Rev. Cancer* 8, 851–864. doi: 10.1038/nrc2501

Wu, J., and Abraham, S. N. (2021). The roles of T cells in bladder pathologies. *Trends Immunol.* 42, 248–260. doi: 10.1016/j.it.2021.01.003

Wu, S., Lin, W., Shen, C., Pan, H., Keh-Bin, W., Chen, Y.-C., et al. (2016a). Melatonin set out to ER stress signaling thwarts epithelial mesenchymal transition and peritoneal dissemination via calpain-mediated C/EBPβ and NFκB cleavage. *J. Pineal Res.* 60, 142–154. doi: 10.1111/jpi.12295

Wu, C., Silvers, C. R., Messing, E. M., and Lee, Y.-F. (2019a). Bladder cancer extracellular vesicles drive tumorigenesis by inducing the unfolded protein response in endoplasmic reticulum of nonmalignant cells. *J. Biol. Chem.* 294, 3207–3218. doi: 10.1074/jbc.RA118.006682

Wu, Y. J., Su, T. R., Dai, G. F., Su, J. H., and Liu, C. (2019b). Flaccidoxide-13-acetate-induced apoptosis in human bladder cancer cells is through activation of p38/JNK, mitochondrial dysfunction, and endoplasmic reticulum stress regulated pathway. *Mar. Drugs* 17:287. doi: 10.3390/md17050287

Wu, Z., Wang, C., Zhang, Z., Liu, W., Xu, H., Wang, H., et al. (2016b). High expression of Derlin-1 is associated with the malignancy of bladder cancer in a Chinese Han population. *PLoS One* 11:e168351. doi: 10.1371/journal.pone.0168351

Xia, Y., Kang, T. W., Jung, Y. D., Zhang, C., and Lian, S. (2019). Sulforaphane inhibits nonmuscle invasive bladder cancer cells proliferation through suppression of HIF-1α-mediated glycolysis in hypoxia. *J. Agric. Food Chem.* 67, 7844–7854. doi: 10.1021/acs.jafc.9b03027

Xie, H., Tang, C., Song, J., Mancuso, A., Del Valle, J. R., Cao, J., et al. (2018). IRE1α RNase-dependent lipid homeostasis promotes survival in Myc-transformed cancers. *J. Clin. Invest.* 128, 1300–1316. doi: 10.1172/JCI95864

Xu, S., Sankar, S., and Neamati, N. (2014). Protein disulfide isomerase: a promising target for cancer therapy. *Drug Discov. Today* 19, 222–240. doi: 10.1016/j.drudis.2013.10.017

Xue, M., Chen, W., Xiang, A., Wang, R., Chen, H., Pan, J., et al. (2017). Hypoxic exosomes facilitate bladder tumor growth and development through transferring long non-coding RNA-UCA1. *Mol. Cancer* 16:143. doi: 10.1186/s12943-017-0714-8

Xue, Y., Tong, L., Liuanwei-Liu, F., Liu, A., Zeng, S., Xiong, Q., et al. (2019). Tumor-infiltrating M2 macrophages driven by specific genomic alterations are associated with prognosis in bladder cancer. *Oncol. Rep.* 42, 581–594. doi: 10.3892/or.2019.7196

Yamamoto, K., Yoshida, H., Kokame, K., Kaufman, R. J., and Mori, K. (2004). Differential contributions of ATF6 and XBP1 to the activation of endoplasmic reticulum stress-responsive cis-acting elements ERSE, UPRE and ERSE-II. *J. Biochem.* 136, 343–350. doi: 10.1093/jb/mvh122

Yan, D., Wang, H., Bowman, R. L., and Joyce, J. A. (2016). STAT3 and STAT6 signaling pathways synergize to promote Cathepsin secretion from macrophages via IRE1α activation. *Cell Rep.* 16, 2914–2927. doi: 10.1016/j.celrep.2016.08.035

Yang, G., Shen, W., Zhang, Y., Liu, M., Zhang, L., Liu, Q., et al. (2017a). Accumulation of myeloid-derived suppressor cells (MDSCs) induced by low levels of IL-6 correlates with poor prognosis in bladder cancer. *Oncotarget* 8, 38378–38388. doi: 10.18632/oncotarget.16386

Yang, F., Tang, X. Y., Liu, H., and Jiang, Z. W. (2016). Inhibition of mitogen-activated protein kinase signaling pathway sensitizes breast cancer cells to endoplasmic reticulum stress-induced apoptosis. *Oncol. Rep.* 35, 2113–2120. doi: 10.3892/or.2016.4580

Yang, L., Taylor, J., Eustace, A., Irlam, J. J., Denley, H., Hoskin, P. J., et al. (2017b). A gene signature for selecting benefit from hypoxia modification of radiotherapy for high-risk bladder cancer patients. *Clin. Cancer Res.* 23, 4761–4768. doi: 10.1158/1078-0432.CCR-17-0038

Yang, X., Yin, H., Zhang, Y., Li, X., Tong, H., Zeng, Y., et al. (2018). Hypoxia-induced autophagy promotes gemcitabine resistance in human bladder cancer cells through hypoxia-inducible factor 1α activation. *Int. J. Oncol.* 53, 215–224. doi: 10.3892/ijo.2018.4376

Yarapureddy, S., Abril, J., Foote, J., Kumar, S., Asad, O., Sharath, V., et al. (2019). ATF6α activation enhances survival against chemotherapy and serves as a prognostic indicator in osteosarcoma. *Neoplasia* 21, 516–532. doi: 10.1016/j.neo.2019.02.004

Yu, Z., Luo, X., Wang, C., Ye, J., Liu, S., Xie, L., et al. (2016a). Baicalin promoted site-2 protease and not site-1 protease in endoplasmic reticulum stress-induced apoptosis of human hepatocellular carcinoma cells. *FEBS Open Bio.* 6, 1093–1101. doi: 10.1002/2211-5463.12130

Yu, N., Sun, Y., Xm, S., He, M., Dai, B., and Kang, J. (2016b). Melatonin attenuates TGFβ1-induced epithelial-mesenchymal transition in lung alveolar epithelial cells. *Mol. Med. Rep.* 14, 5567–5572. doi: 10.3892/mmr.2016.5950

Yu, Q., Zhao, B., Gui, J., Katlinski, K. V., Brice, A., Gao, Y., et al. (2015). Type I interferons mediate pancreatic toxicities of PERK inhibition. *Proc. Natl. Acad. Sci. U.S.A.* 112, 15420–15425. doi: 10.1073/pnas.1516362112

Yuan, X., Li, D., Zhao, H., Jiang, J., Wang, P., Ma, X., et al. (2013). Licochalcone A-induced human bladder cancer T24 cells apoptosis triggered by mitochondria dysfunction and endoplasmic reticulum stress. *Biomed. Res. Int.* 2013:474272. doi: 10.1155/2013/474272

Zhang, M., Du, H., Huang, Z., Zhang, P., Yue, Y., Wang, W., et al. (2018). Thymoquinone induces apoptosis in bladder cancer cell via endoplasmic reticulum stress-dependent mitochondrial pathway. *Chem. Biol. Interact.* 292, 65–75. doi: 10.1016/j.cbi.2018.06.013

Zhang, J., Duan, H., Feng, Z., Han, X., and Gu, C. (2020). Acetyl-CoA synthetase 3 promotes bladder cancer cell growth under metabolic stress. *Oncogene* 9:46. doi: 10.1038/s41389-020-0230-3

Zhang, K., and Kaufman, R. J. (2008). From endoplasmic-reticulum stress to the inflammatory response. *Nature* 454, 455–462. doi: 10.1038/nature07203

Zhang, H., Li, C., Ren, J. -W., Liu, L., Du, X. H., Gao, J., et al. (2021). OTUB1 facilitates bladder cancer progression by stabilizing ATF6 in response to ER stress. *Cancer Sci.* doi: 10.1111/cas.14876 [Epub ahead of print]

Zhang, H., Lu, C., Fang, M., Yan, W., Chen, M., Ji, Y., et al. (2016a). HIF-1α activates hypoxia-induced PFKFB4 expression in human bladder cancer cells. *Biochem. Biophys. Res. Commun.* 476, 146–152. doi: 10.1016/j.bbrc.2016.05.026

Zhang, J., Pavlova, N. N., and Thompson, C. B. (2017a). Cancer cell metabolism: the essential role of the nonessential amino acid, glutamine. *EMBO J.* 36, 1302–1315. doi: 10.15252/embj.201696151

Zhang, J., Sun, A., Xu, R., Tao, X., Dong, Y., Lv, X., et al. (2016b). Cell-penetrating and endoplasmic reticulum-locating TAT-IL-24-KDEL fusion protein induces tumor apoptosis. *J. Cell. Physiol.* 231, 84–93. doi: 10.1002/jcp.25054

Zhang, X.-Q., Yang, Z., and Benedict, W. F. (2011). Direct gene transfer of adenoviral-mediated interferon α into human bladder cancer cells but not the bystander factors produced induces endoplasmic reticulum stress-related cytotoxicity. *Cancer Gene Ther.* 18, 260–264. doi: 10.1038/cgt.2010.76

Zhang, H., Ye, Y. L., Li, M.-X., Ye, S.-B., Huang, W.-R., Cai, T., et al. (2017b). CXCL2/MIF-CXCR2 signaling promotes the recruitment of myeloid-derived suppressor cells and is correlated with prognosis in bladder cancer. *Oncogene* 36, 2095–2104. doi: 10.1038/onc.2016.367

Zhao, N., Cao, J., Xu, L., Tang, Q., Le, D., Lv, X., et al. (2018). Pharmacological targeting of MYC-regulated IRE1/XBP1 pathway suppresses MYC-driven breast cancer. *J. Clin. Invest.* 128, 1283–1299. doi: 10.1172/JCI95873

Conflict of Interest: The authors declare that the research was conducted in the absence of any commercial or financial relationships that could be construed as a potential conflict of interest.

frontiers in Cell and Developmental Biology

MINI REVIEW
published: 11 June 2021
doi: 10.3389/fcell.2021.676342

The Emerging Roles of Pericytes in Modulating Tumor Microenvironment

*Ruipu Sun[1,2], Xiangzhan Kong[1,2], Xiaoyi Qiu[1,2], Cheng Huang[1,2] and Ping-Pui Wong[1,2]**

[1] Guangdong Provincial Key Laboratory of Malignant Tumor Epigenetics and Gene Regulation, Guangdong-Hong Kong Joint Laboratory for RNA Medicine, Sun Yat-sen Memorial Hospital, Sun Yat-sen University, Guangzhou, China, [2] Medical Research Center, Sun Yat-sen Memorial Hospital, Sun Yat-sen University, Guangzhou, China

Pericytes (PCs), known as mural cells, play an important blood vessel (BV) supporting role in regulating vascular stabilization, permeability and blood flow in microcirculation as well as blood brain barrier. In carcinogenesis, defective interaction between PCs and endothelial cells (ECs) contributes to the formation of leaky, chaotic and dysfunctional vasculature in tumors. However, recent works from other laboratories and our own demonstrate that the direct interaction between PCs and other stromal cells/cancer cells can modulate tumor microenvironment (TME) to favor cancer growth and progression, independent of its BV supporting role. Furthermore, accumulating evidence suggests that PCs have an immunomodulatory role. In the current review, we focus on recent advancement in understanding PC's regulatory role in the TME by communicating with ECs, immune cells, and tumor cells, and discuss how we can target PC's functions to re-model TME for an improved cancer treatment strategy.

Keywords: pericyte, mural cell, tumor microenvironment, angiogenesis, immunomodulation

OPEN ACCESS

Edited by:
Liu Yang,
Zhejiang Provincial People's Hospital, China

Reviewed by:
Walter J. Storkus,
University of Pittsburgh, United States
Anantha Koteswararao Kanugula,
University of Massachusetts Medical School, United States
John Chappell,
Fralin Biomedical Research Institute, Virginia Tech Carilion, United States

***Correspondence:**
Ping-Pui Wong
huangbp3@mail.sysu.edu.cn

Specialty section:
This article was submitted to Molecular and Cellular Oncology, a section of the journal Frontiers in Cell and Developmental Biology

Received: *05 March 2021*
Accepted: *06 April 2021*
Published: *11 June 2021*

Citation:
Sun R, Kong X, Qiu X, Huang C and Wong P-P (2021) The Emerging Roles of Pericytes in Modulating Tumor Microenvironment. Front. Cell Dev. Biol. 9:676342. doi: 10.3389/fcell.2021.676342

INTRODUCTION

Pericytes (PCs) are embedded in the basement membrane of blood microvessels (Bergers and Song, 2005), which play a vital role in regulating physiological and pathological events, including vascular development, homeostasis, fibrosis, and stroke. Generally, PCs are responsible for the regulation of vascular stabilization, vascular permeability, blood flow, and angiogenesis along with endothelial cells (ECs) in blood vessels (BVs) (Hellstrom et al., 2001; Pallone and Silldorff, 2001; Enge et al., 2002). In angiogenesis, sprouting ECs secrete platelet derived growth factor (PDGF) to recruit platelet derived growth factor receptor-beta (PDGFR-β) positive mural cells (including PCs), which then interact with ECs and stabilize the newly formed BVs (Carmeliet and Jain, 2000). Unlike other stromal cells, PCs can be distinguished by dynamic molecular marker expression pattern under different conditions, such as PDGFR-β, CD13 (alanine aminopeptidase), Cluster of differentiation 146 (CD146), alpha-smooth muscle actin (α-SMA) (Dermietzel and Krause, 1991; Lindahl et al., 1997; Ozerdem et al., 2001). In recent years, PCs are defined as heterogeneous, tissue-specific, and multipotent cell population in BVs (Ferland-McCollough et al., 2017), which are mainly due to their tissue/organ-specific roles (Shepro and Morel, 1993; Armulik et al., 2005;

Corselli et al., 2013; Kitano and Bloomston, 2016) and ability to give rise to various cell populations (Dore-Duffy et al., 2006; Dellavalle et al., 2007; Crisan et al., 2008; Olson and Soriano, 2011). During tumor angiogenesis, defective EC–PC interaction is one of the major causes of the formation of dysfunctional tumor vasculature and hypoxic tumor microenvironment (TME), which favors cancer growth and metastasis (Song et al., 2005). Therefore, it is important to investigate the underlying role of PCs in modulating tumor angiogenesis and TME in order to develop an improved anti-cancer treatment.

Anti-angiogenetic therapy is recognized as a promising treatment strategy for cancer, while many anti-angiogenic drugs have been approved for certain types of cancers, including anti-vascular endothelial growth factor (VEGF) drug (i.e., Bevacizumab, Ranibizumab) and some tyrosine kinase inhibitors (i.e., Sorafenib, Sunitinib) (Meng et al., 2015; Ramjiawan et al., 2017; Li et al., 2018). However, the resistance to anti-angiogenetic therapy have jeopardized their clinical benefits in cancer patients (Ramjiawan et al., 2017; Li et al., 2018). Previous studies suggested that PCs can protect ECs from anti-angiogenic therapies probably by secreting pro-angiogenic factors (Franco et al., 2011) or soluble factors (Prete et al., 2018). In addition, PCs may increase their coverage around tumor BVs adaptively and cause resistance to anti-angiogenetic therapy in preclinical models (Benjamin et al., 1999; Bergers and Hanahan, 2008). Nevertheless, combination treatment with PDGF receptor kinase inhibitor erlotinib/imatinib and bevacizumab showed very limited benefits in the clinical trials and even displayed an additive toxicity in some cancer patients (Hainsworth et al., 2007). The failure behind these trials suggests that PC may have other potential roles in controlling tumor growth and progression. Indeed, recent work from our laboratory shows that PC can regulate tumor cell growth via paracrine signals controlled by β3-integrin (Wong et al., 2020), independent of its BV supporting function, suggesting that its regulatory role in the TME is far more complicated than we previously thought.

In this review, we will exploit the current progress of understanding the role of PC in regulating TME, and discuss its functions in regulating tumor cells and other stromal cells to dictate cancer growth and progression. For comprehensive reviews of its role in BV formation and supporting function, please see Betsholtz and Crivellato (Armulik et al., 2011; Ribatti et al., 2011).

CROSSTALK BETWEEN PERICYTES AND TUMOR/STROMAL CELLS IN TUMOR MICROENVIRONMENT

Although the composition of TME varies in different cancer types, some features seem to be typical characteristics in most solid tumors. Indeed, TME consists of cancer cells and some non-malignant cells, including ECs, PCs, immune inflammatory cells, cancer-associated fibroblasts (CAFs), and also extracellular matrix (ECM) components (including cytokines, chemokines, matrix metalloproteinases, integrins, and other secreted molecules) (Hanahan and Weinberg, 2011). In this section, we review and discuss the multifaceted roles of PCs in regulating tumor cell and stromal cell's functions in details.

Abnormal Endothelial Cell–Pericyte Interaction and Signaling in Tumor Vasculature

Endothelial cells are the fundamental cells lining the interior face of BV walls, which are surrounded by quiescent mural cells (including PCs). PCs are capable of interacting with newly proliferating ECs to form nascent BVs and secrete angiogenetic factors to stabilize the newly-formed vessels (Abramsson et al., 2003). In tumorigenesis, defective EC–PC interaction leads to the formation of disorganized tumor vasculature (Ferland-McCollough et al., 2017). This is because PC is an essential mediator to maintain the integrity of tumor BVs, while PDGF-B/PDGFR-β signaling is critical for controlling PC migration during angiogenesis. Preceding findings have suggested that PDGFR-β mediated paracrine loop activates ECs to produce PDGF-B in order to recruit PDGFR-β-positive PCs, which in return releases VEGF-A and Ang-1 to stabilize the newly formed BVs (Armulik et al., 2005). Afterward, Ang-1 regulates the maturation and integrity of BV through binding to the endothelial cell-Tie-2 receptor (Harrell et al., 2018). During sprouting angiogenesis, ECs can also secrete Ang-2 to compete with Ang-1 for the binding to endothelial cell-Tie-2 receptor, which in turn destructs EC–PC interaction and destabilizes BVs (Saharinen et al., 2017). Interestingly, overexpression of PDGF-B by ECs causes an increase in PC coverage and vascular stability as well as accelerated tumor progression (Guo et al., 2003; Furuhashi et al., 2004). Moreover, tumor-derived PDGF-B induces endothelial cell-SDF-1α secretion, which then promotes PC migration and recruitment during tumor angiogenesis (Song et al., 2009). Furthermore, EC- and PC-derived HB-EGF (heparin-binding epidermal growth factor-like growth factor) activates EGFR (epidermal growth factor receptor) specifically in tumor-associated perivascular cells, resulting in increased PC coverage and enhanced angiogenesis (Nolan-Stevaux et al., 2010). Conversely, it has been suggested that inadequate PDGF-B in the stroma results in inappropriate attachment of PCs to ECs (Raza et al., 2010). Previous works have demonstrated that the blockade of Notch signaling inhibits vascular co-option and disrupts the EC-PC interaction during tumor angiogenesis (Hernandez et al., 2013), while Jagged-1 expression and Notch signaling are shown to be important for the growth of ECs and PCs as well as the maintenance of EC–PC interaction (Tattersall et al., 2016). In the study of Meng et al. (2015), they discover that ECs and PCs can build an "EC-PC shield" to protect tumor cells from cancer-directed therapy and immune surveillance in the TME, while the maintenance of BV integrity ensures an adequate oxygen and nutrient supply to tumor cells, which in turn promotes cancer growth and progression (Ferland-McCollough et al., 2017). Indeed, clinical studies show that high BV's PC coverage is associated with increased tumor growth and poor prognosis (Furuhashi et al., 2004), while it is correlated with reduced distant metastasis in colorectal cancer patients (Yonenaga et al., 2005). Overall, these findings suggest that PC overabundance and

deficiency occur in different tumor types during vascularization with mixed clinical outcome, implying that targeting PC coverage may not be an ideal strategy for anti-cancer treatment. Instead, our recent study indicates that PC-derived paracrine signals can modulate tumor cell growth independent of its BV supporting role and coverage (Wong et al., 2020), suggesting that targeting PC derived paracrine signals could be an alternative method for cancer therapy.

Direct Paracrine Crosstalk Between Tumor Cells and Pericytes Determines Cancer Growth and Progression

Although PCs have been considered as a critical compartment of the TME, the underlying mechanism of tumor cell–PC interaction has yet to be elucidated. Recently, we have shown that high percentage of mural-β3-integrin negative BVs correlates with increased tumor size and progression in multiple cancers (Wong et al., 2020), while PC specific knock out of β3-integrin expression enhances tumor growth independent of its BV supporting role. Further mechanistic study shows that loss of PC-β3-integrin expression increases the production of paracrine factors, including CCL2, CXCL1, and TIMP1, via activation of the FAK-HGFR-Akt-NF-κB signaling pathway, while PC-derived CCL2 enhances MEK1-ERK1/2-ROCK2 mediated tumor growth, suggesting that inhibition of ROCK in tumors with low PC-β3-integrin expression could potentially control cancer growth (Wong et al., 2020). Interestingly, a recent study from Lechertier et al. (2020) show that loss of PC FAK enhances p-Pyk2-Gas6-Axl-Akt signaling and its downstream Cyr61 expression to stimulate tumor angiogenesis, while PC-derived Cyr61 is also able to enhance tissue factor expression in tumor cells and its mediated cell proliferation. This work provides first evidence that PCs can crosstalk with ECs and tumor cells via the same paracrine signal (Lechertier et al., 2020). Furthermore, Caspani et al. study shows that a pathogenic crosstalk between PCs and tumor cells determines glioblastoma progression in mouse models (Caspani et al., 2014).

Pericytes Modulate Immunosuppressive Tumor Microenvironment

Inflammatory cells, an important component in the TME, are often associated with the inflammatory and immune responses in carcinogenesis. It is known that solid tumors are infiltrated by various innate and adaptive immune cells with both pro-tumor and anti-tumor functions (Turley et al., 2015). Previous works have shown that PCs release chemokines and cytokines in response to the pro-inflammatory stimulus, such as CCL2, CCL3, CXCL1, IFN-γ, and IL-8 (Navarro et al., 2016), while they also express some functional pattern-recognition receptors (i.e., TLR4, TLR2, NOD1) and macrophage markers (i.e., ED-2), implying that they may also have a role in modulating immune response (Navarro et al., 2016). Interestingly, PCs display phagocytic and pinocytic ability and regulate different types of leukocytes trafficking (Navarro et al., 2016). Accordingly, tumor PCs have distinct effects on tumor-associated macrophages (TAMs) in TME, while IL-33 produced by PDGF-BB-stimulated PCs has been shown to recruit TAMs in order to promote cancer metastasis in several human and mouse xenograft models (**Figure 1**, process ①) (Yang et al., 2016). PC-derived chemokine CXCL12 (SDF-1) can trigger the EGF/CSF-1 paracrine invasion loop to mediate the co-migration of TAM and tumor cells, after binding to its receptor CXCR4 on both TAMs and tumor cells (**Figure 1**, process ②) (Qian and Pollard, 2010). Meanwhile, crosstalk between M2-like macrophages and PCs in glioblastoma (GBM) promotes PC recruitment and upregulates the expression of the proangiogenic ECM component periostin deposition in PCs through the CECR1–PDGF-B–PDGFR-β signaling pathway (Zhu et al., 2017). In the *pdgfb*$^{ret/ret}$ mouse model, PCs deficiency-driven hypoxia result in IL-6 upregulation and an increased myeloid-derived suppressor cell (MDSC) transmigration in tumors, and the MDSC accumulation leads to increased tumor growth, while the amounts of circulating malignant cells can be abrogated upon the recovery of PC coverage (**Figure 1**, process ③) (Hong et al., 2015).

Newer evidence suggests that tumor-derived PCs regulate the activity and proliferation of T lymphocytes in TME (**Figure 1**). In a mouse spontaneous model of pancreatic cancer (RIP1-Tag5), knocking out *RGS5 (*regulator of G-protein signaling 5) gene results in PC maturation, vascular normalization and consequently a marked reduction in tumor hypoxia and vessel leakiness, while these changes enhance immune cell infiltration and extend the survival of tumor bearing mice (Hamzah et al., 2008). Furthermore, PC-RGS5 overexpression has been observed in several types of human tumors including kidney, liver, and head and neck cancers (Furuya et al., 2004; Hamzah et al., 2008). Coincidently, Bose et al. show that the expression of PC-RGS5 is upregulated after co-cultured with tumor-derived supernatant or established subcutaneous tumors (Bose et al., 2013). Tumor derived PCs inhibit $CD4^+$ T cell proliferation and activation while promoting $CD4^+$ T cell anergy *in vitro*, which is also regulated by RGS5- and IL-6-dependent signaling pathways (**Figure 1**, process ④). In addition, the expression of PD-L1 is up-regulated in PCs after co-cultured with tumor fragments (Bose et al., 2013). These results suggest that the combined effect of PC-PD-L1 and RGS5 expression might protect tumor cells from cytotoxic T cells. In a different study, the authors show that human malignant glioma-derived pericytes (HMGP), which co-expressed CD90, CD248, and PDGFR-β, are capable of inhibiting the proliferation of mitogen- and allogeneic-stimulated T cells via the release of prostaglandin E2 (PGE2), serum human leukocyte antigen G (sHLA-G), hepatocyte growth factor (HGF), and transforming growth factor-beta (TGF-β) (**Figure 1**, process ⑤). Clinically, the expression level of CD90 in perivascular cells positively correlates with glioma malignancy, while it is negatively associated with BV-associated leukocytes and $CD8^+$ T cell infiltration (Ochs et al., 2013). Recently, Valdor et al. report that GBM-conditioned-pericytes (GBC-PCs) can secrete a high level of anti-inflammatory cytokines and immunosuppressive molecules while reducing their surface co-stimulatory molecule expression, which in turn suppresses $CD4^+$ T cell response and IL-2 production *in vitro* (**Figure 1**, process ⑥) (Valdor et al., 2017). Further study shows that

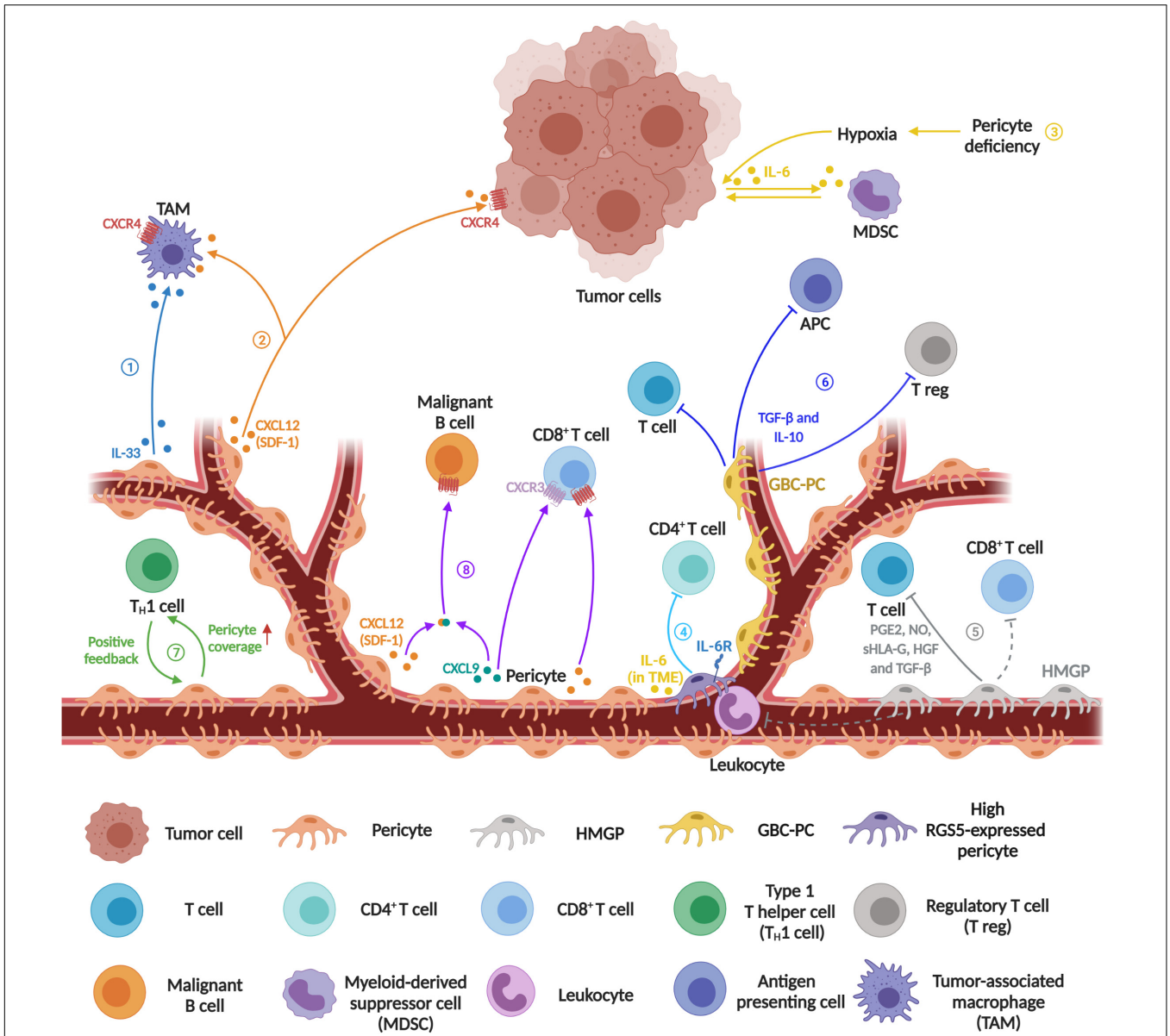

FIGURE 1 | Schematics diagram represents the emerging immunomodulatory role of pericytes in tumor microenvironment. ①Recruitment of tumor-associated macrophage (TAM). PDGF-BB-stimulated PCs release IL-33 to recruit more TAMs. ② Increased co-migration of TAMs and tumor cells. PC-derived chemokine CXCL12 (SDF-1) contributes to the co-migration of TAMs and tumor cells during innate immune response. ③ Increased myeloid-derived suppressor cells (MDSCs) transmigration. PC loss causes leaky blood vessels and inadequate oxygen supply leading to tumor hypoxia, which then induces IL-6 expression in tumor cells to increase MDSC transmigration, resulting in suppression of the T cell-mediated anti-tumor response. ④ Induced $CD4^+$ T cell anergy. Tumor PCs act as negative regulators of $CD4^+$ T cell activity. ⑤ Inhibition of mitogen- and allogeneic-stimulated T cell proliferation. Human malignant glioma-derived pericyte (HMGP) releases PGE2, NO, sHLA-G, HGF, and TDF-β to suppress T cell proliferation, while CD90-positive PCs may function as suppressors of the infiltration of leukocytes and $CD8^+$ T cells in malignant glioma. ⑥ Inhibition of T cell and antigen presenting cell activity, and increased recruitment of regulatory T cells. Glioblastoma conditioned-pericyte (GBC-PC) not only negatively regulates T cell and antigen presenting cell (APC) but also recruits regulatory T cell (T reg). ⑦ Regulation of blood vessel normalization and immune cell infiltration. In the positive feedback loop between type 1 T helper (T_H1) and blood vessel normalization, PC coverage has a certain impact on T_H1-mediated immune cell infiltration. ⑧ Enhanced $CD8^+$ T cell recruitment and malignant B cell migration. Perivascular cell derived CXCL9 and CXCL12 can recruit $CD8^+$ T cell effectors by binding to their corresponding receptor CXCR3 and CXCR4 respectively. Besides, CXCL9 forms a heterocomplex with CXCL12, which then enhances CXCR4-dependent malignant B cell migration to accumulate on the vessel wall (Created with BioRender.com).

GBC-PCs upregulate chaperone-mediated autophagy (CMA) to enhance the expression of anti-inflammatory cytokines TGF-β and IL-10, which then inhibit T cell and antigen presenting cell activity and recruit regulatory T cells (**Figure 1**, process ⑥) (Valdor et al., 2019). Additionally, PCs contribute to the subsequent positive feedback loop of type 1 T helper cells-mediated vessel normalization and immune response (**Figure 1**, process ⑦) (Tian et al., 2017).

TABLE 1 | Phase 3 clinical trials of Pericyte-related antitumor therapy.

Cancer type	Treatment	Targets	Results	References
Temozolomide-resistant progressive GBM	Imatinib + hydroxyurea vs hydroxyurea	PDGFR, c-Kit, and BCR-Abl	Imatinib does not improve PFS in combination therapy.	Dresemann et al., 2010
GIST (failure of imatinib and sunitinib treatment)	Imatinib vs placebo		Resumption of imatinib improves PFS and disease control at 12 weeks.	Kang et al., 2013
Unresectable or metastatic GIST	Imatinib vs nilotinib	PDGFR, c-Kit, and BCR-Abl; PDGFR, BCR-Abl, DDR1, and c-Kit	PFS is higher in the imatinib group than in the nilotinib group.	Blay et al., 2015
Radioiodine-refractory thyroid cancer	Lenvatinib vs placebo	PDGFR,VEGFR, FGFR, c-Kit, and Ret	Lenvatinib improves in PFS and the response rate but has more adverse effects.	Schlumberger et al., 2015
Advanced HCC	Sorafenib vs placebo	PDGFR, VEGFR, Raf, and c-Kit	Sorafenib prolongs median survival and time-to-radiologic-progression in patients.	Rimassa and Santoro, 2009
Advanced HCC	Sorafenib vs placebo		Sorafenib improves median OS significantly.	Cheng et al., 2009
HCC	Sorafenib vs placebo		Sorafenib therapy is not efficacious after HCC resection or ablation.	Bruix et al., 2015
Radioiodine-refractory, locally advanced or metastatic differentiated thyroid cancer	Sorafenib vs placebo		Sorafenib significantly improves PFS.	Brose et al., 2014
Non-metastatic RCC	Sorafenib or sunitinib vs placebo	PDGFR, VEGFR, Raf, and c-Kit; PDGFR, VEGFR, c-Kit, Flt3, CSF-1R, and Ret	Sorafenib or sunitinib adjuvant treatment shows no survival benefit relative to placebo.	Haas et al., 2016
Advanced GIST	Sunitinib vs placebo	PDGFR, VEGFR, c-Kit, Flt3, CSF-1R, and Ret	Sunitinib shows significant clinical benefit.	Demetri et al., 2006
PNET	Sunitinib vs placebo		Sunitinib improves PFS and OS.	Raymond et al., 2011
ccRCC	Sunitinib vs placebo		Sunitinib improves the median duration of disease-free survival.	Ravaud et al., 2016
Metastatic RCC	Sunitinib vs interferon α	PDGFR, VEGFR, c-Kit, Flt3, CSF-1R, and Ret	Sunitinib improves PFS and response rates.	Motzer et al., 2007
Advanced RCC	Axitinib vs sorafenib	VEGFR; PDGFR, VEGFR, Raf, and c-Kit	Axitinib results in prolonged PFS.	Rini et al., 2011
Advanced NSCLC	Anlotinib vs placebo	PDGFR, VEGFR, FGFR, c-Kit, and Ret	Prolongs OS and PFS.	Han et al., 2018
Advanced or metastatic RCC	Pazopanib vs placebo	PDGFR, VEGFR, FGFR, and c-Kit	Pazopanib improves PFS and tumor response.	Sternberg et al., 2010
Metastatic non-adipocytic soft-tissue sarcoma (failure of standard chemotherapy)	Pazopanib vs placebo		Pazopanib improves PFS significantly.	van der Graaf et al., 2012
Soft tissue sarcoma	Pazopanib vs placebo		Pazopanib improves PFS significantly.	Kawai et al., 2016
Metastatic CRC	Regorafenib vs placebo	PDGFR, VEGFR, Tie2, FGFR, c-Kit, Ret, and Raf	Regorafenib shows survival benefits.	Grothey et al., 2013
HCC (progressed on sorafenib)	Regorafenib vs placebo		Regorafenib provides survival benefits.	Bruix et al., 2017
Advanced GIST (failure of imatinib and sunitinib)	Regorafenib vs placebo		Regorafenib improves PFS.	Demetri et al., 2013
Advanced ovarian cancer	Carboplatin and paclitaxel + placebo vs carboplatin and paclitaxel + nintedanib	PDGFR, VEGFR, and FGFR	Nintedanib in combination with carboplatin and paclitaxel increases PFS.	du Bois et al., 2016
Recurrent ovarian cancer	Paclitaxel + placebo vs paclitaxel + trebananbib	Ang-1 and Ang-2	Trebananib prolongs PFS in paclitaxel treatment.	Monk et al., 2014
Recurrent partially platinum-sensitive/resistant ovarian cancer	Pegylated liposomal doxorubicin + placebo vs Pegylated liposomal doxorubicin + trebananbib		Trebananbib improves ORR and DOR but does not improve the PFS.	Marth et al., 2017
Advanced ovarian cancer	Carboplatin and paclitaxel + placebo vs carboplatin and paclitaxel + trebananbib		Trebananbib does not improve PFS.	Vergote et al., 2019

ccRCC, clear cell renal cell carcinoma; CRC, colorectal cancer; CSF-1R, colony-stimulating factor 1; DDR1, discoidin domain receptor 1; DOR, duration of response; FGFR, fibroblast growth factor receptor; GBM, glioblastoma; GIST, gastrointestinal stromal tumor; HCC, hepatocellular carcinoma; NSCLC, non-small-cell lung cancer; ORR, objective response rate; OS, overall survival; PDGFR, platelet-derived growth factor receptor; PFS, progression-free survival; PNET, pancreatic neuroendocrine tumor; RCC, renal cell carcinoma.

Interestingly, Daniel et al., show that PCs may also possess a potential regulatory role of malignant B cell recruitment in primary central nervous system lymphoma (**Figure 1**, process ⑧). Clinically, the localization and density of activated $CD8^+$ T cells within tumors is correlated with the expression level of inflammatory chemokine CXC chemokine ligand 9 (CXCL9), which is an agonist of the CXC chemokine receptor 3 (CXCR3), mainly secreted by PCs and perivascular macrophages. In the perivascular TME, CXCL9 can form heterocomplex with B-cell chemoattractant CXCL12 to enhance CXCL12-induced $CD8^+$ T cell as well as malignant B cell recruitment toward BV walls in the primary central nervous system lymphomas (Venetz et al., 2010). In addition, our recent work shows that β3-integrin controls the secretion of CCL2, CXCL1, and TIMP1 from PCs via the FAK-HGFR-Akt-NF-κB signaling (Wong et al., 2020), while these cytokines have been linked to immune cell infiltration and activity in TME (Navarro et al., 2016), suggesting that targeting PC-β3-integrin and its downstream signaling pathway can be a potential strategy to modulate immunosuppressive TME.

The Role of Pericytes-Fibroblast Transition in Tumor Microenvironment

As a fundamental component of the tumor stroma, cancer associated fibroblast (CAFs) have a role in modulating TME and changing the behavior of neoplastic cells in either a tumor-promoting or tumor-inhibiting manner (Kalluri, 2016). In the tumor-promoting property, CAFs support carcinogenesis through secretion of cytokine, growth factors and angiogenic factors, production and remodeling of the ECM, as well as suppression of immune surveillance in the TME (Matsuda and Seki, 2020). Recently, PC is considered to be one of the major sources of CAFs in tumors and fibrosis (Öhlund et al., 2014; Kalluri, 2016). A novel finding reveals that PDGF-BB-PDGFRβ signaling can induce pericytes-fibroblast transition (PFT), while the detached PCs from tumor microvasculature can transdifferentiate to fibroblasts that significantly contributed to tumor invasion and metastasis (Hosaka et al., 2016).

TARGETING PERICYTES AS A CANCER TREATMENT STRATEGY: CHALLENGES VS OPPORTUNITIES

It has become a research hot topic for developing direct/indirect PC-targeted agents against angiogenesis and cancer growth in the last decades (**Supplementary Table 1**). However, majority of these agents showed modest or no effect on tumor growth and progression as a single agent in preclinical animal models, especially for PDGFR-targeted therapy. Combining anti-PDGFR agent with chemotherapy or other agent-targeted therapy displayed slightly better anti-tumor effect in mouse models of certain cancer types (**Supplementary Table 1**). Furthermore, the phase 3 clinical trials of PC-related antitumor therapy have so far shown modest clinical benefits in certain cancers (**Table 1**). Besides, the combination therapy of anti-PDGFB and anti-VEGF had very limited effect in the clinical trials and even showed additive side effects in some patients (Hainsworth et al., 2007). After interpreting these studies, we speculate that drug dosing strategy is a critical variable which may determine whether PC-targeted drugs promote vascular function and immune cell infiltration or induce tumor vasculature destruction and cancer metastasis. Therefore, it is a clinically unmet need to investigate how to target PC coverage or recondition PC functions (i.e., immunomodulatory role) for preferred immunobiology/vascular function in TME. Apart from targeting PCs directly, Cantelmo et al. show that inhibition of the glycolytic activator PFKFB3 in ECs induces tumor vessel normalization to improve PC coverage and chemotherapy delivery in the preclinical models. The authors also claimed that depletion of PFKFB3 significantly inhibits placenta derived PC proliferation, while improves PC coverage and adherence to ECs in tumor BVs (Cantelmo et al., 2016). However, the short-term effect of BV normalization raises a question about its application in the clinic (Wong et al., 2015). Recently, we discover that loss of mural-β3-integrin expression significantly enhances FAK-p-HGFR-p-Akt-p-p65 mediated CCL2 cytokine production, which in turn activates CCR2-MEK1-ROCK2 dependent tumor growth (Wong et al., 2020). These findings suggest that cancer patients with low PC-β3-integrin expression can be potentially treated with CCR2 or ROCK inhibitors.

CONCLUSION

As an obligatory constituent of the TME, PCs modulate the TME by interacting with tumor cells, ECs, immune cells, and CAFs, beyond their BV supporting role. Recent work supports direct cross-talk between PCs and tumor cells in the TME, which can promote tumor growth independent of tumor angiogenesis. Also, the interplay between ECs and PCs in regulating vascular formation and remodeling has been demonstrated in numerous studies. Disrupting EC-PC interactions in tumor vasculature not only affects PC coverage on tumor BVs but also alter vascular and perivascular TME to influence the efficacy of anti-tumor therapies. Indeed, new studies have highlighted that PCs protect tumor cells from immune surveillance through suppressing the proliferation or response of inflammatory cells around the tumor parenchyma, which could be a new potential target for cancer immunotherapy. Besides, the observation of PC-fibroblast transition suggests the potential progenitor cell property of PC in the TME. In this review, we provide new information to support an integral role for PCs in promoting tumor progression in part through their regulatory activities of tumor cells and dominated stromal cells, suggesting that PCs can serve as a therapeutic target for anticancer treatment in addition to anti-angiogenesis. Meanwhile, the stromal cells within TME may also provide potential therapeutic targets for intending anti-angiogenesis combination therapy since their underlying relationships with PCs. Future studies should focus on exploring the underlying mechanisms of PC-stromal cell/tumor cell interaction in the TME in order to identify new therapeutic targets for an improved cancer treatment strategy.

AUTHOR CONTRIBUTIONS

RS wrote the manuscript and made the figure as well as the table. XK, XQ, and CH reviewed the manuscript. P-PW conceptualized, wrote, and reviewed the final version. All authors approved the submission for publication.

FUNDING

This work was supported by the Natural Science Foundation of China (81920108028 and 81872142), Guangzhou Science and Technology Program (201904020008), Guangdong Science and Technology Department (2020A0505100029, 2020B1212060018, and 2020B1212030004), and the Key Training Program for Young Scholars of Sun Yat-sen University (18ykzd07).

SUPPLEMENTARY MATERIAL

The Supplementary Material for this article can be found online at: https://www.frontiersin.org/articles/10.3389/fcell.2021.676342/full#supplementary-material

Supplementary Table 1 | Preclinical testing of Pericyte-targeted antitumor therapy.

REFERENCES

Abramsson, A., Lindblom, P., and Betsholtz, C. (2003). Endothelial and nonendothelial sources of PDGF-B regulate pericyte recruitment and influence vascular pattern formation in tumors. *J. Clin. Invest.* 112, 1142–1151. doi: 10.1172/jci18549

Armulik, A., Abramsson, A., and Betsholtz, C. (2005). Endothelial/pericyte interactions. *Circ. Res.* 97, 512–523. doi: 10.1161/01.RES.0000182903.16652.d7

Armulik, A., Genove, G., and Betsholtz, C. (2011). Pericytes: developmental, physiological, and pathological perspectives, problems, and promises. *Dev. Cell* 21, 193–215. doi: 10.1016/j.devcel.2011.07.001

Benjamin, L. E., Golijanin, D., Itin, A., Pode, D., and Keshet, E. (1999). Selective ablation of immature blood vessels in established human tumors follows vascular endothelial growth factor withdrawal. *J. Clin. Invest.* 103, 159–165. doi: 10.1172/JCI5028

Bergers, G., and Hanahan, D. (2008). Modes of resistance to anti-angiogenic therapy. *Nat. Rev. Cancer* 8, 592–603. doi: 10.1038/nrc2442

Bergers, G., and Song, S. (2005). The role of pericytes in blood-vessel formation and maintenance. *Neuro Oncol.* 7, 452–464. doi: 10.1215/S1152851705000232

Bergers, G., Song, S., Meyer-Morse, N., Bergsland, E., and Hanahan, D. (2003). Benefits of targeting both pericytes and endothelial cells in the tumor vasculature with kinase inhibitors. *J. Clin. Invest.* 111, 1287–1295. doi: 10.1172/JCI17929

Blay, J. Y., Shen, L., Kang, Y. K., Rutkowski, P., Qin, S., Nosov, D., et al. (2015). Nilotinib versus imatinib as first-line therapy for patients with unresectable or metastatic gastrointestinal stromal tumours (ENESTg1): a randomised phase 3 trial. *Lancet Oncol.* 16, 550–560. doi: 10.1016/s1470-2045(15)70105-1

Bose, A., Barik, S., Banerjee, S., Ghosh, T., Mallick, A., Bhattacharyya Majumdar, S., et al. (2013). Tumor-derived vascular pericytes anergize Th cells. *J. Immunol.* 191, 971–981. doi: 10.4049/jimmunol.1300280

Brand, C., Schliemann, C., Ring, J., Kessler, T., Baumer, S., Angenendt, L., et al. (2016). NG2 proteoglycan as a pericyte target for anticancer therapy by tumor vessel infarction with retargeted tissue factor. *Oncotarget* 7, 6774–6789. doi: 10.18632/oncotarget.6725

Brose, M. S., Nutting, C. M., Jarzab, B., Elisei, R., Siena, S., Bastholt, L., et al. (2014). Sorafenib in radioactive iodine-refractory, locally advanced or metastatic differentiated thyroid cancer: a randomised, double-blind, phase 3 trial. *Lancet* 384, 319–328. doi: 10.1016/s0140-6736(14)60421-9

Bruix, J., Qin, S., Merle, P., Granito, A., Huang, Y. H., Bodoky, G., et al. (2017). Regorafenib for patients with hepatocellular carcinoma who progressed on sorafenib treatment (RESORCE): a randomised, double-blind, placebo-controlled, phase 3 trial. *Lancet* 389, 56–66. doi: 10.1016/s0140-6736(16)32453-9

Bruix, J., Takayama, T., Mazzaferro, V., Chau, G. Y., Yang, J., Kudo, M., et al. (2015). Adjuvant sorafenib for hepatocellular carcinoma after resection or ablation (STORM): a phase 3, randomised, double-blind, placebo-controlled trial. *Lancet Oncol.* 16, 1344–1354. doi: 10.1016/s1470-2045(15)00198-9

Cantelmo, A. R., Conradi, L. C., Brajic, A., Goveia, J., Kalucka, J., Pircher, A., et al. (2016). Inhibition of the glycolytic activator PFKFB3 in endothelium induces tumor vessel normalization, impairs metastasis, and improves chemotherapy. *Cancer Cell* 30, 968–985. doi: 10.1016/j.ccell.2016.10.006

Carmeliet, P., and Jain, R. K. (2000). Angiogenesis in cancer and other diseases. *Nature* 407, 249–257. doi: 10.1038/35025220

Caspani, E. M., Crossley, P. H., Redondo-Garcia, C., and Martinez, S. (2014). Glioblastoma: a pathogenic crosstalk between tumor cells and pericytes. *PLoS One* 9:e101402. doi: 10.1371/journal.pone.0101402

Chen, M., Lei, X., Shi, C., Huang, M., Li, X., Wu, B., et al. (2017). Pericyte-targeting prodrug overcomes tumor resistance to vascular disrupting agents. *J. Clin. Invest.* 127, 3689–3701. doi: 10.1172/jci94258

Cheng, A. L., Kang, Y. K., Chen, Z., Tsao, C. J., Qin, S., Kim, J. S., et al. (2009). Efficacy and safety of sorafenib in patients in the Asia-Pacific region with advanced hepatocellular carcinoma: a phase III randomised, double-blind, placebo-controlled trial. *Lancet Oncol.* 10, 25–34. doi: 10.1016/s1470-2045(08)70285-7

Chi Sabins, N., Taylor, J. L., Fabian, K. P., Appleman, L. J., Maranchie, J. K., Stolz, D. B., et al. (2013). DLK1: a novel target for immunotherapeutic remodeling of the tumor blood vasculature. *Mol. Ther.* 21, 1958–1968. doi: 10.1038/mt.2013.133

Corselli, M., Chin, C. J., Parekh, C., Sahaghian, A., Wang, W., Ge, S., et al. (2013). Perivascular support of human hematopoietic stem/progenitor cells. *Blood* 121, 2891–2901. doi: 10.1182/blood-2012-08-451864

Crisan, M., Yap, S., Casteilla, L., Chen, C. W., Corselli, M., Park, T. S., et al. (2008). A perivascular origin for mesenchymal stem cells in multiple human organs. *Cell Stem Cell* 3, 301–313. doi: 10.1016/j.stem.2008.07.003

Dellavalle, A., Sampaolesi, M., Tonlorenzi, R., Tagliafico, E., Sacchetti, B., Perani, L., et al. (2007). Pericytes of human skeletal muscle are myogenic precursors distinct from satellite cells. *Nat. Cell Biol.* 9, 255–267. doi: 10.1038/ncb1542

Demetri, G. D., Reichardt, P., Kang, Y. K., Blay, J. Y., Rutkowski, P., Gelderblom, H., et al. (2013). Efficacy and safety of regorafenib for advanced gastrointestinal stromal tumours after failure of imatinib and sunitinib (GRID): an international, multicentre, randomised, placebo-controlled, phase 3 trial. *Lancet* 381, 295–302. doi: 10.1016/s0140-6736(12)61857-1

Demetri, G. D., van Oosterom, A. T., Garrett, C. R., Blackstein, M. E., Shah, M. H., Verweij, J., et al. (2006). Efficacy and safety of sunitinib in patients with advanced gastrointestinal stromal tumour after failure of imatinib: a randomised controlled trial. *Lancet* 368, 1329–1338. doi: 10.1016/s0140-6736(06)69446-4

Dermietzel, R., and Krause, D. (1991). Molecular anatomy of the blood-brain barrier as defined by immunocytochemistry. *Intern. Rev. Cytol.* 127, 57–109. doi: 10.1016/s0074-7696(08)60692-0

Dore-Duffy, P., Katychev, A., Wang, X., and Van Buren, E. (2006). CNS microvascular pericytes exhibit multipotential stem cell activity. *J. Cereb. Blood Flow Metab.* 26, 613–624. doi: 10.1038/sj.jcbfm.9600272

Dresemann, G., Weller, M., Rosenthal, M. A., Wedding, U., Wagner, W., Engel, E., et al. (2010). Imatinib in combination with hydroxyurea versus hydroxyurea alone as oral therapy in patients with progressive pretreated glioblastoma resistant to standard dose temozolomide. *J. Neurooncol.* 96, 393–402. doi: 10.1007/s11060-009-9976-3

du Bois, A., Kristensen, G., Ray-Coquard, I., Reuss, A., Pignata, S., Colombo, N., et al. (2016). Standard first-line chemotherapy with or without nintedanib for advanced ovarian cancer (AGO-OVAR 12): a randomised, double-blind,

placebo-controlled phase 3 trial. *Lancet Oncol.* 17, 78–89. doi: 10.1016/s1470-2045(15)00366-6

Edwards, A. K., Glithero, K., Grzesik, P., Kitajewski, A. A., Munabi, N. C., Hardy, K., et al. (2017). NOTCH3 regulates stem-to-mural cell differentiation in infantile hemangioma. *JCI Insight.* 2, 93764. doi: 10.1172/jci.insight.93764

Enge, M., Bjarnegard, M., Gerhardt, H., Gustafsson, E., Kalen, M., Asker, N., et al. (2002). Endothelium-specific platelet-derived growth factor-B ablation mimics diabetic retinopathy. *EMBO J.* 21, 4307–4316. doi: 10.1093/emboj/cdf418

Fabian, K. P. L., Chi-Sabins, N., Taylor, J. L., Fecek, R., Weinstein, A., and Storkus, W. J. (2017). Therapeutic efficacy of combined vaccination against tumor pericyte-associated antigens DLK1 and DLK2 in mice. *OncoImmunology* 6:e1290035. doi: 10.1080/2162402X.2017.1290035

Falcon, B. L., Hashizume, H., Koumoutsakos, P., Chou, J., Bready, J. V., Coxon, A., et al. (2009). Contrasting actions of selective inhibitors of angiopoietin-1 and angiopoietin-2 on the normalization of tumor blood vessels. *Am. J. Pathol.* 175, 2159–2170. doi: 10.2353/ajpath.2009.090391

Falcon, B. L., Pietras, K., Chou, J., Chen, D., Sennino, B., Hanahan, D., et al. (2011). Increased vascular delivery and efficacy of chemotherapy after inhibition of platelet-derived growth factor-B. *Am. J. Pathol.* 178, 2920–2930. doi: 10.1016/j.ajpath.2011.02.019

Ferland-McCollough, D., Slater, S., Richard, J., Reni, C., and Mangialardi, G. (2017). Pericytes, an overlooked player in vascular pathobiology. *Pharmacol. Ther.* 171, 30–42. doi: 10.1016/j.pharmthera.2016.11.008

Franco, M., Roswall, P., Cortez, E., Hanahan, D., and Pietras, K. (2011). Pericytes promote endothelial cell survival through induction of autocrine VEGF-A signaling and Bcl-w expression. *Blood* 118, 2906–2917. doi: 10.1182/blood-2011-01-331694

Furuhashi, M., Sjöblom, T., Abramsson, A., Ellingsen, J., Micke, P., Li, H., et al. (2004). Platelet-derived growth factor production by B16 melanoma cells leads to increased pericyte abundance in tumors and an associated increase in tumor growth rate. *Cancer Res.* 64, 2725–2733. doi: 10.1158/0008-5472.can-03-1489

Furuya, M., Nishiyama, M., Kimura, S., Suyama, T., Naya, Y., Ito, H., et al. (2004). Expression of regulator of G protein signalling protein 5 (RGS5) in the tumour vasculature of human renal cell carcinoma. *J. Pathol.* 203, 551–558. doi: 10.1002/path.1543

Grothey, A., Van Cutsem, E., Sobrero, A., Siena, S., Falcone, A., Ychou, M., et al. (2013). Regorafenib monotherapy for previously treated metastatic colorectal cancer (CORRECT): an international, multicentre, randomised, placebo-controlled, phase 3 trial. *Lancet* 381, 303–312. doi: 10.1016/s0140-6736(12)61900-x

Guan, Y. Y., Luan, X., Xu, J. R., Liu, Y. R., Lu, Q., Wang, C., et al. (2014). Selective eradication of tumor vascular pericytes by peptide-conjugated nanoparticles for antiangiogenic therapy of melanoma lung metastasis. *Biomaterials* 35, 3060–3070. doi: 10.1016/j.biomaterials.2013.12.027

Guo, P., Hu, B., Gu, W., Xu, L., Wang, D., Huang, H. J., et al. (2003). Platelet-derived growth factor-B enhances glioma angiogenesis by stimulating vascular endothelial growth factor expression in tumor endothelia and by promoting pericyte recruitment. *Am. J. Pathol.* 162, 1083–1093. doi: 10.1016/s0002-9440(10)63905-3

Haas, N. B., Manola, J., Uzzo, R. G., Flaherty, K. T., Wood, C. G., Kane, C., et al. (2016). Adjuvant sunitinib or sorafenib for high-risk, non-metastatic renal-cell carcinoma (ECOG-ACRIN E2805): a double-blind, placebo-controlled, randomised, phase 3 trial. *Lancet* 387, 2008–2016. doi: 10.1016/s0140-6736(16)00559-6

Hainsworth, J. D., Spigel, D. R., Sosman, J. A., Burris, H. A. III, Farley, C., Cucullu, H., et al. (2007). Treatment of advanced renal cell carcinoma with the combination bevacizumab/erlotinib/imatinib: a phase I/II trial. *Clin. Genitourin. Cancer* 5, 427–432. doi: 10.3816/CGC.2007.n.030

Hamzah, J., Jugold, M., Kiessling, F., Rigby, P., Manzur, M., Marti, H. H., et al. (2008). Vascular normalization in Rgs5-deficient tumours promotes immune destruction. *Nature* 453, 410–414. doi: 10.1038/nature06868

Han, B., Li, K., Wang, Q., Zhang, L., Shi, J., Wang, Z., et al. (2018). Effect of anlotinib as a third-line or further treatment on overall survival of patients with advanced non-small cell lung cancer: the alter 0303 phase 3 randomized clinical trial. *JAMA Oncol.* 4, 1569–1575. doi: 10.1001/jamaoncol.2018.3039

Hanahan, D., and Weinberg, R. A. (2011). Hallmarks of cancer: the next generation. *Cell* 144, 646–674. doi: 10.1016/j.cell.2011.02.013

Harrell, C. R., Simovic Markovic, B., Fellabaum, C., Arsenijevic, A., Djonov, V., and Volarevic, V. (2018). Molecular mechanisms underlying therapeutic potential of pericytes. *J. Biomed. Sci.* 25:21. doi: 10.1186/s12929-018-0423-7

Hellstrom, M., Gerhardt, H., Kalen, M., Li, X., Eriksson, U., Wolburg, H., et al. (2001). Lack of pericytes leads to endothelial hyperplasia and abnormal vascular morphogenesis. *J. Cell Biol.* 153, 543–553. doi: 10.1083/jcb.153.3.543

Hernandez, S. L., Banerjee, D., Garcia, A., Kangsamaksin, T., Cheng, W.-Y., Anastassiou, D., et al. (2013). Notch and VEGF pathways play distinct but complementary roles in tumor angiogenesis. *Vasc. Cell* 5:17. doi: 10.1186/2045-824X-5-17

Hong, J., Tobin, N. P., Rundqvist, H., Li, T., Lavergne, M., García-Ibáñez, Y., et al. (2015). Role of tumor pericytes in the recruitment of myeloid-derived suppressor cells. *J. Natl. Cancer Instit.* 107:djv209. doi: 10.1093/jnci/djv209

Hosaka, K., Yang, Y., Seki, T., Fischer, C., Dubey, O., Fredlund, E., et al. (2016). Pericyte-fibroblast transition promotes tumor growth and metastasis. *Proc. Natl. Acad. Sci. U.S.A.* 113, E5618–E5627. doi: 10.1073/pnas.1608384113

Kalluri, R. (2016). The biology and function of fibroblasts in cancer. *Nat. Rev. Cancer* 16, 582–598. doi: 10.1038/nrc.2016.73

Kang, Y. K., Ryu, M. H., Yoo, C., Ryoo, B. Y., Kim, H. J., Lee, J. J., et al. (2013). Resumption of imatinib to control metastatic or unresectable gastrointestinal stromal tumours after failure of imatinib and sunitinib (RIGHT): a randomised, placebo-controlled, phase 3 trial. *Lancet Oncol.* 14, 1175–1182. doi: 10.1016/s1470-2045(13)70453-4

Kawai, A., Araki, N., Hiraga, H., Sugiura, H., Matsumine, A., Ozaki, T., et al. (2016). A randomized, double-blind, placebo-controlled, Phase III study of pazopanib in patients with soft tissue sarcoma: results from the Japanese subgroup. *Jpn. J. Clin. Oncol.* 46, 248–253. doi: 10.1093/jjco/hyv184

Keskin, D., Kim, J., Cooke, V. G., Wu, C. C., Sugimoto, H., Gu, C., et al. (2015). Targeting vascular pericytes in hypoxic tumors increases lung metastasis via angiopoietin-2. *Cell Rep.* 10, 1066–1081. doi: 10.1016/j.celrep.2015.01.035

Kitano, M., and Bloomston, P. M. (2016). Hepatic stellate cells and microRNAs in pathogenesis of liver fibrosis. *J. Clin. Med.* 5:38. doi: 10.3390/jcm5030038

Kłosowska-Wardega, A., Hasumi, Y., Burmakin, M., Ahgren, A., Stuhr, L., Moen, I., et al. (2009). Combined anti-angiogenic therapy targeting PDGF and VEGF receptors lowers the interstitial fluid pressure in a murine experimental carcinoma. *PLoS One* 4:e8149. doi: 10.1371/journal.pone.0008149

Kuhnert, F., Tam, B. Y., Sennino, B., Gray, J. T., Yuan, J., Jocson, A., et al. (2008). Soluble receptor-mediated selective inhibition of VEGFR and PDGFRbeta signaling during physiologic and tumor angiogenesis. *Proc. Natl. Acad. Sci. U.S.A.* 105, 10185–10190. doi: 10.1073/pnas.0803194105

Lechertier, T., Reynolds, L. E., Kim, H., Pedrosa, A. R., Gómez-Escudero, J., Muñoz-Félix, J. M., et al. (2020). Pericyte FAK negatively regulates Gas6/Axl signalling to suppress tumour angiogenesis and tumour growth. *Nat. Commun.* 11:2810. doi: 10.1038/s41467-020-16618-6

Lederle, W., Linde, N., Heusel, J., Bzyl, J., Woenne, E. C., Zwick, S., et al. (2010). Platelet-derived growth factor-B normalizes micromorphology and vessel function in vascular endothelial growth factor-A-induced squamous cell carcinomas. *Am. J. Pathol.* 176, 981–994. doi: 10.2353/ajpath.2010.080998

Leow, C. C., Coffman, K., Inigo, I., Breen, S., Czapiga, M., Soukharev, S., et al. (2012). MEDI3617, a human anti-angiopoietin 2 monoclonal antibody, inhibits angiogenesis and tumor growth in human tumor xenograft models. *Int. J. Oncol.* 40, 1321–1330. doi: 10.3892/ijo.2012.1366

Li, T., Kang, G., Wang, T., and Huang, H. (2018). Tumor angiogenesis and anti-angiogenic gene therapy for cancer. *Oncol. Lett.* 16, 687–702. doi: 10.3892/ol.2018.8733

Lindahl, P., Johansson, B. R., Leveen, P., and Betsholtz, C. (1997). Pericyte loss and microaneurysm formation in PDGF-B-deficient mice. *Science* 277, 242–245. doi: 10.1126/science.277.5323.242

Lu, C., Kamat, A. A., Lin, Y. G., Merritt, W. M., Landen, C. N., Kim, T. J., et al. (2007). Dual targeting of endothelial cells and pericytes in antivascular therapy for ovarian carcinoma. *Clin. Cancer Res.* 13, 4209–4217. doi: 10.1158/1078-0432.CCR-07-0197

Lu, C., Shahzad, M. M., Moreno-Smith, M., Lin, Y. G., Jennings, N. B., Allen, J. K., et al. (2010). Targeting pericytes with a PDGF-B aptamer in human ovarian carcinoma models. *Cancer Biol. Ther.* 9, 176–182. doi: 10.4161/cbt.9.3.10635

Marth, C., Vergote, I., Scambia, G., Oberaigner, W., Clamp, A., Berger, R., et al. (2017). ENGOT-ov-6/TRINOVA-2: randomised, double-blind, phase 3 study

of pegylated liposomal doxorubicin plus trebananib or placebo in women with recurrent partially platinum-sensitive or resistant ovarian cancer. *Eur. J. Cancer* 70, 111–121. doi: 10.1016/j.ejca.2016.09.004

Matsuda, M., and Seki, E. (2020). Hepatic stellate cell-macrophage crosstalk in liver fibrosis and carcinogenesis. *Semin. Liver Dis.* 40, 307–320. doi: 10.1055/s-0040-1708876

McCarty, M. F., Somcio, R. J., Stoeltzing, O., Wey, J., Fan, F., Liu, W., et al. (2007). Overexpression of PDGF-BB decreases colorectal and pancreatic cancer growth by increasing tumor pericyte content. *J. Clin. Invest.* 117, 2114–2122. doi: 10.1172/JCI31334

Meng, M. B., Zaorsky, N. G., Deng, L., Wang, H. H., Chao, J., Zhao, L. J., et al. (2015). Pericytes: a double-edged sword in cancer therapy. *Future Oncol.* 11, 169–179. doi: 10.2217/fon.14.123

Miljkovic-Licina, M., Hammel, P., Garrido-Urbani, S., Lee, B. P., Meguenani, M., Chaabane, C., et al. (2012). Targeting olfactomedin-like 3 inhibits tumor growth by impairing angiogenesis and pericyte coverage. *Mol. Cancer Ther.* 11, 2588–2599. doi: 10.1158/1535-7163.MCT-12-0245

Monk, B. J., Poveda, A., Vergote, I., Raspagliesi, F., Fujiwara, K., Bae, D. S., et al. (2014). Anti-angiopoietin therapy with trebananib for recurrent ovarian cancer (TRINOVA-1): a randomised, multicentre, double-blind, placebo-controlled phase 3 trial. *Lancet Oncol.* 15, 799–808. doi: 10.1016/s1470-2045(14)70244-x

Motzer, R. J., Hutson, T. E., Tomczak, P., Michaelson, M. D., Bukowski, R. M., Rixe, O., et al. (2007). Sunitinib versus interferon alfa in metastatic renal-cell carcinoma. *N. Engl. J. Med.* 356, 115–124. doi: 10.1056/NEJMoa065044

Nasarre, P., Thomas, M., Kruse, K., Helfrich, I., Wolter, V., Deppermann, C., et al. (2009). Host-derived angiopoietin-2 affects early stages of tumor development and vessel maturation but is dispensable for later stages of tumor growth. *Cancer Res.* 69, 1324–1333. doi: 10.1158/0008-5472.CAN-08-3030

Navarro, R., Compte, M., Álvarez-Vallina, L., and Sanz, L. (2016). Immune regulation by pericytes: modulating innate and adaptive immunity. *Front. Immunol.* 7:480. doi: 10.3389/fimmu.2016.00480

Nisancioglu, M. H., Betsholtz, C., and Genove, G. (2010). The absence of pericytes does not increase the sensitivity of tumor vasculature to vascular endothelial growth factor-A blockade. *Cancer Res.* 70, 5109–5115. doi: 10.1158/0008-5472.CAN-09-4245

Nolan-Stevaux, O., Truitt, M. C., Pahler, J. C., Olson, P., Guinto, C., Lee, D. C., et al. (2010). Differential contribution to neuroendocrine tumorigenesis of parallel egfr signaling in cancer cells and pericytes. *Genes Cancer* 1, 125–141. doi: 10.1177/1947601909358722

Ochs, K., Sahm, F., Opitz, C. A., Lanz, T. V., Oezen, I., Couraud, P.-O., et al. (2013). Immature mesenchymal stem cell-like pericytes as mediators of immunosuppression in human malignant glioma. *J. Neuroimmunol.* 265, 106–116. doi: 10.1016/j.jneuroim.2013.09.011

Öhlund, D., Elyada, E., and Tuveson, D. (2014). Fibroblast heterogeneity in the cancer wound. *J. Exper. Med.* 211, 1503–1523. doi: 10.1084/jem.20140692

Olson, L. E., and Soriano, P. (2011). PDGFRbeta signaling regulates mural cell plasticity and inhibits fat development. *Dev. Cell* 20, 815–826. doi: 10.1016/j.devcel.2011.04.019

Onoyama, M., Kitadai, Y., Tanaka, Y., Yuge, R., Shinagawa, K., Tanaka, S., et al. (2013). Combining molecular targeted drugs to inhibit both cancer cells and activated stromal cells in gastric cancer. *Neoplasia* 15, 1391–1399. doi: 10.1593/neo.131668

Ozerdem, U., Grako, K. A., Dahlin-Huppe, K., Monosov, E., and Stallcup, W. B. (2001). NG2 proteoglycan is expressed exclusively by mural cells during vascular morphogenesis. *Dev. Dynam.* 222, 218–227. doi: 10.1002/dvdy.1200

Pallone, T. L., and Silldorff, E. P. (2001). Pericyte regulation of renal medullary blood flow. *Exp. Nephrol.* 9, 165–170. doi: 10.1159/000052608

Pietras, K., and Hanahan, D. (2005). A multitargeted, metronomic, and maximum-tolerated dose "chemo-switch" regimen is antiangiogenic, producing objective responses and survival benefit in a mouse model of cancer. *J. Clin. Oncol.* 23, 939–952. doi: 10.1200/jco.2005.07.093

Pietras, K., Pahler, J., Bergers, G., and Hanahan, D. (2008). Functions of paracrine PDGF signaling in the proangiogenic tumor stroma revealed by pharmacological targeting. *PLoS Med.* 5:e19. doi: 10.1371/journal.pmed.0050019

Prete, A., Lo, A. S., Sadow, P. M., Bhasin, S. S., Antonello, Z. A., Vodopivec, D. M., et al. (2018). Pericytes elicit resistance to Vemurafenib and Sorafenib therapy in thyroid carcinoma via the TSP-1/TGFβ1 Axis. *Clin. Cancer Res.* 24, 6078–6097. doi: 10.1158/1078-0432.CCR-18-0693

Qian, B. Z., and Pollard, J. W. (2010). Macrophage diversity enhances tumor progression and metastasis. *Cell* 141, 39–51. doi: 10.1016/j.cell.2010.03.014

Ramjiawan, R. R., Griffioen, A. W., and Duda, D. G. (2017). Anti-angiogenesis for cancer revisited: is there a role for combinations with immunotherapy? *Angiogenesis* 20, 185–204. doi: 10.1007/s10456-017-9552-y

Ravaud, A., Motzer, R. J., Pandha, H. S., George, D. J., Pantuck, A. J., Patel, A., et al. (2016). Adjuvant sunitinib in high-risk renal-cell carcinoma after nephrectomy. *N. Engl. J. Med.* 375, 2246–2254. doi: 10.1056/NEJMoa1611406

Raymond, E., Dahan, L., Raoul, J. L., Bang, Y. J., Borbath, I., Lombard-Bohas, C., et al. (2011). Sunitinib malate for the treatment of pancreatic neuroendocrine tumors. *N. Engl. J. Med.* 364, 501–513. doi: 10.1056/NEJMoa1003825

Raza, A., Franklin, M. J., and Dudek, A. Z. (2010). Pericytes and vessel maturation during tumor angiogenesis and metastasis. *Am. J. Hematol.* 85, 593–598. doi: 10.1002/ajh.21745

Ribatti, D., Nico, B., and Crivellato, E. (2011). The role of pericytes in angiogenesis. *Int. J. Dev. Biol.* 55, 261–268. doi: 10.1387/ijdb.103167dr

Rimassa, L., and Santoro, A. (2009). Sorafenib therapy in advanced hepatocellular carcinoma: the SHARP trial. *Expert. Rev. Anticancer Ther.* 9, 739–745. doi: 10.1586/era.09.41

Rini, B. I., Escudier, B., Tomczak, P., Kaprin, A., Szczylik, C., Hutson, T. E., et al. (2011). Comparative effectiveness of axitinib versus sorafenib in advanced renal cell carcinoma (AXIS): a randomised phase 3 trial. *Lancet* 378, 1931–1939. doi: 10.1016/s0140-6736(11)61613-9

Ruan, J., Luo, M., Wang, C., Fan, L., Yang, S. N., Cardenas, M., et al. (2013). Imatinib disrupts lymphoma angiogenesis by targeting vascular pericytes. *Blood* 121, 5192–5202. doi: 10.1182/blood-2013-03-490763

Rybinski, K., Imtiyaz, H. Z., Mittica, B., Drozdowski, B., Fulmer, J., Furuuchi, K., et al. (2015). Targeting endosialin/CD248 through antibody-mediated internalization results in impaired pericyte maturation and dysfunctional tumor microvasculature. *Oncotarget* 6, 25429–25440. doi: 10.18632/oncotarget.4559

Saharinen, P., Eklund, L., and Alitalo, K. (2017). Therapeutic targeting of the angiopoietin-TIE pathway. *Nat. Rev. Drug Discov.* 16, 635–661. doi: 10.1038/nrd.2016.278

Schiffmann, L. M., Brunold, M., Liwschitz, M., Goede, V., Loges, S., Wroblewski, M., et al. (2017). A combination of low-dose bevacizumab and imatinib enhances vascular normalisation without inducing extracellular matrix deposition. *Br. J. Cancer* 116, 600–608. doi: 10.1038/bjc.2017.13

Schlumberger, M., Tahara, M., Wirth, L. J., Robinson, B., Brose, M. S., Elisei, R., et al. (2015). Lenvatinib versus placebo in radioiodine-refractory thyroid cancer. *N. Engl. J. Med.* 372, 621–630. doi: 10.1056/NEJMoa1406470

Scholz, A., Harter, P. N., Cremer, S., Yalcin, B. H., Gurnik, S., Yamaji, M., et al. (2016). Endothelial cell-derived angiopoietin-2 is a therapeutic target in treatment-naive and bevacizumab-resistant glioblastoma. *EMBO Mol. Med.* 8, 39–57. doi: 10.15252/emmm.201505505

Sennino, B., Falcon, B. L., McCauley, D., Le, T., McCauley, T., Kurz, J. C., et al. (2007). Sequential loss of tumor vessel pericytes and endothelial cells after inhibition of platelet-derived growth factor B by selective aptamer AX102. *Cancer Res.* 67, 7358–7367. doi: 10.1158/0008-5472.CAN-07-0293

Shen, J., Vil, M. D., Prewett, M., Damoci, C., Zhang, H., Li, H., et al. (2009). Development of a fully human anti-PDGFRbeta antibody that suppresses growth of human tumor xenografts and enhances antitumor activity of an anti-VEGFR2 antibody. *Neoplasia* 11, 594–604. doi: 10.1593/neo.09278

Shepro, D., and Morel, N. M. (1993). Pericyte physiology. *FASEB J.* 7, 1031–1038. doi: 10.1096/fasebj.7.11.8370472

Song, N., Huang, Y., Shi, H., Yuan, S., Ding, Y., Song, X., et al. (2009). Overexpression of platelet-derived growth factor-BB increases tumor pericyte content via stromal-derived factor-1alpha/CXCR4 axis. *Cancer Res.* 69, 6057–6064. doi: 10.1158/0008-5472.Can-08-2007

Song, S., Ewald, A. J., Stallcup, W., Werb, Z., and Bergers, G. (2005). PDGFRbeta+ perivascular progenitor cells in tumours regulate pericyte differentiation and vascular survival. *Nat. Cell Biol.* 7, 870–879. doi: 10.1038/ncb1288

Sternberg, C. N., Davis, I. D., Mardiak, J., Szczylik, C., Lee, E., Wagstaff, J., et al. (2010). Pazopanib in locally advanced or metastatic renal cell carcinoma: results of a randomized phase III trial. *J. Clin. Oncol.* 28, 1061–1068. doi: 10.1200/jco.2009.23.9764

Taeger, J., Moser, C., Hellerbrand, C., Mycielska, M. E., Glockzin, G., Schlitt, H. J., et al. (2011). Targeting FGFR/PDGFR/VEGFR impairs tumor growth, angiogenesis, and metastasis by effects on tumor cells, endothelial cells, and pericytes in pancreatic cancer. *Mol. Cancer Ther.* 10, 2157–2167. doi: 10.1158/1535-7163.MCT-11-0312

Tao, Z., Yang, H., Shi, Q., Fan, Q., Wan, L., and Lu, X. (2017). Targeted delivery to tumor-associated Pericytes via an Affibody with High Affinity for PDGFRβ enhances the in vivo antitumor effects of human TRAIL. *Theranostics* 7, 2261–2276. doi: 10.7150/thno.19091

Tattersall, I. W., Du, J., Cong, Z., Cho, B. S., Klein, A. M., Dieck, C. L., et al. (2016). In vitro modeling of endothelial interaction with macrophages and pericytes demonstrates Notch signaling function in the vascular microenvironment. *Angiogenesis* 19, 201–215. doi: 10.1007/s10456-016-9501-1

Thijssen, V. L. J. L., Paulis, Y. W. J., Nowak-Sliwinska, P., Deumelandt, K. L., Hosaka, K., Soetekouw, P. M. M. B., et al. (2018). Targeting PDGF-mediated recruitment of pericytes blocks vascular mimicry and tumor growth. *J. Pathol.* 246, 447–458. doi: 10.1002/path.5152

Tian, L., Goldstein, A., Wang, H., Ching, L. H., Sun, K. I., Welte, T., et al. (2017). Mutual regulation of tumour vessel normalization and immunostimulatory reprogramming. *Nature* 544, 250–254. doi: 10.1038/nature21724

Turley, S. J., Cremasco, V., and Astarita, J. L. (2015). Immunological hallmarks of stromal cells in the tumour microenvironment. *Nat. Rev. Immunol.* 15, 669–682. doi: 10.1038/nri3902

Valdor, R., García-Bernal, D., Bueno, C., Ródenas, M., Moraleda, J. M., Macian, F., et al. (2017). Glioblastoma progression is assisted by induction of immunosuppressive function of pericytes through interaction with tumor cells. *Oncotarget* 8, 68614–68626. doi: 10.18632/oncotarget.19804

Valdor, R., García-Bernal, D., Riquelme, D., Martinez, C. M., Moraleda, J. M., Cuervo, A. M., et al. (2019). Glioblastoma ablates pericytes antitumor immune function through aberrant up-regulation of chaperone-mediated autophagy. *Proc. Natl. Acad. Sci. U.S.A.* 116, 20655–20665. doi: 10.1073/pnas.1903542116

van der Graaf, W. T., Blay, J. Y., Chawla, S. P., Kim, D. W., Bui-Nguyen, B., Casali, P. G., et al. (2012). Pazopanib for metastatic soft-tissue sarcoma (PALETTE): a randomised, double-blind, placebo-controlled phase 3 trial. *Lancet* 379, 1879–1886. doi: 10.1016/s0140-6736(12)60651-5

Venetz, D., Ponzoni, M., Schiraldi, M., Ferreri, A. J., Bertoni, F., Doglioni, C., et al. (2010). Perivascular expression of CXCL9 and CXCL12 in primary central nervous system lymphoma: T-cell infiltration and positioning of malignant B cells. *Int. J. Cancer* 127, 2300–2312. doi: 10.1002/ijc.25236

Vergote, I., Scambia, G., O'Malley, D. M., Van Calster, B., Park, S. Y., Del Campo, J. M., et al. (2019). Trebananib or placebo plus carboplatin and paclitaxel as first-line treatment for advanced ovarian cancer (TRINOVA-3/ENGOT-ov2/GOG-3001): a randomised, double-blind, phase 3 trial. *Lancet Oncol.* 20, 862–876. doi: 10.1016/s1470-2045(19)30178-0

Wong, P. P., Demircioglu, F., Ghazaly, E., Alrawashdeh, W., Stratford, M. R., Scudamore, C. L., et al. (2015). Dual-action combination therapy enhances angiogenesis while reducing tumor growth and spread. *Cancer Cell* 27, 123–137. doi: 10.1016/j.ccell.2014.10.015

Wong, P. P., Munoz-Felix, J. M., Hijazi, M., Kim, H., Robinson, S. D., De Luxan-Delgado, B., et al. (2020). Cancer burden is controlled by mural cell-beta3-integrin regulated crosstalk with tumor cells. *Cell* 181, 1346–1363.e1321. doi: 10.1016/j.cell.2020.02.003

Yang, Y., Andersson, P., Hosaka, K., Zhang, Y., Cao, R., Iwamoto, H., et al. (2016). The PDGF-BB-SOX7 axis-modulated IL-33 in pericytes and stromal cells promotes metastasis through tumour-associated macrophages. *Nat. Commun.* 7:11385. doi: 10.1038/ncomms11385

Yin, L., He, J., Xue, J., Na, F., Tong, R., Wang, J., et al. (2018). PDGFR-beta inhibitor slows tumor growth but increases metastasis in combined radiotherapy and Endostar therapy. *Biomed. Pharmacother.* 99, 615–621. doi: 10.1016/j.biopha.2018.01.095

Yonenaga, Y., Mori, A., Onodera, H., Yasuda, S., Oe, H., Fujimoto, A., et al. (2005). Absence of smooth muscle actin-positive pericyte coverage of tumor vessels correlates with hematogenous metastasis and prognosis of colorectal cancer patients. *Oncology* 69, 159–166. doi: 10.1159/000087840

Zhou, W., Chen, C., Shi, Y., Wu, Q., Gimple, R. C., Fang, X., et al. (2017). Targeting Glioma stem cell-derived Pericytes disrupts the blood-tumor barrier and improves chemotherapeutic efficacy. *Cell Stem Cell* 21, 591–603.e594. doi: 10.1016/j.stem.2017.10.002

Zhu, C., Chrifi, I., Mustafa, D., van der Weiden, M., Leenen, P. J. M., Duncker, D. J., et al. (2017). CECR1-mediated cross talk between macrophages and vascular mural cells promotes neovascularization in malignant glioma. *Oncogene* 36, 5356–5368. doi: 10.1038/onc.2017.145

Conflict of Interest: The authors declare that the research was conducted in the absence of any commercial or financial relationships that could be construed as a potential conflict of interest.

frontiers in Oncology

MINI REVIEW
published: 14 June 2021
doi: 10.3389/fonc.2021.689829

The Role of PARP Inhibitors in the Ovarian Cancer Microenvironment: Moving Forward From Synthetic Lethality

Margherita Turinetto[1,2], *Giulia Scotto*[1,2], *Valentina Tuninetti*[1,2], *Gaia Giannone*[1,2] *and Giorgio Valabrega*[1,2*]

[1] Department of Oncology, University of Torino, Torino, Italy, [2] Candiolo Cancer Institute, FPO-IRCCS, Candiolo, Italy

OPEN ACCESS

Edited by:
Chao Ni,
Zhejiang University, China

Reviewed by:
Guang Peng,
University of Texas MD Anderson Cancer Center, United States
Fernanda Ortis,
University of São Paulo, Brazil

***Correspondence:**
Giorgio Valabrega
giorgio.valabrega@ircc.it

Specialty section:
This article was submitted to Molecular and Cellular Oncology, a section of the journal Frontiers in Oncology

Received: *01 April 2021*
Accepted: *27 May 2021*
Published: *14 June 2021*

Citation:
Turinetto M, Scotto G, Tuninetti V, Giannone G and Valabrega G (2021) The Role of PARP Inhibitors in the Ovarian Cancer Microenvironment: Moving Forward From Synthetic Lethality. Front. Oncol. 11:689829. doi: 10.3389/fonc.2021.689829

PARP inhibitors (PARPi) have shown promising clinical results and have revolutionized the landscape of ovarian cancer management in the last few years. While the core mechanism of action of these drugs has been largely analyzed, the interaction between PARP inhibitors and the microenvironment has been scarcely researched so far. Recent data shows a variety of mechanism through which PARPi might influence the tumor microenvironment and especially the immune system response, that might even partly be the reason behind PARPi efficacy. One of many pathways that are affected is the cGAS-cGAMP-STING; the upregulation of STING (stimulator of interferon genes), produces more Interferon ϒ and pro inflammatory cytokines, thus increasing intratumoral CD4+ and CD8+ T cells. Upregulation of immune checkpoints such as PD1-PDL1 has also been observed. Another interesting mechanism of interaction between PARPi and microenvironment is the ability of PARPi to kill hypoxic cells, as these cells show an intrinsic reduction in the expression and function of the proteins involved in HR. This process has been defined "contextual synthetic lethality". Despite ovarian cancer having always been considered a poor responder to immune therapy, data is now shedding a new light on the matter. First, OC is much more heterogenous than previously thought, therefore it is fundamental to select predictive biomarkers for target therapies. While single agent therapies have not yielded significant results on the long term, influencing the immune system and the tumor microenvironment *via* the concomitant use of PARPi and other target therapies might be a more successful approach.

Keywords: PARP inhibitors, ovarian cancer, tumor microenvironment, immune checkpoint inhibitors, immune system response

BACKGROUND AND STATE OF THE ART

Over the past decade, poly(ADP-ribose) polymerase inhibitors (PARPi) have completely revolutionized the landscape of Ovarian Cancer (OC) treatment. The phase III trials [NOVA (1), SOLO2 (2), and ARIEL3 (3)] conducted for PARPi as maintenance treatment after platinum-based chemotherapy have shown remarkable results in terms of progression free survival PFS, and while the SOLO2 long term analysis didn't show an improvement in OS that was statistically significant, it was interpreted as clinically significant (2). This is incredibly important when considering the lack of alternatives to chemotherapy aforementioned and the tolerable and manageable side effects demonstrated by PARPi.

Currently, PARPi have been implemented in the clinical standards as maintenance therapy in first line BRCA mutated high grade serous ovarian cancer (HGSOC) stages III and IV after partial or complete response to platinum salts, in II line and onward for platinum sensitive relapsed high grade serous or endometrioid OC (4).

While the association between chemotherapy and PARPi has been proven to be burdened by greater toxicities, there are currently a number of trials focusing on PARPi in other scenarios; in the single agent setting [ARIEL4 for Rucaparib (5) and SOLO3 for Olaparib (6)], and in association with other target therapies such as Cediranib, an anti VEGFR [ICON9 (7)] or ICI such as Nivolumab (ATHENA) (8).

Despite the efforts made, immunotherapy is still in the sidelines when it comes to the treatment of OC, at the moment considered a poor responder.

Even if the biology of the tumor suggests that patients might benefit from immunotherapy, the clinical data is not as promising as expected (9).

The use of single agents such as anti PDL1 or anti CTLA4 showed a median response rate (RR) of just 10–15% (10).

In the JAVELIN PARP 200, patients with platinum refractory or resistant OC were treated with PLD or Avelumab single therapy, or Avelumab + PLD, and there was no significant improvement of PFS or OS in the experimental arms compared to PLD alone.

So far combination regimens have not showed any significant benefit; in the phase III IMAGYN050 patients affected by stage III/IV OC were randomized to receive Carboplatin-Taxol-Bevacizumab + Atezolizumab or placebo. The progression free survival (PFS) in the intention to treat (ITT) population did not show any difference in the two cohorts (18.4 months with placebo *vs* 19.5 months with Atezolizumab), overall survival (OS) seems to be similar as well, even though the results are still maturing (11).

The JAVELIN PARP 100 enrolled patients with advanced or metastatic OC, treating the population with Carboplatin-Taxol + Avelumab or placebo, followed by maintenance therapy with Avelumab and Talazoparib. It was discontinued after an interim data analysis indicated the PFS primary endpoint would not be met (12).

There is increasing evidence for their important role in modifying tumor microenvironment (13).

Besides HRD, replication fork instability is another major mechanism through which PARPis are effective, because PARP1 is implicated in fork protection, cooperating with BRCA2 (14). In the absence of restored HR, the replication fork stability has recently been identified as a resistance mechanism (15).

As we will discuss later on, this may be relevant for combining PARPi with immunotherapy (16).

Given the increased T cell inflammation in HRD positive tumors as well as preclinical studies showing the synergistic anti-tumor effects of PARP inhibitors and CTLA or PD(L)1 blockade in EOC carrying BRCA mutations (17) several trials exploring the same combination are ongoing in BRCA mutated and BRCA wild-type patients, respectively (NCT02571725; NCT02485990; NCT02953457).

In this review we will discuss how the effect of PARPi on the tumor environment might boost response to ICI.

BRCA: DIFFERENT IMMUNE-MODULATORY EFFECT AT GENOMIC LEVEL OF BRCA1 MUTATION COMPARED TO BRCA2

Although the majority of OC are sporadic (18), a pathogenic mutation in either BRCA1 or BRCA2 confers respectively 36 to 60% and 16 to 27% (19). Loss of BRCA1 function has also been documented through its promoter methylation in about 10% of high grade serous ovarian cancer (HGSOC) patients. Although to a lower extent, alterations in other genes of the homologous DNA repair pathway like ATM, ATR and Fanconi anemia genes can also cause DNA homologous repair deficiency (HRD) (20). Epigenetic silencing of BRCA1 and RAD51C expression through DNA hypermethylation also results in a DNA homologous repair deficiency (HRD) (21) (22) (23).

BRCA1/2-mutated HGSOCs exhibit a higher mutational load and a unique mutational signature thus harboring more tumor-specific neoantigens that stimulate recruitment of an increased number of tumor-infiltrating lymphocytes (TILs), which is counterbalanced by overexpression of immune checkpoints such as PD-1 or PD-L1.

While both genes have pleiotropic effects on the genesis of the tumor, recent data highlights that they affect in different manners the tumorigenesis, the microenvironment, and the immune response, resulting in contradistinctive mutational landscapes.

Samstein et al. analyzed this in murine models how the two mutations differ in their functional impact on the tumor microenvironment. BRCA2 mutation has a known core function in homologous recombination (HR), one of the most commonly altered DNA damage pathways in cancer, which results in a higher tumor mutational load. Another indicator of genetic instability, mismatch repair deficiency (MRD) has already been approved by FDA as a predictive marker for response to ICI (24); the lack of success of immunotherapy in OC may therefore be a result of our incomplete knowledge of other factors influencing the microenvironment and the immune response rather than a failed therapy approach.

Further analysis of the BRCA2mut murine orthotopic breast cancer cell line compared to a syngeneic BRCA2wt line showed increased CD4+ and CD8+ in tumor infiltrating lymphocytes, NK mediated cytotoxicity, α-interferon, and cytokine signaling. Angiogenesis and epithelial to mesenchymal transition (EMT) were also influenced. When exposed to ICI, specifically anti PD1 or anti CTLA4 and anti PD1, the BRCA2mut mammal tumor exhibited a greater response, with significant growth delay, compared to the BRCA2wt cell line. This was not the case with the syngeneic BRCA1 mut murine model; the difference in elicited response to ICI is the result of a dissimilar effect in both adaptive and innate immune activation, further proven by direct examination between BRCA1 and BRCA2 mut yielded tumor programs.

BRCA1 mutation also showed an upregulation of immunosuppressive and regulatory genes, while BRCA2 mutation had an increased expression of immune cell activation genes.

In recent preclinical mouse model studies, it was observed that also PI3K pathway inhibition resulted in genomic instability, and cancer cells with reduced activity in this pathway are more sensitive to PARP inhibition (25, 26). These results have prompted investigators to test the combination of PI3K and PARP inhibitors in OC (27); PI3K, mTORc1/2, and AKT selective inhibitors have been tested with Olaparib (28).

These results, provided the preclinical aspect and the lack of EOC models, may give an insight on a more heterogeneous landscape of responses to both PARPi and ICI in OC, that requires the identification of reliable predictive markers (29).

PARP ROLE IN THE IMMUNE SYSTEM

In murine models, the T cell development has been shown to require PARP efficiency in all its stages; PARP2 deficiency decreases the number of thymocytes, causing a higher number of apoptosis during the maturation process. PARP1 and 2 deficiency causes a reduction in both CD4+ and CD8+ peripheric population (30).

PARP is also involved in cell activation; PARP1 deficiency seems to direct T cells to the Th1 (31) and Treg phenotype rather than Th2 (32).

B lymphocytes are affected as well, although the reasons are not yet completely clear; dual deficiency affects the peripheric population is the same way it does with T cells, proving to be consistent with the hypothesis that PARP preventing the accumulation of DNA damage is needed during cell proliferation.

PARP plays a role in the activation and recruitment of neutrophils (33), the expression of pro inflammatory cytokines such as IL-6, TNF by macrophages (34) and the recruitment of dendritic cells (in which PARP1 is involved, but PARP2's role remains unclear) (35).

The effects of PARP inhibition are therefore complex and overlapping.

PARP INHIBITORS EFFECTS: MOVING FORWARD FROM SYNTHETIC LETHALITY

Hypoxia

Solid tumors display different levels of oxygenation, especially when characterized by a high cellular replication. It is possible to identify areas where angiogenesis is not able to provide enough oxygen for the quickly growing mass, which will cause varying degrees of hypoxia, from chronic low levels to severe. It's widely known how this characteristic has a negative prognostic impact, because it is a sign of fast proliferation of the tumor and because it is linked to resistance to chemotherapy, radiotherapy, decrease of DNA repair, and increase of the risk of metastatic spreading.

Both severe and chronic hypoxia cause a disruption in the HR pathway, vital for DNA double strand breaks repair, by decreasing the translation of proteins like RAD51, BRCA1, and BRCA2 (36); Chan et al. (37) confirmed this theory *via* the observation of RAD51 activity in hypoxic cells in murine models; RAD51 remained suppressed even at chronically moderate levels of hypoxia. Notably, this was the first mechanism observed that was independent from hypoxia inducing factor 1 alfa (HIF1alfa). It was afterwards theorized how HR defective hypoxic cells could be sensitive to PARPi, irrespective of their BRCA status, which was proven true in various cell lines. The most effective result was observed in cells subjected to severe hypoxia, followed by reoxygenation, probably because of the synergistic effect of reactive oxygen species (ROS) toxicity and PARP inhibition.

Thus far PARPi have been considered effective in BRCA mutated and HRD defective cells; the new concept of contextual synthetic lethality, whereby external conditions such as hypoxia can alter the tumor cell mechanisms rendering them susceptible to target therapies, is surely worth exploring further and can offer new scenarios for clinical setting that were previously thought to be immune to PARPi (38).

Aiming at creating contextual synthetic lethality within the tumor microenvironment, several studies are testing the effect of anti-angiogenic therapy in combination with PARP inhibitors [i.e. PAOLA1 (39) and AVANOVA2 (40) with already available results, MITO25 (41) and CONCERTO (42) currently ongoing].

STING Pathway

There is increasing evidence that the interaction between DNA damage and the immune system plays an important role in the success of cancer treatment. One of many pathways that are affected is the cGAS-cGAMP-STING; the presence of pathogenic DNA elicits the upregulation of STING (stimulator of interferon genes), thus producing more Interferon ϒ and pro inflammatory cytokines.

Ding et al.'s work delves further into this concept, using murine models engrafted with high grade serous ovarian cancer with concurrent loss of p53 and Brca1 and overexpression of c-Myc. Treatment of these models with Olaparib showed significant responses, which were proven to be also driven by the host immune response because they were significantly less noticeable when introducing an anti CD8 antibody or other means of immune suppression.

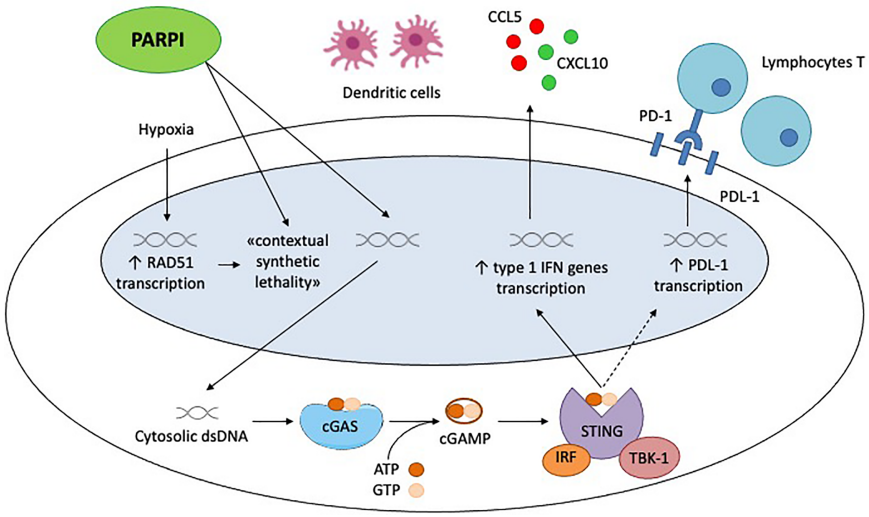

FIGURE 1 | Effect of PARP inhibitors on tumor cells and microenvironment. Chronic hypoxia decreases transcription of homologous recombination proteins, as RAD51, rendering the tumor cells susceptible to PARP inhibitors. This is the concept of «contextual synthetic lethality». Cytosolic double-strand DNA (dsDNA) fragments, generated by the effect of Parpi on tumor cells, activate cGAS-cGAMP-STING pathway, leading to the transcription of type 1 IFN genes and the production of pro inflammatory cytokines. This generates a significant immune response, recruiting activated lymphocytes T and dendritic cells. STING pathway activates also the PDL-1 transcription, inhibiting the immune system through PD-1/PDL-1 interaction.

Specifically, it was observed that Olaparib increased intratumoral CD4+ and CD8+ cells, decreased the production of inhibitory receptors, increased the recruitment and activity of tumor associated dendritic cells, therefore providing a robust immune activation both innate and adaptive.

The importance of STING upregulation for the immune stimulating activity of Olaparib was proven by the significant reduction of response observed in STING knock out mice (43).

The STING pathway was also the focus of Shapiro et al.'s paper. BRCA1 deficient triple negative breast tumor cells were engrafted in mice models; through the activation of the STING pathway, Olaparib significantly increased CD3+ and CD8+ T cells. Granzyme B in CD8+ cells and in NK was also increased, indicative of cytolytic action. While CD4+ T cells were incremented, the Treg phenotype was not found to be more expressed, thus suggesting a higher T helper differentiation. mRNA levels of INFβ, CCL5, and CXCL10, potent proinflammatory signals that correlate to T cell infiltration, were found to be overexpressed. This was not the case in a BRCA1 proficient setting. These findings suggest that PARPi is a potent inductor of both cytotoxic cells recruitment and activation, but the effect is a lot more prominent in a HRD deficient or BRCA mutated models (44, 45).

Upregulation of PDL-1

Immune checkpoints are now recognized to be of fundamental importance in carcinogenesis; a wide range of tumor cells express both PDL1 and 2, and their overexpression contributes to impairment of multiple signaling pathways of the adaptive immune system (46).

An upregulation of PD-L1 after Olaparib treatment in the murine models was also detected in Dyng et al.'s research; while anti PD-L1 alone provided little to no response, combination of Olaparib and PD-L1 showed significant effect (43).

A similar mechanism was studied by Shen et al., through a model that differed from Dyng's in regard to HR deficiency; in a HR proficient setting, Talazoparib was used in synergy with anti PDL1, observing once again an increased level of PDL1 and a significant response to the combination (47).

Besides indirect stimulation through immune signaling, PARPi may induce upregulation of PD-L1 levels through inactivation of GSK3β, which was further proven in Jiao's work by the lack of increase in PD-L1 in GSK3β knock out murine models when treated with Olaparib (48). The hindering of T cell killing caused by higher PD-L1 and PD1 levels seems to reverse when PARPi therapy is combined with ICI.

While expression of PD-L1 on tumor cells is a predictive biomarker of response to ICIs in other cancer types (i.e., NSCLC and urothelial cancers), its expression in EOC is not very frequent (10–33%) suggesting that not all tumors rely on this pathway for immune evasion and its prognostic role in EOC is still controverted. Some data suggest that expression of PD-L1 correlates with worse prognosis (49), while in other series a higher expression correlates with better PFS (50).

In the TOPACIO trial, exploratory analyses of subpopulations did not reveal any difference in clinical activity

TABLE 1 | Ongoing trials regarding ICI + PARPi in ovarian cancer.

Clinical trial identifier	Phase	Agents	Design	Status	Outcome
NCT02571725	Phase I	Tremelimumab + Olaparib	BRCAm ROC	Results published	No DLT or grade 3 AE ORR 100%
NCT02484404	Phase II	Durvalumab + Olaparib	Platinum-resistant ROC	Results published	ORR 14% Acceptable toxicity
TOPACIO NCT02657889	Phase II	Pembrolizumab + Niraparib	Platinum-resistant ROC	Results published	ORR 18% PFS 3.4 months Acceptable toxicity
MEDIOLA NCT02734004	Phase II	Durvalumab + Olaparib	BRCAm platinum-sensitive OC	Results published	ORR 63% Acceptable toxicity
NCT04034927	Phase II	Tremetinib + Niraparib	Platinum-sensitive advanced OC	Recruiting	
KEYLYNK-001 NCT03740165	Phase II	Pembrolizumab + Niraparib	BRCAwt advanced OC	Recruiting	
NCT02484404	Phase I-II	Durvalumab + Niraparib	Advanced, recurrent, or metastatic ovarian, triple negative breast, lung, prostate, colorectal carcinoma or solid tumors	Recruiting	
DUO-O NCT03737643	Phase III	Durvalumab + Niraparib	Advanced OC	Recruiting	
GUIDE2REPAIR NCT04169841	Phase II	Durvalumab + Tremelimumab + Niraparib	HRR-mutated advanced or metastatic solid tumors	Not yet recruiting	
NCT02953457	Phase I-II	Durvalumab + Tremelimumab + Niraparib	DDR-mutated recurrent or refractory OC	Recruiting	
FIRST NCT03602859	Phase III	Durvalumab + Niraparib	Stage III or IV non-mucinous OC	Recruiting	
MOONSTONE NCT03955471	Phase II	Dostarlimab + Niraparib	Advanced platinum-resistant OC	Recruiting	
NCT03806049	Phase III	Dostarlimab + Niraparib	Advanced or recurrent platinum-sensitive OC	Not yet recruiting	
NCT03695380	Phase I	Atezolizumab + Niraparib	Advanced OC	Recruiting	
ANITA NCT03598270	Phase III	Atezolizumab + Niraparib	Recurrent OC	Recruiting	
JAVELIN NCT03642132	Phase III	Avelumab + Niraparib	Advanced OC	Not recruiting	
NCT02873962	Phase II	Nivolumab + Rucaparib	Relapsed OC	Recruiting	
ATHENA NCT03522246	Phase III	Nivolumab + Rucaparib	Advanced OC	Recruiting	
ARIES NCT03824704	Phase II	Nivolumab + Rucaparib	Platinum treated advanced OC	Recruiting	
NCT03101280	Phase I	Atezolizumab + Rucaparib	Advanced or metastatic platinum-sensitive ovarian or endometrial cancer or triple negative breast cancer	Not recruiting	
NITCHE NCT04679064	Phase II	Dostarlimab + Niraparib	Recurrent resistant OC not fit for platinum	Recruiting	

of the duet Pembrolizumab + Niraparib between PD-1 high and PD-1 low tumor status, thus not indicating PD-1 level of expression as a predictive biomarker (51).

DISCUSSION

PARPi have undoubtedly revolutionized the landscape of OC cancer, but new treatments need to be explored as up to 70% of advanced OC eventually relapse.

As discussed in the review, PARPi have numerous ancillary and off target effects; the inhibition of DNA repair and subsequent accumulation of double strand breaks increases the neoantigen load and stimulates the immune system, as well as through the STING pathway (28, 43) (**Figure 1**). In addition to this core action, PARPi have a profound influence on the tumor microenvironment, which in turn is determined by a much more complicated and overlapping series of factors than originally thought, BRCA mutation and HRD being perfect examples (29).

OC has always been considered a poor responder to ICI, but data is now shedding a new light on the matter. Influencing the immune system and the tumor microenvironment *via* the concomitant use of PARPi and other target therapies might be a more successful approach.

So far preclinical studies have produced robust evidence on the association between ICI and PARPi; the combination of anti CTLA4 and PARPi in BRCA1 mutated ovarian cancer models promotes long term responses, due to the local increase of IFNγ in the tumor environment and consequent recruitment and activation of T cells and cytokine production.

The synergistic effects of the combination therapy could be explained by a multiple phases process: firstly, PARP inhibition directly induces tumor cell damage, which increases the neoantigen load and therefore an antitumor T-cell response, a process that is amplified by ICI blockade. Secondly, local activated T cells produce increased levels of IFNγ above a threshold required to enhance the cytotoxic efficacy of PARP inhibition, resulting in additional therapeutic benefit through cell-intrinsic pathways. This indicates that the therapeutic benefit of PARP inhibition can be significantly amplified (17).

This is further proven by the fact that inhibition of T cell recruitment greatly affects response rates to Olaparib in models, suggesting how the benefit is not only dependent on parp depletion but at least partly due to the adaptive immune system (52).

Another very important point is that many preclinical and clinical trials are highlighting how heterogenous OC is, even BRCA1 mutation compared to BRCA2 mutation seem to create different characteristics and therefore different responses to therapies.

Currently, a high tumor mutational burden (TMB) is one of the hallmarks of ICI responders. Growing data points to a correlation between TMB and DDR deficiency, which might explain why BRCA mutated tumors have a higher response rate to ICI and show a stronger immune activation when treated with PARPi, as BRCA is one of the key components of HR; although it needs to be further researched, HRD appears to be a promising predictive biomarker for response to ICI + PARPi (53).

Many clinical trials regarding ICI + PARPi in ovarian cancer are ongoing (**Table 1**), a few with already available and promising data. In a phase II study, in heavily pretreated mostly platinum resistant patients, Durvalumab + Olaparib yielded a 53% disease control rate at 4 months, with good tolerance (54).

The MEDIOLA basket trial (55) assessed Durvalumab + Olaparib in BRCA mutated OC, breast cancer, and gastric cancer; ovarian cancer patients were platinum sensitive and achieved an 81% disease control rate (DCR) at 12 weeks; furthermore, patients with fewer previous therapy lines had better outcomes. A triplet cohort, adding Bevacizumab to Olaparib and Durvalumab in non-germinal BRCA mutated platinum sensitive OC, was later added. The first results have recently been presented and are very promising, with 77.4 *vs* 28.1% DCR at 24 weeks when compared to the duplet cohort, and similar side effects.

In the TOPACIO trial, platinum resistant OC and triple negative breast cancer patients were treated with Niraparib + Pembrolizumab. ORR was 25%, increasing to 45% in the BRCAmut population.

So far, the data is complex and at times contradictory, which clearly shows the need for further research and for further differentiation of the tumor genetic and environmental signature. This will eventually allow the identification of more accurate predictive biomarkers; this is currently an unmet need, and it highlights how important translation endpoints are in clinical trials in order to bring forward a critical change in patient outcomes; finding reliable predictive markers in such a heterogeneous cancer type is key to correctly selecting patients who will benefit from ICI + PARPi therapy, and to identify strategies to counteract primary and secondary resistance.

AUTHOR CONTRIBUTIONS

MT: conceptualization, drafting of the manuscript, and final approval. GS: conceptualization, review and editing, and final approval. VT: review and editing and final approval. GG: review and editing and final approval. GV: conceptualization, supervision, and final approval. All authors contributed to the article and approved the submitted version.

FUNDING

This article was partially funded by Italian Ministry of Health, Ricerca Corrente 2021, FPRC 5xmille 2015 MIUR, progetto FUTURO to GV.

ACKNOWLEDGMENTS

We would like to extend our gratitude to Dr. Eleonora Ghisoni for the useful prompts and revision of the article.

REFERENCES

1. Del Campo JM, Matulonis UA, Malander S, Provencher D, Mahner S, Follana P, et al. Niraparib Maintenance Therapy in Patients With Recurrent Ovarian Cancer After a Partial Response to the Last Platinum-Based Chemotherapy in the ENGOT-OV16/NOVA Trial. *J Clin Oncol* (2019) 37(32):JCO1802238. doi: 10.1200/JCO.18.02238
2. Pujade-Lauraine E, Ledermann JA, Selle F, Gebski V, Penson RT, Oza AM, et al. Olaparib Tablets as Maintenance Therapy in Patients With Platinum-Sensitive, Relapsed Ovarian Cancer and a BRCA1/2 Mutation (SOLO2/ENGOT-Ov21): A Double-Blind, Randomised, Placebo-Controlled, Phase 3 Trial. *Lancet Oncol* (2017) 18(9):1274–84. doi: 10.1016/S1470-2045(21)00073-5
3. Coleman RL, Oza AM, Lorusso D, Aghajanian C, Oaknin A, Dean A, et al. Rucaparib Maintenance Treatment for Recurrent Ovarian Carcinoma After Response to Platinum Therapy (ARIEL3): A Randomised, Double-Blind, Placebo-Controlled, Phase 3 Trial. *Lancet* (2017) 390(10106):1949–61. doi: 10.1016/S0140-6736(17)32440-6
4. Tew WP, Lacchetti C, Ellis A, Maxian K, Banerjee S, Bookman M, et al. Parp Inhibitors in the Management of Ovarian Cancer: ASCO Guideline. *J Clin Oncol* (2020) 38(30):3468–93. doi: 10.1200/JCO.20.01924
5. ARIEL4. *A Study of Rucaparib Versus Chemotherapy Brca Mutant Ovarian, Fallopian Tube, or Primary Peritoneal Cancer Patients*. Available at: https://clinicaltrials.gov/ct2/show/NCT02855944 (Accessed 15/03/2021).
6. Penson RT, Valencia RV, Cibula D, Colombo N, Leath CA, Bidziński M, et al. Solo3: Olaparib Versus Nonplatinum Chemotherapy in Patients With Platinum-Sensitive Relapsed Ovarian Cancer and a Germline Brca1/2 Mutation: A Randomized Phase III Trial (Access 15/03/2021). *J Clin Oncol* (2020) 38(11):1164–74. doi: 10.1200/JCO.19.02745
7. Elyashiv O, Ledermann J, Parmar G, Farrelly L, Counsell N, Feeney A, et al. ICON 9-an International Phase III Randomized Study to Evaluate the Efficacy

of Maintenance Therapy With Olaparib and Cediranib or Olaparib Alone in Patients With Relapsed Platinum-Sensitive Ovarian Cancer Following a Response to Platinum-Based Chemotherapy. *Int J Gynecol Cancer* (2021) 31(1):134–8. doi: 10.1136/ijgc-2020-002073

8. ATHENA. *(a Multicenter, Randomized, Double-Blind, Placebo-Controlled Phase 3 Study in Ovarian Cancer Patients Evaluating Rucaparib and Nivolumab as Maintenance Treatment Following Response to Front-Line Platinum-Based Chemotherapy)*. Available at: https://clinicaltrials.gov/ct2/show/NCT03522246 (Accessed 15/03/2021).
9. Palaia I, Tomao F, Sassu CM, Musacchio L, Benedetti Panici P. Immunotherapy For Ovarian Cancer: Recent Advances and Combination Therapeutic Approaches. *Onco Targets Ther* (2020) 13:6109–29. doi: 10.2147/OTT.S205950
10. Ghisoni E, Imbimbo M, Zimmermann S, Valabrega G. Ovarian Cancer Immunotherapy: Turning Up the Heat. *Int J Mol Sci* (2019) 20(12)2927. doi: 10.3390/ijms20122927
11. Moore KN. Lba31 Primary Results From IMagyn050/GOG 3015/Engot-OV39, a Double-Blind Placebo (Pbo)-Controlled Randomised Phase III Trial of Bevacizumab (Bev)-Containing Therapy +/- Atezolizumab (Atezo) for Newly Diagnosed Stage III/IV Ovarian Cancer (OC). *Ann Oncol* (2020) 31: S1161–2. doi: 10.1016/j.annonc.2020.08.2261
12. Eskander RN, Ledermann JA, Birrer MJ, Fujiwara K, Gaillard S, Richardson GE, et al. JAVELIN Ovarian PARP 100 Study Design: Phase III Trial of Avelumab + Chemotherapy Followed by Avelumab + Talazoparib Maintenance in Previously Untreated Epithelial Ovarian Cancer. *J Clin Oncol* (2019) 37(8_suppl):TPS9–TPS. doi: 10.1200/JCO.2019.37.8_suppl.TPS9
13. Alhmoud JF, Woolley JF, Al Moustafa AE, Malki MI. Dna Damage/Repair Management in Cancers. *Cancers (Basel)* (2020) 12(4)1050. doi: 10.3390/cancers12041050
14. Ying S, Hamdy FC, Helleday T. Mre11-Dependent Degradation of Stalled DNA Replication Forks Is Prevented by BRCA2 and PARP1. *Cancer Res* (2012) 72(11):2814–21. doi: 10.1158/0008-5472.CAN-11-3417
15. Haynes B, Murai J, Lee JM. Restored Replication Fork Stabilization, a Mechanism of PARP Inhibitor Resistance, Can Be Overcome by Cell Cycle Checkpoint Inhibition. *Cancer Treat Rev* (2018) 71:1–7. doi: 10.1016/j.ctrv.2018.09.003
16. Mirza MR, Pignata S, Ledermann JA. Latest Clinical Evidence and Further Development of PARP Inhibitors in Ovarian Cancer. *Ann Oncol* (2018) 29 (6):1366–76. doi: 10.1093/annonc/mdy174
17. Higuchi T, Flies DB, Marjon NA, Mantia-Smaldone G, Ronner L, Gimotty PA, et al. Ctla-4 Blockade Synergizes Therapeutically With PARP Inhibition in BRCA1-Deficient Ovarian Cancer. *Cancer Immunol Res* (2015) 3 (11):1257–68. doi: 10.1158/2326-6066.CIR-15-0044
18. Konstantinopoulos PA, Norquist B, Lacchetti C, Armstrong D, Grisham RN, Goodfellow PJ, et al. Germline and Somatic Tumor Testing in Epithelial Ovarian Cancer: Asco Guideline. *J Clin Oncol* (2020) 38(11):1222–45. doi: 10.1200/JCO.19.02960
19. Venkitaraman AR. Cancer Susceptibility and the Functions of BRCA1 and BRCA2. *Cell* (2002) 108(2):171–82. doi: 10.1016/S0092-8674(02)00615-3
20. Stover EH, Fuh K, Konstantinopoulos PA, Matulonis UA, Liu JF. Clinical Assays for Assessment of Homologous Recombination DNA Repair Deficiency. *Gynecol Oncol* (2020) 159(3):887–98. doi: 10.1016/j.ygyno.2020.09.029
21. Konstantinopoulos PA, Ceccaldi R, Shapiro GI, D'Andrea AD. Homologous Recombination Deficiency: Exploiting the Fundamental Vulnerability of Ovarian Cancer. *Cancer Discov* (2015) 5(11):1137–54. doi: 10.1158/2159-8290.CD-15-0714
22. Network CGAR. Integrated Genomic Analyses of Ovarian Carcinoma. *Nature* (2011) 474(7353):609–15. doi: 10.1038/nature10166
23. Macintyre G, Goranova TE, De Silva D, Ennis D, Piskorz AM, Eldridge M, et al. Copy Number Signatures and Mutational Processes in Ovarian Carcinoma. *Nat Genet* (2018) 50(9):1262–70. doi: 10.1038/s41588-018-0179-8
24. Le DT, Durham JN, Smith KN, Wang H, Bartlett BR, Aulakh LK, et al. Mismatch Repair Deficiency Predicts Response of Solid Tumors to PD-1 Blockade. *Science* (2017) 357(6349):409–13. doi: 10.1126/science.aan6733
25. Ibrahim YH, García-García C, Serra V, He L, Torres-Lockhart K, Prat A, et al. PI3K Inhibition Impairs BRCA1/2 Expression and Sensitizes BRCA-Proficient Triple-Negative Breast Cancer to PARP Inhibition. *Cancer Discov* (2012) 2(11):1036–47. doi: 10.1158/2159-8290.CD-11-0348
26. Wang D, Wang M, Jiang N, Zhang Y, Bian X, Wang X, et al. Effective Use of PI3K Inhibitor BKM120 and PARP Inhibitor Olaparib to Treat PIK3CA Mutant Ovarian Cancer. *Oncotarget* (2016) 7(11):13153–66. doi: 10.18632/oncotarget.7549
27. Matulonis UA, Wulf GM, Barry WT, Birrer M, Westin SN, Farooq S, et al. Phase I Dose Escalation Study of the PI3kinase Pathway Inhibitor BKM120 and the Oral Poly (ADP Ribose) Polymerase (PARP) Inhibitor Olaparib for the Treatment of High-Grade Serous Ovarian and Breast Cancer. *Ann Oncol* (2017) 28(3):512–8. doi: 10.1093/annonc/mdw672
28. Konstantinopoulos PA, Barry WT, Birrer M, Westin SN, Cadoo KA, Shapiro GI, et al. Olaparib and α-Specific PI3K Inhibitor Alpelisib for Patients With Epithelial Ovarian Cancer: A Dose-Escalation and Dose-Expansion Phase 1b Trial. *Lancet Oncol* (2019) 20(4):570–80. doi: 10.1016/S1470-2045(18)30905-7
29. Samstein RM, Krishna C, Ma X, Pei X, Lee K-W, Makarov V, et al. Mutations in *BRCA1* and *BRCA2* Differentially Affect the Tumor Microenvironment and Response to Checkpoint Blockade Immunotherapy. *Nat Cancer* (2020) 1 (12):1188–203. doi: 10.1038/s43018-020-00139-8
30. Navarro J, Gozalbo-López B, Méndez AC, Dantzer F, Schreiber V, Martínez C, et al. Parp-1/PARP-2 Double Deficiency in Mouse T Cells Results in Faulty Immune Responses and T Lymphomas. *Sci Rep* (2017) 7:41962. doi: 10.1038/srep41962
31. Saenz L, Lozano JJ, Valdor R, Baroja-Mazo A, Ramirez P, Parrilla P, et al. Transcriptional Regulation by Poly(ADP-Ribose) Polymerase-1 During T Cell Activation. *BMC Genomics* (2008) 9:171. doi: 10.1186/1471-2164-9-171
32. Nasta F, Laudisi F, Sambucci M, Rosado MM, Pioli C. Increased Foxp3+ Regulatory T Cells in Poly(ADP-Ribose) Polymerase-1 Deficiency. *J Immunol* (2010) 184(7):3470–7. doi: 10.4049/jimmunol.0901568
33. Dharwal V, Naura AS. PARP-1 Inhibition Ameliorates Elastase Induced Lung Inflammation and Emphysema in Mice. *Biochem Pharmacol* (2018) 150:24–34. doi: 10.1016/j.bcp.2018.01.027
34. Hauschildt S, Scheipers P, Bessler W, Schwarz K, Ullmer A, Flad HD, et al. Role of ADP-ribosylation in Activated Monocytes/Macrophages. *Adv Exp Med Biol* (1997) 419:249–52. doi: 10.1007/978-1-4419-8632-0_31
35. Echeverri Tirado LC, Ghonim MA, Wang J, Al-Khami AA, Wyczechowska D, Luu HH, et al. Parp-1 Is Critical for Recruitment of Dendritic Cells to the Lung in a Mouse Model of Asthma But Dispensable for Their Differentiation and Function. *Mediators Inflamm* (2019) 2019:1656484. doi: 10.1155/2019/1656484
36. Chan N, Koritzinsky M, Zhao H, Bindra R, Glazer PM, Powell S, et al. Chronic Hypoxia Decreases Synthesis of Homologous Recombination Proteins to Offset Chemoresistance and Radioresistance. *Cancer Res* (2008) 68(2):605–14. doi: 10.1158/0008-5472.CAN-07-5472
37. Chan N, Pires IM, Bencokova Z, Coackley C, Luoto KR, Bhogal N, et al. Contextual Synthetic Lethality of Cancer Cell Kill Based on the Tumor Microenvironment. *Cancer Res* (2010) 70(20):8045–54. doi: 10.1158/0008-5472.CAN-10-2352
38. Lord CJ, Ashworth A. PARP Inhibitors: Synthetic Lethality in the Clinic. *Science* (2017) 355(6330):1152–8. doi: 10.1126/science.aam7344
39. Ray-Coquard I, Pautier P, Pignata S, Pérol D, González-Martín A, Berger R, et al. Olaparib Plus Bevacizumab as First-Line Maintenance in Ovarian Cancer. *N Engl J Med* (2019) 381(25):2416–28. doi: 10.1056/NEJMoa1911361
40. Mirza MR, Åvall Lundqvist E, Birrer MJ, dePont Christensen R, Nyvang GB, Malander S, et al. Niraparib Plus Bevacizumab Versus Niraparib Alone for Platinum-Sensitive Recurrent Ovarian Cancer (NSGO-AVANOVA2/ENGOT-ov24): A Randomised, Phase 2, Superiority Trial. *Lancet Oncol* (2019) 20(10):1409–19. doi: 10.1016/S1470-2045(19)30515-7
41. MITO 25.1. *A Randomized, Molecular Driven Phase II Trial of Carboplatin-Paclitaxel-Bevacizumab vs Carboplatin-Paclitaxel-Bevacizumab-Rucaparib vs Carboplatin-Paclitaxel-Rucaparib, Selected According to HRD Status, in Patients With Advanced (Stage III B-C-IV) Ovarian, Primary Peritoneal and Fallopian Tube Cancer Preceded by a Phase I Dose Escalation Study on Rucaparib-Bevacizumab Combination*. Available at: https://clinicaltrials.gov/ct2/show/NCT03462212 (Accessed 15/03/2021).
42. Lee J, Moore RC, Ghamande SA, Park MS, John Paul Diaz JP, Chapman JA, et al. Cediranib in Combination With Olaparib in Patients Without a Germline BRCA1/2 Mutation With Recurrent Platinum-Resistant Ovarian Cancer: Phase Iib CONCERTO Trial. *J Clin Oncol* (2020) 38(15_suppl):6056–6056. doi: 10.1200/JCO.2020.38.15_suppl.6056

43. Ding L, Kim HJ, Wang Q, Kearns M, Jiang T, Ohlson CE, et al. Parp Inhibition Elicits STING-Dependent Antitumor Immunity in Brca1-Deficient Ovarian Cancer. *Cell Rep* (2018) 25(11):2972–80.e5. doi: 10.1016/j.celrep.2018.11.054
44. Pantelidou C, Sonzogni O, De Oliveria Taveira M, Mehta AK, Kothari A, Wang D, et al. Parp Inhibitor Efficacy Depends on CD8. *Cancer Discov* (2019) 9(6):722–37. doi: 10.1158/2159-8290.CD-18-1218
45. Huang J, Wang L, Cong Z, Amoozgar Z, Kiner E, Xing D, et al. The PARP1 Inhibitor BMN 673 Exhibits Immunoregulatory Effects in a Brca1(-/-) Murine Model of Ovarian Cancer. *Biochem Biophys Res Commun* (2015) 463(4):551–6. doi: 10.1016/j.bbrc.2015.05.083
46. Currie AJ, Prosser A, McDonnell A, Cleaver AL, Robinson BW, Freeman GJ, et al. Dual Control of Antitumor CD8 T Cells Through the Programmed Death-1/Programmed Death-Ligand 1 Pathway and Immunosuppressive CD4 T Cells: Regulation and Counterregulation. *J Immunol* (2009) 183 (12):7898–908. doi: 10.4049/jimmunol.0901060
47. Shen J, Zhao W, Ju Z, Wang L, Peng Y, Labrie M, et al. Parpi Triggers the STING-Dependent Immune Response and Enhances the Therapeutic Efficacy of Immune Checkpoint Blockade Independent of Brcaness. *Cancer Res* (2019) 79(2):311–9. doi: 10.1158/0008-5472.CAN-18-1003
48. Jiao S, Xia W, Yamaguchi H, Wei Y, Chen MK, Hsu JM, et al. Parp Inhibitor Upregulates PD-L1 Expression and Enhances Cancer-Associated Immunosuppression. *Clin Cancer Res* (2017) 23(14):3711–20. doi: 10.1158/1078-0432.CCR-16-3215
49. Piao J, Lim HJ, Lee M. Prognostic Value of Programmed Cell Death Ligand-1 Expression in Ovarian Cancer: An Updated Meta-Analysis. *Obstet Gynecol Sci* (2020) 63(3):346–56. doi: 10.5468/ogs.2020.63.3.346
50. Martin de la Fuente L, Westbom-Fremer S, Arildsen NS, Hartman L, Malander S, Kannisto P, et al. Pd-1/Pd-L1 Expression and Tumor-Infiltrating Lymphocytes Are Prognostically Favorable in Advanced High-Grade Serous Ovarian Carcinoma. *Virchows Arch* (2020) 477(1):83–91. doi: 10.1007/s00428-020-02751-6
51. Konstantinopoulos PA, Waggoner S, Vidal GA, Mita M, Moroney JW, Holloway R, et al. Single-Arm Phases 1 and 2 Trial of Niraparib in Combination With Pembrolizumab in Patients With Recurrent Platinum-Resistant Ovarian Carcinoma. *JAMA Oncol* (2019) 5(8):1141–9. doi: 10.1001/jamaoncol.2019.1048
52. Mittica G, Capellero S, Genta S, Cagnazzo C, Aglietta M, Sangiolo D, et al. Adoptive Immunotherapy Against Ovarian Cancer. *J Ovarian Res* (2016) 9 (1):30. doi: 10.1186/s13048-016-0236-9
53. Peyraud F, Italiano A. Combined PARP Inhibition and Immune Checkpoint Therapy in Solid Tumors. *Cancers (Basel)* (2020) 12(6):1502. doi: 10.3390/cancers12061502
54. Lampert EJ, Zimmer A, Padget M, Cimino-Mathews A, Nair JR, Liu Y, et al. Combination of PARP Inhibitor Olaparib, and PD-L1 Inhibitor Durvalumab, in Recurrent Ovarian Cancer: A Proof-of-Concept Phase II Study. *Clin Cancer Res* (2020) 26(16):4268–79. doi: 10.1158/1078-0432.CCR-20-0056
55. Drew Y KB, Banerjee S, Kaufman B, Lortholary A, Hong SH, Park YH, et al. Phase II Study of Olaparib + Durvalumab (MEDIOLA): Updated Results in Germline BRCA-mutated Platinum-Sensitive Relapsed (PSR) Ovarian Cancer (OC). *Ann Oncol* (2019) 30(Supplement_5):mdz253.016. doi: 10.1093/annonc/mdz253.016

Conflict of Interest: The authors declare that the research was conducted in the absence of any commercial or financial relationships that could be construed as a potential conflict of interest.

frontiers in Oncology

REVIEW
published: 14 July 2021
doi: 10.3389/fonc.2021.698844

The Immune Microenvironment in Brain Metastases of Non-Small Cell Lung Cancer

Lumeng Luo[1,2†], *Peiyi Liu*[3†], *Kuaile Zhao*[1,2], *Weixin Zhao*[1,2*] *and Xiaofei Zhang*[1,2*]

[1] Department of Radiation Oncology, Fudan University Shanghai Cancer Center, Shanghai, China, [2] Department of Oncology, Shanghai Medical College, Fudan University, Shanghai, China, [3] Department of Orthopedics, TongRen Hospital, School of Medicine Shanghai Jiao Tong University, Shanghai, China

OPEN ACCESS

Edited by:
Kevin J. Ni,
St George Hospital, Australia

Reviewed by:
Xiaoxia Chen,
Shanghai Pulmonary Hospital, China
Tianqing Chu,
Shanghai Jiaotong University, China

***Correspondence:**
Xiaofei Zhang
zhxf_1017@163.com
Weixin Zhao
zwx21@126.com

†These authors share first authorship

Specialty section:
This article was submitted to Molecular and Cellular Oncology, a section of the journal Frontiers in Oncology

Received: 22 April 2021
Accepted: 28 May 2021
Published: 14 July 2021

Citation:
Luo L, Liu P, Zhao K, Zhao W and Zhang X (2021) The Immune Microenvironment in Brain Metastases of Non-Small Cell Lung Cancer. Front. Oncol. 11:698844. doi: 10.3389/fonc.2021.698844

Brain metastasis of non-small cell lung cancer is associated with poor survival outcomes and poses rough clinical challenges. At the era of immunotherapy, it is urgent to perform a comprehensive study uncovering the specific immune microenvironment of brain metastases of NSCLC. The immune microenvironment of brain is distinctly different from microenvironments of extracranial lesions. In this review, we summarized the process of brain metastases across the barrier and revealed that brain is not completely immune-privileged. We comprehensively described the specific components of immune microenvironment for brain metastases such as central nervous system-derived antigen-presenting cells, microglia and astrocytes. Besides, the difference of immune microenvironment between brain metastases and primary foci of lung was particularly demonstrated.

Keywords: immune microenvironment, brain metastases, non-small cell lung cancer, immune therapeutics, brain metastases of non-small cell lung cancer

BACKGROUND

Brain metastases are the most common type intracranial tumors, which are commonly metastasized from lung cancer (1). Approximately 50% of brain metastases originate from non-small cell lung cancer (NSCLC). During the progression of NSCLC, about one third of patients may develop brain metastases (1, 2). Current therapeutic strategies for brain metastases of NSCLC are largely limited, and the prognosis is relatively poor because of the specific anatomic and physiologic features of the central nervous system (CNS). Moreover, comprehensive researches on brain metastases of NSCLC are significantly lacked. Immunotherapy has been rapidly adopted for the treatment of NSCLC (3, 4). Recent small-scale clinical studies have shown that some of NSCLC patients can be benefited from immune checkpoint inhibitors (5). However, due to genetic differences between brain metastases and primary tumors, as well as the difference in tumor microenvironment, the response of intracranial and extracranial lesions to systemic immunotherapy may differ a lot. In addition, the difficulty in collecting

intracranial tissues increases the challenge in clarifying the molecular mechanism of brain metastases (6). Therefore, it is urgent to carry out an in-depth exploration on the immune microenvironment of brain metastases, aiming to guide clinical treatment.

THE PROCESS OF BRAIN METASTASES

Cancer metastasis is one of the most significant characteristics of malignant tumors, which is a multistep cell-biological process, called the invasion-metastasis cascade (7). During metastatic progression, tumor cells detach from their primary lesions (locally invasive and intravasate), translocate systemically (survive in the circulation, arrest at a distant tissue and extravasate), and finally form the metastases in the foreign microenvironment of distant organs (**Figure 1**) (7). Although the circulating tumor cells (CTCs) in the hematogenous circulation could disseminate to a variety of secondary loci, it is noticed that the metastases of a certain type of carcinoma could only form in particular target organs (7). In 1889, Stephen Paget proposed the well-known "seed-and-soil" hypothesis of metastases that metastases only develop at those organ sites ("soils"), in which the newly "seeded" metastatic tumor cells are suitably growing (8). The nervous system is one of the most preferential and frequent metastatic sites of NSCLC (9). CTCs infiltrate through the blood circulation at brain capillaries with a slower flow rate, where they interact with microvascular endothelial cells and secrete cytokines. Then, tumor cells with a strong invasiveness ability circulate through the bloodstream, the brain lymphatics or the CSF, and survive and thrive in the parenchymal, leptomeningeal, or epidural areas, thus leading to brain metastases.

THE MOLECULAR MECHANISM OF BRAIN METASTASES OF NSCLC

The molecular mechanisms underlying brain metastases of NSCLC remain largely unknown due to the lack of *in vitro* models that simulate the complex structure and microenvironment of CNS. A previous study established a multi-organ microfluidic bionic chip platform to recapitulate the process of brain metastases. It is found that AKR1B10 can promote the extravasation of lung cancer cells through the blood–brain barrier (BBB) and then induce brain metastases (10). Through comparing genomic sequencing data of a large number of brain metastases and primary lung adenocarcinomas, three novel metastatic drivers with significantly higher amplification frequencies are identified, including MYC, YAP1, and MMP13. Overexpression of them increases the incidence of brain metastases (11, 12). Besides, *in vitro* and *in vivo* experiments demonstrated that cell adhesion molecule 2 (CADMA2), long noncoding RNA MALAT1, and microRNA-330-3p promote the development of brain metastases by inducing epithelial-mesenchymal transition (EMT) in NSCLC (13–15). The transmembrane cell adhesion protein ADAM9 is

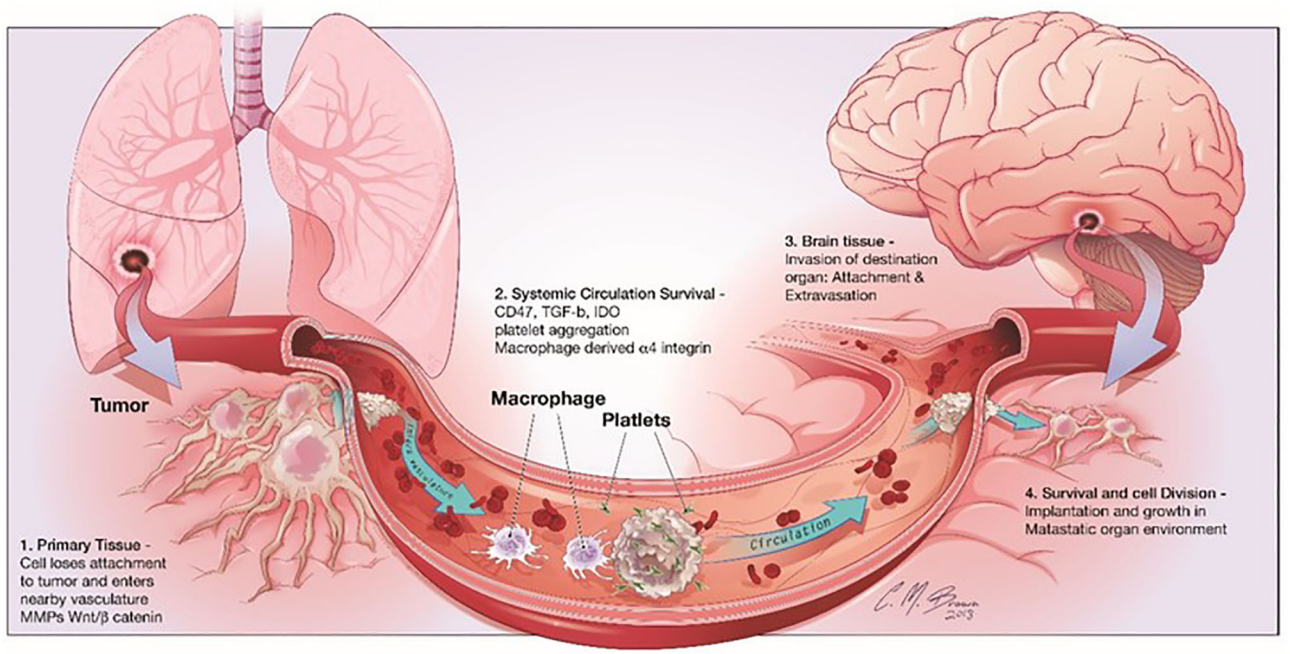

FIGURE 1 | Steps involved in brain metastasis. Brain metastasis cascade involves four major steps: 1) Detachment of the metastatic cell from the primary cancer, 2) Survival in systemic circulation, 3) Invasion in the brain parenchyma and 4) Survival in the CNS microenvironment.

able to promote lung cancer metastases to the brain by a plasminogen activator-based pathway (16). Moreover, activated leukocyte cell adhesion molecule (ALCAM), the tubulin-detyrosinating activity of VASH1, lysophosphatidylcholine acyltransferase 1 (LPCAT1), and the TAZ-AXL-ABL2 feed-forward signaling axis are also essential for the formation of brain metastases from NSCLC (17–20). As for immune-related mechanism, tumor-induced peripheral immunosuppression might promote brain metastases in patients with NSCLC (21). Patients with brain metastatic lung carcinoma exhibit a profound systemic immunosuppression with increased myeloid-derived suppressor cells, regulatory T cell populations, peripheral monocyte PD-L1, myeloid-derived suppressor cells (MDSCs), and regulatory T cells compared to early stage pre-metastatic patients and healthy controls, accompanied by less reactive T cells and worse survival (21).

INCOMPLETELY IMMUNE PRIVILEGED CNS

There are three main barriers in CNS, including the blood–brain barrier (BBB), blood–cerebrospinal fluid (BCSFB) barrier, and the blood– tumor barrier (BTB) (22). In the normal brain, BBB and BCSFB are the initial gatekeepers of CNS, which are formed by the tight junctions of the endothelial cells of capillaries and connective tissues and responsible for protecting CNS from a massive inflammation (brain edema) (23). CTCs could cross the barrier by the transendothelial migration. When the micrometastases (<1 mm) are formed, the BBB still functions normally to protect the micrometastases escaping from the effective anti-cancer drugs, such as water-soluble agents and macromolecules (23, 24). The formation of metastatic tumor in the brain leads to neo-angiogenesis, vascular remodeling, and changes of surface molecules, such as overexpression of the pericyte protein desmin and deficiency of physiological TJ protein (25–27). The changed neurovascular-tumor unit is known as BTB, which is featured by increased permeability, promoting tumor growth, and changing the delivery of anti-cancer agents. Meanwhile, dynamic angiogenesis differs from lesions and regions of the same lesion during metastatic progression (24). As a result, there is a significant heterogeneous permeability in brain metastases, leading to a non-uniform and suboptimal drug distribution and thus promotes drug resistance (28).

CNS is not completely immune-privileged. In the last century, the CNS has been considered as the immune-privileged organ because of the existence of BBB and BCSFB, where immune cells in the blood circulation system are blocked. However, along with the explorations on lymphatic system in the brain and lymphatic ducts of meninges, this conception has been overthrown (29). Experimental data also showed that tumor-infiltrating T lymphocytes and other blood-borne immune cells are observed in the brain metastases (30). Besides, a connection between the blood-borne immune cells and immune components in the brain exists. The specific immune cells of the CNS are able to pass through the endolymphatic system into the cerebrospinal fluid, which further infiltrate to the olfactory bulb, olfactory nerve, cribriform plate, nasal mucosa, and finally reach the deep cervical lymph nodes. Although the BBB limits the penetration of immune cells, they can pass through the tapetum lucidum and lymphatic channels of cerebrospinal fluid (**Figure 2**) (31). Besides, macrophages and CD4-positive memory T cells are residents in the ventricle, pia mater, and perivascular space, which are important for immune monitoring of the CNS (31).

SPECIFIC COMPONENTS OF IMMUNE MICROENVIRONMENT FOR BRAIN METASTASES

CNS-Derived Antigen-Presenting Cells

According to previous studies, CD11c-expressing cells are found as the residents in the juxta vascular parenchyma (32). They are not only recruited from the blood to parenchyma but also derived from an intraneural precursor *in situ* (32). Apart from the CD11c-expressing cells, perivascular and ventricular macrophages, as well as epiplexus cells of the choroid plexus and meninges constitute a main population of antigen-presenting cells (APCs) (CNS-derived APCs) (31). Although they are located outside the parenchyma, they can sample the contents of tumor cells in the parenchyma through the circulating CSF. They express MHC-II molecules, co-stimulatory molecules, and can present antigens to elicit priming and proliferation of CD4+ T cells to activate the adaptive immune response (32).

Microglia

Microglia is another main population of APCs in CNS, playing a vital role in the immune response of CNS. It is the only one type of immune cells existed in healthy CNS parenchyma and unique in CNS. Microglial cells can respond rapidly. As the main resident immune cells in the CNS, microglia is extremely heterogeneous. Microglia can lyse tumor cells by secreting NO and sheltering the brain from the metastatic cell colonization (33). Despite their anti-tumor ability, microglial have shown their tumor-promoting effect. A previous study showed that in brain metastases initiated from lung cancer, a dense accumulation of activated microglia tightly "encapsulate" brain metastases. Microglia can respond rapidly to the metastatic lung cancer cells in the brain and lead to migration and proliferation (34). Since the morphology and molecular markers of activated microglia like MHC-II molecules, CD40 and other co-stimulatory molecules are similar to those of blood-borne macrophages, it is difficult to distinguish the two types of cells (35). Thus, they are classified into the mononuclear-macrophage system, named as microglia-macrophages. Compared with the blood-borne macrophages, microglia accounts for the minority. They express low levels of the accessory molecules required for efficient antigen presentation and present a weak antigen-presenting activity (31, 36–38). According to their functional differences, microglia can be divided into M1-like and M2-like phenotypes based on the polarization (39). As is known, M1 macrophages can either engulf tumor cells or function as APCs to provoke activate CD8+ T cells and the adaptive immune response, thus killing tumor cells.

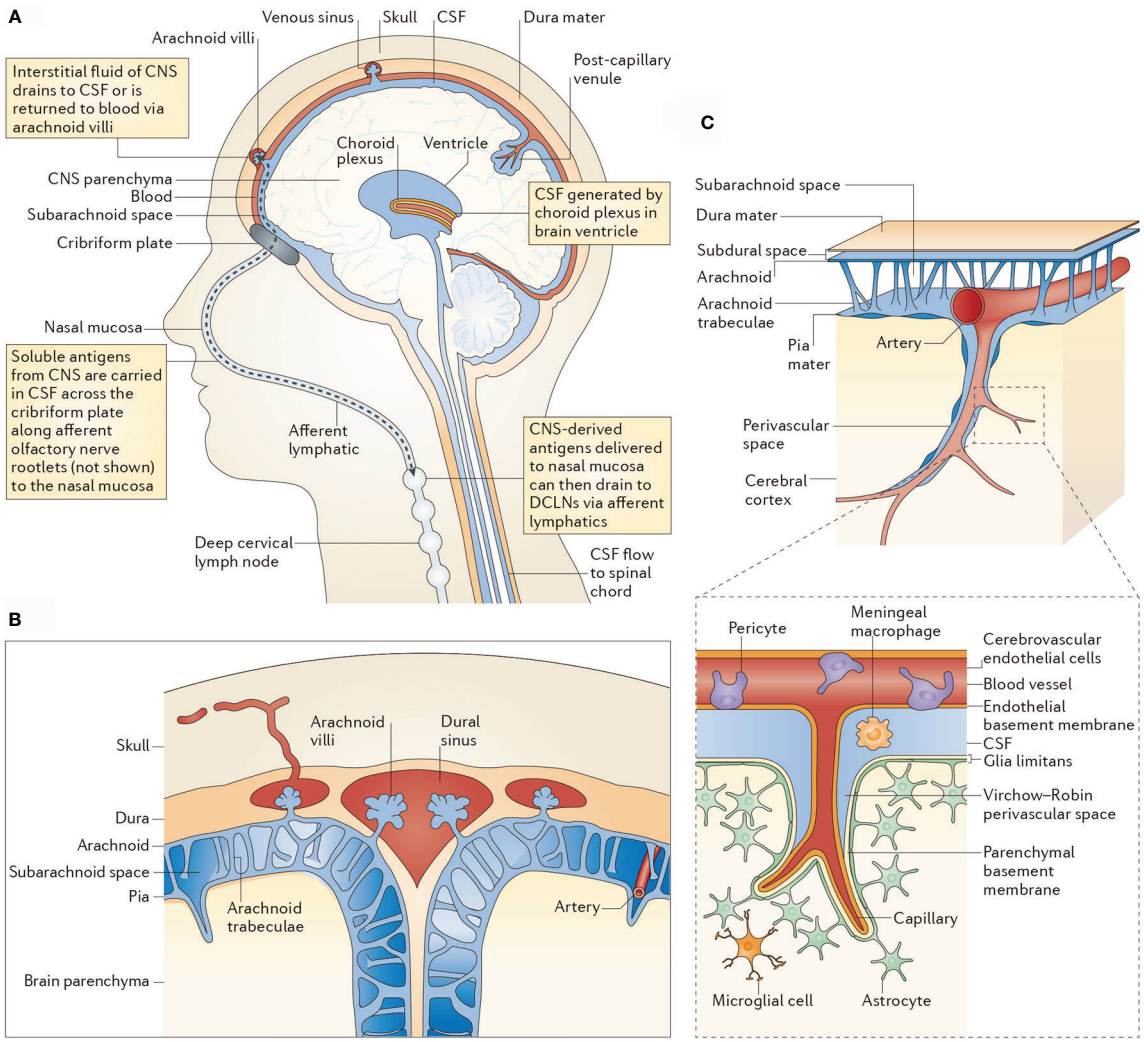

FIGURE 2 | CSF-mediated drainage of interstitial fluid and CNS antigens to deep cervical lymph nodes. **(A)** A human head in midline sagittal section, showing revelant anatomical structures [namely the ventricle, choroid plexus, central nervous system (CNS) parenchyma, lymphatics and deep cervical lymph nodes (DCLNs)] in schematic form. **(B)** Arachnoid granulations in relation to the subarachnoid space and brain parenchyma. **(C)** Subpial vasculature in relation to subarachnoid space and brain parenchyma, indicating the anatomy discussed in the main text. The inset shows the cellular components of cerebral capillaries, the glia limitans and the basement membranes in relation to the perivascular space. CSF, cerebrospinal fluid.

On the contrary, M2 macrophages are immunosuppressive that promote tumor growth by secreting growth factors or facilitating angiogenesis (39). A large population of microglia-macrophages in intracranial tumors are usually similar to M2 macrophages, called M2-like phenotypes. They induce tumor invasion and angiogenesis by interacting with tumor cells (28). At present, microglia in brain metastases of NSCLC have been rarely reported (34, 39). Thus, targeting microglia with M2 macrophages or inhibiting signaling pathways that activate astrocytes might provide novel ideas for immunotherapy of brain metastases of NSCLC.

Astrocytes

Astrocytes are another glial type in CNS besides microglia, accounting for 30% of cells in CNS (40). Responding to injuries or tumors, astrocytes are activated into a reactive state that are responsible for the repair and the formation of glial scars (41). Astrocytes limit metastases without entering in the lesions in the early stage, and in turn, the inflammatory environment caused by brain metastases can activate astrocytes that further promotes tumor growth (42). Lung cancer cells employ protocadherin 7 (PCDH7) to engage astrocytes and promote the establishment of carcinoma-astrocyte gap (43). These channels allow the transfer of cGAMP from cancer cells to astrocytes, thus activating the STING pathway and promoting inflammatory cytokines released by astrocytes, including interferon-α (IFNα) and tumor necrosis factor (TNF), which is an innate immune response pathway to support tumor growth and chemoresistance (43). Besides, latest evidences

have shown that activated astrocytes infiltrating to surrounding tissues are capable of triggering metastasis, in which the STAT3 signaling pathway is a key link for inhibiting intracranial metastases (44).

Other Immune Cells

There exist a small proportion of monocytes in the CSF that comprise about 5% of cells in CSF. They derive from a minority population of CCR1+/CCR5+ monocytes in the blood circulation and are activated and retained in the CNS. For further activation, myeloid monocytes down-regulate CCR1, whereas microglia up-regulate CCR5 (40, 45).

An early study demonstrated that cerebrospinal fluid (CSF) from healthy individuals contains 1,000 to 3,000 leukocytes/ml, which predominantly consist of activated central memory T cells, suggesting that they might be involved in CNS immune surveillance (46). Moreover, it is noticed that CD8+ tissue-resident memory T (Trm) cells have been discovered in the CNS after brain viral infection (46, 47). Although the role of Trm cells in brain immune surveillance as emerged, it is not clear whether they are infiltrated during the brain metastases. To depict the components in immune microenvironment in brain metastases, the overview of immune cells and tumor cells interaction were depicted in **Figure 3**.

TUMOR-INFILTRATING LYMPHOCYTES (TILS) IN BRAIN METASTASES

As is known, TILs are the main component of tumor immune microenvironment and the key subtype of cells involved in the immune response. TILs are subtyped into two categories based on surface molecules, showing anti-cancer function and cancer-promoting effect on the immune escape, respectively (48). During the process of tumor metastasis to the brain, the damaged BBB with increased permeability allows the peripheral lymphatic system passing through the CNS. As a result, TILs can be detected around brain metastases. There are three infiltrating models of TILs, including matrix infiltration, peritumoral infiltration, and diffuse infiltration. Brain metastases of NSCLC are mainly infiltrated as the former two models (49).

TILS FOR BRAIN METASTASES PROGNOSIS

TILs in brain metastases are positively correlated to the prognosis (12). An immunohistochemical analysis involving 61 specimens of brain metastases of lung cancer showed better overall survival in patients with higher ratios of CD3+ T cells, CD8+ T cells, and CD45+ T cells (memory T cells) than those with lower ratios of the three subtypes of T cells (30).

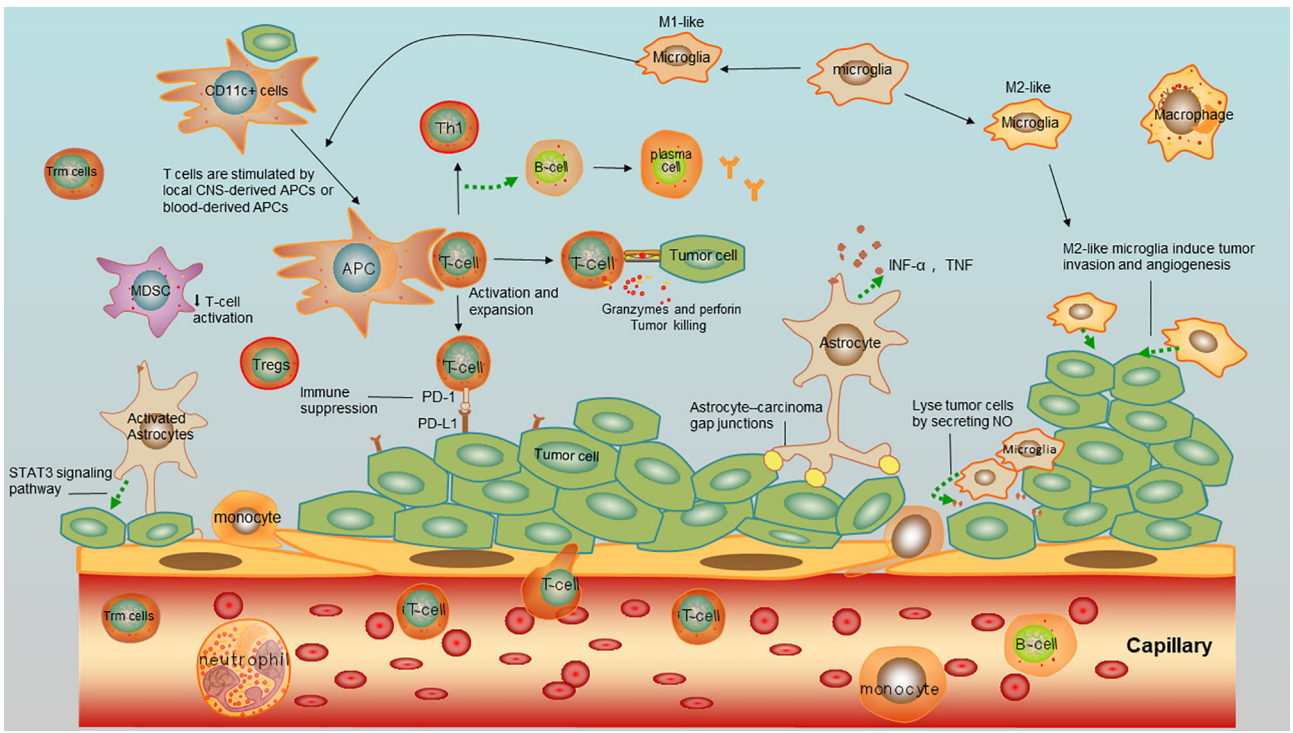

FIGURE 3 | Immnue microenvirment of brain metastases of NSCLC. Tumor cells interact with tumor-infiltrating lymphocytes (TILS), antigen-presenting cells (APCs), astrocytes, microglia, myeloid derived suppressor cells (MDSCs), and macrophages.

Consistently, another study analyzing 25 pairs of primary NSCLC specimens and brain metastases of NSCLC found that the overall density of CD8+ T cells in the parenchyma of brain metastases is higher than that in primary foci, and patients with a lower number of CD8+ TILs in the matrix present a worse prognosis (50).

Comparison Of TILs in Metastases From in Primary FOCI

TILs in brain metastases differ from those in primary foci of lung, and those in the former present a stronger immunosuppressive phenotype in the tumor microenvironment (12). In an analysis of immune gene expression profile involving 78 pairs of primary NSCLC specimens and brain metastases, a total of 161 differentially expressed genes are detected (51). Compared with primary NSCLC specimens, an attenuated antigen presentation function of dendritic cells, reduced lymphocyte extravasation and down-regulated vascular cell adhesion molecule 1 (VCAM1) are examined in brain metastases, indicating that the immunosuppressive microenvironment is more pronounced in brain metastases than that of primary foci (51). Moreover, they estimated the infiltrating level of immune cell subpopulations and lower infiltrating levels of dendritic cells, Th1 cells, and CD8+T cells are examined in brain metastases than those of primary foci. In addition, the overall ratio of infiltrating lymphocytes in brain metastases is lower than that of the primary foci, but that of macrophages is higher, especially M2 macrophages (51).

Comparison of T Cell Receptor Characteristics in Primary Foci and Brain Metastases

It is found that both primary foci and brain metastases share the majority of tumor-associated antigens. However, the density of T cells and T-cell richness in brain metastases are significantly lower than those of primary foci (51). To further investigate T cell phenotypes, T cell clones are assessed by T cell receptor (TCR)-β sequence. In the process of TCR rearrangement, a highly variable region that recognizes antigenic peptides is formed, called complementarity determining region 3 (CDR3). TCR-β-CDR3 sequence contributes to recognize the diversity of TCR, and determines T cell clonality and abundance (52). To compare characteristics of TCR in primary foci and brain metastases, the TCR-β sequencing analysis is performed in 39 pairs of NSCLC specimens and brain metastases (51). No significant difference in the clonality among brain metastases, pulmonary primary tumors, and normal tissues is found. However, the density of T cells and clonal abundance of T cells are significantly lower in brain metastases than those of primary foci (51). Furthermore, the dominant T cell colonies are analyzed, which are shared in most brain metastases and paired primary foci, and the median ratio of shared colonies in brain metastases reaches 100%. Subsequently, the clonal proliferation of T cells in brain metastases is analyzed. Effective clonal proliferation of T cells is found in 64% of brain metastases, with a median frequency of 11.2%. In most cases, for brain metastases and primary tumors, there are tumor-associated antigens. T cell clone amplification can be detected in brain metastases, but insufficient T cell infiltrations and the diversity of TCR in metastases indicate less abundance of T cells in brain metastases (51). An analysis involving 20 cases of brain metastases of lung adenocarcinoma and primary foci consistently identified that T cell colonies and the diversity of T cells are fewer in brain metastases compared with those of primary foci (53).

Comparison of Tumor Mutational Burden Between Primary Foci and Brain Metastases

Although tumor mutational burden (TMB) level is higher in brain metastases, the novel antigen levels do not increase and are similar to those of primary foci. Therefore, using TMB as a single immunotherapy biomarker is not reliable. Mansfield et al. further detected TMB in brain metastases of lung adenocarcinoma and primary foci (53). The average TMB of 13 cases of brain metastases of lung adenocarcinoma and primary foci is 24.9 and 12.5, respectively, indicating more non-identical mutations in intracranial lesions, which are favorable to the immune response. Later, peptides with a strong affinity to MHC are selected from the mutated sequence as new tumor antigen candidates. However, it is found that the number of new tumor antigens does not increase, which may be attributed to the limitation of current methods for predicting new antigens or short mutations generated by non-identical mutations that only a small part of them can be recognized by the immune system. Therefore, some lung adenocarcinoma patients with a relatively high TMB do not respond to immunotherapy. Moreover, it is also suggested that the use of TMB as a single immunotherapy biomarker in either primary foci or brain metastases is not reliable.

EXPRESSION LEVELS OF PD-1 AND PD-L1 IN BRAIN METASTASES

PD-1 is mainly expressed in immune cells, including activated T cells, monocytes, and dendritic cells. After binding to PD-L1, PD-1 inactivates the cytotoxic T cells that recognize tumor cells, thus leading to the immune escape. PD-L1 is mainly expressed in tumor cells and immune cells, including T cells, B cells, macrophages, and dendritic cells (54).

PD-1 and PD-L1 are differentially expressed between brain metastases and primary foci of lung. Mansfield et al. (55) analyzed pathological samples of 73 cases of brain metastases of lung adenocarcinoma and primary foci. The positive expression of PD-L1 is detected in 39% of brain metastasis samples, while the inconsistency rate of positive expression of PD-L1 in paired cancer samples reaches 14%, and that in immune cells is 26%. It is suggested that the spatial heterogeneity of PD-L1 expression in intracranial and extracranial lesions should be taken into consideration. Notably, down-regulation of PD-L1 or loss of PD-L1 can be detected in a considerable number of intracranial lesions compared with that of primary foci. A large number of

brain metastases are non-immune responded (both PD-L1 and TILs are negative).

Therapeutic strategies do not influence expression levels of PD-1/PD-L1 in brain metastases and primary foci. Preoperative radiotherapy, chemotherapy, and hormone therapy generally do not alter expression level of PD-L1 in tumor cells and immune cells of primary foci and brain metastases (56). Up-regulation of PD-1 in immune cells of brain metastases is only detected in 2/61 patients who receive preoperative radiotherapy prior to primary foci resection. Nevertheless, the small sample size limits the reliability of the conclusion that requires to be validated in large-sample studies (56).

Influences of PD-1/PD-L1 levels on therapeutic efficacy of ICI medication in brain metastases need to be further explored as well (12). Currently, a phase III clinical trial of PD-1 inhibitor in the treatment of brain metastases showed that patients with PD-L1 expression ≥ 1% in stromal/immune cells have a longer overall survival than those with PD-L1 <1% (5). Median OS is numerically higher in those with PD-L1 expression ≥ 1% in tumor cells, although no significant difference is obtainable (5). At present, there are multiple studies on immunotherapy for patients with brain metastases, and the therapeutic functions of PD-L1 are waiting to be revealed (12).

CONCLUSIONS

As one of the most protected organs in the body, the brain is still prone to be the distant metastatic organ of NSCLC. Compared with extracranial tumors, the immune microenvironment of intracranial tumors is unique and highly specific. Specific immune cells in the immune microenvironment of intracranial tumors mainly include microglia and astrocytes, showing heterogeneous properties. Compared to the primary foci of lung, the immune microenvironment of brain metastases is overall immunosuppressed. More comprehensive and detailed studies are required to pave the way for developing new immunotherapeutic strategies by targeting their immunosuppressive properties, thus controlling brain metastases of NSCLC.

AUTHOR CONTRIBUTIONS

XZ, PL, and LL were major contributor in writing the manuscript. All authors contributed to the article and approved the submitted version.

REFERENCES

1. Arvold ND, Lee EQ, Mehta MP, Margolin K, Alexander BM, Lin NU, et al. Updates in the Management of Brain Metastases. *Neuro Oncol* (2016) 18 (8):1043–65. doi: 10.1093/neuonc/now127
2. Barnholtz-Sloan JS, Sloan AE, Davis FG, Vigneau FD, Lai P, Sawaya RE. Incidence Proportions of Brain Metastases in Patients Diagnosed (1973 to 2001) in the Metropolitan Detroit Cancer Surveillance System. *J Clin Oncol* (2004) 22(14):2865–72. doi: 10.1200/JCO.2004.12.149
3. Borghaei H, Paz-Ares L, Horn L, Spigel DR, Steins M, Ready NE, et al. Nivolumab Versus Docetaxel in Advanced Nonsquamous Non-Small-Cell Lung Cancer. *N Engl J Med* (2015) 373(17):1627–39. doi: 10.1056/NEJMoa1507643
4. Herbst RS, Baas P, Kim DW, Felip E, Perez-Gracia JL, Han JY, et al. Pembrolizumab Versus Docetaxel for Previously Treated, PD-L1-Positive, Advanced Non-Small-Cell Lung Cancer (KEYNOTE-010): A Randomised Controlled Trial. *Lancet* (2016) 387(10027):1540–50. doi: 10.1016/S0140-6736(15)01281-7
5. Goldberg SB, Schalper KA, Gettinger SN, Mahajan A, Herbst RS, Chiang AC, et al. Pembrolizumab for Management of Patients With NSCLC and Brain Metastases: Long-Term Results and Biomarker Analysis From a non-Randomised, Open-Label, Phase 2 Trial. *Lancet Oncol* (2020) 21(5):655–63. doi: 10.1016/S1470-2045(20)30111-X
6. Boire A, Brastianos PK, Garzia L, Valiente M. Brain Metastasis. *Nat Rev Cancer* (2020) 20(1):4–11. doi: 10.1038/s41568-019-0220-y
7. Valastyan S, Weinberg RA. Tumor Metastasis: Molecular Insights and Evolving Paradigms. *Cell* (2011) 147(2):275–92. doi: 10.1016/j.cell.2011.09.024
8. Fidler IJ. The Pathogenesis of Cancer Metastasis: The 'Seed and Soil' Hypothesis Revisited. *Nat Rev Cancer* (2003) 3(6):453–8. doi: 10.1038/nrc1098
9. Riihimaki M, Hemminki A, Fallah M, Thomsen H, Sundquist K, Sundquist J, et al. Metastatic Sites and Survival in Lung Cancer. *Lung Cancer* (2014) 86 (1):78–84. doi: 10.1016/j.lungcan.2014.07.020
10. Liu W, Song J, Du X, Zhou Y, Li Y, Li R, et al. AKR1B10 (Aldo-Keto Reductase Family 1 B10) Promotes Brain Metastasis of Lung Cancer Cells in a Multi-Organ Microfluidic Chip Model. *Acta Biomater* (2019) 91:195–208. doi: 10.1016/j.actbio.2019.04.053
11. Shih DJH, Nayyar N, Bihun I, Dagogo-Jack I, Gill CM, Aquilanti E, et al. Genomic Characterization of Human Brain Metastases Identifies Drivers of Metastatic Lung Adenocarcinoma. *Nat Genet* (2020) 52(4):371–7.
12. Vilarino N, Bruna J, Bosch-Barrera J, Valiente M, Nadal E. Immunotherapy in NSCLC Patients With Brain Metastases. Understanding Brain Tumor Microenvironment and Dissecting Outcomes From Immune Checkpoint Blockade in the Clinic. *Cancer Treat Rev* (2020) 89:102067. doi: 10.1016/j.ctrv.2020.102067
13. Dai L, Zhao J, Yin J, Fu W, Chen G. Cell Adhesion Molecule 2 (CADM2) Promotes Brain Metastasis by Inducing Epithelial-Mesenchymal Transition (EMT) in Human Non-Small Cell Lung Cancer. *Ann Transl Med* (2020) 8 (7):465. doi: 10.21037/atm.2020.03.85
14. Shen L, Chen L, Wang Y, Jiang X, Xia H, Zhuang Z. Long Noncoding RNA MALAT1 Promotes Brain Metastasis by Inducing Epithelial-Mesenchymal Transition in Lung Cancer. *J Neurooncol* (2015) 121(1):101–8. doi: 10.1007/s11060-014-1613-0
15. Wei C, Zhang R, Cai Q, Gao X, Tong F, Dong J, et al. MicroRNA-330-3p Promotes Brain Metastasis and Epithelial-Mesenchymal Transition Via GRIA3 in Non-Small Cell Lung Cancer. *Aging (Albany NY)* (2019) 11 (17):6734–61. doi: 10.18632/aging.102201
16. Lin CY, Chen HJ, Huang CC, Lai LC, Lu TP, Tseng GC, et al. ADAM9 Promotes Lung Cancer Metastases to Brain by a Plasminogen Activator-Based Pathway. *Cancer Res* (2014) 74(18):5229–43. doi: 10.1158/0008-5472.CAN-13-2995
17. Wang H, Deng Q, Lv Z, Ling Y, Hou X, Chen Z, et al. N6-Methyladenosine Induced miR-143-3p Promotes the Brain Metastasis of Lung Cancer Via Regulation of VASH1. *Mol Cancer* (2019) 18(1):181. doi: 10.1186/s12943-019-1108-x
18. Munsterberg J, Loreth D, Brylka L, Werner S, Karbanova J, Gandrass M, et al. ALCAM Contributes to Brain Metastasis Formation in Non-Small-Cell Lung Cancer Through Interaction With the Vascular Endothelium. *Neuro Oncol* (2020) 22(7):955–66. doi: 10.1093/neuonc/noaa028
19. Wei C, Dong X, Lu H, Tong F, Chen L, Zhang R, et al. LPCAT1 Promotes Brain Metastasis of Lung Adenocarcinoma by Up-Regulating PI3K/AKT/MYC Pathway. *J Exp Clin Cancer Res* (2019) 38(1):95. doi: 10.1186/s13046-019-1092-4
20. Hoj JP, Mayro B, Pendergast AM. A TAZ-AXL-ABL2 Feed-Forward Signaling Axis Promotes Lung Adenocarcinoma Brain Metastasis. *Cell Rep* (2019) 29 (11):3421–34.e8. doi: 10.1016/j.celrep.2019.11.018

21. Li YD, Lamano JB, Lamano JB, Quaggin-Smith J, Veliceasa D, Kaur G, et al. Tumor-Induced Peripheral Immunosuppression Promotes Brain Metastasis in Patients With Non-Small Cell Lung Cancer. *Cancer Immunol Immunother* (2019) 68(9):1501–13. doi: 10.1007/s00262-019-02384-y
22. Lun MP, Monuki ES, Lehtinen MK. Development and Functions of the Choroid Plexus-Cerebrospinal Fluid System. *Nat Rev Neurosci* (2015) 16 (8):445–57. doi: 10.1038/nrn3921
23. Banks WA. From Blood-Brain Barrier to Blood-Brain Interface: New Opportunities for CNS Drug Delivery. *Nat Rev Drug Discov* (2016) 15 (4):275–92. doi: 10.1038/nrd.2015.21
24. Sprowls SA, Arsiwala TA, Bumgarner JR, Shah N, Lateef SS, Kielkowski BN, et al. Improving CNS Delivery to Brain Metastases by Blood-Tumor Barrier Disruption. *Trends Cancer* (2019) 5(8):495–505. doi: 10.1016/j.trecan.2019.06.003
25. Lockman PR, Mittapalli RK, Taskar KS, Rudraraju V, Gril B, Bohn KA, et al. Heterogeneous Blood-Tumor Barrier Permeability Determines Drug Efficacy in Experimental Brain Metastases of Breast Cancer. *Clin Cancer Res* (2010) 16 (23):5664–78. doi: 10.1158/1078-0432.CCR-10-1564
26. Lyle LT, Lockman PR, Adkins CE, Mohammad AS, Sechrest E, Hua E, et al. Alterations in Pericyte Subpopulations Are Associated With Elevated Blood-Tumor Barrier Permeability in Experimental Brain Metastasis of Breast Cancer. *Clin Cancer Res* (2016) 22(21):5287–99. doi: 10.1158/1078-0432.CCR-15-1836
27. Hendricks BK, Cohen-Gadol AA, Miller JC. Novel Delivery Methods Bypassing the Blood-Brain and Blood-Tumor Barriers. *Neurosurg Focus* (2015) 38(3):E10. doi: 10.3171/2015.1.FOCUS14767
28. Soffietti R, Ahluwalia M, Lin N, Ruda R. Management of Brain Metastases According to Molecular Subtypes. *Nat Rev Neurol* (2020) 16(10):557–74. doi: 10.1038/s41582-020-0391-x
29. Korn T, Kallies A. T Cell Responses in the Central Nervous System. *Nat Rev Immunol* (2017) 17(3):179–94. doi: 10.1038/nri.2016.144
30. Berghoff AS, Fuchs E, Ricken G, Mlecnik B, Bindea G, Spanberger T, et al. Density of Tumor-Infiltrating Lymphocytes Correlates With Extent of Brain Edema and Overall Survival Time in Patients With Brain Metastases. *Oncoimmunology* (2016) 5(1):e1057388. doi: 10.1080/2162402X.2015.1057388
31. Ransohoff RM, Engelhardt B. The Anatomical and Cellular Basis of Immune Surveillance in the Central Nervous System. *Nat Rev Immunol* (2012) 12 (9):623–35. doi: 10.1038/nri3265
32. Prodinger C, Bunse J, Kruger M, Schiefenhovel F, Brandt C, Laman JD, et al. CD11c-Expressing Cells Reside in the Juxtavascular Parenchyma and Extend Processes Into the Glia Limitans of the Mouse Nervous System. *Acta Neuropathol* (2011) 121(4):445–58. doi: 10.1007/s00401-010-0774-y
33. Brantley EC, Guo L, Zhang C, Lin Q, Yokoi K, Langley RR, et al. Nitric Oxide-Mediated Tumoricidal Activity of Murine Microglial Cells. *Transl Oncol* (2010) 3(6):380–8. doi: 10.1593/tlo.10208
34. He BP, Wang JJ, Zhang X, Wu Y, Wang M, Bay BH, et al. Differential Reactions of Microglia to Brain Metastasis of Lung Cancer. *Mol Med* (2006) 12 (7-8):161–70. doi: 10.2119/2006-00033.He
35. Utz SG, See P, Mildenberger W, Thion MS, Silvin A, Lutz M, et al. Early Fate Defines Microglia and Non-Parenchymal Brain Macrophage Development. *Cell* (2020) 181(3):557–73.e18. doi: 10.1016/j.cell.2020.03.021
36. Ransohoff RM, Perry VH. Microglial Physiology: Unique Stimuli, Specialized Responses. *Annu Rev Immunol* (2009) 27(119-45). doi: 10.1146/annurev.immunol.021908.132528
37. Ransohoff RM, Cardona AE. The Myeloid Cells of the Central Nervous System Parenchyma. *Nature* (2010) 468(7321):253–62. doi: 10.1038/nature09615
38. Hanisch UK, Kettenmann H. Microglia: Active Sensor and Versatile Effector Cells in the Normal and Pathologic Brain. *Nat Neurosci* (2007) 10(11):1387–94. doi: 10.1038/nn1997
39. Yuan A, Hsiao YJ, Chen HY, Chen HW, Ho CC, Chen YY, et al. Opposite Effects of M1 and M2 Macrophage Subtypes on Lung Cancer Progression. *Sci Rep* (2015) 5:14273. doi: 10.1038/srep14273
40. Liddelow SA, Barres BA. Reactive Astrocytes: Production, Function, and Therapeutic Potential. *Immunity* (2017) 46(6):957–67. doi: 10.1016/j.immuni.2017.06.006
41. Sofroniew MV. Molecular Dissection of Reactive Astrogliosis and Glial Scar Formation. *Trends Neurosci* (2009) 32(12):638–47. doi: 10.1016/j.tins.2009.08.002
42. Anderson MA, Ao Y, Sofroniew MV. Heterogeneity of Reactive Astrocytes. *Neurosci Lett* (2014) 565:23–9. doi: 10.1016/j.neulet.2013.12.030
43. Chen Q, Boire A, Jin X, Valiente M, Er EE, Lopez–Soto A, et al. Carcinoma-Astrocyte Gap Junctions Promote Brain Metastasis by cGAMP Transfer. *Nature* (2016) 533(7604):493–8. doi: 10.1038/nature18268
44. Priego N, Zhu L, Monteiro C, Mulders M, Wasilewski D, Bindeman W, et al. STAT3 Labels a Subpopulation of Reactive Astrocytes Required for Brain Metastasis. *Nat Med* (2018) 24(7):1024–35. doi: 10.1158/1538-7445.AM2019-2746
45. Trebst C, Sorensen TL, Kivisakk P, Cathcart MK, Hesselgesser J, Horuk R, et al. CCR1+/CCR5+ Mononuclear Phagocytes Accumulate in the Central Nervous System of Patients With Multiple Sclerosis. *Am J Pathol* (2001) 159 (5):1701–10. doi: 10.1016/S0002-9440(10)63017-9
46. Kivisakk P, Mahad DJ, Callahan MK, Trebst C, Tucky B, Wei T, et al. Human Cerebrospinal Fluid Central Memory CD4+ T Cells: Evidence for Trafficking Through Choroid Plexus and Meninges Via P-Selectin. *Proc Natl Acad Sci USA* (2003) 100(14):8389–94. doi: 10.1073/pnas.1433000100
47. Wakim LM, Woodward-Davis A, Bevan MJ. Memory T Cells Persisting Within the Brain After Local Infection Show Functional Adaptations to Their Tissue of Residence. *Proc Natl Acad Sci USA* (2010) 107(42):17872–9. doi: 10.1073/pnas.1010201107
48. Schreiber RD, Old LJ, Smyth MJ. Cancer Immunoediting: Integrating Immunity's Roles in Cancer Suppression and Promotion. *Science* (2011) 331(6024):1565–70. doi: 10.1126/science.1203486
49. Harter PN, Bernatz S, Scholz A, Zeiner PS, Zinke J, Kiyose M, et al. Distribution and Prognostic Relevance of Tumor-Infiltrating Lymphocytes (Tils) and PD-1/PD-L1 Immune Checkpoints in Human Brain Metastases. *Oncotarget* (2015) 6(38):40836–49. doi: 10.18632/oncotarget.5696
50. Zhou J, Gong Z, Jia Q, Wu Y, Yang ZZ, Zhu B. Programmed Death Ligand 1 Expression and CD8(+) Tumor-Infiltrating Lymphocyte Density Differences Between Paired Primary and Brain Metastatic Lesions in Non-Small Cell Lung Cancer. *Biochem Biophys Res Commun* (2018) 498(4):751–7. doi: 10.1016/j.bbrc.2018.03.053
51. Kudo Y, Haymaker C, Zhang J, Reuben A, Duose DY, Fujimoto J, et al. Suppressed Immune Microenvironment and Repertoire in Brain Metastases From Patients With Resected Non-Small-Cell Lung Cancer. *Ann Oncol* (2019) 30(9):1521–30. doi: 10.1093/annonc/mdz207
52. Liu P, Liu D, Yang X, Gao J, Chen Y, Xiao X, et al. Characterization of Human AlphabetaTCR Repertoire and Discovery of D-D Fusion in TCRbeta Chains. *Protein Cell* (2014) 5(8):603–15. doi: 10.1007/s13238-014-0060-1
53. Mansfield AS, Ren H, Sutor S, Sarangi V, Nair A, Davila J, et al. Contraction of T Cell Richness in Lung Cancer Brain Metastases. *Sci Rep* (2018) 8(1):2171. doi: 10.1038/s41598-018-20622-8
54. Cha JH, Chan LC, Li CW, Hsu JL, Hung MC. Mechanisms Controlling Pd-L1 Expression in Cancer. *Mol Cell* (2019) 76(3):359–70. doi: 10.1016/j.molcel.2019.09.030
55. Mansfield AS, Aubry MC, Moser JC, Harrington SM, Dronca RS, Park SS, et al. Temporal and Spatial Discordance of Programmed Cell Death-Ligand 1 Expression and Lymphocyte Tumor Infiltration Between Paired Primary Lesions and Brain Metastases in Lung Cancer. *Ann Oncol* (2016) 27 (10):1953–8. doi: 10.1093/annonc/mdw289
56. Teglasi V, Pipek O, Lozsa R, Berta K, Szuts D, Harko T, et al. Pd-L1 Expression of Lung Cancer Cells, Unlike Infiltrating Immune Cells, Is Stable and Unaffected by Therapy During Brain Metastasis. *Clin Lung Cancer* (2019) 20(5):363–9.e2. doi: 10.1016/j.cllc.2019.05.008

Conflict of Interest: The authors declare that the research was conducted in the absence of any commercial or financial relationships that could be construed as a potential conflict of interest.

frontiers in Cell and Developmental Biology

ORIGINAL RESEARCH
published: 19 July 2021
doi: 10.3389/fcell.2021.681240

Effect of ISM1 on the Immune Microenvironment and Epithelial-Mesenchymal Transition in Colorectal Cancer

Yuhui Wu[1†], Xiaojing Liang[1†], Junjie Ni[2†], Rongjie Zhao[1], Shengpeng Shao[3], Si Lu[4], Weidong Han[1] and Liangliang Yu[5*]*

[1] Department of Medical Oncology, Sir Run Run Shaw Hospital, College of Medicine, Zhejiang University, Hangzhou, China, [2] Department of Breast and Thyroid Surgery, Jinhua Municipal Central Hospital, Jinhua, China, [3] Department of Urinary Surgery, The First People's Hospital of Fuyang, Hangzhou, China, [4] Institute of Translational Medicine, Zhejiang University, Hangzhou, China, [5] Department of Gastroenterology, Sir Run Run Shaw Hospital, College of Medicine, Zhejiang University, Hangzhou, China

OPEN ACCESS

Edited by:
Chao Ni,
Zhejiang University, China

Reviewed by:
Jinbo Yue,
Shandong University, China
Na Luo,
Nankai University, China

***Correspondence:**
Weidong Han
hanwd@zju.edu.cn
Liangliang Yu
yudanyu@zju.edu.cn

[†] These authors have contributed equally to this work

Specialty section:
This article was submitted to Molecular and Cellular Oncology, a section of the journal Frontiers in Cell and Developmental Biology

Received: 16 March 2021
Accepted: 28 June 2021
Published: 19 July 2021

Citation:
Wu Y, Liang X, Ni J, Zhao R, Shao S, Lu S, Han W and Yu L (2021) Effect of ISM1 on the Immune Microenvironment and Epithelial-Mesenchymal Transition in Colorectal Cancer. Front. Cell Dev. Biol. 9:681240. doi: 10.3389/fcell.2021.681240

Background: An increasing number of studies have shown that Isthmin 1 (ISM1), a secreted protein, is important in tumorigenesis and invasion, including in colorectal cancer (CRC). However, the mechanisms are still unclear. This study aims to explore the function and prognosis capacity of ISM1 in CRC.

Methods: We investigated the expression of ISM1 in 18 CRC tissues vs. adjacent normal tissues from GSE50760, 473 CRC tissues vs. 41 normal tissues from The Cancer Genome Atlas (TCGA), and across gastrointestinal cancer types. Differences were further confirmed in CRC tissues via quantitative real-time polymerase chain reaction (qRT-PCR). Then, we analyzed correlations between clinicopathologic features and ISM1 expression, including prognostic prediction value, using the Kaplan–Meier method and multivariate Cox regression. Gene set enrichment analysis (GSEA) was performed to identify ISM1-related pathways. *In vitro* experiments were performed to verify the role of ISM1 in epithelial-mesenchymal transition (EMT) and CRC progression.

Results: Multiple datasets showed that ISM1 is upregulated in CRC tissues, which was validated. Patients with higher ISM1 expression had shorter overall survival (OS), and ISM1 expression served as an independent prognostic factor. Enrichment analysis showed that ISM1 upregulation was positively correlated with cancer-related pathways, such as EMT, hypoxia, and the Notch and KRAS signaling pathways. We were exclusively interested in the connection between ISM1 and EMT because 71% of genes in this pathway were significantly positively co-expressed with ISM1, which may account for why patients with higher ISM1 expression are prone to regional lymph node involvement and progression to advanced stages. In addition, we found that ISM1 was positively correlated with multiple immunosuppressive pathways such as IL2/STAT5, TNF-α/NF-κB, and TGF-β, and immune checkpoints, including PD-L1, PD-1, CTLA-4, and LAG3, which may account for upregulation of ISM1 in immunotherapy-resistant

patients. Notably, through *in vitro* experiments, we found that ISM1 promoted EMT and colon cancer cell migration and proliferation.

Conclusion: ISM1 is critical for CRC development and progression, which enhances our understanding of the low response rate of CRC to immunotherapy via immunosuppressive signaling pathways.

Keywords: colorectal cancer, ISM1, EMT, immunosuppressive, microenvironment

INTRODUCTION

Colorectal cancer (CRC) is one of the most common malignant tumors worldwide and the third leading cause of global cancer-related mortality (Bray et al., 2018). Great advancements in clinical diagnosis and comprehensive treatment have partially prolonged survival time, but the prognosis of advanced patients is still very poor (Piawah and Venook, 2019; Sveen et al., 2020). Distant invasion and metastasis are responsible for up to 90% of CRC-related deaths (Arnold et al., 2017). Therefore, searching for reliable biomarkers for early diagnosis is warranted.

Isthmin 1 (ISM1) was a secreted protein, and is important for embryonic and postnatal development (Osório et al., 2014). In recent years, growing evidence has shown that aberrant expression of ISM1 can affect the biological behavior of cancer. For example, ISM1 upregulation mediated by lncRNA H19 enhances carcinogenesis and metastasis of gastric cancer (Li et al., 2014) and can also promote cell proliferation and migration in hepatocellular cancer, regulated by hsa_circ_0091570/miR-1307 (Wang et al., 2019). There has also been a research in CRC. Zheng et al. (2019) reported increased expression of ISM1 in CRC cell lines compared with normal cells and that ISM1 participates in the process of cell proliferation and apoptosis regulated by miR-1307-3p. However, each gene may perform its biological function in a complex regulatory network, and whether there are other mechanisms of ISM1 in CRC deserves further research. In addition, Valle-Rios et al. (2014) reported that ISM1 is expressed in mammalian tissues, such as skin, mucosal, and selected lymphocyte populations, but whether it is related to the tumor microenvironment is still unclear.

To clarify the function of ISM1 in CRC, we gathered RNA-seq data of 491 CRC tissues from GEO and TCGA datasets. Moreover, our findings were verified in mouse models and CRC cell lines. This is the first integrative study to characterize ISM1 expression both molecularly and clinically in CRC.

MATERIALS AND METHODS

Data Preparation

We obtained RNA-seq data from GSE50760 (Kim et al., 2014), which contains 18 primary CRC tissues and paired normal tissues, and from TCGA database[1], which contains 473 CRC tissues and 41 normal tissues in TCGA-COAD cohort. Expression of all genes was normalized in transcripts per million (TPM) format. Then we extracted ISM1 expression data across all samples.

Differential Expression Analysis of the ISM1 Gene and Its Correlation With Clinicopathological Characteristics

We analyzed ISM1 expression changes between normal tissues and CRC in both the GSE50760 and TCGA cohorts. Then, we obtained an expression overview of ISM1 across gastrointestinal cancer types such as esophageal carcinoma, stomach adenocarcinoma, liver hepatocellular carcinoma, cholangiocarcinoma, pancreatic adenocarcinoma, rectum adenocarcinoma, and CRC in GEPIA database (Tang et al., 2017)[2]. TCGA cohort contained 432 cases of CRC with complete clinical information and a follow-up period of more than 30 days. Correlations between ISM1 and clinicopathological characteristics were further analyzed, including age (<60 vs. ≥ 60), gender (male vs. female), T stage (T_{1-2} vs. T_{3-4}), N stage (N_- vs. N_+), stage (stage I–IV), and prior malignancy (yes vs. no). The overall survival (OS) prediction value of ISM1 was also determined using the "maxstat" package[3].

Mouse Models

C57BL/6 mice (male, 8–10 weeks old, Shanghai Institute of Material Medicine, Chinese Academy of Sciences, China) were randomly divided into two groups: groups receiving (A) water only (normal) and (B) DSS for 7 days and water for 14 days (DSS). The induction of CAC was performed according to a previously reported method (Han et al., 2019). First, mice received a single intraperitoneal injection of 10 mg/kg azoxymethane (AOM, MP Biomedicals) and were maintained on a regular diet for 7 days. Then, the mice were continuously fed DSS (2%, MP Biomedicals) for 7 days, followed by a recovery period of 14 days. We cycled the previous steps 3 times. Finally, we sacrificed the mice and removed the colon tumors in preparation for further analysis.

Cell Lines

NCM460, HCT116, HT29, LoVo, DLD1, SW480, and SW620 cells, were purchased from the Chinese Academy of Sciences (Shanghai, China). NCM460, HCT116, LoVo, SW480, SW620, and DLD1 cells were cultured in RPMI 1640 medium (Gibco, United States); HT29 cells were cultured in DMEM with high glucose (Gibco). All of the above media contained 10% fetal

[1]https://portal.gdc.cancer.gov/

[2]http://gepia.cancer-pku.cn/detail.php

[3]https://CRAN.R-project.org/package=maxstat

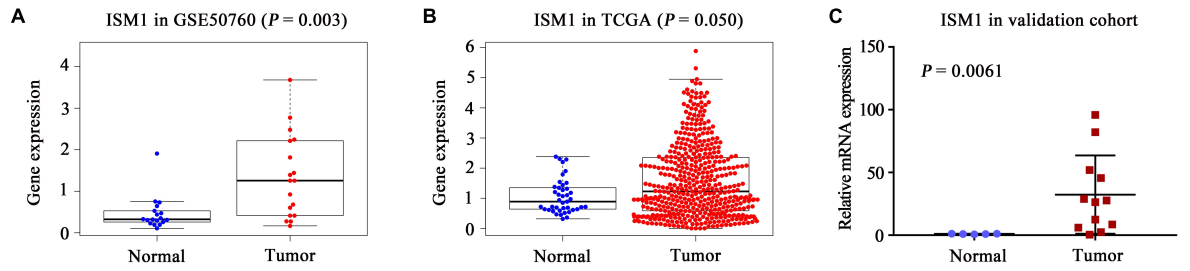

FIGURE 1 | Landscape of ISM1 expression changes. Analysis of differential ISM1 expression between CRC tissues and normal tissues was performed in the **(A)** GSE50760 dataset, **(B)** TCGA dataset, and **(C)** validation cohort.

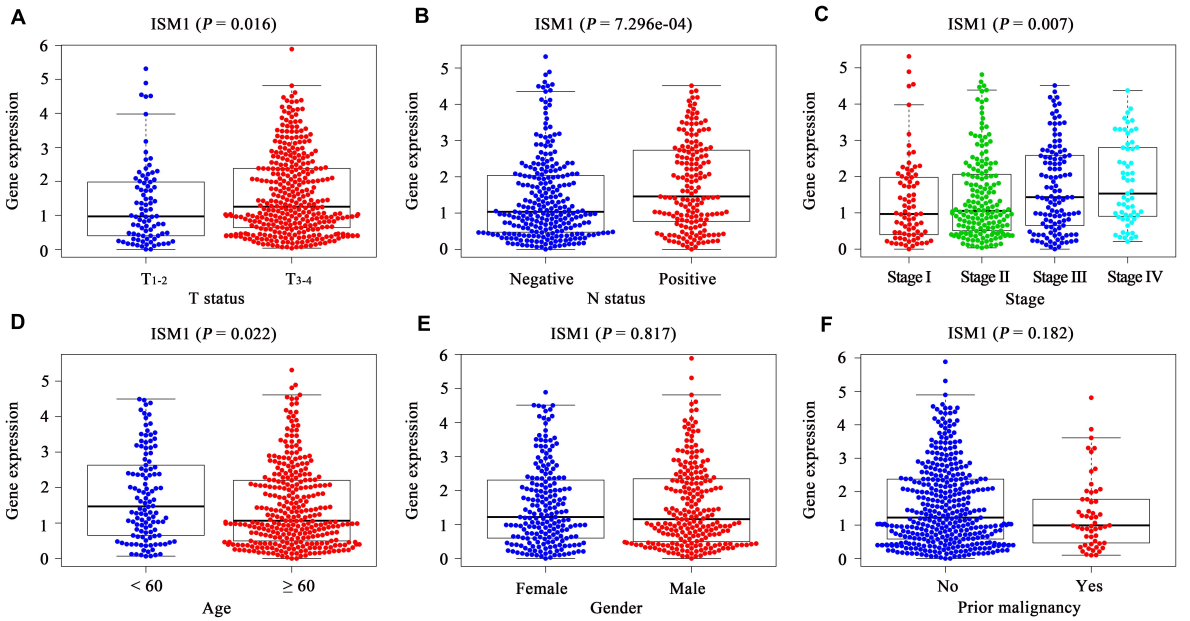

FIGURE 2 | Correlation between clinicopathological characteristics and ISM1 in CRC. **(A–F)** ISM1 expression changes in patients with T_{3-4} (vs. T_{1-2}), lymph node involvement, advanced stages, age <60 (vs. ≥60), and prior malignancy (yes vs. no). $P < 0.05$ is statistically significant.

bovine serum (FBS, Gibco). All cell lines were cultured in a 37°C humidified incubator with 5% CO_2.

RNA Isolation and Quantification

Total RNA from mouse colon tissues or cell lines was extracted using RNA isolate reagent (#R401-01-AA, Vazyme), according to the manufacturer's instructions. Then, the RNA was converted to cDNA using the HiScript II 1st Strand cDNA Synthesis Kit (#R312-02, Vazyme). After that, quantitative real-time polymerase chain reaction (qRT-PCR) was performed using MagicSYBR Mixture (#CW3008M, CWBIO). The relative expression of the ISM1 gene was normalized to that of GAPDH. Primer sequence information was as follows: mouse ISM1: forward primer: 5′-GATGGCCCTGACTCCGAAG-3′; reverse primer: 5′-GGTCCCCACTATTTGTCCTGG-3′; human ISM1: forward primer: 5′-CTTCCCCAGACCGCGATTC-3′; reverse primer: 5′-CGACCACCTCTATGGTGACCT-3′.

Enrichment Analysis of ISM1

To gain further insights into the biological function of ISM1, we calculated the correlation between ISM1 and all other protein-coding genes in 473 CRC tissues from TCGA cohort. Then genes were sorted according to Pearson's correlation to produce a gene list. Gene set enrichment analysis (GSEA) was performed using the "clusterProfiler" package (Subramanian et al., 2005; Yu et al., 2012). Enriched results with adjusted $P < 0.05$ were considered significant. To understand the activity of a certain pathway in CRC, single sample gene set enrichment analysis (ssGSEA) was performed to calculate the activity score in each tissue based on the gene expression profile (Cui et al., 2020). Since 71% genes in epithelial-mesenchymal transition (EMT) pathway were significantly positively co-expressed with ISM1, we focused on the role of EMT in the development and progression of CRC and made a comparison to EMT activity score in tumor tissues vs. paired normal tissues and lymph node involvement vs. non-involvement.

Role of ISM1 in an Immunosuppressive Microenvironment

Enrichment results indicated that ISM1 upregulation was significantly positively associated with multiple immunosuppressive pathways. We further investigated correlations between ISM1 and markers of regulatory T cells (CCR8, TGFB1, STAT5B, and FOXP3), M2 macrophages (CD163, VSIG4, and MS4A4A), and T cell exhaustion (TIM-3, CTLA-4, PD-1, and LAG3) and PD-L1.

To further confirm the suppressive role of ISM1 in immunotherapy, we obtained RNA-seq data and response information from PD-L1 mAb-treated metastatic urothelial cancer patients from IMvigor210 (Mariathasan et al., 2018), which contained 61 complete response (CR)/partial response (PR), and 183 stable disease (SD)/progressive disease (PD) cases. And these patients consisted of three distinct immunological phenotypes: 62 cases of immune inflamed, 113 cases of immune excluded, and 69 cases of immune desert. We compared the expression of ISM1 in patients with different PD-L1 response and immunological phenotypes.

RNA Interference, Plasmid Construction and Transfections

Cells were transfected with siRNA using RNAiMAX (Thermo Fisher Scientific) according to the manufacturer's protocol. siRNAs were purchased from RiboBio (Guangzhou, China), and the target sequences were as follows: si-ISM1-1: 5′–GGCAGAATCCAAATATCCA–3′; si-ISM1-2: 5′–GCAAAAGC GAGTTCTTAAA–3′; and si-ISM1-3: 5′–GACACCACA TCAGAAACCA–3′.

Cells were transfected with plasmids using jetPRIME (Polyplus, United States) according to the manufacturer's protocol. The plasmids used in this study were purchased from GENERAY Biotechnology (Shanghai, China).

Immunoblot Analysis

Proteins in cell lysates were separated via sodium dodecyl sulfate-polyacrylamide gel electrophoresis and transferred to PVDF membranes (Millipore, Bedford, MA, United States). Membranes were blocked with 5% milk in TBST buffer [10 mM Tris–Cl (pH 7.4), 150 mM NaCl, 0.1% Tween 20] at room temperature and incubated overnight at 4°C with the indicated primary antibodies. Then, membranes were incubated with corresponding secondary antibodies at room temperature for 1 h, and proteins were detected with enhanced chemiluminescence reagent (SuperSignal Western Pico Chemiluminescent Substrate; Pierce, United States). Antibodies against the following proteins were used in this study: β-actin (Cell Signaling Technology, CST, United States); ISM1 (Abcam, United States); N-cadherin (CST, United States); E-cadherin (CST, United States); and Snail (CST, United States); ZEB1 (CST, United States).

Transwell Assay

Cells were harvested and resuspended at 1×10^6 cells/mL (LoVo, DLD1) or 5×10^5 cells/mL (HT29) in FBS-free culture medium. Then, 600 μL of culture medium containing 10% FBS was added to the lower chambers and 200 μL of cell suspension was added to the upper chambers containing the cell culture inserts (Corning, United States). After 24 h, cells on the top surface of the inserts were removed with a cotton swab. Cells on the bottom surface of the inserts were fixed with 4% paraformaldehyde for 5 min at room temperature and then washed with PBS. Migrated cells were stained with DAPI for 10 min and then washed with PBS. Migrated cells were visualized and photographed.

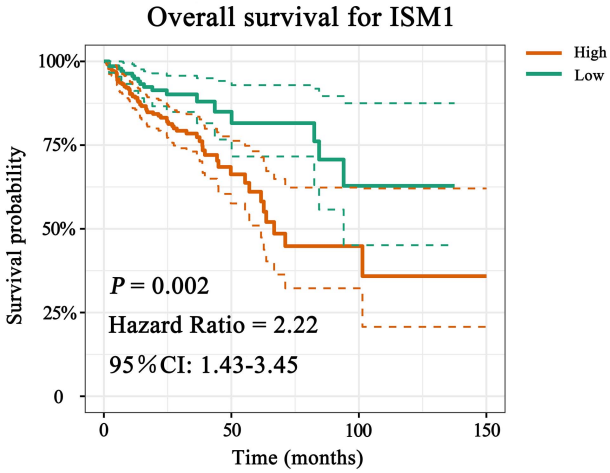

FIGURE 3 | Overall survival (OS) analysis of ISM1. The expression of ISM1 was significantly related to OS in TCGA-CRC cohort. Yellowish brown indicates high ISM1 expression, while dark green indicates low expression. Dotted lines represent confidence intervals. The horizontal axis indicates OS time (months), and the vertical axis is survival probability. $P < 0.05$ is statistically significant.

Cell Counting Kit-8 (CCK8) Assay

The effect of ISM1 expression on human colon cancer cell lines was analyzed using the CCK8 (Meilunbio, Shanghai, China) assay. A 200 μL cell suspension containing 5,000 cells was seeded in each well (96-well plate). At different time points (0, 24, 48, and 72 h), the supernatants were removed, and 100 μL CCK8 solution (10 μL CCK8: 90 μL medium) was added to each well and

TABLE 1 | Univariate and multivariate analysis of clinicopathological characteristics and ISM1 with overall survival in TCGA-COAD cohort.

TCGA-COAD cohort (*n*=432)	Univariate analysis		Multivariate analysis	
	HR (95% CI)	*P*	HR (95% CI)	*P*
Age (vs. <60)	1.303 (0.781–2.175)	0.311		
Gender (vs. female)	1.133 (0.736–1.743)	0.571		
T status (vs. T_{1-2})	4.275 (1.562–11.701)	0.005	2.818 (1.005–7.903)	0.049
N status (vs. N_0)	2.813 (1.805–4.384)	<0.001	2.247 (1.423–3.547)	<0.001
Prior malignancy (vs. yes)	0.612 (0.355–1.055)	0.077		
ISM1 (vs. low)	2.259 (1.334–3.824)	0.002	1.94 (1.140–3.300)	0.014

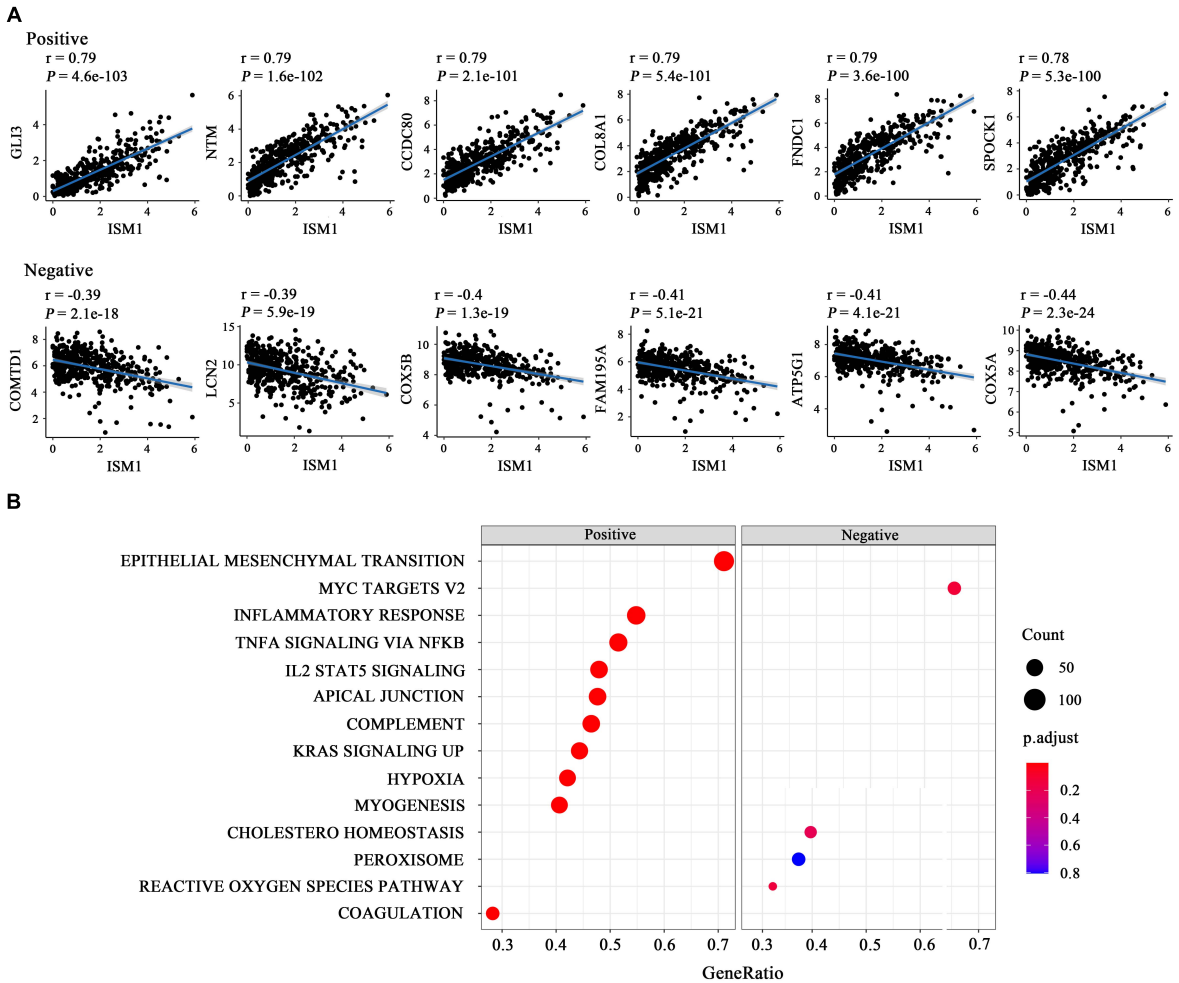

FIGURE 4 | Functional enrichment analysis of ISM1 in CRC. **(A)** Correlation between ISM1 and the remaining 19505 genes. The top six positively and negatively correlated genes are shown. **(B)** GSEA of the 19505 genes was performed using Pearson's correlation, and the top 10 positively and negatively correlated pathways are shown. Pathways in the left box were found to be positively correlated with ISM1, while those in the right box were found to be negative correlated with ISM1. The color of the dots varies from blue to red, representing the significance of changes: red indicates statistical significance. When many genes were found to be correlated with ISM1 in a pathway, the size of the dot larger. The horizontal axis represents the ratio of correlated genes among all the genes in each pathway. $P < 0.05$ is statistically significant.

incubated with the cells for 3 h before analysis. The absorbance at 450 nm was measured.

Statistical Analysis

Differences in ISM1 expression in CRC vs. normal tissues was calculated with a Mann–Whitney test in GraphPad (version 7.00). The role of ISM1 in clinicopathological characteristics and PD-L1 mAb response was calculated with a Wilcoxon test or Kruskal–Wallis test in R software (version 3.5.0). Overall survival rates were calculated using Kaplan–Meier survival curves and a log-rank test. Cox regression was used to determine hazard ratios (HRs) and to identify independent prognostic factors. Connections between ISM1 expression and other genes were determined using Pearson's correlation. EMT activity score differences across cancer types were calculated with paired Wilcoxon tests in R software (version 3.5.0). The EMT activity score difference between lymph node involvement and non-involvement was calculated using a Mann–Whitney test in GraphPad (version 7.00). qRT-PCR data are expressed as the mean ± standard error, and statistical significance was determined with Student's t test. $P < 0.05$ was considered statistically significant.

RESULTS

ISM1 Is Upregulated in CRC vs. Normal Tissues

In both the GSE50760 and TCGA datasets, the expression of ISM1 was significantly higher in CRC tissues than in normal tissues ($P = 0.003$, 0.050; **Figures 1A,B**). To validate the ISM1 expression changes, mice CRC was induced using AOM and

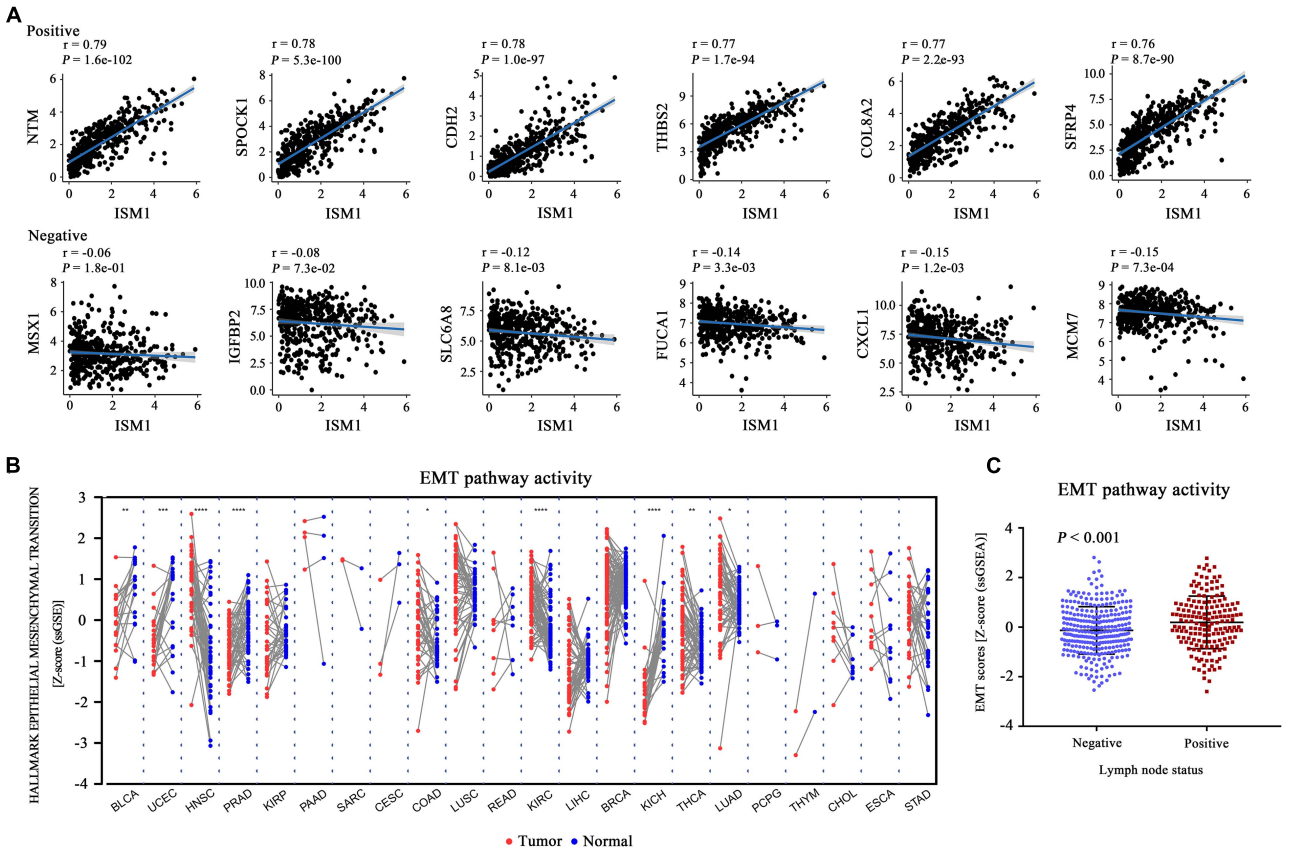

FIGURE 5 | Epithelial-mesenchymal transition (EMT) activity score in all cancer types. **(A)** Pearson's correlation between ISM1 and genes in the EMT pathway was calculated, and the top six positively and negatively correlated genes are shown. **(B)** The pathway activity score for EMT was calculated and compared across 22 cancers from TCGA between tumor tissues (red dot) and paired normal tissues (blue dot). **(C)** EMT activity score for 300 lymph node non-involvement tissues (41 normal tissues and 259 negative lymph node tissues) and 173 lymph node involvement tissues. *$P < 0.05$; **$P < 0.01$; ***$P < 0.001$.

DSS. Then we extracted RNA from CRC or normal colon tissues and performed qRT-PCR and found that ISM1 was consistently significantly higher in CRC tissues than in normal colon tissues ($P = 0.0061$; **Figure 1C**). From the expression landscape across gastrointestinal cancer types, ISM1 showed a higher expression trend in esophageal carcinoma and rectal adenocarcinoma but a lower expression trend in stomach adenocarcinoma, liver hepatocellular carcinoma, cholangiocarcinoma, and pancreatic adenocarcinoma ($P > 0.05$; **Supplementary Figure 1**).

ISM1 Is Correlated With Adverse Clinicopathological Characteristics in CRC

In TCGA cohort, after comparing the expression of ISM1 among cases with different clinicopathological characteristics, we found that expression was higher in patients with age < 60 ($P < 0.05$), a larger tumor size ($P < 0.05$), lymph node involvement ($P < 0.001$), and advanced stages ($P < 0.01$) (**Figures 2A–D**). These differences indicate that ISM1 upregulation is associated with aggressive behavior in CRC patients. Differences were not found in gender or prior malignancy (**Figures 2E,F**).

ISM1 Predicts Shorter OS in CRC

With the method of maximally selected rank statistics, we identified the most effective ISM1 expression cutoff to distinguish CRC prognosis in TCGA cohort ($P = 0.002$, HR = 2.22, 95% CI: 1.43–3.45; **Figure 3**). From the results of Kaplan–Meier curves and Cox regression, higher ISM1 expression indicated a shorter OS. Multivariate analysis showed that ISM1, tumor size and lymph node involvement were all independent prognostic factors (**Table 1**). In this way, ISM1-related aggressive biological behavior may account for its negative effect on OS. Clinically, the prognosis of patients with different clinicopathological features varies greatly, and the treatment they receive is not exactly the same. We further conducted a subgroup analysis based on age, sex, T status, lymph node status, stage, and malignancy history. The results showed that ISM1 overexpression had a better performance in CRC patients with the following characteristics: ≥60 (years), male, T_{3-4}, negative lymph nodes, and prior malignancy, and all of these patients exhibited a shorter OS (**Supplementary Figure 2**). Interestingly, the expression of ISM1 was higher in advanced CRC (**Figure 2C**). However, we found that there was only a slight relationship between ISM1 and OS in the stage II–III subgroups. ISM1 was not related to the prognosis

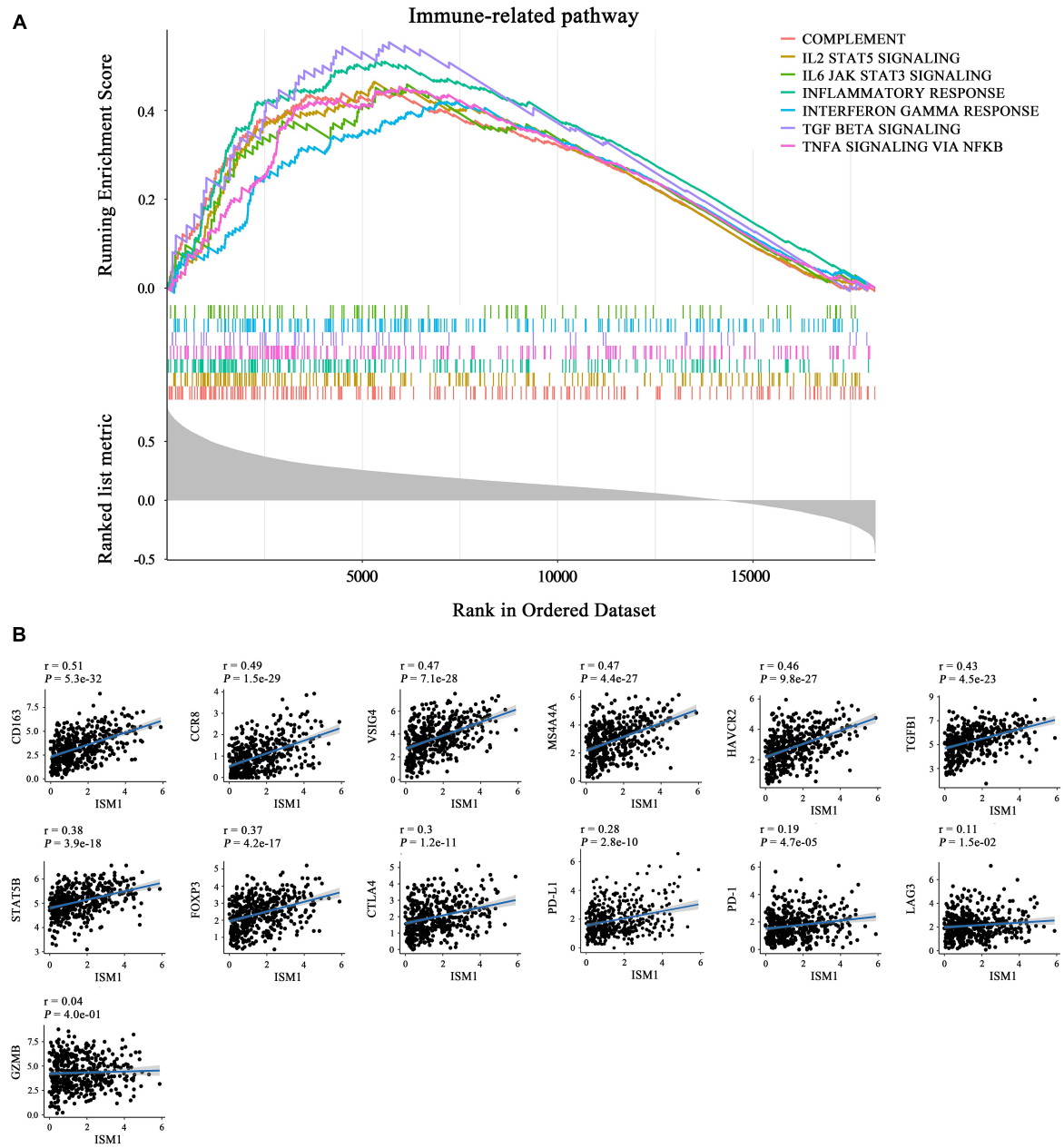

FIGURE 6 | Role of ISM1 in an immunosuppressive microenvironment. **(A)** Seven significantly enriched ISM1-related immunosuppressive pathways in CRC. The short vertical lines in the middle of the figure represent the distribution of ISM1-related genes among the 19505 genes. **(B)** Correlation between ISM1 and immunosuppressive markers of M2 macrophages (CD163, VSIG4, and MS4A4A), Tregs (CCR8, TGFB1, STAT5B, and FOXP3), and T cell exhaustion (TIM-3, CTLA-4, PD-1, and LAG3) and PD-L1. Correlation strength is defined as follows: "0.00–0.29" indicates weak; "0.30–0.59" indicates moderate; "0.60–1.0" indicates strong. $P < 0.05$ is statistically significant.

of patients in stage I/IV, which may be caused by the lower distribution of cases in these subgroups.

ISM1 Is Correlated With Multiple Cancer-Related Pathways

The results mentioned above showed that ISM1 is associated with CRC development and progression. We then performed GSEA to determine ISM1-related biological functions through GSEA based on the Pearson's correlation value for 19505 identified genes. The top six correlated genes (positive and negative) were displayed in the form of a scatter plot (**Figure 4A**). For example, ISM1 showed a positive correlation with GLI3 (cor = 0.79, P = 4.6e-103), CCDC80 (cor = 0.79, P = 2.1e-101), COL8A1 (cor = 0.79, P = 5.4e-101), FNDC1 (cor = 0.79, P = 3.6e-100), and SPOCK1 (cor = 0.78, P = 5.3e-100) but a negative correlation with

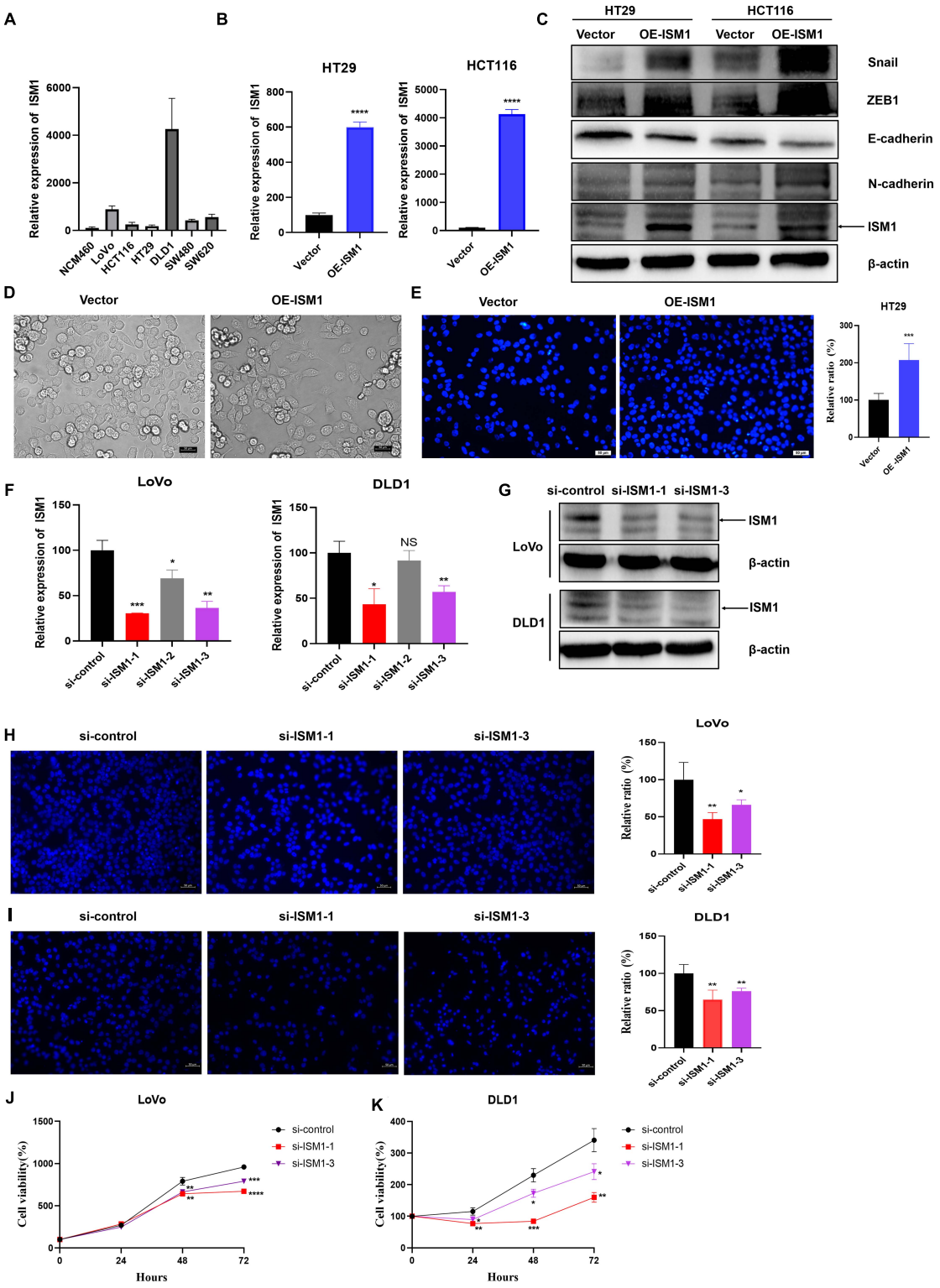

FIGURE 7 | ISM1 promotes EMT and CRC progression *in vitro*. **(A)** Quantitative reverse transcription polymerase chain reaction (qRT-PCR) analysis of ISM1 mRNA levels in NCM460, LoVo, HCT116, HT29, DLD1, SW480, and SW620 cells ($n = 3$, mean ± SD). **(B)** The overexpression (OE) efficiency of ISM1 plasmid (OE-ISM1) in HT29 and HCT116 cells was analyzed via qRT-PCR. Student's *t* test; $^{****}P < 0.0001$; $n = 3$, mean ± SD. **(C)** Immunoblot analysis of ISM1, N-cadherin, E-cadherin, Snail, and ZEB1 in HT29 and HCT116 cells transfected with Vector or OE-ISM1 plasmid. **(D)** Phase contrast images of HT29 cells transfected with Vector or OE-ISM1 plasmid. Scale bars: 50 μm. **(E)** Transwell assay of HT29 cells transfected with Vector or OE-ISM1 plasmid. Student's *t* test; $^{**}P < 0.01$; $n = 5$, mean ± SD. Scale bars: 50 μm. **(F)** The knockdown efficiency of si-ISM1-1, si-ISM1-2 and si-ISM1-3 in LoVo and DLD1 cells was analyzed via qRT-PCR.

(Continued)

FIGURE 7 | Continued
Student's *t* test; $^{*}P < 0.05$, $^{**}P < 0.01$, $^{***}P < 0.001$, NS, no significance; $n = 3$, mean ± SD. **(G)** The knockdown efficiency of si-ISM1-1 and si-ISM1-3 in LoVo and DLD1 cells was analyzed via immunoblot experiments. **(H)** Transwell assay of LoVo cells transfected with si-control, si-ISM1-1, or si-ISM1-3. Student's *t* test; $^{*}P < 0.05$, $^{**}P < 0.01$; $n = 5$, mean ± SD. Scale bars: 50 μm. **(I)** Transwell assay of DLD1 cells transfected with si-control, si-ISM1-1, or si-ISM1-3. Student's *t* test; $^{**}P < 0.01$; $n = 5$, mean ± SD. Scale bars: 50 μm. **(J)** Proliferation of LoVo cells transfected with si-control, si-ISM1-1, or si-ISM1-3 was determined using CCK-8 assays. **(K)** Proliferation of DLD1 cells transfected with si-control, si-ISM1-1, or si-ISM1-3 was determined using CCK-8 assays.

COMTD1 (cor = -0.39, $P = 2.1e\text{-}18$), LCN2 (cor = -0.39, $P = 5.9e\text{-}19$), COX5B (cor = -0.4, $P = 1.3e\text{-}19$), FAM195A (cor = -0.41, $P = 5.1e\text{-}21$), ATP5G1 (cor = -0.41, $P = 4.1e\text{-}21$), and COX5A (cor = -0.44, $P = 2.3e\text{-}24$).

The GSEA results showed that multiple cancer-related pathways were significantly associated with ISM1, including EMT, hypoxia, the KRAS signaling pathway, angiogenesis, the Notch signaling pathway, and the Hedgehog signaling pathway (**Figure 4B** and **Supplementary Figure 3**). Among them, we exclusively focused on the correlation between ISM1 and EMT because 71% of genes in this pathway were significantly positively co-expressed with ISM1. The top six positively correlated genes (NTM, SPOCK1, CDH2, THBS2, COL8A2, and SFRP4, cor > 0.75, $P < 0.001$) and negatively correlated genes (MSX1, IGFBP2, SLC6A8, FUCA1, CXCL1, and MCM7, | cor| : 0.06–0.15, *P:* 0.00073–0.18) in EMT are displayed in **Figure 5A**. Additionally, the EMT activity score was notably increased in CRC vs. paired normal tissues (**Figure 5B** and **Supplementary Table 1**) and in lymph node involvement vs. non-involvement tissues (**Figure 5C**), indicating that the relationship between ISM1 and EMT is vital in CRC progression.

ISM1 Is Correlated With the Immunosuppressive Microenvironment in CRC

The GSEA results also showed that ISM1 was highly associated with immune-related pathways, such as the IL2/STAT5, TNF-α/NF-κB, TGF-β, IFN-γ, and IL6/JAK/STAT3 signaling pathways (**Figure 6A** and **Supplementary Figure 4**). Previous studies have demonstrated that most of these pathways are important to induce strong suppression of the antitumor immune response through Treg cell infiltration (Shi et al., 2018), $CD8^{+}$ T cell exhaustion (Liu et al., 2021), and stabilization of PD-L1 (Lim et al., 2016). However, corresponding reports on ISM1 in immunosuppression are rare. For further understanding, we calculated correlations between ISM1 and immunosuppressive markers. Notably, most correlations were highly significant, including correlations with M2 macrophages (CD163, VSIG4, and MS4A4A, cor: 0.47–0.51, $P < 0.001$) and Tregs (CCR8, TGFB1, STAT5B, and FOXP3, cor: 0.37–0.48, $P < 0.001$). ISM1 showed a weak to moderate positive correlation with the expression of exhausted T cell markers, such as TIM-3, (cor = 0.46, $P < 0.001$), CTLA-4 (cor = 0.30, $P < 0.001$), PD-1 (cor = 0.19, $P < 0.001$), and LAG3 (cor = 0.11, $P < 0.01$). The correlation between PD-L1 and ISM1 was 0.28 ($P < 0.001$) (**Figure 6B**).

Moreover, we analyzed the role of ISM1 in microenvironment in patients treated with PD-L1 mAb, and found it was overexpressed in immune-excluded tumors vs. inflamed (**Supplementary Figure 5A**), and SD/PD patients with immune-excluded tumors vs. CR/PR patients with inflamed tumors (**Supplementary Figure 5B**), indicating that ISM1 may participate in the exclusion of CD8 + T cells entering the parenchyma, which was associated with the activation of TGF-β signaling pathway (Mariathasan et al., 2018). Notably, it supported our previous findings that CRC tissues with overexpressed ISM1 showed a higher activity score of TGF-β signaling pathway (**Supplementary Figure 4A**). We may speculate from these results that high ISM1 expression may create an immunosuppressive microenvironment to drive immune escape and induce resistance to immunotherapy.

In vitro Experiments Confirmed That ISM1 Promotes EMT and CRC Progression

To confirm the role of ISM1 in EMT and CRC progression, *in vitro* experiments were performed. We first detected ISM1 expression levels in a human normal colon epithelial cell line (NCM460) and in colon cancer cell lines (LoVo, HCT116, HT29, DLD1, SW480, and SW620). As shown in **Figure 7A**, the ISM1 level in colon cancer cell lines was higher than that in the normal colon epithelial cell line, which was consistent with previous results showing that the ISM1 expression level is higher in CRC tissues than in normal tissues (**Figures 1A–C**). HT29 and HCT116 cells exhibited lower ISM1 expression, and DLD1 and LoVo cells exhibited higher ISM1 expression. EMT is usually monitored by assessing the protein levels of N-cadherin (mesenchymal marker), E-cadherin (epithelial marker), and the EMT-inducing transcription factors (EMT-TFs) Snail and ZEB (Singh et al., 2018). Therefore, we overexpressed ISM1 in HT29 and HCT116 cells and verified the overexpression (OE) efficiency by qRT-PCR analysis (**Figure 7B**). Then, we detected these important EMT-associated molecules by immunoblot experiments. As shown in **Figure 7C**, ISM1 OE significantly decreased the level of the epithelial marker E-cadherin but increased the levels of the mesenchymal marker N-cadherin and the EMT-inducing transcription factor Snail and ZEB1. We also found that ISM1-overexpressed HT29 cells had an obvious change of cellular morphology (**Figure 7D**). These results suggest that ISM1 promotes EMT.

To further examine the biological function of ISM1 in CRC, we analyzed cell migration ability of HT29 cells transfected with Vector or OE-ISM1 plasmid. As shown in **Figure 7E**, ISM1 OE significantly elevated HT29 cells migration ability, with increase of 1.5-fold. We then generated three small interfering RNAs (siRNAs), namely, si-ISM1-1, si-ISM1-2, and si-ISM1-3. si-ISM1-1 exhibited the highest knockdown (KD) efficiency, followed by si-ISM1-3 and si-ISM1-2 (**Figure 7F**). KD efficiency was

further determined by immunoblot experiments (**Figure 7G**). We then employed si-ISM1-1 and si-ISM1-3 in the ISM1-high colon cancer cell lines LoVo and DLD1. As shown in **Figures 7H,I**, ISM1 KD reduced the migration of LoVo cells by 53.1% (si-ISM1-1, $P < 0.01$) and 33.8% (si-ISM1-3, $P < 0.05$) and of DLD1 cells by 35.1% (si-ISM1-1, $P < 0.01$) and 23.8% (si-ISM1-3, $P < 0.01$) compared with control siRNA (si-control)-transfected cells. We also found that ISM1 KD significantly impaired the proliferation ability of colon cancer cells (**Figures 7J,K**). Thus, our data demonstrate that ISM1 promotes EMT and CRC progression.

DISCUSSION

In our study, we found that the expression of ISM1 was upregulated in CRC tissue (vs. normal) and in patients <60 years of age (vs. those ≥60), T_{3-4} (vs. T_{1-2}), lymph node involvement, and advanced stages and served as an independent OS prediction factor. Enrichment analysis showed that multiple cancer-related pathways and immune-related pathways were closely associated with ISM1.

Previous studies reported that ISM1 is upregulated in CRC cell lines, which is consistent with our results, and participates in the process of cell proliferation and apoptosis regulated by miR-1307-3p (Shi et al., 2018). However, we found that there were more important mechanisms of ISM1 in CRC that have not been reported. In the GSEA results, enriched pathways, such as the EMT, hypoxia, KRAS signaling, angiogenesis, Notch and Hedgehog signaling pathways, were significantly positively associated with ISM1, and most of these pathways are vital to cell proliferation, migration and resistance in cancer (Wang et al., 2020; Andrysik et al., 2021; Cai et al., 2021), including CRC. We exclusively focused on the EMT signaling pathway because 71% of genes in the pathway exhibited a significantly positive correlation with ISM1. Additionally, genes that were highly correlated with ISM1 (cor > 0.7) but not members of the EMT pathway, such as ITGBL1 (Matsuyama et al., 2019), NRP-2 (Liu et al., 2019; Zhang et al., 2019), NOX4 (Shen et al., 2020), and GLI3 (Shen et al., 2021), have already been demonstrated to promote EMT, cell invasion and migration in CRC. EMT is a process during which epithelial cells lose epithelial features and acquire mesenchymal phenotypes and behavior (Yang et al., 2020). EMT is a key process in tumor metastasis, affecting various malignancies (Bai et al., 2021). Cancer cells with EMT also acquire resistance to some chemotherapy. For example, EMT-TFs (ZEB1, SNIAL, SLUG) have been demonstrated to confer resistance to oxaliplatin and cisplatin in breast, ovarian, colon, and pancreatic cancers (Guo et al., 2012; Lim et al., 2013). Interestingly, EMT in cancer cells gives rise to a population of cells with stem-like properties, namely, cancer stem cells (CSCs), which may persist after chemotherapeutic treatment and lead to tumor relapse (Mani et al., 2008; Morel et al., 2008; Shibue and Weinberg, 2017). Additionally, EMT can also modulate immune response. Kudo-Saito et al. (2009) reported that EMT in melanoma induce regulatory T cells and impaired dendritic cells, which leads to resistance to immunotherapy. Therefore, we speculate that EMT induced by ISM1 upregulation played an important role in regional lymph node involvement and advanced stages of CRC. Indeed, our *in vitro* experiments showed that ISM1 could promote EMT. Moreover, ISM1 KD significantly impaired the migration and proliferation abilities of colon cancer cells.

From the assessment of enriched immune-related pathways, including IL2/STAT5, TNF-α/NF-κB, TGF-β, IFN-γ response, and IL6/JAK/STAT3, ISM1 was predicted to be vital in creating an inhibitory immune microenvironment. Shi et al. (2018) found that IL-2/STAT5 was important for maintaining Treg cell homeostasis and migration ability and regulating $CD8^+$ T cell exhaustion (Liu et al., 2021). Owing to the decreased number of intratumoral Tregs, the combination of endoglin antibodies and PD-1 inhibition induced complete regression in 30–40% of CRC mice, producing durable tumor responses (Schoonderwoerd et al., 2020). A high proportion of Treg cells was found to induce resistance to anti-CTLA-4 blocking mAbs in patients with advanced cancer (Coutzac et al., 2020), but such suppression of immunotherapy could be reversed by the TGF-β pathway inhibitor galunisertib (Holmgaard et al., 2018). The TNF-α/NF-κB signaling pathway is a major pathway that stabilizes programmed cell death-ligand 1 (PD-L1) via COP9 signalosome 5 (CSN5), driving cancer cell immunosuppression against T cell surveillance (Lim et al., 2016). The JAK/STAT3 signaling pathway can promote the expression of PD-L1 in CRC (Li et al., 2019). The correlations between ISM1 and markers of suppressive immune cells (M2 macrophages, Tregs, T cell exhaustion) and the overexpression of ISM1 detected in PD1-resistant patients further confirmed our speculation that ISM1 upregulation is potentially involved in immunotherapy resistance via immune-related pathways in CRC.

As mentioned above, research on ISM1 in cancer is still in its infancy. The limitations of this study were also accompanied by advantages. This is the first study to find that ISM1 is associated with multiple important cancer-related pathways, especially EMT, and multiple important immunosuppressive signaling pathways, which provides us with evidence supporting application of ISM1 inhibitors in CRC immunotherapy. However, the mechanisms underlying ISM1 promotion of CRC progression need to be further studied.

In summary, ISM1 plays an important role in CRC development and progression via several pathways, such as EMT. Furthermore, investigating ISM1 and immunosuppressive signaling pathways enhances our understanding of the low response rate of CRC to immunotherapy.

DATA AVAILABILITY STATEMENT

The datasets presented in this study can be found in online repositories. The names of the repository/repositories and accession number(s) can be found in the article/**Supplementary Material**.

ETHICS STATEMENT

The animal study was reviewed and approved by the Experimental Animal Welfare Ethics Review Committee of Zhejiang University.

AUTHOR CONTRIBUTIONS

WH and LY: conceptualization and supervision. YW, XL, and JN: investigation. RZ, YW, SS, XL, and SL: analysis. YW, JN, and RZ: wrote original draft. WH: review, editing, and final approval. All authors contributed to the article and approved the submitted version.

FUNDING

This work was supported by the National Natural Science Foundation of China (81972745), Ten Thousand Plan Youth Talent Support Program of Zhejiang Province (ZJWR0108009), and Zhejiang Medical Innovative Discipline Construction Project-2016.

ACKNOWLEDGMENTS

The authors thank all the researchers and staff who supported The Cancer Genome Atlas Research Network and GSE50760.

SUPPLEMENTARY MATERIAL

The Supplementary Material for this article can be found online at: https://www.frontiersin.org/articles/10.3389/fcell.2021.681240/full#supplementary-material

Supplementary Figure 1 | Expression of ISM1 in gastrointestinal cancers. ESCA, esophageal carcinoma; STAD, stomach adenocarcinoma; LIHC, liver hepatocellular carcinoma; CHOL, cholangiocarcinoma; PAAD, pancreatic adenocarcinoma; COAD, colon adenocarcinoma; READ, rectum adenocarcinoma. $^{*}P < 0.05$.

Supplementary Figure 2 | Subgroup OS analysis of ISM1 expression in CRC. Patients were stratified based on age **(A)**, sex **(B)**, T status **(C)**, lymph node status **(D)**, stage **(E)**, and malignancy history **(F)**. $P < 0.05$ is statistically significant.

Supplementary Figure 3 | Activity score of multiple cancer-related pathways associated with ISM1 expression. **(A–F)** Epithelial mesenchymal transition, angiogenesis, the Hedgehog signaling pathway, the KRAS signaling pathway and hypoxia showed higher activity scores in CRC patients overexpressing ISM1.

Supplementary Figure 4 | Activity score of multiple immune-related pathways associated with ISM1 expression. **(A–F)** TGF-β, inflammatory response, IL2/STAT5, TNF-α/NF-κB, IFN-γ response, and the IL6/JAK/STAT3 signaling pathway showed higher activity scores in CRC patients overexpressing ISM1.

Supplementary Figure 5 | Expression of ISM1 in microenvironment in patients treated with immunotherapy. **(A)** Differentially expressed analysis of ISM1 in three distinct immunological phenotypes, **(B)** SD/PD patients with immune-excluded tumors vs. CR/PR patients with inflamed tumors. Complete response (CR), partial response (PR), and progressive disease (PD). $P < 0.05$ is statistically significant.

Supplementary Table 1 | Information for calculating EMT activity score across 22 cancers from TCGA.

REFERENCES

Andrysik, Z., Bender, H., Galbraith, M. D., and Espinosa, J. M. (2021). Multi-omics analysis reveals contextual tumor suppressive and oncogenic gene modules within the acute hypoxic response. *Nat. Commun.* 12:1375. doi: 10.1038/s41467-021-21687-2

Arnold, M., Sierra, M. S., Laversanne, M., Soerjomataram, I., Jemal, A., and Bray, F. (2017). Global patterns and trends in colorectal cancer incidence and mortality. *Gut* 66, 683–691. doi: 10.1136/gutjnl-2015-310912

Bai, J., Zhang, X., Shi, D., Xiang, Z., Wang, S., Yang, C., et al. (2021). Exosomal miR-128-3p Promotes Epithelial-to-Mesenchymal Transition in Colorectal Cancer Cells by Targeting FOXO4 via TGF-beta/SMAD and JAK/STAT3 Signaling. *Front. Cell Dev. Biol.* 9:568738. doi: 10.3389/fcell.2021.568738

Bray, F., Ferlay, J., Soerjomataram, I., Siegel, R. L., Torre, L. A., and Jemal, A. (2018). Global cancer statistics 2018: GLOBOCAN estimates of incidence and mortality worldwide for 36 cancers in 185 countries. *CA Cancer J. Clin.* 68, 394–424. doi: 10.3322/caac.21492

Cai, H., Chew, S. K., Li, C., Tsai, M. K., Andrejka, L., Murray, C. W., et al. (2021). A functional taxonomy of tumor suppression in oncogenic KRAS-driven lung cancer. *Cancer Discov.* doi: 10.1158/2159-8290.CD-20-1325 [Epub online ahead of print].

Coutzac, C., Jouniaux, J. M., Paci, A., Schmidt, J., Mallardo, D., Seck, A., et al. (2020). Systemic short chain fatty acids limit antitumor effect of CTLA-4 blockade in hosts with cancer. *Nat. Commun.* 11:2168. doi: 10.1038/s41467-020-16079-x

Cui, K., Liu, C., Li, X., Zhang, Q., and Li, Y. (2020). Comprehensive characterization of the rRNA metabolism-related genes in human cancer. *Oncogene* 39, 786–800. doi: 10.1038/s41388-019-1026-9

Guo, W., Keckesova, Z., Donaher, J. L., Shibue, T., Tischler, V., Reinhardt, F., et al. (2012). Slug and Sox9 cooperatively determine the mammary stem cell state. *Cell* 148, 1015–1028. doi: 10.1016/j.cell.2012.02.008

Han, W., Xie, B., Li, Y., Shi, L., Wan, J., Chen, X., et al. (2019). Orally Deliverable Nanotherapeutics for the Synergistic Treatment of Colitis-Associated Colorectal Cancer. *Theranostics* 9, 7458–7473. doi: 10.7150/thno.38081

Holmgaard, R. B., Schaer, D. A., Li, Y., Castaneda, S. P., Murphy, M. Y., Xu, X., et al. (2018). Targeting the TGFbeta pathway with galunisertib, a TGFbetaRI small molecule inhibitor, promotes anti-tumor immunity leading to durable, complete responses, as monotherapy and in combination with checkpoint blockade. *J. Immunother. Cancer* 6:47. doi: 10.1186/s40425-018-0356-4

Kim, S. K., Kim, S. Y., Kim, J. H., Roh, S. A., Cho, D. H., Kim, Y. S., et al. (2014). A nineteen gene-based risk score classifier predicts prognosis of colorectal cancer patients. *Mol. Oncol.* 8, 1653–1666. doi: 10.1016/j.molonc.2014.06.016

Kudo-Saito, C., Shirako, H., Takeuchi, T., and Kawakami, Y. (2009). Cancer metastasis is accelerated through immunosuppression during Snail-induced EMT of cancer cells. *Cancer Cell* 15, 195–206. doi: 10.1016/j.ccr.2009.01.023

Li, H., Yu, B., Li, J., Su, L., Yan, M., Zhu, Z., et al. (2014). Overexpression of lncRNA H19 enhances carcinogenesis and metastasis of gastric cancer. *Oncotarget* 5, 2318–2329. doi: 10.18632/oncotarget.1913

Li, P., Huang, T., Zou, Q., Liu, D., Wang, Y., Tan, X., et al. (2019). FGFR2 Promotes Expression of PD-L1 in Colorectal Cancer via the JAK/STAT3 Signaling Pathway. *J. Immunol.* 202, 3065–3075. doi: 10.4049/jimmunol.1801199

Lim, S., Becker, A., Zimmer, A., Lu, J., Buettner, R., and Kirfel, J. (2013). SNAI1-mediated epithelial-mesenchymal transition confers chemoresistance and cellular plasticity by regulating genes involved in cell death and stem cell maintenance. *PLoS One* 8:e66558. doi: 10.1371/journal.pone.0066558

Lim, S. O., Li, C. W., Xia, W., Cha, J. H., Chan, L. C., Wu, Y., et al. (2016). Deubiquitination and Stabilization of PD-L1 by CSN5. *Cancer Cell* 30, 925–939. doi: 10.1016/j.ccell.2016.10.010

Liu, A., Liu, L., and Lu, H. (2019). LncRNA XIST facilitates proliferation and epithelial-mesenchymal transition of colorectal cancer cells through targeting miR-486-5p and promoting neuropilin-2. *J. Cell Physiol.* 234, 13747–13761. doi: 10.1002/jcp.28054

Liu, Y., Zhou, N., Zhou, L., Wang, J., Zhou, Y., Zhang, T., et al. (2021). IL-2 regulates tumor-reactive CD8(+) T cell exhaustion by activating the aryl hydrocarbon receptor. *Nat. Immunol.* 22, 358–369. doi: 10.1038/s41590-020-00850-9

Mani, S. A., Guo, W., Liao, M. J., Eaton, E. N., Ayyanan, A., Zhou, A. Y., et al. (2008). The epithelial-mesenchymal transition generates cells with properties of stem cells. *Cell* 133, 704–715. doi: 10.1016/j.cell.2008.03.027

Mariathasan, S., Turley, S. J., Nickles, D., Castiglioni, A., Yuen, K., Wang, Y., et al. (2018). TGFbeta attenuates tumour response to PD-L1 blockade by contributing to exclusion of T cells. *Nature* 554, 544–548. doi: 10.1038/nature25501

Matsuyama, T., Ishikawa, T., Takahashi, N., Yamada, Y., Yasuno, M., Kawano, T., et al. (2019). Transcriptomic expression profiling identifies ITGBL1, an epithelial to mesenchymal transition (EMT)-associated gene, is a promising recurrence prediction biomarker in colorectal cancer. *Mol. Cancer* 18:19. doi: 10.1186/s12943-019-0945-y

Morel, A. P., Lièvre, M., Thomas, C., Hinkal, G., Ansieau, S., and Puisieux, A. (2008). Generation of breast cancer stem cells through epithelial-mesenchymal transition. *PLoS One* 3:e2888. doi: 10.1371/journal.pone.0002888

Osório, L., Wu, X., and Zhou, Z. (2014). Distinct spatiotemporal expression of ISM1 during mouse and chick development. *Cell Cycle* 13, 1571–1582. doi: 10.4161/cc.28494

Piawah, S., and Venook, A. P. (2019). Targeted therapy for colorectal cancer metastases: a review of current methods of molecularly targeted therapy and the use of tumor biomarkers in the treatment of metastatic colorectal cancer. *Cancer* 125, 4139–4147. doi: 10.1002/cncr.32163

Schoonderwoerd, M. J. A., Koops, M. F. M., Angela, R. A., Koolmoes, B., Toitou, M., Paauwe, M., et al. (2020). Targeting Endoglin-Expressing Regulatory T Cells in the Tumor Microenvironment Enhances the Effect of PD1 Checkpoint Inhibitor Immunotherapy. *Clin. Cancer Res.* 26, 3831–3842. doi: 10.1158/1078-0432.CCR-19-2889

Shen, C. J., Chang, K. Y., Lin, B. W., Lin, W. T., Su, C. M., Tsai, J. P., et al. (2020). Oleic acid-induced NOX4 is dependent on ANGPTL4 expression to promote human colorectal cancer metastasis. *Theranostics* 10, 7083–7099. doi: 10.7150/thno.44744

Shen, M., Zhang, Z., and Wang, P. (2021). GLI3 Promotes Invasion and Predicts Poor Prognosis in Colorectal Cancer. *Biomed. Res. Int.* 2021:8889986. doi: 10.1155/2021/8889986

Shi, H., Liu, C., Tan, H., Li, Y., Nguyen, T. M., Dhungana, Y., et al. (2018). Hippo Kinases Mst1 and Mst2 Sense and Amplify IL-2R-STAT5 Signaling in Regulatory T Cells to Establish Stable Regulatory Activity. *Immunity* 49, 899–914.e6. doi: 10.1016/j.immuni.2018.10.010

Shibue, T., and Weinberg, R. A. (2017). EMT, CSCs, and drug resistance: the mechanistic link and clinical implications. *Nat. Rev. Clin. Oncol.* 14, 611–629. doi: 10.1038/nrclinonc.2017.44

Singh, M., Yelle, N., Venugopal, C., and Singh, S. K. (2018). EMT: mechanisms and therapeutic implications. *Pharmacol. Ther.* 182, 80–94. doi: 10.1016/j.pharmthera.2017.08.009

Subramanian, A., Tamayo, P., Mootha, V. K., Mukherjee, S., Ebert, B. L., Gillette, M. A., et al. (2005). Gene set enrichment analysis: a knowledge-based approach for interpreting genome-wide expression profiles. *Proc. Natl. Acad. Sci. U. S. A.* 102, 15545–15550. doi: 10.1073/pnas.0506580102

Sveen, A., Kopetz, S., and Lothe, R. A. (2020). Biomarker-guided therapy for colorectal cancer: strength in complexity. *Nat. Rev. Clin. Oncol.* 17, 11–32. doi: 10.1038/s41571-019-0241-1

Tang, Z., Li, C., Kang, B., Gao, G., Li, C., and Zhang, Z. (2017). GEPIA: a web server for cancer and normal gene expression profiling and interactive analyses. *Nucleic Acids Res.* 45, W98–W102. doi: 10.1093/nar/gkx247

Valle-Rios, R., Maravillas-Montero, J. L., Burkhardt, A. M., Martinez, C., Buhren, B. A., Homey, B., et al. (2014). Isthmin 1 is a secreted protein expressed in skin, mucosal tissues, and NK, NKT, and th17 cells. *J. Interferon Cytokine Res.* 34, 795–801. doi: 10.1089/jir.2013.0137

Wang, H., Song, X., Liao, H., Wang, P., Zhang, Y., Che, L., et al. (2020). Overexpression of SMAD7 activates the YAP/NOTCH cascade and promotes liver carcinogenesis in mice and humans. *Hepatology* doi: 10.1002/hep.31692 [Epub online ahead of print].

Wang, Y., Wang, T., Ding, M., Xiang, S., Shi, M., and Zhai, B. (2019). hsa_circ_0091570 acts as a ceRNA to suppress hepatocellular cancer progression by sponging hsa-miR-1307. *Cancer Lett.* 460, 128–138. doi: 10.1016/j.canlet.2019.06.007

Yang, J., Antin, P., Berx, G., Blanpain, C., Brabletz, T., Bronner, M., et al. (2020). Guidelines and definitions for research on epithelial-mesenchymal transition. *Nat. Rev. Mol. Cell Biol.* 21, 341–352. doi: 10.1038/s41580-020-0237-9

Yu, G., Wang, L. G., Han, Y., and He, Q. Y. (2012). clusterProfiler: an R package for comparing biological themes among gene clusters. *OMICS* 16, 284–287. doi: 10.1089/omi.2011.0118

Zhang, H., Wang, R., and Wang, M. (2019). miR-331-3p suppresses cell invasion and migration in colorectal carcinoma by directly targeting NRP2. *Oncol. Lett.* 18, 6501–6508. doi: 10.3892/ol.2019.11029

Zheng, Y., Zheng, Y., Lei, W., Xiang, L., and Chen, M. (2019). miR-1307-3p overexpression inhibits cell proliferation and promotes cell apoptosis by targeting ISM1 in colon cancer. *Mol. Cell. Probes* 48:101445. doi: 10.1016/j.mcp.2019.101445

Conflict of Interest: The authors declare that the research was conducted in the absence of any commercial or financial relationships that could be construed as a potential conflict of interest.

frontiers in Oncology

ORIGINAL RESEARCH
published: 10 August 2021
doi: 10.3389/fonc.2021.712765

Mutational Analysis of PBRM1 and Significance of PBRM1 Mutation in Anti-PD-1 Immunotherapy of Clear Cell Renal Cell Carcinoma

Abudureyimujiang Aili[1], *Jie Wen*[1], *Lixiang Xue*[1,2*] *and Junjie Wang*[1*]

[1] Department of Radiation Oncology, Peking University Third Hospital, Beijing, China, [2] Institute of Medical Innovation and Research, Peking University Third Hospital, Beijing, China

OPEN ACCESS

Edited by:
Hengyu Li,
Second Military Medical University, China

Reviewed by:
Yuyan Zhu,
The First Affiliated Hospital of China Medical University, China
Jinyang Li,
The Rockefeller University, United States
Wen-Hao Xu,
Fudan University, China

***Correspondence:**
Junjie Wang
junjiewang_edu@sina.cn
Lixiang Xue
lixiangxue@bjmu.edu.cn

Specialty section:
This article was submitted to Molecular and Cellular Oncology, a section of the journal Frontiers in Oncology

Received: 21 May 2021
Accepted: 23 July 2021
Published: 10 August 2021

Citation:
Aili A, Wen J, Xue L and Wang J (2021) Mutational Analysis of PBRM1 and Significance of PBRM1 Mutation in Anti-PD-1 Immunotherapy of Clear Cell Renal Cell Carcinoma. Front. Oncol. 11:712765. doi: 10.3389/fonc.2021.712765

Renal cell carcinoma is a common solid tumor. PBRM1 is one of the most mutation-prone genes in clear cell renal cell carcinoma (ccRCC) with the occurrence of mutation in 40% of ccRCC patients. Mutations in PBRM1 have been correlated with the efficacy of immunotherapy. However, the mutation types of PBRM1 are not well characterized. The effects of PBRM1 expression levels in the tumor microenvironment are not well studied. In addition, the mechanism and effect of anti-PD-1 immunotherapy in ccRCC tumor microenvironments are not well clarified. In this study, using bioinformatics methods we analyzed the alternation frequency and expression levels of PBRM1 in various tumors. Next, we experimentally validated their expression levels in ccRCC tissues from human and mouse models. We attempted to clarify the mechanisms of anti-PD-1 immunotherapy in ccRCC with various PBRM1 expression levels. Our results showed that deficiency of PBRM1 protein is correlated with CD4 T cell reduction in human and mouse ccRCC tissues. We also showed that anti-PD-1 Immunotherapy can increase the infiltration of T cells in both PBRM1 high and PBRM1 low tumors but to different degrees. Our study indicates that the reduction of CD4 cells in tumor tissues with low expression of PBRM1 may explain the compromised efficacy of anti-PD-1 immunotherapy in patients with PBRM1 mutated ccRCC. Our study sheds light on the potential of PBRM1 as a therapeutic target in ccRCC.

Keywords: PBRM1 mutation, PBRM1 expression, clear cell renal cell carcinoma, anti-PD-1 immunotherapy, CD4 T cell

Abbreviations: TCGA, The Cancer Genome Atlas; RCC, renal cell carcinoma; ccRCC, clear cell renal cell carcinoma; KIRC, Kidney renal clear cell carcinoma; BRCA, breast invasive carcinoma; COAD, colon adenocarcinoma; LUAD, lung adenocarcinoma; OS, overall survival; DFS, disease free survival; TME, tumor microenvironment.

INTRODUCTION

Renal cell carcinoma(RCC) is a common solid tumor (1) and 75% of RCC is clear cell renal cell carcinoma (ccRCC) (2). Most ccRCC have mutations in genes including VHL, PBRM1, SETD2, etc. (1, 3). Among them, the mutation rate of PBRM1 in ccRCC is about 40% (4). It has been reported that PBRM1 gene encodes the BAF180 protein which is required for the stability of the SWI/SNF chromatin remodeling complex SWI/SNF-B (PBAF) (5). The importance of a gene depends on its function. Functional studies showed that PBRM1 mutation caused genomic instability (6, 7). PBRM1 knockdown has been shown to result in a significant increase in proliferation of RCC cells (8) and loss of PBRM1 contributes to tumor grade in mice (9). It is worth mentioning that VHL mutation is one of the key factors causing ccRCC (10) and PBRM1 restrains VHL loss-driven ccRCC but mutation of the PBRM1 gene alone does not cause ccRCC (11).

Mutation in PBRM1 has been shown to correlate with the clinical benefit of anti-PD-1 therapy (12, 13). However, the characteristics of PBRM1 mutation types are not well studied. Besides, the mechanisms of how PBRM1 mutation affects the tumor microenvironment (TME) and immunotherapies are unclear. It has been reported that the absence or mutation of some genes in tumors may affect tumor-infiltrating T cells (14). The numbers and function of tumor-infiltrating effector T cells are strongly associated with the efficacy of immunotherapy (15). Generally, the higher the number of immune infiltrating effector T cells, the more effective the treatment with immune checkpoint inhibitors (15). Therefore, it is necessary to explore the alternations that occur in PBRM1 and the changes that mutations of PBRM1 cause in tumors. This facilitates the discovery of the features of PBRM1 and it is beneficial to explore its therapeutic targets.

In this study, we analyzed the potential alternations of PBRM1 gene in various tumors using bioinformatics methods and tools. The results showed that PBRM1 is susceptible to mutations in various tumors including ccRCC. We tested its expression levels in different tumors and analyzed the effects on the tumor stages and survival rates. Our results showed that PBRM1 expression is significantly lower in stage IV tumors compared to stage I tumors of ccRCC. We found that mutation, deep deletion and amplification are the three most common types of alternation in the PBRM1 gene. We clarified its mutation types in ccRCC and analyzed the protein-protein interaction network of PBRM1. In addition, we found that mutation or deficiency of PBRM1 protein correlates with CD4 T cell reduction in human and mouse ccRCC tissues. Anti-PD-1 Immunotherapy increase the infiltration of T cells in both high PBRM1 and low PBRM1 tumors but with different levels. This may explain the previous findings that PBRM1 deficiency affects anti-PD-1 therapy (12). Based on our experimental results, we hypothesized that PBRM1 may affect the chemokines that attract T cells to the tumor microenvironment. Further exploration results showed that expression levels of CXCL10, CCL12, ICAM1 and other cell migration-related molecules were decreased. This study explored deeper features of PBRM1 in tumors and shed light on the significance and prospects of PBRM1 to be a potential target in ccRCC.

MATERIALS AND METHODS

Mice

Female BALB/c mice 6–8 weeks of age were purchased from Vital River Lab Animal Technology Company (Beijing, China). All mice were housed and bred in the Peking University Health Science Center animal breeding facilities (Beijing, China) under specific pathogen-free (SPF) conditions. All animal experiments were carried out following the National Institutes of Health guide for the care and use of laboratory animals (NIH Publications No. 8023, revised 1978) and were approved by the Peking University Health Science Center ethics committee.

Tumor Cells

Mouse ccRCC cell line Renca was purchased from ATCC and maintained in RPMI-1640 containing 10% fetal bovine serum, non-essential amino acids (NEAA), and sodium pyruvate according to the ATCC instruction at 37°C with 5% CO_2. PBRM1 knockdown Renca cells were gained using shRNA lentiviral particles (GIDL019025, GENECHEM). Knockdown of PBRM1 was performed as described previously (16).

In Vivo Murine Experiments

5×10^5 Renca cells were suspended in 100 μl Matrigel Matrix (BD PharMingen) diluted with sterile PBS at 1:1, and subcutaneously injected into the backs of BALB/c mice.

Anti-PD-1 immunotherapy in mice was performed as described (17, 18) with some modifications. In brief, anti-PD-1 antibody (RMP1-14, BioXcell) and control antibody were administered on days 6(200μg), 9(100μg), and 12(100μg) post-tumor injection. Mice were sacrificed for analysis 39 days post-tumor injection. Tumors were measured by caliper every 3days and tumor volume calculated as length x width^2 x0.52. At the time of sacrifice for analysis mice were euthanized and subsequent cervical dislocation.

Antibodies and Reagents

For flow cytometry and FACS purification of tumor-infiltrating T cell subsets, the following fluorochrome-conjugated antibodies were used. Anti-CD45, anti-CD3, anti-CD4, anti-CD8, anti-PD-1 were purchased from Biolegend (San Diego, CA). For western-blot anti-PBRM1 (D3F7O, CST) and anti-β-actin (13E5, CST) were used. For multiplex immunohistochemistry assay anti-PBRM1 (D3F7O, CST), anti-CD4 (SP35, Maixin), anti-CD8 (SP16, Maixin) were used.

Opal Multiplex Immunohistochemistry

The human ccRCC detection protocol was approved by Peking University Third Hospital. Human ccRCC Tissue microarrays (TMAs) were generated by OUTDO Biotech (Shanghai, China). The protocol was performed as described previously (12). In brief, TMAs were multiplex immunohistochemically stained

(PBRM1, 690; CD4, 540; CD8, 570) and scanned with the Vectra image scanning system (Caliper Life Sciences). Data were analyzed using inForm Tissue Finder software (Caliper Life Sciences).

Statistical Analysis

The student's unpaired t-test was used for comparing two groups. For survival analyses, Kaplan-Meier survival curves were used and compared using the log-rank test. Data were analyzed with GraphPad Prism 8.0.2. *P<0.05; **P<0.01; ***P<0.001; ns, no significance.

RESULTS

PBRM1 Is Differentially Expressed in Various Tumors

We used the TIMER database to analyze the cancer data in The Cancer Genome Atlas (TCGA) database for PBRM1 expression levels. As shown in **Figure 1A**, in bladder urothelial carcinoma (BLCA), breast invasive carcinoma (BRCA), colon adenocarcinoma (COAD), lung adenocarcinoma (LUAD), kidney renal clear cell carcinoma (KIRC, ccRCC), kidney renal papillary cell carcinoma (KIRP) tumors, there was a significant decrease in the expression level of PBRM1 RNA in cancers compared with normal tissues. Immediately afterward, we used the CPTAC database to validate PBRM1 protein levels in these tumors with differential expression levels (**Figure 1B**). In contrast to the RNA data of TCGA (**Figure 1A**), the expression levels of PBRM1 protein in BRCA, COAD, and LUAD showed a significant difference in the CPTAC database (**Figure 1B**). The results showed that PBRM1 protein level is lower expressed in tumor tissues than in normal tissues only in ccRCC. Next, we analyzed the correlations between tumor grades and PBRM1 expression level (**Figure 1C**). The results showed that the expression level of PBRM1 was lower in COAD in stage IV. In ccRCC, the expression level of PBRM1 showed a decreasing trend with an increasing stage (**Figure 1C**). To further validate, we tested the samples of human ccRCC in Stage I and Stage IV by immunohistochemistry assay in our lab. It showed that PBRM1 was significantly lower in the Stage IV samples (**Figure 1D**). These results suggest that the expression level of PBRM1 varies in different tumors.

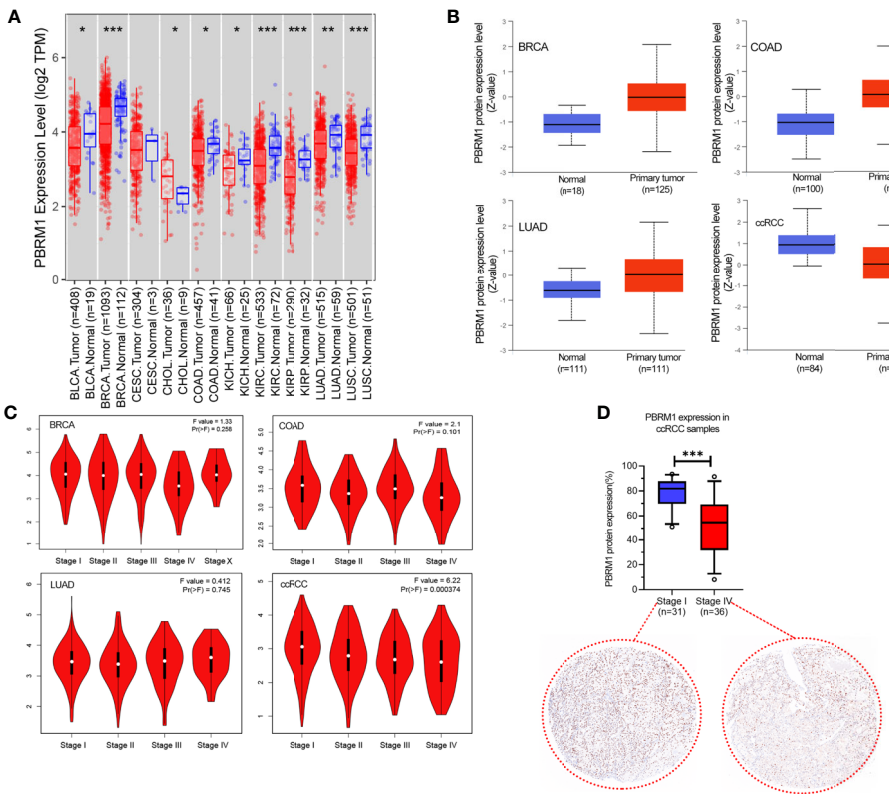

FIGURE 1 | The expression level of PBRM1 varies in different tumors and tumor stages. **(A)** The expression status of the PBRM1 gene in diverse cancer types were analyzed through the TIMER dataset. *P < 0.05; **P < 0.01; ***P < 0.001. **(B)** Based on the CPTAC dataset, the expression level of PBRM1 total protein between normal tissues and primary tumor tissues of breast invasive carcinoma (BRCA), colon adenocarcinoma (COAD), lung adenocarcinoma (LUAD), and kidney renal clear cell carcinoma (KIRC, ccRCC) were analyzed. **(C)** Based on the TCGA data, the expression levels of the PBRM1 gene were analyzed by the main pathological stages (stage I, stage II, stage III, and stage IV) of BRCA, COAD, LUAD, ccRCC. Log2 (TPM+1) was applied for log-scale. **(D)** PBRM1 protein expression levels in Stage I and Stage IV of our ccRCC samples. The expression levels were detected using immunohistochemistry and analyzed by unpaired t-test.

PBRM1 Is Susceptible to Truncating Mutations in ccRCC

To explore the deeper features of alternations of PBR1M, RNA-Seq datasets with corresponding clinical profiles were downloaded from the TCGA database. We used the cBioPortal for Cancer Genomics website (http://www.cbioportal.org) to analyze PBRM1 mutation types in tumors from the TCGA dataset. We found that PBRM1 gene was mutated in a variety of tumors (**Figure 2A**). Interestingly, PBRM1 had the highest probability of mutation in ccRCC (**Figure 2A**). In ccRCC, the most frequent mutation type was truncating mutation (**Figure 2B**). Mutated protein structures may be used to design targeted drugs (19). Thus, we analyzed one of the frequent mutation sites using the cBioPortal website and showed the 3D structure of the site (**Figure 2C**). In addition to considering PBRM1 as a therapeutic target, we can also consider molecules that interact with it as targets. Next, we analyzed the proteins interacting with PBRM1 using STRING (https://string-db.org/cgi/). The top 10 experimentally determined genes ranked by degree were shown (**Figure 2D**). Taken together, these results demonstrated the features of PBRM1 mutations in different tumors and revealed the protein features and protein-protein interaction network of PBRM1. These results revealed the sites of PBRM1 as a potential target.

PBRM1 Expression Correlates With Tumor Stage and Overall Survival

As it's shown above, we analyzed the features of PBRM1 at the molecular level. It demonstrates the potential of PBRM1 as a target. But before treating it as a target, we have to further validate its impact in the clinic.

Next, using the TCGA database, we analyzed the effect of low PBRM1 expression on the overall survival (OS) of BRCA, COAD, LUAD, and KIRC patients with high or low PBRM1 expression levels. The results showed that PBRM1 expression had little effect on overall survival (OS) in the BRCA, LUAD patients (**Figure 3A**). Meanwhile, in the KIRC patients, the patients with high PBRM1 expression had a significantly higher OS (**Figure 3A**). But in the COAD patients, high PBRM1 expression correlates with lower OS (**Figure 3A**). Then we validated the impact of PBRM1 on disease-free survival (DFS) of those patients. In BRCA and COAD patients, lower PBRM1 expression means longer DFS (**Figure 3B**). No significant differences were found in LUAD. However, in the KIRC, lower PBRM1 expression means lower DFS in 80 and 120 months (**Figure 3B**). Finally, we tested the OS of KIRC patients considering PBRM1 expression and tumor grade at the same time. We found that combination analysis predicts the prognosis of ccRCC patients more accurately (**Figure 3C**). These results suggested that the expression level of PBRM1 had an inconsistent effect on survival in different tumors. In ccRCC, low expression of PBRM1 and high tumor grade imply a worse prognosis. It implies that ccRCC patients may benefit from treatment targeting PBRM1.

PBRM1 Expression Correlates With CD4 Infiltration in Human ccRCC

To further investigate the influence of PBRM1 mutations in the tumor microenvironment (TME), we performed a correlation

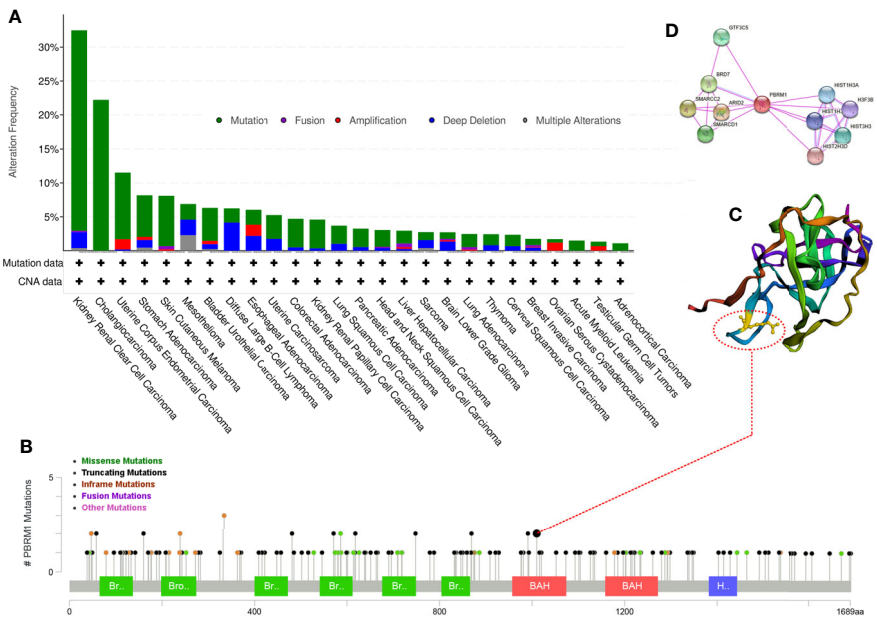

FIGURE 2 | Mutation frequency of PBRM1 in tumors reproduced from the Cancer Genome Atlas (TCGA) database. **(A)** Alternation frequency of PBRM1 in various tumors are shown. **(B)** Mutation types of PBRM1 in ccRCC are shown. **(C)** 3D structure of PBRM1 and the mutation cite is shown. **(D)** Protein-protein interaction network of PBRM1 are shown. The top 10 experimentally determined genes ranked by degree are shown.

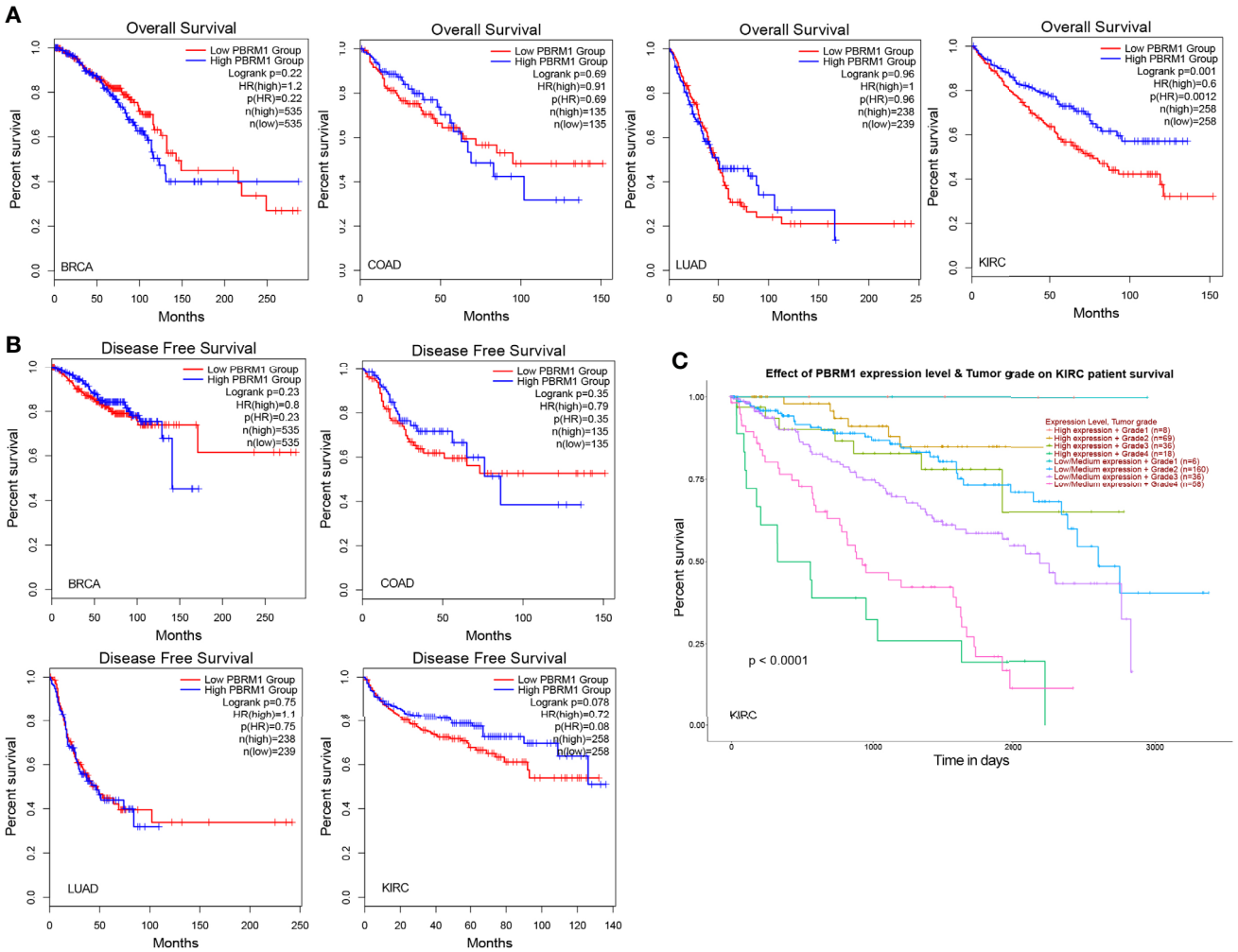

FIGURE 3 | The mutation of PBRM1 affects the survival rates of patients. Overall survival **(A)** and disease-free survival **(B)** of PBRM1 high and PBRM1 low patients in different tumors. GEPIA2 tool was used to analyze the TCGA dataset. BRCA, breast invasive carcinoma; COAD, colon adenocarcinoma; LUAD, lung adenocarcinoma; KIRC, kidney renal clear cell carcinoma (ccRCC). **(C)** Overall survival of KIRC (ccRCC) patients based on the PBRM1 expression level and tumor grade. Kaplan-Meier curves with positive results are given.

analysis of PBRM1 expression levels with CD4 and CD8 cell infiltration using the TIMER database. The analysis showed that CD4 cells positively correlated with the expression levels of PBRM1 in human ccRCC (**Figure 4A**). Meanwhile, the relevance of CD8 cells was not as strong as CD4 cells (**Figure 4A**). To confirm these results, we performed Opal multiplex immunohistochemistry assay of 180 human ccRCC samples. The expression levels of PBRM1 in tumors were classified to High (expression >80%), Medium (expression 50-60%) and Low (expression<20%) groups (**Figure 4B**). We analyzed the number of CD4 and CD8 cells in tumors with different PBRM1 expression levels. We found that in human ccRCC higher level of PBRM1 correlates with more CD4 T cells (**Figure 3C**). Moreover, there was a significant difference in the numbers of CD4 cells between the PBRM1 High group and the PBRM1 Low group (**Figure 4C**). The numbers of CD8 cells also showed a significant difference between the two groups of samples. These results confirmed that PBRM1 mutation affected the tumor microenvironment in human ccRCC.

PBRM1 Knockdown in Mouse ccRCC Model Mimics PBRM1 Mutation in Human ccRCC

To explore the effects of PBRM1 mutation on tumor cells and TME, we set up a mouse ccRCC model using the Renca cell line. The Renca is a spontaneous malignancy cell type that originated from the Balb/c mouse (20). RNA (data not shown) and protein level analysis showed that Renca has normal expression level of PBRM1 (Shown as PBRM1 High in the **Figure 5A**). Therefore, we used short hairpin RNA (shRNA) to knock down PBRM1 molecule (PBRM1 Low) (**Figure 5A**). After knocking down PBRM1, we tested the biological characteristics of the cells and observed similar results as previous studies (21). To get the

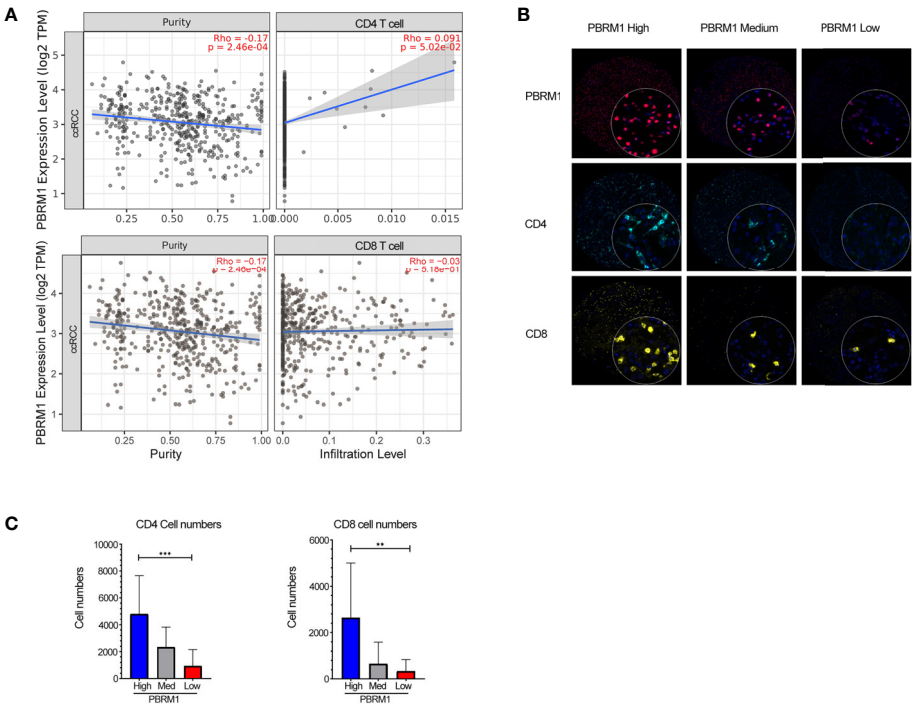

FIGURE 4 | Low expression of PBRM1 correlates with decreased CD4 cells in human ccRCC. **(A)** The correlation of PBRM1 expression with CD4, CD8 within tumors from 533 ccRCC patients were analyzed using the TIMER database. **(B)** Opal Multiplex Immunohistochemistry detection of PBRM1, CD4, CD8 in human ccRCC samples.180 ccRCC samples were tested and classified as High (>80%), Medium (50-60%), Low (<20%) according to the expression level of PBRM1 in the tumor tissues. **(C)** Represents the numbers of CD4, CD8 cells in **(B)**. PBRM1 High, PBRM1 Low groups were calculated by unpaired t-test, $^{**}P < 0.01$; $^{***}P < 0.001$. Data indicates Mean+SD.

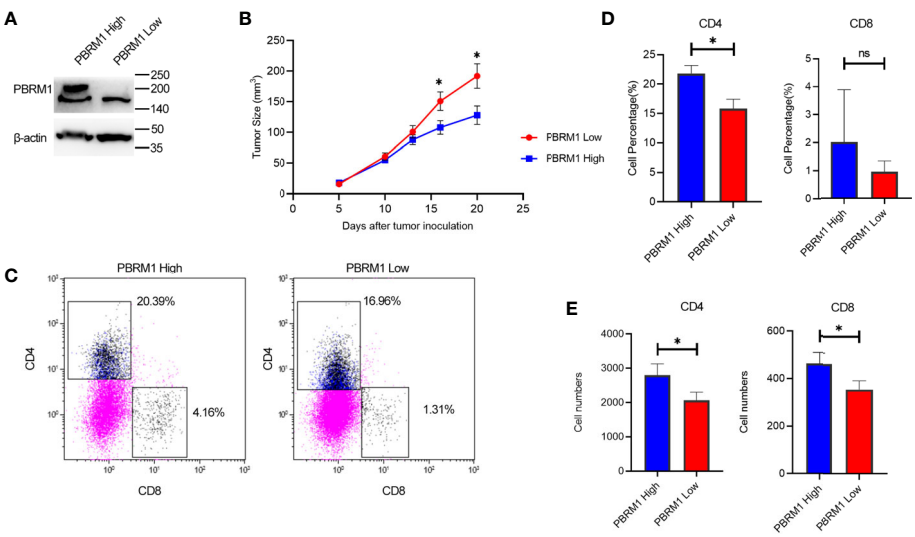

FIGURE 5 | Low expression of PBRM1 causes reduction of tumor-infiltrating CD4 cells in ccRCC mouse model. **(A)** PBRM1 protein expression level in PBRM1 high and PBRM1 low Renca cells were detected by western blot. PBRM1 low Renca cells were obtained using shRNA to PBRM1. β-actin was used as an internal control. **(B)** Growth curves of PBRM1 High and PBRM1 Low tumors in ccRCC mouse model. **(C)** Flow cytometry image of tumor-infiltrating T cells. TIL cells were isolated from tumors and gated $CD45^+$ $CD3^+$cells. Percentage **(D)** and absolute numbers **(E)** of CD4 and CD8 cells in tumors of PBRM1 High and PBRM1 Low mice model. CD4 andCD8 cells gated in $CD45^+$ $CD3^+$ cells. Data represents 3 independent experiments at least 6 mice per group. $^*P < 0.05$; ns, no significance.

ccRCC mouse model, Renca cells were injected subcapsular. The tumor growth and the survival rate of the mice were observed (**Figure 5B**). After euthanasia, tumor-infiltrating lymphocytes were obtained and counted by flow cytometry for the ratio and number of CD4, CD8 T cells (**Figure 5C**). The results showed that in the PBRM1 Low group, the percentage of CD4 cells was about 15.84%; but in the PBRM1 High group, the percentage of CD4 cells was as high as 21.82% (**Figure 5D**). Moreover, the number of CD8 cells was lower in the PBRM1 Low group. Next, we quantified the absolute number of CD4 and CD8 cells with flow cytometry. We found that the number of CD4 cells was lower in the PBRM1 Low group (**Figure 5E**). Our results concluded that decreased PBRM1 expression levels not only lead to the reduction of CD4 and CD8 cells but also to a decrease in the absolute numbers of CD4, CD8 cells.

These data indicated that, PBRM1 deletion causes a decrease in CD4 cells in the tumor microenvironment of ccRCC.PBRM1 knockdown in mouse ccRCC model mimicked PBRM1 mutation in human ccRCC and this mouse model can be used for further research on the precise mechanisms and therapeutic pathways.

PBRM1 Expression Level Affects Anti-PD-1 Immunotherapy Efficiency

The findings above suggest that the deficiency of PBRM1 causes immune cell alterations in the TME. It is known that immune cell alterations in the TME of other tumors affect anti-PD-1 immunotherapy (22–24). Thus, we hypothesized that in mouse models, PBRM1 expression levels affects anti-PD-1 immunotherapy. Besides, we wanted to study the mechanisms and effects of anti-PD-1 immunotherapy in ccRCC mouse model. To test our speculation, we performed anti-PD-1 immunotherapy experiments in mice with ccRCC (**Figure 6A**). The results showed that the deletion of PBRM1 affects anti-PD-1 immunotherapy (**Figure 6B**). Tumor growth was significantly inhibited in mice receiving immunotherapy. PBRM1 High mice showed better efficacy in immunotherapy compared to PBRM1 Low mice. Tumors were better suppressed in PBRM1 High mice. Tumor growth was fastest in mice with PBRM1 Low that did not receive PD-1 treatment. Survival curves also showed that anti-PD-1 treatment significantly improved the survival rate of mice (**Figure 6C**).

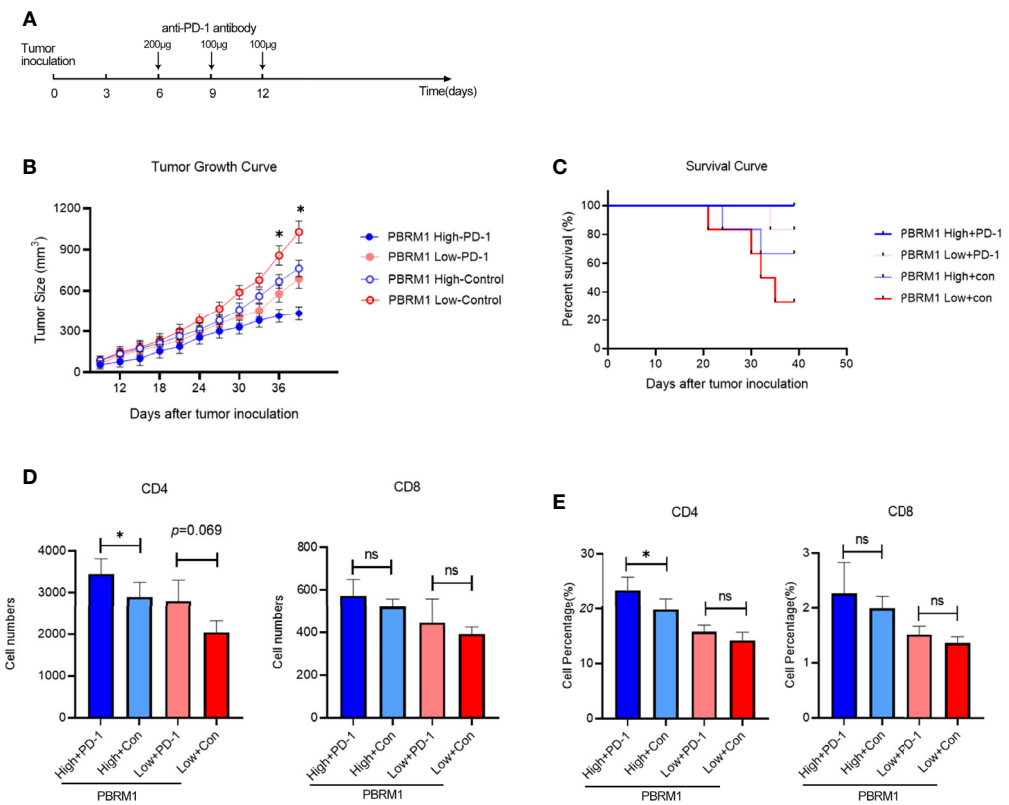

FIGURE 6 | Anti-PD-1 immunotherapy increased CD4 T cell infiltration in ccRCC mouse model. **(A)** Treatment scheme of anti-PD-1 immunotherapy in ccRCC mouse model. Anti-PD-1 antibody and control antibody were administrated at day 6, day 9, and day 12 after tumor inoculation. **(B)** Growth curves of PBRM1 High and PBRM1 Low tumors treated with anti-PD-1 antibody or control isotype antibody in ccRCC mouse model. Test was stopped when mice died or tumors reached 1000mm^3 in size. **(C)** Survival rates of mice in different groups. Data were analyzed with GraphPad Prism 8.0.2. Absolute cell numbers **(D)** and percentages **(E)** of CD4 and CD8 T cells in tumors of different groups were shown. All live mice were euthanized at day39 and tumor infiltrating T cells were detected by Flow Cytometry. Data are presented as mean ± SD with at least 6 mice for each group. *p < 0.05; ns, no significance.

Anti-PD-1 Immunotherapy Increased CD4 T Cell Infiltration in ccRCC

We continued to observe the status of the TME after the immunotherapy was completed. To comply with the experimental ethics and animal welfare, we ended the observation when the tumor grew to 1000mm^3 at day39. Tumor infiltrating T cells were detected with flow cytometry. The results showed that anti-PD-1 immunotherapy increases CD4 T cells in both PBRM1 High and PBRM1 Low groups (**Figures 6D, E**). The deficiency of PBRM1 was associated with a decrease in CD4 and CD8 cells (**Figures 5D, E**). After anti-PD-1 treatment, there was some minor but not significant increase in CD4 and CD8 cells in PBRM1-deficient tumors. However, the PBRM1 High group resulted in a significant increase in CD4 cells after immunotherapy (**Figure 6D**).

The above results showed that the expression level of PBRM1 correlates with the efficiency of anti-PD-1 immunotherapy, and a high expression level of PBRM1 implied a better effectiveness of anti-PD-1 immunotherapy. We found that tumor infiltrating T cells were increased after anti-PD-1 immunotherapy. The increase in the number of infiltrating CD4 and CD8 cells in the TME after anti-PD1 immunotherapy may be one of the mechanisms by which immunotherapy works in ccRCC.

DISCUSSION

Understanding genetic and epigenetic alterations in cancer can identify new disease mechanisms (25) and new therapeutic targets (26). PBRM1 is one of the most frequently mutated genes in ccRCC (3, 27). But its features of genetic and epigenetic alternations, protein-protein interaction network and the consequences caused by the mutation in the tumors are not well studied. One of the consequences caused by the mutation is that TME alters and may affect the mechanisms of immunotherapy.

To explore the role and commonality of PBRM1 on tumor cells, we analyzed the genetic alternation frequency of PBRM1 in various tumors using bioinformatic methods. The results showed that PBRM1 alters in various tumors. We verified the changes in PBRM1 expression levels in several other tumors, which also showed reduced PBRM1 expression levels in ccRCC, BLCA, BRCA, COAD, LUAD, and other tumors (**Figure 1A**). However, after deeper investigation, we found that there was only a difference at the RNA level, but not at the protein level in most of the tumors (**Figure 1B**). But in ccRCC, both RNA and protein levels were lower in tumor than normal tissue. We validated its expression level in ccRCC tissues derived from human. The results showed that PBRM1 was significantly lower in stage IV tumors than stage I tumors (**Figure 1D**). These results drove us to investigate the features of PBRM1 more deeply. After intensive research, we found that mutation, deep deletion and amplification were the three most common types of alternation in PBRM1 gene (**Figure 2A**). Truncation mutations and missense mutations of PBRM1 are very common in ccRCC (**Figure 2B**). These features may be considered when PBRM1 became a direct target of therapy. In order to validate the signaling pathway of PBRM1, we looked up the protein interaction network of the PBRM1. PBRM1 prefers to interact with DNA-binding or chromatin remodeling proteins such as ARID2, SMARCC2, and BRD7 (**Figure 1D**). These results indicate that mutations in PBRM1 are correlated with genome stability, and alternation in the genomic stability has been considered as a cause of cancer (28, 29). But mutations in PBRM1 alone did not cause ccRCC or other cancers (11).

However, mutations in PBRM1 have showed a negative impact on patient survival in ccRCC and BRCA (30–32).By comparing the effects of PBRM1 on OS and DFS in different tumors, we found that PBRM1 has significantly greater effects on ccRCC than in other tumors (**Figure 3A**). Some investigators have proposed PBRM1 as a target for therapy (33). However, these studies did not clarify the specific mechanism of how PBRM1 affects tumor progression or patient survival. This is partly because previous studies of ccRCC have focused more on the roles of the VHL gene in ccRCC (34, 35). The effects of PBRM1 deletion on tumor cells have been studied in human ccRCC tumor cell lines (36), but these experiments were *in vitro* and detached from the tumor microenvironment *in vivo*. Besides, animal models emerged relatively late (37). Therefore, relatively few studies have investigated the effects of gene mutations in ccRCC on the tumor microenvironment.

In our research, we used the Renca subcutaneous model to investigate the effects of PBRM1 in the ccRCC tumor microenvironment (38). PBRM1 high and PBRM1 low cell lines were obtained and inoculated into the flank of immunocompetent BALB/C mice to create a subcutaneous model. In this regard, the results of our model are closer to the environment *in vivo* compared to *in vitro* experiments. But there is also a disadvantage that this is not a spontaneous tumor model or an orthotopic model. It may not fully mimic the human RCC. However, it is sufficient to study the effect of PBRM1 on cancer cells and the tumor microenvironment (37). Our results show that knockdown of PBRM1 in tumor cells causes the reduction of CD4 T cells in the tumor microenvironment. The numbers of CD4 T cells in the tumor microenvironment are related to the efficacy of PD-1 therapy (39). The efficacy of anti-PD-1 immunotherapy will be better if more CD4 cells are available in TME (40, 41). From this perspective, our results may explain the previous findings that PBRM1 deficiency affects anti-PD-1 therapy (12). Our anti-PD-1 immunotherapy experiments showed that PBRM1 expression have impacts on the immunotherapy. Anti-PD-1 immunotherapy can additionally increase the numbers of CD4 and CD8 T cells in PBRM1 high expressed TME (**Figure 6D**).

Chemokines are one of the factors that are influencing tumor-infiltrating immune cells and tumor immunotherapy in the tumor microenvironment (42, 43). Studies have shown that cancer cells can change the immune landscape by secreting chemokines in ccRCC (44).Based on the above results, we hypothesized that PBRM1 may affect the chemokines that attract T cells to the tumor microenvironment. And further

exploration results showed that expression levels of CXCL10 and other cell migration-related molecules were decreased (**Figures S1B, D**). CXCL10 is a chemokine that is involved in attracting CD4 and CD8 cells to the tumor microenvironment in a variety of tumors (43, 45). Based on these facts, it is reasonable to assume that reduction of CXCL10 expression levels in PBRM1 low tumors is one of the factors that is responsible for the reduction of T-cell infiltration. At the same time, we also observed alterations in several other genes and signaling pathways in PBRM1 low tumors (**Figures S1A, C**). Therefore, the exact relationship between the reduction of CD4 cells after PBRM1 deficiency and increase of T cells after anti-PD-1 treatment needs to be further studied.

In conclusion, our work has made three main advances. First of all, we showed RNA and protein levels of PBRM1 in different tumors and the mutation loci of PBRM1 in the ccRCC. This revealed the deeper features of PBRM1 and potentiality of being a therapeutic target in molecular level. Secondly, we analyzed and experimentally proved the variation of PBRM1 protein expression levels within tumors. We also showed that the PBRM1 expression level combined with tumor stage can more accurately reflect the survival rate. This demonstrated the clinical significance of PBRM1 as a target therapy. Thirdly, we have validated the effects of PBRM1 mutations or decreased expression levels on the TME using human and animal samples. We also reported anti-PD-1 immunotherapy of ccRCC causes more T cell infiltration in TME.

Taken together, our data reveals the deeper features of PBRM1 in tumors. PBRM1 mutates in various tumors but it has more significant effect in ccRCC. High PBRM1 expression level and anti-PD-1 immunotherapy imply more T cells in TME. Our study sheds light on the significance of PBRM1 in ccRCC TME and potential of PBRM1 as a therapeutic target in ccRCC.

DATA AVAILABILITY STATEMENT

RNA-Seq datasets of renal clear cell carcinoma with corresponding clinical profiles was downloaded from The Cancer Genome Atlas (TCGA) database (https://portal.gdc.cancer.gov/). The corresponding information related to patients with the PBRM1 mutation was obtained from the cBioPortal for Cancer Genomics website (http://www.cbioportal.org). The protein-protein interaction was analyzed using STRING dataset. The association between PBRM1 expression and immune infiltrates was analyzed *via* the TIMER (http://timer.cistrome.org/) database. GEPIA2 (http://gepia2.cancer-pku.cn/#index) and UALCAN (http://ualcan.path.uab.edu/index.html) tools were used to analyze TCGA, CPTAC, and GTEx datasets. To analyze the differences between PBRM1 high and PBRM1 low ccRCC cells, we also used the GSE 22316 (human), GSE145919 (mice) data from the GEO database. The data were analyzed using GEO2R, an online analysis tool in the GEO database.

ETHICS STATEMENT

The animal study was reviewed and approved by Peking University Health Science Center ethics committee.

AUTHOR CONTRIBUTIONS

AA and LX conceived and designed the study. AA and JW contributed to the experiment and analysis of the data. AA wrote the first draft of manuscript. LX and JJW critically revised the manuscript. All authors contributed to the article and approved the submitted version.

FUNDING

This work was supported by the National Natural Science Foundation of China (no.81902909).

ACKNOWLEDGMENTS

We thank Dr. Yan Song for technical support in multiplex immunohistochemistry assay and data analysis.

SUPPLEMENTARY MATERIAL

The Supplementary Material for this article can be found online at: https://www.frontiersin.org/articles/10.3389/fonc.2021.712765/full#supplementary-material

Supplementary Figure 1 | PBRM1 deficiency caused changes in immune cell-associated signaling pathways. **(A)** Top ten significantly up-regulated and down-regulated genes in PBRM1 low ccRCC cells compared to PBRM1 high ccRCC cells. **(B)** Go analysis and KEGG signaling pathway analysis of PBRM1 low ccRCC cells with PBRM1 high ccRCC cells. Significantly changed (*p < 0.05) pathways are shown. **(C)** Significantly changed (*p < 0.05) transcription factor associated genes in PBRM1 low cells compared with PBRM1 high cells. **(D)** Relative mRNA expression of CXCL10 and CCL12 chemokines in PBRM1 high and PBRM1 low Renca cells. Data represents 5 samples per group. *P < 0.05; **P < 0.01; ***P < 0.001.

REFERENCES

1. Clark DJ, Dhanasekaran SM, Petralia F, Pan J, Song X, Hu Y, et al. Integrated Proteogenomic Characterization of Clear Cell Renal Cell Carcinoma. *Cell* (2019) 179:964–983.e31. doi: 10.1016/j.cell.2019.10.007
2. Jonasch E, Walker CL, Rathmell WK. Clear Cell Renal Cell Carcinoma Ontogeny and Mechanisms of Lethality. *Nat Rev Nephrol* (2021) 17:245–61. doi: 10.1038/s41581-020-00359-2
3. Cancer Genome Atlas Research Network. Comprehensive Molecular Characterization of Clear Cell Renal Cell Carcinoma. *Nature* (2013) 499:43–9. doi: 10.1038/nature12222

4. Espana-Agusti J, Warren A, Chew SK, Adams DJ, Matakidou A. Loss of PBRM1 Rescues VHL Dependent Replication Stress to Promote Renal Carcinogenesis. *Nat Commun* (2017) 8:2026. doi: 10.1038/s41467-017-02245-1
5. Hodges C, Kirkland JG, Crabtree GR. The Many Roles of BAF (mSWI/SNF) and PBAF Complexes in Cancer. *Cold Spring Harb Perspect Med* (2016) 6: a026930. doi: 10.1101/cshperspect.a026930
6. Chabanon RM, Morel D, Eychenne T, Colmet-Daage L, Bajrami I, Dorvault N, et al. PBRM1 Deficiency Confers Synthetic Lethality to DNA Repair Inhibitors in Cancer. *Cancer Res* (2021) 81:2888–902. doi: 10.1158/0008-5472.CAN-21-0628
7. Brownlee PM, Chambers AL, Cloney R, Bianchi A, Downs JA. BAF180 Promotes Cohesion and Prevents Genome Instability and Aneuploidy. *Cell Rep* (2014) 6:973–81. doi: 10.1016/j.celrep.2014.02.012
8. Varela I, Tarpey P, Raine K, Huang D, Ong CK, Stephens P, et al. Exome Sequencing Identifies Frequent Mutation of the SWI/SNF Complex Gene PBRM1 in Renal Carcinoma. *Nature* (2011) 469:539–42. doi: 10.1038/nature09639
9. Gu Y-F, Cohn S, Christie A, McKenzie T, Wolff N, Do QN, et al. Modeling Renal Cell Carcinoma in Mice: Bap1 and Pbrm1 Inactivation Drive Tumor Grade. *Cancer Discov* (2017) 7:900–17. doi: 10.1158/2159-8290.CD-17-0292
10. Gossage L, Eisen T, Maher ER. VHL, the Story of a Tumour Suppressor Gene. *Nat Rev Cancer* (2015) 15:55–64. doi: 10.1038/nrc3844
11. Nargund AM, Pham CG, Dong Y, Wang PI, Osmangeyoglu HU, Xie Y, et al. The SWI/SNF Protein PBRM1 Restrains VHL-Loss-Driven Clear Cell Renal Cell Carcinoma. *Cell Rep* (2017) 18:2893–906. doi: 10.1016/j.celrep.2017.02.074
12. Liu X-D, Kong W, Peterson CB, McGrail DJ, Hoang A, Zhang X, et al. PBRM1 Loss Defines a Nonimmunogenic Tumor Phenotype Associated With Checkpoint Inhibitor Resistance in Renal Carcinoma. *Nat Commun* (2020) 11:2135. doi: 10.1038/s41467-020-15959-6
13. Braun DA, Hou Y, Bakouny Z, Ficial M, Sant' Angelo M, Forman J, et al. Interplay of Somatic Alterations and Immune Infiltration Modulates Response to PD-1 Blockade in Advanced Clear Cell Renal Cell Carcinoma. *Nat Med* (2020) 26:909–18. doi: 10.1038/s41591-020-0839-y
14. McGranahan N, Swanton C. Clonal Heterogeneity and Tumor Evolution: Past, Present, and the Future. *Cell* (2017) 168:613–28. doi: 10.1016/j.cell.2017.01.018
15. Yi M, Jiao D, Xu H, Liu Q, Zhao W, Han X, et al. Biomarkers for Predicting Efficacy of PD-1/PD-L1 Inhibitors. *Mol Cancer* (2018) 17:129. doi: 10.1186/s12943-018-0864-3
16. Ikegami A, Teixeira LFS, Braga MS, Dias MHDS, Lopes EC, Bellini MH. Knockdown of NF-KB1 by shRNA Inhibits the Growth of Renal Cell Carcinoma *In Vitro* and *In Vivo*. *Oncol Res* (2018) 26:743–51. doi: 10.3727/096504017X15120379906339
17. Meng X, Liu X, Guo X, Jiang S, Chen T, Hu Z, et al. FBXO38 Mediates PD-1 Ubiquitination and Regulates Anti-Tumour Immunity of T Cells. *Nature* (2018) 564:130–5. doi: 10.1038/s41586-018-0756-0
18. Wei SC, Levine JH, Cogdill AP, Zhao Y, Anang N-AAS, Andrews MC, et al. Distinct Cellular Mechanisms Underlie Anti-CTLA-4 and Anti-PD-1 Checkpoint Blockade. *Cell* (2017) 170:1120–33.e17. doi: 10.1016/j.cell.2017.07.024
19. Wang S-H, Yu J. Structure-Based Design for Binding Peptides in Anti-Cancer Therapy. *Biomaterials* (2018) 156:1–15. doi: 10.1016/j.biomaterials.2017.11.024
20. Hrushesky WJ, Murphy GP. Investigation of a New Renal Tumor Model. *J Surg Res* (1973) 15:327–36. doi: 10.1016/0022-4804(73)90096-6
21. Hu J, Schokrpur S, Archang M, Hermann K, Sharrow AC, Khanna P, et al. A non-Integrating Lentiviral Approach Overcomes Cas9-Induced Immune Rejection to Establish an Immunocompetent Metastatic Renal Cancer Model. *Mol Ther - Methods Clin Dev* (2018) 9:203–10. doi: 10.1016/j.omtm.2018.02.009
22. Ran X, Xiao J, Zhang Y, Teng H, Cheng F, Chen H, et al. Low Intratumor Heterogeneity Correlates With Increased Response to PD-1 Blockade in Renal Cell Carcinoma. *Ther Adv Med Oncol* (2020) 12:1758835920977117. doi: 10.1177/1758835920977117
23. Molgora M, Esaulova E, Vermi W, Hou J, Chen Y, Luo J, et al. TREM2 Modulation Remodels the Tumor Myeloid Landscape Enhancing Anti-PD-1 Immunotherapy. *Cell* (2020) 182:886–900.e17. doi: 10.1016/j.cell.2020.07.013
24. Li N, Kang Y, Wang L, Huff S, Tang R, Hui H, et al. ALKBH5 Regulates Anti-PD-1 Therapy Response by Modulating Lactate and Suppressive Immune Cell Accumulation in Tumor Microenvironment. *Proc Natl Acad Sci USA* (2020) 117:20159–70. doi: 10.1073/pnas.1918986117
25. Zhou S, Treloar AE, Lupien M. Emergence of the Noncoding Cancer Genome: A Target of Genetic and Epigenetic Alterations. *Cancer Discov* (2016) 6:1215–29. doi: 10.1158/2159-8290.CD-16-0745
26. Berger MF, Mardis ER. The Emerging Clinical Relevance of Genomics in Cancer Medicine. *Nat Rev Clin Oncol* (2018) 15:353–65. doi: 10.1038/s41571-018-0002-6
27. Chevrier S, Levine JH, Zanotelli VRT, Silina K, Schulz D, Bacac M, et al. An Immune Atlas of Clear Cell Renal Cell Carcinoma. *Cell* (2017) 169:736–49.e18. doi: 10.1016/j.cell.2017.04.016
28. Ribeiro-Silva C, Vermeulen W, Lans H. SWI/SNF: Complex Complexes in Genome Stability and Cancer. *DNA Repair (Amst)* (2019) 77:87–95. doi: 10.1016/j.dnarep.2019.03.007
29. Jeggo PA, Pearl LH, Carr AM. DNA Repair, Genome Stability and Cancer: A Historical Perspective. *Nat Rev Cancer* (2016) 16:35–42. doi: 10.1038/nrc.2015.4
30. Carril-Ajuria L, Santos M, Roldán-Romero JM, Rodriguez-Antona C, de Velasco G. Prognostic and Predictive Value of PBRM1 in Clear Cell Renal Cell Carcinoma. *Cancers (Basel)* (2019) 12:16. doi: 10.3390/cancers12010016
31. Yang Q, Shen R, Xu H, Shi X, Xu L, Zhang L, et al. Comprehensive Analyses of PBRM1 in Multiple Cancer Types and Its Association With Clinical Response to Immunotherapy and Immune Infiltrates. *Ann Transl Med* (2021) 9:465. doi: 10.21037/atm-21-289
32. Xia W, Nagase S, Montia AG, Kalachikov SM, Keniry M, Su T, et al. BAF180 Is a Critical Regulator of P21 Induction and a Tumor Suppressor Mutated in Breast Cancer. *Cancer Res* (2008) 68:1667–74. doi: 10.1158/0008-5472.CAN-07-5276
33. Brugarolas J. PBRM1 and BAP1 as Novel Targets for Renal Cell Carcinoma. *Cancer J* (2013) 19:324–32. doi: 10.1097/PPO.0b013e3182a102d1
34. Zhang J, Wu T, Simon J, Takada M, Saito R, Fan C, et al. VHL Substrate Transcription Factor ZHX2 as an Oncogenic Driver in Clear Cell Renal Cell Carcinoma. *Science* (2018) 361:290–5. doi: 10.1126/science.aap8411
35. Yao X, Tan J, Lim KJ, Koh J, Ooi WF, Li Z, et al. VHL Deficiency Drives Enhancer Activation of Oncogenes in Clear Cell Renal Cell Carcinoma. *Cancer Discovery* (2017) 7:1284–305. doi: 10.1158/2159-8290.CD-17-0375
36. Gao W, Li W, Xiao T, Liu XS, Kaelin WG. Inactivation of the PBRM1 Tumor Suppressor Gene Amplifies the HIF-Response in VHL-/- Clear Cell Renal Carcinoma. *Proc Natl Acad Sci USA* (2017) 114:1027–32. doi: 10.1073/pnas.1619726114
37. Sobczuk P, Brodziak A, Khan MI, Chhabra S, Fiedorowicz M, Wełniak-Kamińska M, et al. Choosing the Right Animal Model for Renal Cancer Research. *Trans Oncol* (2020) 13:100745. doi: 10.1016/j.tranon.2020.100745
38. Devaud C, Westwood JA, John LB, Flynn JK, Paquet-Fifield S, Duong CPM, et al. Tissues in Different Anatomical Sites can Sculpt and Vary the Tumor Microenvironment to Affect Responses to Therapy. *Mol Ther* (2014) 22:18–27. doi: 10.1038/mt.2013.219
39. Kagamu H, Kitano S, Yamaguchi O, Yoshimura K, Horimoto K, Kitazawa M, et al. CD4+ T-Cell Immunity in the Peripheral Blood Correlates With Response to Anti-PD-1 Therapy. *Cancer Immunol Res* (2020) 8:334–44. doi: 10.1158/2326-6066.CIR-19-0574
40. Oh DY, Kwek SS, Raju SS, Li T, McCarthy E, Chow E, et al. Intratumoral CD4+ T Cells Mediate Anti-Tumor Cytotoxicity in Human Bladder Cancer. *Cell* (2020) 181:1612–25.e13. doi: 10.1016/j.cell.2020.05.017
41. Giraldo NA, Becht E, Vano Y, Petitprez F, Lacroix L, Validire P, et al. Tumor-Infiltrating and Peripheral Blood T-Cell Immunophenotypes Predict Early Relapse in Localized Clear Cell Renal Cell Carcinoma. *Clin Cancer Res* (2017) 23:4416–28. doi: 10.1158/1078-0432.CCR-16-2848
42. Nagarsheth N, Wicha MS, Zou W. Chemokines in the Cancer Microenvironment and Their Relevance in Cancer Immunotherapy. *Nat Rev Immunol* (2017) 17:559–72. doi: 10.1038/nri.2017.49
43. Karin N. Chemokines and Cancer: New Immune Checkpoints for Cancer Therapy. *Curr Opin Immunol* (2018) 51:140–5. doi: 10.1016/j.coi.2018.03.004

44. Nishida J, Momoi Y, Miyakuni K, Tamura Y, Takahashi K, Koinuma D, et al. Epigenetic Remodelling Shapes Inflammatory Renal Cancer and Neutrophil-Dependent Metastasis. *Nat Cell Biol* (2020) 22:465–75. doi: 10.1038/s41556-020-0491-2
45. Luo R, Firat E, Gaedicke S, Guffart E, Watanabe T, Niedermann G. Cisplatin Facilitates Radiation-Induced Abscopal Effects in Conjunction With PD-1 Checkpoint Blockade Through CXCR3/CXCL10-Mediated T-Cell Recruitment. *Clin Cancer Res* (2019) 25:7243–55. doi: 10.1158/1078-0432.CCR-19-1344

Conflict of Interest: The authors declare that the research was conducted in the absence of any commercial or financial relationships that could be construed as a potential conflict of interest.

Publisher's Note: All claims expressed in this article are solely those of the authors and do not necessarily represent those of their affiliated organizations, or those of the publisher, the editors and the reviewers. Any product that may be evaluated in this article, or claim that may be made by its manufacturer, is not guaranteed or endorsed by the publisher.

frontiers in Cell and Developmental Biology

REVIEW
published: 10 August 2021
doi: 10.3389/fcell.2021.705280

Potential Strategies to Improve the Effectiveness of Drug Therapy by Changing Factors Related to Tumor Microenvironment

Dehong Cao[1†], Xiaokaiti Naiyila[1,2†], Jinze Li[1,2†], Yin Huang[1,2†], Zeyu Chen[1,2], Bo Chen[1,2], Jin Li[1,2], Jianbing Guo[1], Qiang Dong[1], Jianzhong Ai[1], Lu Yang[1], Liangren Liu[1] and Qiang Wei[1]**

[1] Department of Urology/Institute of Urology, West China Hospital, Sichuan University, Chengdu, China, [2] West China School of Medicine, Sichuan University, Chengdu, China

OPEN ACCESS

Edited by:
Kevin J. Ni,
St George Hospital, Australia

Reviewed by:
Tianyi Liu,
University of California,
San Francisco, United States
Bandana Chakravarti,
Sanjay Gandhi Post Graduate Institute
of Medical Sciences (SGPGI), India

***Correspondence:**
Liangren Liu
liuliangren@scu.edu.cn
Qiang Wei
weiqiang339@126.com

[†] These authors have contributed equally to this work

Specialty section:
This article was submitted to Molecular and Cellular Oncology, a section of the journal Frontiers in Cell and Developmental Biology

Received: 05 May 2021
Accepted: 13 July 2021
Published: 10 August 2021

Citation:
Cao D, Naiyila X, Li J, Huang Y, Chen Z, Chen B, Li J, Guo J, Dong Q, Ai J, Yang L, Liu L and Wei Q (2021) Potential Strategies to Improve the Effectiveness of Drug Therapy by Changing Factors Related to Tumor Microenvironment. Front. Cell Dev. Biol. 9:705280. doi: 10.3389/fcell.2021.705280

A tumor microenvironment (TME) is composed of various cell types and extracellular components. It contains tumor cells and is nourished by a network of blood vessels. The TME not only plays a significant role in the occurrence, development, and metastasis of tumors but also has a far-reaching impact on the effect of therapeutics. Continuous interaction between tumor cells and the environment, which is mediated by their environment, may lead to drug resistance. In this review, we focus on the key cellular components of the TME and the potential strategies to improve the effectiveness of drug therapy by changing their related factors.

Keywords: tumor microenvironment, cancer-associated fibroblasts, tumor-associated macrophages, drug therapy, targeted therapy

INTRODUCTION

Tumor microenvironment (TME) refers to the cellular environment in which tumor cells and cancer stem cells (CSCs) exist. It can directly promote angiogenesis, invasion, metastasis, and chronic inflammation, and help maintain the stemness of the tumor (Denton et al., 2018). Different TMEs have not only adverse effects on the occurrence of tumors but also favorable consequences for patients. The composition of TME includes local stromal cells (such as resident fibroblasts and macrophages), remotely recruited cells (such as endothelial cells), immune cells (including myeloid cells and lymphoid cells), bone marrow-derived inflammatory cells, extracellular matrix (ECM), blood vessels, and signal molecules (Del Prete et al., 2017). Among them, tumor-associated myeloid cells (TAMCs) also include five different myeloid cell groups: tumor-associated macrophages (TAMs), monocytes expressing angiopoietin-2 receptor Tie2 (Tie2 expressing monocytes or TEM), myeloid suppressor cells (MDSCs), and tumor-associated dendritic cells (Kim and Bae, 2016). Together, they surround tumor cells while being nourished by a network of blood vessels. The TME plays a key role in the occurrence, development, and metastasis of tumors. It also has a far-reaching impact on the effect of therapeutics, and recent studies have shown that targeted the TME is clinically feasible (**Table 1**). Non-malignant cells in the TME usually stimulate uncontrolled proliferation of cells and play a tumor-promoting function in the overall processes of carcinogenesis. In contrast, malignant cells can metastasize to healthy tissues in other parts of the body through the lymph or circulatory system (Tu et al., 2014). As TME plays a decisive role in the progress of tumor treatment,

it is essential to further understand the components associated with TME in order to provide more precise treatment for different types of cancer.

CANCER STEM CELLS AND TUMOR MICROENVIRONMENT

Bonnet and Dick (1997) first confirmed the existence of CSCs in patients with acute myeloid leukemia and subsequently detected CSCs in other primary tumor tissues and cell lines (Kinugasa et al., 2014; Lau et al., 2017). CSCs refer to the subpopulations of tumor cells present in tumor masses, which are characterized by tumorigenicity and self-renewal properties (Magee et al., 2012). There is increasing evidence that CSCs play a key role in tumor recurrence, metastasis, and therapeutic resistance (Najafi et al., 2019a). TME induces the interaction between cancer cells and a variety of tissue cells. The functional characteristics of CSCs are affected by differentiated cancer cells and activated extracellular signals mediated by fibroblasts, macrophages, epithelial cells, endothelial cells, and blood cells, which provide the necessary growth elements for tumor cells and play an important role in promoting and maintaining the stemness of CSCs (Rafii et al., 2002; Byrne et al., 2005; Kopp et al., 2006; Huang et al., 2010). Recent studies have shown that in addition to changes in proto-oncogenes, the occurrence and metastasis of tumors are closely related to their microenvironment.

In the TME, cancer-associated fibroblasts (CAFs) can promote and maintain the stem cell-like properties of liver cancer cells through the IL-6/STAT3/Notch signaling pathway (Xiong et al., 2018). In contrast, TAMs activate STAT3 and the hedgehog signaling pathway by secreting milk fat globule surface growth factor 8 and IL-6, thereby affecting the self-renewal and chemotherapy resistance of CSCs (Jinushi et al., 2011). Fan et al. (2014) also found that TAMs in liver cancer promote CSC phenotypes through the induction of epithelial–mesenchymal transition (EMT) by transforming growth factor β1 (TGF-β1). Moreover, IL-6 and NO secreted by MDSCs can activate STAT3 and NOTCH signaling pathways, stimulate the expression of microRNA101 in CSCs, and promote the expression of C-terminal binding protein-2 (CtBP2). The CtBP2 protein acts as a transcriptional auxiliary inhibitor factor that can directly target the core genes of stem cells Nanog and Sox2, and ultimately lead to the enhancement of the stemness of CSCs (Cui et al., 2013; Peng et al., 2016). Remarkably, these microenvironmental factors can also maintain the dryness of CSCs through Wntβ-catenin, FGFR, and MEK signaling pathways (Borah et al., 2015; Krishnamurthy and Kurzrock, 2018; Jin, 2020). CSCs can also regulate the expression and/or secretion of cytokines such as NFAT, NF-κB, and STAT signaling pathways through SOX2 and other genes, thereby regulating TME and recruiting TAMs to create an environment for the further development of tumors (Mou et al., 2015; Zeng et al., 2018). This undoubtedly supports the close connection between CSCs and TME. Considering that CSCs play a key role in the process of tumor occurrence, development, and recurrence, the microenvironment regulation strategy for the growth of CSCs is expected to become an effective means of tumor-targeted therapy.

CANCER-RELATED FIBROBLASTS

Cancer-associated fibroblasts are the most common type of host cells in the TME. It is now generally accepted that CAFs are a heterogeneous population with distinct functions which can serve as positive and negative regulators of tumor progression (Kalluri, 2016). Under the influence of the microenvironment, CAFs obtain an activated phenotype that is different from that of normal fibroblasts. It can promote tumor progression and regulate the composition of ECM by secreting soluble factors and interacting with other types of cells (Piccard et al., 2012). In patients with prostate cancer, CAF in the TME can promote cell proliferation and sphere formation through paracrine signals, thus promoting the growth of tumor stem cells. Studies have confirmed that the presence of a large amount of CAF in the tumor stroma is associated with poor prognosis in lung, breast, and pancreatic cancer (Räsänen and Vaheri, 2010). CAF can promote tumor progression by maintaining the continuous proliferation and growth of tumor cells at the metastatic site (Li and Wang, 2011).

Source and Function of CAF

Most activated CAFs originate from resident fibroblasts, which can recruit and activate many growth factors and cytokines, such as transforming growth factor β, fibroblast growth factor-2, and platelet-derived growth factor (PDGF). It has been found that these growth factors and cytokines are abundant in TME (Räsänen and Vaheri, 2010). CAFs can also be derived from bone marrow mesenchymal stem cells (**Figure 1**), transforming from resident epithelium or endothelial cells in the tumor stroma via EMT or endothelial–mesenchymal transition (EndMT), respectively (Kidd et al., 2012). The functions of activated CAFs include the synthesis and secretion of ECM and the release of proteolytic enzymes, such as heparanase and matrix metalloproteinases (MMPs), leading to ECM remodeling (Kessenbrock et al., 2010; Wu and Dai, 2017).

Cancer-associated fibroblasts can interact with tumor cells through direct contact and can also secrete a variety of cytokines through paracrine methods to promote the occurrence and development of cancer (Kalluri, 2016; Salimifard et al., 2020). Orimo et al. (2005) have shown that CXCL12 (stromal cell-derived factor-1, SDF-1) secreted by CAFs directly stimulates tumor growth by acting through the cognate receptor, CXCR4, which is expressed by carcinoma cells. In addition, CAF-secreted vascular cell adhesion molecule-1 (VCAM-1) also promotes the proliferation, migration, and invasion of tumor cells by activating the AKT and MAPK signals of lung cancer cells (Zhou et al., 2020). Recently, Seino et al. (2018) found that CAFs can provide a Wnt-producing niche to support the *in vivo* growth of the Wnt-deficient pancreatic ductal adenocarcinoma (PDAC) organoid mode. CAFs are also an important source of growth factors and cytokines [including hepatocyte growth factor (HGF), vascular endothelial growth factor (VEGF), PDGF,

TABLE 1 | Most recent clinical trials of TME targeted therapies.

Target	Inhibitors/antibodies	Clinical trial phase	Reference
Treg cells			
PD-1/PD-L1	Nivolumab (PD-1 inhibitor) Pembrolizumab (PD-1 inhibitor) Durvalumab (PD- L1 inhibitor) Atezolizumab (PD- L1 inhibitor) Avelumab (PD- L1 inhibitor) Cemiplimab (PD-1 inhibitor)	FDA-approved	
CTLA4	Ipilimumab (anti-CTLA4 monoclonal antibody)	FDA-approved	
LAG-3	Relatlimab (anti-LAG-3 mAb) Eftilagimod alpha (LAG-3Ig fusion protein)	Phase I/II clinical trial Phase II clinical trial	NCT01968109 NCT02614833
OX40	MEDI6383 (OX40 agonist)	Phase I clinical trial	NCT02221960
IDO	Navoximod (IDO inhibitor) Linrodostat mesylate (IDO inhibitor)	Phase I clinical trial Phase III clinical trial	NCT02048709 NCT03661320
CAFs			
MMPs	Rebimastat (MMP inhibitor)	Phase II clinical trial	NCT00040755
CXCR2	Reparixin (CXCR1/2 inhibitor)	Phase II clinical trial	NCT01861054
	BMS-813160 (CXCR2 antagonist)	Phase I/II clinical trial	NCT03496662
	AMD3100 (CXCR4 Inhibitor)	Phase I/II clinical trial	Lecavalier-Barsoum et al., 2018
CXCL12/CXCR4	LY2510924 (CXCR4 antagonist)	Phase II clinical trial Phase I clinical trial Phase II clinical trial	NCT01439568 NCT01837095 NCT02826486
	Balixafortide (CXCR4 antagonist) Motixafortide (CXCR4 antagonist)		
TGF-β	GC1008 (anti-TGF-β monoclonal antibody)	Phase II clinical trial	NCT01401062
TAMs			
CSF-1R	PLX3397 (CSF-1R inhibitor)	Phase I/II clinical trial	NCT01596751
CSF-1R	AMG820 (anti-CSF-1R monoclonal antibody)	Phase I/II clinical trial	NCT02713529
Deplete macrophages	Zoledronate, clodronate, ibandronate	Phase III clinical trial	NCT00127205 NCT00009945
TLR7	852A (TLR7 agonist) Imiquimod (TLR7 agonist)	Phase II clinical trial	NCT00319748 NCT00899574 NCT00821964
CCR2	PF-4136309 (CCR2 inhibitor)	Phase I clinical trial	NCT01413022
MDSCs			
PDE-5	Tadalafil (PDE-5 inhibitors)	Phase II clinical trial	NCT00752115
iNOS and arginase	NCX4016 (Nitric oxide-releasing aspirin derivative)	Phase I clinical trial	NCT00331786
MDSC differentiation	All-trans retinoic acid Inducing	Phase II clinical trial	NCT00617409
Hypoxia			
Hypoxia	TH-302 (hypoxia-activated prodrug) AQ4N (hypoxia-activated prodrug)	Phase III clinical trial Phase I/II clinical trial	NCT01746979 NCT00394628
ECM			
Hyaluronan	PEGPH20 (recombinant hyaluronidase)	Phase II clinical trial Phase III clinical trial	NCT01839487 NCT02715804
Tumor vasculatures			
VEGFRs, PDGFRs, KIT	Sorafenib (tyrosine kinase inhibitor) Sunitinib (tyrosine kinase inhibitor)	FDA-approved	
DLL4	OMP21M18 (anti-DLL4 monoclonal antibody)	Phase I clinical trial	NCT01189968
Notch1	OMP52M51 (anti-Notch1 monoclonal antibody)	Phase I clinical trial	NCT01778439
γ -Secretase	MK0752 (γ -secretase inhibitor)	Phase I clinical trial	NCT00106145

PD-1, programmed cell death-1; PD-L1, programmed death-ligand 1; CTLA4, cytotoxic T lymphocyte-associated antigen-4; LAG-3, lymphocyte activation gene-3; IDO, indoleamine 2,3-dioxygenase; CAFs, cancer-associated fibroblasts; MMPs, matrix metalloproteinases; SDF-1, stromal-derived factor 1; CXCR, chemokine (C-X-C motif) receptor; TGF-β, transforming growth factor beta; CSF-1R, stimulating factor-1 receptor; TLR7, Toll-like receptor 7; MDSC, myeloid-derived suppressor cell; PDE-5, phosphodiesterase-5-inhibitor; ECM, extracellular matrix; VEGFR, vascular endothelial growth factor receptor; PDGFR, platelet-derived growth factor receptor; DLL4, Delta-like 4.

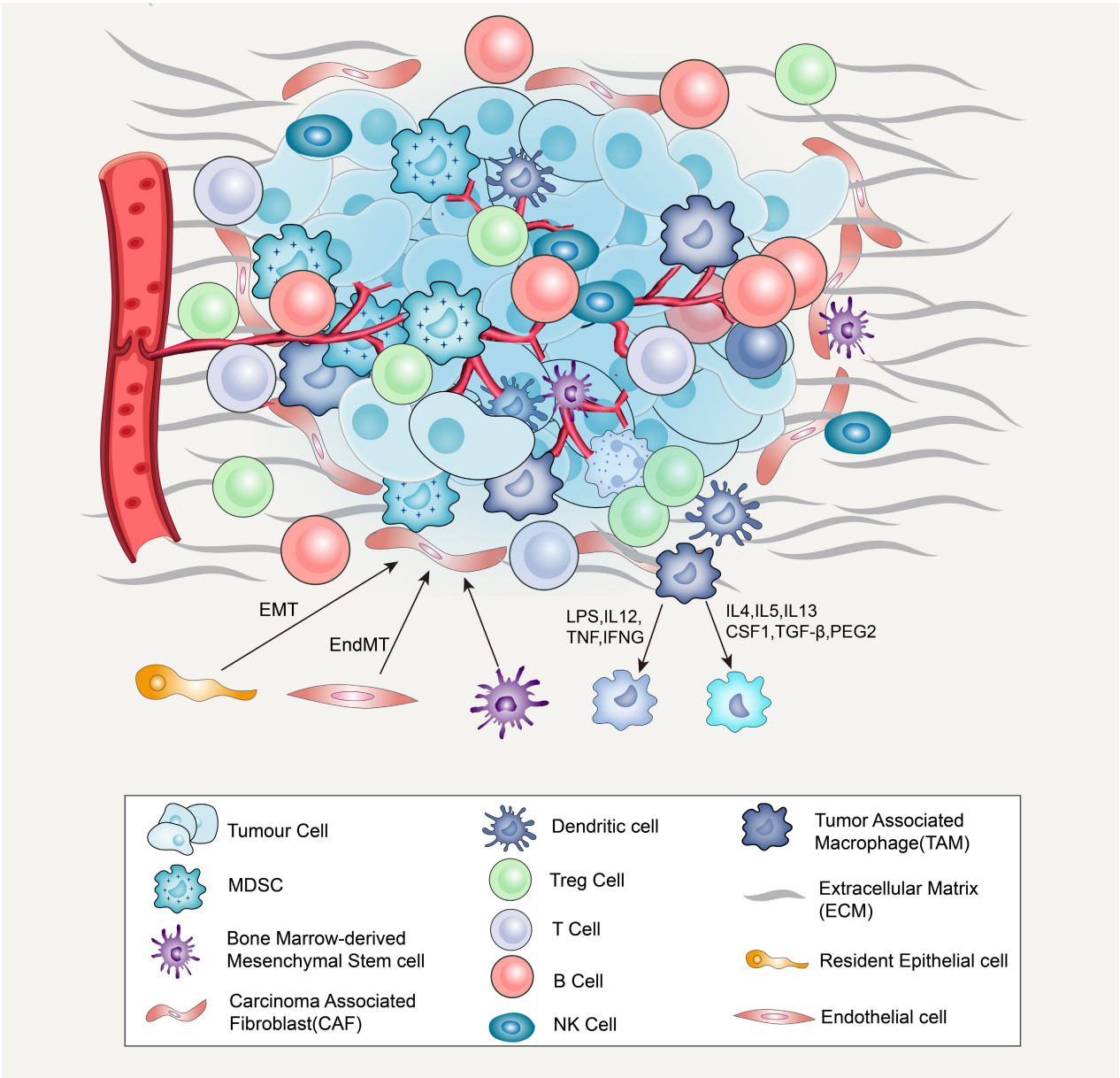

FIGURE 1 | Major cellular constituents and matrix component of the TME, including cancer cells, immune cells (T-cells, B-cells, NK cells, dendritic cells, MDSCs, TAMs), CAFs and ECM. CAF derived from bone marrow mesenchymal stem cells and transform through epithelial–mesenchymal transition (EMT) or endothelial mesenchymal transition (EndMT) from resident epithelium or endothelial cells **(A)**. When macrophages are exposed to LPS, MAMPs, IL12, TNF, IFNG, or another TLR agonists, they will transition to M1-like. When exposed to IL4, IL5, IL10, IL13, CSF1, TGFβ1, and PGE2, it will transition to M2-like state **(B)**.

etc.], which can stimulate the growth of tumor cells *in vitro* and lead to therapeutic drug resistance (Straussman et al., 2012; Erez et al., 2013; Paraiso and Smalley, 2013).

Angiogenesis in tumor tissues can provide oxygen and nutrients for tumor cell metabolism and promote tumor growth and metastasis. Many studies have shown that CAFs can release a variety of stimulating factors that promote angiogenesis and play an important role in the recruitment and proliferation of tumor vascular endothelial cells and the formation of vascular sprouts (Benyahia et al., 2017). CAFs promote angiogenesis by recruiting endothelial progenitor cells (EPCs) into carcinomas, an effect mediated in part by CXCL12 (Orimo et al., 2005). CXCL12 can activate the PI3K/AKT signaling pathway in tumor cells, upregulate the expression of VEGF in tumor tissues, and promote angiogenesis (Wen et al., 2019). VEGF activates the main signaling pathway in tumor angiogenesis by binding to its cognate receptor, VEGFR (Claesson-Welsh and Welsh, 2013). Mirkeshavarz et al. (2017) found that CAFs can secrete interleukin-6 (IL-6) and VEGF to induce angiogenesis in oral cancer, and that IL-6 can induce the secretion of VEGF in

CAF cell lines. CAF can also release active growth factors from the ECM by expressing MMPs, which indirectly promotes angiogenesis (Najafi et al., 2019b) and serves as one of the sources of MMP9 (Boire et al., 2005) and MMP13 (Vosseler et al., 2009). Both these substances have been shown to release VEGF from the ECM to increase angiogenesis in tumors (Lederle et al., 2010).

Cancer-associated fibroblasts interact with tumor cells through inflammatory signals, thereby affecting tumor cell migration and invasion. The CAF-mediated CXCL12/CXCR4 axis plays a key role in tumor cell proliferation, invasion, and migration. The CXCL12/CXCR4 axis can activate the MEK/ERK, PI3K/AKT, and Wnt/β-catenin pathways to promote EMT, thereby promoting tumor invasion and metastasis (Guo et al., 2016; Zhou et al., 2019; Mortezaee, 2020). It also activates the PI3K, MAPK, and ERK1/2 signaling pathways, promotes the secretion of MMPs, reduces the adhesion of tumor cells, and increases their invasion and metastasis ability (Wu and Dai, 2017). In addition, a recent study found that CAF-secreted CXCL-1 can stimulate the migration and invasion of oral cancer cells, that there is an interdependent relationship between CAFs and cancer cells in the oral squamous carcinoma microenvironment, and that CXCL-1 can upregulate MMP-1 in CAF expression and activity (Wei et al., 2019). In addition, CAFs can change the structure and physical properties of the ECM, thereby affecting tumor cell migration and invasion (Egeblad et al., 2010).

Drug Resistance and Targeted Therapy of CAF

The fight against drug resistance remains a major challenge in tumor treatment. CAFs mediate a variety of tumor resistance to chemotherapeutic drugs. CAFs can act on tumor cells by secreting cytokines, activating downstream signaling pathways in tumor cells, and promoting tumor resistance (Chen and Song, 2019). Studies have shown that CAFs can enhance EMT and cisplatin resistance in non-small cell lung cancer induced by transforming growth factor β by releasing high levels of IL-6, while cisplatin, in turn, promotes cancer cells to produce transforming growth factor β, resulting in CAF activation (**Figure 1**). CAFs can also promote chemotherapy resistance in tumor cells by secreting exosomes. Gemcitabine (GEM) is currently a chemotherapy drug that is commonly used in the treatment of pancreatic cancer. Fang et al. (2019) found that exosomal miR-106b derived from CAFs plays an important role in GEM resistance in pancreatic cancer. Recently, Zhang et al. (2020) showed that exosomal miR-522 secreted by CAFs prevents the death of cancer cells by targeting ALOX15 and blocking the accumulation of lipid-ROS. In addition, a new mechanism for obtaining gastric cancer drug resistance through the intercellular signaling pathways of USP7, hnRNPA1, exo-miR-522, and ALOX15 has been observed.

Direct ablation of CAF can promote the regression of immunogenic tumors (Feig et al., 2013), which has been explored in several recent studies, where these cells are cleared by injection of diphtheria toxin or targeting FAP-specific chimeric antigen receptor T cells; direct ablation of CAF, however, can lead to significant side effects due to lack of specificity, such as cachexia and anemia (Roberts et al., 2013; Tran et al., 2013). Because of the lack of specific markers for CAF, this method is not feasible at present, so the need to know more about the mechanism by which CAF works remains important for the development of more targeted treatments.

In a parallel study, pharmacological stimulation of the VDR was successfully performed in activated pancreatic stellate cells (PSCs). VDR is the main genomic inhibitor that is activated by PSCs. In addition, treatment with the VDR ligand calcipotriol induced matrix remodeling, which can inhibit tumor-related inflammation and fibrosis, and also improves the transport of gemcitabine to the tumor area, thus reversing chemotherapy resistance in the pancreatic ductal adenocarcinoma model (Sherman et al., 2014). Due to the complex interaction between CAF and other cells in the tumor environment, targeting some CAF subsets may cause multiple responses in the TME, which may have multiple effects depending on the individual. To eradicate cancer, the synergistic combination of CAF-targeted therapy and other effective treatments (such as immunotherapy) should also be considered.

Furthermore, the CXCL12/CXCR4 axis activates multiple signaling pathways to promote tumor cell proliferation, invasion, distant metastasis, and inhibit apoptosis. Therefore, the screening of antagonists targeting the CXCL12/CXCR4 signaling pathway is a promising target for tumor therapy. Lecavalier-Barsoum et al. (2018) found that the CXCR4 inhibitor AMD3100 can inhibit the CXCL12/CXCR4 axis in the treatment of patients with advanced disseminated high-grade serous ovarian cancer, and the combination of AMD3100 and low-dose paclitaxel can inhibit the growth of ovarian cancer cells. In osteosarcoma, AMD3100 blocks the invasion and metastasis of osteosarcoma to the lung by inhibiting the JNK and AKT pathways (Liao et al., 2015). Another CXCR4 antagonist, AMD3465, can inhibit the proliferation, colony formation, invasion, and migration of bladder cancer cells through the CXCL12/CXCR4/β-catenin axis (Zhang et al., 2018).

Micro RNA and siRNA can silence gene expression through post-transcriptional regulatory mechanisms, which may be another viable way to inhibit CXCR4 expression. In breast cancer cells, siRNA targeting CXCR4 inhibited the migration of breast cancer cells *in vitro* (Burger et al., 2011). miR-126 can also inactivate the RhoA signaling pathway in colon cancer by reducing the expression of CXCR4 and inducing a tumor suppressor effect (Yuan et al., 2016). These studies show that miRNA or siRNA targeting CXCR4 is of great significance in tumor treatment research. CTCE-9908 is composed of dimers of CXCL12, which is a competitive inhibitor of CXCL12 targeting CXCR4 and can inhibit the secretion of CXCL12 (Guo et al., 2016). Huang et al. (2009) reported that CTCE-9908 can target the CXCL12/CXCR4 axis and inhibit primary tumor growth and metastasis of breast cancer. Hassan et al. (2011) also found that CTCE-9908 combined with the anti-angiogenic agent DC101 also reduced the volume of the primary tumor and distant metastasis compared with DC101 alone. Moreover, an *in vitro* experiment proved that CTCE-9908 can inhibit the growth, invasion, and metastasis of prostate cancer (Wong et al., 2014). This evidence

supports CTCE-9908 as an efficacious novel agent to prevent and treat the spread of metastatic cancer. At present, cancer treatment methods targeting CAFs and the CXCL12/CXCR4 axis are being explored and developed rapidly.

TUMOR-ASSOCIATED MACROPHAGE

Tumor-associated macrophages account for a large proportion of most malignant tumors. They promote tumor progression at different levels by promoting genetic instability, cultivating CSCs, supporting metastasis, and taming protective adaptive immunity (Mantovani et al., 2017). TAMs can be divided into M1-like and M2-like types. When macrophages are exposed to cytokines such as bacterial lipopolysaccharide (LPS), microbe-associated molecular patterns (MAMPs), IL12, TNF, interferon-γ (IFNG), or other Toll-like receptor (TLR) agonists, they will be in a pro-inflammatory and anti-tumor state, hence M1-like. When exposed to IL4, IL5, IL10, IL13, CSF1, TFGB1, and prostaglandin E2 (PGE2), it transitions from a pro-inflammatory state to an anti-inflammatory and pro-tumor state, that is, to an M2-like state (Murray et al., 2014). TAMs have a high degree of functional plasticity and can quickly adapt to changing microenvironment (Gubin et al., 2018). The necrotic and anoxic regions of the TME contain M2-like TAMs, with low fluidity, limited antigen presentation ability, and secrete a large number of tumor support factors (Wenes et al., 2016). The metabolic spectrum of TAMs is in a dynamic model, which can change with the nutritional needs of malignant tumor cells and changes in TME. It also has a far-reaching impact on the survival of TAMs, cancer progression, and tumor-targeted immune response.

The most abundant inflammatory or immune cell type is near the CAF-populated areas in the tumor stroma, indicating a close interaction between TAMs and CAF. In prostate cancer, CAF-mediated CXCL12/CXCR4 axis induces the differentiation of monocytes and possibly M1 cells into pro-tumor M2 cells. Conversely, TAMs with the M2 phenotype activate CAFs, thereby promoting tumor malignancy (Augsten et al., 2014; Comito et al., 2014). *In vitro* co-culture experiments showed that CAF-like BM-MSCs enhanced the invasiveness of TAM-like macrophages. These macrophages strongly stimulate the proliferation and invasion of CAFs, thereby synergistically promoting the development of neuroblastoma (Hashimoto et al., 2016).

Tumor-associated macrophages release TNF-α to increase MMPs secreted by tumor cells and tumor stromal cells, destroy basement membrane tissue, and promote tumor metastasis (Shuman Moss et al., 2012). TAMs also stimulate vascular endothelium to secrete VEGF by synthesizing and secreting the Wnt7b protein to regulate angiogenesis (Yeo et al., 2014). TNF-α binds to tumor necrosis factor receptor 1 (TNFR-1), activates the VEGFC/VEGFR3 pathway, and promotes lymphangiogenesis (Ran and Montgomery, 2012). In addition, transforming (TGF-β) secreted by TAMs can induce EMT of colorectal cancer cells, thereby promoting the invasion and metastasis of colorectal cancer cells (Yang et al., 2019). Notably, exosomes are one of the components in TME, which carry a variety of active substances and are the mediator of information transmission between cells (Sun et al., 2018). The exosomes of tumor cells can stimulate TAMs to secrete cytokines and enhance tumor invasion and metastasis (Trivedi et al., 2016).

Drug Resistance and Targeted Therapy of TAM

Tumor-associated macrophages can promote tumor repair response by coordinating tissue damage and limit the anti-tumor activity of conventional chemotherapy and radiotherapy by providing a protective niche for CSCs (Mantovani et al., 2017). There is increasing evidence that macrophages play a central role in both normal and diseased tissue remodeling, including angiogenesis, basement membrane rupture, leukocyte infiltration, and immunosuppression. Therefore, TAMs have become a promising target for the development of new anticancer treatments. These methods are mainly focused on the depletion of M2-like TAMs and/or promotion of their transformation to M1-like phenotype (Cassetta and Pollard, 2018; Pradel et al., 2018). However, the effectiveness of this method may be limited by a variety of factors, such as alternative immunosuppressive cells that can compensate for TAMs, the existence of innate and acquired drug resistance mechanisms, and the emergence of strong immunosuppression after cessation of treatment (Quail and Joyce, 2017). PLX-3397 is a small-molecule inhibitor of the CSF-1 pathway. It is not only an effective tyrosine kinase inhibitor of CSF-1R, but also targeted at cKit and FLT3. Blocking CSF-1/CSF-1R can reduce TAMS and reprogramming TAMS in the TME and enhance the activation of T cells in the TME by enhancing antigen presentation. The downstream effect blocked by CSF-1/CSF-1R hinders the growth of the tumor (Zhu et al., 2014). In a mouse model of preclinical lung adenocarcinoma, PLX-3397 has been shown to change the distribution of TAMs in the TME and reduce tumor load (Cuccarese et al., 2017). In the syngeneic mouse model of BRAFV600E mutant melanoma, PLX-3397 combined with adoptive cell metastasis immunotherapy showed a decrease in TAMs (Mok et al., 2014). In similar melanoma mouse models, PLX-3397 combined with BRAF inhibitor PLX4032 significantly reduced M2 phenotypic macrophage recruitment, resulting in significant tumor growth inhibition (Ngiow et al., 2016). In addition, recent studies have shown that M2-like TAMs, which seem to be regulators of lysosomal pH, express high levels of vacuolar ATP enzymes and are expected to become a new drug target (Kuchuk et al., 2018; Liu et al., 2019). Targeting TAMs has proven to be a promising strategy, and with the deepening of preclinical development of TAM-targeted drugs and the new progress in the study of TAM mechanism, TAM-targeted therapy will become an important supplement to anticancer drugs.

MYELOGENOUS SUPPRESSOR CELLS

Myelogenous suppressor cells (MDSCs) are a heterogeneous population composed of bone marrow progenitor cells and immature bone marrow cells (IMCs) (Gabrilovich et al., 2012). Under normal physiological conditions, IMCs produced in the

bone marrow can rapidly differentiate into mature granulocytes, macrophages, or dendritic cells. In tumors and other pathological conditions, IMCs cannot normally differentiate into mature bone marrow cells under the action of cytokines, thus forming MDSCs with immunosuppressive functions, including T cell suppression and innate immune regulation (Kumar et al., 2016). In the TME, immunosuppressive cytokines such as IL-10 and TGF-β secreted by MDSCs are important factors that inhibit the anti-tumor immune response and promote tumor progression (Yaseen et al., 2020; Salminen, 2021). Studies have shown that TGF-β can inhibit the cytotoxic activity of cytotoxic T and NK cells by reducing the production of interferon-γ (IFN-γ). On the other hand, TGF-β can also inhibit the proliferation of anti-tumor immune active cells and inhibit anti-tumor immunity from the root (Salminen et al., 2018). Bone marrow mesenchymal stem cells play a role in inducing proliferation in the TME due to the interaction between cytokines and chemokines in the tumor inflammatory environment. Conversely, MDSCs can stimulate angiogenesis by producing matrix metalloproteinase 9, pro-factor 2, and VEGF, which further induces the migration of cancer cells to endothelial cells and promotes the metastasis of cancer cells (Lee et al., 2018; Yang et al., 2020).

Myelogenous suppressor cells produce high levels of inhibitory molecules, such as Arg1, reactive oxygen species (ROS), inducible nitric oxide synthase (iNOS), and prostaglandin E2 (PGE2), to directly inhibit the anti-tumor immune response induced by effector T cells (Kusmartsev et al., 2004; Gabrilovich and Nagaraj, 2009; Condamine et al., 2015; He et al., 2018). MDSCs can also inhibit the immune response by inducing regulatory T cells (Tregs), promoting the development of macrophages into M2 phenotypes, and differentiating into TAMs (Huang et al., 2006; Weber et al., 2018). Deng et al. (2017) found that MDSC-exosomes can directly accelerate the proliferation and metastasis of tumor cells by delivering miR-126a, which indicates that MDSCs have a new regulatory mechanism on tumor cells. MDSC-induced immunosuppression promotes tumor progression by promoting EMT, accelerating immune escape, and enhancing the formation of metastatic lesions (Veglia et al., 2018). Additionally, MDSCs enhance the stemness of tumor cells, promote angiogenesis by secreting IL6 and NO, and promote tumor growth, invasion, and metastasis directly or indirectly by inhibiting T cells or natural killer cells (Condamine et al., 2015, 2016).

Drug Resistance and Targeted Therapy of MDSC

The key roles played by MDSCs in the TME show that it is necessary to target them effectively by blocking or deleting them. Although they play a key role in tumor progression, there are no FDA-approved drugs or treatments that directly target MDSCs. At present, clinical trials are underway to target the activities of iNOS Arg1 and STAT3, metabolism through CD36, transport through CXCR2, and other mechanisms for different types of cancer (Fleming et al., 2018). The antisense oligonucleotide STAT3 inhibitor AZD9150 has been used in phase 1b clinical trials of diffuse large B-cell lymphoma in combination with immune checkpoint inhibitors. Systemic administration of AZD9150 significantly decreased granulocyte MDSCs in peripheral blood mononuclear cells (PBMCs) (Reilley et al., 2018). Current targeting strategies mainly include induction of differentiation into mature cells, inhibiting its expansion and recruitment, and blocking its immune characteristics. Studies have shown that some neutralizing antibodies or inhibitors targeting chemokine systems (CXCR4, CXCR2, and CCL2) and tumor-derived factors (CSF1, GM-CSF, and IL-6) can inhibit the expansion or recruitment of MDSC (Bayne et al., 2012; Sumida et al., 2012; Highfill et al., 2014). For example, the chemokine receptor CCR5 plays a key role in the chemotaxis of MDSCs to TME (Weber et al., 2018). However, not all MDSCs express CCR5. In melanoma mice, MDSCs expressing CCR5 have stronger immunosuppressive ability than MDSCs that do not express CCR5. Blocking CCR5 can inhibit the recruitment and immunosuppressive activity of MDSCs and improve the survival rate of melanoma patients (Blattner et al., 2018).

It has been found that some drugs, such as phosphodiesterase-5 inhibitors (sildenafil, cyclooxygenase-2 inhibitors (acetylsalicylic acid and celecoxib), vardenafil and tadalafil and bardoxolone methyl, can directly block the immunosuppressive activity of MDSCs and restore T cell response (Serafini et al., 2006; Nagaraj et al., 2010; Fujita et al., 2011; Obermajer et al., 2011). Recent studies have found that MDSC-specific peptide-Fc fusion protein therapy can completely deplete MDSCs in the blood, spleen, and tumor without affecting other immune cells, and inhibit tumor growth process (Qin et al., 2014), which provides a new idea for inhibiting tumor growth *in vivo*. In patients and animal models, the failure of anti-angiogenic therapy based on inhibition of the VEGF pathway is often concomitant with an increase in the number of MDSCs or TAMs infiltrating tumor tissues (Lu-Emerson et al., 2013; Gabrusiewicz et al., 2014). Along this line of thinking, anti-VEGF therapy is thought to upregulate alternative angiogenic factors (prokinin-1 and proagonin-2) produced by myeloid cells, which may accidentally produce anti-angiogenic effects and limit tumor recurrence.

Recent studies have shown that the accumulation of MDSCs in tumors limits the effect of anti-programmed death 1 (PD1) in the treatment of rhabdomyosarcoma checkpoint blockage. Inhibition of MDSC metastasis with an anti-CXCR2 antibody can enhance the efficacy of anti-PD1 (Highfill et al., 2014). In a tumor model of tolerant mice, the removal of MDSCs with gemcitabine combined with immunotherapy can effectively break the self-tolerance and induce strong anti-tumor immunity (Ko et al., 2007). Several chemotherapeutic drugs, such as anthracyclines, platinum derivatives, and doxorubicin, can induce immunogenic cell death, thus activating an effective anti-tumor adaptive response (Kroemer et al., 2013). The chemical process for enhancing the anticancer effect of these drugs includes increasing the antigen presentation ability of dendritic cells and the subsequent CD8+ T cell response (Bracci et al., 2014). Although the current targeted therapy targeting only MDSCs does not strengthen clinical outcomes, it may play an important role in anticancer immunotherapy in the future.

CONCLUSION

Most of the treatments are focused on a certain aspect of the TME. Although some of these therapeutic responses have produced positive results, a more effective way is to promote inflammatory innate immune cells, such as CD8+ T cells, and to alter many aspects of TME through a strong inflammatory response. Breakthrough drug resistance remains a major clinical challenge. The response of tumor cells to treatment depends not only on the regulation of the TME but also on the aberration of its genome. Targeted therapy cannot focus on the complete depletion of all inherent cells in the TME, as this may cause severe complications in the patient. The solution must be a complex combination, with focus on developing multidrug management that targets both tumor cells and TME to overcome resistance and improve prognosis as much as possible.

AUTHOR CONTRIBUTIONS

DC, XN, JL, YH, ZC, BC, JL, and JG: wrote the review article prepared and assembled the figure and table. QD, JA, LL, and QW: critically organized and revised the manuscript by incorporating significant reports. All authors contributed to the article and approved the submitted version.

FUNDING

This work was funded by the National Natural Science Foundation of China (Grant No. 82000721), Post-Doctor Research Project, West China Hospital, Sichuan University (Grant No. 2019HXBH089), Health commission of Sichuan province (Grant No. 20PJ036), and Programs from the Department of Science and Technology of Sichuan Province (Grant No. 2020YJ0054).

REFERENCES

Augsten, M., Sjöberg, E., Frings, O., Vorrink, S. U., Frijhoff, J., and Olsson, E. (2014). Borg Å, Östman A: cancer-associated fibroblasts expressing CXCL14 rely upon NOS1-derived nitric oxide signaling for their tumor-supporting properties. *Cancer Res.* 74, 2999–3010. doi: 10.1158/0008-5472.can-13-2740

Bayne, L. J., Beatty, G. L., Jhala, N., Clark, C. E., Rhim, A. D., Stanger, B. Z., et al. (2012). Tumor-derived granulocyte-macrophage colony-stimulating factor regulates myeloid inflammation and T cell immunity in pancreatic cancer. *Cancer Cell* 21, 822–835. doi: 10.1016/j.ccr.2012.04.025

Benyahia, Z., Dussault, N., Cayol, M., Sigaud, R., Berenguer-Daizé, C., Delfino, C., et al. (2017). Stromal fibroblasts present in breast carcinomas promote tumor growth and angiogenesis through adrenomedullin secretion. *Oncotarget* 8, 15744–15762. doi: 10.18632/oncotarget.14999

Blattner, C., Fleming, V., Weber, R., Himmelhan, B., Altevogt, P., Gebhardt, C., et al. (2018). CCR5(+) Myeloid-Derived Suppressor Cells Are Enriched and Activated in Melanoma Lesions. *Cancer Res.* 78, 157–167. doi: 10.1158/0008-5472.can-17-0348

Boire, A., Covic, L., Agarwal, A., Jacques, S., Sherifi, S., and Kuliopulos, A. (2005). PAR1 is a matrix metalloprotease-1 receptor that promotes invasion and tumorigenesis of breast cancer cells. *Cell* 120, 303–313. doi: 10.1016/j.cell.2004.12.018

Bonnet, D., and Dick, J. E. (1997). Human acute myeloid leukemia is organized as a hierarchy that originates from a primitive hematopoietic cell. *Nat. Med.* 3, 730–737. doi: 10.1038/nm0797-730

Borah, A., Raveendran, S., Rochani, A., Maekawa, T., and Kumar, D. S. (2015). Targeting self-renewal pathways in cancer stem cells: clinical implications for cancer therapy. *Oncogenesis* 4:e177. doi: 10.1038/oncsis.2015.35

Bracci, L., Schiavoni, G., Sistigu, A., and Belardelli, F. (2014). Immune-based mechanisms of cytotoxic chemotherapy: implications for the design of novel and rationale-based combined treatments against cancer. *Cell Death Differ.* 21, 15–25. doi: 10.1038/cdd.2013.67

Burger, J. A., Stewart, D. J., Wald, O., and Peled, A. (2011). Potential of CXCR4 antagonists for the treatment of metastatic lung cancer. *Expert Rev. Anticancer Ther.* 11, 621–630. doi: 10.1586/era.11.11

Byrne, A. M., Bouchier-Hayes, D. J., and Harmey, J. H. (2005). Angiogenic and cell survival functions of vascular endothelial growth factor (VEGF). *J. Cell. Mol. Med.* 9, 777–794. doi: 10.1111/j.1582-4934.2005.tb00379.x

Cassetta, L., and Pollard, J. W. (2018). Targeting macrophages: therapeutic approaches in cancer. *Nat. Rev. Drug Discov.* 17, 887–904. doi: 10.1038/nrd.2018.169

Chen, X., and Song, E. (2019). Turning foes to friends: targeting cancer-associated fibroblasts. *Nat. Rev. Drug Discov.* 18, 99–115. doi: 10.1038/s41573-018-0004-1

Claesson-Welsh, L., and Welsh, M. (2013). VEGFA and tumour angiogenesis. *J. Intern. Med.* 273, 114–127. doi: 10.1111/joim.12019

Comito, G., Giannoni, E., Segura, C. P., Barcellos-de-Souza, P., Raspollini, M. R., Baroni, G., et al. (2014). Cancer-associated fibroblasts and M2-polarized macrophages synergize during prostate carcinoma progression. *Oncogene* 33, 2423–2431. doi: 10.1038/onc.2013.191

Condamine, T., Dominguez, G. A., Youn, J. I., Kossenkov, A. V., Mony, S., Alicea-Torres, K., et al. (2016). Lectin-type oxidized LDL receptor-1 distinguishes population of human polymorphonuclear myeloid-derived suppressor cells in cancer patients. *Sci. Immunol.* 1:aaf8943. doi: 10.1126/sciimmunol.aaf8943

Condamine, T., Ramachandran, I., Youn, J. I., and Gabrilovich, D. I. (2015). Regulation of tumor metastasis by myeloid-derived suppressor cells. *Annu. Rev. Med.* 66, 97–110. doi: 10.1146/annurev-med-051013-052304

Cuccarese, M. F., Dubach, J. M., Pfirschke, C., Engblom, C., Garris, C., Miller, M. A., et al. (2017). Heterogeneity of macrophage infiltration and therapeutic response in lung carcinoma revealed by 3D organ imaging. *Nat. Commun.* 8:14293.

Cui, T. X., Kryczek, I., Zhao, L., Zhao, E., Kuick, R., Roh, M. H., et al. (2013). Myeloid-derived suppressor cells enhance stemness of cancer cells by inducing microRNA101 and suppressing the corepressor CtBP2. *Immunity* 39, 611–621. doi: 10.1016/j.immuni.2013.08.025

Del Prete, A., Schioppa, T., Tiberio, L., Stabile, H., and Sozzani, S. (2017). Leukocyte trafficking in tumor microenvironment. *Curr. Opin. Pharmacol.* 35, 40–47. doi: 10.1016/j.coph.2017.05.004

Deng, Z., Rong, Y., Teng, Y., Zhuang, X., Samykutty, A., Mu, J., et al. (2017). Exosomes miR-126a released from MDSC induced by DOX treatment promotes lung metastasis. *Oncogene* 36, 639–651. doi: 10.1038/onc.2016.229

Denton, A. E., Roberts, E. W., and Fearon, D. T. (2018). Stromal Cells in the Tumor Microenvironment. *Adv. Exp. Med. Biol.* 1060, 99–114.

Egeblad, M., Rasch, M. G., and Weaver, V. M. (2010). Dynamic interplay between the collagen scaffold and tumor evolution. *Curr. Opin. Cell Biol.* 22, 697–706. doi: 10.1016/j.ceb.2010.08.015

Erez, N., Glanz, S., Raz, Y., Avivi, C., and Barshack, I. (2013). Cancer associated fibroblasts express pro-inflammatory factors in human breast and ovarian tumors. *Biochem. Biophys. Res. Commun.* 437, 397–402. doi: 10.1016/j.bbrc.2013.06.089

Fan, Q. M., Jing, Y. Y., Yu, G. F., Kou, X. R., Ye, F., Gao, L., et al. (2014). Tumor-associated macrophages promote cancer stem cell-like properties via transforming growth factor-beta1-induced epithelial-mesenchymal transition in hepatocellular carcinoma. *Cancer Lett.* 352, 160–168. doi: 10.1016/j.canlet.2014.05.008

Fang, Y., Zhou, W., Rong, Y., Kuang, T., Xu, X., Wu, W., et al. (2019). Exosomal miRNA-106b from cancer-associated fibroblast promotes

gemcitabine resistance in pancreatic cancer. *Exp. Cell Res.* 383:111543. doi: 10.1016/j.yexcr.2019.111543

Feig, C., Jones, J. O., Kraman, M., Wells, R. J., Deonarine, A., Chan, D. S., et al. (2013). Targeting CXCL12 from FAP-expressing carcinoma-associated fibroblasts synergizes with anti-PD-L1 immunotherapy in pancreatic cancer. *Proc. Natl. Acad. Sci. U. S. A.* 110, 20212–20217. doi: 10.1073/pnas.1320318110

Fleming, V., Hu, X., Weber, R., Nagibin, V., Groth, C., Altevogt, P., et al. (2018). Targeting Myeloid-Derived Suppressor Cells to Bypass Tumor-Induced Immunosuppression. *Front. Immunol.* 9:398. doi: 10.3389/fimmu.2018.00398

Fujita, M., Kohanbash, G., Fellows-Mayle, W., Hamilton, R. L., Komohara, Y., Decker, S. A., et al. (2011). COX-2 blockade suppresses gliomagenesis by inhibiting myeloid-derived suppressor cells. *Cancer Res.* 71, 2664–2674. doi: 10.1158/0008-5472.can-10-3055

Gabrilovich, D. I., and Nagaraj, S. (2009). Myeloid-derived suppressor cells as regulators of the immune system. *Nat. Rev. Immunol.* 9, 162–174. doi: 10.1038/nri2506

Gabrilovich, D. I., Ostrand-Rosenberg, S., and Bronte, V. (2012). Coordinated regulation of myeloid cells by tumours. *Nat. Rev. Immunol.* 12, 253–268. doi: 10.1038/nri3175

Gabrusiewicz, K., Liu, D., Cortes-Santiago, N., Hossain, M. B., Conrad, C. A., Aldape, K. D., et al. (2014). Anti-vascular endothelial growth factor therapy-induced glioma invasion is associated with accumulation of Tie2-expressing monocytes. *Oncotarget* 5, 2208–2220. doi: 10.18632/oncotarget.1893

Gubin, M. M., Esaulova, E., Ward, J. P., Malkova, O. N., Runci, D., Wong, P., et al. (2018). High-Dimensional Analysis Delineates Myeloid and Lymphoid Compartment Remodeling during Successful Immune-Checkpoint Cancer Therapy. *Cell* 175, 1014–1030.e19.

Guo, F., Wang, Y., Liu, J., Mok, S. C., Xue, F., and Zhang, W. (2016). CXCL12/CXCR4: a symbiotic bridge linking cancer cells and their stromal neighbors in oncogenic communication networks. *Oncogene* 35, 816–826. doi: 10.1038/onc.2015.139

Hashimoto, O., Yoshida, M., Koma, Y., Yanai, T., Hasegawa, D., Kosaka, Y., et al. (2016). Collaboration of cancer-associated fibroblasts and tumour-associated macrophages for neuroblastoma development. *J. Pathol.* 240, 211–223. doi: 10.1002/path.4769

Hassan, S., Buchanan, M., Jahan, K., Aguilar-Mahecha, A., Gaboury, L., Muller, W. J., et al. (2011). CXCR4 peptide antagonist inhibits primary breast tumor growth, metastasis and enhances the efficacy of anti-VEGF treatment or docetaxel in a transgenic mouse model. *Int. J. Cancer* 129, 225–232. doi: 10.1002/ijc.25665

He, Y. M., Li, X., Perego, M., Nefedova, Y., Kossenkov, A. V., Jensen, E. A., et al. (2018). Transitory presence of myeloid-derived suppressor cells in neonates is critical for control of inflammation. *Nat. Med.* 24, 224–231. doi: 10.1038/nm.4467

Highfill, S. L., Cui, Y., Giles, A. J., Smith, J. P., Zhang, H., Morse, E., et al. (2014). Disruption of CXCR2-mediated MDSC tumor trafficking enhances anti-PD1 efficacy. *Sci. Transl. Med.* 6:237ra267.

Huang, B., Pan, P. Y., Li, Q., Sato, A. I., Levy, D. E., Bromberg, J., et al. (2006). Gr-1+CD115+ immature myeloid suppressor cells mediate the development of tumor-induced T regulatory cells and T-cell anergy in tumor-bearing host. *Cancer Res.* 66, 1123–1131. doi: 10.1158/0008-5472.can-05-1299

Huang, E. H., Singh, B., Cristofanilli, M., Gelovani, J., Wei, C., Vincent, L., et al. (2009). A CXCR4 antagonist CTCE-9908 inhibits primary tumor growth and metastasis of breast cancer. *J. Surg. Res.* 155, 231–236. doi: 10.1016/j.jss.2008.06.044

Huang, M., Li, Y., Zhang, H., and Nan, F. (2010). Breast cancer stromal fibroblasts promote the generation of CD44+CD24- cells through SDF-1/CXCR4 interaction. *J. Exp. Clin. Cancer Res.* 29:80.

Jin, W. (2020). Role of JAK/STAT3 Signaling in the Regulation of Metastasis, the Transition of Cancer Stem Cells, and Chemoresistance of Cancer by Epithelial-Mesenchymal Transition. *Cells* 9:217. doi: 10.3390/cells9010217

Jinushi, M., Chiba, S., Yoshiyama, H., Masutomi, K., Kinoshita, I., Dosaka-Akita, H., et al. (2011). Tumor-associated macrophages regulate tumorigenicity and anticancer drug responses of cancer stem/initiating cells. *Proc. Natl. Acad. Sci. U. S. A.* 108, 12425–12430. doi: 10.1073/pnas.1106645108

Kalluri, R. (2016). The biology and function of fibroblasts in cancer. *Nat. Rev. Cancer* 16, 582–598. doi: 10.1038/nrc.2016.73

Kessenbrock, K., Plaks, V., and Werb, Z. (2010). Matrix metalloproteinases: regulators of the tumor microenvironment. *Cell* 141, 52–67. doi: 10.1016/j.cell.2010.03.015

Kidd, S., Spaeth, E., Watson, K., Burks, J., Lu, H., Klopp, A., et al. (2012). Origins of the tumor microenvironment: quantitative assessment of adipose-derived and bone marrow-derived stroma. *PLoS One* 7:e30563. doi: 10.1371/journal.pone.0030563

Kim, J., and Bae, J. S. (2016). Tumor-Associated Macrophages and Neutrophils in Tumor Microenvironment. *Mediators Inflamm.* 2016:6058147.

Kinugasa, Y., Matsui, T., and Takakura, N. (2014). CD44 expressed on cancer-associated fibroblasts is a functional molecule supporting the stemness and drug resistance of malignant cancer cells in the tumor microenvironment. *Stem Cells* 32, 145–156. doi: 10.1002/stem.1556

Ko, H. J., Kim, Y. J., Kim, Y. S., Chang, W. S., Ko, S. Y., Chang, S. Y., et al. (2007). A combination of chemoimmunotherapies can efficiently break self-tolerance and induce antitumor immunity in a tolerogenic murine tumor model. *Cancer Res.* 67, 7477–7486. doi: 10.1158/0008-5472.can-06-4639

Kopp, H. G., Ramos, C. A., and Rafii, S. (2006). Contribution of endothelial progenitors and proangiogenic hematopoietic cells to vascularization of tumor and ischemic tissue. *Curr. Opin. Hematol.* 13, 175–181. doi: 10.1097/01.moh.0000219664.26528.da

Krishnamurthy, N., and Kurzrock, R. (2018). Targeting the Wnt/beta-catenin pathway in cancer: update on effectors and inhibitors. *Cancer Treat. Rev.* 62, 50–60. doi: 10.1016/j.ctrv.2017.11.002

Kroemer, G., Galluzzi, L., Kepp, O., and Zitvogel, L. (2013). Immunogenic cell death in cancer therapy. *Annu. Rev. Immunol.* 31, 51–72.

Kuchuk, O., Tuccitto, A., Citterio, D., Huber, V., Camisaschi, C., Milione, M., et al. (2018). pH regulators to target the tumor immune microenvironment in human hepatocellular carcinoma. *Oncoimmunology* 7:e1445452. doi: 10.1080/2162402x.2018.1445452

Kumar, V., Patel, S., Tcyganov, E., and Gabrilovich, D. I. (2016). The Nature of Myeloid-Derived Suppressor Cells in the Tumor Microenvironment. *Trends Immunol.* 37, 208–220.

Kusmartsev, S., Nefedova, Y., Yoder, D., and Gabrilovich, D. I. (2004). Antigen-specific inhibition of CD8+ T cell response by immature myeloid cells in cancer is mediated by reactive oxygen species. *J. Immunol.* 172, 989–999. doi: 10.4049/jimmunol.172.2.989

Lau, E. Y., Ho, N. P., and Lee, T. K. (2017). Cancer Stem Cells and Their Microenvironment: biology and Therapeutic Implications. *Stem Cells Int.* 2017:3714190.

Lecavalier-Barsoum, M., Chaudary, N., Han, K., Koritzinsky, M., Hill, R., and Milosevic, M. (2018). Targeting the CXCL12/CXCR4 pathway and myeloid cells to improve radiation treatment of locally advanced cervical cancer. *Int. J. Cancer* 143, 1017–1028. doi: 10.1002/ijc.31297

Lederle, W., Hartenstein, B., Meides, A., Kunzelmann, H., Werb, Z., Angel, P., et al. (2010). MMP13 as a stromal mediator in controlling persistent angiogenesis in skin carcinoma. *Carcinogenesis* 31, 1175–1184. doi: 10.1093/carcin/bgp248

Lee, S. E., Lim, J. Y., Kim, T. W., Jeon, Y. W., Yoon, J. H., Cho, B. S., et al. (2018). Matrix Metalloproteinase-9 in Monocytic Myeloid-Derived Suppressor Cells Correlate with Early Infections and Clinical Outcomes in Allogeneic Hematopoietic Stem Cell Transplantation. *Biol. Blood Marrow Transplant.* 24, 32–42. doi: 10.1016/j.bbmt.2017.08.017

Li, B., and Wang, J. H. (2011). Fibroblasts and myofibroblasts in wound healing: force generation and measurement. *J. Tissue Viability* 20, 108–120. doi: 10.1016/j.jtv.2009.11.004

Liao, Y. X., Fu, Z. Z., Zhou, C. H., Shan, L. C., Wang, Z. Y., Yin, F., et al. (2015). AMD3100 reduces CXCR4-mediated survival and metastasis of osteosarcoma by inhibiting JNK and Akt, but not p38 or Erk1/2, pathways in in vitro and mouse experiments. *Oncol. Rep.* 34, 33–42. doi: 10.3892/or.2015.3992

Liu, N., Luo, J., Kuang, D., Xu, S., Duan, Y., Xia, Y., et al. (2019). Lactate inhibits ATP6V0d2 expression in tumor-associated macrophages to promote HIF-2α-mediated tumor progression. *J. Clin. Invest.* 129, 631–646. doi: 10.1172/jci123027

Lu-Emerson, C., Snuderl, M., Kirkpatrick, N. D., Goveia, J., Davidson, C., Huang, Y., et al. (2013). Increase in tumor-associated macrophages after antiangiogenic

therapy is associated with poor survival among patients with recurrent glioblastoma. *Neuro Oncol.* 15, 1079–1087. doi: 10.1093/neuonc/not082

Magee, J. A., Piskounova, E., and Morrison, S. J. (2012). Cancer stem cells: impact, heterogeneity, and uncertainty. *Cancer Cell* 21, 283–296. doi: 10.1016/j.ccr.2012.03.003

Mantovani, A., Marchesi, F., Malesci, A., Laghi, L., and Allavena, P. (2017). Tumour-associated macrophages as treatment targets in oncology. *Nat. Rev. Clin. Oncol.* 14, 399–416. doi: 10.1038/nrclinonc.2016.217

Mirkeshavarz, M., Ganjibakhsh, M., Aminishakib, P., Farzaneh, P., Mahdavi, N., Vakhshiteh, F., et al. (2017). Interleukin-6 secreted by oral cancer- associated fibroblast accelerated VEGF expression in tumor and stroma cells. *Cell. Mol. Biol.* 63, 131–136. doi: 10.14715/cmb/2017.63.10.21

Mok, S., Koya, R. C., Tsui, C., Xu, J., Robert, L., Wu, L., et al. (2014). Inhibition of CSF-1 receptor improves the antitumor efficacy of adoptive cell transfer immunotherapy. *Cancer Res.* 74, 153–161. doi: 10.1158/0008-5472.can-13-1816

Mortezaee, K. (2020). CXCL12/CXCR4 axis in the microenvironment of solid tumors: a critical mediator of metastasis. *Life Sci.* 249:117534. doi: 10.1016/j.lfs.2020.117534

Mou, W., Xu, Y., Ye, Y., Chen, S., Li, X., Gong, K., et al. (2015). Expression of Sox2 in breast cancer cells promotes the recruitment of M2 macrophages to tumor microenvironment. *Cancer Lett.* 358, 115–123. doi: 10.1016/j.canlet.2014.11.004

Murray, P. J., Allen, J. E., Biswas, S. K., Fisher, E. A., Gilroy, D. W., Goerdt, S., et al. (2014). Macrophage activation and polarization: nomenclature and experimental guidelines. *Immunity* 41, 14–20. doi: 10.1016/j.immuni.2014.06.008

Nagaraj, S., Youn, J. I., Weber, H., Iclozan, C., Lu, L., Cotter, M. J., et al. (2010). Anti-inflammatory triterpenoid blocks immune suppressive function of MDSCs and improves immune response in cancer. *Clin. Cancer Res.* 16, 1812–1823. doi: 10.1158/1078-0432.ccr-09-3272

Najafi, M., Farhood, B., and Mortezaee, K. (2019a). Cancer stem cells (CSCs) in cancer progression and therapy. *J. Cell. Physiol* 234, 8381–8395. doi: 10.1002/jcp.27740

Najafi, M., Farhood, B., and Mortezaee, K. (2019b). Extracellular matrix (ECM) stiffness and degradation as cancer drivers. *J. Cell. Biochem.* 120, 2782–2790. doi: 10.1002/jcb.27681

Ngiow, S. F., Meeth, K. M., Stannard, K., Barkauskas, D. S., Bollag, G., Bosenberg, M., et al. (2016). Co-inhibition of colony stimulating factor-1 receptor and BRAF oncogene in mouse models of BRAF(V600E) melanoma. *Oncoimmunology* 5:e1089381. doi: 10.1080/2162402x.2015.1089381

Obermajer, N., Muthuswamy, R., Odunsi, K., Edwards, R. P., and Kalinski, P. (2011). PGE(2)-induced CXCL12 production and CXCR4 expression controls the accumulation of human MDSCs in ovarian cancer environment. *Cancer Res.* 71, 7463–7470. doi: 10.1158/0008-5472.can-11-2449

Orimo, A., Gupta, P. B., Sgroi, D. C., Arenzana-Seisdedos, F., Delaunay, T., Naeem, R., et al. (2005). Stromal fibroblasts present in invasive human breast carcinomas promote tumor growth and angiogenesis through elevated SDF-1/CXCL12 secretion. *Cell* 121, 335–348. doi: 10.1016/j.cell.2005.02.034

Paraiso, K. H., and Smalley, K. S. (2013). Fibroblast-mediated drug resistance in cancer. *Biochem. Pharmacol.* 85, 1033–1041. doi: 10.1016/j.bcp.2013.01.018

Peng, D., Tanikawa, T., Li, W., Zhao, L., Vatan, L., Szeliga, W., et al. (2016). Myeloid-Derived Suppressor Cells Endow Stem-like Qualities to Breast Cancer Cells through IL6/STAT3 and NO/NOTCH Cross-talk Signaling. *Cancer Res.* 76, 3156–3165. doi: 10.1158/0008-5472.can-15-2528

Piccard, H., Muschel, R. J., and Opdenakker, G. (2012). On the dual roles and polarized phenotypes of neutrophils in tumor development and progression. *Crit. Rev. Oncol. Hematol.* 82, 296–309. doi: 10.1016/j.critrevonc.2011.06.004

Pradel, L. P., Franke, A., and Ries, C. H. (2018). Effects of IL-10 and T(h) 2 cytokines on human Mφ phenotype and response to CSF1R inhibitor. *J. Leukoc. Biol.* 103, 545–558. doi: 10.1002/jlb.5ma0717-282r

Qin, H., Lerman, B., Sakamaki, I., Wei, G., Cha, S. C., Rao, S. S., et al. (2014). Generation of a new therapeutic peptide that depletes myeloid-derived suppressor cells in tumor-bearing mice. *Nat. Med.* 20, 676–681. doi: 10.1038/nm.3560

Quail, D. F., and Joyce, J. A. (2017). Molecular Pathways: deciphering Mechanisms of Resistance to Macrophage-Targeted Therapies. *Clin. Cancer Res.* 23, 876–884. doi: 10.1158/1078-0432.ccr-16-0133

Rafii, S., Lyden, D., Benezra, R., Hattori, K., and Heissig, B. (2002). Vascular and haematopoietic stem cells: novel targets for anti-angiogenesis therapy? *Nat. Rev. Cancer* 2, 826–835. doi: 10.1038/nrc925

Ran, S., and Montgomery, K. E. (2012). Macrophage-mediated lymphangiogenesis: the emerging role of macrophages as lymphatic endothelial progenitors. *Cancers* 4, 618–657. doi: 10.3390/cancers4030618

Räsänen, K., and Vaheri, A. (2010). Activation of fibroblasts in cancer stroma. *Exp. Cell Res.* 316, 2713–2722. doi: 10.1016/j.yexcr.2010.04.032

Reilley, M. J., McCoon, P., Cook, C., Lyne, P., Kurzrock, R., Kim, Y., et al. (2018). STAT3 antisense oligonucleotide AZD9150 in a subset of patients with heavily pretreated lymphoma: results of a phase 1b trial. *J. Immunother. Cancer* 6:119.

Roberts, E. W., Deonarine, A., Jones, J. O., Denton, A. E., Feig, C., Lyons, S. K., et al. (2013). Depletion of stromal cells expressing fibroblast activation protein-α from skeletal muscle and bone marrow results in cachexia and anemia. *J. Exp. Med.* 210, 1137–1151. doi: 10.1084/jem.20122344

Salimifard, S., Masjedi, A., Hojjat-Farsangi, M., Ghalamfarsa, G., Irandoust, M., Azizi, G., et al. (2020). Cancer associated fibroblasts as novel promising therapeutic targets in breast cancer. *Pathol. Res. Pract.* 216:152915. doi: 10.1016/j.prp.2020.152915

Salminen, A. (2021). Increased immunosuppression impairs tissue homeostasis with aging and age-related diseases. *J. Mol. Med.* 99, 1–20. doi: 10.1007/s00109-020-01988-7

Salminen, A., Kauppinen, A., and Kaarniranta, K. (2018). Myeloid-derived suppressor cells (MDSC): an important partner in cellular/tissue senescence. *Biogerontology* 19, 325–339. doi: 10.1007/s10522-018-9762-8

Seino, T., Kawasaki, S., Shimokawa, M., Tamagawa, H., Toshimitsu, K., Fujii, M., et al. (2018). Human Pancreatic Tumor Organoids Reveal Loss of Stem Cell Niche Factor Dependence during Disease Progression. *Cell Stem Cell* 22, 454–467.e6.

Serafini, P., Meckel, K., Kelso, M., Noonan, K., Califano, J., Koch, W., et al. (2006). Phosphodiesterase-5 inhibition augments endogenous antitumor immunity by reducing myeloid-derived suppressor cell function. *J. Exp. Med.* 203, 2691–2702. doi: 10.1084/jem.20061104

Sherman, M. H., Yu, R. T., Engle, D. D., Ding, N., Atkins, A. R., Tiriac, H., et al. (2014). Vitamin D receptor-mediated stromal reprogramming suppresses pancreatitis and enhances pancreatic cancer therapy. *Cell* 159, 80–93. doi: 10.1016/j.cell.2014.08.007

Shuman Moss, L. A., Jensen-Taubman, S., and Stetler-Stevenson, W. G. (2012). Matrix metalloproteinases: changing roles in tumor progression and metastasis. *Am. J. Pathol.* 181, 1895–1899.

Straussman, R., Morikawa, T., Shee, K., Barzily-Rokni, M., Qian, Z. R., Du, J., et al. (2012). Tumour micro-environment elicits innate resistance to RAF inhibitors through HGF secretion. *Nature* 487, 500–504. doi: 10.1038/nature11183

Sumida, K., Wakita, D., Narita, Y., Masuko, K., Terada, S., Watanabe, K., et al. (2012). Anti-IL-6 receptor mAb eliminates myeloid-derived suppressor cells and inhibits tumor growth by enhancing T-cell responses. *Eur. J. Immunol.* 42, 2060–2072. doi: 10.1002/eji.201142335

Sun, W., Luo, J. D., Jiang, H., and Duan, D. D. (2018). Tumor exosomes: a double-edged sword in cancer therapy. *Acta Pharmacol. Sin.* 39, 534–541. doi: 10.1038/aps.2018.17

Tran, E., Chinnasamy, D., Yu, Z., Morgan, R. A., Lee, C. C., Restifo, N. P., et al. (2013). Immune targeting of fibroblast activation protein triggers recognition of multipotent bone marrow stromal cells and cachexia. *J. Exp. Med.* 210, 1125–1135. doi: 10.1084/jem.20130110

Trivedi, M., Talekar, M., Shah, P., Ouyang, Q., and Amiji, M. (2016). Modification of tumor cell exosome content by transfection with wt-p53 and microRNA-125b expressing plasmid DNA and its effect on macrophage polarization. *Oncogenesis* 5:e250. doi: 10.1038/oncsis.2016.52

Tu, E., Chia, P. Z., and Chen, W. (2014). TGFβ in T cell biology and tumor immunity: angel or devil? *Cytokine Growth Factor Rev.* 25, 423–435. doi: 10.1016/j.cytogfr.2014.07.014

Veglia, F., Perego, M., and Gabrilovich, D. (2018). Myeloid-derived suppressor cells coming of age. *Nat. Immunol.* 19, 108–119. doi: 10.1038/s41590-017-0022-x

Vosseler, S., Lederle, W., Airola, K., Obermueller, E., Fusenig, N. E., and Mueller, M. M. (2009). Distinct progression-associated expression of tumor and stromal MMPs in HaCaT skin SCCs correlates with onset of invasion. *Int. J. Cancer* 125, 2296–2306. doi: 10.1002/ijc.24589

Weber, R., Fleming, V., Hu, X., Nagibin, V., Groth, C., Altevogt, P., et al. (2018). Myeloid-Derived Suppressor Cells Hinder the Anti-Cancer Activity of Immune Checkpoint Inhibitors. *Front. Immunol.* 9:1310. doi: 10.3389/fimmu.2018.01310

Wei, L. Y., Lee, J. J., Yeh, C. Y., Yang, C. J., Kok, S. H., Ko, J. Y., et al. (2019). Reciprocal activation of cancer-associated fibroblasts and oral squamous carcinoma cells through CXCL1. *Oral Oncol.* 88, 115–123. doi: 10.1016/j.oraloncology.2018.11.002

Wen, N., Guo, B., Zheng, H., Xu, L., Liang, H., Wang, Q., et al. (2019). Bromodomain inhibitor jq1 induces cell cycle arrest and apoptosis of glioma stem cells through the VEGF/PI3K/AKT signaling pathway. *Int. J. Oncol.* 55, 879–895.

Wenes, M., Shang, M., Di Matteo, M., Goveia, J., Martín-Pérez, R., Serneels, J., et al. (2016). Macrophage Metabolism Controls Tumor Blood Vessel Morphogenesis and Metastasis. *Cell Metab.* 24, 701–715. doi: 10.1016/j.cmet.2016.09.008

Wong, D., Kandagatla, P., Korz, W., and Chinni, S. R. (2014). Targeting CXCR4 with CTCE-9908 inhibits prostate tumor metastasis. *BMC Urol.* 14:12. doi: 10.1186/1471-2490-14-12

Wu, T., and Dai, Y. (2017). Tumor microenvironment and therapeutic response. *Cancer Lett.* 387, 61–68. doi: 10.1016/j.canlet.2016.01.043

Xiong, S., Wang, R., Chen, Q., Luo, J., Wang, J., Zhao, Z., et al. (2018). Cancer-associated fibroblasts promote stem cell-like properties of hepatocellular carcinoma cells through IL-6/STAT3/Notch signaling. *Am. J. Cancer Res.* 8, 302–316.

Yang, C., Wei, C., Wang, S., Shi, D., Zhang, C., Lin, X., et al. (2019). Elevated CD163(+)/CD68(+) Ratio at Tumor Invasive Front is Closely Associated with Aggressive Phenotype and Poor Prognosis in Colorectal Cancer. *Int. J. Biol. Sci.* 15, 984–998. doi: 10.7150/ijbs.29836

Yang, Z., Guo, J., Cui, K., Du, Y., Zhao, H., Zhu, L., et al. (2020). Thymosin alpha-1 blocks the accumulation of myeloid suppressor cells in NSCLC by inhibiting VEGF production. *Biomed. Pharmacother.* 131:110740. doi: 10.1016/j.biopha.2020.110740

Yaseen, M. M., Abuharfeil, N. M., Darmani, H., and Daoud, A. (2020). Mechanisms of immune suppression by myeloid-derived suppressor cells: the role of interleukin-10 as a key immunoregulatory cytokine. *Open Biol.* 10:200111. doi: 10.1098/rsob.200111

Yeo, E. J., Cassetta, L., Qian, B. Z., Lewkowich, I., Li, J. F., Stefater, J. A. III, et al. (2014). Myeloid WNT7b mediates the angiogenic switch and metastasis in breast cancer. *Cancer Res.* 74, 2962–2973. doi: 10.1158/0008-5472.can-13-2421

Yuan, W., Guo, Y. Q., Li, X. Y., Deng, M. Z., Shen, Z. H., Bo, C. B., et al. (2016). MicroRNA-126 inhibits colon cancer cell proliferation and invasion by targeting the chemokine (C-X-C motif) receptor 4 and Ras homolog gene family, member A, signaling pathway. *Oncotarget* 7, 60230–60244. doi: 10.18632/oncotarget.11176

Zeng, J., Liu, Z., Sun, S., Xie, J., Cao, L., Lv, P., et al. (2018). Tumor-associated macrophages recruited by periostin in intrahepatic cholangiocarcinoma stem cells. *Oncol. Lett.* 15, 8681–8686.

Zhang, H., Deng, T., Liu, R., Ning, T., Yang, H., Liu, D., et al. (2020). CAF secreted miR-522 suppresses ferroptosis and promotes acquired chemo-resistance in gastric cancer. *Mol. Cancer* 19:43.

Zhang, T., Yang, F., Li, W., Liu, B., Li, W., Chen, Z., et al. (2018). Suppression of the SDF-1/CXCR4/β−catenin axis contributes to bladder cancer cell growth inhibition in vitro and in vivo. *Oncol. Rep.* 40, 1666–1674.

Zhou, W., Guo, S., Liu, M., Burow, M. E., and Wang, G. (2019). Targeting CXCL12/CXCR4 Axis in Tumor Immunotherapy. *Curr. Med. Chem.* 26, 3026–3041. doi: 10.2174/0929867324666170830111531

Zhou, Z., Zhou, Q., Wu, X., Xu, S., Hu, X., Tao, X., et al. (2020). VCAM-1 secreted from cancer-associated fibroblasts enhances the growth and invasion of lung cancer cells through AKT and MAPK signaling. *Cancer Lett.* 473, 62–73. doi: 10.1016/j.canlet.2019.12.039

Zhu, Y., Knolhoff, B. L., Meyer, M. A., Nywening, T. M., West, B. L., Luo, J., et al. (2014). CSF1/CSF1R blockade reprograms tumor-infiltrating macrophages and improves response to T-cell checkpoint immunotherapy in pancreatic cancer models. *Cancer Res.* 74, 5057–5069. doi: 10.1158/0008-5472.can-13-3723

Conflict of Interest: The authors declare that the research was conducted in the absence of any commercial or financial relationships that could be construed as a potential conflict of interest.

Publisher's Note: All claims expressed in this article are solely those of the authors and do not necessarily represent those of their affiliated organizations, or those of the publisher, the editors and the reviewers. Any product that may be evaluated in this article, or claim that may be made by its manufacturer, is not guaranteed or endorsed by the publisher.

frontiers in Cell and Developmental Biology

REVIEW
published: 26 August 2021
doi: 10.3389/fcell.2021.684966

Targeting the Microenvironment in Esophageal Cancer

Lei Wang[1,2†], Huiqiong Han[1,2†], Zehua Wang[1,2], Litong Shi[1,2], Mei Yang[1,2] and Yanru Qin[1,2]*

[1] Department of Oncology, The First Affiliated Hospital of Zhengzhou University, Zhengzhou, China, [2] State Key Laboratory of Esophageal Cancer Prevention and Treatment, Zhengzhou University, Zhengzhou, China

Esophageal cancer (EC) is the eighth most common type of cancer and the sixth leading cause of cancer-related deaths worldwide. At present, the clinical treatment for EC is based mainly on radical surgery, chemotherapy, and radiotherapy. However, due to the limited efficacy of conventional treatments and the serious adverse reactions, the outcome is still unsatisfactory (the 5-year survival rate for patients is less than 25%). Thus, it is extremely important and urgent to identify new therapeutic targets. The concept of tumor microenvironment (TME) has attracted increased attention since it was proposed. Recent studies have shown that TME is an important therapeutic target for EC. Microenvironment-targeting therapies such as immunotherapy and antiangiogenic therapy have played an indispensable role in prolonging survival and improving the prognosis of patients with EC. In addition, many new drugs and therapies that have been developed to target microenvironment may become treatment options in the future. We summarize the microenvironment of EC and the latest advances in microenvironment-targeting therapies in this review.

Keywords: esophageal cancer, tumor microenvironment, vascular endothelial growth factor, PD-1/PD-L1, cancer associated fibroblasts

OPEN ACCESS

Edited by:
Chao Ni,
Zhejiang University, China

Reviewed by:
Richa Shrivastava,
Birla Institute of Technology and Science, India
Carmen Veríssima Ferreira Halder,
State University of Campinas, Brazil

***Correspondence:**
Yanru Qin
yanruqin@zzu.edu.cn

† These authors have contributed equally to this work and share first authorship

Specialty section:
This article was submitted to Molecular and Cellular Oncology, a section of the journal Frontiers in Cell and Developmental Biology

Received: *24 March 2021*
Accepted: *27 July 2021*
Published: *26 August 2021*

Citation:
Wang L, Han H, Wang Z, Shi L, Yang M and Qin Y (2021) Targeting the Microenvironment in Esophageal Cancer. Front. Cell Dev. Biol. 9:684966. doi: 10.3389/fcell.2021.684966

INTRODUCTION

Esophageal cancer (EC) is one of the most common malignancies and is a major global health challenge. In 2018, new cases of EC accounted for 3.2% of the total cancer cases and EC-related deaths accounted for 5.3% of the total cancer deaths (Bray et al., 2018; Wang L. et al., 2021). EC consists of two main pathologies—esophageal squamous cell carcinoma (ESCC) and esophageal adenocarcinoma (EAC). ESCC is the most common, mainly in East Asia and Africa, while EAC is mainly prevalent in North America and Europe (Arnold et al., 2015; Torre et al., 2015). Geographical distribution of EC is associated with diet and genetics (Smyth et al., 2017). More than half of patients with EC are often at an advanced stage when first diagnosed, and extensive metastasis makes radical surgery, which is currently the only cure for EC, impossible (Ohashi et al., 2015). At present, the treatment for advanced EC include chemotherapy, radiotherapy, and a few targeted drugs. Although great strides have been made in diagnosis and treatment, the 5-year survival rate for patients with advanced EC is still very poor; no more than 25% (Enzinger and Mayer, 2003). The high mortality rate in EC patients indicates that better treatment methods and targets are needed.

The "seed and soil" hypothesis proposed by Paget (1989) is the prototype for the tumor microenvironment (TME). Subsequent complementary studies have found that TME is composed of a variety of different cells and proteins, including immune cells, extracellular matrix (ECM), and

tumor blood vessels (Polyak et al., 2009). In addition, TME has several important characteristics, including hypoxia, acidosis, chronic inflammation, and immunosuppression, which are associated with tumor proliferation, migration, apoptosis, immune evasion, and angiogenesis (Sung and Chung, 2002; Whiteside, 2008). Moreover, TME is not invariant, but involves constant remodeling of cells and their secretions to make them more suitable for tumor survival (Han et al., 2020). This is partly responsible for the development of resistance to conventional treatments (Luan et al., 2021). All these indicate that the "soil" of EC is important for tumor survival and may be an avenue for overcoming neoplastic disease.

Cells in the microenvironment have better gene stability, suggesting that TME-targeted treatments may have better effects and lower chances of drug resistance. To date, the most popular therapies targeting TME in EC include antiangiogenic therapy (anti-VEGF) and immunotherapy (PD-1/PD-L1 inhibitors) (Kojima et al., 2020; Yang Y. M. et al., 2020; Zhang B. et al., 2020). Both monotherapy and combination therapies further improved treatment efficacy and prolonged survival in patients with EC. In addition, anti-inflammatory reoxygenation combined with radiotherapy or photodynamic therapy, tumor vaccine, blocking microenvironment signal transduction, and other new therapies prevent occurrence and improve the prognosis of EC (Huang and Fu, 2019; Liu J. et al., 2020; Yamamoto and Kato, 2020; Yang Y. M. et al., 2020). Moreover, many cells and factors in the microenvironment can be used as important indicators to judge the prognosis of EC (Lin et al., 2016; Han et al., 2020). This review summarizes the EC microenvironment and related targeted therapies.

SUPPRESSING INFLAMMATION PREVENTS ESOPHAGEAL CANCER

The relationship between inflammation and cancer has been a key focus of research, and long-term inflammatory stimulation is an important inducer of EC (Coussens and Werb, 2002). The EC microenvironment is filled with a variety of pro-inflammatory cytokines and inflammatory substances, all of which are closely associated with tumor occurrence, proliferation, and migration (Bhat et al., 2021). Systematic activation of inflammatory pathway signals promotes the progression of EC. Nuclear factor-kappa B (NF-κB) consists of a family of structurally related transcription factors (Zhang et al., 2019), and its elevated expression is considered a marker of inflammation-induced tumorigenesis (Karin et al., 2002; Izzo et al., 2006). In addition to the NF-κB signaling pathway, interleukin-6 (IL-6)/STAT3 signaling pathway was also found to be upregulated in EC (Wang et al., 2004; Groblewska et al., 2012a). IL-6 is a cytokine that signals by binding to gp130 *via* its receptor, IL-6Rα, to trigger downstream pathways and activate important molecules such as Ras-MAPK, SHP2, PI3K, STAT1, and STAT3. Activation of these pathways gives tumor cells the ability to survive in a highly toxic inflammatory environment and inhibits the effects of immunotherapy (Karin et al., 2002; Hodge et al., 2005).

There are several differences in the inflammatory microenvironment of ESCC and EAC. ESCC is the most common pathological type of EC in East Asia (Smyth et al., 2017), and several well-known carcinogenic factors, such as alcohol and smoking (Enzinger and Mayer, 2003; Rustgi and El-Serag, 2014), cause chronic irritation and subsequent inflammation of the esophageal epithelium through direct toxic effects and reactive oxygen species (ROS) production (Radojicic et al., 2012; Kubo et al., 2014). Epidemiological studies of high-risk populations in China have found that frequent consumption of superheated foods also increases the incidence of ESCC, which is thought to damage the esophageal epithelium and lead to increased inflammation (Shen et al., 2020). Thus, there is little doubt that chronic inflammation is a risk factor for ESCC. Barrett's esophagus is a precancerous lesion of EAC in which chronic gastroesophageal reflux (GERD) causes esophageal epithelial cells to be replaced by goblet cells (Dvorak et al., 2007). Gastric acid reflux directly damages the esophagus and promotes ROS production. Direct injury can trigger sonic hedgehog (SHH) signaling between the damaged epithelium and adjacent stroma, leading to intestinal metaplasia (Wang et al., 2010). Infiltrating inflammatory cells also produce high quantities of ROS to promote epithelial cell transformation and the production of ROS directly leads to DNA damage, causing tumor-initiation mutations (Poulsen et al., 1998; Farhadi et al., 2002). Epidemiological studies have linked obesity to EC (Kamat et al., 2009; Rustgi and El-Serag, 2014). Obesity is in fact a systemic inflammation and a metabolic disorder, which is thought to play an important role in the origin of malignant diseases (Bianchini et al., 2002). There are several mechanisms that can explain the association between obesity and EC, including increased incidence of GERD, increased secretion of proinflammatory adipocytokines in the serum, causing insulin and insulin-like growth factor secretion disorder, and leptin (Eusebi et al., 2012; Greer et al., 2012; Mokrowiecka et al., 2012). In addition to obesity, microbes are also important factors. The imbalance in the oral and intestinal flora can lead to inflammation and gastroesophageal reflux. Based on analysis of high-risk populations, this imbalance is mainly manifested as a decrease in gram-positive bacteria and an increase in gram-negative bacteria (Yang L. et al., 2012; Walker and Talley, 2014).

Normal cells are more likely to mutate in an environment filled with inflammatory cells and cytokines, leading to the development of tumors (Coussens and Werb, 2002). Therefore, anti-inflammatory therapy is a very effective preventive measure. Primary prevention of EC involves improving lifestyle, that is, keeping away from the risk factors for inflammation, including avoiding smoking, consuming moderate quantities of alcohol, and maintaining a healthy weight. For patients with esophagitis or Barrett's esophagus, secondary prevention includes medication with proton pump inhibitors (PPIs) and prokinetics (e.g., Domperidone and Itopride). Anti-reflux surgery is also a form of primary prophylaxis. Some meta-analyses and cohort studies have shown that patients with Barrett's esophagus who were treated with PPIs had a lower incidence of dysplasia and EAC compared with those patients who were not treated with PPIs

(Nguyen et al., 2009; Kastelein et al., 2013). Several drugs have also been shown to inhibit the production of inflammatory factors, thereby inhibiting inflammation. Curcumin, which is found in the household spice turmeric, can inhibit acid-induced IL-6 and IL-8 production by inhibiting activation of the MAPK and PKC signaling pathways, as well as NF-κB (Rafiee et al., 2009). This drug is expected to treat esophagitis caused by GERD. In addition to prevention, inhibition of inflammation can increase the sensitivity of radiation and chemotherapy *in vivo* and *in vitro* and forms one approach for comprehensively treating EC (Li et al., 2018; Liao et al., 2020).

ANTI-ANGIOGENESIS IS A CLASSIC MICROENVIRONMENT-TARGETING THERAPY

Angiogenesis plays an essential role in the development of most solid tumors, including EC, by delivering oxygen and nutrients to the tumor. Tumor angiogenesis is regulated by a variety of angiogenic factors such as vascular endothelial growth factor (VEGF), hepatocyte growth factor (HGF), transforming growth factor-beta (TGF-β), and hypoxia-inducible factor-1 (HIF-1) (Ladeira et al., 2018). Hypoxia, acidosis, and nutritional deficiency can all upregulate the expression of VEGF and promote angiogenesis. Distant metastasis through blood vessels is an additional pathway for tumor progression. As early as Folkman (1971) speculated that blocking tumor blood vessels could inhibit tumor growth. Anti-angiogenic therapies, particularly VEGF inhibitors, have gradually improved following years of research and have played an important role in clinical treatment.

The key mediator of angiogenesis is VEGF, including VEGF-A/B/C/D/E and placental growth factor (PIGF) (Roskoski, 2007). As shown in **Figure 1**, activation of VEGF/VEGFR and VEGF/NRP pathways not only promote the proliferation of vascular endothelial cells and accelerate angiogenesis but also play an important role in promoting lymphangiogenesis (Ding et al., 2006). VEGFR is also expressed in tumor cells. The binding of VEGF to VEGFR triggers multiple downstream signaling pathways, such as ERK1/2 and PI3K/Akt, to promote cell proliferation (Olsson et al., 2006; Chrzanowska-Wodnicka et al., 2008). Therefore, the VEGF/VEGFR signaling pathway is an effective target for the treatment of EC. A variety of VEGF/VEGFR inhibitors have been developed, including anlotinib, apatinib, sorafenib, sunitinib, ramucirumab, and bevacizumab (**Table 1**). Of these, anlotinib, apatinib, sorafenib, and ramucirumab have been shown to have clinical benefits in patients with EC during clinical trials (Wilke et al., 2014; Xu et al., 2014; Janjigian et al., 2015; Moehler et al., 2016; Cunningham et al., 2017; Liu G. et al., 2020; Yang Y. M. et al., 2020; Huang et al., 2021). The positive effect of Endostar combined with radiotherapy and chemotherapy in the treatment of ESCC has been reported and similar clinical trials are ongoing (Xu et al., 2014). Anlotinib and apatinib are included in the Chinese Society of Clinical Oncology (CSCO)-EC guidelines as important treatments for EC. Ramucirumab is also included in the National Comprehensive Cancer Network (NCCN) guidelines for the treatment of gastroesophageal junction (GEJ) adenocarcinoma (Bang et al., 2020). In addition to monotherapy, combination with chemotherapy, immunotherapy, or radiotherapy can result in a better curative effect. Researchers successfully treated a patient with advanced ESCC using apatinib in combination with the PD-1 inhibitor camrelizumab (Yan et al., 2020). Li et al. (2019) showed that the combined use of apatinib and docetaxel significantly prolonged patients' survival and had controllable side effects. Currently, additional studies are exploring the use of combinations of anti-angiogenesis therapy and traditional therapies such as radiotherapy and chemotherapy. On the other hand, tumor blood vessels are structurally and functionally abnormal. This abnormality makes effective drug delivery become difficult and creates an abnormal microenvironment (e.g., hypoxia) that reduces the effectiveness of radiotherapy and chemotherapy. Researchers have found that using anti-angiogenic drugs can induce normalization of blood vessels, then making patients more sensitive to chemotherapy (Batchelor et al., 2007).

However, anti-angiogenesis therapy has some limitations. In addition to several manageable side effects such as hypertension, renal dysfunction, thrombosis, and wound-healing complications, anti-angiogenic drugs are suspected of affecting the spread of other chemotherapeutic drugs *in vivo* (Ye, 2016). Using positron emission tomography (PET), Van der Veldt and others observed that anti-angiogenic drugs could inhibit the delivery of cytotoxic drugs to the tumor site (Van der Veldt et al., 2012). This is not consistent with our previous theory that anti-angiogenic therapy induces structural and functional changes in tumor blood vessels that make them more similar to normal blood vessels, leading to increased blood flow and easier access of cytotoxic drugs into tumors (Batchelor et al., 2007). Zhao et al. (2019) found that small doses of apatinib could regulate TME, alleviate hypoxia, and increase the number of T cells at tumor sites, then enhance the efficacy of PD-1/PD-L1 inhibitors. Excessive doses do not have this effect. This theory has not yet been tested in EC, but it shows that adjusting the order and dosage of medication during treatment is necessary to obtain better efficacy. Current research suggests that anti-angiogenesis therapy combined with other treatments can achieve better therapeutic effects; thus, actively developing new angiogenesis inhibitors and exploring additional drug combination regimens is still the main focus of research efforts.

MATURATION OF IMMUNOTHERAPY

Immunotherapy may be the most significant breakthrough in the history of tumor treatment. In-depth study of the immune microenvironment of EC and accurate intervention has become a consensus among most people. The components of the immune microenvironment of EC are complex and diverse. As shown in **Figure 2**, tumor cells can inhibit the anti-tumor immune response by recruiting a variety of immune cell populations or expressing inhibitory molecular factors (Lin et al., 2016). Smart tumor cells disguise themselves and

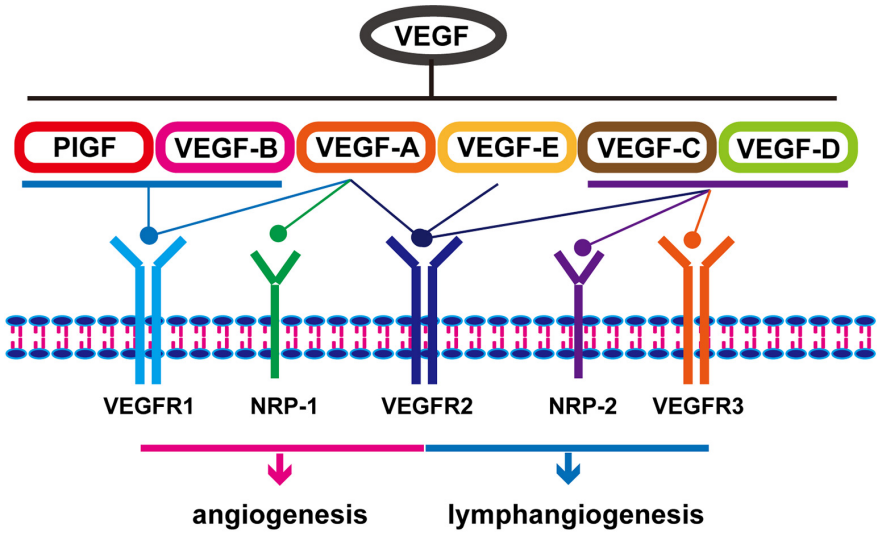

FIGURE 1 | Classification and function of vascular endothelial growth factors.

TABLE 1 | Vascular endothelial growth factor inhibitors applied to esophageal cancer.

Molecule	NCT	Target	Strategy	Type	Result	References
Bevacizumab	NCT00450203	VEGF-A	Combination	EAC	Failure	Cunningham et al., 2017
Ramucirumab	NCT01170663	VEGFR2	Combination	GEJ	Success	Wilke et al., 2014
	NCT01246960	VEGFR2	Combination	EAC/GEJ	Failure	Yoon et al., 2016
	NCT02314117	VEGFR2	Combination	GEJ	Failure	Fuchs et al., 2019
Sunitinib	NCT00702884	VEGFRs	Monotherapy	GEJ	Failure	Wu et al., 2015
	NCT00730353	VEGFRs	Combination	EC/GEJ	Failure	Schmitt et al., 2012
Sorafenib	NCT00917462	VEGFRs	Monotherapy	GEJ	Success	Janjigian et al., 2015
	NCT00253370	VEGFRs	Combination	GEJ	Success	Sun et al., 2010
Apatinib	NCT03274011	VEGFR2	Monotherapy	ESCC	Ongoing	U.S. National Library of Medicine, 2021a
	NCT03603756	VEGFR2	Combination	ESCC	Success	Zhang B. et al., 2020
	NCT02942329	VEGFR2	Combination	GEJ	Success	Xu et al., 2019
Anlotinib	NCT02649361	VEGFRs	Monotherapy	ESCC	Success	Huang et al., 2021
Endostar	NCT03797625	VEGFs	Combination	ESCC	Ongoing	U.S. National Library of Medicine, 2021b

secrete a variety of cytokines to escape attack by T cells. Immunotherapy suppresses the expression of related pathways or provides immune system-specific tumor antigens that restore the immune system function and eliminates tumor cells. Mainstream immunotherapies include inhibition of immune checkpoints (PD-1/PD-L1), tumor vaccination, and adoptive T-cell therapy. These are described in detail below.

Immune Checkpoint Blockade

Programmed death-1 (PD-1) is an immune checkpoint for T cells that can deactivate their immune function. Two ligands, PD-L1 and PD-L2, bind to PD-1 receptors, induce PD-1 signal and associated T-cell depletion, and reversibly inhibit T-cell activation and proliferation (Zou et al., 2016). Activation of the PD-1/PD-L1 signaling pathway can inhibit the function of CTL, while inhibition of this signaling pathway can restore T lymphocyte function and enhance the immune response (Chen and Mellman, 2017). Based on this principle, PD-1/PD-L1 blockers were developed for the treatment of tumors and have shown promise in the treatment of multiple malignancies (Topalian et al., 2012).

Programmed death-1 inhibitors such as pembrolizumab and camrelizumab have recently been approved for the treatment of EC following extensive clinical trials. KEYNOTE-181 is a global multicenter, randomized, controlled, open, phase III clinical trial including 628 patients with advanced or metastatic EC. Final experimental results showed that, compared with chemotherapy, pembrolizumab prolonged overall survival when used as a second-line therapy for advanced EC in patients with PD-L1 $\geq$ 10, with fewer treatment-related adverse events being reported (Kojima et al., 2020). In the latest KEYNOTE-590 study, pembrolizumab combined with cisplatin-fluoropyrimidine chemotherapy as first-line therapy significantly improved overall survival in patients with EC compared with placebo (Smyth et al., 2021). Another PD-1 inhibitor invented in China, camrelizumab, was approved for the treatment of advanced ESCC in 2019 (Zhang B. et al., 2020). In addition to

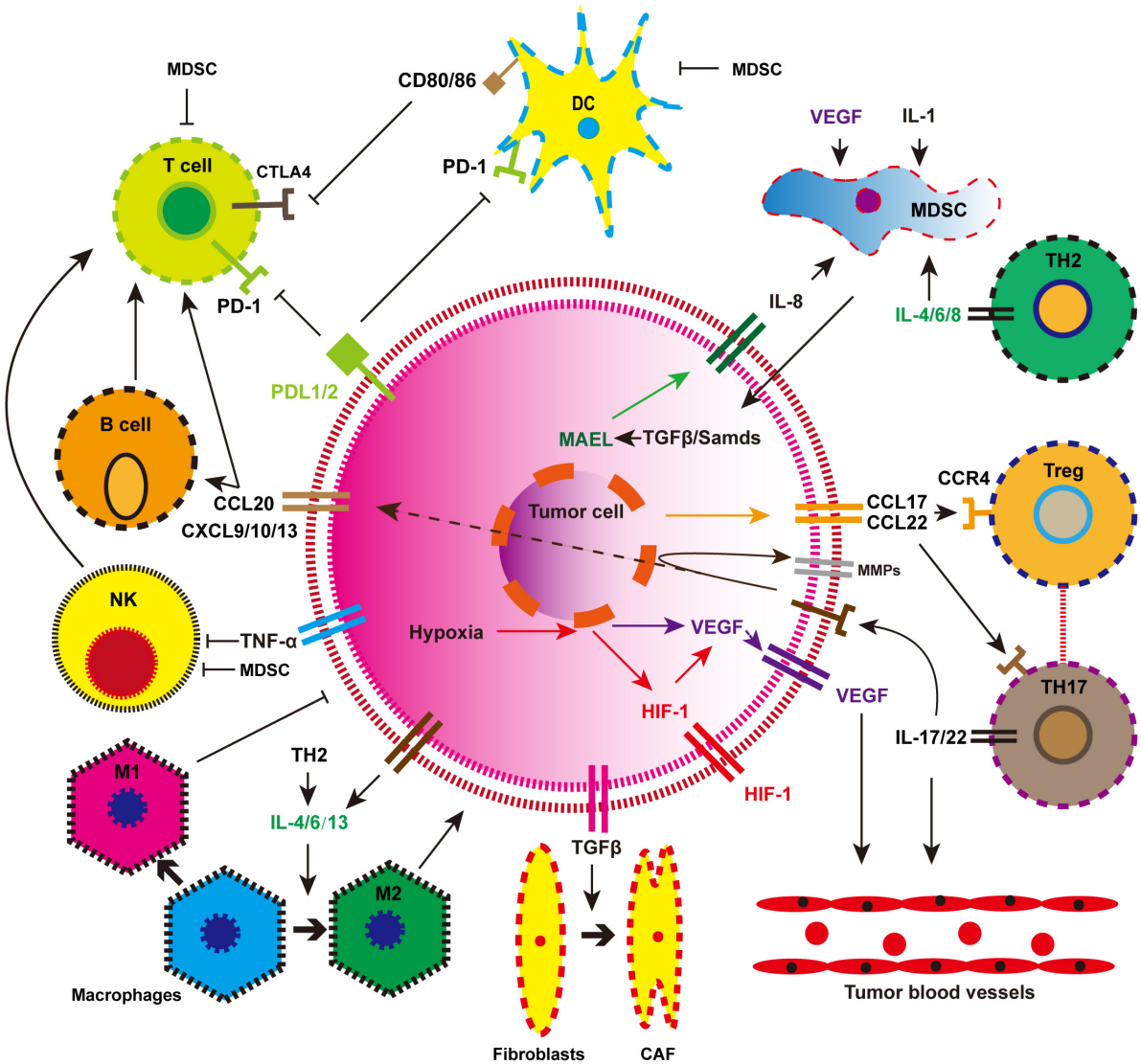

FIGURE 2 | The immune landscape of esophageal cancer. MDSC, myeloid-derived suppressor cell; DC, mature dendritic cell; NK, natural killer cell; Treg, regulatory T cell; M1, tumor suppressor macrophages; M2, tumor-promoting macrophages; CAF, cancer-associated fibroblasts.

the two PD-1 inhibitors mentioned above, there are multiple PD-1/PD-L1 inhibitors undergoing experimental verification, which will provide more options for immunotherapy in EC patients (Yamamoto and Kato, 2020). Compared with traditional chemotherapy, PD-1/PD-L1 inhibitors have fewer side effects and are more effective.

In clinical practice, most patients do not get better survival outcomes following the administration of PD-1 inhibitors. Therefore, predictive biomarkers are needed to determine whether patients are more likely to respond to PD-1/PD-L1 inhibitors. In KEYNOTE-181, researchers found that, compared with chemotherapy, pembrolizumab significantly increased overall survival in PD-L1-positive patients. This may indicate that PD-L1 expression is a direct biological predictor. Disappointingly, PD-L1 status was not associated with objective response rates (ORR) in Chinese ESCC patients (Huang et al., 2018). Thus, we cannot predict therapeutic effect based only on the expression of PD-L1 in patients. Mismatch repair (MMR) defect, tumor mutation load (TML), and microsatellite instability (MSI) have been identified as predictive biomarkers in non-small cell lung cancer, but their role in EC needs to be validated (Yang H. et al., 2020). Li et al. (2021) recently found that upregulation of Laminin γ2 (Ln-γ2) resulted in worse anti-PD-1 treatment outcome, which could be an effective biological predictor in the future. CAF-derived TGF-β1 signaling leads to T-cell exclusion by increasing the expression of Ln-γ2 in ESCC cells, thereby constructing a protective barrier to the tumor, preventing immune cells from penetrating into tumor parenchyma, and weakening the response to anti-PD-1 therapy. In addition, analysis of 260 patients with ESCC

showed that Ln-γ2 is also an independent prognostic predictor. Furthermore, biometric analysis of several serological indicators and a variety of genes including HSPA6, CACYBP, DKK1, EGF, FGF19, GAST, OSM, and ANGPTL3 has also been implicated in having predictive significance (Guo et al., 2020). In fact, it is not very accurate to use a single indicator to predict the efficacy of immunotherapy. Lee and Ruppin found that comprehensive analysis of CD8 T-cell abundance, TML, and PD-1 gene expression can give a more accurate prognosis (Lee and Ruppin, 2019). Whether the comprehensive use of the above indicators can accurately screen out immunotherapy-sensitive populations requires further exploration.

The expression of cytotoxic T-lymphocyte-associated antigen 4 (CTLA4) reduces T-cell activity by inhibiting T-cell receptor (TCR) signaling. A number of studies have shown that overexpression of CTLA4 can block the T-cell cycle, thereby reducing the body's specific immune function and leading to immune evasion of cancer cells (Krummel and Allison, 1995). Interestingly, CTLA4 is not only expressed by tumor infiltrating immune cells (TIICs) in EC, but is also expressed on cancer cells, which is an important part of tumor cell immune escape (Huang and Fu, 2019). Several studies have proven that CTLA4-targeted therapy can produce good survival benefits and fewer side effects. Currently available drugs for CTLA4 include ipilimumab and tremlimumab, of which tremlimumab has been proven to have a therapeutic effect on EC in clinical trials (Ralph et al., 2010). PD-1 and CTLA4 have different mechanisms for reducing T-cell activation and the combined use of these two immune checkpoint inhibitors may yield better results. This synergistic effect (ipilimumab-nivolumab combination) has been demonstrated in melanoma; it is unproven but promising in EC (Weber et al., 2015).

Cancer Vaccines

Tumor-testicular antigens (TTA) are the most well-studied tumor-associated antigens (TAA) that are highly expressed in EC, including New York esophageal squamous cell carcinoma 1 (NY-ESO-1), melanoma-associated antigen-A (MAGE-A), TTK protein kinase (TTK), and Cancer-testis antigen 2 (CTAG2; also known as LAGE1) (Huang and Fu, 2019). Cancer vaccines induce an immune response through these specific antigens, stimulating CTLs to recognize and attack tumor cells. Several peptide vaccines are already in clinical trials (Kantoff et al., 2010; Kageyama et al., 2013). Cancer vaccines containing a combination of multiple peptides derived from TTK, lymphocyte antigen 6 complex locus K (LY6K), and insulin-like growth factor-II mRNA binding protein 3 (IMP3) were tested in phase II clinical trials for treatment of advanced EC (Kono et al., 2012). Results demonstrated that vaccine-induced immune responses in patients with advanced ESCC are associated with better outcomes, suggesting that tumor vaccine therapy using multiple epitope peptides as monotherapy may provide clinical benefits for EC patients. Another vaccine is DC vaccine pulsed with peptides. The powerful antigen-presenting function of DC cells enables the body to produce a stronger immune response which kills the tumor. Sadanaga et al. generated autologous DCs *ex vivo* and pulsed them with MAGE-3 peptide (Sadanaga et al., 2001). This was the first report of DC vaccination of EC patients with MAGE-3 peptide. No toxicity was observed *in vivo*, and tumor regression was induced by an immune response to MAGE-3 peptide. At present, tumor vaccines are not formally used in clinical practice, but their strong and specific anti-tumor function requires further study.

Chimeric Antigen Receptor T-Cell Therapy

Chimeric antigen receptor-T cell therapy refers to the modification of T cells into chimeric antigen receptor (CAR) T cells through genetic engineering to specifically recognize and attack tumor cells. CAR-T cell therapy is more commonly used in hematologic tumors such as leukemia and lymphoma. In recent years, CAR-T cells have been explored as a therapy against solid tumors, including EC (Kiesgen et al., 2018). Studies have shown that ephrin type A receptor 2 (EphA2) and human epidermal growth factor receptor 2 (HER2) are highly expressed in ESCC which are common targets for CAR-T cell therapies (Shi et al., 2018; Yu et al., 2020). Both CAR-T cell therapies have been demonstrated to effectively identify, bind, and destroy ESCC cell lines and release high levels of pro-inflammatory cytokines (Shi et al., 2018; Yu et al., 2020). Kagoya et al. (2018) recently designed a new generation of CAR-T cells with enhanced specificity, persistence, and anti-tumor ability by modifying the previous domain. Based on the CAR-T cell design described above, Zhang H. et al. (2020) designed enhanced MUC1-CAR-T cells for eliminating EC, which were shown to have significant antitumor activity. This enhanced MUC1-CAR-T cells have a longer survival time in mice, which means that they can have sustained anti-tumor ability. The enhanced CAR-T cells seem to be able to overcome the limitations of traditional CAR-T cells. The application of CAR-T cells in solid tumors still has certain limitations, including in the selection of solid tumor-specific antigens and the delivery of CAR-T cells (Akhoundi et al., 2021). Therefore, additional breakthroughs are needed in these areas.

Oncolytic Viruses

Recently, Challenor and Tucker (2021) reported the case of one patient with Hodgkin's lymphoma whose tumor disappeared after being infected with SARS-CoV-2. They hypothesized that the SARS-CoV-2 triggered a tumor immune response that allowed T cells to attack cancer cells. This is a special case, but it suggests that viral therapy may be effective. Oncolytic viruses are potential antitumor agents with unique therapeutic mechanisms, including the ability to directly lyse tumors and induce antitumor immunity. Since the first oncolytic virus (*Talimogene laherparepvec*) was approved for the treatment of melanoma, its use has been broadened, including in multiple experiments on EC (Andtbacka et al., 2015). Ma et al. (2012) confirmed that trichostatin enhanced the antitumor activity of oncolytic adenovirus H101 by activating the MAPK/ERK pathway. Another study used radiotherapy in combination with OBP-301, an attenuate type 5 adenovirus with oncolytic potential that contains the human telomerase reverse transcriptase

promoter, to regulate viral replication, which is important for the treatment of EC (Kuroda et al., 2010).

EXTRACELLULAR MATRIX AND SIGNAL TRANSDUCTION ACCELERATE TUMOR PROGRESSION

The ECM is an important component of the TME, a network of proteins and glycosaminoglycan (Aguado et al., 2016; Hoshiba and Tanaka, 2016). ECM continues to be remodeled to adapt to the survival and progression of tumors. Easily occurring metastasis is one of the characteristics of malignant tumors and one of the reasons why tumors cannot be cured. Many studies have shown that the dynamic changes in ECM promote tumor metastasis.

Stromal Components

The most abundant component in ECM is type I collagen, which is secreted by tumor-associated fibroblasts (TAFs) or cancer-associated fibroblasts (CAFs), fills the gaps between cancer cells, and enhances the stiffness of the tumor (Kai et al., 2019). Dense ECM can inhibit the diffusion, penetration, and transportation of therapeutic drugs; thus, ECM becomes an obstacle to drug delivery (Cun et al., 2015; Jena et al., 2016). Another very important molecule is glycoproteins, which are involved in cell-to-cell adhesion and which can be altered to facilitate migration of cancer cells (Palumbo et al., 2020). For example, deletion of E-cadherin, which is responsible for cell-cell adhesion and communication, has been shown to be associated with increased aggressiveness of tumor cells (Canel et al., 2013). Integrins are a family of transmembrane glycoprotein adhesion receptors that regulate extracellular matrix and cellular adhesion. Kwon et al. (2013) inhibited the proliferation and invasion of EC cells by knocking out integrin alpha 6 (ITGA6) *in vitro*, proving that ITGA6 could be a new therapeutic target. So, it is generally believed that the improvement in tumor stiffness and structure is directly associated with tumor invasion.

Remodeling of ECM is dependent on matrix degradable proteolytic enzymes, which mainly include matrix metalloproteinases (MMPs), plasminogen activators, atypical proteinases (e.g., intracellular cathepsin), and glycolytic enzymes (heparinase and hyaluronidase) (Piperigkou et al., 2021). MMPs are characterized by multi-domain zinc-dependent endopeptidases, which play an indispensable role in the continuous remodeling of ECM (Lei et al., 2020). Through ECM remodeling, MMPs regulate the proliferation, migration, and angiogenesis of tumor cells. More than 30 types of MMP have been identified, among which MMP-2 and MMP-9 are the most closely related to EC (Groblewska et al., 2012b). Overexpression of MMP-2 and MMP-9 results in poor prognosis in EC patients due to type IV collagen basement membrane rupture and is associated with advanced tumor stage, local invasion, and metastasis (Groblewska et al., 2012b). MMPs are regulated by their endogenous natural inhibitors (TIMPs), but in EC, this regulation mechanism is abnormal. The decrease in TIMPs expression and the increase in MMPs expression indicate poor prognosis in patients with EC (Groblewska et al., 2012b). Researchers are currently trying to synthesize exogenous MMP inhibitors (MMPIs) that inhibit tumor progression. Thanks to progress in drug technology, MMPIs now have higher specificity and lower toxic and side effects, and their related therapeutic effects have been verified in the treatments of periodontal disease, multiple sclerosis, and gastric cancer and may also be a new target for the treatment of EC (Fields, 2019). Another very important enzyme is lysyl oxidase (LOX), which catalyzes the cross-linking of collagen and elastin. Kalikawe et al. (2019) found that silencing LOX could inhibit the proliferation of ESCC cells and reduce their invasion and migration ability. Understanding the mechanism of these enzymes will benefit our clinical treatment.

Cancer-associated fibroblast is involved in the development of cancer (**Figure 3**). In Barrett's esophagus, reflux of stomach acid can stimulate the production of IL-6 by esophageal fibroblasts and increase inflammation (Rieder et al., 2007). CAFs are activated by cytokines secreted by tumor cells such as TGF-β. More importantly, fibroblast-derived factor can induce esophageal epithelial metaplasia (Eda et al., 2003). CAFs can secrete a variety of important cytokines, including HGF, fibroblast growth factor (FGF), CXCL12, and TGFβ1, which play an important role in promoting the progression of EC. Subsequent studies confirmed that CAFs can also express VEGF, suggesting that it may be involved in EC angiogenesis (Nie et al., 2014). CAFs are also promoters of tumor invasion and metastasis. They produce factors such as Wnt2 that induce epithelial-mesenchymal transformation (EMT) of EC cells and thus increase cell motility (Fu et al., 2011). CAFs are strongly implicated in tumor progression; thus, eliminating CAFs as a way of inhibiting tumor progression may be a good idea. *In vitro* and animal model studies showed that EC cells co-cultured with CAFs were more prone to metastasis and that cell migration reduced after removal of CAFs (Kashima et al., 2019). In recent years, researchers have tried to inhibit tumor progression by eliminating or inhibiting CAFs. For example, near-infrared photoimmunotherapy (NIR-PIT) was proposed by Mitsunaga et al. (2011) as a new cancer treatment method using highly selective monoclonal antibody (mAb)-photosensitizer conjugate (APC). CAF elimination using CAF-targeted NIR-PIT effectively interferes with the progression of EC and overcomes therapeutic resistance (Katsube et al., 2021). Combining the new CAF-targeted NIR-PIT with traditional anticancer drugs is expected to provide a more effective treatment strategy.

Important Signaling Pathways

FGF/FGFR Pathway

Fibroblast growth factors are known to play a crucial role in regulating excessive development during the embryonic and adult stages of life. When FGF binds to FGFRS, the downstream Ras-MAPK, PI3K-Akt, and PLC-γ-PKC pathways are activated, inducing cell proliferation, differentiation, and tumor formation (Liu G. et al., 2021). Analysis of the ESCC gene database showed that FGF12 expression was elevated, meaning that it can be used as a biomarker (Bhushan et al., 2017). Analysis

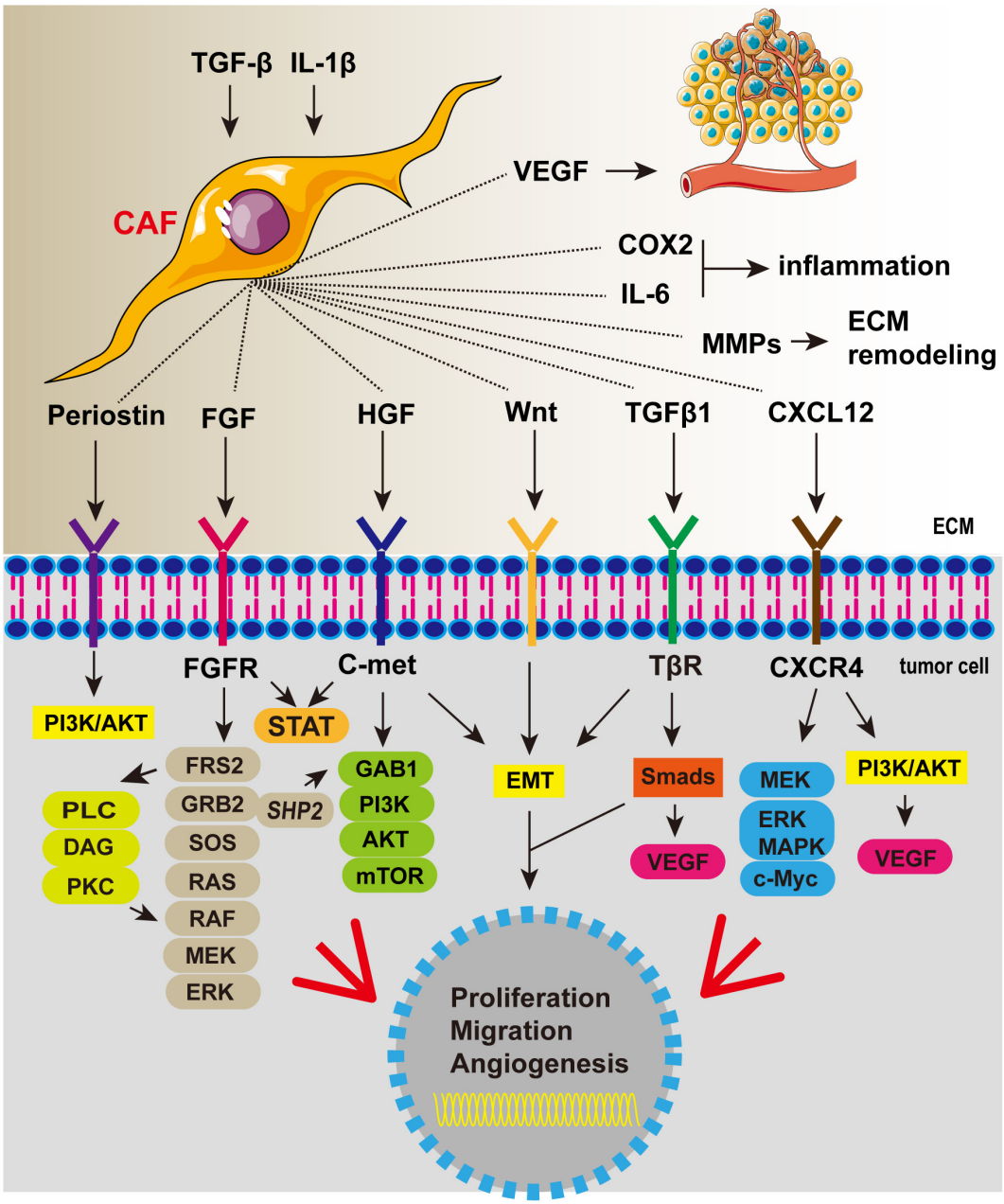

FIGURE 3 | Cancer-associated fibroblasts secrete a variety of cytokines that promote tumor proliferation, invasion, and angiogenesis and aggravate inflammation.

of ESCC samples also showed that the level of FGFR3IIIC, an FGF receptor, was elevated and tumor cell proliferation was increased (Ueno et al., 2016). In conclusion, systemic activation of the FGF/FGFR signaling pathway is important for the progression of EC. FGF/FGFR signaling plays a role in tumorigenesis, and a large number of drugs targeting this signaling pathway have been developed. Erdafitinib, a potent tyrosine kinase inhibitor of FGFR1/2/3/4, has been approved for the treatment of metastatic urothelial carcinoma (Loriot et al., 2019). Another FGFR inhibitor, pemigatinib, has also been shown to prolong survival in people with advanced cholangiocarcinoma (Abou-Alfa et al., 2020). A phase 2 clinical trial in EC patients using brivanib (FGF and VEGF inhibitors) showed an objective therapeutic effect on gastroesophageal cancer, but the data was insufficient to support the application of this drug in clinical treatment (Jones et al., 2019). Additional data is therefore needed to verify the effectiveness of FGF/FGFR inhibitors in EC.

HGF/c-Met Pathway

The binding of HGF to its high-affinity receptor, c-Met, can initiate the proliferation, migration, and angiogenesis of various tumors and promote tumor progression (Wang et al., 2020).

TABLE 2 | Factors and cells associated with poor esophageal cancer prognosis and their mechanisms of action.

Predictor	Mechanism	Expression	References
NF-κB	Induces the expression of IL-8 and IL-1β, intensifies inflammation, and inhibits tumor immunity	Up	Izzo et al., 2007, 2009
C-reactive protein	Directly reflect the degree of inflammation in the body	Up	Suzuki et al., 2020
Gram-negative bacteria	Its increase produces more lipopolysaccharides, which leads to increased inflammation and reflux	Down	Yang L. et al., 2012
IL-6	IL-6 activates downstream STAT3 expression after binding to its receptor. This allows tumor cells to survive in a highly toxic inflammatory environment	Up	Oka et al., 1996; Maeda et al., 2020
STAT3		Up	Hodge et al., 2005
IL-1β	It is two important pro-inflammatory cytokines, which promote tumor invasion and tumor-mediated immunosuppression	Up	Fitzgerald et al., 2002
IL-8		Up	Ogura et al., 2013
COX-2	COX-2 is an inflammatory enzyme responsible for the production of prostaglandin, which is associated with inflammation associated with gastrointestinal cancer	Up	Akutsu et al., 2011
MDSCs	MDSCs directly inhibits T cell activation, NK cell killing, and secretion of a large number of inflammatory cytokines to inhibit tumor immunity	Up	Chen et al., 2014
Tregs	Tregs may play a dual role in the occurrence of tumors, inhibiting inflammation in the early stage and inhibiting cytotoxic T cell function in the late stage, leading to immune escape	Up	Nabeki et al., 2015
M2 macrophage	Macrophages can differentiate into two completely different functional cell types: tumor-suppressing macrophages (M1) and tumor-promoting macrophages (M2). M1 macrophages play a role in tumor rejection, while M2 macrophages promote tumor progression	Up	Shigeoka et al., 2013
Th17	Th17 can directly or indirectly promote tumor growth. Th17 can express extracellular nucleotide enzymes CD39 and CD73, release adenosine, and inhibit CD8+T cells	Up	Chen et al., 2012
PD-L1	When they bind to PD-1, they inhibit T cell activation and promote immune escape	Up	Ohigashi et al., 2005
PD-L2		Up	
CAFs	CAFs secrete a variety of factors to promote tumor invasion and angiogenesis and promote immune evasion	Up	Underwood et al., 2015
TGF-β (Later stage)	TGF-β signaling appears to have a dual role in regulating tumorigenesis: in early stages it is a growth suppressor, but in later stages it promotes EMT and metastasis	Up	von Rahden et al., 2006
HGF	HGF induces the activation of oncogene signaling pathways by binding to its receptor c-Met and promotes tumor cell invasion and angiogenesis	Up	Takada et al., 1995
VEGFs	Trigger endothelial cell proliferation, migration, and breakdown of ECM to build new blood vessels	Up	Lord et al., 2003
MMP-2/7/9	Participate in extracellular matrix remodeling and promote tumor invasion	Up	Gu et al., 2005
CXCL12	The binding of its receptors CXCR4 and CXCR7 to tumor cells can induce tumor cell growth and promote angiogenesis and invasion	Up	Kaifi et al., 2005

HGF secreted by mesenchymal cells is also considered an important angiogenic factor. It binds to c-Met (mainly expressed in epithelial cells) exclusively and induces the activation of oncogenic pathways, angiogenesis, and scattering of cells, leading to metastasis (Ladeira et al., 2018). Additionally, upregulation of the HGF/c-Met signaling pathway can lead to activation of the β-catenin and PI3K/Akt pathways and deactivation of the E-cadherin pathway, promoting tumor invasion (Anderson et al., 2006). Several HGF/c-Met inhibitors which inhibit downstream signaling by either blocking HGF binding to c-Met or directly targeting c-Met are currently in clinical trials. Obinutuzumab and rilotumumab are humanized monoclonal antibodies that target HGF and inhibit its binding to c-Met (Shah et al., 2016; Catenacci et al., 2017). Unfortunately, using rilotumumab combined with cisplatin, capecitabine, and epirubicin as first-line treatment for MET-positive gastroesophageal adenocarcinoma did not give survival benefits (Catenacci et al., 2017). Obinutuzumab also failed in Phase III clinical trials. However, several c-Met inhibitors have been shown to be effective at inhibiting HGF/c-Met signaling by directly targeting c-Met. For example, AMG337, a highly selective small-molecule MET inhibitor, can effectively prevent c-Met/HGF binding. In a multi-center phase II study, AMG337, used as a single agent, showed significant anti-tumor activity in MET-amplified EAC patients

(Van Cutsem et al., 2019). Additional data is needed to verify the effectiveness of HGF/c-Met inhibitors.

TGF-β Pathway

Many studies have clarified the important role of TGF-β in tumor regulation, including proliferation, angiogenesis, immune escape, and cell differentiation (Derynck et al., 2001). Interestingly, TGF-β plays a dual role in tumor progression, acting as a negative regulator in the early stage of tumor development but inducing epithelial mesenchymal transformation (EMT) and promoting migration in the late stages of development (Wojtowicz-Praga, 2003). Typically, TGF-β blocks the normal cell cycle in the G1 phase by inhibiting c-Myc and increasing the expression of P21 and P15, which are considered major regulators of the cell cycle (Wang L. et al., 2021). Activation of TGF-β/Smads inhibits the expression of cyclin-dependent kinase (CDK) inhibitors in advanced tumor cells and simultaneously activates the PI3K/Akt pathway, thereby preventing FoxO and Smad3 recombination. Ras/MAP kinases are also activated to induce EMT by bypassing TGF-β inhibition (Haque and Morris, 2017). As mentioned above, activation of the TGF-β signaling pathway can promote tumor progression and is therefore a potential therapeutic target. The most common inhibitors use the following mechanisms: (1) interferes with TGF-β synthesis, (2) blocks TGF-β signaling and downstream regulatory molecules, and (3) increases TGF-β endogenous or exogenous inhibitors. There are currently multiple TGF-β inhibitors in clinical trials. For example, Galunisertib, a small molecule inhibitor that directly targets TGFBR1 kinase, has shown satisfactory therapeutic effects in phase I clinical trials of advanced liver, pancreatic, breast, and colorectal cancers (Ahmadi et al., 2019). Unfortunately, TGF-β inhibitors have not been reported for EC. Moreover, TGF-β's complex regulatory signals and dual effects also present challenges in its targeted therapy. However, TGF-β has shown anti-tumor effects in other cancer types, leading us to believe that it has great potential for use in the treatment of EC.

IMPROVING THE HYPOXIC MICROENVIRONMENT

Hypoxia and acidosis are common phenomena in a variety of solid tumors, including EC, and lead to a series of physiological changes. Tumor cells rapidly proliferate and consume large volumes of oxygen. In addition, solid tumors compress blood vessels around the tumor and cause blood vessel blockages, which results in insufficient oxygen supply to the center of the tumor (Masoud and Li, 2015; Bhattarai et al., 2018). Normally differentiated cells rely mainly on the oxidative phosphorylation of mitochondria to provide energy for the cells, while most tumor cells depend on aerobic glycolysis, a phenomenon called Warburg effect (Vander Heiden et al., 2009). This phenomenon exacerbates hypoxia and lactic acid accumulation in solid tumors and promotes tumor metastasis. Under hypoxic conditions, the functional inactivation of prolyl-hydroxylase 2 (PHD-2) leads to reduced degradation of HIF-1, which is an important regulator of hypoxic microenvironments (Masoud and Li, 2015). Overexpression of HIF-1α upregulates GLUTs, hexokinase isoform 2 (HK2), pyruvate kinase isoform M (PKM), and other key factors, leading to tumor aerobic glycolytic metabolism (Kato et al., 2018; Sormendi and Wielockx, 2018; Han et al., 2020). The phenomenon is also applicable to EC, where several important regulatory factors such as HIF-1α, GLUT-1, and PKM2 have been found to be elevated (Xiaoyu et al., 2018). Another endogenous hypoxia marker, Carbonic anhydrase IX (CAIX), is also overexpressed in EC (Jomrich et al., 2014). In addition, the increased expression of HIF-1α can also directly upregulate VEGF and PD-L1, which are associated with tumor angiogenesis and immune escape, respectively (Augustin et al., 2020). In the hypoxic microenvironment, many immune cells are affected by HIF-1α, which reduces the immune response and promotes the proliferation of tumors. Moreover, hypoxia can also lead to genetic mutations that inhibit the effects of radiotherapy; downregulation of homologous recombinant proteins BRCA1 and BRCA2 in EC cells promoted G0-G1 cell cycle arrest and thus reduced the response to radiotherapy (Nguyen et al., 2013). A recent study using single-cell sequencing showed that HIF-1 expression decreased in paclitaxel-resistant EC cells, but this phenomenon was reversed with carfilzomib (Wu et al., 2018).

Hypoxia is one of the characteristics of solid tumors and is therefore a potential therapeutic target. Several approaches have been targeted at the hypoxic microenvironment, including HIF-1α targeted therapy, CAIX antagonists, nanomedicine, and traditional Chinese medicine (Wang et al., 2016; Wigerup et al., 2016; Chen et al., 2018; Li et al., 2018; Pan et al., 2018; Yu et al., 2018). Dihydroartemisinin, which is a derivative of artemisinin, can enhance the sensitivity of other treatments by inhibiting the expression of HIF-1α (Li et al., 2018). Chinese herbal medicine has thus proved unique in improving the hypoxic microenvironment and treating EC, but the specific underlying mechanism still requires in-depth analysis. EC can also be treated using phototherapy (Wang B. et al., 2021; Xiang et al., 2021). Recently, Liu J. et al. (2020) designed a cage-like carbon-manganese nanozyme which can not only improve the hypoxic microenvironment but also deliver a lot of photosensitizers to the tumor site, making it useful for real-time tumor imaging and enhancing the efficacy of phototherapy. This new nanomedicine has been verified in both *in vivo* and *in vitro* experiments. Improving the hypoxic microenvironment is an essential part of treating EC. At present, there are few treatment methods targeting the hypoxic microenvironment of EC and most of them are still in preclinical studies.

RELATIONSHIP BETWEEN MICROENVIRONMENT INDICATORS AND PROGNOSIS

Multiple factors in the microenvironment play an indispensable role in EC development. Therefore, the detection of microenvironment indicators can predict the prognosis of patients to a certain extent. These prognostic indicators are summarized in **Table 2**.

CONCLUSION

In this review, we summarized a variety of microenvironment-targeted therapies. At present, traditional therapies such as surgery, chemotherapy, and radiotherapy are still the main treatments for EC. Due to the drug resistance and side effects of traditional treatment, the current therapeutic effect does not meet our requirements. In a recent review, Luan et al. (2021) detailed the relationship between microenvironment and drug resistance in EC, suggesting that microenvironment-targeted therapy may be a breakthrough point for drug resistance. These results highlight the function of TME as a therapeutic target.

Some microenvironment-targeted drugs, such as PD-1/PD-L1 inhibitors and anti-angiogenesis drugs, have entered the clinic and shown good outcomes. New immunotherapies, such as CAR-T therapy, tumor vaccines, and oncolytic viruses, are undergoing clinical trials and have demonstrated initial therapeutic value. In addition, inhibition of the inflammatory microenvironment and improvement of hypoxia are also helpful for patient outcomes. However, existing treatment regimens have many limitations and are not sufficient to cure malignancies; thus, additional research is needed. First, enhancing the effectiveness of existing drugs, e.g., using biomarkers to identify drug-sensitive patients or combining drugs to enhance efficacy, is the simplest way of extending patient survival. Second, many microenvironment-targeted drugs that have shown significant anticancer effects in other tumors can also be used to treat EC. For example, TGF-β pathway inhibitors can not only directly inhibit the tumor but also enhance human immunity. Tests can be performed on EC to determine drug efficacy. Finally, in addition to the targets mentioned above, there are many mechanisms of the microenvironment that are currently unknown. Further studies of these mechanisms and active research and development of new drugs are important for achieving breakthroughs in EC. We believe that microenvironment-targeted therapy can achieve greater survival benefits for patients with EC and its specific mechanism requires further exploration.

AUTHOR CONTRIBUTIONS

YQ designed the study and reviewed the manuscript. LW and HH participated in study design and wrote the original draft of the manuscript. LW was mainly responsible for the design of the image. ZW, LS, and MY were involved in document retrieval and review. All authors agreed to the submission of the final manuscript.

FUNDING

This study was supported by the National Natural Science Foundation of China (Grant No. 81872264).

ACKNOWLEDGMENTS

We acknowledge Haiyu Wang, Chi Qin, Longxiao Zhang, Haonan Xu, and Hongyi Li for their support during this study.

REFERENCES

Abou-Alfa, G. K., Sahai, V., Hollebecque, A., Vaccaro, G., Melisi, D., Al-Rajabi, R., et al. (2020). Pemigatinib for previously treated, locally advanced or metastatic cholangiocarcinoma: a multicentre, open-label, phase 2 study. *Lancet Oncol.* 21, 671–684. doi: 10.1016/s1470-2045(20)30109-1

Aguado, B. A., Caffe, J. R., Nanavati, D., Rao, S. S., Bushnell, G. G., Azarin, S. M., et al. (2016). Extracellular matrix mediators of metastatic cell colonization characterized using scaffold mimics of the pre-metastatic niche. *Acta Biomater.* 33, 13–24. doi: 10.1016/j.actbio.2016.01.043

Ahmadi, A., Najafi, M., Farhood, B., and Mortezaee, K. (2019). Transforming growth factor-β signaling: tumorigenesis and targeting for cancer therapy. *J. Cell Physiol.* 234, 12173–12187. doi: 10.1002/jcp.27955

Akhoundi, M., Mohammadi, M., Sahraei, S. S., Sheykhhasan, M., and Fayazi, N. (2021). CAR T cell therapy as a promising approach in cancer immunotherapy: challenges and opportunities. *Cell Oncol. (Dordr.)* 44, 495-523. doi: 10.1007/s13402-021-00593-1

Akutsu, Y., Hanari, N., Yusup, G., Komatsu-Akimoto, A., Ikeda, N., Mori, M., et al. (2011). COX2 expression predicts resistance to chemoradiotherapy in esophageal squamous cell carcinoma. *Ann. Surg. Oncol.* 18, 2946–2951. doi: 10.1245/s10434-011-1645-z

Anderson, M. R., Harrison, R., Atherfold, P. A., Campbell, M. J., Darnton, S. J., Obszynska, J., et al. (2006). Met receptor signaling: a key effector in esophageal adenocarcinoma. *Clin. Cancer Res.* 12(20 Pt 1), 5936–5943. doi: 10.1158/1078-0432.Ccr-06-1208

Andtbacka, R. H., Kaufman, H. L., Collichio, F., Amatruda, T., Senzer, N., Chesney, J., et al. (2015). Talimogene laherparepvec improves durable response rate in patients with advanced melanoma. *J. Clin. Oncol.* 33, 2780–2788. doi: 10.1200/jco.2014.58.3377

Arnold, M., Soerjomataram, I., Ferlay, J., and Forman, D. (2015). Global incidence of oesophageal cancer by histological subtype in 2012. *Gut* 64, 381–387. doi: 10.1136/gutjnl-2014-308124

Augustin, R. C., Delgoffe, G. M., and Najjar, Y. G. (2020). Characteristics of the tumor microenvironment that influence immune cell functions: hypoxia, oxidative stress, metabolic alterations. *Cancers (Basel)* 12:3802. doi: 10.3390/cancers12123802

Bang, Y. J., Golan, T., Dahan, L., Fu, S., Moreno, V., Park, K., et al. (2020). Ramucirumab and durvalumab for previously treated, advanced non-small-cell lung cancer, gastric/gastro-oesophageal junction adenocarcinoma, or hepatocellular carcinoma: an open-label, phase Ia/b study (JVDJ). *Eur. J. Cancer* 137, 272–284. doi: 10.1016/j.ejca.2020.06.007

Batchelor, T. T., Sorensen, A. G., di Tomaso, E., Zhang, W. T., Duda, D. G., Cohen, K. S., et al. (2007). AZD2171, a pan-VEGF receptor tyrosine kinase inhibitor, normalizes tumor vasculature and alleviates edema in glioblastoma patients. *Cancer Cell* 11, 83–95. doi: 10.1016/j.ccr.2006.11.021

Bhat, A. A., Nisar, S., Maacha, S., Carneiro-Lobo, T. C., Akhtar, S., Siveen, K. S., et al. (2021). Cytokine-chemokine network driven metastasis in esophageal cancer; promising avenue for targeted therapy. *Mol. Cancer* 20:2. doi: 10.1186/s12943-020-01294-3

Bhattarai, D., Xu, X., and Lee, K. (2018). Hypoxia-inducible factor-1 (HIF-1) inhibitors from the last decade (2007 to 2016): a "structure-activity relationship" perspective. *Med. Res. Rev.* 38, 1404–1442. doi: 10.1002/med.21477

Bhushan, A., Singh, A., Kapur, S., Borthakar, B. B., Sharma, J., Rai, A. K., et al. (2017). Identification and validation of fibroblast growth factor 12 gene as a novel potential biomarker in esophageal cancer using cancer genomic datasets. *Omics* 21, 616–631. doi: 10.1089/omi.2017.0116

Bianchini, F., Kaaks, R., and Vainio, H. (2002). Overweight, obesity, and cancer risk. *Lancet Oncol.* 3, 565–574. doi: 10.1016/s1470-2045(02)00849-5

Bray, F., Ferlay, J., Soerjomataram, I., Siegel, R. L., Torre, L. A., and Jemal, A. (2018). Global cancer statistics 2018: GLOBOCAN estimates of incidence and mortality worldwide for 36 cancers in 185 countries. *CA Cancer J. Clin.* 68, 394–424. doi: 10.3322/caac.21492

Canel, M., Serrels, A., Frame, M. C., and Brunton, V. G. (2013). E-cadherin-integrin crosstalk in cancer invasion and metastasis. *J. Cell Sci.* 126(Pt 2), 393–401. doi: 10.1242/jcs.100115

Catenacci, D. V. T., Tebbutt, N. C., Davidenko, I., Murad, A. M., Al-Batran, S. E., Ilson, D. H., et al. (2017). Rilotumumab plus epirubicin, cisplatin, and capecitabine as first-line therapy in advanced MET-positive gastric or gastro-oesophageal junction cancer (RILOMET-1): a randomised, double-blind, placebo-controlled, phase 3 trial. *Lancet Oncol.* 18, 1467–1482. doi: 10.1016/s1470-2045(17)30566-1

Challenor, S., and Tucker, D. (2021). SARS-CoV-2-induced remission of *Hodgkin lymphoma*. *Br. J. Haematol.* 192:415. doi: 10.1111/bjh.17116

Chen, D. S., and Mellman, I. (2017). Elements of cancer immunity and the cancer-immune set point. *Nature* 541, 321–330. doi: 10.1038/nature21349

Chen, D., Hu, Q., Mao, C., Jiao, Z., Wang, S., Yu, L., et al. (2012). Increased IL-17-producing CD4(+) T cells in patients with esophageal cancer. *Cell Immunol.* 272, 166–174. doi: 10.1016/j.cellimm.2011.10.015

Chen, H., Liu, P., Zhang, T., Gao, Y., Zhang, Y., Shen, X., et al. (2018). Effects of diphyllin as a novel V-ATPase inhibitor on TE-1 and ECA-109 cells. *Oncol. Rep.* 39, 921–928. doi: 10.3892/or.2018.6191

Chen, M. F., Kuan, F. C., Yen, T. C., Lu, M. S., Lin, P. Y., Chung, Y. H., et al. (2014). IL-6-stimulated CD11b+ CD14+ HLA-DR- myeloid-derived suppressor cells, are associated with progression and poor prognosis in squamous cell carcinoma of the esophagus. *Oncotarget* 5, 8716–8728. doi: 10.18632/oncotarget.2368

Chrzanowska-Wodnicka, M., Kraus, A. E., Gale, D., White, G. C. II, and Vansluys, J. (2008). Defective angiogenesis, endothelial migration, proliferation, and MAPK signaling in Rap1b-deficient mice. *Blood* 111, 2647–2656. doi: 10.1182/blood-2007-08-109710

Coussens, L. M., and Werb, Z. (2002). Inflammation and cancer. *Nature* 420, 860–867. doi: 10.1038/nature01322

Cun, X., Chen, J., Ruan, S., Zhang, L., Wan, J., He, Q., et al. (2015). A novel strategy through combining iRGD peptide with tumor-microenvironment-responsive and multistage nanoparticles for deep tumor penetration. *ACS Appl. Mater. Interfaces* 7, 27458–27466. doi: 10.1021/acsami.5b09391

Cunningham, D., Stenning, S. P., Smyth, E. C., Okines, A. F., Allum, W. H., Rowley, S., et al. (2017). Peri-operative chemotherapy with or without bevacizumab in operable oesophagogastric adenocarcinoma (UK Medical Research Council ST03): primary analysis results of a multicentre, open-label, randomised phase 2-3 trial. *Lancet Oncol.* 18, 357–370. doi: 10.1016/s1470-2045(17)30043-8

Derynck, R., Akhurst, R. J., and Balmain, A. (2001). TGF-beta signaling in tumor suppression and cancer progression. *Nat. Genet.* 29, 117–129. doi: 10.1038/ng1001-117

Ding, M. X., Lin, X. Q., Fu, X. Y., Zhang, N., and Li, J. C. (2006). Expression of vascular endothelial growth factor-C and angiogenesis in esophageal squamous cell carcinoma. *World J. Gastroenterol.* 12, 4582–4585. doi: 10.3748/wjg.v12.i28.4582

Dvorak, K., Payne, C. M., Chavarria, M., Ramsey, L., Dvorakova, B., Bernstein, H., et al. (2007). Bile acids in combination with low pH induce oxidative stress and oxidative DNA damage: relevance to the pathogenesis of Barrett's oesophagus. *Gut* 56, 763–771. doi: 10.1136/gut.2006.103697

Eda, A., Osawa, H., Satoh, K., Yanaka, I., Kihira, K., Ishino, Y., et al. (2003). Aberrant expression of CDX2 in Barrett's epithelium and inflammatory esophageal mucosa. *J. Gastroenterol.* 38, 14–22. doi: 10.1007/s005350300001

Enzinger, P. C., and Mayer, R. J. (2003). Esophageal cancer. *N. Engl. J. Med.* 349, 2241–2252. doi: 10.1056/NEJMra035010

Eusebi, L. H., Fuccio, L., and Bazzoli, F. (2012). The role of obesity in gastroesophageal reflux disease and Barrett's esophagus. *Dig. Dis.* 30, 154–157. doi: 10.1159/000336668

Farhadi, A., Fields, J., Banan, A., and Keshavarzian, A. (2002). Reactive oxygen species: are they involved in the pathogenesis of GERD, Barrett's esophagus, and the latter's progression toward esophageal cancer? *Am. J. Gastroenterol.* 97, 22–26. doi: 10.1111/j.1572-0241.2002.05444.x

Fields, G. B. (2019). The rebirth of matrix metalloproteinase inhibitors: moving beyond the dogma. *Cells* 8:984. doi: 10.3390/cells8090984

Fitzgerald, R. C., Abdalla, S., Onwuegbusi, B. A., Sirieix, P., Saeed, I. T., Burnham, W. R., et al. (2002). Inflammatory gradient in Barrett's oesophagus: implications for disease complications. *Gut* 51, 316–322. doi: 10.1136/gut.51.3.316

Folkman, J. (1971). Tumor angiogenesis: therapeutic implications. *N. Engl. J. Med.* 285, 1182–1186. doi: 10.1056/nejm197111182852108

Fu, L., Zhang, C., Zhang, L. Y., Dong, S. S., Lu, L. H., Chen, J., et al. (2011). Wnt2 secreted by tumour fibroblasts promotes tumour progression in oesophageal cancer by activation of the Wnt/β-catenin signalling pathway. *Gut* 60, 1635–1643. doi: 10.1136/gut.2011.241638

Fuchs, C. S., Shitara, K., Di Bartolomeo, M., Lonardi, S., Al-Batran, S. E., Van Cutsem, E., et al. (2019). Ramucirumab with cisplatin and fluoropyrimidine as first-line therapy in patients with metastatic gastric or junctional adenocarcinoma (RAINFALL): a double-blind, randomised, placebo-controlled, phase 3 trial. *Lancet Oncol.* 20, 420–435. doi: 10.1016/s1470-2045(18)30791-5

Greer, K. B., Thompson, C. L., Brenner, L., Bednarchik, B., Dawson, D., Willis, J., et al. (2012). Association of insulin and insulin-like growth factors with Barrett's oesophagus. *Gut* 61, 665–672. doi: 10.1136/gutjnl-2011-300641

Groblewska, M., Mroczko, B., Sosnowska, D., and Szmitkowski, M. (2012a). Interleukin 6 and C-reactive protein in esophageal cancer. *Clin. Chim. Acta* 413, 1583–1590. doi: 10.1016/j.cca.2012.05.009

Groblewska, M., Siewko, M., Mroczko, B., and Szmitkowski, M. (2012b). The role of matrix metalloproteinases (MMPs) and their inhibitors (TIMPs) in the development of esophageal cancer. *Folia Histochem. Cytobiol.* 50, 12–19. doi: 10.2478/18691

Gu, Z. D., Li, J. Y., Li, M., Gu, J., Shi, X. T., Ke, Y., et al. (2005). Matrix metalloproteinases expression correlates with survival in patients with esophageal squamous cell carcinoma. *Am. J. Gastroenterol.* 100, 1835–1843. doi: 10.1111/j.1572-0241.2005.50018.x

Guo, X., Wang, Y., Zhang, H., Qin, C., Cheng, A., Liu, J., et al. (2020). Identification of the prognostic value of immune-related genes in esophageal cancer. *Front. Genet.* 11:989. doi: 10.3389/fgene.2020.00989

Han, P., Cao, P., Hu, S., Kong, K., Deng, Y., Zhao, B., et al. (2020). Esophageal microenvironment: from precursor microenvironment to premetastatic niche. *Cancer Manag. Res.* 12, 5857–5879. doi: 10.2147/cmar.S258215

Haque, S., and Morris, J. C. (2017). Transforming growth factor-β: a therapeutic target for cancer. *Hum. Vaccin. Immunother.* 13, 1741–1750. doi: 10.1080/21645515.2017.1327107

Hodge, D. R., Hurt, E. M., and Farrar, W. L. (2005). The role of IL-6 and STAT3 in inflammation and cancer. *Eur. J. Cancer* 41, 2502–2512. doi: 10.1016/j.ejca.2005.08.016

Hoshiba, T., and Tanaka, M. (2016). Decellularized matrices as in vitro models of extracellular matrix in tumor tissues at different malignant levels: mechanism of 5-fluorouracil resistance in colorectal tumor cells. *Biochim. Biophys. Acta* 1863, 2749–2757. doi: 10.1016/j.bbamcr.2016.08.009

Huang, J., Xiao, J., Fang, W., Lu, P., Fan, Q., Shu, Y., et al. (2021). Anlotinib for previously treated advanced or metastatic esophageal squamous cell carcinoma: a double-blind randomized phase 2 trial. *Cancer Med.* 10, 1681–1689. doi: 10.1002/cam4.3771

Huang, J., Xu, B., Mo, H., Zhang, W., Chen, X., Wu, D., et al. (2018). Safety, activity, and biomarkers of SHR-1210, an Anti-PD-1 antibody, for patients with advanced esophageal carcinoma. *Clin. Cancer Res.* 24, 1296–1304. doi: 10.1158/1078-0432.Ccr-17-2439

Huang, T. X., and Fu, L. (2019). The immune landscape of esophageal cancer. *Cancer Commun. (Lond.)* 39:79. doi: 10.1186/s40880-019-0427-z

Izzo, J. G., Correa, A. M., Wu, T. T., Malhotra, U., Chao, C. K., Luthra, R., et al. (2006). Pretherapy nuclear factor-kappaB status, chemoradiation resistance, and metastatic progression in esophageal carcinoma. *Mol. Cancer Ther.* 5, 2844–2850. doi: 10.1158/1535-7163.Mct-06-0351

Izzo, J. G., Malhotra, U., Wu, T. T., Luthra, R., Correa, A. M., Swisher, S. G., et al. (2007). Clinical biology of esophageal adenocarcinoma after surgery is influenced by nuclear factor-kappaB expression. *Cancer Epidemiol. Biomarkers Prev.* 16, 1200–1205. doi: 10.1158/1055-9965.Epi-06-1083

Izzo, J. G., Wu, X., Wu, T. T., Huang, P., Lee, J. S., Liao, Z., et al. (2009). Therapy-induced expression of NF-kappaB portends poor prognosis in patients with localized esophageal cancer undergoing preoperative chemoradiation. *Dis. Esophagus.* 22, 127–132. doi: 10.1111/j.1442-2050.2008.00884.x

Janjigian, Y. Y., Vakiani, E., Ku, G. Y., Herrera, J. M., Tang, L. H., Bouvier, N., et al. (2015). Phase II trial of sorafenib in patients with chemotherapy refractory metastatic esophageal and gastroesophageal (ge) junction cancer. *PLoS One* 10:e0134731. doi: 10.1371/journal.pone.0134731

Jena, P. V., Shamay, Y., Shah, J., Roxbury, D., Paknejad, N., and Heller, D. A. (2016). Photoluminescent carbon nanotubes interrogate the permeability of multicellular tumor spheroids. *Carbon N. Y.* 97, 99–109. doi: 10.1016/j.carbon.2015.08.024

Jomrich, G., Jesch, B., Birner, P., Schwameis, K., Paireder, M., Asari, R., et al. (2014). Stromal expression of carbonic anhydrase IX in esophageal cancer. *Clin. Transl. Oncol.* 16, 966–972. doi: 10.1007/s12094-014-1180-z

Jones, R. L., Ratain, M. J., O'Dwyer, P. J., Siu, L. L., Jassem, J., Medioni, J., et al. (2019). Phase II randomised discontinuation trial of brivanib in patients with advanced solid tumours. *Eur. J. Cancer* 120, 132–139. doi: 10.1016/j.ejca.2019.07.024

Kageyama, S., Wada, H., Muro, K., Niwa, Y., Ueda, S., Miyata, H., et al. (2013). Dose-dependent effects of NY-ESO-1 protein vaccine complexed with cholesteryl pullulan (CHP-NY-ESO-1) on immune responses and survival benefits of esophageal cancer patients. *J. Transl. Med.* 11:246. doi: 10.1186/1479-5876-11-246

Kagoya, Y., Tanaka, S., Guo, T., Anczurowski, M., Wang, C. H., Saso, K., et al. (2018). A novel chimeric antigen receptor containing a JAK-STAT signaling domain mediates superior antitumor effects. *Nat. Med.* 24, 352–359. doi: 10.1038/nm.4478

Kai, F., Drain, A. P., and Weaver, V. M. (2019). The extracellular matrix modulates the metastatic journey. *Dev. Cell* 49, 332–346. doi: 10.1016/j.devcel.2019.03.026

Kaifi, J. T., Yekebas, E. F., Schurr, P., Obonyo, D., Wachowiak, R., Busch, P., et al. (2005). Tumor-cell homing to lymph nodes and bone marrow and CXCR4 expression in esophageal cancer. *J. Natl. Cancer Inst.* 97, 1840–1847. doi: 10.1093/jnci/dji431

Kalikawe, R., Baba, Y., Nomoto, D., Okadome, K., Miyake, K., Eto, K., et al. (2019). Lysyl oxidase impacts disease outcomes and correlates with global DNA hypomethylation in esophageal cancer. *Cancer Sci.* 110, 3727–3737. doi: 10.1111/cas.14214

Kamat, P., Wen, S., Morris, J., and Anandasabapathy, S. (2009). Exploring the association between elevated body mass index and Barrett's esophagus: a systematic review and meta-analysis. *Ann. Thorac. Surg.* 87, 655–662. doi: 10.1016/j.athoracsur.2008.08.003

Kantoff, P. W., Higano, C. S., Shore, N. D., Berger, E. R., Small, E. J., Penson, D. F., et al. (2010). Sipuleucel-T immunotherapy for castration-resistant prostate cancer. *N. Engl. J. Med.* 363, 411–422. doi: 10.1056/NEJMoa1001294

Karin, M., Cao, Y., Greten, F. R., and Li, Z. W. (2002). NF-kappaB in cancer: from innocent bystander to major culprit. *Nat. Rev. Cancer* 2, 301–310. doi: 10.1038/nrc780

Kashima, H., Noma, K., Ohara, T., Kato, T., Katsura, Y., Komoto, S., et al. (2019). Cancer-associated fibroblasts (CAFs) promote the lymph node metastasis of esophageal squamous cell carcinoma. *Int. J. Cancer* 144, 828–840. doi: 10.1002/ijc.31953

Kastelein, F., Spaander, M. C., Steyerberg, E. W., Biermann, K., Valkhoff, V. E., Kuipers, E. J., et al. (2013). Proton pump inhibitors reduce the risk of neoplastic progression in patients with Barrett's esophagus. *Clin. Gastroenterol. Hepatol.* 11, 382–388. doi: 10.1016/j.cgh.2012.11.014

Kato, Y., Maeda, T., Suzuki, A., and Baba, Y. (2018). Cancer metabolism: new insights into classic characteristics. *Jpn. Dent. Sci. Rev.* 54, 8–21. doi: 10.1016/j.jdsr.2017.08.003

Katsube, R., Noma, K., Ohara, T., Nishiwaki, N., Kobayashi, T., Komoto, S., et al. (2021). Fibroblast activation protein targeted near infrared photoimmunotherapy (NIR PIT) overcomes therapeutic resistance in human esophageal cancer. *Sci. Rep.* 11:1693. doi: 10.1038/s41598-021-81465-4

Kiesgen, S., Chicaybam, L., Chintala, N. K., and Adusumilli, P. S. (2018). Chimeric antigen receptor (CAR) T-cell therapy for thoracic malignancies. *J. Thorac. Oncol.* 13, 16–26. doi: 10.1016/j.jtho.2017.10.001

Kojima, T., Shah, M. A., Muro, K., Francois, E., Adenis, A., Hsu, C. H., et al. (2020). Randomized phase III KEYNOTE-181 study of pembrolizumab versus chemotherapy in advanced esophageal cancer. *J. Clin. Oncol.* 38, 4138–4148. doi: 10.1200/jco.20.01888

Kono, K., Iinuma, H., Akutsu, Y., Tanaka, H., Hayashi, N., Uchikado, Y., et al. (2012). Multicenter, phase II clinical trial of cancer vaccination for advanced esophageal cancer with three peptides derived from novel cancer-testis antigens. *J. Transl. Med.* 10:141. doi: 10.1186/1479-5876-10-141

Krummel, M. F., and Allison, J. P. (1995). CD28 and CTLA-4 have opposing effects on the response of T cells to stimulation. *J. Exp. Med.* 182, 459–465. doi: 10.1084/jem.182.2.459

Kubo, N., Morita, M., Nakashima, Y., Kitao, H., Egashira, A., Saeki, H., et al. (2014). Oxidative DNA damage in human esophageal cancer: clinicopathological analysis of 8-hydroxydeoxyguanosine and its repair enzyme. *Dis. Esophagus.* 27, 285–293. doi: 10.1111/dote.12107

Kuroda, S., Fujiwara, T., Shirakawa, Y., Yamasaki, Y., Yano, S., Uno, F., et al. (2010). Telomerase-dependent oncolytic adenovirus sensitizes human cancer cells to ionizing radiation via inhibition of DNA repair machinery. *Cancer Res.* 70, 9339–9348. doi: 10.1158/0008-5472.Can-10-2333

Kwon, J., Lee, T. S., Lee, H. W., Kang, M. C., Yoon, H. J., Kim, J. H., et al. (2013). Integrin alpha 6: a novel therapeutic target in esophageal squamous cell carcinoma. *Int. J. Oncol.* 43, 1523–1530. doi: 10.3892/ijo.2013.2097

Ladeira, K., Macedo, F., Longatto-Filho, A., and Martins, S. F. (2018). Angiogenic factors: role in esophageal cancer, a brief review. *Esophagus* 15, 53–58. doi: 10.1007/s10388-017-0597-1

Lee, J. S., and Ruppin, E. (2019). Multiomics prediction of response rates to therapies to inhibit programmed cell death 1 and programmed cell death 1 ligand 1. *JAMA Oncol.* 5, 1614–1618. doi: 10.1001/jamaoncol.2019.2311

Lei, Z., Jian, M., Li, X., Wei, J., Meng, X., and Wang, Z. (2020). Biosensors and bioassays for determination of matrix metalloproteinases: state of the art and recent advances. *J. Mater. Chem. B* 8, 3261–3291. doi: 10.1039/c9tb02189b

Li, J., Jia, Y., Gao, Y., Chang, Z., Han, H., Yan, J., et al. (2019). Clinical efficacy and survival analysis of apatinib combined with docetaxel in advanced esophageal cancer. *Onco. Targets Ther.* 12, 2577–2583. doi: 10.2147/ott.S191736

Li, L., Wei, J. R., Dong, J., Lin, Q. G., Tang, H., Jia, Y. X., et al. (2021). Laminin γ2-mediating T cell exclusion attenuates response to anti-PD-1 therapy. *Sci. Adv.* 7:eabc8346. doi: 10.1126/sciadv.abc8346

Li, Y., Sui, H., Jiang, C., Li, S., Han, Y., Huang, P., et al. (2018). Dihydroartemisinin increases the sensitivity of photodynamic therapy via NF-κB/HIF-1α/VEGF pathway in esophageal cancer cell in vitro and in vivo. *Cell Physiol. Biochem.* 48, 2035–2045. doi: 10.1159/000492541

Liao, X., Gao, Y., Liu, J., Tao, L., Xie, J., Gu, Y., et al. (2020). Combination of tanshinone IIA and cisplatin inhibits esophageal cancer by downregulating NF-κB/COX-2/VEGF pathway. *Front. Oncol.* 10:1756. doi: 10.3389/fonc.2020.01756

Lin, E. W., Karakasheva, T. A., Hicks, P. D., Bass, A. J., and Rustgi, A. K. (2016). The tumor microenvironment in esophageal cancer. *Oncogene* 35, 5337–5349. doi: 10.1038/onc.2016.34

Liu, G., Chen, T., Ding, Z., Wang, Y., Wei, Y., and Wei, X. (2021). Inhibition of FGF-FGFR and VEGF-VEGFR signalling in cancer treatment. *Cell Prolif.* 54:e13009. doi: 10.1111/cpr.13009

Liu, G., Wang, Y., Wang, C., He, Y., and E M. (2020). Clinical efficacy and safety of apatinib as maintenance treatment in patients with advanced esophageal squamous cell carcinoma. *Expert. Rev. Clin. Pharmacol.* 13, 1423–1430. doi: 10.1080/17512433.2020.1844004

Liu, J., Gao, J., Zhang, A., Guo, Y., Fan, S., He, Y., et al. (2020). Carbon nanocage-based nanozyme as an endogenous H(2)O(2)-activated oxygenerator for real-time bimodal imaging and enhanced phototherapy of esophageal cancer. *Nanoscale* 12, 21674–21686. doi: 10.1039/d0nr05945e

Lord, R. V., Park, J. M., Wickramasinghe, K., DeMeester, S. R., Oberg, S., Salonga, D., et al. (2003). Vascular endothelial growth factor and basic fibroblast growth factor expression in esophageal adenocarcinoma and *Barrett esophagus*. *J. Thorac. Cardiovasc. Surg.* 125, 246–253. doi: 10.1067/mtc.2003.203

Loriot, Y., Necchi, A., Park, S. H., Garcia-Donas, J., Huddart, R., Burgess, E., et al. (2019). Erdafitinib in locally advanced or metastatic urothelial carcinoma. *N. Engl. J. Med.* 381, 338–348. doi: 10.1056/NEJMoa1817323

Luan, S., Zeng, X., Zhang, C., Qiu, J., Yang, Y., Mao, C., et al. (2021). Advances in drug resistance of esophageal cancer: from the perspective of tumor microenvironment. *Front. Cell Dev. Biol.* 9:664816. doi: 10.3389/fcell.2021.664816

Ma, J., Zhao, J., Lu, J., Jiang, Y., Yang, H., Li, P., et al. (2012). Coxsackievirus and adenovirus receptor promotes antitumor activity of oncolytic adenovirus H101 in esophageal cancer. *Int. J. Mol. Med.* 30, 1403–1409. doi: 10.3892/ijmm.2012.1133

Maeda, Y., Takeuchi, H., Matsuda, S., Okamura, A., Fukuda, K., Miyasho, T., et al. (2020). Clinical significance of preoperative serum concentrations of interleukin-6 as a prognostic marker in patients with esophageal cancer. *Esophagus* 17, 279–288. doi: 10.1007/s10388-019-00708-6

Masoud, G. N., and Li, W. (2015). HIF-1α pathway: role, regulation and intervention for cancer therapy. *Acta Pharm. Sin. B* 5, 378–389. doi: 10.1016/j.apsb.2015.05.007

Mitsunaga, M., Ogawa, M., Kosaka, N., Rosenblum, L. T., Choyke, P. L., and Kobayashi, H. (2011). Cancer cell-selective in vivo near infrared photoimmunotherapy targeting specific membrane molecules. *Nat. Med.* 17, 1685–1691. doi: 10.1038/nm.2554

Moehler, M., Gepfner-Tuma, I., Maderer, A., Thuss-Patience, P. C., Ruessel, J., Hegewisch-Becker, S., et al. (2016). Sunitinib added to FOLFIRI versus FOLFIRI in patients with chemorefractory advanced adenocarcinoma of the stomach or lower esophagus: a randomized, placebo-controlled phase II AIO trial with serum biomarker program. *BMC Cancer* 16:699. doi: 10.1186/s12885-016-2736-9

Mokrowiecka, A., Daniel, P., Jasinska, A., Pietruczuk, M., Pawlowski, M., Szczesniak, P., et al. (2012). Serum adiponectin, resistin, leptin concentration and central adiposity parameters in Barrett's esophagus patients with and without intestinal metaplasia in comparison to healthy controls and patients with GERD. *Hepatogastroenterology* 59, 2395–2399. doi: 10.5754/hge12587

Nabeki, B., Ishigami, S., Uchikado, Y., Sasaki, K., Kita, Y., Okumura, H., et al. (2015). Interleukin-32 expression and Treg infiltration in esophageal squamous cell carcinoma. *Anticancer Res.* 35, 2941–2947.

Nguyen, D. M., El-Serag, H. B., Henderson, L., Stein, D., Bhattacharyya, A., and Sampliner, R. E. (2009). Medication usage and the risk of neoplasia in patients with Barrett's esophagus. *Clin. Gastroenterol. Hepatol.* 7, 1299–1304. doi: 10.1016/j.cgh.2009.06.001

Nguyen, M. P., Lee, S., and Lee, Y. M. (2013). Epigenetic regulation of hypoxia inducible factor in diseases and therapeutics. *Arch. Pharm. Res.* 36, 252–263. doi: 10.1007/s12272-013-0058-x

Nie, L., Lyros, O., Medda, R., Jovanovic, N., Schmidt, J. L., Otterson, M. F., et al. (2014). Endothelial-mesenchymal transition in normal human esophageal endothelial cells cocultured with esophageal adenocarcinoma cells: role of IL-1β and TGF-β2. *Am. J. Physiol. Cell Physiol.* 307, C859–C877. doi: 10.1152/ajpcell.00081.2014

Ogura, M., Takeuchi, H., Kawakubo, H., Nishi, T., Fukuda, K., Nakamura, R., et al. (2013). Clinical significance of CXCL-8/CXCR-2 network in esophageal squamous cell carcinoma. *Surgery* 154, 512–520. doi: 10.1016/j.surg.2013.06.013

Ohashi, S., Miyamoto, S., Kikuchi, O., Goto, T., Amanuma, Y., and Muto, M. (2015). Recent advances from basic and clinical studies of esophageal squamous cell carcinoma. *Gastroenterology* 149, 1700–1715. doi: 10.1053/j.gastro.2015.08.054

Ohigashi, Y., Sho, M., Yamada, Y., Tsurui, Y., Hamada, K., Ikeda, N., et al. (2005). Clinical significance of programmed death-1 ligand-1 and programmed death-1 ligand-2 expression in human esophageal cancer. *Clin. Cancer Res.* 11, 2947–2953. doi: 10.1158/1078-0432.Ccr-04-1469

Oka, M., Iizuka, N., Yamamoto, K., Gondo, T., Abe, T., Hazama, S., et al. (1996). The influence of interleukin-6 on the growth of human esophageal cancer cell lines. *J. Interferon. Cytokine Res.* 16, 1001–1006. doi: 10.1089/jir.1996.16.1001

Olsson, A. K., Dimberg, A., Kreuger, J., and Claesson-Welsh, L. (2006). VEGF receptor signalling - in control of vascular function. *Nat. Rev. Mol. Cell Biol.* 7, 359–371. doi: 10.1038/nrm1911

Paget, S. (1989). The distribution of secondary growths in cancer of the breast. 1889. *Cancer Metastasis Rev.* 8, 98–101.

Palumbo, A. Jr., Meireles Da Costa, N., Pontes, B., Leite, de Oliveira, F., Lohan Codeço, M., et al. (2020). Esophageal cancer development: crucial clues arising from the extracellular matrix. *Cells* 9:455. doi: 10.3390/cells9020455

Pan, P., Yang, B. X., and Ge, X. L. (2018). *Brucea javanica* seed oil enhances the radiosensitivity of esophageal cancer by inhibiting hypoxia-inducible factor 1α, in vitro and in vivo. *Oncol. Lett.* 15, 3870–3875. doi: 10.3892/ol.2018.7779

Piperigkou, Z., Kyriakopoulou, K., Koutsakis, C., Mastronikolis, S., and Karamanos, N. K. (2021). Key matrix remodeling enzymes: functions and targeting in cancer. *Cancers (Basel)* 13:1441. doi: 10.3390/cancers13061441

Polyak, K., Haviv, I., and Campbell, I. G. (2009). Co-evolution of tumor cells and their microenvironment. *Trends Genet.* 25, 30–38. doi: 10.1016/j.tig.2008.10.012

Poulsen, H. E., Prieme, H., and Loft, S. (1998). Role of oxidative DNA damage in cancer initiation and promotion. *Eur. J. Cancer Prev.* 7, 9–16.

Radojicic, J., Zaravinos, A., and Spandidos, D. A. (2012). HPV, KRAS mutations, alcohol consumption and tobacco smoking effects on esophageal squamous-cell carcinoma carcinogenesis. *Int. J. Biol. Markers* 27, 1–12. doi: 10.5301/jbm.2011.8737

Rafiee, P., Nelson, V. M., Manley, S., Wellner, M., Floer, M., Binion, D. G., et al. (2009). Effect of curcumin on acidic pH-induced expression of IL-6 and IL-8 in human esophageal epithelial cells (HET-1A): role of PKC, MAPKs, and NF-kappaB. *Am. J. Physiol. Gastrointest. Liver Physiol.* 296, G388–G398. doi: 10.1152/ajpgi.90428.2008

Ralph, C., Elkord, E., Burt, D. J., O'Dwyer, J. F., Austin, E. B., Stern, P. L., et al. (2010). Modulation of lymphocyte regulation for cancer therapy: a phase II trial of tremelimumab in advanced gastric and esophageal adenocarcinoma. *Clin. Cancer Res.* 16, 1662–1672. doi: 10.1158/1078-0432.Ccr-09-2870

Rieder, F., Cheng, L., Harnett, K. M., Chak, A., Cooper, G. S., Isenberg, G., et al. (2007). Gastroesophageal reflux disease-associated esophagitis induces endogenous cytokine production leading to motor abnormalities. *Gastroenterology* 132, 154–165. doi: 10.1053/j.gastro.2006.10.009

Roskoski, R. Jr. (2007). Vascular endothelial growth factor (VEGF) signaling in tumor progression. *Crit. Rev. Oncol. Hematol.* 62, 179–213. doi: 10.1016/j.critrevonc.2007.01.006

Rustgi, A. K., and El-Serag, H. B. (2014). Esophageal carcinoma. *N. Engl. J. Med.* 371, 2499–2509. doi: 10.1056/NEJMra1314530

Sadanaga, N., Nagashima, H., Mashino, K., Tahara, K., Yamaguchi, H., Ohta, M., et al. (2001). Dendritic cell vaccination with MAGE peptide is a novel therapeutic approach for gastrointestinal carcinomas. *Clin. Cancer Res.* 7, 2277–2284.

Schmitt, J. M., Sommers, S. R., Fisher, W., Ansari, R., Robin, E., Koneru, K., et al. (2012). Sunitinib plus paclitaxel in patients with advanced esophageal cancer: a phase II study from the Hoosier Oncology Group. *J. Thorac. Oncol.* 7, 760–763. doi: 10.1097/JTO.0b013e31824abc7c

Shah, M. A., Cho, J. Y., Tan, I. B., Tebbutt, N. C., Yen, C. J., Kang, A., et al. (2016). A randomized phase II study of folfox with or without the MET inhibitor onartuzumab in advanced adenocarcinoma of the stomach and gastroesophageal junction. *Oncologist* 21, 1085–1090. doi: 10.1634/theoncologist.2016-0038

Shen, Y., Xie, S., Zhao, L., Song, G., Shao, Y., Hao, C., et al. (2020). Estimating individualized absolute risk for esophageal squamous cell carcinoma: a population-based study in high-risk areas of china. *Front. Oncol.* 10:598603. doi: 10.3389/fonc.2020.598603

Shi, H., Yu, F., Mao, Y., Ju, Q., Wu, Y., Bai, W., et al. (2018). EphA2 chimeric antigen receptor-modified T cells for the immunotherapy of esophageal squamous cell carcinoma. *J. Thorac. Dis.* 10, 2779–2788. doi: 10.21037/jtd.2018.04.91

Shigeoka, M., Urakawa, N., Nakamura, T., Nishio, M., Watajima, T., Kuroda, D., et al. (2013). Tumor associated macrophage expressing CD204 is associated with tumor aggressiveness of esophageal squamous cell carcinoma. *Cancer Sci.* 104, 1112–1119. doi: 10.1111/cas.12188

Smyth, E. C., Gambardella, V., Cervantes, A., and Fleitas, T. (2021). Checkpoint inhibitors for gastroesophageal cancers: dissecting heterogeneity to better understand their role in first line and adjuvant therapy. *Ann. Oncol.* 32, 590-599. doi: 10.1016/j.annonc.2021.02.004

Smyth, E. C., Lagergren, J., Fitzgerald, R. C., Lordick, F., Shah, M. A., Lagergren, P., et al. (2017). Oesophageal cancer. *Nat. Rev. Dis. Primers* 3:17048. doi: 10.1038/nrdp.2017.48

Sormendi, S., and Wielockx, B. (2018). Hypoxia pathway proteins as central mediators of metabolism in the tumor cells and their microenvironment. *Front. Immunol.* 9:40. doi: 10.3389/fimmu.2018.00040

Sun, W., Powell, M., O'Dwyer, P. J., Catalano, P., Ansari, R. H., and Benson, A. B. III (2010). Phase II study of sorafenib in combination with docetaxel and cisplatin in the treatment of metastatic or advanced gastric and gastroesophageal junction adenocarcinoma: ECOG 5203. *J. Clin. Oncol.* 28, 2947–2951. doi: 10.1200/jco.2009.27.7988

Sung, S. Y., and Chung, L. W. (2002). Prostate tumor-stroma interaction: molecular mechanisms and opportunities for therapeutic targeting. *Differentiation* 70, 506–521. doi: 10.1046/j.1432-0436.2002.700905.x

Suzuki, T., Ishibashi, Y., Tsujimoto, H., Nomura, S., Kouzu, K., Itazaki, Y., et al. (2020). A novel systemic inflammatory score combined with immunoinflammatory markers accurately reflects prognosis in patients with esophageal cancer. *In Vivo* 34, 3705–3711. doi: 10.21873/invivo.12218

Takada, N., Yano, Y., Matsuda, T., Otani, S., Osugi, H., Higashino, M., et al. (1995). Expression of immunoreactive human hepatocyte growth factor in human esophageal squamous cell carcinomas. *Cancer Lett.* 97, 145–148. doi: 10.1016/0304-3835(95)03967-2

Topalian, S. L., Hodi, F. S., Brahmer, J. R., Gettinger, S. N., Smith, D. C., McDermott, D. F., et al. (2012). Safety, activity, and immune correlates of anti-PD-1 antibody in cancer. *N. Engl. J. Med.* 366, 2443–2454. doi: 10.1056/NEJMoa1200690

Torre, L. A., Bray, F., Siegel, R. L., Ferlay, J., Lortet-Tieulent, J., and Jemal, A. (2015). Global cancer statistics, 2012. *CA Cancer J. Clin.* 65, 87–108. doi: 10.3322/caac.21262

U.S. National Library of Medicine (2021a). Available online at: https://clinicaltrials.gov/ct2/show/NCT03274011?term=NCT03274011&draw=2&rank=1 (accessed January 26, 2021).

U.S. National Library of Medicine (2021b). Available online at: https://clinicaltrials.gov/ct2/show/NCT03797625?term=NCT03797625&draw=2&rank=1 (accessed January 9, 2019).

Ueno, N., Shimizu, A., Kanai, M., Iwaya, Y., Ueda, S., Nakayama, J., et al. (2016). Enhanced expression of fibroblast growth factor receptor 3 iiic promotes human esophageal carcinoma cell proliferation. *J. Histochem. Cytochem.* 64, 7–17. doi: 10.1369/0022155415616161

Underwood, T. J., Hayden, A. L., Derouet, M., Garcia, E., Noble, F., White, M. J., et al. (2015). Cancer-associated fibroblasts predict poor outcome and promote periostin-dependent invasion in oesophageal adenocarcinoma. *J. Pathol.* 235, 466–477. doi: 10.1002/path.4467

Van Cutsem, E., Karaszewska, B., Kang, Y. K., Chung, H. C., Shankaran, V., Siena, S., et al. (2019). A multicenter phase II study of amg 337 in patients with MET-amplified gastric/gastroesophageal junction/esophageal adenocarcinoma and other MET-amplified solid tumors. *Clin. Cancer Res.* 25, 2414–2423. doi: 10.1158/1078-0432.Ccr-18-1337

Van der Veldt, A. A., Lubberink, M., Bahce, I., Walraven, M., de Boer, M. P., Greuter, H. N., et al. (2012). Rapid decrease in delivery of chemotherapy to tumors after anti-VEGF therapy: implications for scheduling of anti-angiogenic drugs. *Cancer Cell* 21, 82–91. doi: 10.1016/j.ccr.2011.11.023

Vander Heiden, M. G., Cantley, L. C., and Thompson, C. B. (2009). Understanding the warburg effect: the metabolic requirements of cell proliferation. *Science* 324, 1029–1033. doi: 10.1126/science.1160809

von Rahden, B. H., Stein, H. J., Feith, M., Pühringer, F., Theisen, J., Siewert, J. R., et al. (2006). Overexpression of TGF-beta1 in esophageal (Barrett's) adenocarcinoma is associated with advanced stage of disease and poor prognosis. *Mol. Carcinog.* 45, 786–794. doi: 10.1002/mc.20259

Walker, M. M., and Talley, N. J. (2014). Review article: bacteria and pathogenesis of disease in the upper gastrointestinal tract–beyond the era of *Helicobacter pylori*. *Aliment. Pharmacol. Ther.* 39, 767–779. doi: 10.1111/apt.12666

Wang, B., Zhao, Q., Zhang, Y., Liu, Z., Zheng, Z., Liu, S., et al. (2021). Targeting hypoxia in the tumor microenvironment: a potential strategy to improve cancer immunotherapy. *J. Exp. Clin. Cancer Res.* 40:24. doi: 10.1186/s13046-020-01820-7

Wang, D. H., Clemons, N. J., Miyashita, T., Dupuy, A. J., Zhang, W., Szczepny, A., et al. (2010). Aberrant epithelial-mesenchymal Hedgehog signaling characterizes Barrett's metaplasia. *Gastroenterology* 138, 1810–1822. doi: 10.1053/j.gastro.2010.01.048

Wang, D., Qin, Q., Jiang, Q. J., and Wang, D. F. (2016). Bortezomib sensitizes esophageal squamous cancer cells to radiotherapy by suppressing the expression of HIF-1α and apoptosis proteins. *J. Xray Sci. Technol.* 24, 639–646. doi: 10.3233/xst-160571

Wang, H., Rao, B., Lou, J., Li, J., Liu, Z., Li, A., et al. (2020). The Function of the HGF/c-met axis in hepatocellular carcinoma. *Front. Cell Dev. Biol.* 8:55. doi: 10.3389/fcell.2020.00055

Wang, L., Han, H., Dong, L., Wang, Z., and Qin, Y. (2021). Function of p21 and its therapeutic effects in esophageal cancer. *Oncol. Lett.* 21:136. doi: 10.3892/ol.2020.12397

Wang, T., Niu, G., Kortylewski, M., Burdelya, L., Shain, K., Zhang, S., et al. (2004). Regulation of the innate and adaptive immune responses by Stat-3 signaling in tumor cells. *Nat. Med.* 10, 48–54. doi: 10.1038/nm976

Weber, J. S., D'Angelo, S. P., Minor, D., Hodi, F. S., Gutzmer, R., Neyns, B., et al. (2015). Nivolumab versus chemotherapy in patients with advanced melanoma who progressed after anti-CTLA-4 treatment (CheckMate 037): a randomised, controlled, open-label, phase 3 trial. *Lancet Oncol.* 16, 375–384. doi: 10.1016/s1470-2045(15)70076-8

Whiteside, T. L. (2008). The tumor microenvironment and its role in promoting tumor growth. *Oncogene* 27, 5904–5912. doi: 10.1038/onc.2008.271

Wigerup, C., Påhlman, S., and Bexell, D. (2016). Therapeutic targeting of hypoxia and hypoxia-inducible factors in cancer. *Pharmacol. Ther.* 164, 152–169. doi: 10.1016/j.pharmthera.2016.04.009

Wilke, H., Muro, K., Van Cutsem, E., Oh, S. C., Bodoky, G., Shimada, Y., et al. (2014). Ramucirumab plus paclitaxel versus placebo plus paclitaxel in patients with previously treated advanced gastric or gastro-oesophageal junction adenocarcinoma (RAINBOW): a double-blind, randomised phase 3 trial. *Lancet Oncol.* 15, 1224–1235. doi: 10.1016/s1470-2045(14)70420-6

Wojtowicz-Praga, S. (2003). Reversal of tumor-induced immunosuppression by TGF-beta inhibitors. *Invest. New Drugs* 21, 21–32. doi: 10.1023/a:1022951824806

Wu, C., Mikhail, S., Wei, L., Timmers, C., Tahiri, S., Neal, A., et al. (2015). A phase II and pharmacodynamic study of sunitinib in relapsed/refractory oesophageal and gastro-oesophageal cancers. *Br. J. Cancer* 113, 220–225. doi: 10.1038/bjc.2015.197

Wu, H., Chen, S., Yu, J., Li, Y., Zhang, X. Y., Yang, L., et al. (2018). Single-cell transcriptome analyses reveal molecular signals to intrinsic and acquired paclitaxel resistance in esophageal squamous cancer cells. *Cancer Lett.* 420, 156–167. doi: 10.1016/j.canlet.2018.01.059

Xiang, Q., Qiao, B., Luo, Y., Cao, J., Fan, K., Hu, X., et al. (2021). Increased photodynamic therapy sensitization in tumors using a nitric oxide-based nanoplatform with ATP-production blocking capability. *Theranostics* 11, 1953–1969. doi: 10.7150/thno.52997

Xiaoyu, H., Yiru, Y., Shuisheng, S., Keyan, C., Zixing, Y., Shanglin, C., et al. (2018). The mTOR pathway regulates PKM2 to affect glycolysis in esophageal squamous cell carcinoma. *Technol. Cancer Res. Treat.* 17:1533033818780063. doi: 10.1177/1533033818780063

Xu, J., Zhang, Y., Jia, R., Yue, C., Chang, L., Liu, R., et al. (2019). Anti-PD-1 Antibody SHR-1210 combined with apatinib for advanced hepatocellular carcinoma, gastric, or esophagogastric junction cancer: an open-label, dose escalation and expansion study. *Clin. Cancer Res.* 25, 515–523. doi: 10.1158/1078-0432.Ccr-18-2484

Xu, M., Huang, H., Xiong, Y., Peng, B., Zhou, Z., Wang, D., et al. (2014). Combined chemotherapy plus endostar with sequential stereotactic radiotherapy as salvage treatment for recurrent esophageal cancer with severe dyspnea: a case report and review of the literature. *Oncol. Lett.* 8, 291–294. doi: 10.3892/ol.2014.2087

Yamamoto, S., and Kato, K. (2020). Immuno-oncology for esophageal cancer. *Future Oncol.* 16, 2673–2681. doi: 10.2217/fon-2020-0545

Yan, Z., Yao, Z. H., Yao, S. N., Wang, H. Y., Chu, J. F., Song, M., et al. (2020). Camrelizumab plus apatinib successfully treated a patient with advanced esophageal squamous cell carcinoma. *Immunotherapy* 12, 1161–1166. doi: 10.2217/imt-2020-0197

Yang, H., Wang, K., Wang, T., Li, M., Li, B., Li, S., et al. (2020). The combination options and predictive biomarkers of PD-1/PD-L1 inhibitors in esophageal cancer. *Front. Oncol.* 10:300. doi: 10.3389/fonc.2020.00300

Yang, L., Francois, F., and Pei, Z. (2012). Molecular pathways: pathogenesis and clinical implications of microbiome alteration in esophagitis and *Barrett esophagus*. *Clin. Cancer Res.* 18, 2138–2144. doi: 10.1158/1078-0432.Ccr-11-0934

Yang, Y. M., Hong, P., Xu, W. W., He, Q. Y., and Li, B. (2020). Advances in targeted therapy for esophageal cancer. *Signal. Transduct. Target Ther.* 5:229. doi: 10.1038/s41392-020-00323-3

Ye, W. (2016). The complexity of translating anti-angiogenesis therapy from basic science to the clinic. *Dev. Cell* 37, 114–125. doi: 10.1016/j.devcel.2016.03.015

Yoon, H. H., Bendell, J. C., Braiteh, F. S., Firdaus, I., Philip, P. A., Cohn, A. L., et al. (2016). Ramucirumab combined with FOLFOX as front-line therapy for advanced esophageal, gastroesophageal junction, or gastric adenocarcinoma: a randomized, double-blind, multicenter Phase II trial. *Ann. Oncol.* 27, 2196–2203. doi: 10.1093/annonc/mdw423

Yu, F., Wang, X., Shi, H., Jiang, M., Xu, J., Sun, M., et al. (2020). Development of chimeric antigen receptor-modified T cells for the treatment of esophageal cancer. *Tumori* 107, 341-352. doi: 10.1177/0300891620960223

Yu, Y., Li, X., Xu, H., Liu, J., Dong, M., Yang, J., et al. (2018). Correlation of hypoxia status with radiosensitizing effects of sodium glycididazole: a preclinical study. *Oncol. Lett.* 15, 6481–6488. doi: 10.3892/ol.2018.8096

Zhang, B., Qi, L., Wang, X., Xu, J., Liu, Y., Mu, L., et al. (2020). Phase II clinical trial using camrelizumab combined with apatinib and chemotherapy as the first-line treatment of advanced esophageal squamous cell carcinoma. *Cancer Commun. (Lond.)* 40, 711–720. doi: 10.1002/cac2.12119

Zhang, H., Zhao, H., He, X., Xi, F., and Liu, J. (2020). JAK-STAT domain enhanced MUC1-CAR-T cells induced esophageal cancer elimination. *Cancer Manag. Res.* 12, 9813–9824. doi: 10.2147/cmar.S264358

Zhang, L., Xiao, X., Arnold, P. R., and Li, X. C. (2019). Transcriptional and epigenetic regulation of immune tolerance: roles of the NF-κB family members. *Cell Mol. Immunol.* 16, 315–323. doi: 10.1038/s41423-019-0202-8

Zhao, S., Ren, S., Jiang, T., Zhu, B., Li, X., Zhao, C., et al. (2019). Low-dose apatinib optimizes tumor microenvironment and potentiates antitumor effect of PD-1/PD-L1 blockade in lung cancer. *Cancer Immunol. Res.* 7, 630–643. doi: 10.1158/2326-6066.Cir-17-0640

Zou, W., Wolchok, J. D., and Chen, L. (2016). PD-L1 (B7-H1) and PD-1 pathway blockade for cancer therapy: mechanisms, response biomarkers, and combinations. *Sci. Transl. Med.* 8:328rv324. doi: 10.1126/scitranslmed.aad7118

Conflict of Interest: The authors declare that the research was conducted in the absence of any commercial or financial relationships that could be construed as a potential conflict of interest.

Publisher's Note: All claims expressed in this article are solely those of the authors and do not necessarily represent those of their affiliated organizations, or those of the publisher, the editors and the reviewers. Any product that may be evaluated in this article, or claim that may be made by its manufacturer, is not guaranteed or endorsed by the publisher.

frontiers in Cell and Developmental Biology

ORIGINAL RESEARCH
published: 08 September 2021
doi: 10.3389/fcell.2021.654504

Role of CXCR4 as a Prognostic Biomarker Associated With the Tumor Immune Microenvironment in Gastric Cancer

Yuyang Gu[1†], Wenyue Gu[2†], Rongrong Xie[1], Zhi Chen[1], Tongpeng Xu[3] and Zhenghua Fei[1]**

[1] Department of Oncology, The First Affiliated Hospital of Wenzhou Medical University, Wenzhou, China, [2] Yancheng Third People's Hospital, The Sixth Affiliated Hospital of Nantong University, Yancheng, China, [3] Department of Oncology, The First Affiliated Hospital of Nanjing Medical University, Nanjing, China

Background: Gastric cancer (GC) is a leading cause of cancer-related deaths worldwide, accounting for high rates of morbidity and mortality in the population. The tumor microenvironment (TME), which plays a crucial role in GC progression, may serve as an optimal prognostic predictor of GC. In this study, we identified CXC motif chemokine receptor 4 (*CXCR4*) as a TME-related gene among thousands of differentially expressed genes (DEGs). We showed that *CXCR4* can be used to predict the effect of immunotherapy in patients with GC.

Methods: GC samples obtained from The Cancer Genome Atlas (TCGA) were analyzed for the presence of stroma (stromal score), the infiltration of immune cells (immune score) in tumor tissues, and the tumor purity (estimate score) using the ESTIMATE (Estimation of STromal and Immune cells in MAlignant Tumor tissues using Expression data) algorithm. DEGs were sorted based on differences in the values of the three scores. Furthermore, Gene Ontology (GO) and Kyoto Encyclopedia of Genes and Genomes (KEGG) analyses were performed to determine the biological processes and pathways enriched in these DEGs. The correlations of scores with clinicopathological features and overall survival (OS) of patients with GC were assessed by the Kaplan–Meier survival and Cox regression analyses. Through subsequent protein–protein interaction (PPI) network and univariate Cox regression analyses, CXCR4 was identified as a TME-related gene. Gene Set Enrichment Analysis (GSEA) was performed to assess the role of CXCR4 in the TME of GC. The CIBERSORT algorithm was used to further explore the correlation between tumor-infiltrating immune cells (TIICs) and CXCR4. Finally, the TISIDB database was used to predict the efficacy of immunotherapy in patients with GC.

Results: We extracted 1231 TME-related DEGs and by an overlapping screening of PPI network and univariate Cox regression, CXCR4 was identified as a biomarker of TME, which deeply engaged in immune-related biological processes of gastric cancer and have close association with several immunocompetent cells.

Conclusion: CXCR4 may be a useful biomarker of prognosis and an indicator of the TME in GC.

Keywords: CXCR4, tumor microenvironment, gastric cancer, ESTIMATE algorithm, CIBERSORT algorithm

OPEN ACCESS

Edited by:
Liu Yang,
Zhejiang Provincial People's Hospital, China

Reviewed by:
Raphael Carmo Valente,
Federal University of Rio de Janeiro, Brazil
Xiaodong Liang,
Zhejiang Provincial People's Hospital, China

***Correspondence:**
Tongpeng Xu
tongpeng_xu_njmu@163.com
Zhenghua Fei
940077455@qq.com

[†] These authors have contributed equally to this work

Specialty section:
This article was submitted to Molecular and Cellular Oncology, a section of the journal Frontiers in Cell and Developmental Biology

Received: *16 January 2021*
Accepted: *19 August 2021*
Published: *08 September 2021*

Citation:
Gu Y, Gu W, Xie R, Chen Z, Xu T and Fei Z (2021) Role of CXCR4 as a Prognostic Biomarker Associated With the Tumor Immune Microenvironment in Gastric Cancer. Front. Cell Dev. Biol. 9:654504. doi: 10.3389/fcell.2021.654504

INTRODUCTION

Gastric cancer (GC) is one of the most common malignant tumors of the alimentary system, with growing incidences worldwide. Globally, GC is the sixth most frequently diagnosed cancer and the third leading cause of cancer-related deaths (Sitarz et al., 2018). More than 1,000,000 new cases are diagnosed, and approximately 783,000 deaths occur annually (Bray et al., 2018; Global Burden of Disease Cancer Collaboration, Fitzmaurice et al., 2019). Although surgical resection remains the primary curative treatment for GC, the incidence of postoperative tumor recurrence is high. In particular, the 5-year survival rate of patients with stage II, III, and IV GC is approximately 31, 13, and 3%, respectively (Akhondi-Meybodi et al., 2017). Despite remarkable progress in treatment modalities in recent years, the mortality rate of patients with GC remains high (Rawla and Barsouk, 2019). Therefore, it is necessary and urgent to develop novel strategies for the early diagnosis and prognostic prediction to reduce the high mortality and recurrence rates of patients with GC.

Previous investigations have demonstrated that the characteristics of the tumor microenvironment (TME) are closely associated with the progression and prognosis of GC (Wang et al., 2019). The significance of the TME in cancer initiation and progression has drawn increasing attention in recent years. Research has shown that the TME is an active promoter of cancer progression, as opposed to its previous designation as a silent bystander during cancer (Bussard et al., 2016). Emerging evidence has indicated that the TME, which is mainly composed of the extracellular matrix, stromal cells, blood vessels, and lymphatic networks, plays a key role in tumor development and metastasis (Hanahan and Coussens, 2012; Junttila and de Sauvage, 2013; Quail and Joyce, 2013). The type and proportion of stromal cells are related to the physiological state of the TME (Alkasalias et al., 2018). Moreover, tumor-infiltrating immune cells (TIICs), such as CD8+ T cells, regulatory T cells (Tregs), and tumor-associated macrophages (TAMs), positively affect the clinical outcome of patients with various malignancies, including melanoma, lung cancer, breast cancer, and GC (Adams et al., 2013; Massi et al., 2015; Bremnes et al., 2016; Jiang et al., 2017). The dynamic interplay between stromal cells and immune cells in the TME involves several cellular events and physiological processes (Lee et al., 2014). Further investigations of various components and pathways of GC in the TME may facilitate targeted therapy.

Recently, ESTIMATE (Estimation of STromal and Immune cells in MAlignant Tumor tissues using Expression data), a novel algorithm, has been developed to calculate stromal and immune scores, which are used to assess the extent of stromal and immune cells infiltrating into tumor tissues. The ESTIMATE algorithm helps present a better picture of the numbers of stromal and immune cells in the TME (Yoshihara et al., 2013). Thus, based on the scores calculated by ESTIMATE, the clinical outcomes of patients with GC may be predicted (Liu et al., 2018).

In this article, we collected the gene expression profiles of patients with GC from The Cancer Genome Atlas (TCGA) and used the ESTIMATE algorithm to calculate immune and stromal scores of the TME in GC. Moreover, we investigated the correlation between the risk scores obtained from differentially expressed genes (DEGs) and the clinicopathological characteristics of patients with GC. Furthermore, we constructed a protein–protein interaction (PPI) network and conducted a functional enrichment analysis of the identified DEGs to explore their potential correlations with TIICs.

MATERIALS AND METHODS

Microarray Data Collection and Processing

From the TCGA dataset, transcriptome and relevant clinical data of 373 patients with GC (343 tumor samples vs. 30 normal samples) were collected, and the ESTIMATE algorithm was employed to evaluate the composition of the TME. The results were represented as three scores, namely immune score, stromal score, and estimate score, corresponding to the proportion of immune cells, stromal cells, and both immune and stromal cells, respectively. All genes of tumor samples were ranked by their expression levels, and DEGs were screened out using the "limma" package in R. DEGs were identified based on the following criteria: an absolute value of log2 fold change ($|\log2FC| > 1$ and false discovery rate (FDR) < 0.05. Furthermore, the "VennDiagram" package was used to screen for genes with similar expression levels in both stromal and immune cells. The "pheatmap" package was used to produce heatmaps of TME-related DEGs.

Functional Enrichment Analysis of TME-Related DEGs

tumor microenvironment-related DEGs were performed Kyoto Encyclopedia of Genes and Genomes (KEGG) and Gene Ontology (GO) analysis, which revealed the function of DEGs in the biologic process, molecular function, and showing the pathway enrichment result. The "ggplot2," "enrichplot," and "clusterProfiler" packages in R were used to perform GO and KEGG analyses. Statistical significance was set at $P < 0.05$ and $q < 0.05$.

Correlation Between Scores With Clinicopathological Characteristics and Survival

The clinicopathological characteristics of each sample were evaluated by the Wilcoxon rank-sum and Kruskal–Wallis rank-sum test, clarifying the correlation between scores and the clinical stage. Samples were divided into high- and low-score groups by compared to media value and executed survival analysis. R packages "survival" and "survminer" were applied and $P < 0.05$ was identified as significant difference.

PPI Network and Cox Regression Analysis

Next, to explore the relationship among DEGs, the STRING platform[1] was used to establish a PPI network, and nodes were employed to reconstruct the network with the confidence of interactive relationship greater than 0.95. The Cytoscape software was used to identify the top 30 hub genes. Univariate Cox regression was performed using the "survival" package in R to select DEGs associated with the prognosis of GC. The top 50 genes ranked according to log-rank test *P*-values in univariate Cox analysis are shown in the plot. Finally, based on the results of the intersection analysis of the PPI network and Cox regression analysis, only the CXC motif chemokine receptor 4 (*CXCR4*) gene was found to meet all the above-mentioned metrics.

Correlation Between CXCR4 Expression and Clinicopathological Characteristics

Kaplan–Meier survival analysis was performed to illustrate the differences in the overall survival (OS) between the GC groups with low and high expression. Next, correlation analysis was performed between clinical characteristics and *CXCR4* expression levels, which were contrasted by univariate analysis. Statistical analysis was performed using SPSS 22.0, and statistical significance was set at $P < 0.05$.

Further Analysis of the Relationship Between CXCR4 and Tumor Immunoreaction

To explore the role of CXCR4 in the TME of GC, Gene Set Enrichment Analysis (GSEA) was performed to verify the results of KEGG pathway enrichment analysis using GSEA version 3.0 (Broad Institute, Cambridge, MA, United States). Differences were considered significant if NOM *P*-value < 0.05 and FDR < 0.25. In addition, to determine the relative abundance of TIICs in GC samples, the extent of infiltration was estimated using the CIBERSORT algorithm. Samples with $P < 0.05$ were identified to have significantly different immune cell infiltration between the two groups. Furthermore, correlation analyses between the expression of *CXCR4* and immune cell infiltration in the TME were performed. Additionally, the correlation of the expression levels of CXCR4 with those of immune checkpoint molecules in GC was identified by the TISIDB web portal[2]. Statistical significance was set at $P < 0.05$.

RESULTS

Identification and Functional Analysis of DEGs

ImmuneScore, StromalScore, and ESTIMATEScore were dissected by Kaplan–Meier survival analysis. The high- and low-score samples were analyzed and compared to determine the differences in gene expression patterns in immune and stromal components. A total of 2143 DEGs were obtained based on the immune score, out of which 1553 genes were upregulated and 580 genes were downregulated (**Figures 1A,C,D**). Similarly, 2454 DEGs were acquired based on the stromal score, out of which 2152 genes were upregulated and 302 genes were downregulated (**Figures 1B,C,D**). Furthermore, the Venn plot identified 1051 upregulated genes and 180 downregulated genes in both the immune and stromal components. These 1231 DEGs were identified as TME-related DEGs. The results of GO analysis demonstrated that these DEGs were mostly engaged in immune-related functions, such as the regulation of lymphocyte activation and lymphocyte-mediated immunity (**Figures 2A,C**). Moreover, the results of KEGG analysis demonstrated the involvement of DEGs in certain immune-related functions, including cytokine-cytokine receptor interaction and chemokine signaling pathway (**Figures 2B,D**).

Correlation Between Scores and Clinicopathological Features of Patients With GC

To ascertain the correlation between stromal and immune scores with the clinicopathological characteristics of patients with GC, commensurable clinical features of patients with GC acquired from TCGA were analyzed. The immune score was found to be significantly and positively correlated with the T stage of the tumor ($P = 0.00086$) (**Figure 3D**) and the cancer grade ($P = 0.016$) (**Figure 3M**). Moreover, the stromal scores were significantly correlated with the T stage of the tumor ($P < 0.001$) (**Figure 3E**) and the cancer stage ($P = 0.02$) (**Figure 3B**). Furthermore, the estimate score was closely associated with the T and N stages of the tumor ($P = 0.024$, $P < 0.001$, and $P = 0.036$, respectively) (**Figures 3C,F,L**). However, all three scores were not significantly associated with the M stage of the tumor ($P = 0.49$, $P = 0.61$, and $P = 0.04$, respectively) (**Figures 3G–I**) while immune score was not statistically significantly correlated with N stage ($P = 0.068$) (**Figure 3J**) or the stage of tumor ($P = 0.13$) (**Figure 3A**). Neither stromal score or estimate score were associated with gender ($P = 0.49$, $P = 0.37$, respectively) (**Figures 3N,O**). Besides, there was no significant correlation between stromal score and N stage ($P = 0.067$) (**Figure 3K**). The correlation of immune, stromal, and estimate scores with patient survival was analyzed by the Kaplan–Meier survival method, and the correlation of each score with the survival rate was assessed. As shown in **Figure 4C**, the amount of the stromal constituent was negatively correlated with the OS of patients with GC ($P = 0.005$). However, the immune and estimate scores had no significant correlation with the OS (**Figure 4A**, $P = 0.233$; **Figure 4B**, $P = 0.476$). These results suggest that the stromal components in the TME are significantly associated with the prognosis of patients with GC.

Intersection Analysis of Univariate Cox Regression and PPI Network

Next, we thoroughly investigated the interactions among DEGs. We constructed a PPI network using the STRING database in Cytoscape. The correlation between each DEG and the top 30 genes ranked by the nodes was displayed in **Figures 5A,B**. The results of univariate Cox regression analysis showed that 50 genes were associated with the prognosis of GC (**Figure 5C**). The

[1] http://string-db.org/

[2] http://cis.hku.hk/TISIDB/index.php

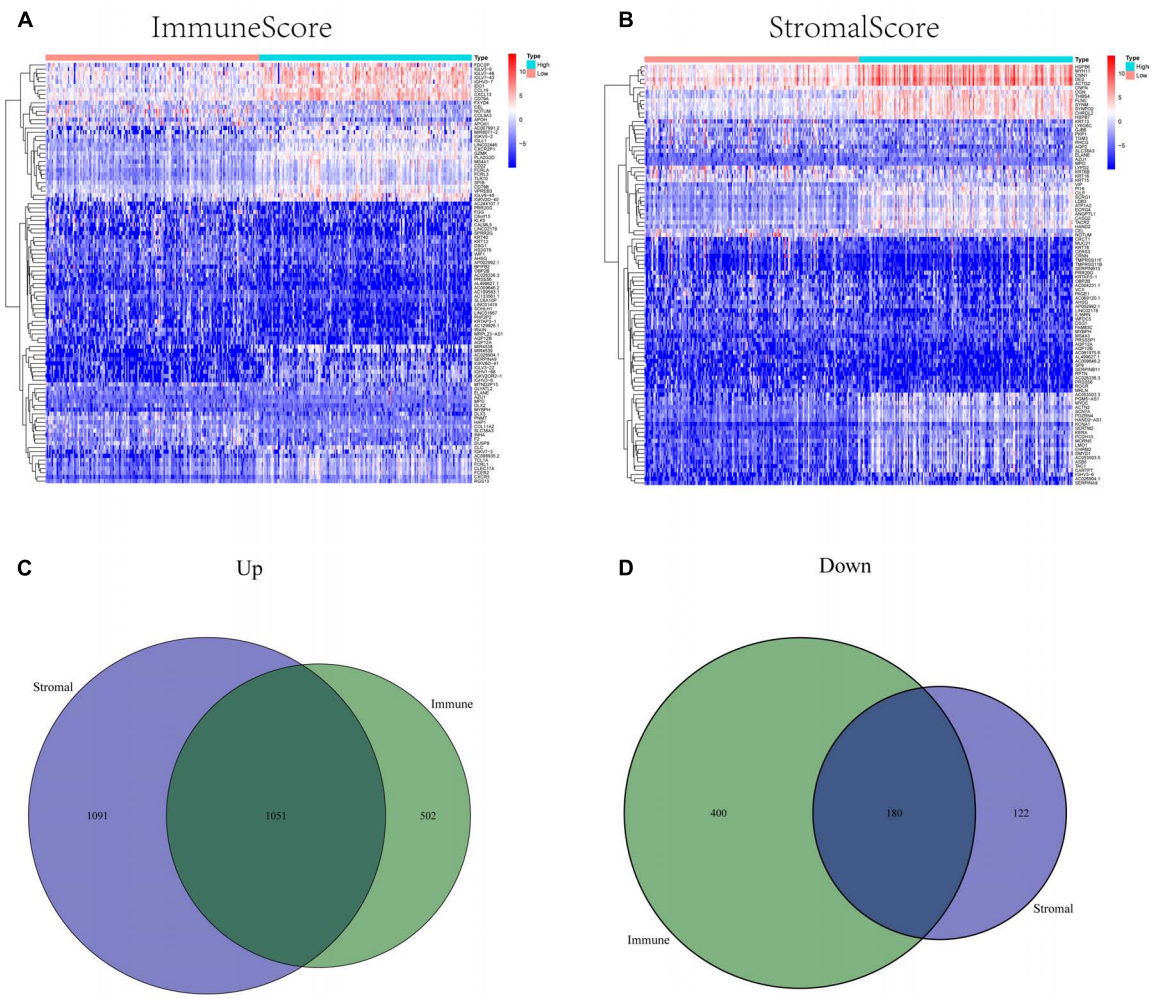

FIGURE 1 | Heatmaps and Venn plots of differentially expressed genes (DEGs). **(A)** A heatmap of immune-related DEGs between the high- and low *CXCR4* expression groups. **(B)** A heatmap of stromal-related DEGs between the high- and low *CXCR4* expression groups. **(C)** A Venn diagram of commonly upregulated DEGs in the stromal and immune components. **(D)** A Venn diagram of commonly downregulated DEGs in the stromal and immune components.

results of intersection analysis between the 30 hub genes and 50 prognostic DEGs revealed *CXCR4* as the only overlapping gene (**Figure 5D**).

Association Between CXCR4 Expression With Clinicopathological Factors and Disease Progression

In the present study, GC samples were divided into high CXCR4 and low CXCR4 groups using the median expression value of *CXCR4* as the threshold value. Survival analysis showed that GC patients with low *CXCR4* expression had a longer survival time than those with high *CXCR4* expression (**Figure 6C**, $P = 0.010$). Results of the Wilcoxon rank-sum test demonstrated that the level of CXCR4 in tumor tissues was significantly higher than that in healthy tissues in both paired or unpaired samples (**Figure 6B**, $P = 0.045$; **Figure 6A**, $P = 0.008$). In addition, the expression of CXCR4 was significantly different between different age groups (**Figure 6I**, $P = 0.042$). Additionally, the level of CXCR4 was inextricably linked to the T stage (**Figure 6D**, $P = 2.4e\text{-}06$) and the stage of cancer (**Figures 6G**, $P = 0.0036$). However, there were no significant differences between the expression level of CXCR4 and the M stage (**Figures 6F**, $P = 0.089$), N stage (**Figures 6E**, $P = 0.089$), grade (**Figure 6H**, $P = 0.17$), or sex (**Figures 6J**, $P = 0.15$).

Role of CXCR4 in the TME of Gastric Cancer

As shown in **Figure 7**, *CXCR4* was mainly engaged in immune-related activities, such as an intestinal immune network for IgA production, JAK-STAT signaling pathway, natural killer cell-mediated cytotoxicity, and Toll-like receptor signaling pathway. Using the CIBERSORT algorithm, we identified the infiltrating profiles of 22 different types of immune cells in tumor tissues (**Figures 8A,B**). A total of six types of TIICs were found to be strongly correlated with *CXCR4* expression in the TME of

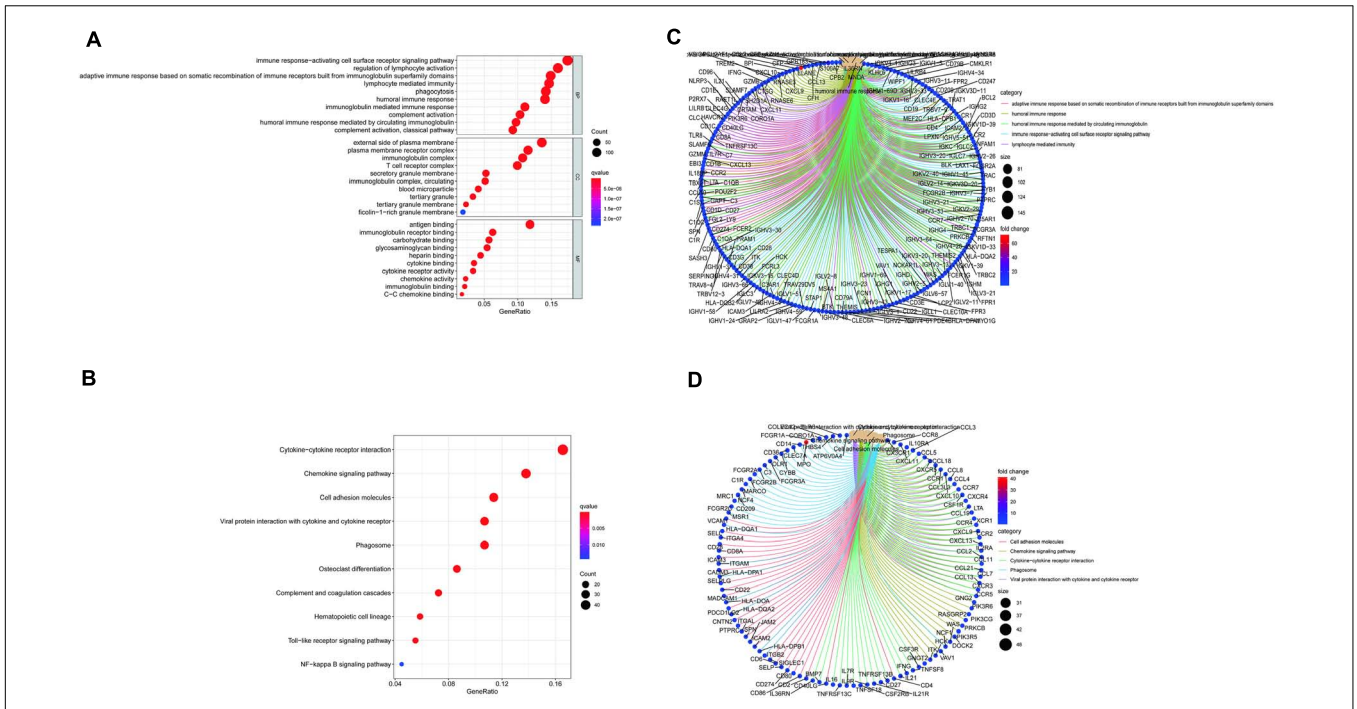

FIGURE 2 | Gene Ontology (GO) and Kyoto Encyclopedia of Genes and Genomes (KEGG) enrichment analysis of differentially expressed genes (DEGs) **(A–D)**.

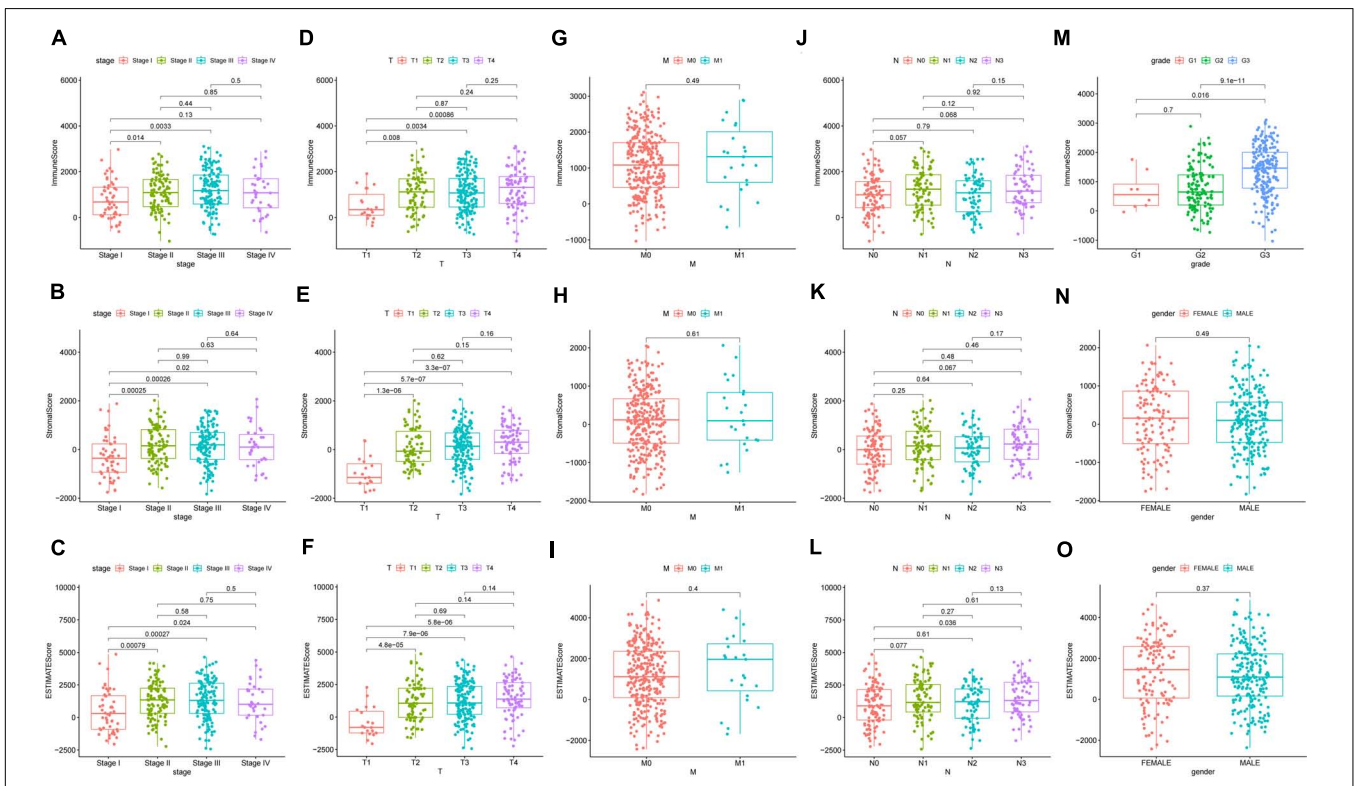

FIGURE 3 | Correlation of clinicopathological characteristics with immune, stromal, and estimate scores **(A–O)**.

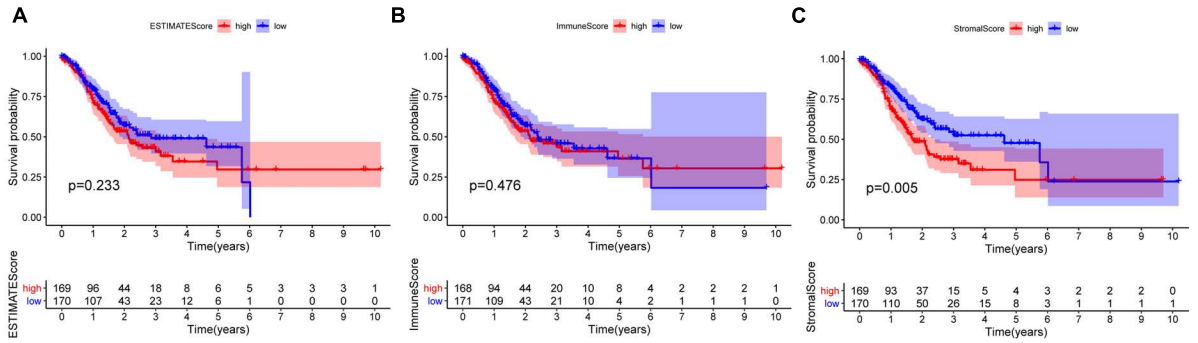

FIGURE 4 | Correlation of each estimate, immune, and stromal score with the survival outcome of patients with gastric cancer **(A–C)**.

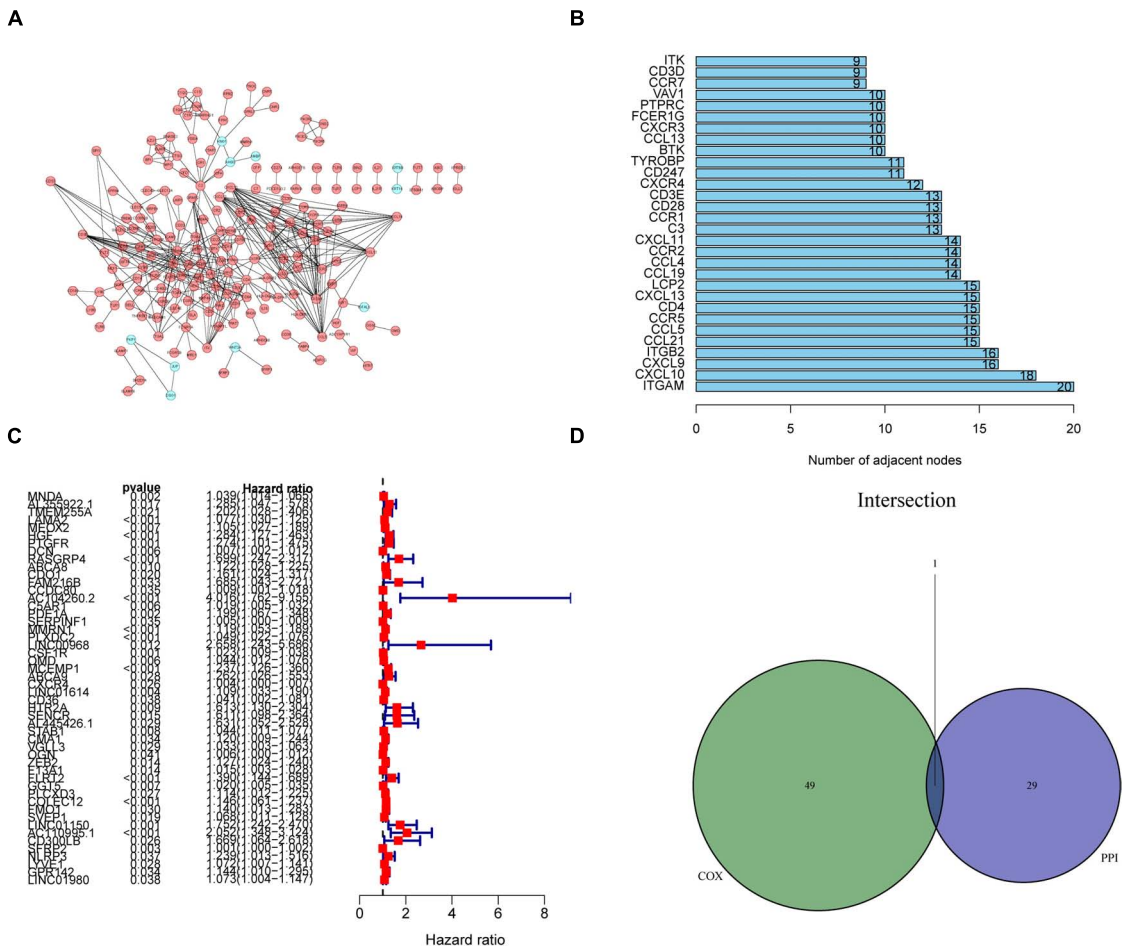

FIGURE 5 | Protein–protein interaction (PPI) network and univariate Cox regression analysis. **(A)** Construction of the PPI network of 1231 differentially expressed genes (DEGs). **(B)** The top 30 genes ranked by the number of adjacent nodes of the PPI network. **(C)** Results of univariate Cox regression analysis with selected DEGs, with the top 50 genes displayed in the forest plot. **(D)** A Venn diagram showing *CXCR4* as the most commonly expressed DEG in gastric cancer by combination analysis of the top 30 genes in the PPI network and the top 50 prognostic genes from the results of Cox regression analysis.

GC cells (**Figure 9**). Immune cells such as memory B cells, resting dendritic cells, CD8+ T cells, monocytes, and Tregs were positively related with the expression of *CXCR4*, while decreased activation of mast cells was negatively correlated with *CXCR4* expression. Furthermore, we characterized the interactions between *CXCR4* with 22 immune control genes. As shown in **Figure 10**, the expression level of *CXCR4* was positively correlated with that of 20 immune checkpoint molecules,

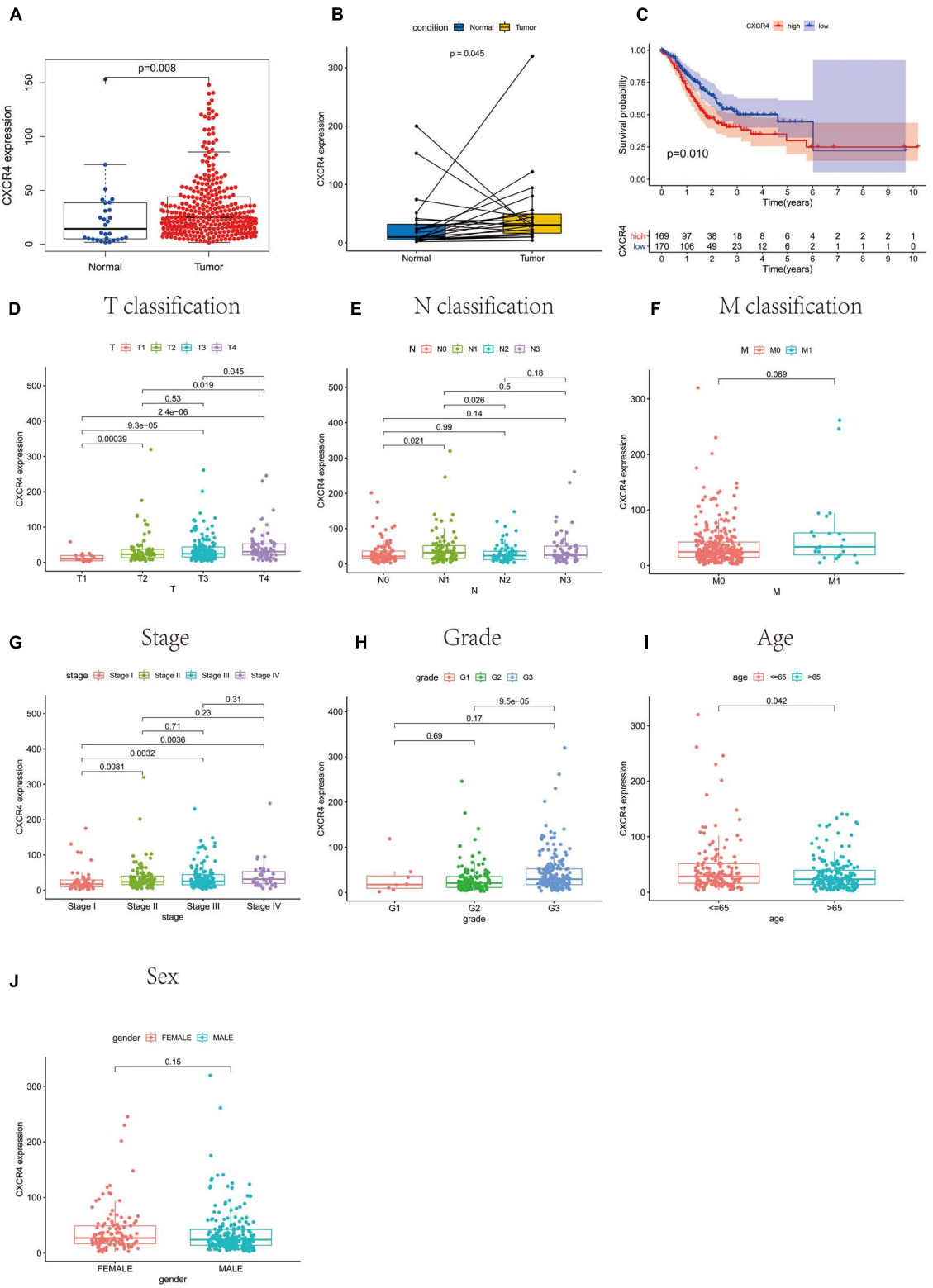

FIGURE 6 | The relationship between *CXCR4* expression with survival rate, clinical and pathological characteristics of patients with gastric cancer. **(A)** unpaired samples, **(B)** paired samples, **(C)** survival rate, **(D)** T classification, **(E)** N classification, **(F)** M classification, **(G)** stage, **(H)** grade, **(I)** age, and **(J)** sex.

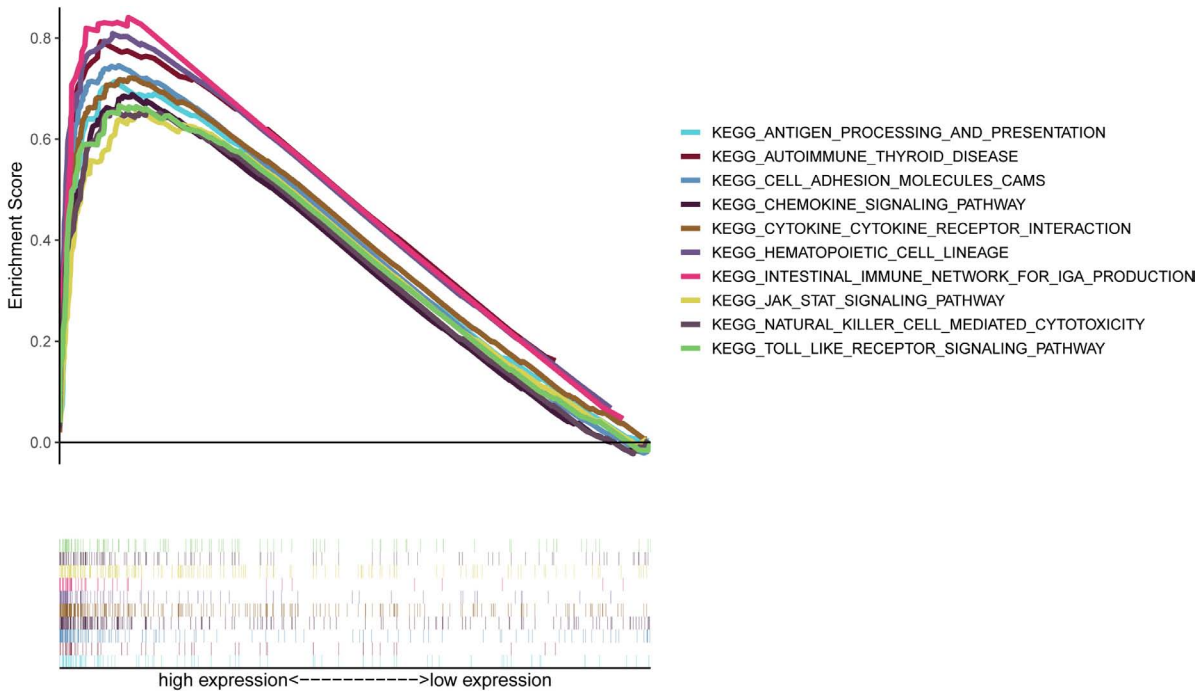

FIGURE 7 | Gene set enrichment analysis of *CXCR4*.

including *CD274*, *CTLA-4*, and *LAG3*, among others. Therefore, these results indicate that CXCR4 plays an important role in the immune evasion of GC cells.

DISCUSSION

Great advances in whole-genome sequencing have facilitated the development of molecular classification systems and treatment strategies for cancer. In the present study, we identified *CXCR4* as a TME-related gene associated with survival and TMN-stage classification in GC samples gathered from TCGA database.

CXC motif chemokine receptor 4, the receptor for chemokine CXCL12/SDF-1 and a member of the G protein-coupled receptor superfamily, is overexpressed in various types of solid cancers, including non-small-cell lung cancer (NSCLC), breast cancer, colorectal cancer, and GC. Previous studies have demonstrated that CXCR4 accelerates the metastasis, invasion, growth, and therapeutic resistance of cancer (Zhao et al., 2010; Otsuka et al., 2011; Ying et al., 2012; Mukherjee and Zhao, 2013; Xu et al., 2018). Moreover, CXCR4 affects the migration of GC cells via the ERK/Akt signaling pathway (Cheng et al., 2017). Cheng et al. (2020) found that the positive crosstalk between CXCR4 and EGFR promotes GC metastasis via the NF-kB pathway. Another study revealed that CXCR4 activates the NF-kB pathway and upregulates the expression of serine proteinase inhibitor clade B member 3, thereby facilitating the migration and invasion of GC cells (Gong et al., 2020). CXCR4 also plays a critical role in tumor angiogenesis in GC by activating the JAK2/STAT3 (Zhang et al., 2017). Furthermore, it promotes the proliferation and invasion processes via the Wnt/β-catenin pathway (Lin et al., 2017). Thus, inhibition of CXCR4 can disrupt multiple processes that facilitate the growth and spread of GC tumors. Therefore, given its multiple functions, CXCR4 may prove to be a promising target for immunotherapy.

Tumor progression is determined not only by cancer cells but also by the TME, which is the internal environment of malignant tumor progression. The TME can reduce the resistance of cancer cells to chemotherapy and immunotherapy (Russi et al., 2019). Epithelial-mesenchymal transition (EMT), a major modulator of tumor metastasis, may be involved in the interaction between tumor cells and the TME (Zheng et al., 2015; Suarez-Carmona et al., 2017; Hsieh et al., 2018). Compelling evidence indicates that CXCR4 regulates tumor EMT together with the c-MET signaling pathway (Quail and Joyce, 2013). The stromal component, another key component of the TME, primarily consists of cancer-associated fibroblasts (CAFs), which drive the growth, metastasis, and malignancy of cancer cells (Cheng et al., 2018). One study showed that CXCL12 secreted from CAFs promotes GC cell invasion by enhancing the clustering of integrin β1 in GC cells (Daisuke et al., 2015). In addition, CXCL12 mainly stems from the stromal part, which directly stimulates the proliferation and migration of CXCR4-expressing cells. Thus, the specific interaction between stromal cells and tumor cells might be one of the causes of drug resistance. Fortunately, AMD300, a CXCR4 inhibitor approved by the United States Food and Drug Administration (FDA), has already been shown to disrupt tumor-stromal interactions, sensitizing cancer cells to docetaxel-based chemotherapy in prostate cancer (Domanska et al., 2012). Currently, AMD300 is the most frequently used drug targeting the CXCL12-CXCR4 axis in clinical trials for solid gastrointestinal tumors, and

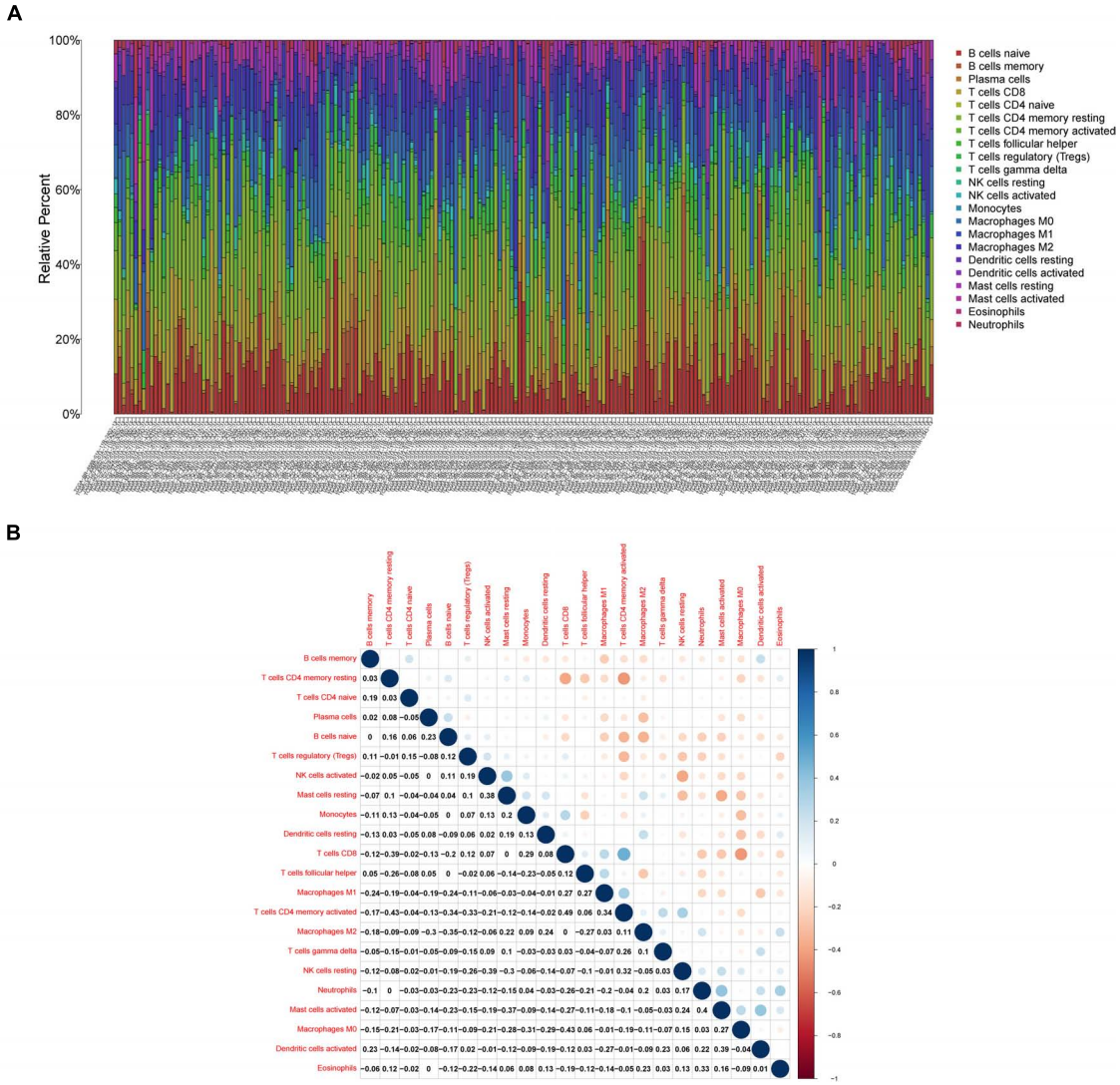

FIGURE 8 | Profiles of tumor-infiltrating immune cells (TIICs) in gastric cancer (GC) samples and their correlation analysis. **(A)** Barplot showing the proportion of 21 different types of TIICs in GC tumor samples. **(B)** A heatmap showing the correlation between 21 different types of TIICs.

therefore, CXCR4 might be a promising candidate target for GC immunotherapy.

In this study, the CIBERSORT algorithm was used to analyze the proportion of TIICs. The results showed that Tregs, dendritic cells, eosinophils, and CD8+ T cells were significantly positively correlated with *CXCR4* expression in patients with GC, which is concurrent with our hypothesis that *CXCR4* may be the hub gene of the TME in GC. Previous studies have revealed that CD8+ T cells are associated with poor prognosis in GC (Thompson et al., 2017). Similarly, Tregs are known to play an immunosuppressive role in the TME. Further reports have indicated that Tregs derived from patients with cancer usually express diverse chemokine receptors, which contributes to their migration into tumors in response to the signals stemming from the TME (Yan et al., 2011). However, some studies argued that Treg infiltration predicts favorable outcomes for patients with GC. For example, Li et al. (2016) reported that lower FOXP3+ and GARP+ Treg levels after neoadjuvant chemotherapy are associated with good outcomes in progressive GC. Thus, Treg infiltration may play a subtle yet vital role in GC progression. Nevertheless, more subset and related molecule regulation mechanisms of Tregs should to investigated thoroughly to better evaluate the prognosis of patients with GC (Liu et al., 2019).

Moreover, we have attempted to characterized the correlation between the expression levels of *CXCR4* with that of immune checkpoint molecules. The results revealed moderate positive correlations between the expression of *CXCR4* with that of PD-L1 (CD274) or CTLA4 in GC, which, in some ways, may be exploited for improving the efficacy of immunotherapy. Previous evidence indicated that suppression of CXCR4 promotes anti-PD-1/PD-L1

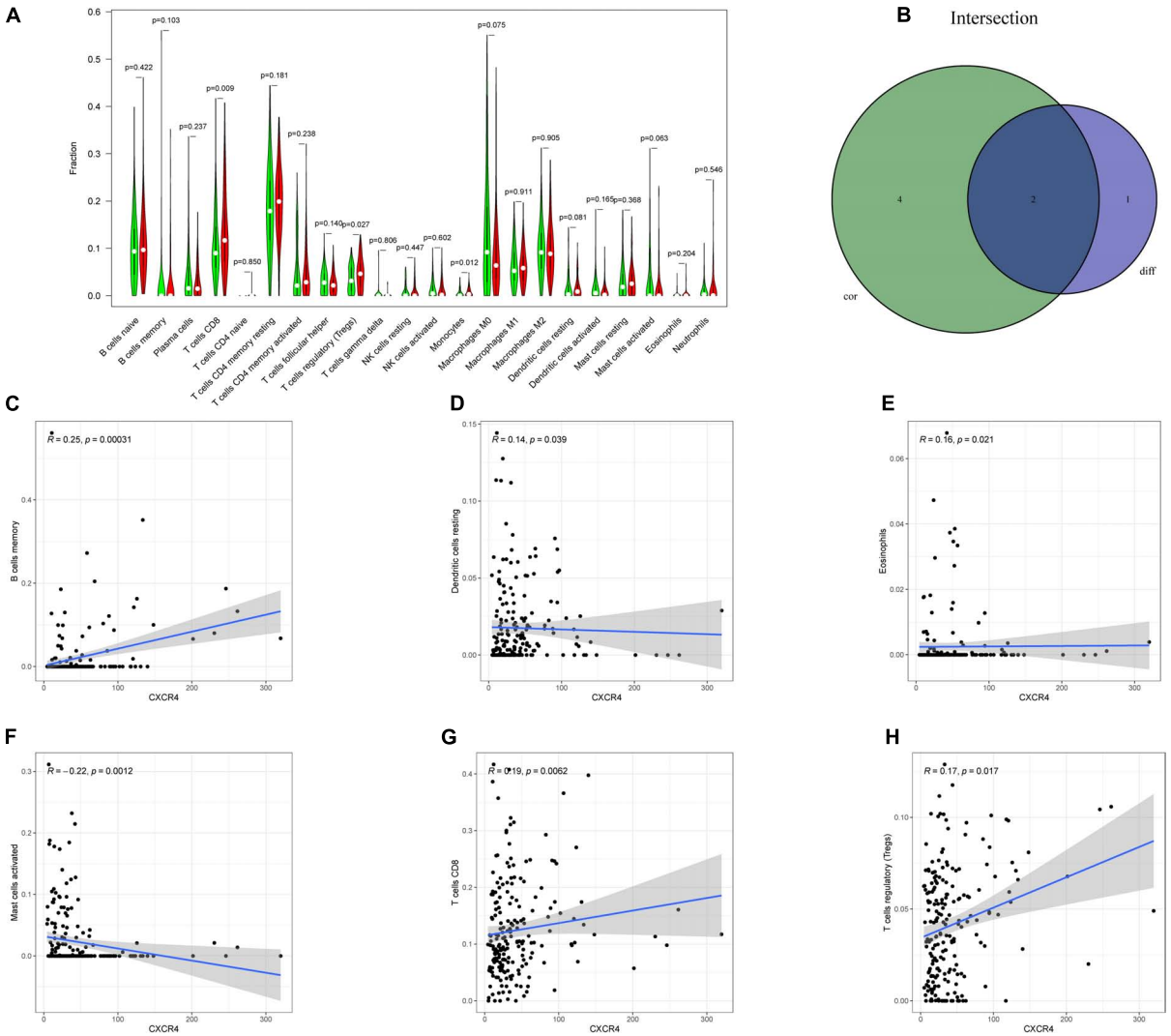

FIGURE 9 | Relation between the expression of *CXCR4* and proportion of tumor-infiltrating immune cells (TIICs). **(A)** A violin plot showing the differences in the proportions of 21 different types of immune cells in GC tumor samples with low or high *CXCR4* expression. **(B)** A Venn plot displaying the differences and correlation between two types of TIICs associated with *CXCR4* expression. **(C–H)** A scatter plot showing the correlation of the proportions of TIICs with *CXCR4* expression.

efficacy by reshaping the TME in hepatocellular carcinoma (Chen et al., 2015). A similar conclusion was observed in osteosarcoma, where Feig et al. (2013) showed that the SDF-1/CXCR4 axis facilitates the accumulation of myeloid-derived suppressor cells in the TME to abate the response to anti-PD-1 therapy. Another study discovered that in patients with colorectal cancer liver metastases, the expression of *CXCR4 CXCR7*, *TLR2/TLR4*, and *PD-1/PD-L1* was significantly increased in metastatic liver tissues compared to unaffected liver tissues (D'Alterio et al., 2016). Interestingly, our study found that CXCR4 was closely related to the Toll-like receptor signaling pathway (**Figure 10**). However, more experiments should be conducted to elaborate the interaction of CXCR4, TLRs, and PD-1/PD-L1 in GC. Furthermore, Pep R, a novel CXCR4 antagonist, has been found to enhance the efficiency of anti-PD-1 in various models (D'Alterio et al., 2019). X4-136, another CXCR4 inhibitor, could serve as a monotherapy or combined with immune checkpoint inhibitors in the treatment of melanoma and renal cell carcinoma (Saxena et al., 2020). In addition, a few studies have demonstrated that the combined blockade of CXCL12-CXCR4 and PD-1- PD-L1 pathways could provide survival benefits by regulating the TME of various solid tumors (Feig et al., 2013; Wu et al., 2019; Zeng et al., 2019; Seo et al., 2019) shedding light on CXCR4/PD-1-targeting combination therapy in GC. Given these advances, although the correlation between the expression of CXCR4 and PD-1/PD-L1 was moderate, we theorized that it has far-reaching clinical implications and relevance, which needs further experimental verification.

This study has some limitations that need to be acknowledged. First, as the clinical data were mainly acquired from TCGA database, result biases were unavoidable. Additionally, we did not conduct experimental research to inspect the function of

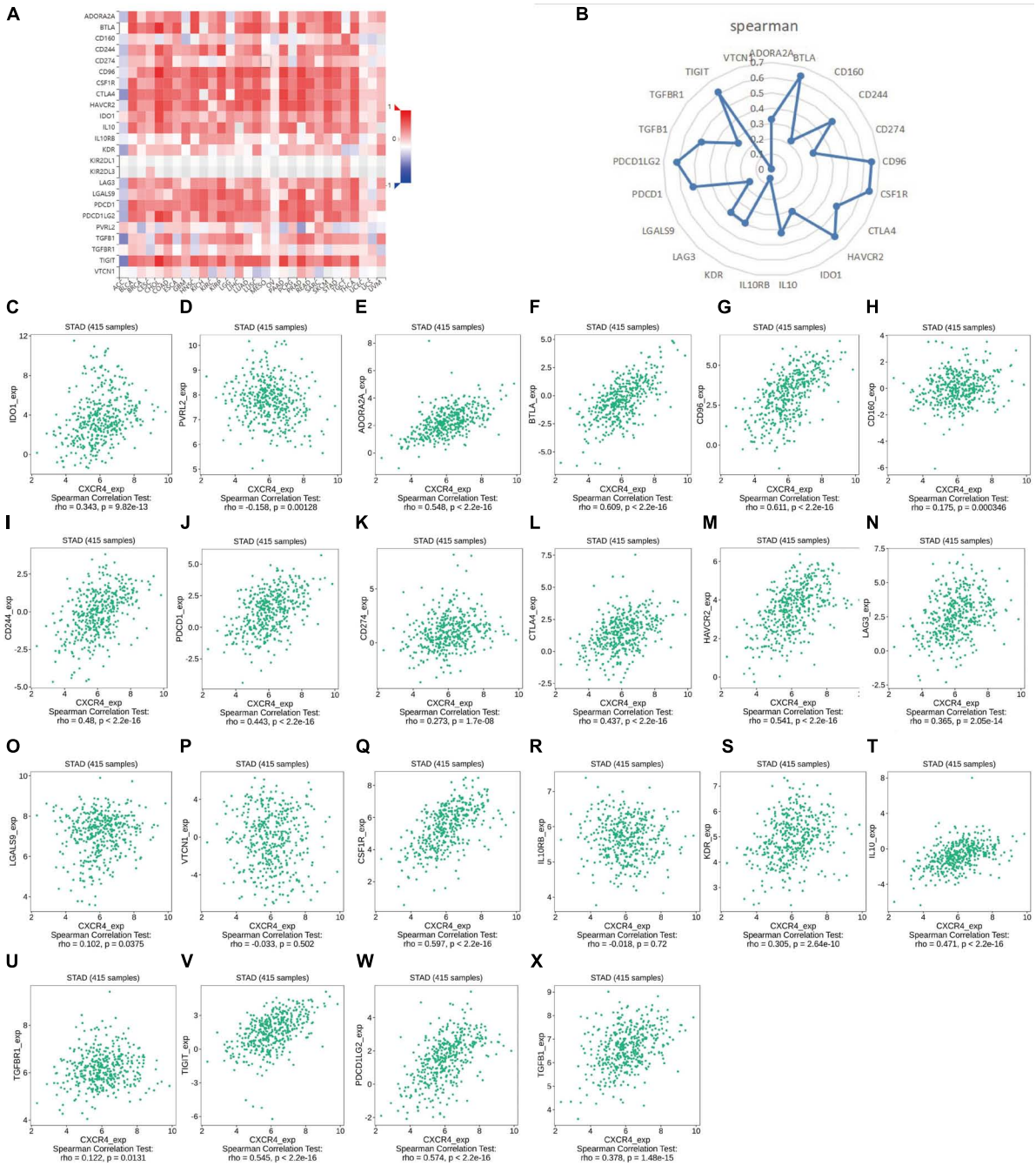

FIGURE 10 | Correlation analysis of the expression of *CXCR4* expression with that of immune checkpoint genes. **(A,B)** Correlation analysis of the expression levels of *CXCR4* with those of 22 common immune checkpoint genes in gastric cancer. **(C–X)** The relationship between the expression of *CXCR4* with that of *IDO1*, *PVRL2*, *ADORA2A*, *BTLA*, *CD96*, *CD160*, *CD244*, *PDCD1*, *CD274*, *CTLA4*, *HAVCR2*, *LAG3*, *LGALS9*, *VTCN1*, *CSF1R*, *IL10RB*, *KDR*, *IL10*, *TGFBR1*, *TIGIT*, *PDCD1LG2*, and *TGFB1*.

CXCR4 in GC. The combined application of CXCR4 blocker and PD-1 inhibitor may prolong the survival time of GC. However, more evidence is needed to prove the mechanism of combined immunotherapy.

In summary, we employed the ESTIMATE algorithm to identify genes that were associated with the TME in GC samples gathered from TCGA database. Consequently, CXCR4 was discovered as a promising prognostic target for patients with GC. Nevertheless, more experimental research is warranted to explore the underlying molecular mechanisms and potential clinical value of CXCR4 for the early diagnosis of tumor micrometastasis.

CONCLUSION

Overall, the ESTIMATE algorithm was used to calculate the immune, stromal, and estimate scores of GC samples acquired from TCGA. Stromal and immune cells that infiltrated into the TME were closely related to tumor growth. We identified a few TME-related DEGs, out of which *CXCR4*, was significantly associated with the regulation of the immune-active status in the TME. Therefore, CXCR4 might be a latent biomarker in GC, which determines the efficacy of cancer immunotherapy. The results of the present study may provide new insights into the development of effective therapeutic strategies targeted against GC.

DATA AVAILABILITY STATEMENT

Publicly available datasets were analyzed in this study. This data can be found here: the datasets analyzed for this study can be found in the TCGA (https://cancergenome.nih.gov/) and ImmPort (https://www.immport.org).

AUTHOR CONTRIBUTIONS

TX and ZF conceived and devised the study and gave aid in writing the manuscript. YG and WG performed the data analyses and contributed to the writing of the manuscript. ZC and RX reviewed the original manuscript. All authors reviewed the manuscript.

FUNDING

This study was supported by grant from the Natural Science Foundation of Zhejiang Province (No. LY21H280012).

REFERENCES

Adams, S., Gray, R. J., Demaria, S., Goldstein, L. J., and Badve, S. S. (2013). Abstract S1-07: prognostic value of tumor-infiltrating lymphocytes (TILs) in two phase III randomized adjuvant breast cancer trials: ECOG 2197 and ECOG 1199. *Cancer Res.* 73, S1–S07.

Akhondi-Meybodi, M., Ghane, M., Akhondi-Meybodi, S., and Dashti, G. (2017). Five-year survival rate for gastric cancer in Yazd Province, Central Iran, from 2001 to 2008. *Middle East J. Dig. Dis.* 9, 39–48. doi: 10.15171/mejdd.2016.50

Alkasalias, T., Moyano-Galceran, L., Arsenian-Henriksson, M., and Lehti, K. (2018). Fibroblasts in the tumor microenvironment: shield or spear. *Int. J. Mol. Sci.* 19:1532. doi: 10.3390/ijms19051532

Bray, F., Ferlay, J., Soerjomataram, I., Siegel, R. L., Torre, L. A., and Jemal, A. (2018). Global cancer statistics 2018: GLOBOCAN estimates of incidence and mortality worldwide for 36 cancers in 185 countries. *CA Cancer J. Clin.* 68, 394–424. doi: 10.3322/caac.21492

Bremnes, R. M., Busund, L. T., Kilvær, T. L., Andersen, S., Richardsen, E., Paulsen, E. E., et al. (2016). The role of tumor-infiltrating lymphocytes in development, progression, and prognosis of non-small cell lung cancer. *J. Thorac. Oncol.* 11, 789–800. doi: 10.1016/j.jtho.2016.01.015

Bussard, K. M., Mutkus, L., Stumpf, K., Gomez-Manzano, C., and Marini, F. C. (2016). Tumor-associated stromal cells as key contributors to the tumor microenvironment. *Breast Cancer Res.* 18:84. doi: 10.1186/s13058-016-0740-2

Chen, Y., Ramjiawan, R. R., Reiberger, T., Ng, M. R., Hato, T., Huang, Y., et al. (2015). CXCR4 inhibition in tumor microenvironment facilitates anti-programmed death receptor-1 immunotherapy in sorafenib-treated hepatocellular carcinoma in mice. *Hepatology* 61, 1591–1602. doi: 10.1002/hep.27665

Cheng, Y., Che, X., Zhang, S., Guo, T., He, X., Liu, Y., et al. (2020). Positive cross-talk between CXC chemokine receptor 4 (CXCR4) and epidermal growth factor receptor (EGFR) promotes gastric cancer metastasis via the nuclear factor kappa B (NF-kB)-dependent pathway. *Med. Sci. Monit.* 26:e925019. doi: 10.12659/MSM.925019

Cheng, Y., Qu, J., Che, X., Xu, L., Song, N., Ma, Y., et al. (2017). CXCL12/SDF-1α induces migration via SRC-mediated CXCR4-EGFR cross-talk in gastric cancer cells. *Oncol. Lett.* 14, 2103–2110. doi: 10.3892/ol.2017.6389

Cheng, Y., Song, Y., Qu, J., Che, X., Song, N., Fan, Y., et al. (2018). The chemokine receptor CXCR4 and c-MET cooperatively promote epithelial-mesenchymal transition in gastric cancer cells. *Transl. Oncol.* 11, 487–497. doi: 10.1016/j.tranon.2018.02.002

Daisuke, I., Ishimoto, T., Miyake, K., Sugihara, H., Eto, K., Sawayama, H., et al. (2015). CXCL12/CXCR4 activation by cancer-associated fibroblasts promotes integrin β1 clustering and invasiveness in gastric cancer. *Int. J. Cancer* 138, 1207-19.

D'Alterio, C., Buoncervello, M., Ieranó, C., Napolitano, M., Portella, L., Rea, G., et al. (2019). Targeting CXCR4 potentiates anti-PD-1 efficacy modifying the tumor microenvironment and inhibiting neoplastic PD-1. *J. Exp. Clin. Cancer Res.* 38:432. doi: 10.1186/s13046-019-1420-8

D'Alterio, C., Nasti, G., Polimeno, M., Ottaiano, A., Conson, M., Circelli, L., et al. (2016). CXCR4-CXCL12-CXCR7, TLR2-TLR4, and PD-1/PD-L1 in colorectal cancer liver metastases from neoadjuvant-treated patients. *Oncoimmunology* 5:e1254313. doi: 10.1080/2162402X.2016.1254313

Domanska, U. M., Timmer-Bosscha, H., Nagengast, W. B., Oude Munnink, T. H., Kruizinga, R. C., Ananias, H. J., et al. (2012). CXCR4 inhibition with AMD3100 sensitizes prostate cancer to docetaxel chemotherapy. *Neoplasia* 14, 709–718. doi: 10.1593/neo.12324

Feig, C., Jones, J. O., Kraman, M., Wells, R. J., Deonarine, A., Chan, D. S., et al. (2013). Targeting CXCL12 from FAP-expressing carcinoma-associated fibroblasts synergizes with anti-PD-L1 immunotherapy in pancreatic cancer. *Proc. Natl. Acad. Sci. U.S.A.* 110, 20212–20217. doi: 10.1073/pnas.1320318110

Global Burden of Disease Cancer Collaboration, Fitzmaurice, C., Abate, D., Abbasi, N., Abbastabar, H., Abd-Allah, F., et al. (2019). Global, regional, and national cancer incidence, mortality, years of life lost, years lived with disability, and disability-adjusted life-years for 29 cancer groups, 1990 to 2017: a systematic analysis for the global burden of disease study. *JAMA Oncol.* 5, 1749–1768. doi: 10.1001/jamaoncol.2019.2996

Gong, J., Song, Y., Xu, L., Che, X., Hou, K., Guo, T., et al. (2020). Upregulation of serine proteinase inhibitor clade B member 3 (SERPINB3) expression by stromal cell-derived factor (SDF-1)/CXCR4/nuclear factor kappa B (NF-κB) promotes migration and invasion of gastric cancer cells. *Med. Sci. Monit.* 26:e927411. doi: 10.12659/MSM.927411

Hanahan, D., and Coussens, L. M. (2012). Accessories to the crime: functions of cells recruited to the tumor microenvironment. *Cancer Cell* 21, 309–322. doi: 10.1016/j.ccr.2012.02.022

Hsieh, C. H., Tai, S. K., and Yang, M. H. (2018). Snail-overexpressing cancer cells promote M2-like polarization of tumor-associated macrophages by delivering MiR-21-abundant exosomes. *Neoplasia* 20, 775–788. doi: 10.1016/j.neo.2018.06.004

Jiang, W., Liu, K., Guo, Q., Cheng, J., Shen, L., Cao, Y., et al. (2017). Tumor-infiltrating immune cells and prognosis in gastric cancer: a systematic review and meta-analysis. *Oncotarget* 8, 62312–62329. doi: 10.18632/oncotarget.17602

Junttila, M. R., and de Sauvage, F. J. (2013). Influence of tumour microenvironment heterogeneity on therapeutic response. *Nature* 501, 346–354. doi: 10.1038/nature12626

Lee, K., Hwang, H., and Nam, K. T. (2014). Immune response and the tumor microenvironment: how they communicate to regulate gastric cancer. *Gut Liver* 8, 131–139. doi: 10.5009/gnl.2014.8.2.131

Li, K., Chen, F., and Xie, H. (2016). Decreased FOXP3+ and GARP+ Tregs to neoadjuvant chemotherapy associated with favorable prognosis in advanced gastric cancer. *Onco Targets Ther.* 9, 3525–3533. doi: 10.2147/OTT.S101884

Lin, X. L., Xu, Q., Tang, L., Sun, L., Han, T., Wang, L. W., et al. (2017). Regorafenib inhibited gastric cancer cells growth and invasion via CXCR4 activated Wnt pathway. *PLoS One* 12:e0177335. doi: 10.1371/journal.pone.0177335

Liu, W., Ye, H., Liu, Y., Xu, C., Zhong, Y., Tian, T., et al. (2018). Transcriptome-derived stromal and immune scores infer clinical outcomes of patients with cancer. *Oncol. Lett.* 15, 4351–4357.

Liu, X., Zhang, Z., and Zhao, G. (2019). Recent advances in the study of regulatory T cells in gastric cancer. *Int. Immunopharmacol.* 73, 560–567. doi: 10.1016/j.intimp.2019.05.009

Massi, D., Brusa, D., Merelli, B., Falcone, C., Xue, G., Carobbio, A., et al. (2015). The status of PD-L1 and tumor-infiltrating immune cells predict resistance and poor prognosis in BRAFi-treated melanoma patients harboring mutant BRAFV600. *Ann. Oncol.* 26, 1980–1987. doi: 10.1093/annonc/mdv255

Mukherjee, D., and Zhao, J. (2013). The Role of chemokine receptor CXCR4 in breast cancer metastasis. *Am. J. Cancer Res.* 3, 46–57.

Otsuka, S., Klimowicz, A. C., Kopciuk, K., Petrillo, S. K., Konno, M., Hao, D., et al. (2011). CXCR4 overexpression is associated with poor outcome in females diagnosed with stage IV non-small cell lung cancer. *J. Thorac. Oncol.* 6, 1169–1178. doi: 10.1097/JTO.0b013e3182199a99

Quail, D. F., and Joyce, J. A. (2013). Microenvironmental regulation of tumor progression and metastasis. *Nat. Med.* 19, 1423–1437. doi: 10.1038/nm.3394

Rawla, P., and Barsouk, A. (2019). Epidemiology of gastric cancer: global trends, risk factors and prevention. *Prz. Gastroenterol.* 14, 26–38. doi: 10.5114/pg.2018.80001

Russi, S., Verma, H. K., Laurino, S., Mazzone, P., Storto, G., Nardelli, A., et al. (2019). Adapting and surviving: intra and extra-cellular remodeling in drug-resistant gastric cancer cells. *Int. J. Mol. Sci.* 20:3736. doi: 10.3390/ijms20153736

Saxena, R., Wang, Y., and Mier, J. W. (2020). CXCR4 inhibition modulates the tumor microenvironment and retards the growth of B16-OVA melanoma and Renca tumors. *Melanoma Res.* 30, 14–25. doi: 10.1097/CMR.0000000000000639

Seo, Y. D., Jiang, X., Sullivan, K. M., Jalikis, F. G., Smythe, K. S., Abbasi, A., et al. (2019). Mobilization of CD^{8+} T cells via CXCR4 blockade facilitates PD-1 checkpoint therapy in human pancreatic cancer. *Clin. Cancer Res.* 25, 3934–3945. doi: 10.1158/1078-0432.CCR-19-0081

Sitarz, R., Skierucha, M., Mielko, J., Offerhaus, G., Maciejewski, R., and Polkowski, W. P. (2018). Gastric cancer: epidemiology, prevention, classification, and treatment. *Cancer Manag. Res.* 10, 239–248. doi: 10.2147/CMAR.S149619

Suarez-Carmona, M., Lesage, J., Cataldo, D., and Gilles, C. (2017). EMT and inflammation: inseparable actors of cancer progression. *Mol. Oncol.* 11, 805–823. doi: 10.1002/1878-0261.12095

Thompson, E. D., Zahurak, M., Murphy, A., Cornish, T., Cuka, N., Abdelfatah, E., et al. (2017). Patterns of PD-L1 expression and CD8 T cell infiltration in gastric adenocarcinomas and associated immune stroma. *Gut* 66, 794–801. doi: 10.1136/gutjnl-2015-310839

Wang, H., Wu, X., and Chen, Y. (2019). Stromal-immune score-based gene signature: a prognosis stratification tool in gastric cancer. *Front. Oncol.* 9:1212. doi: 10.3389/fonc.2019.01212

Wu, A., Maxwell, R., Xia, Y., Cardarelli, P., Oyasu, M., Belcaid, Z., et al. (2019). Combination anti-CXCR4 and anti-PD-1 immunotherapy provides survival benefit in glioblastoma through immune cell modulation of tumor microenvironment. *J. Neurooncol.* 143, 241–249. doi: 10.1007/s11060-019-03172-5

Xu, C., Zheng, L., Li, D., Chen, G., Gu, J., Chen, J., et al. (2018). CXCR4 overexpression is correlated with poor prognosis in colorectal cancer. *Life Sci.* 208, 333–340. doi: 10.1016/j.lfs.2018.04.050

Yan, M., Jene, N., Byrne, D., Millar, E. K., O'Toole, S. A., McNeil, C. M., et al. (2011). Recruitment of regulatory T cells is correlated with hypoxia-induced CXCR4 expression, and is associated with poor prognosis in basal-like breast cancers. *Breast Cancer Res.* 13:R47. doi: 10.1186/bcr2869

Ying, J., Xu, Q., Zhang, G., Liu, B., and Zhu, L. (2012). The expression of CXCL12 and CXCR4 in gastric cancer and their correlation to lymph node metastasis. *Med. Oncol.* 29, 1716–1722. doi: 10.1007/s12032-011-9990-0

Yoshihara, K., Shahmoradgoli, M., Martínez, E., Vegesna, R., Kim, H., Torres-Garcia, W., et al. (2013). Inferring tumour purity and stromal and immune cell admixture from expression data. *Nat. Commun.* 4:2612. doi: 10.1038/ncomms3612

Zeng, Y., Li, B., Liang, Y., Reeves, P. M., Qu, X., Ran, C., et al. (2019). Dual blockade of CXCL12-CXCR4 and PD-1-PD-L1 pathways prolongs survival of ovarian tumor-bearing mice by prevention of immunosuppression in the tumor microenvironment. *FASEB J.* 33, 6596–6608. doi: 10.1096/fj.201802067RR

Zhang, Q., Xu, F., Shi, Y., Chen, Y. W., Wang, H. P., Yu, X., et al. (2017). C-X-C motif chemokine receptor 4 promotes tumor angiogenesis in gastric cancer via activation of JAK2/STAT3. *Cell Biol. Int.* 41, 854–862. doi: 10.1002/cbin.10794

Zhao, C., Lu, X., Bu, X., Zhang, N., and Wang, W. (2010). Involvement of tumor necrosis factor-alpha in the upregulation of CXCR4 expression in gastric cancer induced by *Helicobacter* pylori. *BMC Cancer* 10:419. doi: 10.1186/1471-2407-10-419

Zheng, X., Carstens, J. L., Kim, J., Scheible, M., Kaye, J., Sugimoto, H., et al. (2015). Epithelial-to-mesenchymal transition is dispensable for metastasis but induces chemoresistance in pancreatic cancer. *Nature* 527, 525–530. doi: 10.1038/nature16064

Conflict of Interest: The authors declare that the research was conducted in the absence of any commercial or financial relationships that could be construed as a potential conflict of interest.

Publisher's Note: All claims expressed in this article are solely those of the authors and do not necessarily represent those of their affiliated organizations, or those of the publisher, the editors and the reviewers. Any product that may be evaluated in this article, or claim that may be made by its manufacturer, is not guaranteed or endorsed by the publisher.

frontiers in Cell and Developmental Biology

ORIGINAL RESEARCH
published: 14 September 2021
doi: 10.3389/fcell.2021.711348

Characterization of Molecular Subtypes in Head and Neck Squamous Cell Carcinoma With Distinct Prognosis and Treatment Responsiveness

Pei Zhang[1†], Shue Li[2,3†], Tingting Zhang[4], Fengzhen Cui[4], Ji-Hua Shi[5], Faming Zhao[4*] and Xia Sheng[4*]*

[1] Department of Stomatology, The First Affiliated Hospital of Zhengzhou University, Zhengzhou, China, [2] Department of Stomatology, Union Hospital, Tongji Medical College, Huazhong University of Science and Technology, Wuhan, China, [3] Hubei Province Key Laboratory of Oral and Maxillofacial Development and Regeneration, Wuhan, China, [4] Key Laboratory of Environment and Health, Ministry of Education & Ministry of Environmental Protection, State Key Laboratory of Environmental Health (Incubation), School of Public Health, Tongji Medical College, Huazhong University of Science and Technology, Wuhan, China, [5] Department of Hepatobiliary and Pancreatic Surgery, Henan Key Laboratory of Digestive Organ Transplantation, The First Affiliated Hospital of Zhengzhou University, Zhengzhou, China

Head and neck squamous cell carcinoma (HNSCC) is one of the most aggressive malignancies with complex phenotypic, etiological, biological, and clinical heterogeneities. Previous studies have proposed different clinically relevant subtypes of HNSCC, but little is known about its corresponding prognosis or suitable treatment strategy. Here, we identified 101 core genes from three prognostic pathways, including mTORC1 signaling, unfold protein response, and UV response UP, in 124 pairs of tumor and matched normal tissues of HNSCC. Moreover, we identified three robust subtypes associated with distinct molecular characteristics and clinical outcomes using consensus clustering based on the gene expression profiles of 944 HNSCC patients from four independent datasets. We then integrated the genomic information of The Cancer Genome Atlas (TCGA) HNSCC cohort to comprehensively evaluate the molecular features of different subtypes and screen for potentially effective therapeutic agents. Cluster 1 had more arrested oncogenic signaling, the highest immune cell infiltration, the highest immunotherapy and chemotherapeutic responsiveness, and the best prognosis. By contrast, Cluster 3 showed more activated oncogenic signaling, the lowest immune cell infiltration, the lowest immunotherapy and chemotherapy responsiveness, and the worst prognosis. Our findings corroborate the molecular diversity of HNSCC tumors and provide a novel classification strategy that may guide for prognosis and treatment allocation.

Keywords: head and neck squamous cell carcinoma, molecular subgroups, gene expression, tumor immune microenvironment, prognosis

OPEN ACCESS

Edited by:
Liu Yang,
Zhejiang Provincial People's Hospital, China

Reviewed by:
Ildikò Szabò,
University of Padua, Italy
Concetta Saponaro,
Istituto Tumori Bari Giovanni Paolo II, Istituto Nazionale dei Tumori (IRCCS), Italy

***Correspondence:**
Pei Zhang
zpzxd99@163.com
Faming Zhao
famingzhao@hust.edu.cn
Xia Sheng
xiasheng@hust.edu.cn

† These authors have contributed equally to this work

Specialty section:
This article was submitted to Molecular and Cellular Oncology, a section of the journal Frontiers in Cell and Developmental Biology

Received: *18 May 2021*
Accepted: *10 August 2021*
Published: *14 September 2021*

Citation:
Zhang P, Li S, Zhang T, Cui F, Shi J-H, Zhao F and Sheng X (2021) Characterization of Molecular Subtypes in Head and Neck Squamous Cell Carcinoma With Distinct Prognosis and Treatment Responsiveness. Front. Cell Dev. Biol. 9:711348. doi: 10.3389/fcell.2021.711348

INTRODUCTION

Head and neck squamous cell carcinoma (HNSCC) is a primary malignant tumor that develops from the mucosal epithelium in the pharynx, larynx, and oral cavity, causing 600,000 new cases worldwide each year (Cancer Genome Atlas Network, 2015; Alsahafi et al., 2019; Canning et al., 2019). HNSCC is generally categorized into four subgroups, namely, basal, mesenchymal, atypical, and classical subtypes (Chung et al., 2004; Walter et al., 2013; Cancer Genome Atlas Network, 2015). Recent large-scale transcriptomic profiling has uncovered the molecular landscape of HNSCC, where genes involved in receptor tyrosine kinase (RTK)/RAS/PI3K signaling, cell cycle, cell death, and immunity signaling pathways are found frequently altered (Cancer Genome Atlas Network, 2015). These studies, on the one hand, underscored the complexity and heterogeneity of HNSCC tumors and, on the other hand, alerted that the prognosis and treatment strategy may be highly variable among tumors of different molecular features (Cancer Genome Atlas Network, 2015).

The current treatment of HNSCC includes surgery, radiation therapy, targeted therapy [epidermal growth factor receptor (EGFR)-targeting monoclonal antibody cetuximab], and chemotherapy with cytotoxic agents (such as cisplatin, methotrexate, gemcitabine, and bleomycin) (Johnson et al., 2020). Unfortunately, the current available treatments are largely ineffective and can cause severe toxicity (Alsahafi et al., 2019). Furthermore, approximately 50% of the patients experience recurrence (Leemans et al., 2018). Recent studies have shown that awakening the immune system with anti-PD1 and anti-CTLA4 therapies may be promising for recurrent/metastatic patients (Jie et al., 2015; Seiwert et al., 2016). However, a major limitation of these immune checkpoint inhibitors (ICIs) is the low responsive rate (Ferris et al., 2016; Burtness et al., 2019). Therefore, there is an urgent need to develop validated biomarkers to stratify HNSCC patients with potentially different survival outcome and treatment responsiveness and to reduce undesirable side effects.

To this end, we interrogated the publicly available gene expression datasets of HNSCC patients and screened for prognosis-related pathways by gene set variation analysis (GSVA) of paired tumor and normal samples. This led to the identification of three prognostic pathways and 101 core genes within which categorized the HNSCC patients into different subgroups with distinct prognosis. We then integrated the genomic information of 502 HNSCC samples to comprehensively evaluate the molecular features of different subtypes. Finally, we identified several potential immunotherapeutic and chemotherapeutic agents that may be of selected responsiveness for specific subtypes of HNSCC. Together, our findings corroborate the molecular diversity of HNSCC tumors while proposing a novel system of patient stratification with diverse prognosis and treatment option.

MATERIALS AND METHODS

Dataset Selection and Preparation

The RNA-sequencing data (raw read count and FPKM normalized) and full clinical annotation of The Cancer Genome Atlas (TCGA)-HNSCC project (n = 546) were downloaded from Xena Public Data Hubs (Goldman et al., 2020). Somatic mutation data were obtained from the cBioPortal database.[1] Gene expression profiles of GSE107591 (n = 46), GSE127165 (n = 114), GSE41613 (n = 97), GSE65858 (n = 270), and GSE427433 (n = 75) were downloaded from the Gene Expression Omnibus (GEO).[2] The normal and tumor samples were already defined in the datasets analyzed, for example, for TCGA-HNSCC project (tumor = 402 and matched normal = 44), defining a sample as tumoral or healthy sample according to TCGA barcode, with tumors ranging from 01 to 09 and normal types from 10 to 19.

Gene Set Variation Analysis and Functional Annotation

Pathway analyses were predominantly performed on the 50 hallmark gene sets (Liberzon et al., 2015). The enrichment scores of molecular pathways were evaluated by GSVA (Hanzelmann et al., 2013), which is commonly employed for estimating the variation in pathway and biological process activities in the samples of an expression dataset. To reduce pathway redundancies and overlaps, each gene set in 50 hallmark pathways was trimmed to only contain unique genes, and all genes associated with two or more pathways were excluded (Lambrechts et al., 2018). Most gene sets retained more than 70% of their associated genes. The GSVA was conducted on the gene profile through "GSVA" R packages, and differential pathways were identified using the R package "Limma" (Liu et al., 2015). Adjusted p-value < 0.05 was considered statistically significant. Univariate Cox analysis of overall survival (OS) was then performed to screen prognostic-related pathways.

Functional annotations were implemented by the "clusterProfiler" R package (Yu et al., 2012). Firstly, the log fold change of whole gene expression was acquired by paired differential expression analysis using DEseq2 R package (Love et al., 2014) between paired tumor and normal samples. Next, the gene set enrichment analysis (GSEA) was applied to verify the activation of the mTORC1 signaling, unfolded protein response (UPR) pathway, and UV response UP, which led to the identification of 101 common core genes from TCGA, GSE107591, and GSE127165. Gene Ontology (GO) and Kyoto Encyclopedia of Genes and Genomes (KEGG) analyses were further employed for functional annotations of these core genes. Adjusted p-value less than 0.05 was considered as statistically significant.

[1] http://www.cbioportal.org/datasets
[2] https://www.ncbi.nlm.nih.gov/gds

Identification of Core Gene Expression-Based Subtypes

To functionally elucidate the biological characteristics of the core genes from mTORC1 signaling, UPR pathway, and UV response UP, unsupervised clustering was performed using the "ConsensusClusterPlus" R package (Wilkerson and Hayes, 2010) to classify HNSCC patients into different subtypes. We first normalized the expression of each gene by log transform across all tumors before applying a robustified *z*-score transformation (median-centered and mad-scaled) per sample. Then we extracted the normalized expression data of the 101 core genes for consensus cluster analysis. And 80% item resampling, 100 resamplings, a maximum evaluated K of 8, and ward2 algorithm (Murtagh and Legendre, 2014) were selected for clustering. The cumulative distribution function (CDF) and consensus heatmap were used to assess the optimal K.

Estimation of Tumor Purity and Immune Cell Type Fractions

R package "estimate" was used to evaluate the stromal score, immune score, and tumor purity of each patient (Yoshihara et al., 2013). The immune infiltration of 22 immune cell types was explored using the CIBERSORT algorithm, in combination with the LM22 signature matrix (Newman et al., 2015).

Therapeutic Response Prediction

To identify potential targets for immunotherapy, the gene expression profile of T-cell signaling pathway was examined (Chen et al., 2017). Furthermore, the Tumor Immune Dysfunction and Exclusion (TIDE) algorithm (Jiang et al., 2018) and immune-related genetic prognostic index (IRGPI) score (Chen et al., 2021) were used to predict ICI response for HNSCC. Besides, unsupervised subclass mapping method (SubMap) algorithms (Hoshida et al., 2007) were used to predict PD-1 and CTLA4 in three subtypes identified by us with another published dataset containing 47 melanoma patients who responded to immunotherapies (Roh et al., 2017).

"pRRophetic" R package was used to predict half-maximal inhibitory concentration (IC50) for each sample by ridge regression, and the prediction accuracy was evaluated by 10-fold cross-validation based on the Genomics of Drug Sensitivity in Cancer (GDSC) training set (Geeleher et al., 2014). The GDSC[3] is one of the largest publicly available pharmacogenomics databases. All parameters were set by the default values with transcripts per kilobase million data. p-Value < 0.05 was considered statistically significant.

Statistical Analysis

All data analyses were performed in the R platform (x64, version 4.0.2). Student's t-test or Wilcoxon rank-sum test was performed to compare continuous variables between two groups. Chi-square test or Fisher's exact test was used for categorical data. One-way ANOVA or Kruskal–Wallis tests were used to conduct difference comparisons of three groups. Kaplan–Meier analysis with log-rank tests was performed to assess survival difference between groups *via* "survminer" R package. The mutation landscape in HNSCC patients with different subtypes was exhibited using "maftools" R package. All statistical p-values were two-sided, and $p < 0.05$ was considered statistically significant.

[3]https://www.cancerrxgene.org/

RESULTS

Identification of the Prognostic Pathways and Core Genes for Overall Survival in Head and Neck Squamous Cell Carcinoma

To screen for robust oncogenic signaling across different HNSCC cohorts, we applied GSVA based on the expression profile and identified several differentially activated pathways between paired tumor and normal samples in TCGA (n = 44), GSE107591 (n = 23), and GSE127165 (n = 57) datasets (**Figure 1A** and **Supplementary Figure 1A**). A Venn diagram showed the 13 commonly altered oncogenic pathways, including eight upregulated pathways (such as mTORC1 signaling) and five downregulated pathways (such as notch signaling) (**Supplementary Figure 1B**). Univariate Cox regression of OS based on GSVA scores in TCGA HNSCC cohort (patients n = 502) then identified three candidate prognostic pathways with statistical significance, including mTORC1 signaling (HR = 0.65, 95% CI = 0.49–0.84, $p < 0.01$), UPR pathway (HR = 0.73, 95% CI = 0.57–0.93, $p < 0.01$), and UV response UP (HR = 0.75, 95% CI = 0.57–0.98, $p = 0.03$) (**Figure 1B**). Interestingly, Kaplan–Meier survival analysis showed that the OS and progression-free survival (PFS) of the high GSVA score group was significantly shorter than those of the low GSVA score group in TCGA cohort (**Figures 1C,D**).

To further verify the activation of the three oncogenic pathways in HNSCC samples, GSEA was performed between paired tumor and normal samples in TCGA, GSE107591, and GSE127165 cohorts. As expected, the three oncogenic pathways were all significantly enriched in tumor samples (**Figure 2A** and **Supplementary Figure 1C**). Furthermore, 101 significantly deregulated genes within the three pathways were identified, 11 of which belonged to multiple pathways due to their functional diversity (**Figure 2B** and **Supplementary Table 1**). Interestingly, KEGG analyses of the core genes showed the highest score of Epstein–Barr virus (EBV) infection (**Figure 2C**), one of the established risk factors leading to nasopharyngeal carcinoma (Fernandes et al., 2018). This indicates that the core genes selected are highly relevant to HNSCC. Besides, KEGG and GO analyses also demonstrated that the core genes were involved in processes such as endoplasmic reticulum (ER) stress, hypoxia, cell cycle, DNA damage, and repair (**Figures 2C,D**).

Identification of Three Distinct Subtypes of Head and Neck Squamous Cell Carcinoma

In addition to identifying key genes and pathways, cancer subtyping is critical to improving personalized treatment (Berger et al., 2018). Toward this goal, we utilized unsupervised consensus clustering based on the expression profile of these

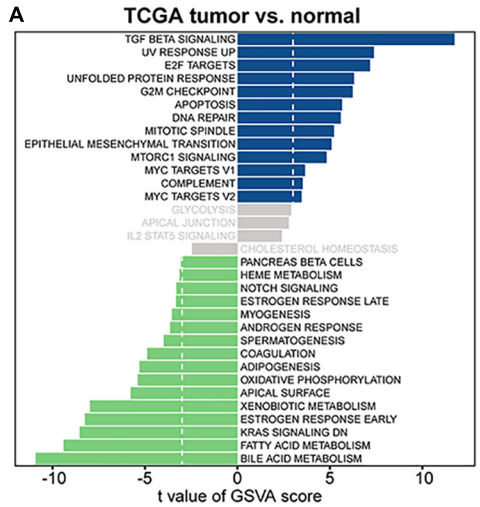

B Univariate Cox analysis

Pathway UP	HR (95%CI)	p-value
MTORC1 SIGNALING	0.64 (0.49−0.84)	< 0.01
UNFOLDED PROTEIN RESPONSE	0.73 (0.57−0.93)	< 0.01
UV RESPONSE UP	0.75 (0.57−0.98)	0.03
MYC TARGETS V2	0.82 (0.63−1.07)	0.15
TGF BETA SIGNALING	0.91 (0.69−1.19)	0.47
EPITHELIAL MESENCHYMAL TRANSITION	0.95 (0.73−1.24)	0.7
G2M CHECKPOINT	1.04 (0.8−1.36)	0.78
E2F TARGETS	1.04 (0.79−1.35)	0.8
Pathway DN	**HR (95%CI)**	**p-value**
NOTCH SIGNALING	0.78 (0.59−1.02)	0.06
XENOBIOTIC METABOLISM	0.84 (0.64−1.1)	0.2
BILE ACID METABOLISM	1.15 (0.88−1.5)	0.31
FATTY ACID METABOLISM	1.07 (0.82−1.4)	0.61
ESTROGEN RESPONSE EARLY	1.04 (0.8−1.36)	0.74

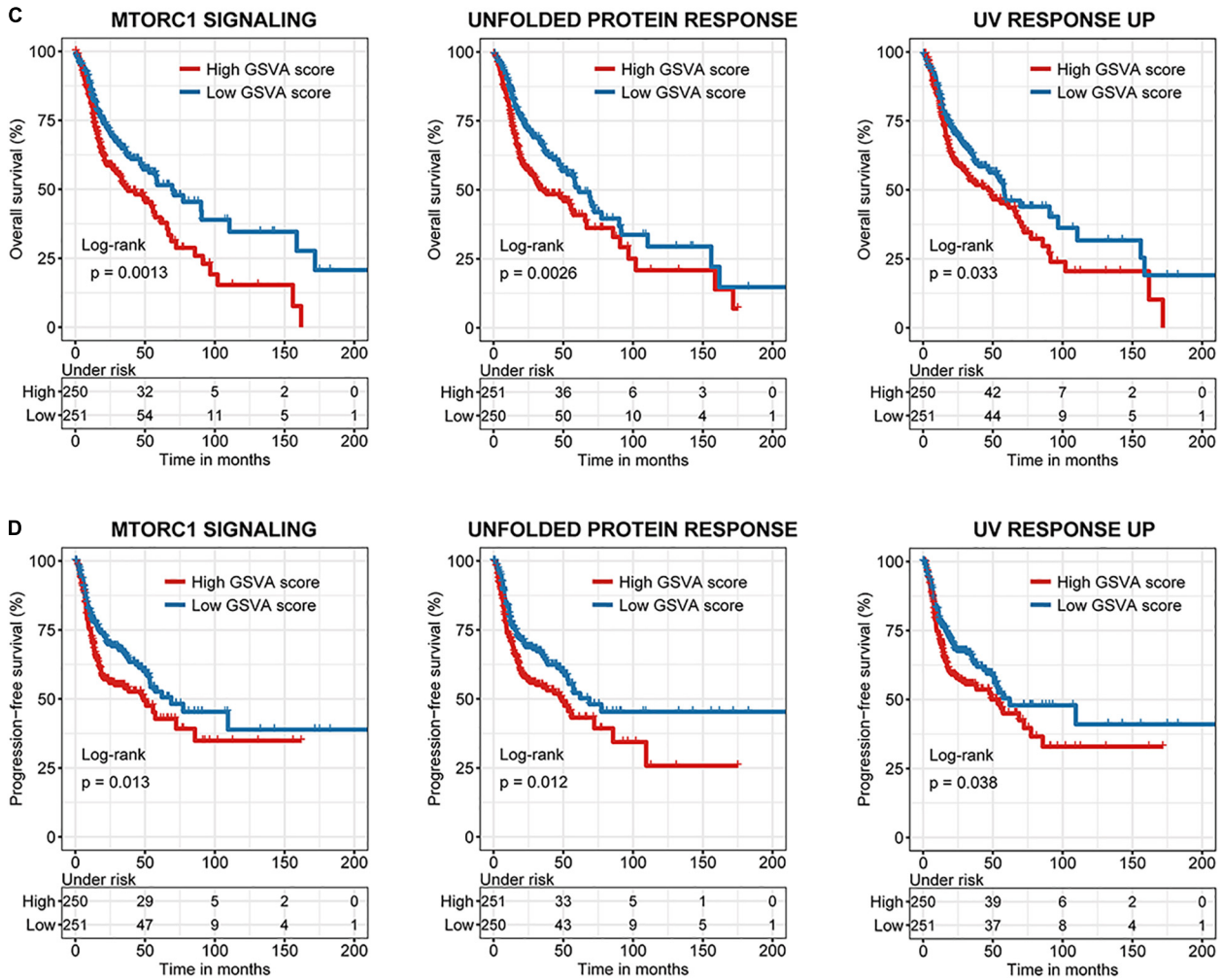

FIGURE 1 | The major prognostic pathways in head and neck squamous cell carcinoma (HNSCC) identified by gene set variation analysis (GSVA). **(A)** Differences in pathway activities scored per sample by GSVA between paired tumor and normal HNSCC in The Cancer Genome Atlas (TCGA) (*n* = 44). Shown are *t*-values from a linear model, corrected for patient of origin. dn, down; UV, ultraviolet; v1, version 1; v2, version 2. **(B)** Univariate Cox regression analysis among various hallmarks of cancer. Kaplan–Meier curves of overall **(C)** and progression-free **(D)** survival for HNSCC patients in the two groups divided by GSVA pathway score.

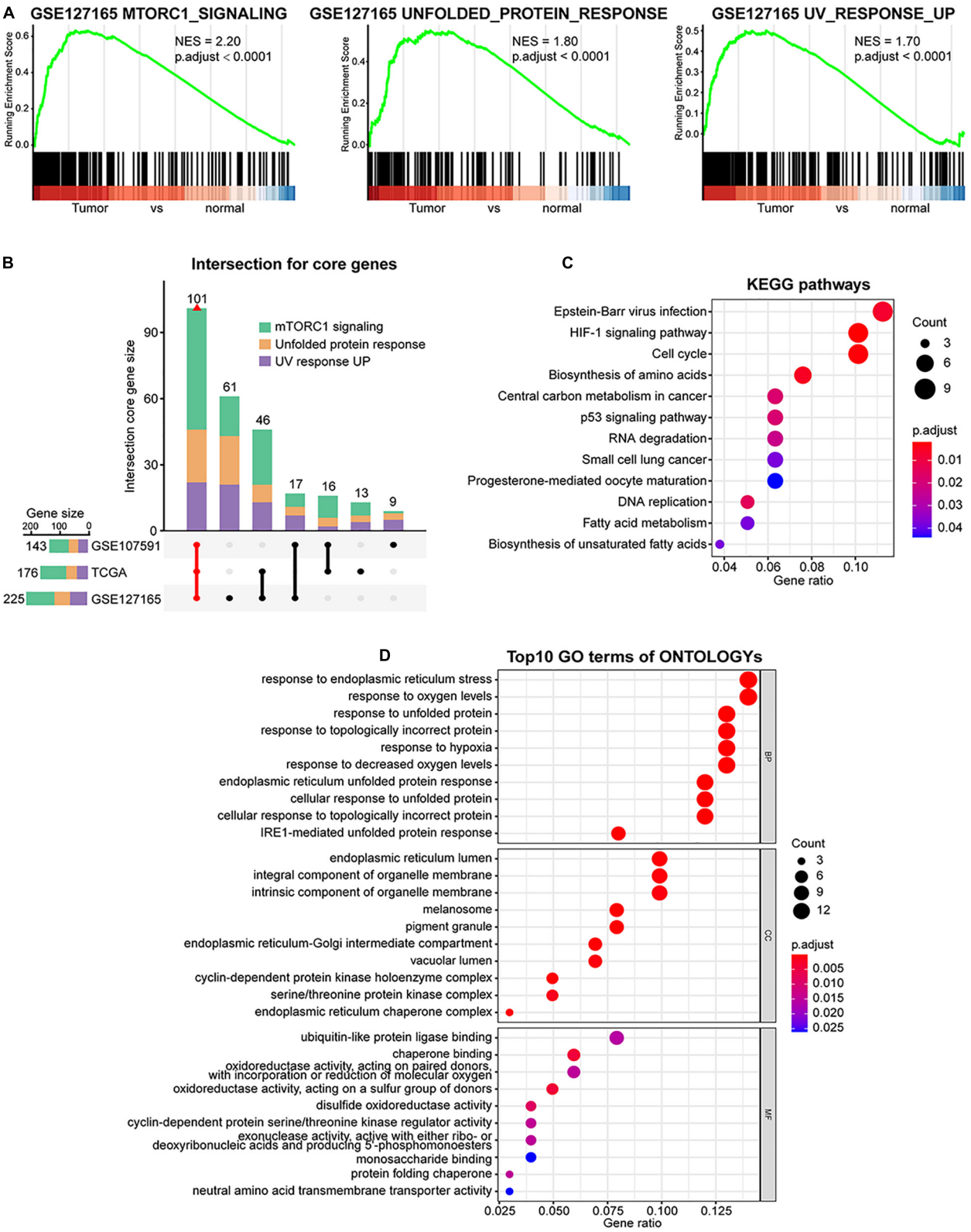

FIGURE 2 | Identification of the core genes in mTORC1 signaling, unfolded protein response (UPR), and UV response UP gene sets. **(A)** Gene set enrichment analysis (GSEA) shows that mTORC1 signaling, UPR, and UV response UP are significantly enriched in GSE127165 cohort. **(B)** Intersection of core genes based on GSEA from three databases is indicated in red. Kyoto Encyclopedia of Genes and Genomes (KEGG) **(C)** and Gene Ontology (GO) **(D)** analysis of the common core genes. BP, biological processes; CC, cellular components; MF, molecular function.

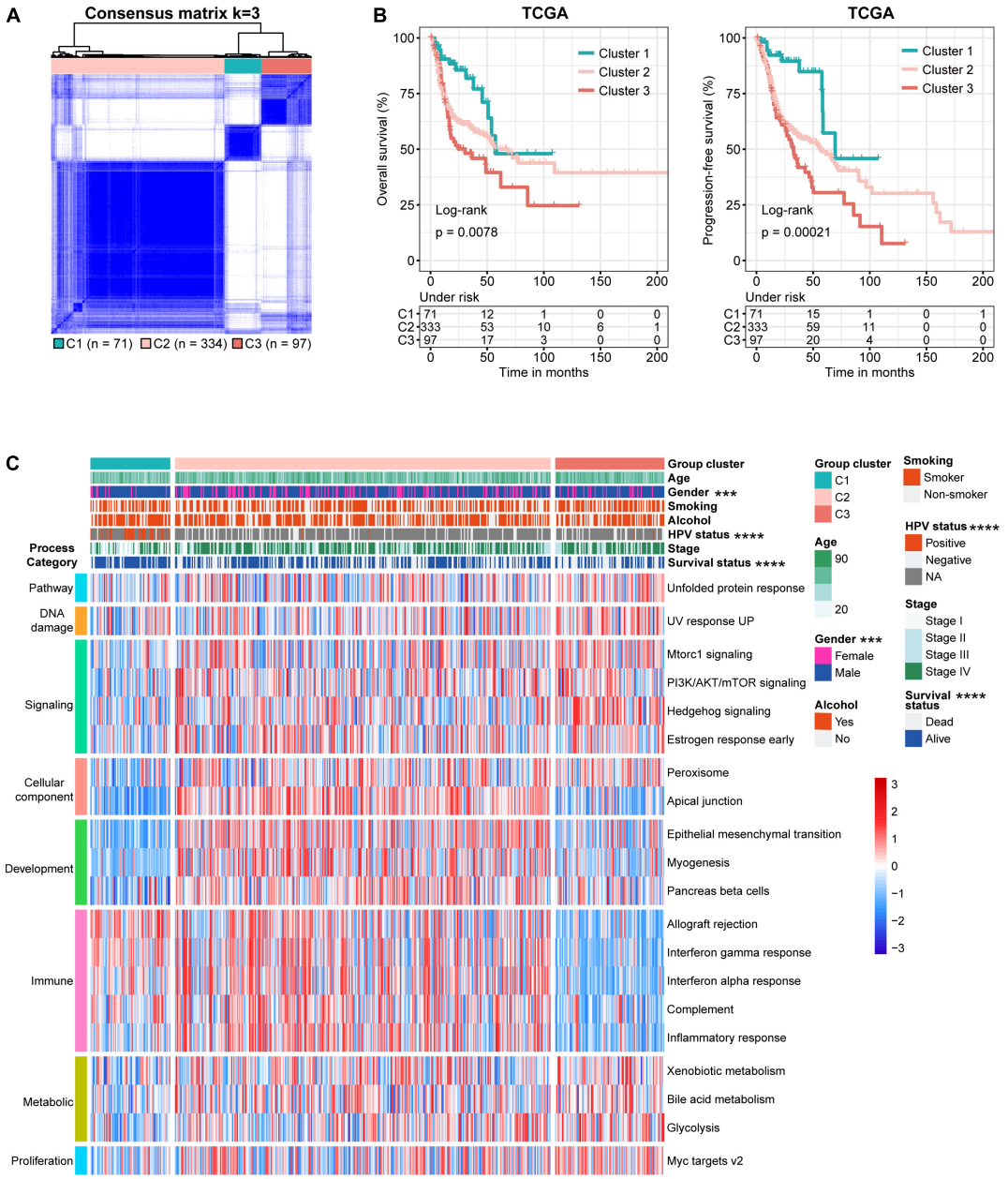

FIGURE 3 | Identification of three molecular subtypes of head and neck squamous cell carcinoma (HNSCC) in The Cancer Genome Atlas (TCGA) discovery dataset. **(A)** Consensus matrix heatmaps (k = 3) of common core genes in The Cancer Genome Atlas (TCGA) cohort. **(B)** Kaplan–Meier curves of overall (left, OS) and progression-free (right, PFS) survival for HNSCC patients in different subtypes. **(C)** Heatmap of differentially activated pathways based on gene set variation analysis (GSVA) score and clinicopathological features of the three subtypes.

core genes, where a total of 502 patients from TCGA cohort were clustered into three subtypes, namely, Cluster 1 (C1, n = 71), Cluster 2 (C2, n = 334), and Cluster 3 (C3, n = 97) (**Figure 3A** and **Supplementary Figure 2A**). Upon comparison of the survival rates among the three subtypes, we found that the C1 patients showed the best OS and PFS (**Figure 3B**). To validate this correlation, we performed the same analysis in additional HNSCC datasets, where a distinct survival rate of OS or PFS showed in different subtypes in GSE41613 (n = 97), GSE65858 (n = 270), and GSE42743 (n = 74) (**Supplementary Figures 2B–D**). Interestingly, the C1 subtype displayed the lowest GSVA score of several pathways that are known to be oncogenic or activated in cancers, such as mTORC1 signaling, UPR, and UV response UP pathways (**Supplementary Figures 2E, 3A**). Furthermore, according to the differential analysis of pathway GSVA scores, the C1 and C2 subgroups showed stronger enrichment of immune pathways, such as inflammatory response, and lower enrichment of oncogenic processes, such as DNA damage, and metabolic and

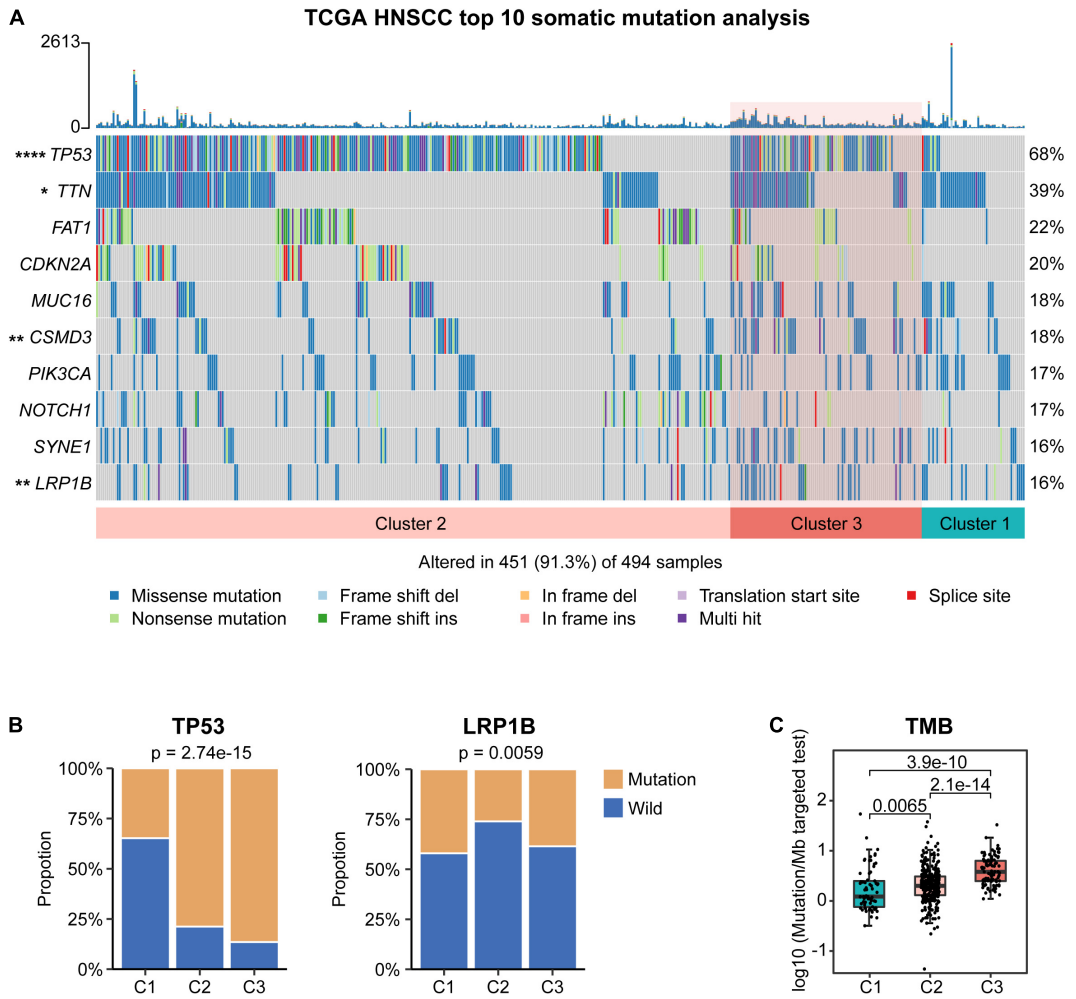

FIGURE 4 | Association between different molecular subtypes and tumor somatic mutation in The Cancer Genome Atlas (TCGA) cohort. **(A)** Top 10 highly mutated genes in head and neck squamous cell carcinoma (HNSCC) subtypes. **(B)** The proportion of *TP53* and *LRP1B* mutation in different subtypes. **(C)** Tumor mutational burden (TMB) of different subtypes.

proliferation pathways, than did C3 subgroup (**Figure 3C**). We also noted no difference in age, smoking status, alcohol history, and cancer stage among different subtypes in TCGA cohort, despite more male and human papillomavirus (HPV)-positive patients in the C1 subtype (**Figure 3C** and **Supplementary Figure 3B**). Taken together, these results demonstrate that the status of 101 core genes identified from the UPR, UV response UP, and mTORC1 signaling is able to distinguish the HNSCC patients with different molecular features and survival outcomes.

Comparison of the Mutational Profile and Burden Between the Three Subtypes

To investigate the difference in somatic mutation among these subtypes, we examined the mutect2-processed mutation dataset in TCGA. As shown in **Figure 4A**, the landscape of top 10 genes with the most frequent genomic alterations in HNSCC is displayed. Four of the top 10 mutation genes (*TP53*, *TTN*, *CSMD3*, and *LRP1B*) showed a distinct mutation rate among the three subtypes. For instance, the canonical tumor suppressor gene *TP53* was more frequently mutated in C2 and C3 patients than in C1 patients (p = 2.74e−15, Chi-square test), whereas another frequently deleted gene in HNSCC *LRP1B* showed a lower mutation rate in C2 compared with C1 and C3 (p = 0.0059, Chi-square test) (**Figure 4B**). Compared with C1 and C2, C3 showed significantly higher tumor mutational burden (TMB) (**Figure 4C**), a parameter correlated with unfavorable immune expression signatures and poor clinical outcomes in HNSCC patients (Chen et al., 2019; Eder et al., 2019).

Characterization of Immunological Features Among Different Subtypes

Given that these subtypes exhibited marked difference in immune-related pathways and TMB, we further explored the characteristics of the tumor microenvironment within different subtypes. To do so, we first examined the distribution of stromal score, immune score, and tumor purity of different subgroups

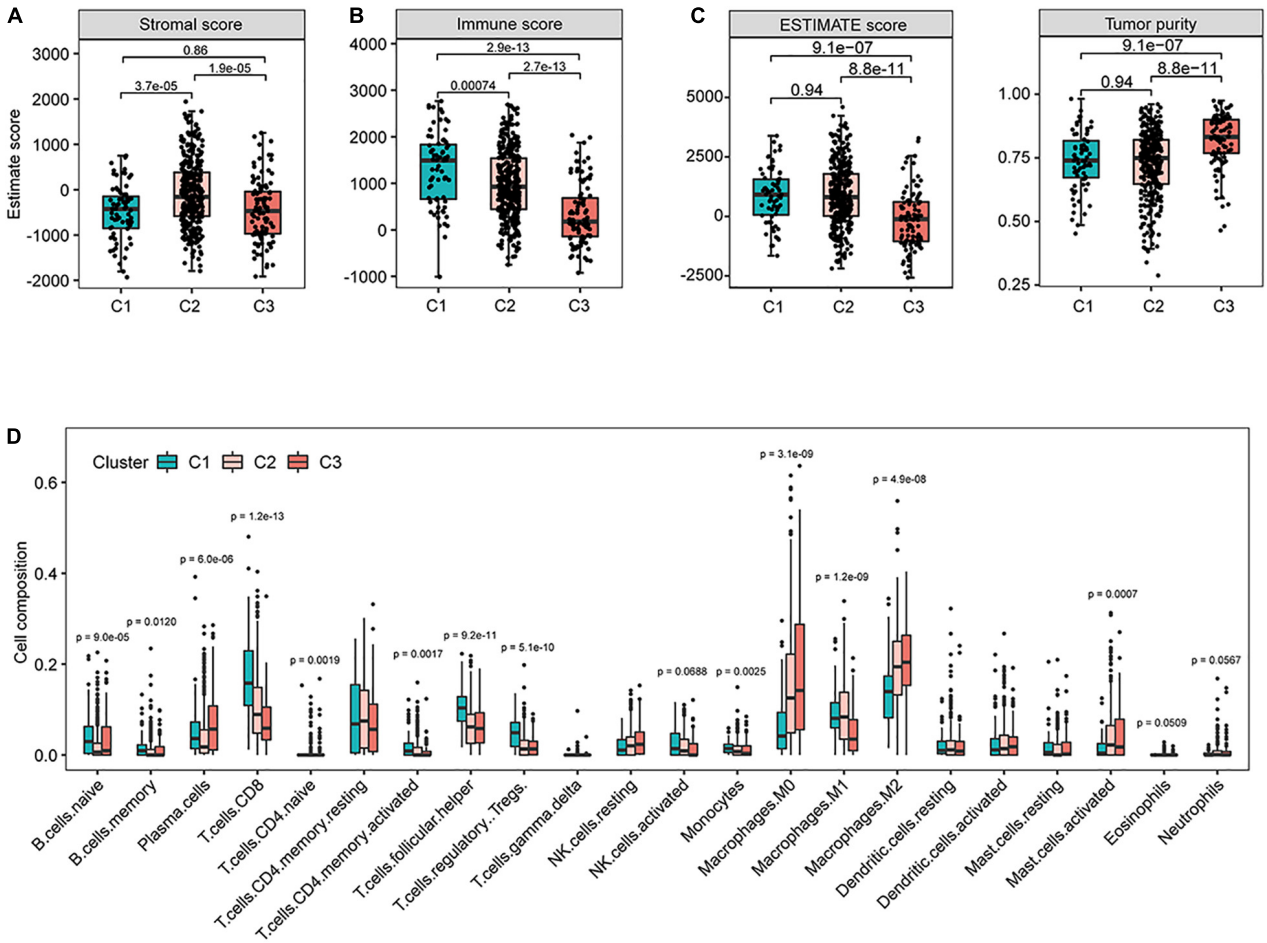

FIGURE 5 | Identification of immune characteristics for different subtypes in The Cancer Genome Atlas (TCGA) cohort. The distribution of stromal score **(A)**, immune score **(B)**, ESTIMATE score, and tumor purity **(C)** for patients in different subtypes. **(D)** The infiltrating levels of 22 immune cell types in different subtypes in The Cancer Genome Atlas (TCGA) cohort.

by computing the ESTIMATE algorithm (Yoshihara et al., 2013). C2 showed the highest stromal score (**Figure 5A**), suggesting the highest stromal content in C2 tumors. C2 subtype also exhibited higher immune scores than C3 (**Figure 5B**), indicative of the higher infiltration of immune cells. Moreover, the ESTIMATE score (combining the stromal and immune scores) of C3 was significantly lower compared with that of other subtypes, whereas its tumor purity was the highest (**Figure 5C**). These data suggest that low immune infiltration may be a phenotypic feature of C3 tumors.

To gain further insight in this regard, we performed CIBERSORT method to estimate the differences in the infiltration of 22 common immune cell types. In line with the immune score results, C3 tumors showed the lowest proportions of lymphocyte infiltration including $CD8^+$ T cells, CD4 memory-activated T cells, regulatory T cells, and activated NK cells (**Figure 5D**). Tumor-associated macrophages polarize into different subtypes that may either promote (M2 subtype) or inhibit (M1 subtype) tumor growth (Anderson et al., 2021). We found that C3 had the highest proportions of resting M0 and polarized M2 macrophages and the lowest level of M1 macrophages (**Figure 5D**). Together, these findings suggest potentially diverse immunological profiles among different subtypes of HNSCC tumors.

Prediction of Potentially Responsive Treatment Strategies for Different Subtypes

Building upon these findings, we speculate that these subtypes of HNSCC tumors may respond to different therapies. To identify potential targets for immunotherapy, the gene expression profile of T-cell signaling pathway was examined (Chen et al., 2017). Interestingly, we found that the expression of several canonical immune checkpoints was markedly elevated in C1 than in C3 (**Figure 6A** and **Supplementary Figure 4A**), such as *CD274* (PD-L1), *PDCD1LG2* (PD-L2), *PDCD1* (PD1), and *CTLA4* (CD152), potentiating the effectiveness of ICI in C1 tumors.

To validate this, we assessed the potential clinical efficacy of immunotherapy in different subtypes by TIDE, whose score

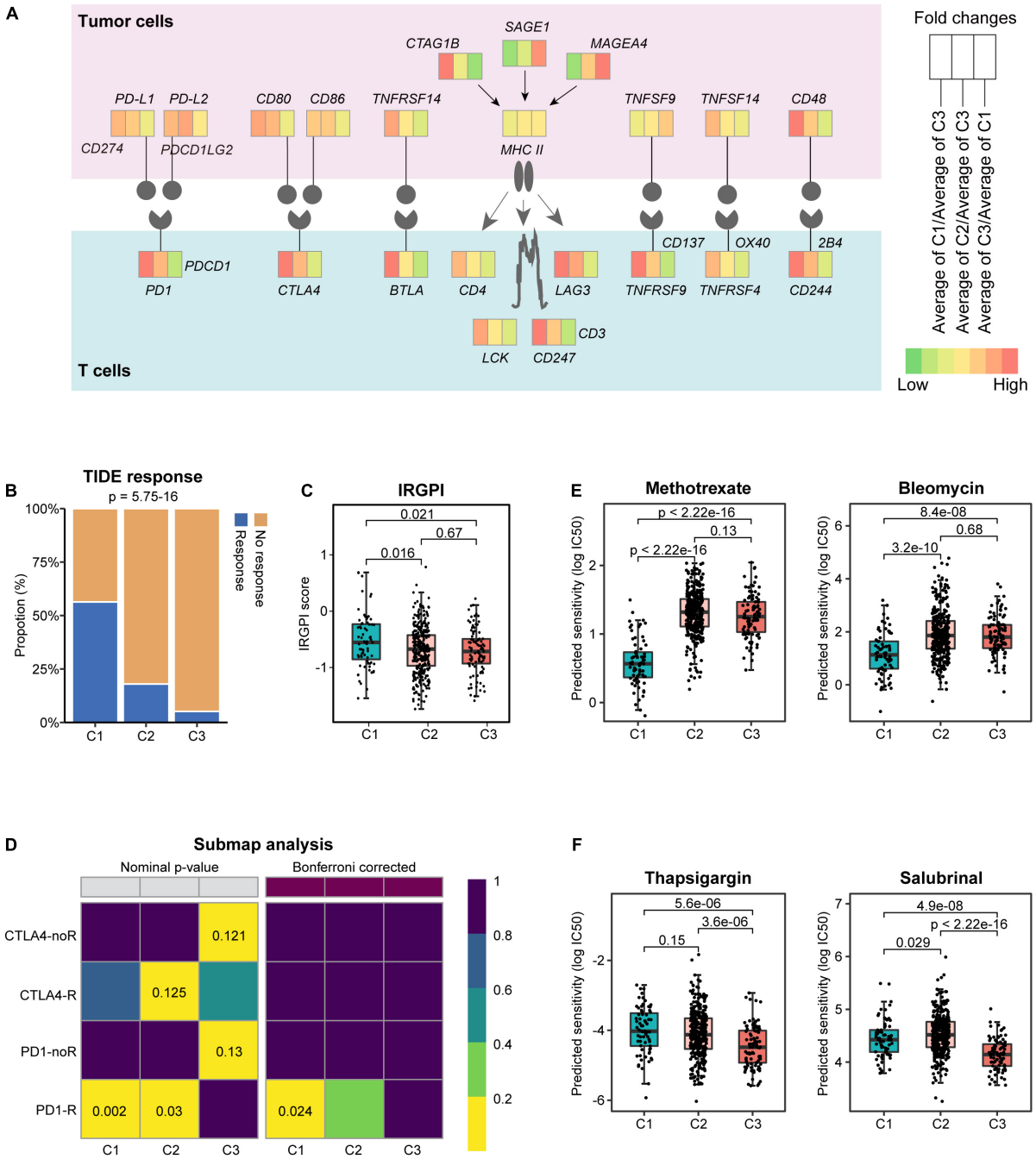

FIGURE 6 | Prediction of response to immunotherapeutic and therapeutic agents for different subtypes. **(A)** Diagram of the immune checkpoint pathway, comparing tumors in different subtypes. Tumor Immune Dysfunction and Exclusion (TIDE) response **(B)** and immune-related genetic prognostic index (IRGPI) score **(C)** in different subtypes. **(D)** Subclass mapping method (SubMap) analysis predicted the sensitivities of different subtypes to the four immune checkpoint inhibitors. noR, no response; R, response. The box plots depict the estimated IC50 for methotrexate, bleomycin **(E)**, and thapsigargin and salubrinal **(F)**.

can be predictive of the potential for immune evasion (Jiang et al., 2018). Our analysis found that C1 tumors had the highest response rate to immunotherapy (**Figure 6B**) and the lowest TIDE score (**Supplementary Figure 4B**). In addition to the TIDE prediction, IRGPI score was recently proposed as a promising immune-related prognostic biomarker in HNSCC (Chen et al., 2021). In keeping with the previous findings, C1 tumors showed significantly higher IRGPI score than C2 and C3 tumors (**Figure 6C**). These results suggested that patients of C1 subtype were more likely to benefit from ICI therapy than those of C2 and C3 subtypes. To examine this in a more detailed manner, SubMap analysis was conducted, and the results indicated that

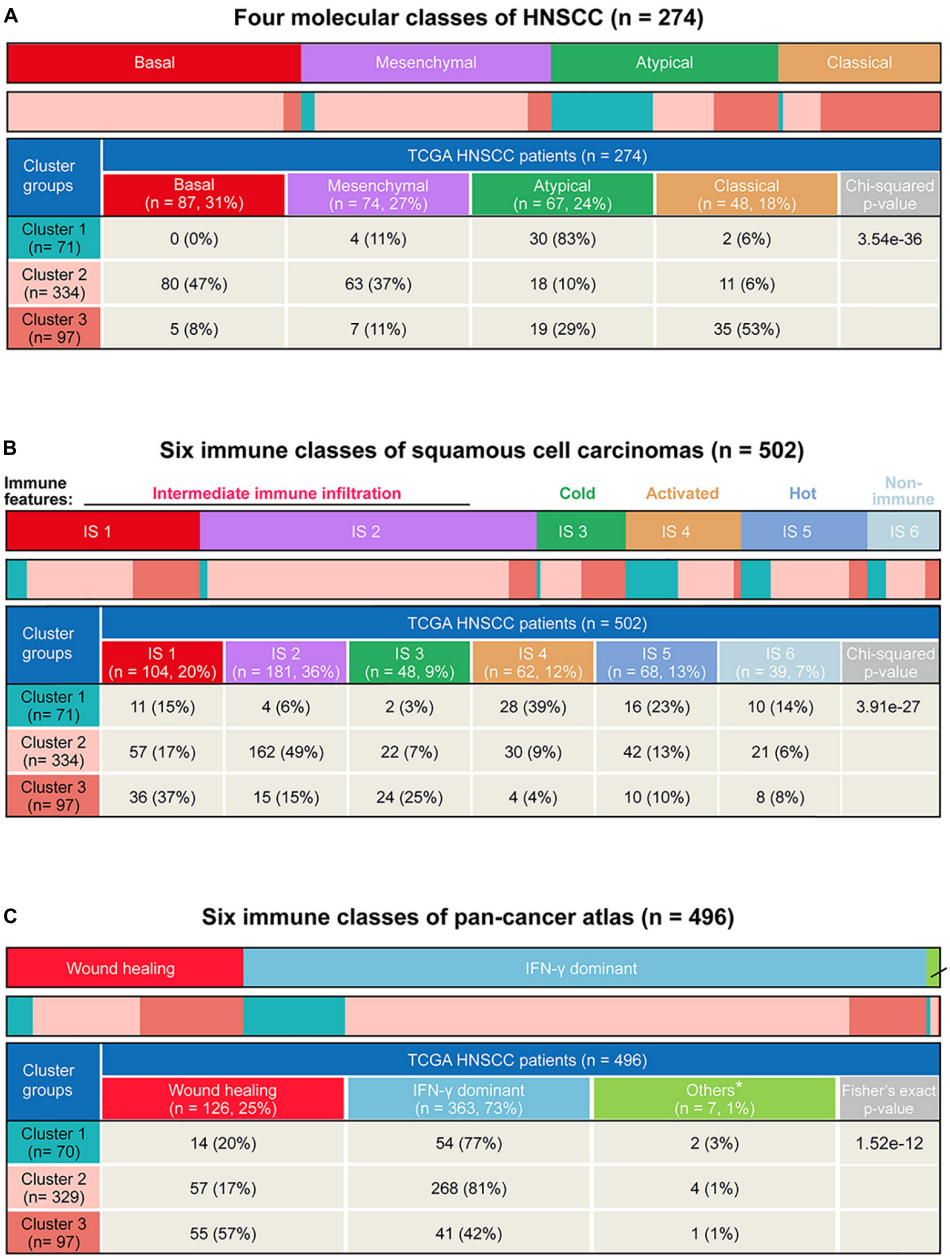

Cluster groups	TCGA HNSCC patients (n = 274)				
	Basal (n = 87, 31%)	Mesenchymal (n = 74, 27%)	Atypical (n = 67, 24%)	Classical (n = 48, 18%)	Chi-squared p-value
Cluster 1 (n= 71)	0 (0%)	4 (11%)	30 (83%)	2 (6%)	3.54e-36
Cluster 2 (n= 334)	80 (47%)	63 (37%)	18 (10%)	11 (6%)	
Cluster 3 (n= 97)	5 (8%)	7 (11%)	19 (29%)	35 (53%)	

Cluster groups	TCGA HNSCC patients (n = 502)						
	IS 1 (n = 104, 20%)	IS 2 (n = 181, 36%)	IS 3 (n = 48, 9%)	IS 4 (n = 62, 12%)	IS 5 (n = 68, 13%)	IS 6 (n = 39, 7%)	Chi-squared p-value
Cluster 1 (n= 71)	11 (15%)	4 (6%)	2 (3%)	28 (39%)	16 (23%)	10 (14%)	3.91e-27
Cluster 2 (n= 334)	57 (17%)	162 (49%)	22 (7%)	30 (9%)	42 (13%)	21 (6%)	
Cluster 3 (n= 97)	36 (37%)	15 (15%)	24 (25%)	4 (4%)	10 (10%)	8 (8%)	

Cluster groups	TCGA HNSCC patients (n = 496)			
	Wound healing (n = 126, 25%)	IFN-γ dominant (n = 363, 73%)	Others* (n = 7, 1%)	Fisher's exact p-value
Cluster 1 (n= 70)	14 (20%)	54 (77%)	2 (3%)	1.52e-12
Cluster 2 (n= 329)	57 (17%)	268 (81%)	4 (1%)	
Cluster 3 (n= 97)	55 (57%)	41 (42%)	1 (1%)	

FIGURE 7 | Comparison of the three subtypes in our study with existing immune and molecular classes. **(A)** Heatmap and table showing distribution of four head and neck squamous cell carcinoma (HNSCC) molecular classes (basal, mesenchymal, atypical, and classic) in different subtypes. **(B)** Heatmap and table showing the distribution of pan-squamous cell carcinomas (SCC) immune classes (IS1, IS2, IS3, IS4, IS5, and IS6) between the three subtypes. **(C)** Heatmap and table showing distribution of six pan-cancer immune classes in different subtypes. *Other immune classes include inflammatory, lymphocyte depleted, immunologically quiet, and TGF-β dominant.

C1 tumors were more likely to respond to anti-PD1 therapy (**Figure 6D**; Bonferroni-corrected $p = 0.024$).

Furthermore, we assessed the potential responsiveness of the subtypes to the existing HNSCC drugs by estimating the drug IC50 for each sample in TCGA cohort through 10-fold cross-validation based on the GDSC training set (Geeleher et al., 2014). Interestingly, compared with C2 and C3 tumors, C1 showed markedly lower estimated IC50 of chemotherapeutic drugs, such as methotrexate, bleomycin, cisplatin, gemcitabine, and entinostat (**Figure 6E** and **Supplementary Figure 4C**), suggesting a selective sensitivity of these tumors to chemotherapy. Besides these clinical drugs, further interrogation of the GDSC database found that C2 tumors may be responsive to the HSP90 inhibitor luminespib, and the MEK 1/2 inhibitor selumetinib (**Supplementary Figure 4D**), whereas C3 tumors were predicted to be sensitive

to agents disrupting ER homeostasis, such as the SERCA pump inhibitor thapsigargin and the eIF2α phosphatase inhibitor salubrinal (**Figure 6F**), as well as the mTOR inhibitor AZD8055 (**Supplementary Figure 4D**).

Integration of the Three Subgroups With Other Immune and Molecular Classes

Head and neck squamous cell carcinoma tumors can be grouped as basal, mesenchymal, atypical, and classical subtypes according to statistically significant chromosomal gains and losses and differential cell of origin expression patterns (Chung et al., 2004; Walter et al., 2013; Cancer Genome Atlas Network, 2015). The basal class demonstrates inactivation of *NOTCH1* with intact oxidative stress signaling and fewer alterations of chromosome 3q. The mesenchymal subtype, characterized by either the presence of fibroblasts or a strong desmoplastic response, displays common alterations in innate immunity genes. The atypical class is a less aggressive subtype associated with a strong immune signature and a lack of chromosome 7 amplifications. In addition, the classical subtype shows high *TP53* mutation rate and alterations of oxidative stress genes. Based on the subtyping of HNSCC tumors, we detected the highest proportion of the atypical class (83%) within C1 (**Figure 7A**). Moreover, C2 was a mixed subtype composed of mesenchymal and basal samples, whereas C3 had more classical samples (p = 3.54e−36, Chi-squared test) (**Figure 7A**).

A squamous cell carcinoma immune subtype classification has described the immune landscape of HNSCC according to consensus clustering of immune-related gene expression profiles and has summarized six immune subtypes (Li et al., 2019). In line with the previous immunological profile analysis, there were more IS4 (immune-activated phenotype, 39%) and IS5 (immune-hot phenotype, 23%) classes in C1 while more IS1 (immune-suppressive phenotype, 37%) and IS3 (immune-cold phenotype, 25%) classes in C3 (p = 3.91e−27, Chi-square test) (**Figure 7B**).

Lastly, we also integrated our results with the six pan-cancer immune subtypes (Thorsson et al., 2018). Among these, the Wound healing class is defined by elevated expression of angiogenic genes and a Th2 cell bias to the adaptive immune infiltrate, while the IFN-γ dominant class is defined by the highest M1/M2 macrophage polarization and a strong CD8 signal. We found that C1 (77%) and C2 (81%) had significantly higher proportion of IFN-γ dominant class, whereas C3 showed the highest proportion of the Wound healing class (p = 1.52e−12, Fisher's exact test) (**Figure 7C**). Taken together, by comparing our subtypes with previously established molecular and immunological classifications, these results corroborated that the C1 tumors were characterized by an active immune response and lower tumor aggressiveness, while the C3 tumor was characterized by an immune-suppressive response and higher aggressiveness.

DISCUSSION

Head and neck squamous cell carcinoma is an aggressive malignancy, whose highly heterogeneous nature leads to disparities in prognosis and therapeutic response irrespective of clinical stage (Cancer Genome Atlas Network, 2015; Canning et al., 2019). Therefore, identifying biomarkers to stratify patients into clinically meaningful subtypes and selecting effective targeted therapies for different subtypes has become the primary focus of the field (Berger et al., 2018). In this study, by comprehensive bioinformatics analysis of the published datasets, we identified three subtypes of HNSCC tumors with distinct molecular features and survival outcomes, and we proposed potentially suitable therapeutic agents for specific subtypes (**Figure 8**), which may facilitate patient stratification and tailored treatment strategies in HNSCC.

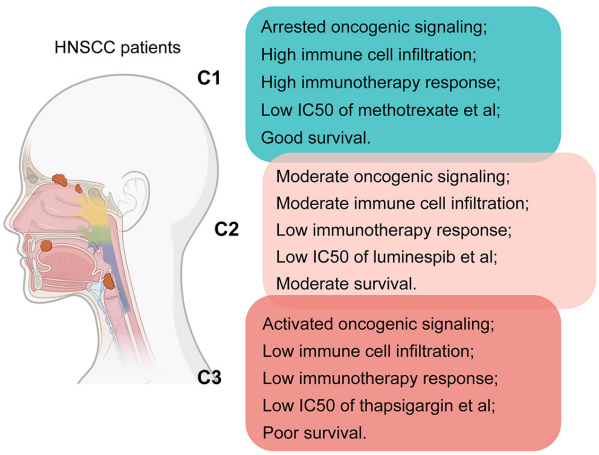

FIGURE 8 | Summary of features for patients of the three subtypes in this study.

Recently, several large-scale comprehensive studies have advanced our understanding in the molecular landscape of HNSCC and uncovered frequently altered genes and pathways (Chung et al., 2004; Walter et al., 2013; Cancer Genome Atlas Network, 2015). To identify the gene sets that are relevant to prognosis, we compared the paired tumor and normal samples from these publicly available datasets by GSVA and found that mTORC1 signaling, UPR, and UV response UP were the most significantly enriched upregulated pathways ($p < 0.05$). As a central regulator of metabolism, activation of mTORC1 signaling has been linked with poor prognosis in various malignancies, including HNSCC (Tan et al., 2019). Hyper-activated mTORC1 phosphorylates 4E-BP1, which stabilizes p21 and affects HNSCC clinical outcome (Llanos et al., 2016). Clinical trials of mTORC1 inhibitors used either alone or in combination with chemotherapy or radiotherapy showed encouraging results in HNSCC. Therefore, from a precision treatment standpoint, identifying the patients who may benefit from mTORC1 inhibitors is of clinical significance (Tan et al., 2019). Genes involved in the UPR and UV response are vital for maintaining proteostasis and genome stability (Mansilla et al., 2013; Strozyk and Kulms, 2013; Wang et al., 2019; Zhang et al., 2020). Previous evidence has functionally implicated these homeostatic mechanisms in HNSCC by regulating key tumor biology processes including cancer cell survival and therapy

resistance, while their activities have also been associated with HNSCC prognosis (Pluquet and Galmiche, 2019; Psyrri et al., 2021). Furthermore, by overlapping the genes in these three pathways across different cohorts, we identified 101 core genes that were able to subgroup the patients with distinct survival outcomes and molecular profiles. Patients with the best prognosis (C1) were associated with arrested oncogenic pathways, such as PI3K/AKT/mTOR signaling and Myc targets. These results, at least in concept, provide a novel strategy to classify the HNSCC patients with divergent survival outcomes. Further refinement of the gene set is needed to generate biomarkers that may be of clinical utility.

To gain further biological insight into the molecular characteristics of three subtypes, we examined the mutect2-processed mutation dataset in TCGA, and we identified four commonly altered genes in HNSCC (*TP53*, *TTN*, *CSMD3*, and *LRP1B*) with distinct mutation rate among the three subtypes. As the single most commonly reported genetic abnormality in cancers, *TP53* aberration is also a molecular hallmark of HNSCC. The reported alteration frequency in HNSCC ranged from 20 to 90%, depending on the methodologies used, types of tumor materials sampled, and heterogeneity of tumor sites examined (Zhou et al., 2016). *TP53* encodes for a nuclear phosphoprotein that acts as a sequence-specific transcription factor and is involved in a plethora of processes, including cell cycle regulation, cellular response to DNA damage, senescence, and apoptosis (Zhou et al., 2016). *LRP1B* belongs to the gene family of low-density lipoprotein receptor and is also reputed as a tumor suppressor gene. Its frequent mutation has been observed in several cancer types, including HNSCC, and is associated with tumor HPV status and response to ICI (Cao et al., 2021). *TTN* encodes the large muscle protein titin that is primarily responsible for stabilization of cytoskeletal filaments (Lee et al., 2021), while *CSMD3* encodes for a large transmembrane protein with CUB and sushi multiple domains (Shimizu et al., 2003). Despite the frequent aberrations observed in HNSCC, neither of their functional role is clear so far. Studies even indicate that high alteration frequencies of *TTN* and *CSMD3* are likely due to heterogeneous mutation rates at different chromosome locations (Lawrence et al., 2013, 2014). Immunotherapies are a valuable addition to the arsenal of HNSCC treatments. However, the complexity in tumor microenvironment and immunity across different tumors has hindered its effectiveness in HNSCC. Here, we evaluated the immune-related parameters of different subtypes by computing multiple previously established algorithms. The results showed that C1 patients with the best prognosis displayed the highest immune, ESTIMATE, and IRGPI scores and the lowest TIDE response and score. The composition of activated cytotoxic T cells and NK cells was the highest in C1, whereas that of M2 macrophage was the lowest. These findings suggest that C1 subtype may represent the immunologically "hot" tumors that would likely benefit from ICI. In keeping with this, our drug response analysis predicted that C1 tumors were significantly more sensitive to chemotherapeutic and immunotherapeutic agents. By contrast, our analysis suggested that the immunologically "cold" C3 tumors may not directly benefit from either chemotherapy or immunotherapy but may be selectively sensitive to compounds disrupting ER homeostasis. This is consistent with the observation that UPR activity is the highest in these tumors. It would be of interest to dissect the role of different UPR branches in HNSCC experimentally and to evaluate the therapeutic value using branch-specific inhibitors that have been under extensive preclinical and clinical development (Hetz et al., 2019; Sheng et al., 2019; Torres et al., 2019).

CONCLUSION

In conclusion, as an effort toward patient stratification and individualized treatment, we performed comprehensive bioinformatics analysis of the published datasets of HNSCC, and we proposed a novel classification strategy that can effectively categorize patients with different survival outcomes, molecular features, and immunological profiles. We also identified potentially suitable drugs and therapeutic strategies for each subtype. Our findings gain new insight into the heterogeneous nature of HNSCC and offer priorities for future experimental investigations.

DATA AVAILABILITY STATEMENT

The datasets presented in this study can be found in online repositories. The names of the repository/repositories and accession number(s) can be found in the article/ **Supplementary Material**.

AUTHOR CONTRIBUTIONS

PZ, SL, and FZ designed the study and conducted the bioinformatics analysis. TZ and J-HS helped in the data analysis and revised the manuscript. XS and FZ wrote the manuscript and supervised the project. All authors read and approved the final manuscript.

FUNDING

This work was supported by the Medical Science and Technology Program of Henan Province, China (LHGJ20190193) to PZ and the National Natural Science Foundation of China (81802546) to XS.

ACKNOWLEDGMENTS

Figure 8 was made in part with BioRender.com.

SUPPLEMENTARY MATERIAL

The Supplementary Material for this article can be found online at: https://www.frontiersin.org/articles/10.3389/fcell.2021.711348/full#supplementary-material

REFERENCES

Alsahafi, E., Begg, K., Amelio, I., Raulf, N., Lucarelli, P., Sauter, T., et al. (2019). Clinical update on head and neck cancer: molecular biology and ongoing challenges. *Cell Death Dis.* 10:540. doi: 10.1038/s41419-019-1769-9

Anderson, N. R., Minutolo, N. G., Gill, S., and Klichinsky, M. (2021). Macrophage-based approaches for cancer immunotherapy. *Cancer Res.* 81, 1201–1208. doi: 10.1158/0008-5472.CAN-20-2990

Berger, A. C., Korkut, A., Kanchi, R. S., Hegde, A. M., Lenoir, W., Liu, W., et al. (2018). A comprehensive pan-cancer molecular study of gynecologic and breast cancers. *Cancer Cell* 33, 690.e699–705.e699. doi: 10.1016/j.ccell.2018.03.014

Burtness, B., Harrington, K. J., Greil, R., Soulieres, D., Tahara, M., de Castro, G. Jr., et al. (2019). Pembrolizumab alone or with chemotherapy versus cetuximab with chemotherapy for recurrent or metastatic squamous cell carcinoma of the head and neck (KEYNOTE-048): a randomised, open-label, phase 3 study. *Lancet* 394, 1915–1928. doi: 10.1016/S0140-6736(19)32591-7

Cancer Genome Atlas Network (2015). Comprehensive genomic characterization of head and neck squamous cell carcinomas. *Nature* 517, 576–582. doi: 10.1038/nature14129

Canning, M., Guo, G., Yu, M., Myint, C., Groves, M. W., Byrd, J. K., et al. (2019). Heterogeneity of the head and neck squamous cell carcinoma immune landscape and its impact on immunotherapy. *Front. Cell Dev. Biol.* 7:52. doi: 10.3389/fcell.2019.00052

Cao, C. H., Liu, R., Lin, X. R., Luo, J. Q., Cao, L. J., Zhang, Q. J., et al. (2021). LRP1B mutation is associated with tumor HPV status and promotes poor disease outcomes with a higher mutation count in HPV-related cervical carcinoma and head & neck squamous cell carcinoma. *Int. J. Biol. Sci.* 17, 1744–1756. doi: 10.7150/ijbs.56970

Chen, F., Zhang, Y., Parra, E., Rodriguez, J., Behrens, C., Akbani, R., et al. (2017). Multiplatform-based molecular subtypes of non-small-cell lung cancer. *Oncogene* 36, 1384–1393. doi: 10.1038/onc.2016.303

Chen, Y. P., Wang, Y. Q., Lv, J. W., Li, Y. Q., Chua, M. L. K., Le, Q. T., et al. (2019). Identification and validation of novel microenvironment-based immune molecular subgroups of head and neck squamous cell carcinoma: implications for immunotherapy. *Ann. Oncol.* 30, 68–75. doi: 10.1093/annonc/mdy470

Chen, Y., Li, Z. Y., Zhou, G. Q., and Sun, Y. (2021). An immune-related gene prognostic index for head and neck squamous cell carcinoma. *Clin. Cancer Res.* 27, 330–341. doi: 10.1158/1078-0432.CCR-20-2166

Chung, C. H., Parker, J. S., Karaca, G., Wu, J., Funkhouser, W. K., Moore, D., et al. (2004). Molecular classification of head and neck squamous cell carcinomas using patterns of gene expression. *Cancer Cell* 5, 489–500. doi: 10.1016/s1535-6108(04)00112-6

Eder, T., Hess, A. K., Konschak, R., Stromberger, C., Johrens, K., Fleischer, V., et al. (2019). Interference of tumour mutational burden with outcome of patients with head and neck cancer treated with definitive chemoradiation: a multicentre retrospective study of the german cancer consortium radiation oncology group. *Eur. J. Cancer* 116, 67–76. doi: 10.1016/j.ejca.2019.04.015

Fernandes, Q., Merhi, M., Raza, A., Inchakalody, V. P., Abdelouahab, N., Zar Gul, A. R., et al. (2018). Role of epstein-barr virus in the pathogenesis of head and neck cancers and its potential as an immunotherapeutic target. *Front. Oncol.* 8:257. doi: 10.3389/fonc.2018.00257

Ferris, R. L., Blumenschein, G. Jr., Fayette, J., Guigay, J., Colevas, A. D., Licitra, L., et al. (2016). Nivolumab for recurrent squamous-cell carcinoma of the head and neck. *N. Engl. J. Med.* 375, 1856–1867. doi: 10.1056/NEJMoa1602252

Geeleher, P., Cox, N. J., and Huang, R. S. (2014). Clinical drug response can be predicted using baseline gene expression levels and in vitro drug sensitivity in cell lines. *Genome Biol.* 15:R47. doi: 10.1186/gb-2014-15-3-r47

Goldman, M. J., Craft, B., Hastie, M., Repecka, K., McDade, F., Kamath, A., et al. (2020). Visualizing and interpreting cancer genomics data via the Xena platform. *Nat. Biotechnol.* 38, 675–678. doi: 10.1038/s41587-020-0546-8

Hanzelmann, S., Castelo, R., and Guinney, J. (2013). GSVA: gene set variation analysis for microarray and RNA-seq data. *BMC Bioinformatics* 14:7. doi: 10.1186/1471-2105-14-7

Hetz, C., Axten, J. M., and Patterson, J. B. (2019). Pharmacological targeting of the unfolded protein response for disease intervention. *Nat. Chem. Biol.* 15, 764–775. doi: 10.1038/s41589-019-0326-2

Hoshida, Y., Brunet, J. P., Tamayo, P., Golub, T. R., and Mesirov, J. P. (2007). Subclass mapping: identifying common subtypes in independent disease data sets. *PLoS One* 2:e1195. doi: 10.1371/journal.pone.0001195

Jiang, P., Gu, S., Pan, D., Fu, J., Sahu, A., Hu, X., et al. (2018). Signatures of T cell dysfunction and exclusion predict cancer immunotherapy response. *Nat. Med.* 24, 1550–1558. doi: 10.1038/s41591-018-0136-1

Jie, H. B., Schuler, P. J., Lee, S. C., Srivastava, R. M., Argiris, A., Ferrone, S., et al. (2015). CTLA-4(+) regulatory T cells increased in cetuximab-treated head and neck cancer patients suppress NK cell cytotoxicity and correlate with poor prognosis. *Cancer Res.* 75, 2200–2210. doi: 10.1158/0008-5472.CAN-14-2788

Johnson, D. E., Burtness, B., Leemans, C. R., Lui, V. W. Y., Bauman, J. E., and Grandis, J. R. (2020). Head and neck squamous cell carcinoma. *Nat. Rev. Dis. Primers* 6:92. doi: 10.1038/s41572-020-00224-3

Lambrechts, D., Wauters, E., Boeckx, B., Aibar, S., Nittner, D., Burton, O., et al. (2018). Phenotype molding of stromal cells in the lung tumor microenvironment. *Nat. Med.* 24, 1277–1289. doi: 10.1038/s41591-018-0096-5

Lawrence, M. S., Stojanov, P., Mermel, C. H., Robinson, J. T., Garraway, L. A., Golub, T. R., et al. (2014). Discovery and saturation analysis of cancer genes across 21 tumour types. *Nature* 505, 495–501. doi: 10.1038/nature12912

Lawrence, M. S., Stojanov, P., Polak, P., Kryukov, G. V., Cibulskis, K., Sivachenko, A., et al. (2013). Mutational heterogeneity in cancer and the search for new cancer-associated genes. *Nature* 499, 214–218. doi: 10.1038/nature12213

Lee, D. Y., Kang, Y., Im, N. R., Kim, B., Kwon, T. K., Jung, K. Y., et al. (2021). Actin-associated gene expression is associated with early regional metastasis of tongue cancer. *Laryngoscope* 131, 813–819. doi: 10.1002/lary.29025

Leemans, C. R., Snijders, P. J. F., and Brakenhoff, R. H. (2018). The molecular landscape of head and neck cancer. *Nat. Rev. Cancer* 18, 269–282. doi: 10.1038/nrc.2018.11

Li, B., Cui, Y., Nambiar, D. K., Sunwoo, J. B., and Li, R. (2019). The immune subtypes and landscape of squamous cell carcinoma. *Clin Cancer Res.* 25, 3528–3537. doi: 10.1158/1078-0432.CCR-18-4085

Liberzon, A., Birger, C., Thorvaldsdottir, H., Ghandi, M., Mesirov, J. P., and Tamayo, P. (2015). The molecular signatures database (MSigDB) hallmark gene set collection. *Cell Syst.* 1, 417–425. doi: 10.1016/j.cels.2015.12.004

Liu, R., Holik, A. Z., Su, S., Jansz, N., Chen, K., Leong, H. S., et al. (2015). Why weight? Modelling sample and observational level variability improves power in RNA-seq analyses. *Nucleic Acids Res.* 43:e97. doi: 10.1093/nar/gkv412

Llanos, S., Garcia-Pedrero, J. M., Morgado-Palacin, L., Rodrigo, J. P., and Serrano, M. (2016). Stabilization of p21 by mTORC1/4E-BP1 predicts clinical outcome of head and neck cancers. *Nat. Commun.* 7:10438. doi: 10.1038/ncomms10438

Love, M. I., Huber, W., and Anders, S. (2014). Moderated estimation of fold change and dispersion for RNA-seq data with DESeq2. *Genome Biol.* 15:550. doi: 10.1186/s13059-014-0550-8

Mansilla, S. F., Soria, G., Vallerga, M. B., Habif, M., Martinez-Lopez, W., Prives, C., et al. (2013). UV-triggered p21 degradation facilitates damaged-DNA replication and preserves genomic stability. *Nucleic Acids Res.* 41, 6942–6951. doi: 10.1093/nar/gkt475

Murtagh, F., and Legendre, P. (2014). Ward's hierarchical agglomerative clustering method: which algorithms implement ward's criterion? *J. Classif.* 31, 274–295. doi: 10.1007/s00357-014-9161-z

Newman, A. M., Liu, C. L., Green, M. R., Gentles, A. J., Feng, W., Xu, Y., et al. (2015). Robust enumeration of cell subsets from tissue expression profiles. *Nat. Methods* 12, 453–457. doi: 10.1038/nmeth.3337

Pluquet, O., and Galmiche, A. (2019). Impact and relevance of the unfolded protein response in HNSCC. *Int. J. Mol. Sci.* 20:2654. doi: 10.3390/ijms20112654

Psyrri, A., Gkotzamanidou, M., Papaxoinis, G., Krikoni, L., Economopoulou, P., Kotsantis, I., et al. (2021). The DNA damage response network in the treatment of head and neck squamous cell carcinoma. *ESMO Open* 6:100075. doi: 10.1016/j.esmoop.2021.100075

Roh, W., Chen, P. L., Reuben, A., Spencer, C. N., Prieto, P. A., Miller, J. P., et al. (2017). Integrated molecular analysis of tumor biopsies on sequential CTLA-4 and PD-1 blockade reveals markers of response and resistance. *Sci. Transl. Med.* 9:eaah3560. doi: 10.1126/scitranslmed.aah3560

Seiwert, T. Y., Burtness, B., Mehra, R., Weiss, J., Berger, R., Eder, J. P., et al. (2016). Safety and clinical activity of pembrolizumab for treatment of recurrent or metastatic squamous cell carcinoma of the head and neck (KEYNOTE-012): an open-label, multicentre, phase 1b trial. *Lancet Oncol.* 17, 956–965. doi: 10.1016/S1470-2045(16)30066-3

Sheng, X., Nenseth, H. Z., Qu, S., Kuzu, O. F., Frahnow, T., Simon, L., et al. (2019). IRE1alpha-XBP1s pathway promotes prostate cancer by activating c-MYC signaling. *Nat. Commun.* 10:323. doi: 10.1038/s41467-018-08152-3

Shimizu, A., Asakawa, S., Sasaki, T., Yamazaki, S., Yamagata, H., Kudoh, J., et al. (2003). A novel giant gene CSMD3 encoding a protein with CUB and sushi multiple domains: a candidate gene for benign adult familial myoclonic epilepsy on human chromosome 8q23.3-q24.1. *Biochem. Biophys. Res. Commun.* 309, 143–154. doi: 10.1016/s0006-291x(03)01555-9

Strozyk, E., and Kulms, D. (2013). The role of AKT/mTOR pathway in stress response to UV-irradiation: implication in skin carcinogenesis by regulation of apoptosis, autophagy and senescence. *Int. J. Mol. Sci.* 14, 15260–15285. doi: 10.3390/ijms140815260

Tan, F. H., Bai, Y., Saintigny, P., and Darido, C. (2019). mTOR signalling in head and neck cancer: heads up. *Cells* 8:333. doi: 10.3390/cells8040333

Thorsson, V., Gibbs, D. L., Brown, S. D., Wolf, D., Bortone, D. S., Ou Yang, T. H., et al. (2018). The immune landscape of cancer. *Immunity* 48, 812.e814–830.e814. doi: 10.1016/j.immuni.2018.03.023

Torres, S. E., Gallagher, C. M., Plate, L., Gupta, M., Liem, C. R., Guo, X., et al. (2019). Ceapins block the unfolded protein response sensor ATF6alpha by inducing a neomorphic inter-organelle tether. *Elife* 8:e46595. doi: 10.7554/eLife.46595

Walter, V., Yin, X., Wilkerson, M. D., Cabanski, C. R., Zhao, N., Du, Y., et al. (2013). Molecular subtypes in head and neck cancer exhibit distinct patterns of chromosomal gain and loss of canonical cancer genes. *PLoS One* 8:e56823. doi: 10.1371/journal.pone.0056823

Wang, Y., Wang, K., Jin, Y., and Sheng, X. (2019). Endoplasmic reticulum proteostasis control and gastric cancer. *Cancer Lett.* 449, 263–271. doi: 10.1016/j.canlet.2019.01.034

Wilkerson, M. D., and Hayes, D. N. (2010). ConsensusClusterPlus: a class discovery tool with confidence assessments and item tracking. *Bioinformatics* 26, 1572–1573. doi: 10.1093/bioinformatics/btq170

Yoshihara, K., Shahmoradgoli, M., Martinez, E., Vegesna, R., Kim, H., Torres-Garcia, W., et al. (2013). Inferring tumour purity and stromal and immune cell admixture from expression data. *Nat. Commun.* 4:2612. doi: 10.1038/ncomms3612

Yu, G., Wang, L. G., Han, Y., and He, Q. Y. (2012). clusterProfiler: an R package for comparing biological themes among gene clusters. *OMICS* 16, 284–287. doi: 10.1089/omi.2011.0118

Zhang, T., Li, N., Sun, C., Jin, Y., and Sheng, X. (2020). MYC and the unfolded protein response in cancer: synthetic lethal partners in crime? *EMBO Mol. Med.* 12:e11845. doi: 10.15252/emmm.201911845

Zhou, G., Liu, Z., and Myers, J. N. (2016). TP53 Mutations in head and neck squamous cell carcinoma and their impact on disease progression and treatment response. *J. Cell Biochem.* 117, 2682–2692. doi: 10.1002/jcb.25592

Conflict of Interest: The authors declare that the research was conducted in the absence of any commercial or financial relationships that could be construed as a potential conflict of interest.

Publisher's Note: All claims expressed in this article are solely those of the authors and do not necessarily represent those of their affiliated organizations, or those of the publisher, the editors and the reviewers. Any product that may be evaluated in this article, or claim that may be made by its manufacturer, is not guaranteed or endorsed by the publisher.

frontiers in Oncology

REVIEW
published: 30 September 2021
doi: 10.3389/fonc.2021.690115

Immunotherapy and Targeting the Tumor Microenvironment: Current Place and New Insights in Primary Pulmonary NUT Carcinoma

Xiang Li[1†], Hui Shi[1†], Wei Zhang[1], Chong Bai[1], Miaoxia He[2*], Na Ta[2], Haidong Huang[1], Yunye Ning[1], Chen Fang[1], Hao Qin[1] and Yuchao Dong[1]*

[1] Department of Respiratory and Critical Care Medicine, Changhai Hospital (The First Affiliated Hospital of Naval Medical University), Naval Medical University (Second Military Medical University), Shanghai, China, [2] Department of Pathology, Changhai Hospital (The First Affiliated Hospital of Naval Medical University), Naval Medical University (Second Military Medical University), Shanghai, China

Primary pulmonary nuclear protein of testis carcinoma is a rare and highly aggressive malignant tumor. It accounts for approximately 0.22% of primary thoracic tumors and is little known, so it is often misdiagnosed as pulmonary squamous cell carcinoma. No effective treatment has been formed yet, and the prognosis is extremely poor. This review aims to summarize the etiology, pathogenesis, diagnosis, treatment, and prognosis of primary pulmonary nuclear protein of testis carcinoma in order to better recognize it and discuss the current and innovative strategies to overcome it. With the increasing importance of cancer immunotherapy and tumor microenvironment, the review also discusses whether immunotherapy and targeting the tumor microenvironment can improve the prognosis of primary pulmonary nuclear protein of testis carcinoma and possible treatment strategies. We reviewed and summarized the clinicopathological features of all patients with primary pulmonary nuclear protein of testis carcinoma who received immunotherapy, including initial misdiagnosis, disease stage, immunohistochemical markers related to tumor neovascularization, and biomarkers related to immunotherapy, such as PD-L1 (programmed death-ligand 1) and TMB (tumor mutational burden). In the meanwhile, we summarized and analyzed the progression-free survival (PFS) and the overall survival (OS) of patients with primary pulmonary nuclear protein of testis carcinoma treated with PD-1 (programmed cell death protein 1)/PD-L1 inhibitors and explored potential population that may benefit from immunotherapy. To the best of our knowledge, this is the first review on the exploration of the tumor microenvironment and immunotherapy effectiveness in primary pulmonary nuclear protein of testis carcinoma.

Keywords: nuclear protein of testis carcinoma, NUT carcinoma, midline carcinoma, pulmonary, tumor microenvironment, immunotherapy, immune checkpoint inhibitor

OPEN ACCESS

Edited by:
Jian Huang,
Zhejiang University, China

Reviewed by:
Weifeng He,
Army Medical University, China
Jinhan Wang,
Peking Union Medical College, China
Tao Han,
Northern Theater General Hospital, China

***Correspondence:**
Chong Bai
bc7878@sohu.com
Miaoxia He
hmm26@163.com

[†]These authors have contributed equally to this work and share first authorship

Specialty section:
This article was submitted to Molecular and Cellular Oncology, a section of the journal Frontiers in Oncology

Received: *02 April 2021*
Accepted: *13 September 2021*
Published: *30 September 2021*

Citation:
Li X, Shi H, Zhang W, Bai C, He M, Ta N, Huang H, Ning Y, Fang C, Qin H and Dong Y (2021) Immunotherapy and Targeting the Tumor Microenvironment: Current Place and New Insights in Primary Pulmonary NUT Carcinoma. Front. Oncol. 11:690115. doi: 10.3389/fonc.2021.690115

1 INTRODUCTION

The nuclear protein of testis (NUT) carcinoma is defined by the *NUT* (also known as *NUTM1*) gene rearrangement. The typical *BRD4-NUT* fusion gene is formed by the translocation rearrangement of the *NUT* gene on chromosome 15q and the *BRD4* gene on chromosome 19p (1), which accounts for at least 2/3 of NUT carcinoma (2). The *BRD3* gene on chromosome 9q (3)and the *NSD3* gene on chromosome 8p (4) are often fused with the *NUT* gene (5, 6). In recent years, with the rapid development of molecular technologies such as next-generation sequencing (NGS), rare fusion partners such as *ZNF532* (7), *ZNF592* (8), *MXD4* (9), *CIC* (10), *MGA* (11), *YAP1* (12), *CHRM5* (13)have been discovered one after another.

Since t (15; 19)(q15;p13) chromosome was first discovered in thymic carcinoma in 1991 (14), NUT carcinoma has always been regarded as a tumor inseparable from the midline structure, so it was called "NUT midline carcinoma". However, as "NUT midline carcinoma" is successively discovered in structures or organs outside the midline, such as lungs (15), salivary glands (16, 17), kidneys (18, 19), adrenal glands (20) and soft tissues (18), the World Health Organization (WHO) has changed its name from "NUT midline carcinoma" to "NUT carcinoma" (21).

There is no gender difference in the prevalence of NUT carcinoma, which could be seen in any age group, but mainly children and young adults (5). The median age of NUT carcinoma patients is 23.6 years old (range=18days-80years) and is 30 years old (range=21years-68years) for primary pulmonary NUT carcinoma, respectively (6, 15).

NUT carcinoma is extremely aggressive, with rapid disease progression, poor treatment effect, high recurrence and mortality rate. The median OS (mOS) in NUT carcinoma is 6.5 months (6), while the mOS in primary pulmonary NUT carcinoma is only 2.2 months (15). Until the year of 2020, there were about 55 cases of primary pulmonary NUT carcinoma had been published in English (22). In order to have better treatment outcome and prognosis for patients with primary pulmonary NUT carcinoma, this article reviewed the latest diagnosis and treatment method, particularly the immunotherapy.

2 ETIOLOGY AND PATHOGENESIS

2.1 Etiology

Due to the lack of cohort or large samples studies of primary pulmonary NUT carcinoma, the etiology remains unclear. Although some patients have a history of smoking, current evidences suggest that primary pulmonary NUT carcinoma occurs far more common among non-smokers (15). However, environmental factors and viral infections, such as Epstein-Barr virus, human papilloma virus, are not discovered to be related to primary pulmonary NUT carcinoma (13, 23, 24).

2.2 Pathogenesis

BRD4-NUT fusion oncoprotein (3, 5)contains parts of the BRD4 protein and the NUT protein. The BRD4 protein is a bromodomain and extraterminal domain (BET) protein. It binds BRD4-NUT fusion oncoprotein to histone acetylated lysine residues in chromatin *via* two bromodomains. The NUT protein can recruit the histone acetyltransferase (HAT) p300. It acetylates adjacent histones, which in turn allows more BRD4-NUT fusion oncoproteins to bind to chromatin and recruit transcription factors, such as positive transcription elongation factor b (P-TEFb) (25, 26). BRD4-NUT fusion oncoprotein sequesters histone acetyltransferases (HATs) and other transcriptional co-factors to the chromatin regions that transcribe pro-proliferative and anti-differentiation genes, such as *MYC*, *TP63*, *SOX2 (*27–29). It also leads to the silencing of differentiation-promoting genes and hypoacetylation of the whole genome, thereby inhibiting differentiation and promoting proliferation (27, 30–34) (**Figure 1**).

The carcinogenic mechanism of BRD3-NUT fusion oncoprotein is similar to BRD4-NUT (35). The pathogenic mechanism of NSD3-NUT and ZNF532-NUT fusion oncoproteins was once thought to be similar to BRD4-NUT fusion oncoprotein (4, 7), but in recent years, it has been proposed that BRD4/BRD3, NSD3 and "Z4", which consists of ZNF592, ZNF532, ZMYND8 and ZNF68, are combined into "BRD4-NUT complex". Any component can directly bind to the NUT protein and recruit HAT p300. The complex then causes local chromatin lahyperacetylation, which promotes tumor growth and inhibition differentiation (8, 35).

3 CLINICAL MANIFESTATION

The clinical manifestations of primary pulmonary NUT carcinoma are similar to those of lung cancer and are often closely related to tumor size, location, presence or absence of complications or metastases. Some patients are even asymptomatic, only founded in routine physical examination (36). The common symptoms included cough, chest pain, hemoptysis, wheezing, dyspnea, fever, etc., among which cough is the most common, and dyspnea caused by moderate to large pleural effusion is also frequently present (13, 15, 36).

4 IMAGING CHARACTERISTICS

The chest plain computed tomography (CT) scans showed irregular soft tissue density masses (**Figure 2**), mostly located in the lower lobe of the right lung (15, 37). Enhanced CT scans showed uneven enhancement of the masses. The lesions were large (maximum diameter of 12.7cm), mostly central and often fused with ipsilateral hilar and mediastinal lymphadenopathy (**Figure 2**). They often presented withobstructive atelectasis, ipsilateral pleural nodules and moderate or large pleural effusions (**Figure 2**). Supraclavicular, contralateral mediastinal, and subcarinal lymphadenopathy were also frequently present. Except for a small amount of pleural effusions on CT, there is no evidence of disease involvement in the contralateral lung (**Figure 2**). The extrathoracic metastatic sites were

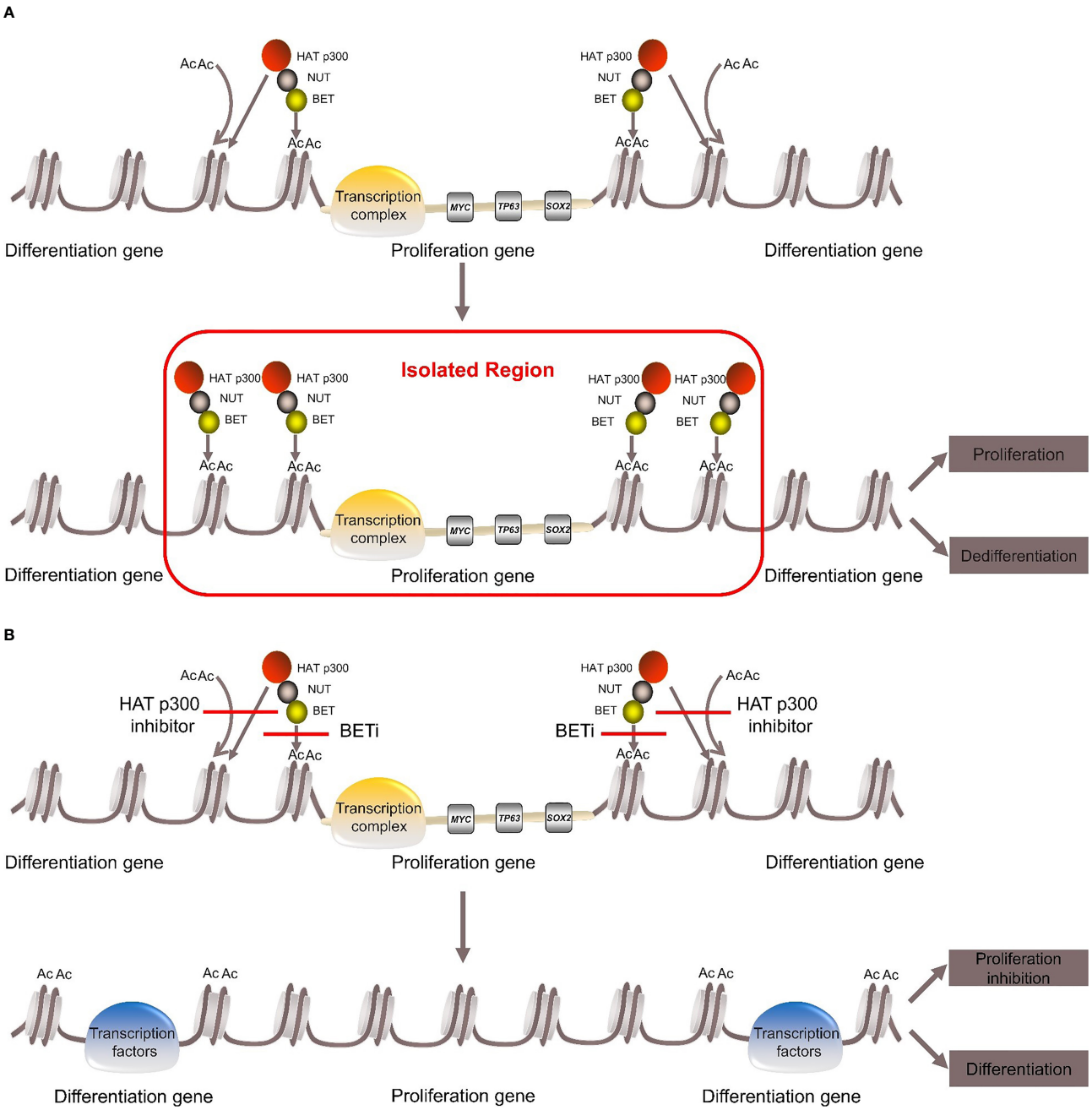

FIGURE 1 | Pathogenesis of NUT carcinoma. **(A)** BRD4-NUT fusion oncoprotein binds to histone acetylated lysine residues in chromatin and recruits the histone acetyltransferase (HAT) p300. HAT p300 makes adjacent histones acetylated, which allows more BRD4-NUT fusion oncoproteins to bind to chromatin and recruit transcription factors to form transcription complex. The transcription complex is sequestered to regions of the chromatin that transcribe pro-proliferative and anti-differentiation genes, such as MYC, TP63, SOX. While it leads to the silencing of differentiation genes, thereby repressing differentiation and promoting proliferation. **(B)** With the use of BETi or HAT p300 inhibitor can induce differentiation and inhibit proliferation.

predominantly bones, with osteolytic changes on CT. Liver, adrenal gland, soft tissue involvement has also been reported.To our knowledge, case of brain metastasis in primary pulmonary NUT carcinoma has not been reported so far (13, 15, 38, 39).

PET/CT (positron emission tomography/CT) facilitated the staging and early detection of metastases. The 18F-flurodeoxyglucose (18F-FDG) of the pulmonary lesion was often highly concentrated (the standard uptake value (SUV) can be as high as 18.6). If the SUV in the center of the lesion

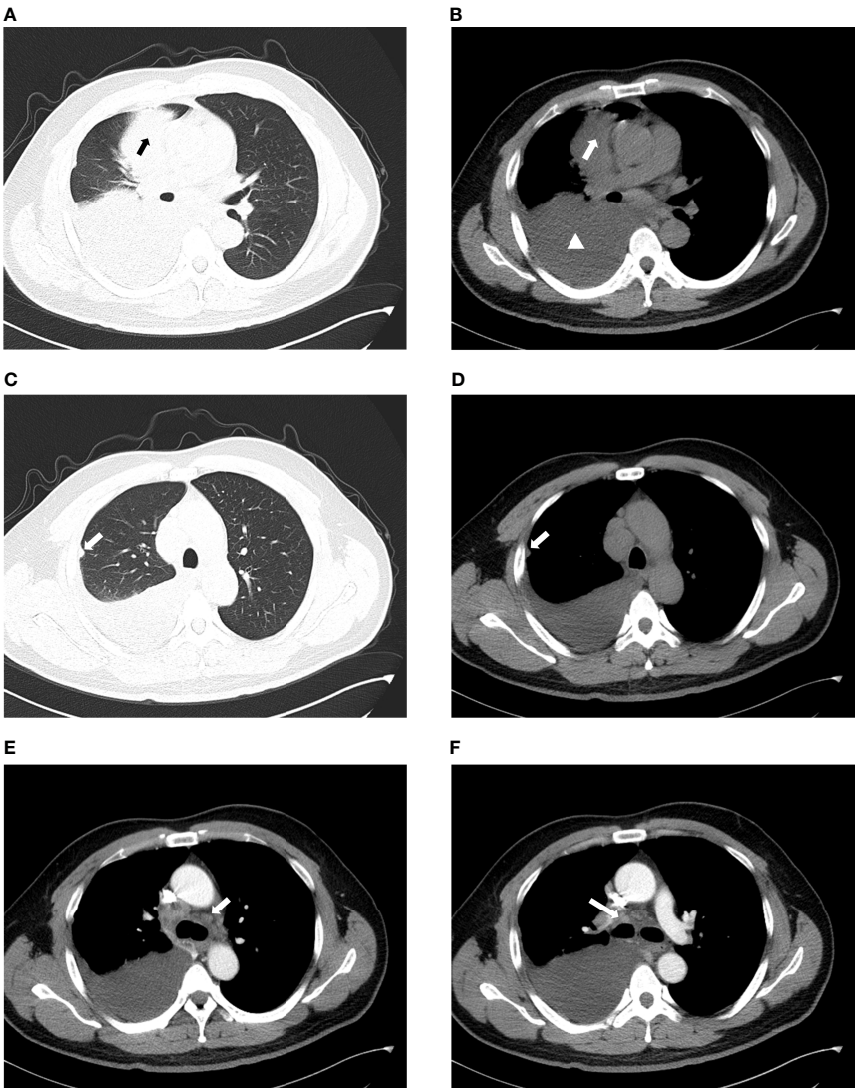

FIGURE 2 | Imaging characteristics of chest CT. **(A, B)** The mass is located in the right upper lobe and is of central type with moderate to large pleural effusion on the right (arrow: mass, triangle: pleural effusion). **(C, D)** They show the ipsilateral pleural nodule but no involvement of the contralateral lung (arrow:pleural nodule). **(E)** Contralateral mediastinal lymphadenopathy. **(F)** Ipsilateral hilar lymphadenopathy.

decreased, it indicates necrosis of the lesion. In addition, PET/CT has good sensitivity for detecting bone metastases that cannot be detected by bone scintigraphy (15, 40).

Although the imaging findings of primary pulmonary NUT carcinoma show some characteristics, they are still not specific.

5 DIAGNOSIS AND PATHOLOGY

Since the etiology of primary pulmonary NUT carcinoma is still unclear, and the clinical manifestations, laboratory tests and imaging characteristics are non-specific, pathology is still the cornerstone of its diagnosis. Primary pulmonary NUT carcinoma was once considered as a subtype of lung squamous cell cancer (13, 41), but the WHO classified it as "other and unclassified carcinomas" in lung cancer in 2015 and 2021.

5.1 Gross Pathology

NUT carcinoma is extremely aggressive. Over 50% of patients have presented withorgans and/or lymph nodes metastases at the time of diagnosis (6, 41). Therefore, most patients cannot undergo surgery. In addition, the incidence of primary pulmonary NUT carcinoma is extremely low. Therefore, to date, there are few case reports on gross pathology. The gross examinations revealed an irregular solid tumor, which was not clearly demarcated from the surrounding tissues. Together with enlarged intralobar lymph nodes, they can cause airway compression and mucus obstruction. The cut surface of the

tumor was brown and white or white and may be accompanied by hemorrhage and necrosis (22, 37, 42–44).

5.2 Cytology

5.2.1 Pulmonary Mass and Lymph Node Needle Aspiration Cytology

The tumor cells were medium in size and relatively monotonous, with sheet-like arrangement. The nuclei were large and hyperchromatic, which could be round, ovoid or irregular (45–47) (**Figures 3A, B**). Scattered bare nuclei were also observed (46, 47). The nucleoli was prominent and nuclear chromatin was fine to granular (45, 47, 48). Mitoses and apoptotic nuclei were frequent (46, 47).

5.2.2 Pleural Effusion Cytology

Monomorphic tumor cells were arranged in isolation or clusters, with irregular nuclear contours, prominent nucleoli and coarse chromatin granules (49).

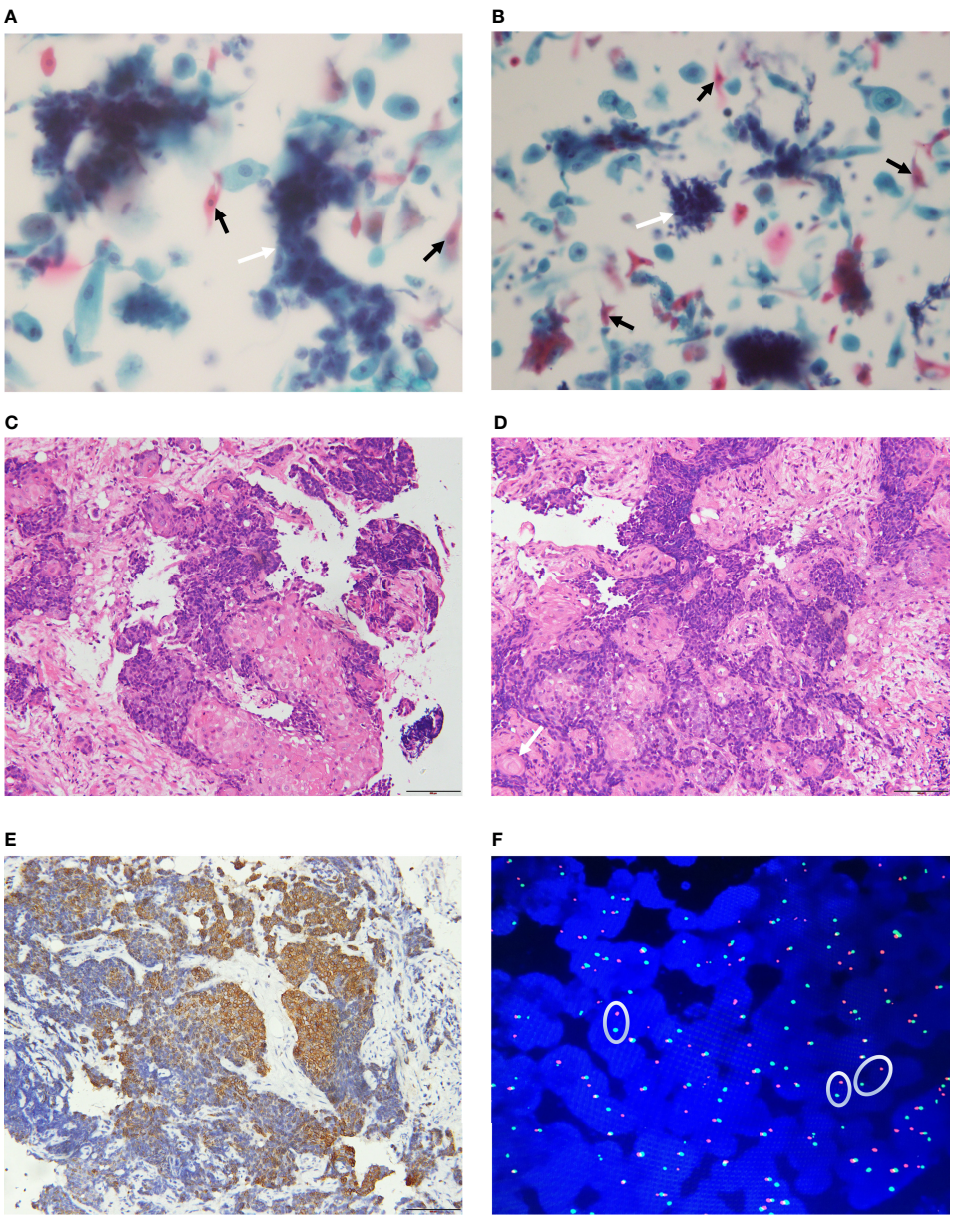

FIGURE 3 | Pathological features of NUT carcinoma. **(A, B)**: The tumor cells are nested or sheet-like arrangement (white arrow). The nuclei are large and hyperchromatic. Tumor cells of squamous epithelial differentiation can be seen (black arrow). **(C, D)** (H&E staining): The tumor is poorly differentiated and shows infiltrative growth. The tumor cells are irregular nest-like, polygonal, large nucleus and heteromorphic. There are abrupt squamous epithelial differentiation and keratinized bead (arrow). **(E)** (IHC): CK5/6 (+) **(F)** (FISH): Dual-color split probes targeting both sides of the NUT gene breakpoint are seperated (oval).

5.3 Histology

Most primary pulmonary NUT carcinoma were poorly differentiated or undifferentiated neoplasm (50–52). The tumors had invasive growth and could invade the bronchial walls or blood vessels (53, 54). The tumour cells were medium in size, relatively monotonous and could be round, epithelioid or polygonal. They were arranged in nested or sheeted pattern (39, 49) and could be accompanied by obvious proliferation of interstitial connective tissues (42, 44, 53, 54). Neutrophil infiltration and necrosis may occur in the background (44, 47–51, 53). The nuclei may be round, oval or irregular, with prominent nucleoli, open chromatin, which were granular to coarse. The cytoplasm was scarce and the nucleocytoplasmic ratio was high (15, 22, 44, 48, 50, 52, 55). Mitotic figures were evident (22, 50, 51, 53, 54). The representative pathological changes of primary pulmonary NUT carcinoma are abrupt differentiation of squamous epithelial and keratinized beads (**Figures 3C, D**) (51, 54).

5.4 Immunohistochemistry

Most primary pulmonary NUT carcinoma cases were positive for cytokeratins (AE1/AE3, CAM5.2, CK5/6, pan-cytokeratin were more common) (**Figure 3E**), P63, P40, and NUT (37, 56, 57). TTF-1 and a variety of neuroendocrine markers were mostly negative (13, 39, 55, 58). Ki-67 (13, 37, 45, 48), EMA (22, 47, 54), and C-MYC (58) were positive in some cases. Clinicians and pathologists lack relevant knowledge of primary pulmonary NUT carcinoma. Relatively speaking, there is no consistent selection criteria for immunohistochemical staining markers for primary pulmonary NUT carcinoma. Therefore, the results of immunohistochemical staining varied widely among the literatures. Using highly specific anti-NUT monoclonal antibody C52 for Immunohistochemical staining, the sensitivity of the diagnosis of NUT carcinoma is 87% and the specificity is 100% (59), but the fusion partner of the NUT gene cannot be identified.

5.5 Molecular Pathology

In addition to classic cytogenetic karyotype analysis (14, 60), fluorescence *in situ* hybridization (FISH) (22, 50, 61), reverse transcription polymerase chain reaction (RT-PCR) (52, 55, 57) and NGS, including RNA sequencing (4, 7), Archer FusionPlex (8, 18) as well as whole-genome sequencing (WGS) (62) are effective diagnostic methods (**Table 1**). However, various diagnostic methods have certain limitations (23): (1) Cytogenetic was the traditional method for discovering classic t (15;19)(q14; p13.1) fusion. It was undoubtedly the "gold standard", but its high cost and the need for fresh live tumor greatly limited its application. (2) RT-PCR: Due to the need to use known specific primers, it is impossible to identify rare, unknown, and non-classical fusion genes, which can easily lead to missed diagnosis or misdiagnosis. (3) Archer FusionPlex and whole-genome sequencing: Although it can identify any fusion partner of NUTM1, detect gene mutations and TMB, it is costly and requires a large amount of tumor tissues. (4)FISH: The NUTM1 dual-color translocation rearrangement FISH probes targeting the NUT breakpoint and the fusion-partner breakpoint can detect the fusion of corresponding genes(two separate probes are close to each other). They can confirm the diagnosis of NUT carcinoma and the type of known fusion partners (30, 50). Moreover, the NUTM1 dual-color split probes were also used for diagnosis (**Figure 3F**) (13, 58, 61, 63), but the fusion partners could not be identified. False negative FISH results have been reported (59, 64), so it is recommended to use a probe spanning NUTM1 (59) or a combination of conventional IHC and C52 antibody for diagnosis. The sensitivity of FISH combined with C52 IHC in diagnosing NUT carcinoma can reach 100% (59, 65).

6 DIFFERENTIAL DIAGNOSIS

Primary pulmonary NUT carcinoma is very aggressive and is undifferentiated or poorly differentiated. Early diagnosis is of great significance for prognostic judgment. Histology shows squamous differentiation and formation of keratinized beads. Immunohistochemical staining is mostly positive for cytokeratins, p63 and P40. So it is easily misdiagnosed as poorly differentiated squamous cell carcinoma. However, primary pulmonary NUT carcinoma shows abrupt squamous differentiation and immunohistochemical staining with anti-NUT monoclonal antibody is positive. Both primary pulmonary NUT carcinoma and small cell lung cancer (SCLC) show scarce cytoplasm and high Ki-67 proliferation index, but the latter has no obvious nucleoli and no focal squamous cell differentiation. Immunohistochemical staining is positive for chromogranin and synaptophysin, negative for NUT (46, 63).

TABLE 1 | Various diagnostic methods of molecular pathology.

Diagnostic Methods	Advantages	Limitations
Cytogenetic	Gold standard	High cost The need for fresh live tumor
RT-PCR	Fast	The need for using known specific primers Impossible to identify rare, unknown, and non-classical fusion genes
NGS	Identify any fusion partner Detect gene mutations and TMB	High cost The need for a large amount of tumor tissues
FISH	Can be used on multiple sample types (frozen tumor, air dried, or FFPE)	Fusion partners cannot be identified using the NUTM1 dual-color split probes False negative*

**The sensitivity of FISH combined with C52 IHC in diagnosing NUT carcinoma can reach 100%.*

Differentiation of poorly differentiated lung adenocarcinoma and primary pulmonary NUT carcinoma mainly relies on immunohistochemistry. Immunohistochemical staining of adenocarcinomais positive for TTF-1 and Napsin A, negative for p40, p63 and NUT. Patients with poorly differentiated or undifferentiated lung tumor, especially those who are young, nonsmokers or lack of other high-risk factors, should be alert to primary pulmonary NUT carcinoma. In particular, patients with rapid disease progression, extensive invasions and poor response to initial treatment, anti-NUT monoclonal antibody immunohistochemical staining should be performed as soon as possible, combined with FISH if necessary.

7 THERAPY STRATEGIES

The treatment of primary pulmonary NUT carcinoma mainly included surgery, chemotherapy and radiotherapy. In recent years, targeted therapy, antiangiogenic therapy and immunotherapy have also been reported (13, 57, 66). In addition, novel targeted drugs such as BET inhibitor (BETi), p300/CBP HAT inhibitor, histone deacetylase inhibitor (HDACi) and dual HDAC/PI3K inhibitor are also considered as potential treatments (32, 58, 67–72).

7.1 Surgery

Surgery is the first choice for almost all solid malignant tumors. However, due to the aggressive nature of NUT carcinoma, most patients have missed the best timing when they were diagnosed and even lost the opportunity for surgical treatment, which greatly reduces the rate of radical operation. However, early radical operation can still significantly improve the PFS and OS of NUT carcinoma (2, 6, 41). It has been reported (66, 73) that the disease free survival (DFS) of a patient staged as T1bN0M0 with primary pulmonary NUT carcinoma and treated with first-line radical surgery and adjuvant chemotherapy is up to 30 months, far exceeding 2.2 months of mOS, as well as long-term survival. One patient at T3N1M0 stage underwent radical lobectomy and regional lymphadenectomy, with adjuvant etoposide and platinum combined with bevacizumab. As of the publication of the literature, DFS has reached 10 months (66). It is suggested that radical surgery and adjuvant chemotherapy (combined with antiangiogenic therapy in locally advanced-stage patients) in early-stage patients can significantly improve the prognosis.

7.2 Chemoradiotherapy and Chemotherapy

Up to now, most of the cases who had lost the opportunity for surgery have received chemoradiotherapy or chemotherapy. In patients receiving chemoradiotherapy, the shorter OS was 2 months to 4 months (39, 55), and the longer OS reached 148weeks (47, 54, 57, 61). The OS was significantly higher than the mOS of primary pulmonary NUT carcinoma. It is consistent with the conclusion that radiotherapy can improve the prognosis of NUT carcinoma (2, 6, 41). For patients receiving chemotherapy, after a short-term response or stable disease, they often progressed rapidly (13, 57). According to the literatures, the longest PFS was 5 months (74) and the longest OS was 13 months (75). However, until now, no chemotherapy regimen with definite therapeutic effect has been recognized.

Therefore, for patients who have lost the opportunity for surgery, chemoradiotherapy may significantly benefit patients, but the exact effective regimens still need to be further explored.

7.3 Targeted Therapy

Because primary pulmonary NUT carcinoma was often misdiagnosed as undifferentiated or squamous cell lung cancer, driver genes were rarely detected. As far as we know, there are few reports of EGFR mutation cases (13, 63) and none of ALK and ROS1 rearrangements cases have been reported. Xiaohong Xie et al. reported a patient with EGFR exon 19 deletion, who received gefitinib in the second-line (the PFS was 2 weeks) apatinib in the third-line (the PFS was 1 month). The OS was 4.1 months (13). Although the results were not satisfactory, it provided a possible idea for the treatment of primary pulmonary NUT carcinoma.

Clinical trials of BET inhibitors have been carried out in recent years. Although several BETi have showed certain anti-NUT carcinoma activity, the efficacy of single-agent was limited (76, 77). The response rate in NUT carcinoma was only 20-30% (67, 68). In preclinical trials, p300/CBP HAT inhibitor has been shown to have inhibitory effects in NUT carcinoma. The combination of p300/CBP HAT inhibitor and BETi even has synergistic effects (32, 67, 68). The anti-NUT carcinoma activity of HDACi was also confirmed in animal models and two cases of NUT carcinoma in children (69, 70). Moreover, the anti-NUT carcinoma activity of CUDC-907 (dual HDAC/PI3K inhibitor) has been demonstrated *in vitro* and animal models, even better than HDACi (58, 71, 72).

In general, targeted therapy significantly improves the prognosis of lung cancer with targetable driver oncogenes. If patients with primary pulmonary NUT carcinoma have targetable driver oncogenes, targeted therapy may be a potential treatment option. In addition, novel targeted drugs have appeared in the treatment of NUT carcinoma and are worth looking forward to in the future.

7.4 Immunotherapy

Since the Food and Drug Administration (FDA) first approved Nivolumab for the treatment of advanced lung cancer in 2015, immunotherapy has developed so rapidly to significantly improved the prognosis.

7.4.1 The Main Mechanism of PD-1 or PD-L1 Inhibitors

PD-1 is expressed on the surface of T cells. Its ligands are PD-L1 or PD-L2 on the surface of tumor cells and PD-L1 on the surface of antigen-presenting cells (APCs), mainly including dendritic cells (DCs) and macrophages. The combination of PD-1 and its ligand can activate the PI3K-Akt-mTOR pathway in tumor cells, resulting in a decrease in T effector cells and T memory cells with immunostimulatory effects and an increase in T regulatory cells (Treg) and T exhausted cells (Tex) with immunosuppressive

effects, leading to immune escape of tumor cells (78). PD-1 inhibitors or PD-L1 inhibitors can block the binding of PD-1 to its ligand and restore the immune killing of tumor cells (**Figures 4**, **5**).

7.4.2 The Present Condition of Immunotherapy in Primary Pulmonary NUT Carcinoma

In recent years, cases of primary pulmonary NUT carcinoma receiving immunotherapy have also been reported (see **Table 2**

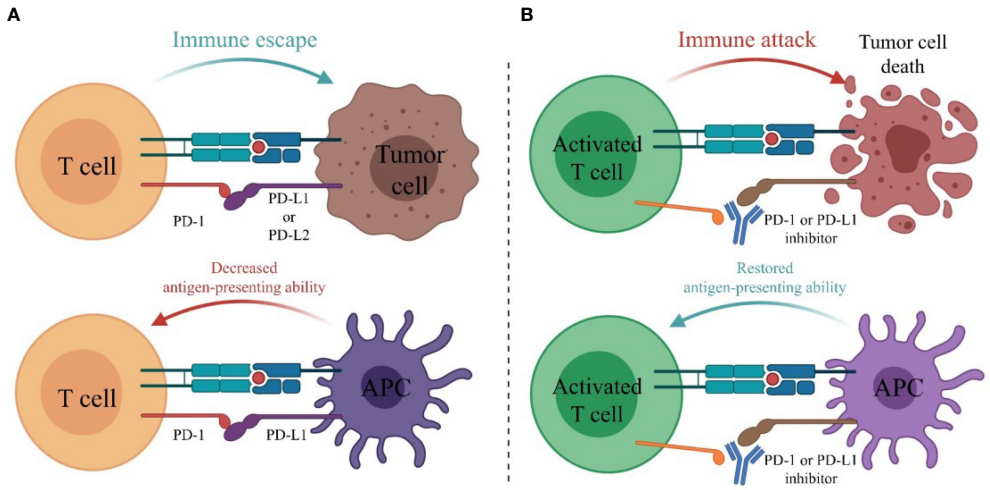

FIGURE 4 | The main mechanism of PD-1 or PD-L1 inhibitors. **(A)** PD-1 is expressed on the surface of T cells. Its ligands are PD-L1 or PD-L2 on the surface of tumor cells and PD-L1 on the surface of antigen-presenting cells (APCs). The combination of PD-1 and its ligand inhibits the activation of T cells, leading to immune escape of tumor cells. **(B)** PD-1 or PD-L1 inhibitors block the binding of PD-1 to its ligands and restore the immune killing of tumor cells.

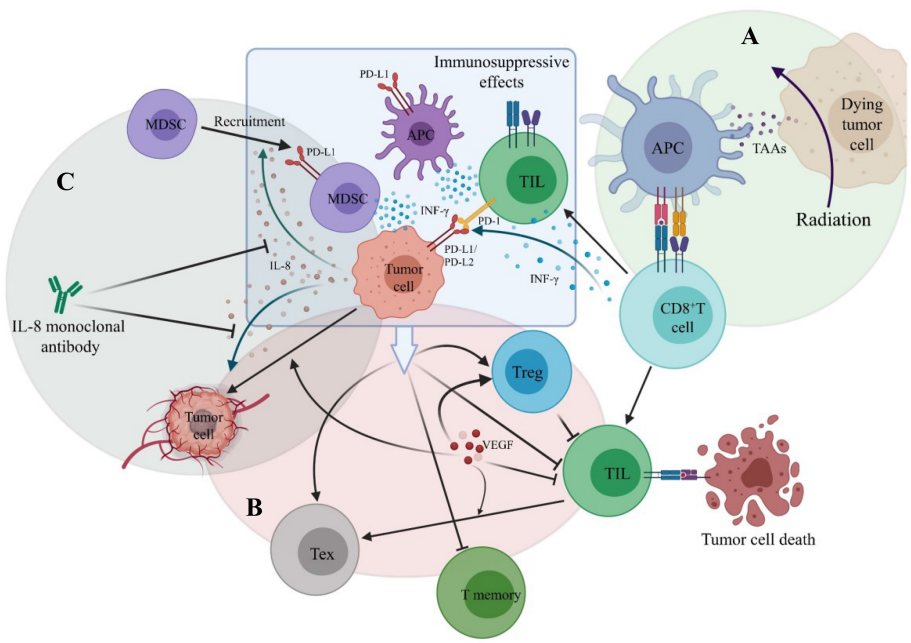

FIGURE 5 | The main mechanisms of combination therapy with PD-1/PD-L1 inhibitors. **(A)** Radition results in tumor cell death. Tumor-associated antigens (TAAs) are released and antigen-presenting cell is activated. CD8+ T cell is then primed by binding to APC. **(B)** VEGF stimulates angiogenesis, promotes the infiltration of T regulatory cell (Treg), decreases TIL infiltration and promotes the formation of T exhausted cell (Tex). **(C)** Tumor-derived IL-8 can promote tumor angiogenesis and recruit MDSC to suppress anti-tumor immune responses.

TABLE 2 | Clinicopathological features, immunotherapy and outcomes.

Patients	Age (years)/ Gender	Initial diagnosis	TNM staging‡	PD-L1	TMB (muts/ Mb)	Treatment1	PFS1	Treatment2	PFS2	Treatment3	PFS3	Treatment4	PFS4	Treatment5	PFS5	OS	NUTM1-fusion	Reference
1	23/M	Mucinous epithelial carcinoma	IVA (T3N2M1b)	ND	11.55	Operation	1 mo	Atezo	2w	–	–	–	–	–	–	1.5 mo	ND	(13)
2	30/F	SCC	IVA (T4N3M1b)	ND	ND	TP*	6w	T	3w	T + Nivo	3w	–	–	–	–	3 mo	ND	(13)
3	74/M	NC	IVA (T3N3M1a)	ND	High	RT	1 mo	Pembro	21w	Support care	13 mo	–	–	–	–	19.5mo	ND	(13)
4	58/F	NC	IIIC (T4N3M0)	ND	73.81	Cet+RT+DP	18w	Support care	18 mo	Pembro +Cet	3mo	Pembro +Oxaliplatin	3w	Support care	–	26.7mo	ND	(13)
5	31/F	NC	IIIA (T4N1M0)	ND	1.75	DP+ Cet	6w	T +Gemcitabine +Nivo Pembro+ T +Gemcitabine +Nivo	2w 4w	Nivo+Iri +Platinum	3w	Pembro+ Carboplatin + RT	3mo	Support care	–	12mo+	CHRM5	(13)
6	45/M	NC	IIIA	70%	ND	AC†+Pembro	NA	NA	NA	NA	NA	NA	NA	NA	NA	12mo+	ND	(36)
7	48/F	SCC	IIIA	0%	ND	Genexol+ Carboplatin + Pembro, Lobectomy +Pembro	NA	NA	NA	NA	NA	NA	NA	NA	NA	12mo+	ND	(36)
8	31/M	NA	IV	ND	ND	CRT,Atezo**	NA	NA	NA	NA	NA	NA	NA	NA	NA	2.2mo	NSD3	(39)
9	53/M	NA	III	ND	ND	CRT,Nivo,HDAC inhibitor**	NA	NA	NA	NA	NA	NA	NA	NA	NA	11.6mo	BRD3	(39)
10	57/M	PD SCC	IVA (T4N3M1a)	ND	ND	DP	6w	Nivo	6w	–	–	–	–	–	–	4mo	ND	(49)
11	31/F	SCC	IA (T1bN0M0)	10% (SP263)	ND	Lobectomy adjuvant TP§	30mo (DFS)	Observed off-treatment	7mo	Nivo	29 mo	Nivo	13mo	NA	NA	79mo+	ND	(73)
12	34/F	NC	IVB	Negative	ND	TP*	5mo	Pembro	Lost	–	–	–	–	–	–	Lost	ND	(74)

CD34 expression and MSI status were not detected in all patients.

‡Using IASLC Eighth Edition of the TNM Classification for Lung Cancer to re-staging the cases with detailed data, while directly quoting the staging in the original literatures for the cases with insufficient data.

**nab-Paclitaxel(T)+Carboplatin, §Paclitaxel+Carboplatin, †AC: Pemetrexed+Carboplatin, **The treatment protocol was not described in detail.*

Atezo, Atezolizumab; Cet, cetuximab; CRT, chemotherapy+radiotherapy; F, female; Iri, irinotecan; Lost, lost follow-up; mo, months; M, male; NA, data not available; NC, NUT carcinoma; ND, not done; Nivo, Nivotuzumab; PD, poorly differentiated; Pembro, Pembrolizumab; RT, radiotherapy; SCC, squamous cell carcinoma; w, weeks.

for clinicopathological features, treatments methods and survival results). The immunotherapy drugs mentioned in the reported literature for patients with primary pulmonary NUT carcinoma included PD-1 inhibitors (Nivolumab, Pembrolizumab) or PD-L1 inhibitor (Atezolizumab). The vast majority of patients received immunotherapy as second-line or beyond (subsequent) treatment.

The best OS of patients stage IVA who underwent surgery or chemoradiotherapy in the first-line and Atezolizumab in the second-line was only 2.2 months (13, 39), which is similar to the mOS of primary pulmonary NUT carcinoma. Atezolizumab does not seem to improve the prognosis of advanced patients.

One patient of stage IA (Patient 11 in **Table 2**) was reported to receive radical surgery and adjuvant chemotherapy in the first-line and Nivolumab monotherapy in the third-line. The PFS reached 29 months and the OS was at least 79 months (73). So far, this patient had the longest survival time among the primary pulmonary NUT carcinoma patients retrieved in the literatures, who had received immunotherapy. Two patients received the combination treatment including Pembrolizumab as the first-line treatment, the OS had exceeded 12 months (36), suggesting that first-line use of Pembrolizumab may improve the prognosis. The OS of two non-surgical patients staging III who had previously received chemoradiotherapy and then received Nivolumab or Pembrolizumab was significantly prolonged [11.6 months (39), 26.7 months (13) respectively]. The OS of one non-surgical patient staging IVA who received chemotherapy in the first-line and Nivolumab in the second-line (The PFS was 6 weeks) was 4 months (49), and that of one non-surgical patient staging IVA who received radiotherapy in the first-line and Pembrolizumab in the second-line (The PFS was 21 weeks) was 19.5 months (13). Therefore, it seems that patients, whose tumor are unresectable or not fit for surgery, are likely to benefit more from Pembrolizumab than Nivolumab, especially those who ever received chemoradiotherapy or radiotherapy. This seems to be consistent with the view that radiotherapy combined with immunotherapy can achieve a benefit in overall survival in lung cancer (79, 80). The probable mechanisms (**Figure 5**) are that after receiving radiotherapy, dead tumor cells release tumor-associated antigens (TAAs) and inflammatory cytokines. Dendritic cells recognize them and are activated, promoting antigen presentation to cells of the immune system, and $CD8^+$ T cells are then primed and recruited to the tumor site, thereby killing tumor cells (81, 82). In the meanwhile, radiotherapy can upregulate the expression of PD-L1 on tumor cells *via* IFN-γ released by $CD8^+$ T cells and the PD-1 levels on $CD8^+$ tumor infiltrating lymphocytes (TILs) (78, 82), which enhance the effect of PD-1 inhibitors. Although the optimal PFS of PD-1 inhibitors in non-surgical patients was only 21 weeks, which was similar to that of chemotherapy. However, compared with chemotherapy, the OS of non-surgical patients was significantly prolonged.

7.4.3 The Recommendations for the Application of Immunotherapy in Primary Pulmonary NUT Carcinoma

(1) Atezolizumab does not seem to improve the prognosis of advanced patients. (2) For early-stage patients, PD-1 inhibitors used in the second-line, after radical surgery and adjuvant chemotherapy in the first-line, could distinctly prolong the PFS and the OS. (3) For advanced-stage patients or whose tumor is surgically unresectable, if they ever received chemoradiotherapy or radiotherapy, PD-1 inhibitors could significantly prolong the OS, and Pembrolizumab may be better than Nivolumab. (4) Combination therapy with Pembrolizumab or Pembrolizumab monotherapy in first-line may improve the OS.

7.4.4 PD-1 Inhibitor in Combination With BETi

In mouse models and a wide variety of human tumor cell lines, BETi inhibited constitutive and IFN-γ induced PD-L1 expression on tumor cells and tumor-associated dendritic cells and macrophages, which correlated with an increase in the activity of TILs (83, 84). Moreover, the combination of PD-1 inhibitor and BETi caused synergistic effects in mice (83, 84).

Therefore, patients with primary pulmonary NUT carcinoma may benefit from the combination treatment of PD-1 inhibitor with BETi. However, this inference needs more basic researches and clinical trial results to testify.

8 TARGETING THE TUMOR MICROENVIRONMENT

8.1 Tumor Angiogenesis and VEGF (Vascular Endothelial Growth Factor)

Tumor angiogenesis is closely related to the growth and metastasis of cancer. In addition to stimulating endothelial cell growth and angiogenesis, VEGF can also decrease TILs infiltration, promote the infiltration of Tregs (**Figure 5**), and increase the expression of inhibitory receptors contributing to $CD8^+$ TILs exhaustion (85, 86). As a antigen of vascular endothelial cell, after immunohistochemical staining, CD34 can be used as a marker of angiogenesis to count microvessel density (MVD) and the degree of neoangiogenesis (87, 88). High expression of CD34 or high MVD is closely correlated to the tumor progression and poor prognosis (88–90). Moreover, it has been indicated that the inhibition of CD34 expression may repress neoangiogenesis, tumor growth and invasion (91).

8.2 The Relationship Between the Prognosis and CD34 Expression in Primary Pulmonary NUT Carcinoma

Cases of primary pulmonary NUT carcinoma involving CD34 expression have also been successively reported in recent years (Clinicopathological features, treatments, and survival outcomes are shown in **Table 3**). The best OS for non-surgical patients of stage IV with primary pulmonary NUT carcinoma, with CD34-positive staining, was at least 100 weeks (61, 92). The worst OS in stage IIIC non-surgical patients with CD34-negative staining was 2 months (93), while the best OS in stage IV non-surgical patients with CD34-negative staining was 148 weeks (52, 61). Therefore, the published literatures have not found significant correlation between CD34 expression and the prognosis of patients with primary pulmonary NUT carcinoma, which needs more patients data for further evaluation.

TABLE 3 | Clinical features, immunohistochemistry CD34 staining, treatments and outcomes.

Patients	Age (years)/ Gender	Initial diagnosis	TNM staging‡‡	CD34	PD-L1	TMB (muts/ Mb)	MSI	Treatment1	PFS1	Treatment2	PFS2	OS	NUTM1-fusion	Reference
1	36/M	Nonseminomatous Primary mediastinal germ cell tumor	T3N3Mx	Negative	ND	ND	ND	I/E/Cisplatin	2cylces	RT,BETi	2cylces	2mo	BRD4	(30)
2	34/M	Spindle cell neoplasm	IV	Positive	80%	ND	ND	CRT(Genexol/Carboplatin), Pembro	Lost	–	–	Lost	ND	(36)
3	48/M	NC	T4N2M0 (IIIB)	Negative	ND	ND	ND	Radical operation	2mo	Palliative RT (right scapula)	NA	6mo	ND	(43)
4	66/M	NC	T4NxM1c	Negative	ND	ND	ND	Palliative care	NA	NA	NA	1mo	ND	(54)
5	14/M	Unspecified sarcoma or undifferentiated arcinoma	T4NxMx	Negative	ND	ND	ND	IRS III regimen 36(VCR/E/ CTX/Cisplatin)	NA	I/Carboplatin/E, Lobectomy+ I/ Carboplatin/E	NA	12mo	BRD4	(55)
6	7/F	Undifferentiated SCC	IV	Negative	ND	ND	ND	CRT (TP)	NA	NA	NA	4mo	BRD4	(55)
7	16/F	PD carcinoma	IV	Positive	ND	ND	ND	CRT	NA	NA	NA	100w+	ND	(61)
8	16/M	SCC	IVB	Negative	ND	ND	ND	CRT	NA	NA	NA	148w	BRD4	(61)
9	26/M	NA	T4NxMx	Negative	ND	ND	ND	E	NA	NA	NA	5mo	ND	(63)
10	69/M	NA	T2NxMx	Negative	ND	ND	ND	E	NA	NA	NA	6mo	ND	(63)
11	69/M	Neuroendocrine carcinoma with adenocarcinoma	T3N1M0 (IIIA)	ND	Negative (22C3)	1.6	Stable	Radical operation adjuvant EP (1^{th}-3^{th} cycle)/EC(4^{th}cycle) and Avastin	10mo+(DFS)	–	–	Not reached	ND	(66)
12	17/M	NC	IVB	Positive	ND	ND	ND	SSG IX	NA	NA	NA	5mo	ND	(92)
13	23/F	Non-Hodgkin's lymphoma	T4NxMx	Negative	ND	ND	ND	DP,Vorinostat‡	NA	NA	NA	2mo	BRD4	(93)

‡‡*Using IASLC Eighth Edition of the TNM Classification for Lung Cancer to re-staging the cases with detailed data, while directly quoting the staging in the original literatures for the cases with insufficient data.*

‡Vorinostat, an HDAC inhibitor; CRT, chemotherapy+radiotherapy; CTX, Cyclophosphamide; E, Etoposide; F, female; I, Ifosfamide; Lost, lost follow-up; mo, months; M, male; NA, data not available; NC, NUT carcinoma; ND, not done; PD, poorly differentiated; Pembro, Pembrolizumab; RT, radiotherapy; SCC, squamous cell carcinoma; VCR, Vincristine; w, weeks.

8.3 The Rationale for Anti-VEGF Therapy and the Present Condition of Anti-VEGF Therapy

By inhibiting VEGF-mediated suppression of dendritic cells maturation, Bevacizumab can trigger and activate T-cell response (94). In addition, Bevacizumab downregulates PD-1 expression on $CD8^+$ TILs and results in an increased infiltration of T cells into the tumor by normalising the tumor vasculature (95–99). In the meanwhile, Bevacizumab reprogrammes the tumor microenvironment by inhibiting the activity of myeloid derived suppressor cells (MDSCs) and Treg cells (98, 100–102). One patient with primary pulmonary NUT carcinoma (patient 11 in **Table 3**, TNM staging:T3N1M0-IIIA) received radical lobectomy, regional lymphadenectomy and adjuvant EP (etoposide and platinum) combined with Bevacizumab (Avastin) for 4 cycles. The DFS had reached at least 10 months by the time of literature publication (66). Regrettably, the expression of CD34 was not tested in the patient. In addition, two patients with orbital NUT carcinoma, who had undergone operation, received anlotinib in third-line. The OS was beyond 15 months and 8 months, respectively (103, 104).

According to IMpower150 research, compared with Bevacizumab combined with paclitaxel plus carboplatin, Atezolizumab plus Bevacizumab combined with paclitaxel plus carboplatin significantly improved the PFS and OS in lung cancer, regardless of PD-L1 expression. Therefore, we consider that anti-VEGF therapy combined with PD-1/PD-L1 inhibitor plus chemotherapy may be beneficial to patients with primary pulmonary NUT carcinoma.

In summary, anti-VEGF therapy may be a potential treatment for primary pulmonary NUT carcinoma, especially in postoperative adjuvant treatment and combination application with PD-1/PD-L1 inhibitor (particularly Pembrolizumab) plus chemotherapy.

8.4 Immunosuppressive Effects of Interleukin-8 (IL-8)

As the correlation between IL-8 and tumor is being investigated in full swing, the impacts of tumor-derived IL-8 on the tumor microenvironment have been clearer (105, 106). It has been confirmed that tumor-derived IL-8 can promote tumor angiogenesis, recruit MDSCs to suppress anti-tumor immune responses (**Figure 5**) and maintain the epithelial mesenchymal transition phenotype of tumor cells, thereby participating in the proliferation and metastasis of tumor cells (107–110).

8.5 IL-8 and Prognosis on Immunotherapy

Low baseline serum IL-8 (sIL-8) level and early decline of sIL-8 are in correlation with the benefit from immune checkpoint inhibitors as well as better cancer prognosis. The mOS of patients undergoing Nivolumab with low (<23 pg ml^{-1}) baseline sIL-8 levels was as 2 to 3 times as high (≥23 pg ml^{-1}) baseline sIL-8 levels. The decline of sIL-8 levels, 2-4 weeks after starting treatment, was significantly correlation with response to PD-1 inhibitor. The mOS of patients receiving PD-1 inhibitor with sIL-8 decrease over baseline was not reached, while that of those with sIL-8 increase over baseline was 8 months. Besides, the decline of sIL-8 can help judge immunotherapy pseudoprogression when imaging evaluation is progressive disease. In addition, levels of sIL-8 are not correlated with the PD-1 and PD-L1 expression (111–113).

Therefore, based on sIL-8 levels, we will consider whether to choose immune checkpoint inhibitor for treatment and estimate the prognosis in primary pulmonary NUT carcinoma.

8.6 IL-8 Monoclonal Antibody

It has been demonstrated that IL-8 monoclonal antibody can suppress tumor angiogenesis (**Figure 5**), significantly reduce tumor size *in vitro* and animal models (114, 115), and decrease recruitment of MDSCs to the tumor (116). Even more exciting is that a Phase I trial of patients with metastatic or unresectable solid tumors showed that sIL-8 significantly decreased on the third day of IL-8 monoclonal antibody monotherapy. Among 73% of patients, their disease was stable, with the median treatment duration of 24 weeks (117). For patients with higher sIL-8 level in primary pulmonary NUT carcinoma, it is good news. The combination of IL-8 monoclonal antibody with immune checkpoint inhibitor or anti-VEGF therapy, may be new directions for the treatment in the future. This is consistent with the results of previous laboratory studies (116, 118). We look forward to further clinical trials results of IL-8 monoclonal antibody in the treatment of tumor.

8.7 Neutrophil/Lymphocyte Ratio (NLR) and Immunotherapy

In multiple studies of patients receiving PD-1/PD-L1 inhibitors, it was found that lower baseline NLR in the blood was associated with better response, PFS and OS. The cutoff value of NLR was 5 in most of studies. In addition, the decline of NLR during treatment often indicated that immunotherapy was effective (119–122).

Therefore, baseline NLR levels and dynamic NLR changes may also be biomarkers for determining whether patients with primary pulmonary NUT carcinoma can benefit from immunotherapy.

9 PROGNOSIS

One study (6) that included 124 patients of NUT carcinoma found that the mOS of nonthoracic primary NUT carcinoma was significantly better than that of thoracic primary NUT carcinomas, and patients with BRD4-NUT fusion had worse mOS than those with BRD3-NUT or NSD3-NUT fusion. It was consistent with the conclusions of previous reports (41, 61). The mOS of NUT carcinoma is 6.7 months (41), whereas the mOS of primary pulmonary NUT carcinoma is only 2.2 months (15).

It is well known that PD-L1 expression level has a certain correlation with the benefit from immunotherapy. Few cases on PD-L1 expression level of primary pulmonary NUT carcinoma have been reported, and PD-L1 TPS (Tumor Proportion Score) varied from 0-80% (36, 73). However, due to the uneven quality of cases data, it is impossible to precisely evaluate the relationship

between PD-L1 expression level and the benefit from immunotherapy or prognosis in primary pulmonary NUT carcinoma. In addition, TMB, microsatellite instability (MSI) and DNA mismatch repair (MMR) do not seem to be associated with the prognosis (13, 66, 123).

10 CONCLUSION

Although primary pulmonary NUT carcinoma is rare, it is recognized gradually in recent years with the application and development of immunohistochemistry and molecular pathology. However, there is still a lack of general understanding and clear awareness in clinical practice. Patients with poorly differentiated or undifferentiated lung tumors who are youthful, nonsmokers, and lack of other high-risk factors for lung cancer, particularly those with sudden squamous epithelial differentiation with or without keratosis beads formation, should be highly alert to primary pulmonary NUT carcinoma. In addition, for patients with central lung mass, moderate to large pleural effusion ipsilaterally, extensive infiltrating lesions, rapid disease progression and poor response to initial therapy, anti-NUT monoclonal antibody immunohistochemical staining should be performed as soon as possible, if necessary, combined with FISH (using the NUTM1 dual-color translocation rearrangement probes and the sensitivity of combining FISH with C52 IHC for diagnosing NUT carcinoma can reach 100%), NGS or whole genome sequencing.

Many attempts have been made in the treatment of primary pulmonary NUT carcinoma in recent years, but a standard and consistently effective treatment has not yet been established.

For early-stage or locally advanced patients, radical surgery and adjuvant chemotherapy (for locally advanced-stage patients, combined with anti-VEGF therapy, in the meanwhile) could distinctly prolong the PFS and the survival time. The OS can be further extended using PD-1 inhibitor as the second-line treatment.

Patients who have lost the opportunity for surgery can significantly benefit from chemoradiotherapy. For advanced-stage or patients with tumors unresectable, who have received chemoradiotherapy or radiotherapy, PD-1 inhibitor could significantly prolong the OS, and Pembrolizumab is likely to be superior to Nivolumab. Combination therapy with Pembrolizumab or Pembrolizumab monotherapy in first-line may prolong the OS. Moreover, based on NLR levels and sIL-8 levels, we may decide whether to choose immune checkpoint inhibitor as the treatment option and estimate the benefit from immunotherapy as well as the prognosis.

However, the above inferences mainly came from case reports or small sample studies and more animal experiments and clinical trial results are needed to help further confirm our insights.

In addition, the detection of targetable driver oncogenes could be attempted, and targeted therapy may be a potential treatment option. At the same time, we look forward to the clinical efficacy data of new targeted drugs, such as BETi, p300/CBP HAT inhibitor, HDACi, and dual HDAC/PI3K inhibitor.

Meanwhile, we proposed the possibility of anti-VEGF therapy combined with PD-1/PD-L1 inhibitor plus chemotherapy, PD-1 inhibitor combined with BETi, and IL-8 monoclonal antibody combined with immune checkpoint inhibitor to improve the prognosis in primary pulmonary NUT carcinoma.

AUTHOR CONTRIBUTIONS

XL and HS determined the writing direction and were responsible for the manuscript writing and modification. XL was responsible for literature collection and collation. WZ, CB, HH, and MH gave ideas and suggestions on selecting directions. MH and NT provided advice on pathology writing. YN, CF, and HQ took part in making charts. CB and YD provided financial support, and reviewed and revised the manuscript. All authors contributed to the article and approved the submitted version.

FUNDING

This work was partially supported by the National Natural and Science Foundation of China(NO.82000102) and the Collaborative Innovation Cluster Foundation of Shanghai Health Commission(NO.2020CXJQ03).

REFERENCES

1. French CA, Miyoshi I, Kubonishi I, Grier HE, Perez-Atayde AR, Fletcher JA. BRD4-NUT Fusion Oncogene: A Novel Mechanism in Aggressive Carcinoma. *Cancer Res* (2003) 63:304–7.
2. Chau NG, Hurwitz S, Mitchell CM, Aserlind A, Grunfeld N, Kaplan L, et al. Intensive Treatment and Survival Outcomes in NUT Midline Carcinoma of the Head and Neck. *CANCER-AM Cancer Soc* (2016) 122:3632–40. doi: 10.1002/cncr.30242
3. French CA, Ramirez CL, Kolmakova J, Hickman TT, Cameron MJ, Thyne ME, et al. BRD–NUT Oncoproteins: A Family of Closely Related Nuclear Proteins That Block Epithelial Differentiation and Maintain the Growth of Carcinoma Cells. *Oncogene* (2008) 27:2237–42. doi: 10.1038/sj.onc.1210852
4. French CA, Rahman S, Walsh EM, Kühnle S, Grayson AR, Lemieux ME, et al. NSD3–NUT Fusion Oncoprotein in NUT Midline Carcinoma: Implications for a Novel Oncogenic Mechanism. *Cancer Discov* (2014) 4:928–41. doi: 10.1158/2159-8290.CD-14-0014
5. Huang QW, He LJ, Zheng S, Liu T, Peng BN. An Overview of Molecular Mechanism, Clinicopathological Factors, and Treatment in NUT Carcinoma. *BioMed Res Int* (2019) 2019:1–6. doi: 10.1155/2019/1018439
6. Chau NG, Ma C, Danga K, Al-Sayegh H, Nardi V, Barrette R, et al. An Anatomical Site and Genetic-Based Prognostic Model for Patients With Nuclear Protein in Testis (NUT) Midline Carcinoma: Analysis of 124 Patients. *JNCI Cancer Spectr* (2020) 4:z94. doi: 10.1093/jncics/pkz094
7. Alekseyenko AA, Walsh EM, Zee BM, Pakozdi T, Hsi P, Lemieux ME, et al. Ectopic Protein Interactions Within BRD4–Chromatin Complexes Drive Oncogenic Megadomain Formation in NUT Midline Carcinoma. *Proc Natl Acad Sci* (2017) 114:E4184–92. doi: 10.1073/pnas.1702086114
8. Shiota H, Elya JE, Alekseyenko AA, Chou PM, Gorman SA, Barbash O, et al. "Z4" Complex Member Fusions in NUT Carcinoma: Implications for a

Novel Oncogenic Mechanism. *Mol Cancer Res* (2018) 16:1826–33. doi: 10.1158/1541-7786.MCR-18-0474
9. Tamura R, Nakaoka H, Yoshihara K, Mori Y, Yachida N, Nishikawa N, et al. Novel MXD4–NUTM1 Fusion Transcript Identified in Primary Ovarian Undifferentiated Small Round Cell Sarcoma. *Gene Chromosome Canc* (2018) 57:557–63. doi: 10.1002/gcc.22668
10. Schaefer IM, Dal Cin P, Landry LM, Fletcher CDM, Hanna GJ, French CA. CIC-NUTM1 Fusion: A Case Which Expands the Spectrum of NUT-Rearranged Epithelioid Malignancies. *Gene Chromosome Canc* (2018) 57:446–51. doi: 10.1002/gcc.3
11. Diolaiti D, Dela Cruz FS, Gundem G, Bouvier N, Boulad M, Zhang Y, et al. A Recurrent Novel MGA–NUTM1 Fusion Identifies a New Subtype of High-Grade Spindle Cell Sarcoma. *Mol Case Stud* (2018) 4:a3194. doi: 10.1101/mcs.a003194
12. Agaimy A, Togel L, Haller F, Zenk J, Hornung J, Markl B. YAP1-NUTM1 Gene Fusion in Porocarcinoma of the External Auditory Canal. *Head Neck Pathol* (2020) 14:982–90. doi: 10.1007/s12105-020-01173-9
13. Xie XH, Wang LQ, Qin YY, Lin XQ, Xie ZH, Liu M, et al. Clinical Features, Treatment, and Survival Outcome of Primary Pulmonary NUT Midline Carcinoma. *Orphanet J Rare Dis* (2020) 15:183. doi: 10.1186/s13023-020-01449-x
14. Kubonishi I, Takehara N, Iwata J, Sonobe H, Ohtsuki Y, Abe T, et al. Novel T (15;19)(Q15;P13) Chromosome Abnormality in a Thymic Carcinoma. *Cancer Res (Chicago Ill.)* (1991) 51:3327–8.
15. Sholl LM, Nishino M, Pokharel S, Mino-Kenudson M, French CA, Janne PA, et al. Primary Pulmonary NUT Midline Carcinoma: Clinical, Radiographic, and Pathologic Characterizations. *J Thorac Oncol* (2015) 10:951–9. doi: 10.1097/JTO.0000000000000545
16. Ziai J, French CA, Zambrano E. NUT Gene Rearrangement in a Poorly-Differentiated Carcinoma of the Submandibular Gland. *Head Neck Pathol (Totowa N.J.)* (2010) 4:163–8. doi: 10.1007/s12105-010-0174-6
17. den Bakker MA, Beverloo BH, van den Heuvel-Eibrink MM, Meeuwis CA, Tan LM, Johnson LA, et al. NUT Midline Carcinoma of the Parotid Gland With Mesenchymal Differentiation. *Am J Surg Pathol* (2009) 33:1253–8. doi: 10.1097/PAS.0b013e3181abe120
18. Dickson BC, Sung Y, Rosenblum MK, Reuter VE, Harb M, Wunder JS, et al. NUTM1 Gene Fusions Characterize a Subset of Undifferentiated Soft Tissue and Visceral Tumors. *Am J Surg Pathol* (2018) 42:636–45. doi: 10.1097/PAS.0000000000001021
19. Bishop JA, French CA, Ali SZ. Cytopathologic Features of NUT Midline Carcinoma: A Series of 26 Specimens From 13 Patients. *Cancer Cytopathol* (2016) 124:901–8. doi: 10.1002/cncy.21761
20. French CA. Pathogenesis of NUT Midline Carcinoma. *Annu Rev Pathol: Mech Dis* (2012) 7:247–65. doi: 10.1146/annurev-pathol-011811-132438
21. Agaimy A, Fonseca I, Martins C, Thway K, Barrette R, Harrington KJ, et al. NUT Carcinoma of the Salivary Glands: Clinicopathologic and Molecular Analysis of 3 Cases and a Survey of NUT Expression in Salivary Gland Carcinomas. *Am J Surg Pathol* (2018) 42:877–84. doi: 10.1097/PAS.0000000000001046
22. Numakura S, Saito K, Motoi N, Mori T, Saito Y, Yokote F, et al. P63-Negative Pulmonary NUT Carcinoma Arising in the Elderly: A Case Report. *Diagn Pathol* (2020) 15:134. doi: 10.1186/s13000-020-01053-4
23. French CA. NUT Carcinoma: Clinicopathologic Features, Pathogenesis, and Treatment. *Pathol Int* (2018) 68:583–95. doi: 10.1111/pin.12727
24. Maffini F, French CA, Cameron MJ, Stufano V, Barberis M, Pisa E, et al. A Case of NUT Midline Carcinoma With No HPV Infection, Slight EWSR1 Rearrangement and Strong Expression of EGFR. *Tumori* (2013) 99:e152. doi: 10.1700/1361.15114
25. Wang R, You J. Mechanistic Analysis of the Role of Bromodomain-Containing Protein 4 (BRD4) in BRD4-NUT Oncoprotein-Induced Transcriptional Activation. *J Biol Chem* (2015) 290:2744–58. doi: 10.1074/jbc.M114.600759
26. Yan J, Diaz J, Jiao J, Wang R, You J. Perturbation of BRD4 Protein Function by BRD4-NUT Protein Abrogates Cellular Differentiation in NUT Midline Carcinoma*. *J Biol Chem* (2011) 286:27663–75. doi: 10.1074/jbc.M111.246975
27. Grayson AR, Walsh EM, Cameron MJ, Godec J, Ashworth T, Ambrose JM, et al. MYC, a Downstream Target of BRD-NUT, Is Necessary and Sufficient for the Blockade of Differentiation in NUT Midline Carcinoma. *Oncogene* (2014) 33:1736–42. doi: 10.1038/onc.2013.126
28. Stelow EB, French CA. Carcinomas of the Upper Aerodigestive Tract With Rearrangement of the Nuclear Protein of the Testis (NUT) Gene (NUT Midline Carcinomas). *Adv Anat Pathol* (2009) 16:92–6. doi: 10.1097/PAP.0b013e31819923e4
29. Wang R, Liu W, Helfer CM, Bradner JE, Hornick JL, Janicki SM, et al. Activation of SOX2 Expression by BRD4-NUT Oncogenic Fusion Drives Neoplastic Transformation in NUT Midline Carcinoma. *Cancer Res* (2014) 74:3332–43. doi: 10.1158/0008-5472.CAN-13-2658
30. Parikh SA, French CA, Costello BA, Marks RS, Dronca RS, Nerby CL, et al. Nut Midline Carcinoma: An Aggressive Intrathoracic Neoplasm. *J Thorac Oncol* (2013) 8:1335–8. doi: 10.1097/JTO.0b013e3182a00f41
31. French CA. The Importance of Diagnosing NUT Midline Carcinoma. *Head Neck Pathol (Totowa N.J.)* (2013) 7:11–6. doi: 10.1007/s12105-013-0428-1
32. Morrison-Smith CD, Knox TM, Filic I, Soroko KM, Eschle BK, Wilkens MK, et al. Combined Targeting of the BRD4–NUT–P300 Axis in NUT Midline Carcinoma by Dual Selective Bromodomain Inhibitor, NEO2734. *Mol Cancer Ther* (2020) 19:1406–14. doi: 10.1158/1535-7163.MCT-20-0087
33. Alekseyenko AA, Walsh EM, Wang X, Grayson AR, Hsi PT, Kharchenko PV, et al. The Oncogenic BRD4-NUT Chromatin Regulator Drives Aberrant Transcription Within Large Topological Domains. *Gene Dev* (2015) 29:1507–23. doi: 10.1101/gad.267583.115
34. French C. NUT Midline Carcinoma. *Nat Rev Cancer* (2014) 14:149–50. doi: 10.1038/nrc3659
35. McEvoy CR, Fox SB, Prall OWJ. Emerging Entities in NUTM1-Rearranged Neoplasms. *Genes Chromosomes Cancer* (2020) 59:375–85. doi: 10.1002/gcc.22838
36. Cho YA, Choi YL, Hwang I, Lee K, Cho JH, Han J. Clinicopathological Characteristics of Primary Lung Nuclear Protein in Testis Carcinoma: A Single-Institute Experience of 10 Cases. *Thorac Cancer* (2020) 11:3205–12. doi: 10.1111/1759-7714.13648
37. Harms A, Herpel E, Pfarr N, Penzel R, Heussel CP, Herth FJ, et al. NUT Carcinoma of the Thorax: Case Report and Review of the Literature. *Lung Cancer* (2015) 90:484–91. doi: 10.1016/j.lungcan.2015.10.001
38. Virarkar M, Saleh M, Ramani NS, Morani AC, Bhosale P. Imaging Spectrum of NUT Carcinomas. *Clin Imag* (2020) 67:198–206. doi: 10.1016/j.clinimag.2020.07.025
39. Hung YP, Chen AL, Taylor MS, Huynh TG, Kem M, Selig MK, et al. Thoracic NUT Carcinoma: Expanded Pathologic Spectrum With Expression of TTF-1 and Neuroendocrine Markers. *Histopathology* (2020) 78:896–904. doi: 10.1111/his.14306
40. Rosenbaum DG, Teruya-Feldstein J, Price AP, Meyers P, Abramson S. Radiologic Features of NUT Midline Carcinoma in an Adolescent. *Pediatr Radiol* (2012) 42:249–52. doi: 10.1007/s00247-011-2288-8
41. Bauer DE, Mitchell CM, Strait KM, Lathan CS, Stelow EB, Lüer SC, et al. Clinicopathologic Features and Long-Term Outcomes of NUT Midline Carcinoma. *Clin Cancer Res* (2012) 18:5773–9. doi: 10.1158/1078-0432.CCR-12-1153
42. Wasserman JK, Purgina B, Sekhon H, Gomes MM, Lai C. The Gross Appearance of a NUT Midline Carcinoma. *Int J Surg Pathol* (2015) 24:85–8. doi: 10.1177/1066896915606970
43. Cao J, Chen D, Yang F, Yao J, Zhu W, Zhao C. NUT Midline Carcinoma as a Primary Lung Tumor: A Case Report. *J Thorac Dis* (2017) 9:E1045–9. doi: 10.21037/jtd.2017.11.50
44. Pezzuto F, Fortarezza F, Mammana M, Pasello G, Pelosi G, Rea F, et al. Immunohistochemical Neuroendocrine Marker Expression in Primary Pulmonary NUT Carcinoma: A Diagnostic Pitfall. *Histopathology* (2020) 77:508–10. doi: 10.1111/his.14166
45. Lee T, Choi S, Han J, Choi Y, Lee K. Abrupt Dyskeratotic and Squamoid Cells in Poorly Differentiated Carcinoma: Case Study of Two Thoracic NUT Midline Carcinomas With Cytohistologic Correlation. *J Pathol Trans Med* (2018) 52:349–53. doi: 10.4132/jptm.2018.07.16
46. Dutta R, Nambirajan A, Mittal S, Roy Chowdhuri S, Jain D. Cytomorphology of Primary Pulmonary NUT Carcinoma in Different Cytology Preparations. *Cancer Cytopathol* (2020) 129:53–61. doi: 10.1002/cncy.22342
47. Kuroda S, Suzuki S, Kurita A, Muraki M, Aoshima Y, Tanioka F, et al. Cytological Features of a Variant NUT Midline Carcinoma of the Lung

Harboring the NSD3-NUT Fusion Gene: A Case Report and Literature Review. *Case Rep Pathol* (2015) 2015:1–5. doi: 10.1155/2015/572951
48. Policarpio-Nicolas MLC, de Leon EMB, Jagirdar J. Cytologic Findings of NUT Midline Carcinoma in the Hilum of the Lung. *Diagn Cytopathol* (2015) 43:739–42. doi: 10.1002/dc.23291
49. Maruyama N, Hikiishi A, Suginaka M, Furukawa K, Ogawa K, Nakamura N, et al. Nuclear Protein in Testis Carcinoma of the Thorax. *Internal Med* (2018) 57:3169–73. doi: 10.2169/internalmedicine.0434-17
50. Suzuki S, Kurabe N, Ohnishi I, Yasuda K, Aoshima Y, Naito M, et al. NSD3-NUT-Expressing Midline Carcinoma of the Lung: First Characterization of Primary Cancer Tissue. *Pathol - Res Pract* (2015) 211:404–8. doi: 10.1016/j.prp.2014.10.013
51. Raza A, Cao H, Conrad R, Cobb C, Castelino-Prabhu S, Mirshahidi S, et al. Nuclear Protein in Testis Midline Carcinoma With Unusual Elevation of α-Fetoprotein and Synaptophysin Positivity: A Case Report and Review of the Literature. *Expert Rev Anticanc* (2015) 15:1199–213. doi: 10.1586/14737140.2015.1082909
52. Mao N, Liao Z, Wu J, Liang K, Wang S, Qin S, et al. Diagnosis of NUT Carcinoma of Lung Origin by Next-Generation Sequencing: Case Report and Review of the Literature. *Cancer Biol Ther* (2018) 20:150–6. doi: 10.1080/15384047.2018.1523852
53. Karakuş E, Poyraz A, Oğuz Erdogan AS, Emir S, Özyörük D. NUT Midline Carcinoma of the Lung in a Six-Year-Old Child. *Fetal Pediatr Pathol* (2017) 36:472–4. doi: 10.1080/15513815.2017.1392662
54. Reddy R, Woods TR, Allan RW, Malhotra P, Mehta HJ, Sarkar PK, et al. NUT (Nuclear Protein in Testis) Carcinoma: A Report of Two Cases With Different Histopathologic Features. *Int J Surg Pathol* (2019) 27:225–9. doi: 10.1177/1066896918796606
55. Tanaka M, Kato K, Gomi K, Yoshida M, Niwa T, Aida N, et al. NUT Midline Carcinoma: Report of 2 Cases Suggestive of Pulmonary Origin. *Am J Surg Pathol* (2012) 36:381–8. doi: 10.1097/PAS.0b013e31824230a8
56. Inamura K. Update on Immunohistochemistry for the Diagnosis of Lung Cancer. *Cancers* (2018) 10:72. doi: 10.3390/cancers10030072
57. Lemelle L, Pierron G, Fréneaux P, Huybrechts S, Spiegel A, Plantaz D, et al. NUT Carcinoma in Children and Adults: A Multicenter Retrospective Study. *Pediatr Blood Cancer* (2017) 64:e26693. doi: 10.1002/pbc.26693
58. Jung M, Kim S, Lee JK, Yoon SO, Park HS, Hong SW, et al. Clinicopathological and Preclinical Findings of NUT Carcinoma: A Multicenter Study. *Oncologist* (2019) 24:e740–8. doi: 10.1634/theoncologist.2018-0477
59. Haack H, Johnson LA, Fry CJ, Crosby K, Polakiewicz RD, Stelow EB, et al. Diagnosis of NUT Midline Carcinoma Using a NUT-Specific Monoclonal Antibody. *Am J Surg Pathol* (2009) 33:984–91. doi: 10.1097/PAS.0b013e318198d666
60. Kees UR, Mulcahy MT, Willoughby ML. Intrathoracic Carcinoma in an 11-Year-Old Girl Showing a Translocation T(15;19). *Am J Pediatr Hematol Oncol* (1991) 13:459–64. doi: 10.1097/00043426-199124000-00011
61. French CA, Kutok JL, Faquin WC, Toretsky JA, Antonescu CR, Griffin CA, et al. Midline Carcinoma of Children and Young Adults With NUT Rearrangement. *J Clin Oncol* (2004) 22:4135–9. doi: 10.1200/JCO.2004.02.107
62. Lee JK, Louzada S, An Y, Kim SY, Kim S, Youk J, et al. Complex Chromosomal Rearrangements by Single Catastrophic Pathogenesis in NUT Midline Carcinoma. *Ann Oncol* (2017) 28:890–7. doi: 10.1093/annonc/mdw686
63. Zhou L, Yong X, Zhou J, Xu J, Wang C. Clinicopathological Analysis of Five Cases of NUT Midline Carcinoma, Including One With the Gingiva. *BioMed Res Int* (2020) 2020:1–6. doi: 10.1155/2020/9791208
64. McLean-Holden AC, Moore SA, Gagan J, French CA, Sher D, Truelson JM, et al. NUT Carcinoma in a Patient With Unusually Long Survival and False Negative FISH Results. *Head Neck Pathol* (2020) 15:698–703. doi: 10.1007/s12105-020-01220-5
65. Shenoy KD, Stanzione N, Caron JE, Fishbein GA, Abtin F, Lluri G, et al. Midline Carcinoma Expressing NUT in Malignant Effusion Cytology. *Diagn Cytopathol* (2019) 47:594–8. doi: 10.1002/dc.24150
66. Liu Y, Li Y, Ke X, Lu Y. The Primary Pulmonary NUT Carcinomas and Some Uncommon Somatic Mutations Identified by Next-Generation Sequencing: A Case Report. *AME Case Rep* (2020) 4:24. doi: 10.21037/acr-19-168
67. Stathis A, Bertoni F. BET Proteins as Targets for Anticancer Treatment. *Cancer Discov* (2018) 8:24–36. doi: 10.1158/2159-8290.CD-17-0605
68. Zhang X, Zegar T, Lucas A, Morrison-Smith C, Knox T, French CA, et al. Therapeutic Targeting of P300/CBP HAT Domain for the Treatment of NUT Midline Carcinoma. *Oncogene* (2020) 39:4770–9. doi: 10.1038/s41388-020-1301-9
69. Schwartz BE, Hofer MD, Lemieux ME, Bauer DE, Cameron MJ, West NH, et al. Differentiation of NUT Midline Carcinoma by Epigenomic Reprogramming. *Cancer Res* (2011) 71:2686–96. doi: 10.1158/0008-5472.CAN-10-3513
70. Maher OM, Christensen AM, Yedururi S, Bell D, Tarek N. Histone Deacetylase Inhibitor for NUT Midline Carcinoma. *Pediatr Blood Cancer* (2015) 62:715–7. doi: 10.1002/pbc.25350
71. Sun K, Atoyan R, Borek MA, Dellarocca S, Samson ME, Ma AW, et al. Dual HDAC and PI3K Inhibitor CUDC-907 Downregulates MYC and Suppresses Growth of MYC-Dependent Cancers. *Mol Cancer Ther* (2017) 16:285–99. doi: 10.1158/1535-7163.MCT-16-0390
72. Napolitano M, Venturelli M, Molinaro E, Toss A. NUT Midline Carcinoma of the Head and Neck: Current Perspectives. *Onco Targets Ther* (2019) 12:3235–44. doi: 10.2147/OTT.S173056
73. Davis A, Mahar A, Wong K, Barnet M, Kao S. Prolonged Disease Control on Nivolumab for Primary Pulmonary NUT Carcinoma. *Clin Lung Cancer* (2020) 22:e665–7. doi: 10.1016/j.cllc.2020.10.016
74. Joel S, Weschenfelder F, Schleussner E, Hofmann GO, Weschenfelder W. NUT Midline Carcinoma in a Young Pregnant Female: A Case Report. *World J Surg Oncol* (2020) 18:290. doi: 10.1186/s12957-020-02065-6
75. Cho HJ, Lee HK. Lung Nuclear Protein in Testis Carcinoma in an Elderly Korean Woman: A Case Report With Cytohistological Analysis. *Thorac Cancer* (2020) 11:1724–7. doi: 10.1111/1759-7714.13438
76. Stathis A, Zucca E, Bekradda M, Gomez-Roca C, Delord JP, de La Motte Rouge T, et al. Clinical Response of Carcinomas Harboring the BRD4–NUT Oncoprotein to the Targeted Bromodomain Inhibitor OTX015/MK-8628. *Cancer Discov* (2016) 6:492–500. doi: 10.1158/2159-8290.CD-15-1335
77. Lewin J, Soria JC, Stathis A, Delord JP, Peters S, Awada A, et al. Phase Ib Trial With Birabresib, a Small-Molecule Inhibitor of Bromodomain and Extraterminal Proteins, in Patients With Selected Advanced Solid Tumors. *J Clin Oncol* (2018) 36:3007–14. doi: 10.1200/JCO.2018.78.2292
78. Boussiotis VA. Molecular and Biochemical Aspects of the PD-1 Checkpoint Pathway. *N Engl J Med* (2016) 375:1767–78. doi: 10.1056/NEJMra1514296
79. Fiorica F, Belluomini L, Stefanelli A, Santini A, Urbini B, Giorgi C, et al. Immune Checkpoint Inhibitor Nivolumab and Radiotherapy in Pretreated Lung Cancer Patients: Efficacy and Safety of Combination. *Am J Clin Oncol* (2018) 41:1101–5. doi: 10.1097/COC.0000000000000428
80. Formenti SC, Rudqvist N, Golden E, Cooper B, Wennerberg E, Lhuillier C, et al. Radiotherapy Induces Responses of Lung Cancer to CTLA-4 Blockade. *Nat Med* (2018) 24:1845–51. doi: 10.1038/s41591-018-0232-2
81. Bernstein MB, Krishnan S, Hodge JW, Chang JY. Immunotherapy and Stereotactic Ablative Radiotherapy (ISABR): A Curative Approach? *Nat Rev Clin Oncol* (2016) 13:516–24. doi: 10.1038/nrclinonc.2016.30
82. Khalifa J, Mazieres J, Gomez-Roca C, Ayyoub M, Moyal EC. Radiotherapy in the Era of Immunotherapy With a Focus on Non-Small-Cell Lung Cancer: Time to Revisit Ancient Dogmas? *Front Oncol* (2021) 11:662236. doi: 10.3389/fonc.2021.662236
83. Hogg SJ, Vervoort SJ, Deswal S, Ott CJ, Li J, Cluse LA, et al. BET-Bromodomain Inhibitors Engage the Host Immune System and Regulate Expression of the Immune Checkpoint Ligand PD-L1. *Cell Rep (Cambridge)* (2017) 18:2162–74. doi: 10.1016/j.celrep.2017.02.011
84. Zhu H, Bengsch F, Svoronos N, Rutkowski MR, Bitler BG, Allegrezza MJ, et al. BET Bromodomain Inhibition Promotes Anti-Tumor Immunity by Suppressing PD-L1 Expression. *Cell Rep* (2016) 16:2829–37. doi: 10.1016/j.celrep.2016.08.032
85. Wang F, Wang S, Zhou Q. The Resistance Mechanisms of Lung Cancer Immunotherapy. *Front Oncol* (2020) 10:568059. doi: 10.3389/fonc.2020.568059
86. Meder L, Schuldt P, Thelen M, Schmitt A, Dietlein F, Klein S, et al. Combined VEGF and PD-L1 Blockade Displays Synergistic Treatment

Effects in an Autochthonous Mouse Model of Small Cell Lung Cancer. *Cancer Res* (2018) 78:4270–81. doi: 10.1158/0008-5472.CAN-17-2176
87. Inda AM, Andrini LB, García MN, García AL, Fernández Blanco A, Furnus CC, et al. Evaluation of Angiogenesis With the Expression of VEGF and CD34 in Human Non-Small Cell Lung Cancer. *J Exp Clin Cancer research: CR* (2007) 26:375–8.
88. Bing Z, Jian-ru Y, Yao-quan J, Shi-feng C. Evaluation of Angiogenesis in Non-Small Cell Lung Carcinoma by CD34 Immunohistochemistry. *Cell Biochem Biophys* (2014) 70:327–31. doi: 10.1007/s12013-014-9916-5
89. Yano T, Tanikawa S, Fujie T, Masutan M. Vascular Endothelial Growth Factor Expression and Neovascularisation in Non-Small Cell Lung Cancer. *Eur J Cancer (Oxford England: 1990)* (2000) 36:601–9. doi: 10.1016/S0959-8049(99)00327-5
90. Ushijima C, Tsukamoto S, Yamazaki K, Yoshino I, Sugio K, Sugimachi K. High Vascularity in the Peripheral Region of Non-Small Cell Lung Cancer Tissue Is Associated With Tumor Progression. *Lung Cancer (Amsterdam Netherlands)* (2001) 34:233–41. doi: 10.1016/S0169-5002(01)00246-X
91. Ene Nicolae CD, Nicolae I. Interleukin 8 Serum Concentration, But Not Lactate Dehydrogenase Activity, Positively Correlates to CD34 Antigen in Melanoma Tumors. *J Immunoassay Immunochemistry* (2016) 37:463–71. doi: 10.1080/15321819.2016.1155996
92. Li W, Chastain K. NUT Midline Carcinoma With Leukemic Presentation Mimicking CD34-Positive Acute Leukemia. *Blood* (2018) 132:456. doi: 10.1182/blood-2017-07-796268
93. Shatavi S, Fawole A, Haberichter K, Jaiyesimi I, French C. Nuclear Protein in Testis (NUT) Midline Carcinoma With a Novel Three-Way Translocation (4;15;19)(Q13;Q14;P13.1). *Pathology* (2016) 48:620–3. doi: 10.1016/j.pathol.2016.06.010
94. Gabrilovich DI, Chen HL, Girgis KR, Cunningham HT, Meny GM, Nadaf S, et al. Production of Vascular Endothelial Growth Factor by Human Tumors Inhibits the Functional Maturation of Dendritic Cells. *Nat Med* (1996) 2:1096–103. doi: 10.1038/nm1096-1096
95. Goel S, Duda DG, Xu L, Munn LL, Boucher Y, Fukumura D, et al. Normalization of the Vasculature for Treatment of Cancer and Other Diseases. *Physiol Rev* (2011) 91:1071–121. doi: 10.1152/physrev.00038.2010
96. Motz GT, Santoro SP, Wang L, Garrabrant T, Lastra RR, Hagemann IS, et al. Tumor Endothelium Fasl Establishes a Selective Immune Barrier Promoting Tolerance in Tumors. *Nat Med* (2014) 20:607–15. doi: 10.1038/nm.3541
97. Hodi FS, Lawrence D, Lezcano C, Wu X, Zhou J, Sasada T, et al. Bevacizumab Plus Ipilimumab in Patients With Metastatic Melanoma. *Cancer Immunol Res* (2014) 2:632–42. doi: 10.1158/2326-6066.CIR-14-0053
98. Wallin JJ, Bendell JC, Funke R, Sznol M, Korski K, Jones S, et al. Atezolizumab in Combination With Bevacizumab Enhances Antigen-Specific T-Cell Migration in Metastatic Renal Cell Carcinoma. *Nat Commun* (2016) 7:12624. doi: 10.1038/ncomms12624
99. Voron T, Colussi O, Marcheteau E, Pernot S, Nizard M, Pointet AL, et al. VEGF-a Modulates Expression of Inhibitory Checkpoints on CD8+ T Cells in Tumors. *J Exp Med* (2015) 212:139–48. doi: 10.1084/jem.20140559
100. Gabrilovich DI, Nagaraj S. Myeloid-Derived Suppressor Cells as Regulators of the Immune System. *Nat Rev Immunol* (2009) 9:162–74. doi: 10.1038/nri2506
101. Roland CL, Lynn KD, Toombs JE, Dineen SP, Udugamasooriya DG, Brekken RA. Cytokine Levels Correlate With Immune Cell Infiltration After Anti-VEGF Therapy in Preclinical Mouse Models of Breast Cancer. *PloS One* (2009) 4:e7669. doi: 10.1371/journal.pone.0007669
102. Facciabene A, Peng X, Hagemann IS, Balint K, Barchetti A, Wang LP, et al. Tumour Hypoxia Promotes Tolerance and Angiogenesis *via* CCL28 and T (Reg) Cells. *NATURE* (2011) 475:226–30. doi: 10.1038/nature10169
103. Ding T, Wang Y, Zhao T, Xu Z, Gao W, Cui Z, et al. NUT Midline Carcinoma in the Right Orbit: A Case Report. *Cancer Biol Ther* (2019) 20:1091–6. doi: 10.1080/15384047.2019.1598761
104. Chai P, Zhou C, Jia R, Wang Y. Orbital Involvement by NUT Midline Carcinoma: New Presentation and Encouraging Outcome Managed by Radiotherapy Combined With Tyrosine Kinase Inhibitor: A Case Report. *Diagn Pathol* (2020) 15:2. doi: 10.1186/s13000-019-0922-1
105. Liu Q, Li A, Tian Y, Wu JD, Liu Y, Li T, et al. The CXCL8-CXCR1/2 Pathways in Cancer. *Cytokine Growth F R* (2016) 31:61–71. doi: 10.1016/j.cytogfr.2016.08.002
106. Alfaro C, Sanmamed MF, Rodríguez-Ruiz ME, Teijeira Á, Oñate C, González Á, et al. Interleukin-8 in Cancer Pathogenesis, Treatment and Follow-Up. *Cancer Treat Rev* (2017) 60:24–31. doi: 10.1016/j.ctrv.2017.08.004
107. Rose JJ, Foley JF, Murphy PM, Venkatesan S. On the Mechanism and Significance of Ligand-Induced Internalization of Human Neutrophil Chemokine Receptors CXCR1 and CXCR2. *J Biol Chem* (2004) 279:24372–86. doi: 10.1074/jbc.M401364200
108. Gonzalez-Aparicio M, Alfaro C. Significance of the IL-8 Pathway for Immunotherapy. *Hum Vacc Immunother* (2020) 16:2312–7. doi: 10.1080/21645515.2019.1696075
109. Fujimura T, Kambayashi Y, Aiba S. Crosstalk Between Regulatory T Cells (Tregs) and Myeloid Derived Suppressor Cells (Mdscs) During Melanoma Growth. *Oncoimmunology* (2012) 1:1433–4. doi: 10.4161/onci.21176
110. Leibowitz-Amit R, Pintilie M, Khoja L, Azad AA, Berger R, Laird AD, et al. Changes in Plasma Biomarkers Following Treatment With Cabozantinib in Metastatic Castration-Resistant Prostate Cancer: A *Post Hoc* Analysis of an Extension Cohort of a Phase II Trial. *J Transl Med* (2016) 14:12. doi: 10.1186/s12967-015-0747-y
111. Sanmamed MF, Perez-Gracia JL, Schalper KA, Fusco JP, Gonzalez A, Rodriguez-Ruiz ME, et al. Changes in Serum Interleukin-8 (IL-8) Levels Reflect and Predict Response to Anti-PD-1 Treatment in Melanoma and Non-Small-Cell Lung Cancer Patients. *Ann Oncol* (2017) 28:1988–95. doi: 10.1093/annonc/mdx190
112. Schalper KA, Carleton M, Zhou M, Chen T, Feng Y, Huang SP, et al. Elevated Serum Interleukin-8 Is Associated With Enhanced Intratumor Neutrophils and Reduced Clinical Benefit of Immune-Checkpoint Inhibitors. *Nat Med* (2020) 26:688–92. doi: 10.1038/s41591-020-0856-x
113. Bakouny Z, Choueiri TK. IL-8 and Cancer Prognosis on Immunotherapy. *Nat Med* (2020) 26:650–1. doi: 10.1038/s41591-020-0873-9
114. Arenberg DA, Kunkel SL, Polverini PJ, Glass M, Burdick MD, Strieter RM. Inhibition of Interleukin-8 Reduces Tumorigenesis of Human Non-Small Cell Lung Cancer in SCID Mice. *J Clin Invest* (1996) 97:2792–802. doi: 10.1172/JCI118734
115. Smith DR, Polverini PJ, Kunkel SL, Orringer MB, Whyte RI, Burdick MD, et al. Inhibition of Interleukin 8 Attenuates Angiogenesis in Bronchogenic Carcinoma. *J Exp Med* (1994) 179:1409–15. doi: 10.1084/jem.179.5.1409
116. Dominguez C, McCampbell KK, David JM, Palena C. Neutralization of IL-8 Decreases Tumor PMN-Mdscs and Reduces Mesenchymalization of Claudin-Low Triple-Negative Breast Cancer. *JCI Insight* (2017) 2:e94296. doi: 10.1172/jci.insight.94296
117. Bilusic M, Heery CR, Collins JM, Donahue RN, Palena C, Madan RA, et al. Phase I Trial of Humax-IL8 (BMS-986253), an Anti-IL-8 Monoclonal Antibody, in Patients With Metastatic or Unresectable Solid Tumors. *J Immunother Cancer* (2019) 7:240. doi: 10.1186/s40425-019-0706-x
118. Highfill SL, Cui Y, Giles AJ, Smith JP, Zhang H, Morse E, et al. Disruption of CXCR2-Mediated MDSC Tumor Trafficking Enhances Anti-PD1 Efficacy. *Sci Transl Med* (2014) 6:237r–67r. doi: 10.1126/scitranslmed.3007974
119. Ameratunga M, Chénard-Poirier M, Moreno Candilejo I, Pedregal M, Lui A, Dolling D, et al. Neutrophil-Lymphocyte Ratio Kinetics in Patients With Advanced Solid Tumours on Phase I Trials of PD-1/PD-L1 Inhibitors. *Eur J Cancer* (2018) 89:56–63. doi: 10.1016/j.ejca.2017.11.012
120. Zer A, Sung MR, Walia P, Khoja L, Maganti M, Labbe C, et al. Correlation of Neutrophil to Lymphocyte Ratio and Absolute Neutrophil Count With Outcomes With PD-1 Axis Inhibitors in Patients With Advanced Non-Small-Cell Lung Cancer. *Clin Lung Cancer* (2018) 19:426–34. doi: 10.1016/j.cllc.2018.04.008
121. Jiang T, Bai Y, Zhou F, Li W, Gao G, Su C, et al. Clinical Value of Neutrophil-to-Lymphocyte Ratio in Patients With Non-Small-Cell Lung Cancer Treated With PD-1/PD-L1 Inhibitors. *Lung Cancer (Amsterdam Netherlands)* (2019) 130:76–83. doi: 10.1016/j.lungcan.2019.02.009
122. Bagley SJ, Kothari S, Aggarwal C, Bauml JM, Alley EW, Evans TL, et al. Pretreatment Neutrophil-to-Lymphocyte Ratio as a Marker of Outcomes in Nivolumab-Treated Patients With Advanced Non-Small-Cell Lung Cancer. *Lung Cancer* (2017) 106:1–7. doi: 10.1016/j.lungcan.2017.01.013
123. He M, Chernock R, Zhou S, Gondim M, Dehner LP, Pfeifer JD. Tumor Mutation Burden and Checkpoint Immunotherapy Markers in NUT Midline

Carcinoma. *Appl Immunohisto M M* (2020) 28:495–500. doi: 10.1097/PAI.0000000000000781

Conflict of Interest: The authors declare that the research was conducted in the absence of any commercial or financial relationships that could be construed as a potential conflict of interest.

Publisher's Note: All claims expressed in this article are solely those of the authors and do not necessarily represent those of their affiliated organizations, or those of the publisher, the editors and the reviewers. Any product that may be evaluated in this article, or claim that may be made by its manufacturer, is not guaranteed or endorsed by the publisher.

Advantages of publishing in Frontiers

OPEN ACCESS
Articles are free to read for greatest visibility and readership

FAST PUBLICATION
Around 90 days from submission to decision

HIGH QUALITY PEER-REVIEW
Rigorous, collaborative, and constructive peer-review

TRANSPARENT PEER-REVIEW
Editors and reviewers acknowledged by name on published articles

Frontiers
Avenue du Tribunal-Fédéral 34
1005 Lausanne | Switzerland

Visit us: www.frontiersin.org
Contact us: frontiersin.org/about/contact

REPRODUCIBILITY OF RESEARCH
Support open data and methods to enhance research reproducibility

DIGITAL PUBLISHING
Articles designed for optimal readership across devices

FOLLOW US
@frontiersin

IMPACT METRICS
Advanced article metrics track visibility across digital media

EXTENSIVE PROMOTION
Marketing and promotion of impactful research

LOOP RESEARCH NETWORK
Our network increases your article's readership